



Novel conjugates of autotaxin
inhibitors for the treatment of ovarian
cancer

Ryan Allan Hemming
School of Science and Technology

A thesis submitted in partial fulfilment of the
requirements of
Nottingham Trent University
for the degree of Doctor of Philosophy

September 2018

Declaration

I confirm that this is my own work and the use of all materials from other sources has been properly and fully acknowledged. No part of this thesis has already been, or is being currently submitted for any such degree, diploma or other qualification.

Ryan Allan Hemming

Signed.....

Date.....

This work is the intellectual property of the author. You may copy up to 5% of this work for private study, or personal, non-commercial research. Any re-use of the information contained within this document should be fully referenced, quoting the author, title, university, degree level and pagination. Queries or requests for any other use, or if a more substantial copy is required, should be directed in the owner of the Intellectual Property Rights

Abstract

Over 7000 women are diagnosed with ovarian cancer each year in the UK. This disease is characterized by a particularly poor survival rate (40% at stage III, after 5 years), leading it to become known as a “silent killer”. This poor survival rate is due, in part, to the biological mechanisms by which cancer cells become resistant to drugs used in chemotherapy. The enzyme autotaxin has been strongly implicated in this process. Whilst many autotaxin inhibitors are extremely potent *in vitro*, when tested *in vivo* they have been found to perform poorly. This is partly because the drugs can be rapidly absorbed from their site of action, through the wall of the peritoneal cavity, before undergoing hepatic metabolism.

Herein we present a novel strategy that is designed to increase the residence time of an autotaxin inhibitor within the peritoneal cavity, using a novel polymer-drug conjugate approach for drug delivery. This was achieved through the attachment of a known autotaxin inhibitor to a high molecular weight polymer (Icodextrin or Inulin), known to be retained within the peritoneal cavity for extended periods of time. To our knowledge, Icodextrin has never been used as a vehicle for drug delivery outside of our research group. This thesis demonstrates the application of this novel drug conjugate approach, across a range of autotaxin inhibitors and polymers. The effect of polymer-drug loading on activity was also investigated, which to our knowledge has never been studied before with the supports used in this study. To facilitate this, a novel conjugation method was developed for the attachment of drug molecules to the polymer, which yielded 11 drug conjugates in total, which were then evaluated for their biological activity. The drug conjugates were found to be highly potent in separate assay types, with IC_{50} values as low as $300 \pm 40 \text{ ng / mL}^{-1}$ for Inulin-drug conjugates and $698 \pm 294 \text{ ng / mL}^{-1}$ for Icodextrin conjugates. This study also revealed the effect of drug loading on biological activity, which gave an unexpected result which could influence the design of polymer-drug conjugates in the future. The peritoneal retention of an Inulin-autotaxin inhibitor conjugate was studied in mice for the first time. The effect of intra polymer cross-linking on biological activity has also been evaluated.

Overall, the work described within this thesis could be used to provide an effective new therapeutic approach for the treatment of ovarian cancer; additionally the polymer therapeutic approach described in this work has the potential to be used in application to treat a variety of diseases.

Dedicated to my grandmother

Maureen Little

“Nannie”

Acknowledgements

I Would like to thank my Mum and Dad for their unconditional love.

I would also like to thank my Supervisor Professor Steve Allin, for his help and guidance throughout my PhD and final year masters project

My co-supervisors: Professor John Wallis, Dr Mike Edwards and Dr Alan Richardson

and Dr Liam Duffy, for his unlimited positivity.

My friends and colleagues: Myles, Jonny and Omar

My friends: Ryan, Jack, Theo, Tom, Amy, James, Abbey, James, Mark, Mike and Kial

I am a better person through having known you all.

I would also like to the Nottingham Trent University Vice Chancellor's Scholarship for the funding of this project and Charnwood Molecular Ltd, for their financial contribution for this project

Additionally, I would also like to thank the National Mass Spectrometry Facility at Swansea University for their superb service throughout the last three years

Associated publications

N. Fisher, M. G. Edwards, R. Hemming, S. M. Allin, J. D. Wallis, P. C. Bulman Page, M. J. McKenzie, S. Jones, M. R. J. Elsegood, J. King-Underwood and A. Richardson, Synthesis and Activity of a Novel Autotaxin Inhibitor-Icodextrin Conjugate, *J. Med. Chem.*, 2018, **61**, 7942–7951

R. A. Hemming, M. Bell, L. J. Duffy, J. Bristow, J. D. Wallis, S. M. Allin and P. C. Bulman Page, A Novel and Highly Stereoselective Route for the Synthesis of Non-racemic 3-Substituted Isoindolin-1-one Targets, *Tetrahedron*, Submitted 2018.

List of commonly used abbreviations

ATX	Autotaxin
DCE	1,2-Dichloroethane
DCM	Dichloromethane
DMAc	Dimethyl acetamide
DMF	N,N-Dimethylformamide
DMSO	Dimethyl sulfoxide
DS	Degree of substitution
EPI	Epichlorohydrin
ESI	Electrospray ionisation
HPLC	High performance liquid chromatography
IDX	Icodextrin
IMS	Industrial methylated spirit
INU	Inulin
IR	Infra-red
LPA	Lysophosphatidic acid
LPA _r	LPA receptor
LPC	Lysophosphatidylcholine
MP	Melting point
MTBE	Methyl tertiary-butyl ether
MWCO	Molecular weight cut off
NMR	Nuclear magnetic resonance
TFA	Trifluoroacetic acid

Table of Contents

Chapter 1: Introduction	2
1.1 Ovarian cancer	2
1.1.1 Ovarian cancer treatments.....	3
1.1.2 Chemoresistance	5
1.2 Autotaxin, introduction.....	6
1.2.1 Autotaxin and its role in ovarian cancer	10
1.2.2 Autotaxin and its role in other diseases	15
1.2.3 Inhibition of ATX.....	16
1.3 Drug delivery and polymer therapeutics	25
1.3.1 Reactive drug delivery systems	26
1.3.2 Passive drug delivery systems	27
1.3.3 Polymer therapeutics in the clinic	30
1.4 The peritoneal cavity	31
1.5 The development of a novel drug delivery strategy for the peritoneal cavity	33
1.5.1 Suitable polymer supports - Icodextrin	36
1.5.2 Suitable polymer supports – Inulin.....	38
1.5.3 Drug attachment methodologies in the literature:	40
1.5.4 Analysis of drug-polymer conjugates	45
1.5.5 Approaches to the synthesis of novel drug-conjugates	47
1.5.6 The use of linker / spacer units in drug polymer conjugates	47
1.6 Relevance to previous work.....	48
1.7 Project outline	50
1.8 Significance of drug-conjugation for potential treatment in the clinic.....	54
1.9 Aims of this work	55
Chapter 2: Synthesis of Icodextrin drug-polymer conjugates	57
2.1 Synthesis of 3-BoA linker analogue, initial route	57
2.1.1 Preparation of Nagano’s heterocycle	60
2.1.2 Synthesis of the boronic ester fragment	62
2.1.3 S _N 2 coupling between both fragments.....	67
2.1.4 Attachment of the linker to phenol 9	71
2.1.5 The conversion of ether 19 to a boronic acid.....	72
2.1.6 Synthesis of 3-BoA linker, summary	75
2.2 The attempted preparation of a 3-BoA-Icodextrin conjugate using the “tosylated IDX method”	77
2.2.1 Tosylated icodextrin approach, model study	79
2.2.2 The attempted preparation of a 3-BoA-Icodextrin conjugate, using the “tosylated drug method”	81
2.2.3 Alternative approaches using the “tosylated-drug method”	84
2.2.4 Tosylated drug approach, model drug study.....	87
2.3 Re-synthesis of HA155 analogue 45	90
2.3.1 Conjugation of 45 to IDX (Conjugate 17).....	92
2.4 The attempted synthesis of a HA155-IDX conjugate, using the “tosylated drug method”	94
2.4.1 The preparation of a boronic acid, HA155 linker analogue.....	94

2.5 The attempted conjugation of a linker analogue of HA155 to IDX	96
2.6 Discussion of the difficulties encountered with attaching drug-linker analogues to IDX	97
2.7 Alternative approaches to the preparation of boronic acid ATX inhibitor-IDX conjugates	100
2.7.1 MIDA protected boronic acid approach	101
2.7.2 Conjugation of 51 to IDX in the presence of water	103
2.7.3 “Late-stage” borylation approach	104
Chapter 3: Synthesis of Inulin drug conjugates and the development of the “epichlorohydrin activation method” for both Inulin and IDX	108
3.1 Attempted preparation of Inulin drug conjugates, using the “tosylated drug method”	108
3.2 The development of the “epichlorohydrin activation method” for Inulin, introduction	111
3.2.1 Trial reactions	113
3.2.2 Attempted preparation of a 3-BoA-Inulin conjugate using the “epichlorohydrin activation method”	117
3.2.3 Preparation of carboxylic acid-ATX inhibitor Inulin conjugates, early method	118
3.3 The development of the “epichlorohydrin activation method” for IDX	119
3.3.1 ¹ H NMR Study of the reaction between epichlorohydrin and IDX over time	122
3.3.2 Refinement of the epichlorohydrin method for IDX	125
3.4 Further refinement of the “epichlorohydrin activation method” for Inulin and IDX	126
3.5 Final reaction optimisation	128
3.6 Synthesis of IDX and Inulin drug conjugates, optimised conditions	129
3.7 Drug loading study	130
3.7.1 Quantification of drug loading: determining the degree of substitution (DS)	132
3.8 Synthesis of a highly crosslinked Icodextrin drug-conjugate	134
3.9 Boronic acid ATX inhibitor IDX / Inulin conjugates, using the epichlorohydrin method	135
3.9.1 Synthesis of boronic acid “free-drug”	137
3.10 Attempted conjugation of GLPG 1690 to IDX and Inulin	139
3.10.1 Introduction	139
3.10.2 Synthesis of GLPG 1690	140
3.10.3 Synthesis of fragment 2	141
3.10.4 Coupling reaction between amine 66 and chloride 62 and proceeding transformations	142
3.10.5 The preparation of fragment 3 and synthesis of GLPG 1690	143
3.11 Attempted attachment of a diethylene glycol linker to GLPG 1690	144
3.12 Summary of Chapter 2 and 3	145
Chapter 4: The biological evaluation of novel ATX inhibitor-IDX and ATX inhibitor-Inulin drug conjugates	147
4.1 Introduction	147
4.2 Autotaxin inhibition assays	147
4.2.1 Bis(<i>para</i> -nitrophenyl) phosphate (Bis- <i>p</i> NPP) artificial substrate assay	148
4.2.2 Fluorogenic substrate-3 (FS-3) artificial substrate assay	154
4.3 Discussion of results	158
4.3.1 The effect of drug loading on activity	161

4.3.2 The effect of intra-polymer cross-linking on biological activity	165
4.4 Peritoneal retention study	166
4.4.1 Introduction	166
4.4.2 Method	166
4.4.3 Discussion of results	167
4.5 Conclusion	167
Chapter 5: Novel approaches to the asymmetric synthesis of 3-substituted isoindolin-1-ones	169
5.1 Introduction	169
5.1.1 Approaches of to the stereoselective synthesis of isoindolinones in the literature	170
5.1.2 Our previous work	172
5.2 Application to the synthesis of a range of 3-substituted isoindolin-1-one targets.....	179
5.2.1 Removal of the chiral auxiliary	181
5.3 Attempted enantioselective synthesis of an isoindolinone drug molecule	181
5.4 Conclusion	185
Chapter 6: Conclusion, future work and final comments.....	187
6.1 Conclusion.....	187
6.2 Future work.....	189
6.3 Concluding remarks	192
Chapter 7: Experimental methodology.....	194
7.1 Synthetic chemistry.....	196
7.1.1 2-(Hydroxymethyl)-4-(4,4,5,5-tetramethyl-1,3,2-dioxaborolan-2-yl)phenol, (7)	196
7.1.2 2-Hydroxy-5-(4,4,5,5-tetramethyl-1,3,2-dioxaborolan-2-yl)benzaldehyde, (8)	197
7.1.3 2-Methyl-4-(4,4,5,5-tetramethyl-1,3,2-dioxaborolan-2-yl)phenol, (4)	198
7.1.4 2-Methyl-4-(4,4,5,5-tetramethyl-1,3,2-dioxaborolan-2-yl)phenyl acetate, (14)	199
7.1.5 2-(Bromomethyl)-4-(4,4,5,5-tetramethyl-1,3,2-dioxaborolan-2-yl)phenyl acetate, (15) ...	200
7.1.6 <i>tert</i> -Butyl piperazine-1-carboxylate, (1)	201
7.1.7 <i>tert</i> -Butyl-(<i>Z</i>)-4-(5-(3,4-dichlorobenzylidene)-4-oxo-4,5-dihydrothiazol-2-yl)piperazine-1-carboxylate, (2)	202
7.1.8 (<i>Z</i>)-5-(3,4-Dichlorobenzylidene)-2-(piperazin-1-yl)thiazol-4(5H)-one, (17)	203
7.1.9 (<i>Z</i>)-2-((4-(5-(3,4-Dichlorobenzylidene)-4-oxo-4,5-dihydrothiazol-2-yl)piperazin-1-yl)methyl)-4-(4,4,5,5-tetramethyl-1,3,2-dioxaborolan-2-yl)phenyl acetate, (16)	205
7.1.10 (<i>Z</i>)-5-(3,4-Dichlorobenzylidene)-2-(4-(2-hydroxy-5-(4,4,5,5-tetramethyl-1,3,2-dioxaborolan-2-yl)benzyl)piperazin-1-yl)thiazol-4(5H)-one, (9)	206
7.1.11 2-(2-Bromoethoxy)ethan-1-ol, (18)	207
7.1.12 (<i>Z</i>)-5-(3,4-Dichlorobenzylidene)-2-(4-(2-(2-(2-hydroxyethoxy)ethoxy)-5-(4,4,5,5-tetramethyl-1,3,2-dioxaborolan-2-yl)benzyl)piperazin-1-yl)thiazol-4(5H)-one, (19)	208
7.1.13 Potassium (<i>Z</i>)-(3-((4-(5-(3,4-dichlorobenzylidene)-4-oxo-4,5-dihydrothiazol-2-yl).....	209
7.1.14 (<i>Z</i>)-(3-((4-(5-(3,4-Dichlorobenzylidene)-4-oxo-4,5-dihydrothiazol-2-yl)piperazin-1-yl)methyl)-4-(2-(2-hydroxyethoxy)ethoxy)phenyl)boronic acid, (22)	210
7.1.15 (<i>Z</i>)-2-(2-(2-((4-(5-(3,4-Dichlorobenzylidene)-4-oxo-4,5-dihydrothiazol-2-yl)piperazin-1-yl)methyl)-4-(4,4,5,5-tetramethyl-1,3,2-dioxaborolan-2-yl)phenoxy)ethoxy)ethyl 4-methylbenzenesulfonate, (31)	211
7.1.16 Potassium (<i>Z</i>)-(3-((4-(5-(3,4-dichlorobenzylidene)-4-oxo-4,5-dihydrothiazol-2-yl)piperazin-1-yl)methyl)-4-(2-(2-(tosyloxy)ethoxy)ethoxy)phenyl)trifluoroborate, (32)	212

7.1.17 (Z)-5-(3,4-Dichlorobenzylidene)-2-(4-(2-(2-(2-(2-hydroxyethoxy)ethoxy)ethoxy)-5-(4,4,5,5-tetramethyl-1,3,2-dioxaborolan-2-yl)benzyl)piperazin-1-yl)thiazol-4(5H)-one, (34)	213
7.1.18 (Z)-2-(2-(2-(2-((4-(5-(3,4-Dichlorobenzylidene)-4-oxo-4,5-dihydrothiazol-2-yl) piperazin-1-yl)methyl)-4-(4,4,5,5-tetramethyl-1,3,2-dioxaborolan-2-yl)phenoxy)ethoxy) ethoxy)ethyl 4-methylbenzenesulfonate, (35)	214
7.1.19 (Z)-2-(2-(2-((4-(5-(3,4-Dichlorobenzylidene)-4-oxo-4,5-dihydrothiazol-2-yl)piperazin-1-yl)methyl)-4-(4,4,5,5-tetramethyl-1,3,2-dioxaborolan-2-yl)phenoxy)ethoxy)ethylmethanesulfonate, (36)	215
7.1.20 2-Methyl-5-(4,4,5,5-tetramethyl-1,3,2-dioxaborolan-2-yl)phenol, (23)	216
7.1.21 2-Methyl-5-(4,4,5,5-tetramethyl-1,3,2-dioxaborolan-2-yl)phenyl acetate, (24)	217
7.1.22 2-(Bromomethyl)-5-(4,4,5,5-tetramethyl-1,3,2-dioxaborolan-2-yl)phenyl acetate, (25)	218
7.1.23 (Z)-2-((4-(5-(3,4-dichlorobenzylidene)-4-oxo-4,5-dihydrothiazol-2-yl)piperazin-1-yl)methyl)-5-(4,4,5,5-tetramethyl-1,3,2-dioxaborolan-2-yl)phenyl acetate, (26)	219
7.1.24 (Z)-5-(3,4-Dichlorobenzylidene)-2-(4-(2-hydroxy-4-(4,4,5,5-tetramethyl-1,3,2-dioxaborolan-2-yl)benzyl)piperazin-1-yl)thiazol-4(5H)-one, (27)	220
7.1.25 (Z)-5-(3,4-Dichlorobenzylidene)-2-(4-(2-(2-(2-hydroxyethoxy)ethoxy)-4-(4,4,5,5-tetramethyl-1,3,2-dioxaborolan-2-yl)benzyl)piperazin-1-yl)thiazol-4(5H)-one, (28)	221
7.1.26 2-(2-(2-Methyl-4-(4,4,5,5-tetramethyl-1,3,2-dioxaborolan-2-yl)phenoxy)ethoxy)	222
7.1.27 Potassium trifluoro(4-(2-(2-hydroxyethoxy)ethoxy)-3-methylphenyl)borate, (29)	223
7.1.28 4-(2-(2-Hydroxyethoxy)ethoxy)-3-methylphenyl)boronic acid, (30)	224
7.1.29 2-(2-(2-Methyl-4-(4,4,5,5-tetramethyl-1,3,2-dioxaborolan-2-yl)phenoxy)ethoxy)ethyl-4-methylbenzenesulfonate, (37)	225
7.1.30 2-(2-(2-methyl-4-(4,4,5,5-tetramethyl-1,3,2-dioxaborolan-2-yl)phenoxy)ethoxy)ethyl 2-chloroacetate, (38)	226
7.1.31 4-((4-Bromobenzyl)oxy)-3-hydroxybenzaldehyde, (46)	227
7.1.32 3-Hydroxy-4-((4-(4,4,5,5-tetramethyl-1,3,2-dioxaborolan-2-yl)benzyl)oxy)benzaldehyde, (47)	228
7.1.33 3-(4-Fluorobenzyl)thiazolidine-2,4-dione, (42)	229
7.1.34 3-(2-(2-hydroxyethoxy)ethoxy)-4-((4-(4,4,5,5-tetramethyl-1,3,2-dioxaborolan-2-yl)benzyl)oxy)benzaldehyde, (48)	230
7.1.35 (Z)-3-(4-Fluorobenzyl)-5-(3-(2-(2-hydroxyethoxy)ethoxy)-4-((4-(4,4,5,5-tetramethyl-1,3,2-dioxaborolan-2-yl)benzyl)oxy)benzylidene)thiazolidine-2,4-dione, (49)	231
7.1.36 (Z)-2-(2-(5-((3-(4-Fluorobenzyl)-2,4-dioxothiazolidin-5-ylidene)methyl)-2-((4-(4,4,5,5-tetramethyl-1,3,2-dioxaborolan-2-yl)benzyl)oxy)phenoxy)ethoxy)ethyl 4-methylbenzenesulfonate, (50)	232
7.1.37 (Z)-4-((4-((3-(4-fluorobenzyl)-2,4-dioxothiazolidin-5-ylidene)methyl)-2-(2-(2-.....	234
7.1.38 Potassium (Z)-trifluoro(4-((4-((3-(4-fluorobenzyl)-2,4-dioxothiazolidin-5-ylidene)	235
7.1.39 Methyl 4-((4-formyl-2-hydroxyphenoxy)methyl)benzoate, (39)	236
7.1.40 Methyl 4-((4-formyl-2-(2-(2-hydroxyethoxy)ethoxy)phenoxy)methyl)benzoate, (40)	237
7.1.41 4-((4-Formyl-2-(2-(2-hydroxyethoxy)ethoxy)phenoxy)methyl)benzoic acid, (41)	238
7.1.42 (Z)-4-((4-((3-(4-Fluorobenzyl)-2,4-dioxothiazolidin-5-ylidene)methyl)-2-(2-(2-hydroxyethoxy)ethoxy)phenoxy)methyl)benzoic acid, (43)	239
7.1.43 Triisopropylsilyl-(Z)-4-((4-((3-(4-fluorobenzyl)-2,4-dioxothiazolidin-5-ylidene)methyl)-2-(2-(2-hydroxyethoxy)ethoxy)phenoxy)methyl)benzoate, (44)	240
7.1.44 Triisopropylsilyl(Z)-4-((4-((3-(4-fluorobenzyl)-2,4-dioxothiazolidin-5-ylidene)methyl)-2-(2-(2-(tosyloxy)ethoxy)ethoxy)phenoxy)methyl)benzoate, (45)	241
7.1.45 Potassium (Z)-trifluoro(4-((4-((3-(4-fluorobenzyl)-2,4-dioxothiazolidin-5-ylidene)	242
7.1.46 (Z)-4-((4-((3-(4-fluorobenzyl)-2,4-dioxothiazolidin-5-ylidene)methyl)-2-(2-(2-hydroxyethoxy)ethoxy)phenoxy)methyl)phenyl)boronic acid, (52)	243
7.1.47 (Z)-2-(4-((4-((3-(4-Fluorobenzyl)-2,4-dioxothiazolidin-5-ylidene)methyl)-2-(2-(2-hydroxyethoxy)ethoxy)phenoxy)methyl)phenyl)-6-methyl-1,3,6,2-dioxazaborocane-4,8-dione, (53)	244

7.1.48	(Z)-2-(2-(5-((3-(4-Fluorobenzyl)-2,4-dioxothiazolidin-5-ylidene)methyl)-2-((4-(6-methyl-4,8-dioxo-1,3,6,2-dioxaborocan-2-yl)benzyl)oxy)phenoxy)ethoxy)ethyl 4-methylbenzenesulfonate, (54)	245
7.1.49	4-((4-bromobenzyl)oxy)-3-(2-(2-hydroxyethoxy)ethoxy)benzaldehyde, (55)	246
7.1.50	(Z)-5-(4-((4-Bromobenzyl)oxy)-3-(2-(2-hydroxyethoxy)ethoxy)benzylidene)-3-(4-fluorobenzyl)thiazolidine-2,4-dione, (56)	247
7.1.51	(Z)-2-(2-(2-((4-Bromobenzyl)oxy)-5-((3-(4-fluorobenzyl)-2,4-dioxothiazolidin-5-ylidene)methyl)phenoxy)ethoxy)ethyl 4-methylbenzenesulfonate, (57)	248
7.1.52	(Z)-3-(4-Fluorobenzyl)-5-(3-hydroxy-4-((4-(4,4,5,5-tetramethyl-1,3,2dioxo	249
7.1.53	(Z)-3-(4-Fluorobenzyl)-5-(3-hydroxy-4-((4-(trifluoro-l4-boranyl)benzyl)	250
7.1.54	(Z)-4-((4-((3-(4-Fluorobenzyl)-2,4-dioxothiazolidin-5-ylidene)methyl)-2-hydroxyphenoxy)methyl)phenyl)boronic acid, (60)	251
7.1.55	Procedure for the isolation of solid Icodextrin from Adept® adhesion reduction solution:	252
7.1.56	Photos to demonstrate dialysis procedure:	253
7.1.57	Benzyl Icodextrin conjugate, (Conjugate 16).....	254
7.1.58	Icodextrin- 44 conjugate, (Conjugate 17).....	255
7.1.59	Inulin- (44) conjugate, (Conjugate 26).....	256
7.1.60	Inulin- (44) conjugate, (Conjugate 35).....	257
7.1.61	Inulin- (44) conjugate, (Conjugate 36).....	258
7.1.62	Inulin- (44) conjugate, (Conjugate 37).....	259
7.1.63	Inulin- (44) conjugate, (Conjugate 38).....	260
7.1.64	Inulin- (44) conjugate, (Conjugate 39).....	261
7.1.65	Inulin- (52) conjugate, (Conjugate 44).....	262
7.1.66	Icodextrin- (44) conjugate, (Conjugate 34)	263
7.1.67	Icodextrin- (44) conjugate, (Conjugate 40)	265
7.1.68	Icodextrin- (44) conjugate, (Conjugate 41)	266
7.1.69	Icodextrin- (44) conjugate, (Conjugate 42)	267
7.1.70	Icodextrin- (44) highly cross-linked conjugate, (Conjugate 43).....	268
7.1.71	Icodextrin- (52) conjugate, (Conjugate 45)	269
7.1.72	2-Amino-4-(4-fluorophenyl)thiazole-5-carbonitrile, (61)	271
7.1.73	2-Chloro-4-(4-fluorophenyl)thiazole-5-carbonitrile, (62)	271
7.1.74	6-Bromo-3-(chloro-l5-azaneyl)-2-ethyl-8-methylimidazo[1,2-a]pyridine, (63)	272
7.1.75	N-(6-Bromo-2-ethyl-8-methylimidazo[1,2-a]pyridin-3-yl)formamide, (64)	273
7.1.76	N-(6-Bromo-2-ethyl-8-methylimidazo[1,2-a]pyridin-3-yl)-N-methylformamide, (65)	274
7.1.77	6-Bromo-2-ethyl-N,8-dimethylimidazo[1,2-a]pyridin-3-amine, (66)	274
7.1.78	2-((6-Bromo-2-ethyl-8-methylimidazo[1,2-a]pyridin-3-yl)(methyl)amino)-4-(4-fluorophenyl)thiazole-5-carbonitrile, (67)	275
7.1.79	tert-Butyl 4-(3-((5-cyano-4-(4-fluorophenyl)thiazol-2-yl)(methyl)amino)-2-ethyl-8-methylimidazo[1,2-a]pyridin-6-yl)piperazine-1-carboxylate, (68)	276
7.1.80	2-((2-Ethyl-8-methyl-6-(piperazin-1-yl)imidazo[1,2-a]pyridin-3-yl)(methyl)amino)-4-(4-fluorophenyl)thiazole-5-carbonitrile, (69)	276
7.1.81	2-Chloro-1-(3-hydroxyazetid-1-yl)ethan-1-one, (70)	277
7.1.82	2-((2-Ethyl-6-(4-(2-(3-hydroxyazetid-1-yl)-2-oxoethyl)piperazin-1-yl)-8-methylimidazo[1,2-a]pyridin-3-yl)(methyl)amino)-4-(4-fluorophenyl)thiazole-5-carbonitrile, (71)	278
7.1.83	(3R,9bS)-3-Phenyl-2,3-dihydrooxazolo[2,3-a]isoindol-5(9bH)-one, (73)	279
7.1.84	(R)-2-((R)-2-Hydroxy-1-phenylethyl)-3-methylisoindolin-1-one, (74a)	279
7.1.85	(R)-3-Ethyl-2-((R)-2-hydroxy-1-phenylethyl)isoindolin-1-one, (74b)	280
7.1.86	(R)-2-((R)-2-Hydroxy-1-phenylethyl)-3-propylisoindolin-1-one, (74c)	282
7.1.87	(R)-3-Allyl-2-((R)-2-hydroxy-1-phenylethyl)isoindolin-1-one, (74d)	283
7.1.88	(R)-3-Benzyl-2-((R)-2-hydroxy-1-phenylethyl)isoindolin-1-one, (74e)	284
7.1.89	(R)-3-(2-Fluorobenzyl)-2-((R)-2-hydroxy-1-phenylethyl)isoindolin-1-one, (74f)	286

7.1.90 (<i>R</i>)-2-((<i>R</i>)-2-Hydroxy-1-phenylethyl)-3-(3-methoxybenzyl)isoindolin-1-one, (74g)	287
7.1.91 Preparation of C-3 racemic compound for chiral HPLC investigation	289
7.1.92 (<i>R</i>)-3-Methylisoindolin-1-one, (75)	289
7.1.93 (3 <i>S</i>)-9b-((1,3-Dioxolan-2-yl)methyl)-3-phenyl-2,3-dihydrooxazolo[2,3- <i>a</i>]isoindol-5(9 <i>bH</i>)-one, (76)	290
7.2 Biological evaluation	291
7.2.1 Bis-pNPP assay	291
7.2.2 FS3 Assay	292
7.2.3 Peritoneal retention	293
Chapter 8: References	294

Living is easy with eyes closed, misunderstanding all you see

-Lennon / McCartney

Chapter 1:

Introduction

Chapter 1: Introduction

1.1 Ovarian cancer

Over 7000 women are diagnosed with ovarian cancer each year in the UK and approximately 240,000 worldwide.^{1,2} Though it is less prevalent than many other cancers, 4200 women die from ovarian cancer each year in the UK and over 100,000 worldwide.^{1,3} Ovarian cancer is typified by a poor chance of survival, often caused by a resurgence in tumour growth after the initial treatment.¹⁻³

Ovarian cancer is characterised by an uncontrolled proliferation of cells, which forms a tumour. Three different cell types have been identified: germ cells, stromal cells and epithelial cells, though epithelial ovarian cancer is the most common.³⁻⁵ These are further divided into five main types: high-grade serous (70%, most prevalent), endometrioid (10%), clear cell (10%), mucinous (3%), and low-grade serous carcinomas (<5%).³⁻⁵ It is reported that these are essentially separate diseases, which will respond differently to chemotherapy, therefore accurate diagnosis of the tumour type is essential for an effective treatment.³ The progression of ovarian cancer is defined by the FIGO system, by Stages 1-4, (Figure 1).^{6,7}

As may be expected, the survival rate decreases for each Stage. At stage 1, 90% of women will survive beyond 5 years, this decreases to 40 % at Stage 2, 20 % at Stage 3 and lastly 5 % at stage 4.^{1,8} Though the outlook is positive at Stage 1, as the cancer spreads the chance of survival rapidly decreases, indeed, in the UK ovarian cancer has the poorest survival rate out of all female only cancers.⁹

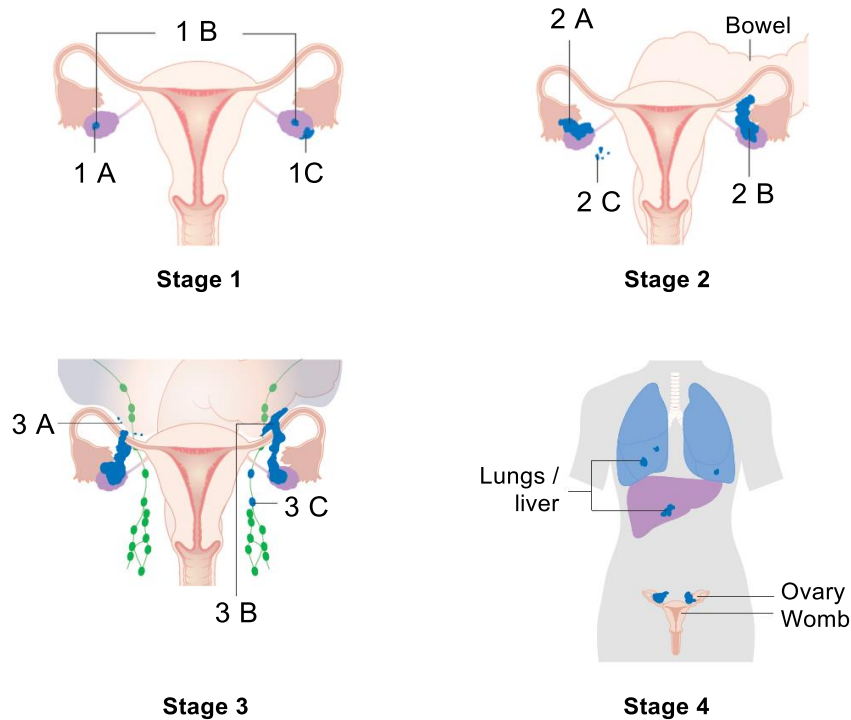


Figure 1 -Stage 1-4 ovarian cancer during the transition from one stage to the next, the severity of ovarian cancer increases. Stage 1 A, the tumour is localised inside one ovary; 1 B, the tumour is localised inside both ovaries; 1 C, the tumour is inside both ovaries and is on the surface of one ovary.^{6,7} Stage 2 A, the tumour has spread to the fallopian tubes; 2 B, the tumour has spread to the bladder or rectum; 2 C, cancer cells are present in the peritoneal cavity.^{6,7} Stage 3 A, cancer cells are present in samples from the peritoneum; 3 B, tumour growths smaller than 2 cm are found on the peritoneum; 3 C tumour growths larger than a diameter of 2 cm are found on the peritoneum.^{6,7} Stage 4 A, the cancer has caused a build-up of fluid in the lungs (known as a plural effusion); 4 B, the tumour has spread to the inside of the liver.^{6,7}

1.1.1 Ovarian cancer treatments

Ovarian cancer treatments follow a similar treatment regime to many other cancer therapies, and typically include a combination of surgery, chemotherapy and radiotherapy. In the case of stage 1 A-B, the preferred route of treatment is surgery to debulk the tumour, known as optimal surgical staging. It is suggested that chemotherapy should not be used while the tumour is localised inside the ovaries.^{10,11} At Stage 1 C, the tumour has spread outside of the ovaries, making surgery suboptimal. In this situation chemotherapy is administered alongside surgery. In late stage ovarian cancer (Stage 2-4) it is recommended that complete resection of all macroscopic disease is carried out before chemotherapy is administered. This is referred to as neoadjuvant chemotherapy and is commonly used when

the tumour is too difficult to remove completely *via* surgery.^{10,11} Radiotherapy is used less extensively in ovarian cancer, due to its impact on fertility; it is advised to use chemotherapy instead.¹¹

The most common chemotherapeutic agents used to treat ovarian cancer are carboplatin (preferred over cisplatin due to it being less toxic), paclitaxel, docetaxel and doxorubicin (Figure 2).^{12,13}

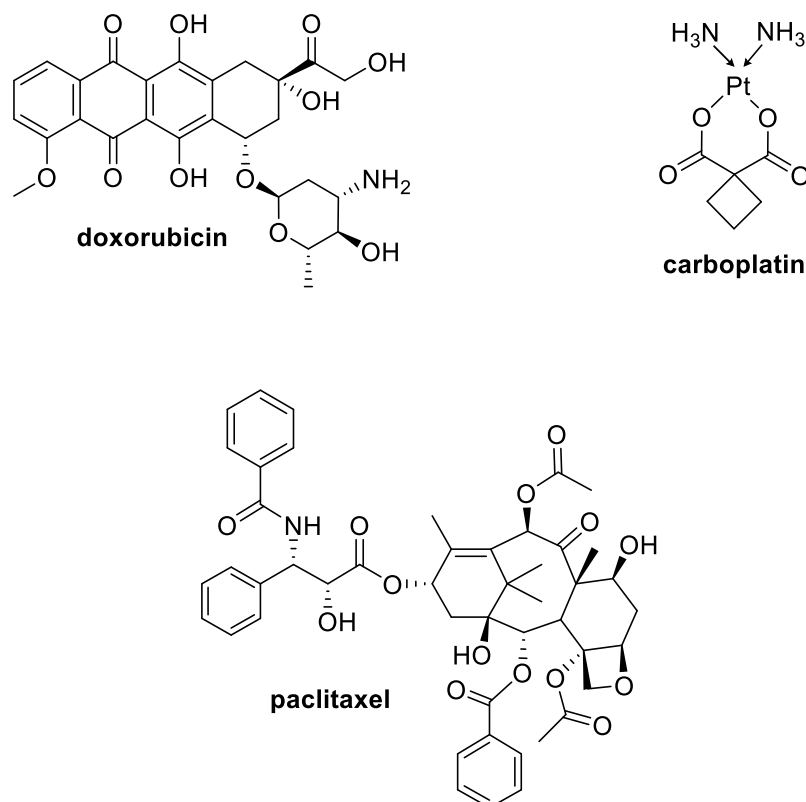


Figure 2 - The most commonly used drugs to treat ovarian cancer

Sometimes two chemotherapeutic agents of different modes of action are administered simultaneously, such as paclitaxel and carboplatin, drug combinations have been shown to be more effective than single drug regimens.¹⁴ Most chemotherapeutic agents for ovarian cancer are administered through an intravenous route, however it has been demonstrated that intraperitoneal administration can result in progression-free survival and longer survival periods, though it is less widely used.¹⁵ Patients are classified according to their “platinum sensitivity”, that is their response to platin drugs after 6 months. If they relapse they are defined as “platinum resistant” and their chemotherapy is adjusted so that an alternative agent is used, such as doxorubicin.¹⁶ The chemotherapeutic agents currently used to treat

ovarian cancer are undoubtedly effective therapies, however, it should be remembered that these drugs are cytotoxic and their use is not without detriment to the patient.^{14,17} There is a clear need for the development of new drugs tailored to ovarian cancer, with greater specificity for ovarian cancer cells.

1.1.2 Chemoresistance

As noted, ovarian cancer has a particularly poor survival rate. There are a number of factors that give rise to this situation. Ovarian cancer is most treatable in the early stages of disease progression (Stage 1 A-B, Figure 1) where it has a good rate of survival.¹¹ Yet, because ovarian cancer is asymptomatic in the early stages, it is most commonly diagnosed at the later Stages of tumour growth (Stage 2-4, Figure 1), when it is less treatable.¹ Additionally, there is a lack of biomarkers for ovarian cancer, which would be useful particularly to assist in early diagnosis of the disease.¹⁸ The most significant contributing factor to the poor survival rate associated with ovarian cancer is chemoresistance or multiple drug resistance (MDR). This phenomenon can occur 6 months or several years after the first round of chemotherapy, at which point tumour cells become less responsive to chemotherapeutic agents, across multiple classes of drugs.^{19,20} Chemoresistance in ovarian cancer originates *via* a number of mechanisms with ATP-Binding Cassette transporters (ABC transporters) being over-expressed in ovarian cancer.^{19,20} This is thought to occur through detoxifying systems being activated in response to exposure to a drug.^{19,20} ABC transporters (such as MDR1 and MRP1) actively transport the drug out of the cell, causing an efflux of the drug, which reduces accumulation and controls apoptosis.^{19,20}

Ovarian cancer cells can also become resistant to paclitaxel. Paclitaxel functions by selectively binding to β -tubulin, causing defects in mitotic spindle assembly, disrupting mitosis which leads to cell death.^{19,21} Ovarian cancer cells have been found to express specific β -tubulin isotypes, that are resistant to the effects of paclitaxel.^{19,21} As stated previously, ovarian cancer cells quickly develop resistance to platinum-based drugs. Cisplatin / carboplatin cause the intercalation of platinum within DNA strands (by cross-linking with purine bases on DNA), causing DNA damage.²² Resistance can occur *via* mechanisms that repair the damage caused by the platin drug, through a process known as nucleotide excision repair (NER), which removes damaged sections of DNA.^{19,23–25} Ovarian cancer cells can also

develop chemoresistance to drugs belonging to the anthracycline class (such as doxorubicin). These drugs target DNA conformation-controlling nuclear enzymes: topoisomerases.^{19,26} Anthracyclines function by stabilizing a reaction intermediate formed during the catalytic cycle of TopoII (referred to as the cleavable complex), which is involved in the transcription and replication of DNA, which leads to DNA damage and cell death.^{19,26} It is postulated that through mutation, resistance occurs by a reduction in cleavable complex formation, resulting in less DNA damage.^{19,26}

Of particular interest to us is the enzyme autotaxin (ATX), which has been identified to play a role in chemoresistance of ovarian cancer cells. ATX has also been noted to contribute to the proliferation, growth and survival of ovarian cancer cells.²⁷ It is now thought of as a promising target for multiple drug resistance in ovarian cancer.²⁷

1.2 Autotaxin, introduction

The glycoprotein autotaxin (ATX) (Figure 3), is a member of the ecto-nucleotide family (ENPP2) and has an important role in lipid signalling, through its function as an enzyme.²⁷⁻³¹ In recent years however, it has received attention regarding the part it plays in cancer and other diseases.²⁷⁻³¹

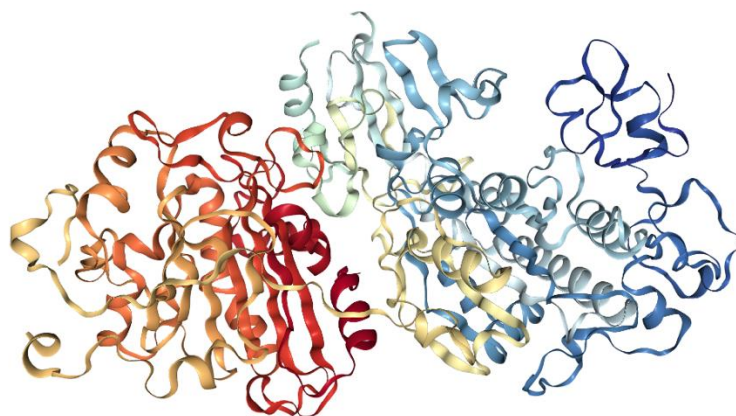


*Figure 3 – The X-ray structure of ATX*³²

The physiological role of autotaxin should not go unrecognised. For example it is involved in the formation of vascular structure within early embryos (ATX-deficient mice were found to die mid-gestation due to reduced blood vessel formation).^{30,33} It is believed that ATX also contributes to the proliferation, growth and survival of ovarian cancer cells through its

unique action as a lysophospholipase D.^{27,33,34} Phospholipids, unlike other chemical messengers, such as neurotransmitters, cannot be stored in vesicles. This is due to their hydrophobic structure they diffuse through membranes. Instead they are synthesised “on-command” from a parent molecule.^{32,33} Autotaxin has a high degree of specificity for the phospholipid lysophosphatidylcholine (LPC).^{31,33,35–38} ATX catalyses the hydrolysis of a phosphodiester bond located on LPC, removing a choline group to expose lysophosphatidic acid (LPA) (Figure 4).^{31,33,35–38} ATX has some limited activity towards sphingosylphosphorylcholine (SPC), hydrolysing SPC to sphingosine-1-phosphate (S1P).^{39–41}

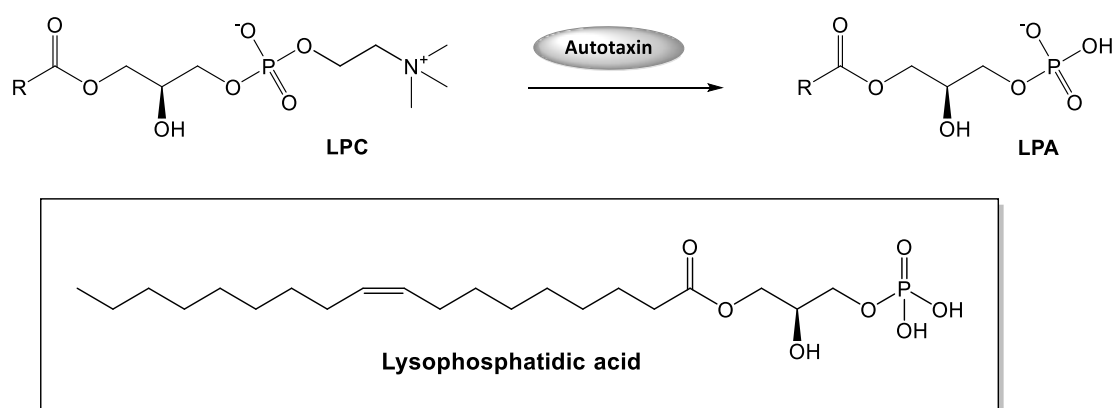


Figure 4- ATX catalyses the hydrolysis of LPC to LPA³³

Whilst other enzymatic processes lead to the production of LPA, such as the enzyme phospholipase A₂. Phospholipase A₂ catalyses the hydrolysis of LPC in the same manner, but despite this ATX is the major contributor of serum LPA.³⁰ A study in which mice were genetically engineered to not carry the gene for autotaxin, it was found that plasma LPA levels had decreased by 95%.³⁰

Understanding of autotaxin was greatly enhanced, when in 2011, the crystal structure for ATX was first reported by Perrakis and colleagues (Figure 3).^{42,43} This study revealed that ATX is comprised of four distinct domains, (Figure 5a).

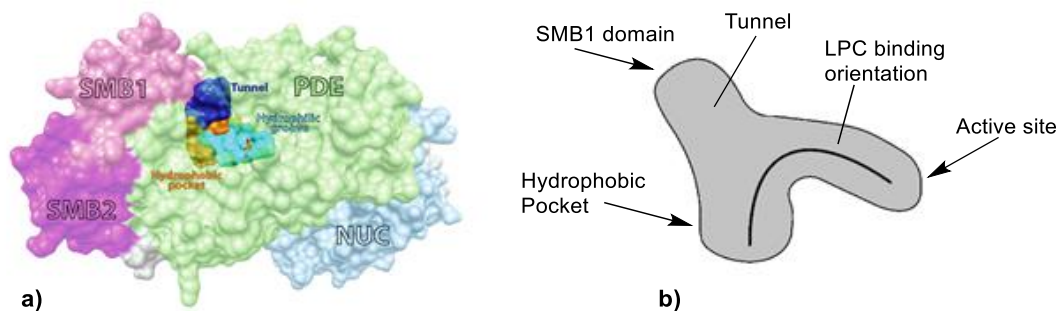
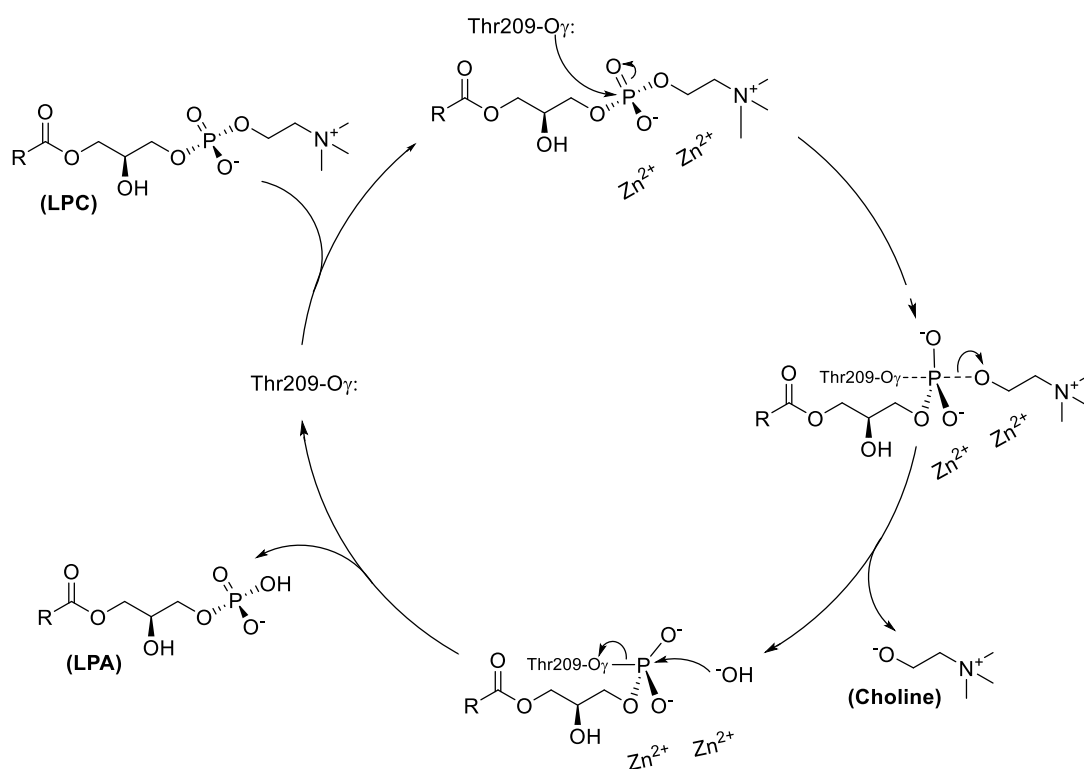


Figure 5 - a) Distinct domains within ATX, b) expansion of the T-shaped catalytic pocket^{29,44}

The PDE domain (phosphodiesterase domain) primarily concerns the catalytic function of ATX, containing the catalytic site.^{32,42,44} The two SMB “like” *N*-terminal domains (somatomedin B) lie next to the PDE domain.^{32,42,44} They both act in a broadly similar way and are known to facilitate protein-protein interactions.^{32,42,44} There is some evidence to suggest that SMB 1 has a role in stimulating LPA-independent cell migration.²⁹ The *C*-terminal nuclease “like” domain (NUC), along with the SMB domains act to encapsulate the PDE domain.^{29,44} This is achieved through two linkages: an *N*-linked glycan and an inter domain disulphide bridge, a “lasso” type loop wraps itself around the NUC domain starting from the PDE domain.^{29,44} These linkages assist in maintaining a conformationally rigid structure.^{29,44} Additionally, an extensive hydrogen bond network (as a consequence of water molecules sitting between the catalytic and NUC domains) and several hydrophilic and hydrophobic interactions act to stabilise the protein.^{29,44}

Within the PDE domain lies the core catalytic site. Unlike other members of the ENPP family, this site contains a hydrophobic pocket, shown in Figure 5b. It is 15 Å deep and has a volume of approximately 800 Å³, is 15 Å deep.^{29,32,42,44} The pocket readily accommodates lysophosphates but appears to have significance in determining the specificity of ATX for LPC. For example, LPC containing a saturated acyl (hydrophobic) chain of 14-16 carbon atoms in length is readily accommodated within the site, however saturated chains, longer than 18 atoms do not fit and are therefore not substrates.²⁹ Unsaturated (*Z*) acyl chains can adopt a “bent” conformation to fit within the pocket.²⁹ Connected to the hydrophobic pocket is a tunnel, (Figure 5b) comprised of both hydrophobic and hydrophilic residues along the tunnel wall.^{29,44} It is proposed that the tunnel acts to eject LPA following its conversion from LPC. The tunnel forms partly within the PDE domain, but also within SMB1.^{29,44}

The active site (Figure 5b) contains two Zn^{2+} atoms and in close proximity, a threonine residue (Thr209), these residues have been found to be essential for the catalytic activity of ATX.^{29,32,42,44} In a recent study by Perrakis and co-workers the hydrolysis of LPC to LPA by autotaxin was investigated.³² The authors suggest that the hydrolysis reaction adopts an associative mechanism in which the nucleophilic Thr209 (likely deprotonated by a neighbouring histidine residue) attacks the phosphodiester. The ligand (choline) then departs, analogous to a $\text{S}_{\text{N}}2$ mechanism.³² The phosphodiester substrate is held in the correct position for nucleophilic attack by Thr209 *via* two zinc atoms. Following the displacement of choline, hydroxide then attacks the phosphoester causing Thr209 to be displaced (Scheme 1).



*Scheme 1 - Proposed catalytic cycle of the hydrolysis of LPC to LPA by autotaxin.*³²

The study by Perrakis and co-workers involved obtaining ATX crystal structures with different substrates that closely match the transition state of the catalytic cycle. In the absence of being able to monitor it in real time, ATX-VO₅ to demonstrate the transition state, prior to choline being expelled (Figure 6). Whilst there is little conformational change in autotaxin during catalysis, the enzyme does act to stabilise the reaction intermediates.³² The O⁻ species

of the phosphodiester is stabilised by an interaction with the two zinc atoms. Additionally, the ligand orientates itself to favour the disassociation of choline.

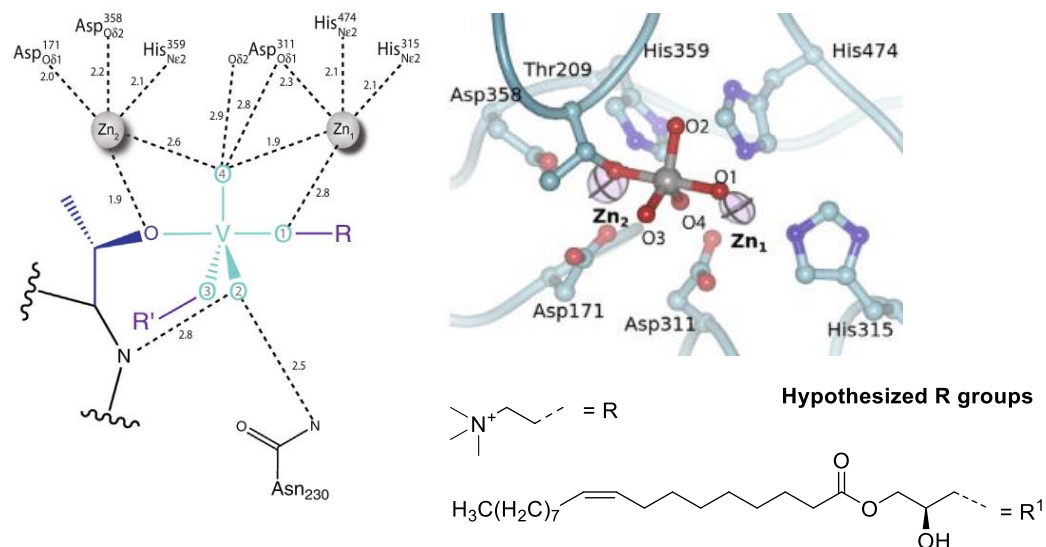


Figure 6 - ATX crystal structure bound to VO_5 , and a diagram to represent the transition state

1.2.1 Autotaxin and its role in ovarian cancer

The significance of autotaxin with regard to ovarian cancer can be largely attributed to its role in the production of LPA.^{31,33,36,38,44,45} Indeed, ovarian cancer patients have been found to have LPA in concentrations of up to 80 μM in their ascites fluid (compared to 7 μM in healthy patients).^{33,45,46} Upon its formation, LPA binds to G-protein coupled receptors: LPA₁₋₆. From there a cascade of different cellular responses is triggered, known to be conducive to the development of ovarian cancer. The extent of LPA signalling is shown in Figure 7.^{31,33,36,44}

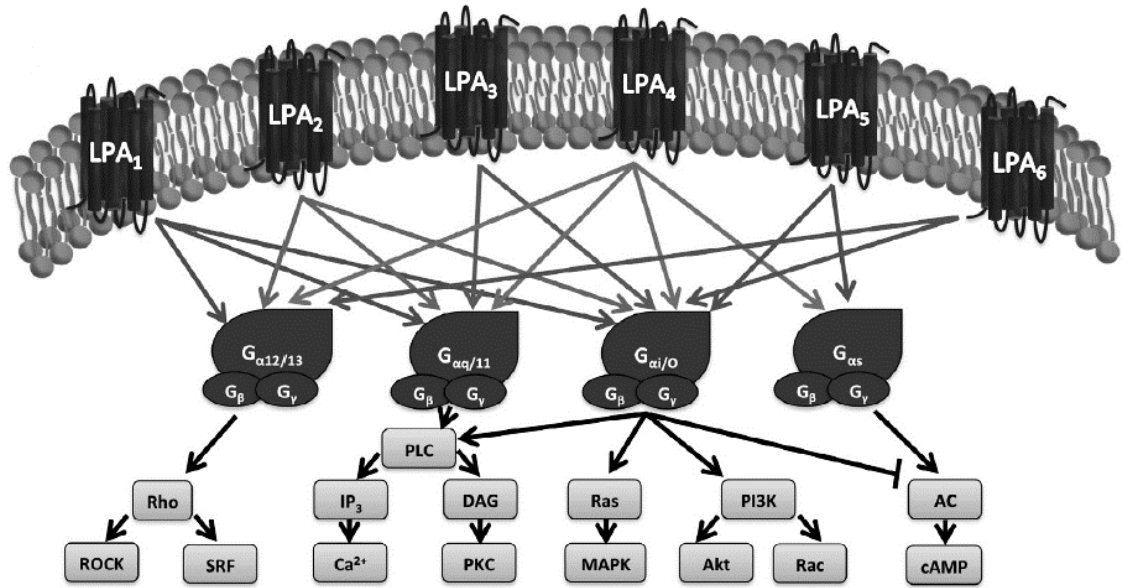


Figure 7 - The ATX / LPA cell signalling pathway³³

The G-protein bound to each receptor determines the response observed. Many of these responses have been identified as the driving force behind the invasion and migration, inhibition of apoptosis, senescence, angiogenesis and chemoresistance of ovarian cancer cells.^{31,33,36,44}

1.2.1.1 Invasion and migration

LPA causes the down-regulation of RhoA, in conjunction with G-protein: $G_{\alpha 12/13}$ (Figure 7).^{47,48} This GTPase is responsible for regulating changes in actin filament (actin filaments are essential for the adhesion, mobility /contraction of cells during division /replication).^{47,48} The down regulation of RhoA results in a loss of adhesion between cells, which leads to an increase in cell motility. This allows the infiltration of invasive cancer cells, within a healthy system.^{47,48} The loss of adhesion causes cancer cells to dislocate from a tumour, allowing the cancer to spread away from the primary site to a secondary site such as the peritoneal cavity.^{27,47,48} LPA also causes the activation of Src kinase, This family of enzymes is known to cause the breakdown of cell-cell junctions (a bridge between two cells or the extracellular matrix), which in a similar way to RhoA, promotes cell scattering, a process by which individual cells detach from cell clusters, allowing cancer cells to invade healthy tissue.^{27,48}

The effect of Src kinase is potentiated by the action of urokinase Plasminogen Activator (uPA).^{27,49,50} LPA causes the secretion of uPA which binds to its specific receptors, and as a result of the interaction, causes the conversion of plasminogen to plasmin. Plasmin degrades the basement membranes of cells (containing fibrin, fibronectin, proteoglycans and laminin).⁵¹

The G_i-Ras-MEKK1 pathway plays a major role in LPA mediated cell migration, through its re-distribution of focal adhesion kinase (FAK) near the focal contacts of cells.^{28,45,48} The activation of LPA receptors coupled to the g-protein g_{ai}/O, causes the activation of Ras, which in turn activates MEKK1 (Figure 7).^{28,33,45,48} MEKK1 facilitates the localisation of FAK near the focal contacts of cells (mechanism not fully understood).^{45,48,52} Increased turnover of focal adhesions (adhesions at the point of contact between a cell and the underlying substrate) leads to cell migration.^{30,45,48}

LPA induces the expression of metalloproteinases, including MMP1, MMP2, MMP7 and MMP9. These proteases contribute to the breakdown of the extracellular matrix, causing the invasion of cancer cells in the basement membrane.²⁷ The damaging effect of MMPs are multiplied by a reduction in the expression of TIMP metalloprotease inhibitors, caused by the presence of LPA.^{27,30,53}

1.2.1.2 Inhibition of apoptosis

The action of LPA is also known to inhibit processes that lead to both intrinsic and extrinsic apoptosis (programmed cell death), which is essential for the survival of cancer cells. For example, LPA causes the translocation of the receptor Fas, from the cancer-cell surface.^{19,27} Fas is a receptor that can initiate apoptosis within a cell. Once activated, Fas receptors initiate an intra-cellular caspase protease cascade to drive apoptosis (protease breaks down proteins to amino acids, resulting in cell death).^{19,27} This means that after its relocation, the receptor is less responsive to stimuli associated with apoptosis.^{19,27} The apoptotic response is muted further by LPA, by its inhibition of caspase-8, through increased expression of cFLIP, an inhibitor of caspase-8.^{27,54} LPA is also known to cause the expression of Fas ligand (FasL) on the surface of cancer cells.²⁷ Fas ligand acts to promote the apoptosis of lymphocytes, meaning the tumour is less likely to be detected by the immune system.⁵⁵

The protein BAD has an important part in the apoptosis of cells. It can cause the permeabilization of the outer mitochondrial matrix, through the activation of pore-forming proteins: Bak and Bax, which leads to cell death.^{19,27,56} LPA inhibits apoptosis by promoting the phosphorylation of BAD, which results in a loss of function.^{19,27,56} In continuation, upon the activation of receptor LPA₂, transcriptional cofactors: NHERF2 and TRIP6 are recruited *via* a zinc finger located within the protein structure (unique to LPA₂).²⁷ NHERF2 and TRIP6 cause the ubiquitination of pro-apoptotic, apoptosis regulatory protein, Siva-1.^{27,57} Thus Siva-1 is deactivated. The significance of this is that Siva-1 is understood to inhibit Bcl-xl.⁵⁷ Bcl-xl acts to inhibit Bak and Bax, which as stated have a significant role within the intrinsic apoptosis pathway.^{19,27} It is also worthy of note that inhibition of Bcl-xl increases the sensitivity of cancer cells to carboplatin.²⁷

RGS proteins act to regulate G-protein signalling, associated with LPA receptor activation.^{30,33,45,47} Upon the stimulation of LPA receptors, RGS proteins release GTPases, which hydrolyse GTP bound α -subunits.^{30,33,45,47} Guanosine triphosphate (GTP) is released in response to LPA. GTP is an important molecule in signal transduction and triggers number of downstream processes including those attributed to the inhibition of apoptosis.^{30,33,45,47} GTPases hydrolyse GTP to guanosine diphosphate (GDP), reducing the amount of GTP present, moderating the signal. LPA can cause the suppression of RGS proteins, which results in a loss of regulation of GTP and a net increase in signalling, amplifying the pathophysiological effects of LPA.^{30,33,45,47} Interestingly, autotaxin has been shown in itself to confer resistance to the apoptosis of fibroblasts by serum starvation.^{27,58}

1.2.1.3 Proliferation and senescence

Senescence refers to a loss of cell growth or division as a consequence of age. This physiological process is an important factor in controlling the proliferation of cells / tumour growth.^{27,45,47} Replicative senescence is regulated by the tumour suppressor p53.^{27,45,47} In response to cellular stress p53, is activated, resulting in many cellular responses, including the senescence of cells.^{27,45,47} In the absence of p53, cells continue to replicate, even when exposed to stress, meaning that they can incur DNA damage.^{27,45,47} LPA is understood to suppress p53 senescence by activation of receptor LPA₂.^{27,45,47}

LPA is known to contribute to the angiogenesis of ovarian cancer cells. Angiogenesis is a process by which new blood vessels form. It follows that such a process is essential for

tumour growth / survival. Angiogenic growth factor, VEGF, has the ability to stimulate the growth of new blood vessels around the tumour and therefore has an important role in the proliferation of ovarian cancer cells.^{27,30,33,34,38} LPA can trigger the production of VEGF, but can also cause increased VEGF receptor expression on endothelial cells.^{27,30,33,38} VEGF can cause the expression of autotaxin by ovarian cancer cells, which leads to increased turnover of extracellular LPA.^{27,30,33,38} Intriguingly, a study by Hu *et al*, found that LPA was able to act as a growth factor by increasing the level of checkpoint regulator, cyclin D1 in ovarian cancer cells, resulting in an increased rate of proliferation.³⁸

LPA has been found to stimulate growth-regulated oncogene α (GRO α), a chemokine commonly associated with angiogenesis.^{19,27,59} In a study by Lee *et al*, it was found that when ovarian cancer cells were starved in serum-free medium they ceased to secrete GRO α .⁵⁹ However, when exposed to LPA, GRO α was once more expressed.⁵⁹ Additionally, LPA has been observed to further aid angiogenesis in cancer cells by causing the expression of IL-8, a pro-angiogenic factor.³⁰

1.2.1.4 Chemoresistance

Ovarian cancer is typically treated with paclitaxel or carboplatin, which in many cases prove to be an effective therapy.²⁷ Paclitaxel (taxol) functions by targeting tubulin, a protein that is a large component of the eukaryotic cytoskeleton. Cells exposed to taxol are found to have defects in their mitotic spindle formation.⁶⁰ These defects result in cancer cells losing their ability to undergo mitosis and eventually leads to cell death.^{27,60} However, over time patients can become less responsive to these chemotherapeutic agents, which accounts for the poor survival rate attributed to ovarian cancer patients over a five-year period.^{19,27,30,57} LPA is known to activate the phosphoinositide 3-kinase (PI3K) pathway, which then triggers several responses down-field. Of particular note is the AKT pathway, known to mediate cell survival signals which act to protect cells from apoptosis.^{19,27,30,45,57} Concerningly, it has been observed that the PI3K pathway has the ability to restore spindle function in cancer cells damaged by paclitaxel.³⁰

In a study by Testa and co-workers, ovarian cancer cells were treated with a PI3K inhibitor (LY294002). Inhibition of PI3K augmented cisplatin-induced apoptosis. Similarly LY294002 has been shown to enhance the effect of taxol on tumour cell growth.⁶¹⁻⁶³ Therefore,

targeting extracellular LPA through the inhibition of ATX may prove to be a beneficial approach to combating chemoresistance in ovarian cancer cells.^{19,27,30,45,57,61–63}

Drug resistance is also conferred by LPA through its role in the deactivation of the pro-apoptosis protein Siva-1, as stated earlier. The inhibition of LPA results in cancer cells becoming resistant to cis-platin.^{27,41}

1.2.1.5 Self-potentialiation

Along with its part in the migration and invasion, proliferation and senescence, inhibition of apoptosis and chemoresistance of ovarian cancer cells, the ATX / LPA signalling pathway has what can be described as a "self-potentiating action".^{27,33} That is, mechanisms exist by which LPA signalling is increased, meaning that the processes linked to the development of ovarian cancer cells will be intensified. For example, LPA has been identified as a growth factor in its own right and has been shown to stimulate the growth of ovarian cancer cells.^{27,33} Ovarian cancer cells have been observed to increase ATX levels, leading to elevated levels of LPA.²⁷ Moreover, cancer cells are known to increase the expression of LPA receptors on their surface, compared to healthy cells.³³ Lastly, LPA under physiological conditions has a short half-life of around 5 minutes.^{29,30} This is due to the action of lipid phosphate phosphatases (LPP) which break down LPA, attenuating its interaction with LPA receptors.^{57,64} Cancer cells are known to down-regulate the expression of LPPs, compared to normal cells, leading to increased LPA.³³ The self-potentiating properties of ATX / LPA, in combination with the down-field response following LPA receptor activation has been described by some as a "perfect storm" for the development of ovarian cancer.³³

1.2.2 Autotaxin and its role in other diseases

Although the role of autotaxin (ATX) in ovarian cancer is the primary focus of this work, it should be stated that ATX has been identified as having a major role within the pathogenesis of a number of other diseases. As the pathways become clearer, it is anticipated that autotaxin will receive greater attention as a target for the treatment of these diseases.³³

In particular, ATX has been linked with Idiopathic Pulmonary Fibrosis (IPF). IPP is a lung disease characterised by a progressive and permanent decline of lung function caused by a thickening and scarring of connective lung tissue (fibrosis).^{33,58,65–68} Treatment options are very limited.^{58,66} A connection between autotaxin and IPF has been established through its role in the synthesis of LPA, and subsequent activation of LPA receptors (LPAr's), in a similar manner to ovarian cancer.^{33,58,65,67,68} Elevated levels of ATX have been found in the synovial fluid of patients with rheumatoid arthritis (RA). The ATX / LPA signalling pathway has been implicated in the progression of RA, through events downstream of LPAr activation. LPAr₁₋₃ have been identified to trigger responses deemed to potentiate RA.^{33,69,70} Aidinis and co-workers showed that when ATX expression was conditionally ablated in mice, inflammation slowed, demonstrating the significance of ATX in rheumatoid arthritis.³³ Autotaxin has also been linked to obesity. Obesity occurs in reaction to excess nutrients and energy *via* the chronic inflammation of metabolic tissue, such as adipose, muscle and liver, through the induction of cytokines. In mice engineered to overexpress ATX, it was discovered that when fed with a high fat feedstock, they took on more fat in comparison to wild type mice.^{33,71}

1.2.3 Inhibition of ATX

Autotaxin has a significant role in the development of ovarian cancer, through the part it plays in the migration and invasion, proliferation and senescence, inhibition of apoptosis and chemoresistance of ovarian cancer cells. It follows that by inhibiting autotaxin, extracellular LPA should be significantly reduced and tumour growth slowed. There is little evidence to suggest ATX inhibition can actually cause cell death to occur. The inhibition of ATX may restore cell sensitivity to existing chemotherapeutic agents such as taxol.^{33,72,73} Therefore, autotaxin inhibitors are likely to be most effective when used in combination with a cytotoxic agent, as evidenced by the work of Banerjee and Samadi *et al.*^{72,73}

One may question whether LPA receptors could make a suitable target for inhibition considering that many of the aforementioned processes occur as a direct consequence of LPA, downstream of autotaxin. However, it is our belief that autotaxin is a much more suitable target for inhibition for two main reasons.

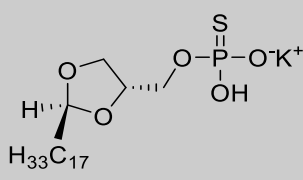
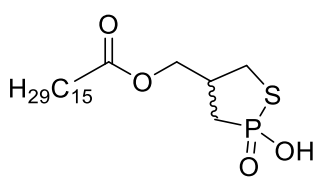
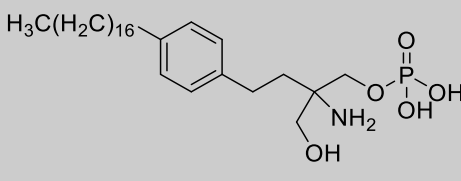
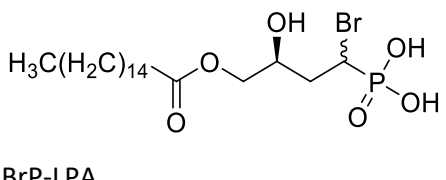
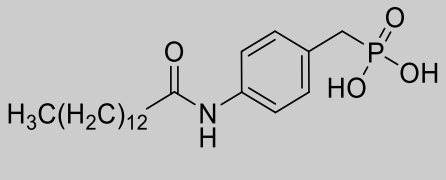
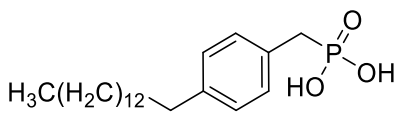
Rather than having a single defined structure, LPA has a number of variants, with regard to its acyl chain, such as chain length and degree of saturation.^{30,74} These differences result in

LPA receptors (LPA_r) having a strong affinity for only certain sub-types of LPA, which varies throughout LPA_r 1-6.^{30,74} For example, LPA₄ has a greater affinity for longer acyl chain lengths on LPA, of around 16-20 carbon atoms, whereas LPA₂ has greater specificity for shorter chains: 12-14 carbon atoms.⁷⁴ For the processes attributed to the development of ovarian cancer to be effectively modulated, every LPA receptor subtype should be inhibited. Owing to their differing substrate specificity there may be considerable challenge in designing an effective antagonist that has wide-reaching LPA_r activity. Allosteric modulation may provide a more effective mode of inhibition but designing a drug for this purpose brings with it other challenges. Secondly LPA signalling has an important physiological role, such as cerebral cortex formation, neuronal cell proliferation and causes the apoptosis of cells.^{75,76} In consideration of this, deactivation of LPA receptors may disrupt important physiological processes within the body and could potentially cause damage. Reducing extracellular LPA levels *via* ATX inhibition will control LPA_r activation and the down-field effects associated with cancer, whilst maintaining physiological function. This is evidenced in a study by Ninou *et al* in which it was suggested that up to 80 % of ATX / LPA signalling could be dispensed with in adult mice whilst still maintaining physiological function.^{58,77}

1.2.3.1 Known ATX inhibitors

Unsurprisingly, over the last 12 years many autotaxin inhibitors have appeared in the literature, and have evolved in structural complexity, from early LPA mimetic type drugs to complex heterocyclic systems that have activity in the low nanomolar range.^{44,78}

The current range of autotaxin inhibitors can be divided into two groups according to their structure: lipid like inhibitors and small-molecule inhibitors (non-lipid-like).^{44,78} With little exception, both classes act as competitive inhibitors.^{44,78} From a historical perspective, lipid inhibitors were the first to be developed, from 2006 onwards, using LPA as a starting point, which in its own right is known to have a weak inhibitory action on ATX.^{78,79} The lipid-like ATX inhibitors developed to date are listed in Table 1.

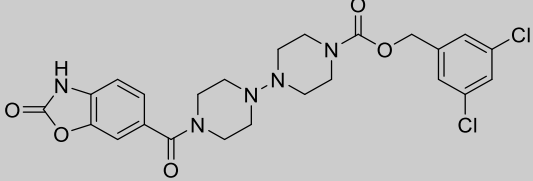
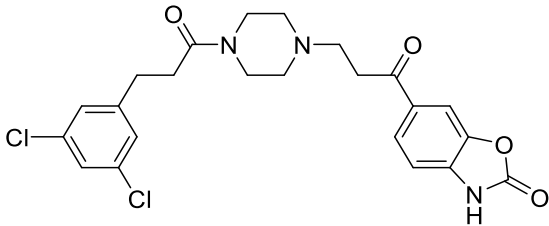
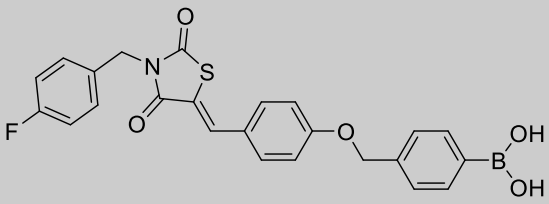
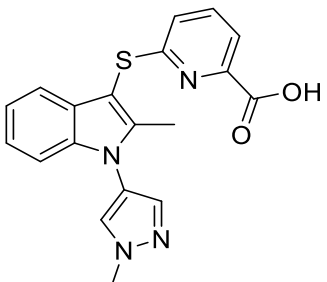
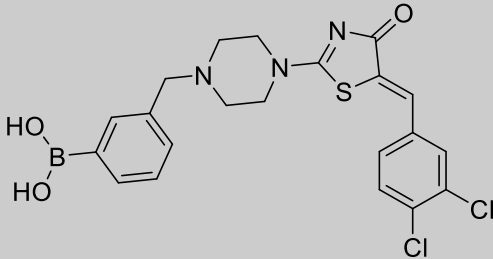
Table entry	Compound structure / Name (if available)	Activity / IC ₅₀	Mr / g / mol	Log P	Publication date
1	 <p>H₃₃C₁₇</p>	252 nM	474.68	7.42	2006 ⁷⁹
2	 <p>H₂₉C₁₅</p>	140 nM	404.54	5.65	2006 ⁸⁰
3	 <p>FTY720-P</p>	350 nM	387.5	4.73	2008 ⁸¹
4	 <p>BrP-LPA</p>	22 nM	487.41	5.58	2008 ^{78,82}
5	 <p>S32826</p>	5.6 nM	397.5	5.5	2008 ⁸³
6	 <p>H₃C(H₂C)₁₂</p>	170 nM	368.5	7.3	2010 ^{33,84,85}

7		1.93 nM	494.3	3.9	2015 ⁸⁶
---	--	------------	-------	-----	--------------------

Table 1 - A summary of lipid like ATX inhibitors published to date

A recurring motif within this class of inhibitor is a phosphate “spearhead,” sometimes substituted for phosphorothioate, that interacts with the active site of ATX, in a similar manner to LPA (discussed in 1.2.1).^{44,78} Additionally, these inhibitors incorporate a long alkyl / alkenyl tail that sits in the hydrophobic pocket, not unlike LPA.^{44,78} Many of these inhibitors have very acceptable potencies. It is speculated that compounds with low nanomolar activity are caused by a covalent bond between the Thr209 residue on ATX and the substrate.^{44,78} The majority of lipid-like compounds in the literature were published from 2006-2010. After that point in time, inhibitors based around “unnatural substrates” were published much more frequently.^{44,78} This was in part due to the X-ray crystal structure of autotaxin being solved in 2011, which was a significant step forward in terms of rational drug-design. With the aid of docking studies and virtual screening many different small molecule inhibitors were quickly developed. The other and perhaps more definitive reason lipid-like inhibitors are less prevalent today is because of their strong structural similarity to LPA. Lipid-like inhibitors can act down-field of autotaxin, meaning the inhibitor has the potential to activate LPA receptors which would negate any therapeutic benefit of ATX inhibition.^{44,78} It has also been found that many of the lipid-like inhibitors, such as S32826 have poor bioavailability and stability *in vivo*.⁸³

A summary of the small molecule ATX inhibitors are listed in Table 2:

Table entry	Compound structure / name (if available)	Activity / IC ₅₀	Mr / (g/mol)	Log P	Publication date
1		<1 μM	534.3	2.6	2009 ⁸⁷
2	 PF-8380	2.8 nM	476.3	3.0	2010 44,78,87
3	 HA155	5.7 nM	463.2	2.7	2011 ⁴³
4		4 nM	364.4	3.6	2012 35,44
5	 3BoA	13 nM	476.1	4.9	2013 ⁸⁸

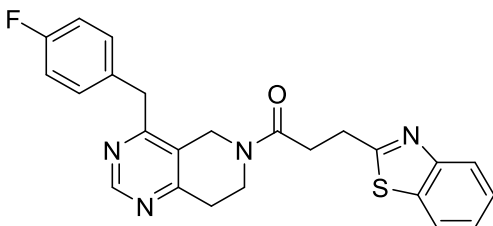
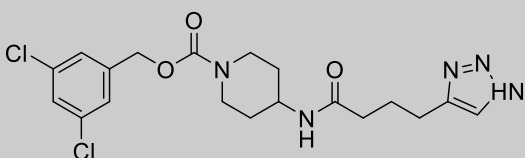
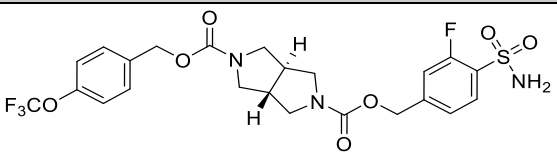
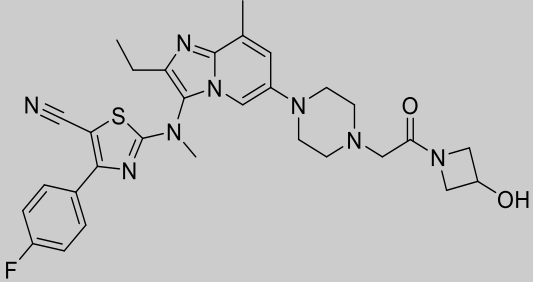
6		1.7 nM	438.5	3.7	2013 44,89
7		2 nM	440.3	2.6	2014 44,90
8		1 nM	561.5	3.5	2014 ⁹¹
9	 GLPG 1690	131 nM	588.7	4.9	2017 ⁶⁷

Table 2 – A summary of small molecule ATX inhibitors

Although each inhibitor shown in Table 2 incorporates different functionality and structural motifs, they do share a common trait regarding their shape. Using PF-8380 as an example. These inhibitors typically contain a lipophilic tail, an acidic head and a spacer group set in the middle, which is in many ways analogous to LPA (Figure 8).⁴⁴

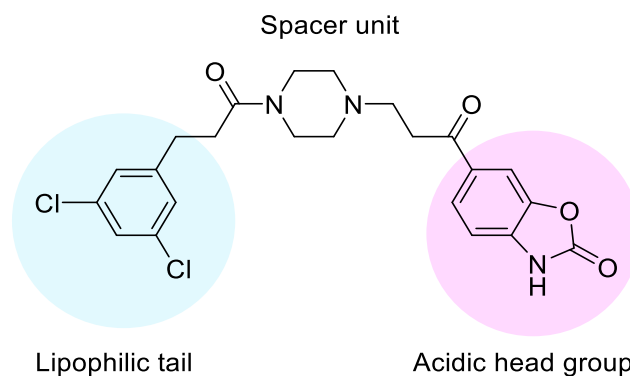


Figure 8 - The common structural features of small-molecule ATX inhibitors. ⁴⁴

These features can be observed throughout the small-molecule inhibitor series, although more recently there appears to be a trend in compounds moving away from using an acidic head group, such as GLPG 1690 (Table 2, entry 9).⁶⁷ It is common for this class of inhibitor to have a high degree of flexibility, particularly in the centre of the structure. This enables the molecule to correctly orientate itself within the hydrophobic pocket of ATX to assist drug binding.^{44,78} Many small molecule ATX inhibitors have a high molecular weight, typically higher than 400 g/mol and a log P value over 4. Whilst these values may be considered unacceptably high under normal circumstances, one must consider the active site of ATX and its natural substrate: LPA. LPA has a high molecular weight of 436.52 g/mol (18:1 carbon chain) and is highly lipophilic, with a log P value of approximately 6.12. Under these circumstances a high molecular weight should be considered acceptable because of the need shown for LPA to fill the hydrophobic pocket of ATX as well as bind to its active site for an effective interaction to occur. To fulfil these two requirements, the drug molecule has to be reasonably long due to the size of the cavity. This will inevitably lead to an increase in molecular weight. Lipophilicity can be controlled by careful drug design and indeed has been brought down to acceptable levels.

For some of the compounds in Table 2 the crystal structure was obtained of the drugs bound to ATX. The X-ray structures revealed information about their binding mode (Figure 9).

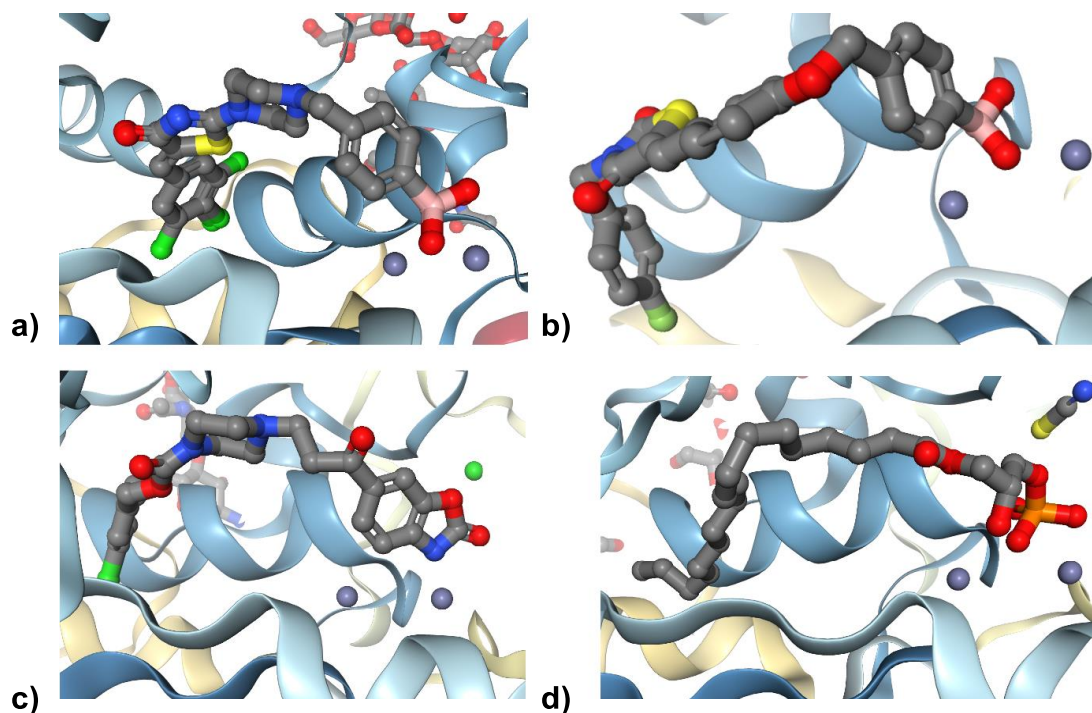


Figure 9 - ATX bound to 4 different inhibitors: a) 3BoA, b) HA155, c) PF-8380 (Table 2, entry 5, 3, 2, respectively) d) LPA^{43,87,88}

Figure 9 shows three different drug molecules bound to ATX. Despite having different structures, each compound adopts a similar binding pose. The acidic head group interacts with two zinc atoms (shown in blue). Figure 9d shows LPA bound to ATX, in a near identical fashion to a-c, suggesting that these inhibitors interact with ATX in a similar way to LPA. It has been suggested that, like LPA, the acidic headgroup is susceptible to nucleophilic attack from the Thr209 residue on ATX, forming a covalent bond.^{44,78} The covalent bond accounts for the high potency observed for all three compounds (low nanomolar). Not all autotaxin inhibitors adopt this binding pose, including the recently published GLPG 1690.⁶⁷

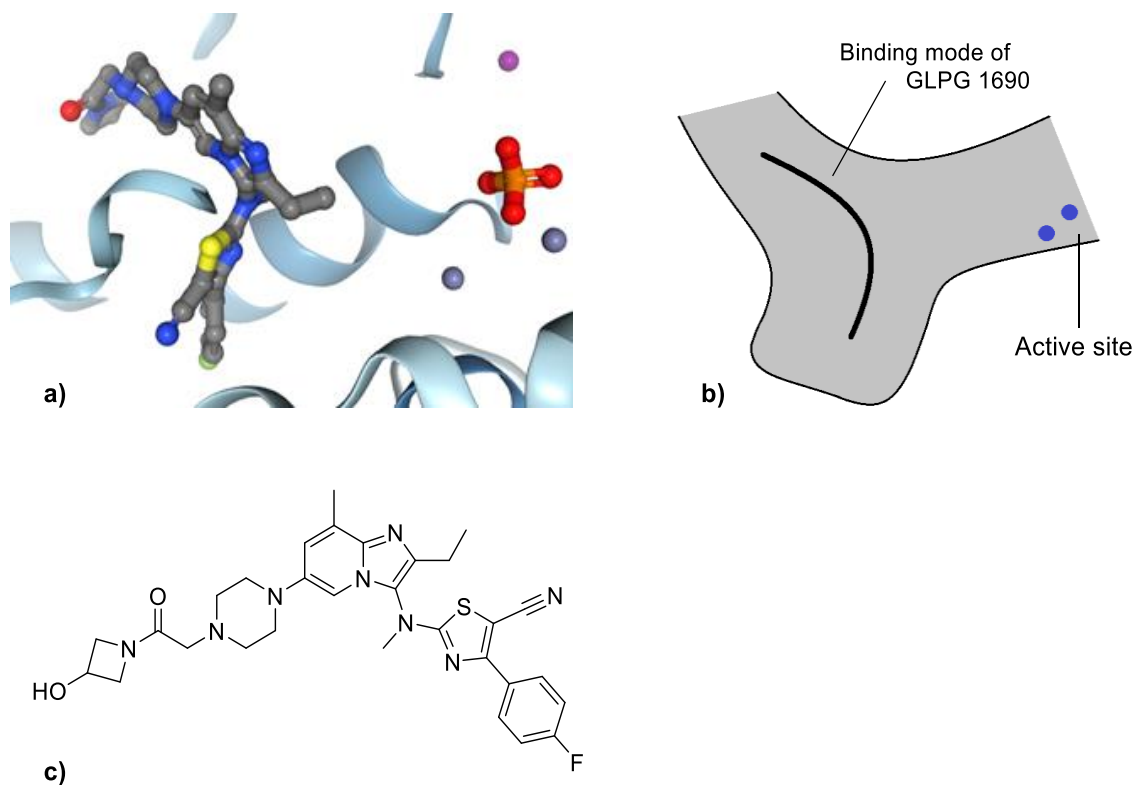


Figure 10 – a) GLPG 1690 bound to ATX, b) the binding mode of GLPG, c) 1690.⁶⁷

The X-ray structure of GLPG 1690 bound to ATX (Figure 10a) shows the drug adopting an alternative binding mode. The fluorobenzyl half sits in the hydrophobic pocket and the hydroxyazetidine portion lies in the tunnel.⁶⁷ Notice that the drug does not appear to interact with zinc atoms (shown in blue) within the active site (i.e. it is not a “zinc binder”). The authors speculate that the reason for the compound being highly potent is that it occupies part of the tunnel.⁶⁷ The tunnel is thought to have a significant role in the removal of LPA (post hydrolysis of LPC). In blocking access to the tunnel, the catalytic cycle is disrupted, leading to inhibition of ATX.⁶⁷

1.2.3.2 Autotaxin inhibitors in the clinic

The past 10 years have seen considerable advancement in the development of autotaxin inhibitors from both industry and academia. The compounds featured in Table and Table 2 are the result of extensive screening and library synthesis over a period of many years, but despite this, as of 2018, there is only one autotaxin inhibitor in clinical trials.^{44,65,67} The

compound in question, GLPG 1690 developed by Galapagos NV, is being investigated as a potential therapy for Idiopathic Pulmonary Fibrosis (IPF).⁶⁷ The drug is orally active, taken once daily and has so far performed very well in clinical trials, advancing to stage III in recent months.⁹²

Despite the apparent success of Galapagos and their flagship compound in this area. ATX inhibitors as treatments for ovarian cancer have unfortunately not progressed past pre-clinical studies.⁴⁴ We speculate that the reason for this is the unique challenge of targeting organs within the peritoneal cavity (discussed in chapter 1.4. The further development of ATX inhibitors for ovarian cancer therapy may be hindered until this problem is overcome. The focus of our research, over the last several years, has been to investigate new methods by which the pharmacokinetic properties of autotaxin inhibitors can be improved, without compromising activity inherent to the drug molecule. This has led us to investigate the use of polymeric drug–delivery strategies as a method to increase peritoneal retention of ATX inhibitors.^{93,94}

1.3 Drug delivery and polymer therapeutics

Novel strategies for drug delivery, in particular polymer-based therapeutics have been of interest since the mid 1970 s.⁹⁵ In principle, these systems have the potential to enhance the physicochemical and pharmacokinetic properties of a drug, which may otherwise have been considered unacceptable within a biological system.^{95,96} Previously, drug delivery systems have been used to change the solubility, toxicity and improve the half-life of drug molecules.^{95,96} Additionally, they can be designed to target a specific area of the body or even particular organs. This ensures that the drug is distributed to where it is needed, which can reduce dosing.^{95,96} Drug delivery should not be confused with formulation approaches in which a drug's properties are modified by an external "technology". This may include using an enteric coating on a pill to prevent the degradation of an acid-labile drug in the stomach.⁹⁷ The difference between this application and a drug delivery approach is that such a modification does not involve any chemical bonding, though we would extend this definition to non-covalent interactions as well.⁹⁶ The majority of drug delivery systems featured in the current literature can be divided into two classifications: reactive and passive.^{98,99}

1.3.1 Reactive drug delivery systems

Reactive drug delivery systems are designed to transport drug molecules to a target area. Then the drug is released through a specific response to the environment (such as a change in pH). Such systems have the potential advantage of being highly specific in the areas that they target but they can be very difficult to design and to get to work effectively. Two common examples of this type of drug delivery approach are encapsulation and targeted drug release.^{96,100,101} Encapsulation is an attractive approach to extend the half-life of a drug and is commonly achieved by functionalising a polymer.^{100,102,103} Under specific conditions the polysaccharide may form a micelle. During the formation of a micelle a drug is introduced into solution it can become entrapped within the structure (Figure 11a).^{99,102,104}

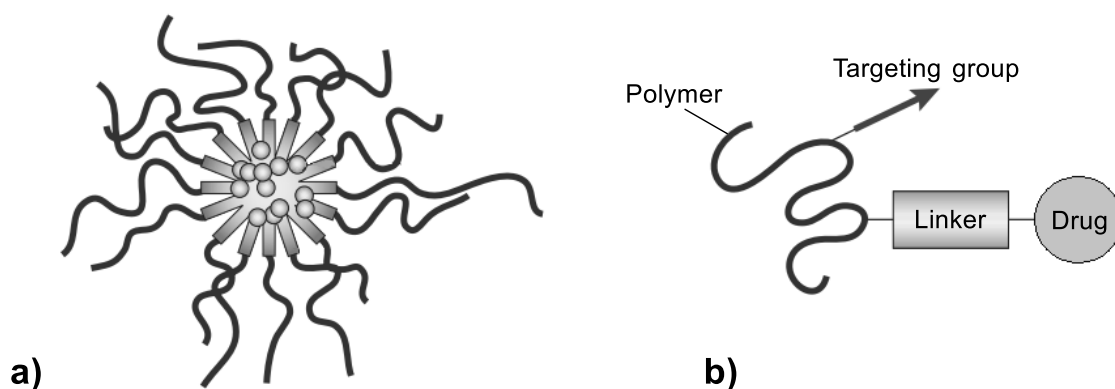


Figure 11 - a) Encapsulated drug delivery system, b) targeted drug release system

The encapsulated drug in response to an external factor, such as temperature, will be slowly released as the micelle deforms, as demonstrated by Zhang and co-workers.¹⁰⁴ Drug molecules can also be encapsulated using supramolecular arrays. However, these have limited use outside of academia due to their poor biocompatibility.¹⁰⁵ One criticism of the use of encapsulation as a drug delivery device is that the drug can be released only very slowly or not at all. This is due to the material being held too tightly within the micelle or liposome, which reduces its therapeutic benefit.¹⁰⁶

Targeted drug release systems are similar to a passive polymer therapeutic approach. However, they differ in that they are designed to transport the drug and then release their payload through a cleavable linker unit (Figure 11b).⁹⁸

These systems often have a targeting molecule attached to the polymer to assist in the site specificity of the drug delivery device. For example, Ojima and co-workers conjugated vitamin B₇ to their Taxane vehicle.¹⁰⁷ Tumour cells are known to over express vitamin receptors on the cell surface, meaning that the device was able to selectively target tumours and release a taxol derivative via a “self-immolating” disulfide linker.^{107,108}

1.3.2 Passive drug delivery systems

Passive drug delivery systems concern the covalent attachment of a drug molecule to a polymer (known as polymer therapeutics). Through this modification the drug molecule can take on some of the properties of the polymer which may enhance its pharmacokinetic profile. The polymer chosen for this purpose is usually inert and does not interact with the biological target by itself. These materials are polydisperse by nature and therefore their use from a therapeutic viewpoint would appear to counter the efforts of the pharmaceutical industry during the last century. Which has pursued monodisperse molecules, rather than a polymer drug conjugate made of many different molecular weight fractions and irregular drug loading. However, provided the polymer is known to be inert and biocompatible, the greatest safety concern in any polymer-based drug delivery system should rest with that of the drug. This is evidenced by polymer therapeutics now routinely being used in the clinic during the last 20 years.⁹⁶

Polymer therapeutics are further divided into two categories: natural and synthetic polymers. Examples of natural polymers include dextrans, chitosans and alginates. These polymers are typically water-soluble materials that contain functionality which can be used to covalently attach (conjugate) drug molecules to their structure.^{95,96} Examples of synthetic polymers include dendrimers, polyethylene glycol (PEG), *N*-(2-hydroxypropyl) methacrylamide (HPMA) and linear polyamidoamines. Synthetic polymers have an advantage over natural polymers in that their polydispersity and physical properties can be controlled, which is desirable from a design viewpoint. Dendrimers can be “grown” by the sequential addition of reagents creating branching. As each layer of branching is added the dendrimer goes through a change in generation, which defines its physical characteristics.¹⁰⁹ It follows that synthetic polymers can be tailored to meet a particular requirement of a drug delivery application.^{109,110} Synthetic polymers have sometimes been found to be cytotoxic

leading them to be withdrawn from clinical trials.¹¹¹ A number of different polymer therapeutic approaches have been applied to a variety of drug types (Figure 12).

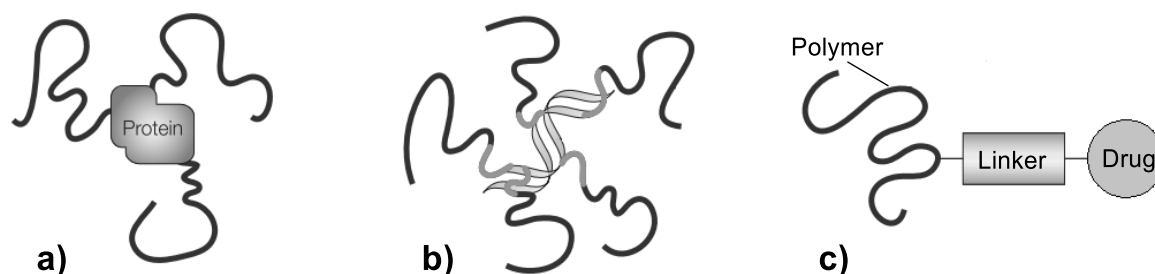


Figure 12 - a) polymer-protein conjugate, b) polymer DNA-complex, and c) polymer drug conjugate

Recombinant DNA and monoclonal antibody technologies have produced a vast reservoir of peptide and protein-based drugs, which have the potential to be effective therapies. However, these can suffer from a short plasma half-life, solubility and stability issues, which have slowed their development. Polymer-protein conjugates (Figure 12a) are a useful way to improve the shortcomings of protein drugs. Abuchowski and co-workers first demonstrated the PEGylation approach in 1977, in which PEG was conjugated to a protein.¹¹² This had a positive effect on the solubility and stability of the protein, starting a whole new field of research and a multi-billion dollar industry.^{96,113}

DNA or oligonucleotides have large therapeutic potential as they have the ability to selectively bind to DNA / RNA sequences and inhibit gene expression and therefore have value in viral and cancer therapy.¹¹⁴ Disappointingly, the clinical progression of this technology has been slow which is most likely due to their low resistance to nucleases.¹¹⁴ DNA polymer conjugates (polyplex) (Figure 12b) have been shown by Liao *et al* and Frederiksen *et al* to be effective gene delivery devices for cancer and viral treatments.^{115,116}

The drug polymer conjugate approach (Figure 12c) is of most relevance to this thesis. Natural and synthetic polymers have been conjugated to a variety of drugs. A drug conjugate approach may attenuate unwanted attributes such as high toxicity, low aqueous solubility, low stability, high acid lability, low plasma half-life and high lipophilicity.⁹⁶ The main principle behind this approach is that because the bulk of the conjugate is a polymer, the drug (covalently bonded) will take on some of the properties of the polymer.¹¹⁷ For example, if the polymer were particularly hydrophilic (such as a polysaccharide) then the drug bound to

the polymer would overall become more hydrophilic. Conversely, because the polymer is not biologically active and has no role in the interaction of the drug with its target, the drug should retain its potency. The drug polymer conjugate approach has been investigated for use in cancer therapy. A study by Peppas and co-workers featured the preparation of a doxorubicin-Inulin conjugate.¹¹⁸ Interestingly, CTI Biopharma have developed a paclitaxel-polyglutamate conjugate (Paclitaxel Poliglumex). This has been shown to increase the solubility of taxol (within the overall drug-conjugate) and decrease administration times.^{96,119,120} Further to this, the material can be administered in higher dosages than taxol alone, Paclitaxel Poliglumex has entered phase III clinical trials in women with ovarian cancer. As part of our own research endeavours in this area, a potent lipid-like ATX inhibitor (S32826) was attached to a 3rd generation PAMAM dendrimer (Figure 13).⁹³ It was envisaged that, after the attachment of the dendrimer to S32826, the drug's bioavailability would be improved along with an increase in the site specificity of the drug, which is a common problem associated with this class of inhibitor.^{78,93} It was found that the drug retained its activity following attachment to the dendrimer ($IC_{50} = 160$ nM). This drug delivery system was not developed further due to toxicity concerns associated with dendrimers. However, the concept explored within the study formed the basis of our future investigations.^{94,121}

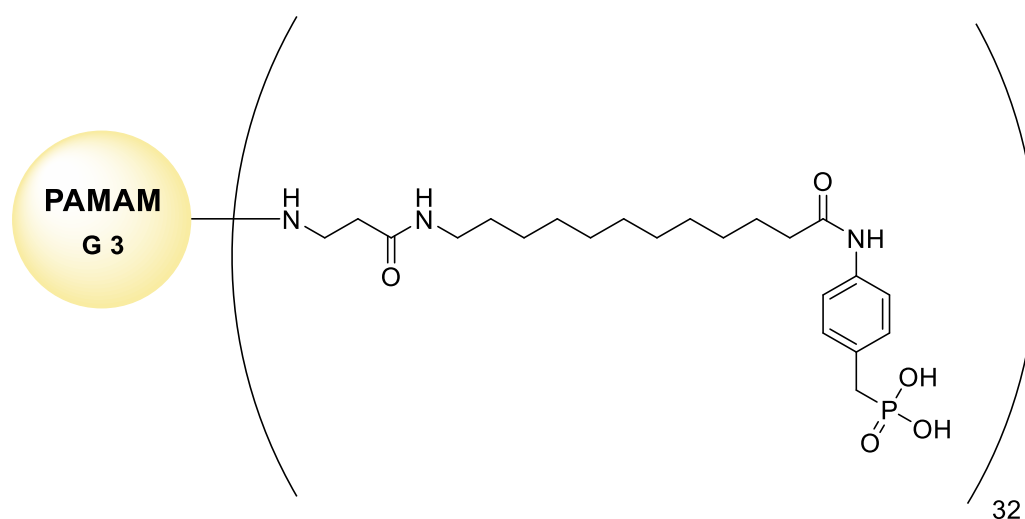


Figure 13 - PAMAM-S32826 dendrimer conjugate

1.3.3 Polymer therapeutics in the clinic

As of 2018, over 10 polymer-drug conjugates are at various stages of clinical development, with many drug conjugates having cleared phase III trials over the last 20 years leading to their widespread adoption in the clinic.¹²² As alluded to earlier, PEGylated proteins dominate the list (Table 3) although taking into account the drug conjugates currently in development, this trend may change over the next decade.^{96,122}

Type	Trade name	Drug	Polymer	Disease
Polymeric drug	Copaxone	Glatiramer acetate	Glu Ala Tryp co polymer	Multiple Sclerosis ¹²²
Polymeric drug	Synvisc	Hyaluronic acid	Hyaluronic acid	Arthritis ¹²²
Polymer protein conjugate	Zinostatin stimalamer	Zinostatin	Lipiodol	Liver cancer ¹²³
PEGylated protein	Cimzia	Anti-TNF Fab	PEG	Chron's disease ¹²⁴
PEGylated protein	Mircera	Epoetin-β	PEG	Anaemia associated with chronic kidney disease ¹²⁵
PEGylated protein	Pegasys	Interferon α 2b	PEG	Hepatitis c ¹²⁶
PEGylated protein	Neulasta	hrGCSF	PEG	Neutropenia caused by chemotherapy ^{96,122}
PEGylated protein	Uricase-PEG20	Uricase	PEG	Gout ¹²⁷
Drug polymer conjugate	Abraxane	Paclitaxel	Albumin	Breast, lung and pancreatic cancer ¹²⁸

Table 3 - Clinically approved polymer-conjugate treatments

It is worth noting that two of the drugs featured in Table 3, Copaxone and Neulasta, have each amassed sales of several billion dollars, and at one stage (2011) featured in the top 10 selling pharmaceutical products in the world.^{96,129,130} This shows that drug-polymer conjugates have progressed significantly from academic curiosities, and are now a widely accepted therapeutic approach by the pharmaceutical industry.

1.4 The peritoneal cavity

As stated in Chapter 1.2.3 it is postulated that one of the reasons that autotaxin inhibitors perform poorly *in vivo* is that they are rapidly eliminated from the peritoneal cavity and therefore away from the location of the tumour. We hypothesised that the properties of an autotaxin inhibitor can be enhanced by the use of a drug delivery strategy, specifically a drug polymer conjugate approach (Figure 12c). We postulated that this modification will significantly increase the residence time of an autotaxin inhibitor within the peritoneal cavity.

The peritoneal cavity (Figure 14) is located in the abdominal area of the body. and exists as potential space, separated by a thin membrane between the abdominal wall and major organs including the small intestine, liver, pancreas and for women, ovaries.^{131,132}

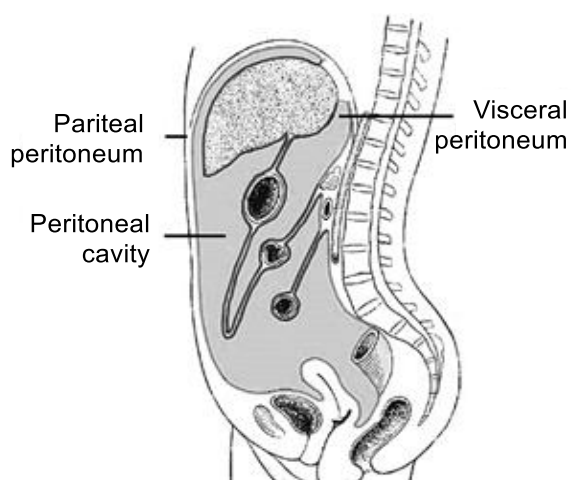


Figure 14- The Peritoneal Cavity (enlarged, for the purposes of the diagram)¹³³

Chemotherapeutic agents may be administered intraperitoneally, meaning the drug is injected directly into the peritoneal cavity.^{15,134} This technique appears to garner superior

results (in terms of drug response) compared to intravenous injection or oral intake.¹⁵ It can be speculated that this is due to establishing a localised concentration of the material near the cancerous area.^{15,134} Additionally, the peritoneal membrane, which acts as barrier between the peritoneal cavity and the rest of the body, contains many capillaries that are ideal site for absorption.^{132,135,136}

The peritoneal membrane (peritoneum) is commonly used medically, in a process known as Peritoneal Dialysis or Ultrafiltration.¹³² Ultrafiltration is the process by which solutes are transported through the peritoneal cavity via the peritoneum (a layer of tissue comprised of many blood vessels).^{131,132} The peritoneum itself is semi-permeable to molecules, depending on their physical properties and clinically this is exploited for peritoneal dialysis.^{15,132,137} Toxins (e.g. methanol) that would otherwise not be metabolised though complications associated with renal failure, are removed from blood.¹³² A typical procedure (Figure 15) involves the introduction of dialysis fluid (typically comprising a high molecular weight dextran polysaccharide dissolved in water) into the peritoneal cavity through a permanent catheter.¹³² Solutes are filtered through the peritoneum and after several hours an equilibrium is established, the fluid is then drained off from the peritoneal cavity, removing many unwanted / toxic solutes.¹³² The entire process can be then repeated. Peritoneal dialysis is often a very effective treatment for those with reduced renal capacity.¹³²

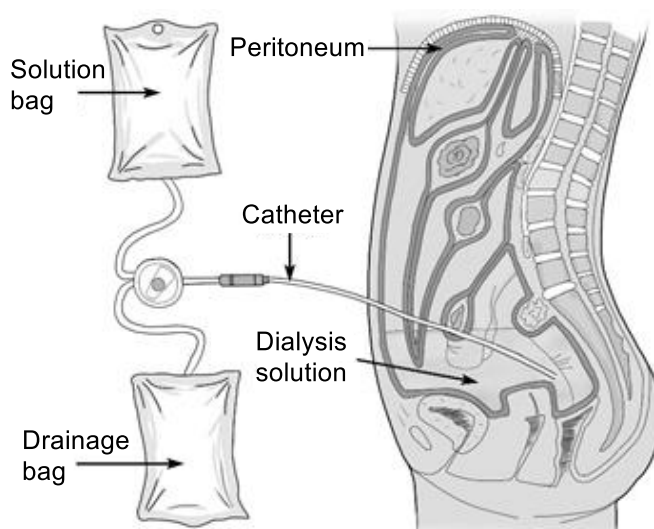


Figure 15- Typical peritoneal dialysis procedure¹³⁸

With reference to ovarian cancer, when the cancer metastasises it can cause irritation of the peritoneum, which triggers the build-up of ascites fluid.⁴⁶ The accumulating fluid puts pressure on the abdomen which can be very painful. Patients suffering with ovarian cancer regularly need to have the ascites fluid drained to alleviate the pressure.⁴⁶

1.5 The development of a novel drug delivery strategy for the peritoneal cavity

Transport of material through the peritoneum, and by extension the intraperitoneal cavity, is a complex process, but to be able to design an effective drug-polymer conjugate it must be understood. There are two ways for a solute to be transported through the peritoneum (away from the peritoneal cavity) namely: diffusive transport and convective transport.¹³²

Diffusive transport is driven by the concentration of a given solute in the capillaries (of the peritoneum) and the peritoneal cavity.¹³² A difference in concentration results in a concentration gradient, which acts to distribute solute molecules within a defined space.¹³² Diffusive transport is an entropically driven process which is directly proportional to temperature.¹³² Molecular weight is a significant factor which affects diffusion; the rate of diffusion for a solute is inversely proportional its molecular weight.^{132,136,139,140} A solute of high molecular weight diffuses at a slower rate than those of a low molecular weight (Figure 16).¹³²

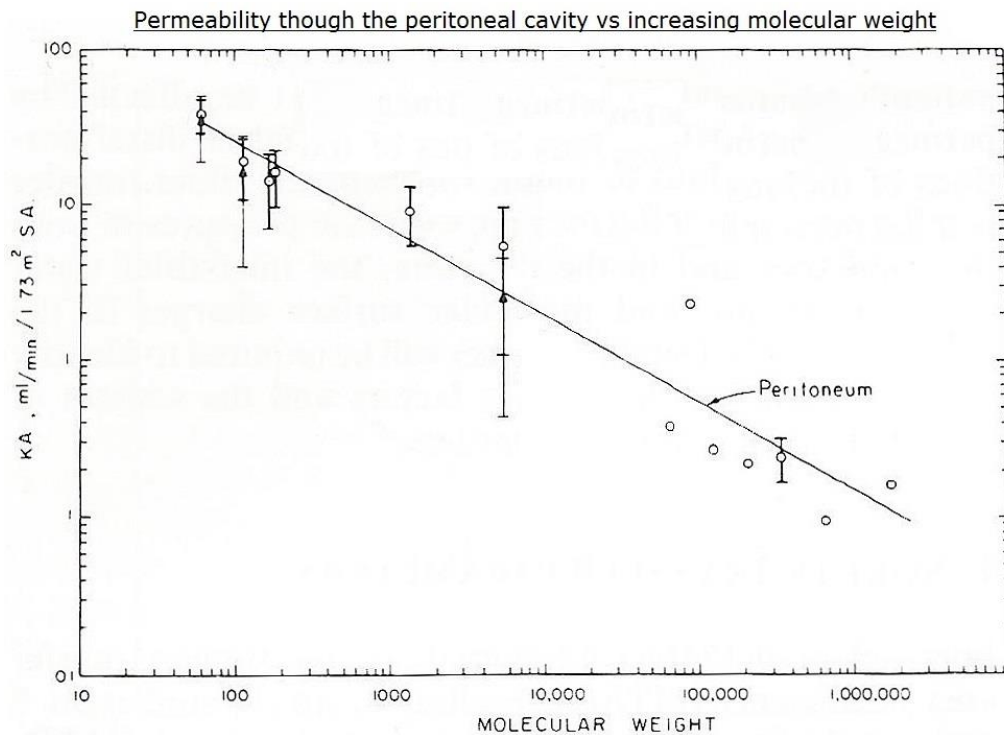


Figure 16 - The effect of increasing molecular weight on the rate diffusion of molecules through the peritoneal membrane ¹³²

This effect is observed regardless of capillary pore size, as increasing pore size acts to reduce the total surface area available for diffusion, and therefore a reduction in transport will be observed.¹³²

Conversely convective transport is largely independent of the molecular weight of the solute. When a solute of high molecular weight accumulates within the peritoneal cavity it would be expected that a concentration gradient would be established, i.e. a high concentration of solute in the peritoneal cavity compared to a low concentration on the outside.^{132,136,139,140} As the osmotic pressure increases against the peritoneal membrane to around 25 mm/Hg it is significant enough to force high molecular weight solutes through the capillary pores (hydrostatic pressure of blood flow = 15 mm/Hg at capillary end).¹³² Inward diffusion of high molecular weight solutes acts to equilibrate the pressure gradient. By establishing a concentration gradient within the peritoneal cavity the rate of ultrafiltration is significantly increased, which explains why dextran solutions are routinely used as an osmotic agent in peritoneal dialysis procedures.^{132,140} The rate of ultrafiltration can be increased further by increasing the concentration of osmotic agent.¹³²

Pappenheimer's theory of restricted diffusion, states that three factors can influence the passage of molecules across capillaries: ^{132,141}

1. Steric hindrance at the entrance to a capillary pore¹⁴¹
2. Friction between molecules moving within a pore, which relates directly to the molecular weight of the solute¹⁴¹
3. Molecular friction within the stationary walls of a pore¹⁴¹

Other factors that affect diffusion across the peritoneal membrane depend on whether the solute carries a charge. This is because the capillary pores are lined with basic amino acid groups as well as phosphate and choline groups. It has been observed that the rate of diffusion for acids / bases decreases across the peritoneum.¹³² Additionally the use of vasodilating drugs significantly increases the rate of diffusion for larger molecular weight solutes.¹³²

By understanding the principles which underlie the transport of molecules through the peritoneal membrane, it should be apparent that the peritoneal cavity presents an inhospitable environment for drug molecules to be able to function correctly. Because of their relatively low molecular weight they are rapidly expelled through the peritoneal membrane and are subsequently metabolised. As a consequence a small-molecule would not be expected to inhibit autotaxin present within the intraperitoneal cavity to any measurable extent.^{132,136}

A suitable polymeric drug carrier would therefore be expected to possess the following characteristics:

- Highly biocompatible, meaning that it is completely inert within the body (containing no toxicophores) and ideally already be approved for use / precedent for its use within the peritoneal cavity.
- Possess a high molecular weight, over 5000 Da
- Have no affinity for autotaxin in its own right
- Contain suitable functionality for the covalent conjugation of drugs
- Not carry any charged species

1.5.1 Suitable polymer supports - Icodextrin

Icodextrin (IDX) (Figure 17) is a polysaccharide with an average molecular weight of approximately 13-19 kDa.^{139,140,142,143} It is comprised entirely of glucose subunits, which are linked at the α (1,4) position and branched by α (1, 6) glycosidic bonds, to a lesser extent.¹⁴⁰

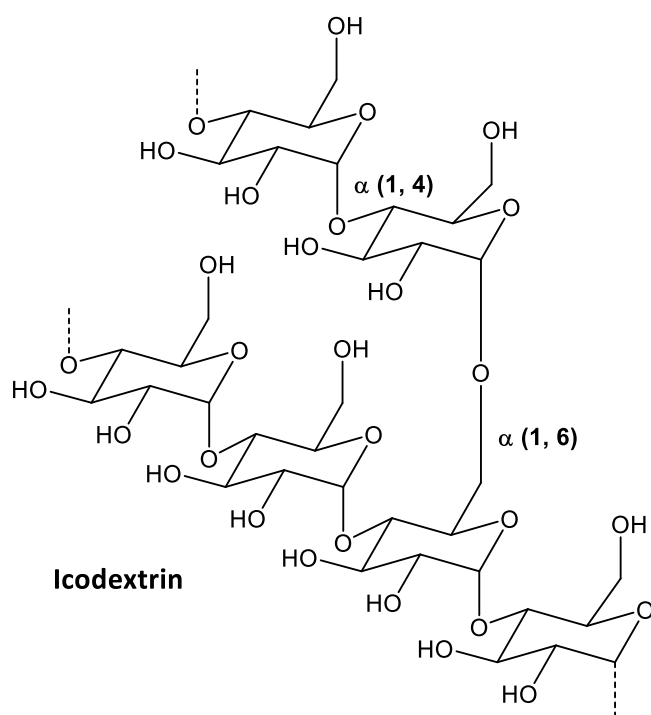


Figure 17 - The structure of Icodextrin

Icodextrin is used commercially, in solution, as an osmotic agent for peritoneal dialysis and as a post-surgery adhesion reductant, under the trade names Extraneal™ and Adept™ respectively, produced by Baxter healthcare.^{139,140,144}

From a synthetic standpoint IDX is potentially very suitable as a polymeric drug support. This is because it can be easily isolated in large quantities as a solid from solution *via* dialysis. Additionally, it contains many free OH groups to which drug molecules can be covalently attached. From a materials viewpoint IDX is also ideally suited as a polymer drug carrier. IDX has been approved in 31 countries for use in the peritoneal cavity and is widely considered to be completely safe / inert.¹⁴⁵ It has also been shown in numerous studies that Icodextrin has a significantly longer retention time in the peritoneal cavity compared to the equivalent monosaccharide glucose (Figure 18).^{139,140,142,145,146}

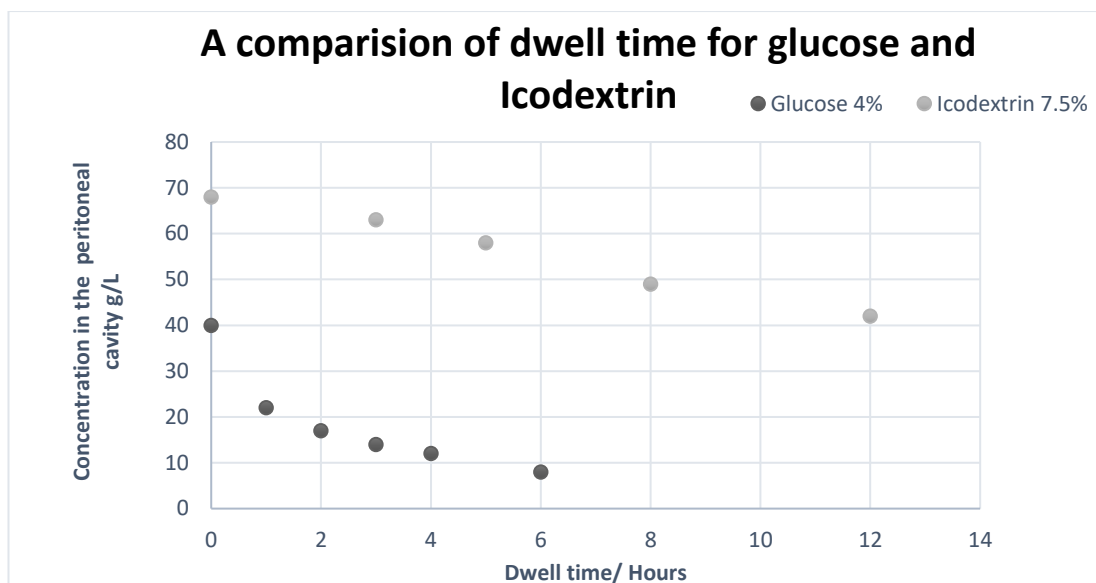


Figure 18 - A graph to show the retention of IDX and glucose in the peritoneal cavity.¹³⁹

Typically, less than 40% of IDX in solution will be absorbed in a 12-hour period and has a median plasma half-life of 14.73 hours.^{139,144} This means that IDX is retained in the peritoneal cavity for up to several days, making it an ideal polymer support to maximise peritoneal retention of a drug molecule. In a study previously conducted by us, an Icodextrin-drug conjugate was shown to be retained within the peritoneal cavity up to 30% of its original concentration, after 24 hours.¹⁴⁷ This significantly increased the residence time of the drug in the peritoneal cavity. In comparison < 0.1 % of the free-drug equivalent was observed after 24 hours.¹⁴⁷ Outside of the research efforts of our group, to our knowledge Icodextrin has never been used as a polymer-drug support.

IDX is not metabolised in the human peritoneal cavity to any extent. Instead it must diffuse through the peritoneal membrane and into the bloodstream. Icodextrin is metabolised by the enzyme α -amylase, of which many subtypes exist, that break down specific glycosidic linkages.^{144,148-150} Icodextrin is metabolised into smaller oligosaccharides (approximately ten units) and then to smaller, soluble carbohydrates that can easily be digested.¹⁵⁰

While in many ways Icodextrin is ideally suited as a polymer drug support, this study will utilise two separate polymers. This decision was taken for two reasons, the first being that it would be beneficial to contrast the performance of Icodextrin to another polymer, as a drug delivery device. It may be observed that there is a difference in peritoneal retention for different polymer drug-conjugates. Additionally, it may be found that using a different

polymer results in a reduction or increase in potency. It could be envisaged that this effect would result from the space occupied by the polymer, causing the drug (pharmacophore) to interact less favourably with the active site of ATX through steric hindrance. Another polymer may cause a less pronounced reduction in potency because of it having a different structure and may not hinder the interaction of ATX and the pharmacophore as significantly. Secondly, as mentioned previously, IDX is metabolised by the enzyme α -amylase.^{148,149,151} In humans this fact is of little significance because it is produced in comparatively low concentrations, contributing to its high residency time in the peritoneal cavity.^{149,151} However, rodents have a much higher concentration of amylase, meaning that certain polysaccharides are metabolised faster, compared to humans. Humans have approximately 7 U/L amylase present in their peritoneal cavity, conversely Rats are known to have 1252 U/L (U = the amount of enzyme that catalyses 1 μ M of substrate per minute).^{151,152} The significance of this is that ultimately animal models will need to be used to demonstrate that the polymer-drug conjugates produced in this project have improved peritoneal retention compared to their free-drug counterparts. If the polymer support is metabolised before the drug can significantly inhibit ATX, there is concern that a false-negative result may be obtained. Paradoxically, because of the increased α -amylase present in rodents, IDX peritoneal retention may be significantly reduced, whereas in human studies this would not be the case.^{151,152}

1.5.2 Suitable polymer supports – Inulin

This reflection points to the need to investigate a second polymer. It should be similar to IDX, such as being a polysaccharide in order for a meaningful comparison between the two to be made. However, the material also needs to be resistant to amylases, so some structural differences would be anticipated. By using two polymers in tandem, the chance of producing effective drug-conjugates would be increased.

Through an extensive examination of the literature it was found that the most suitable alternative polysaccharide was Inulin, a furanose sugar of an average molecular weight of 5 kDa, derived from Jerusalem Artichokes.^{153,154} It can be purchased cheaply from commercial sources and has been tested in the peritoneal cavity, and FDA approved, indeed it is commonly taken as a dietary supplement, highlighting its high biocompatibility.^{153,154} Inulin

(INU) has a similar structure to IDX (Figure 19), the main difference being that IDX is made of pyranose whereas INU is made of fructose, save a terminal glucose unit.^{153,155} The difference is that amylases are only capable of metabolising glycosidic bonds on glucopyranosides, meaning that Inulin is not a substrate of amylase.¹⁴⁸ Further to this Inulin is known to pass through the human body undigested, showing complete stability to a variety of other enzymes.¹⁵⁴

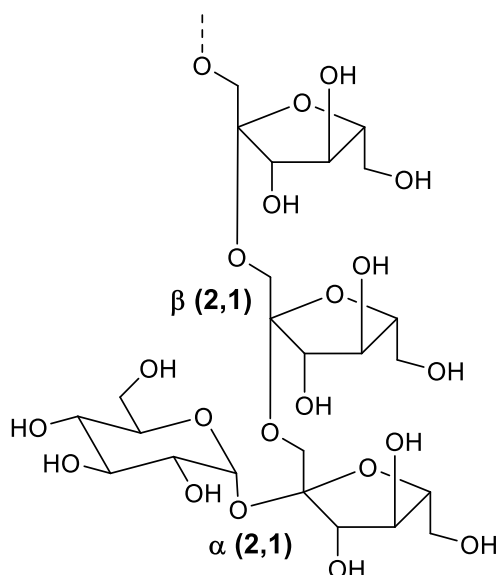


Figure 19 - Shows the structure of Inulin

There is also some evidence to suggest that INU has superior peritoneal retention compared to IDX, which would be beneficial.^{136,156} However it is worth stating that peritoneal retention of IDX and INU have never been evaluated in the same study so the results are not directly comparable.

1.5.2.1 Inulin-drug conjugates in the literature

An added advantage of Inulin is that unlike IDX, there are a wealth of studies that attempt to utilise INU as a polymer support in various capacities. Yang and co-workers conjugated Ibuprofen to inulin through attachment at its carboxylic acid group.¹⁰⁴ The resulting Ibuprofen-Inulin conjugate underwent self-assembly in water, due to the hydrophobic region on Ibuprofen contrasting with the hydrophilic Inulin.¹⁰⁴ This action formed a micelle, allowing the steroid (methylprednisolone) to be encapsulated for the purposes of drug delivery.¹⁰⁴

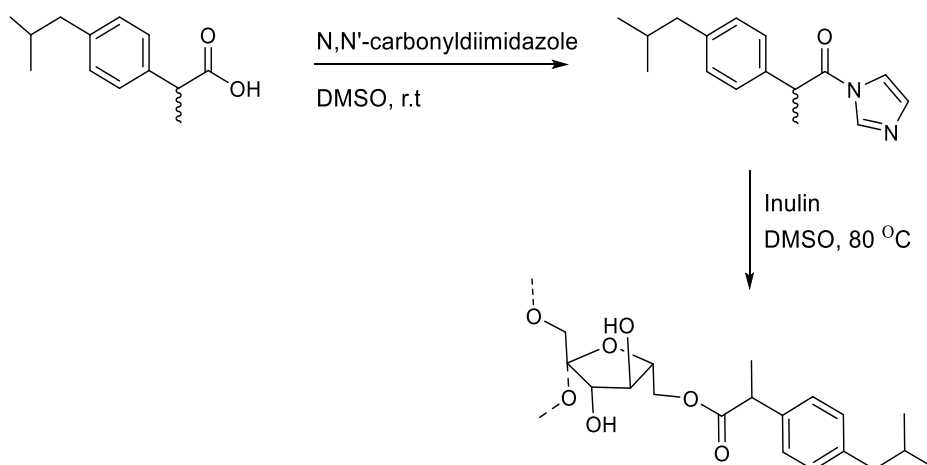
Peppas and co-workers developed a doxorubicin-Inulin conjugate to reduce the cardiotoxicity effects associated with the chemotherapeutic agent.¹¹⁸ Disappointingly, while an increase in potency was observed (compared to the free drug) the toxicity also increased. The authors suggested this was due to increased cell uptake of the conjugate, causing the drug to accumulate.¹¹⁸ Further to this, Giammona and co-workers attempted to encapsulate doxorubicin through the formation of a micelle, *via* ceramide units conjugated to Inulin.¹⁰⁶ The authors were able to show that doxorubicin could be released in a controlled manner in a variety of aqueous media and that cell uptake was increased compared to the unprotected drug.¹⁰⁶ Caron and co-workers demonstrated an Inulin-Triton X-100 conjugate, in an effort to increase the hydrophilic nature of the surfactant.¹⁵⁷ The purpose of this work was to create a surfactant suitable for solubilisation of a biological structure.¹⁵⁷ Based on the preposition that the large polymer support would prevent the hydrophobic component of the surfactant from penetrating the hydrophobic region of the protein and not causing activity to be reduced.¹⁵⁷ This led to limited success in reducing the toxicity of Triton X-100, but not significant enough to constitute further development.¹⁵⁷ Inulin has also been used as a siRNA delivery system, by conjugating diethylenetriamine units to the polymer.¹⁵⁸ In acidic conditions the terminal amine groups are protonated, which allows for an electrostatic interaction between the negatively charged nucleic acid residues of siRNA and ammonium groups of the modified INU.¹⁵⁸ The resulting siRNA conjugates showed improved cell-wall penetration. However, the overall effectiveness of the drug conjugate was questionable because siRNA was unable to detach from the polymer.¹⁵⁸ Inulin hydrogels have been used to deliver the chemotherapeutic agent 2-methoxyestradiol.¹⁵⁹ The drug was entrapped in INU *via* an internal cross-linking reaction between divinyl sulfone (covalently attached to Inulin) and the thiol groups of tris(3-mercaptopropionate), with the cross-linked strands of Inulin acting as a “cage”.¹⁵⁹

1.5.3 Drug attachment methodologies in the literature

As noted, many Inulin drug conjugates feature in the literature. Consequently, a variety of methodologies exist for covalently attaching molecules to Inulin. This is also the case for other polysaccharides such as Dextrans, of which methods should be broadly applicable to both Icodextrin and Inulin.¹⁶⁰ The challenges posed in attaching a drug molecule to a polymer (to prepare a drug-polymer conjugate) are three-fold: the reaction conditions must be

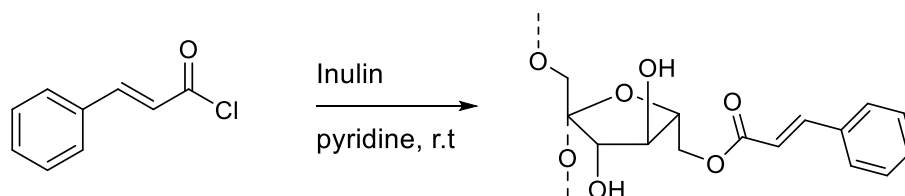
suitably mild so that no degradation occurs within the drug structure, to retain its biological activity. The functionality at the point of attachment should be relatively inert and not be susceptible to acidic hydrolysis. This is to ensure free drug is not deposited in the peritoneal cavity, which would reduce the benefit of polymeric enhancement. Further to this, it would be prudent for the linkage point to have no interaction with ATX, so as not to interfere with the intended pharmacophore. Therefore, only certain methods will be applicable for the attachment of drug-like molecules.

As previously mentioned, in a study by Yang and co-workers, Ibuprofen was conjugated to inulin, first, by reacting carbonyldiimidazole with the carboxylic acid group on Ibuprofen, then Inulin was added to the reaction mixture (Scheme 2).¹⁰⁴ Ibuprofen displaces the imidazole group, which results in the formation of an Ibuprofen-INU conjugate.¹⁰⁴



*Scheme 2 – Synthesis of an Ibuprofen-Inulin conjugate*¹⁰⁴

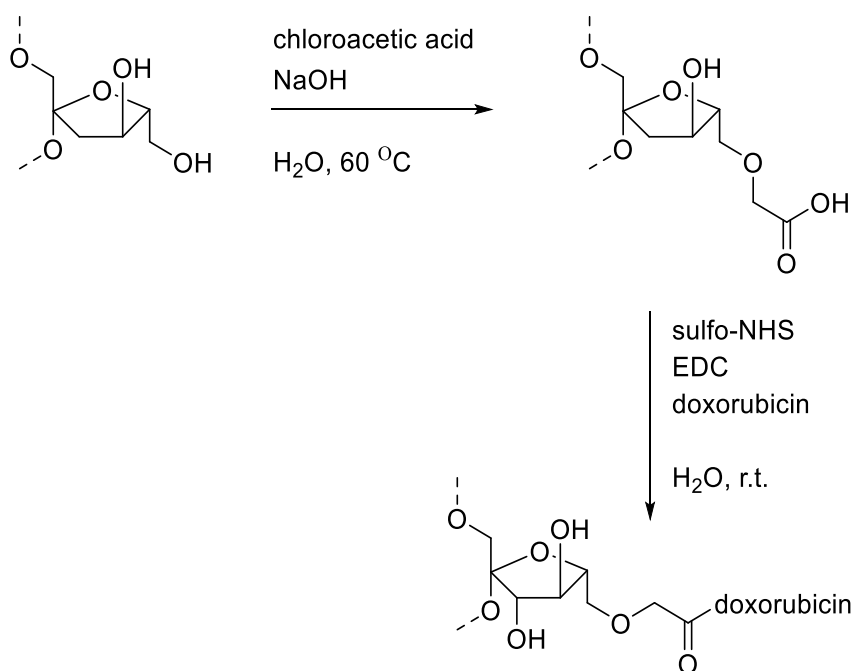
Similarly, Rodríguez-López and co-workers cinnamoylated Inulin by reacting INU with cinnamic acid chloride (Scheme 3).¹⁰³



Scheme 3 – Synthesis of Cinnamoylated-Inulin

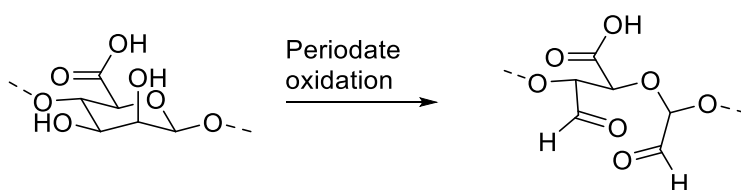
While this method is facile in its inception and is clearly suited to conjugating drug molecules, an ester linkage was felt to be too labile and would be susceptible to hydrolysis within the peritoneal cavity in our proposed study.¹⁶¹

Another attractive method is to pre-functionalize inulin by reacting it with chloroacetic acid. As demonstrated by Peppas and co-workers this can be conjugated to an amino acid unit of a drug (such as doxorubicin) using standard peptide coupling conditions (Scheme 4).¹¹⁸



*Scheme 4 - Synthesis of doxorubicin-Inulin Conjugate*¹¹⁸

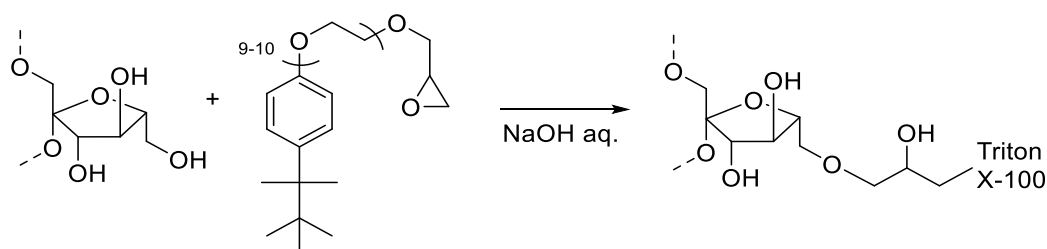
While being suitable for many applications, the amide moiety would be susceptible to hydrolysis and be unsuitable for our own work.¹⁶¹ Alternatively, some polysaccharides are known to undergo oxidation to an aldehyde (1° alcohol position), in the presence of galactose-6-oxidase or oxidative cleavage of cis 1,2-diols using sodium periodate (Scheme 5).^{160,162}



*Scheme 5 - Periodate oxidation of a polysaccharide*¹⁶⁰

The newly formed aldehyde provides a useful synthetic handle from which reductive amination with an amine can be used to attach drug molecules.^{160,163} The downside is that, in the case of oxidative cleavage, the polysaccharide undergoes significant derivatisation.¹⁶⁰

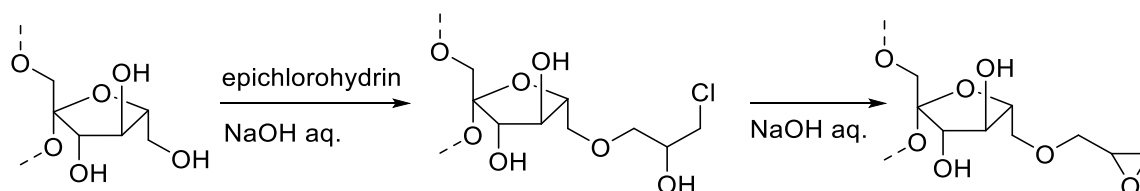
Epoxides are a particularly useful functionality for conjugating molecules to polysaccharides.¹⁶⁰ One approach is to modify the intended substrate by attaching an epoxide group, often using epichlorohydrin such as in the work by Caron and co-workers.¹⁵⁷ The epoxide intermediate can then be reacted with Inulin in basic media (Scheme 6).¹⁵⁷



*Scheme 6 - Conjugation of Triton X-100 to Inulin*¹⁵⁷

The advantage of this method is that it employs an ether linkage for attachment, which is comparatively inert and provides a stable backbone for conjugation. The ether-alcohol unit also closely mimics the polysaccharide structure, so is unlikely to interfere with the pharmacodynamics of the drug-conjugate. The stability of the epoxide-drug molecule would be of concern though, due to the highly reactive nature of epoxides.¹⁶¹

This method has also been used in “reverse” by Moltini who first activated Inulin by reacting it with epichlorohydrin. Then, in a basic environment, a second epoxide forms by an intramolecular displacement of chloride via the neighbouring hydroxyl group (Scheme 7).^{164,165}

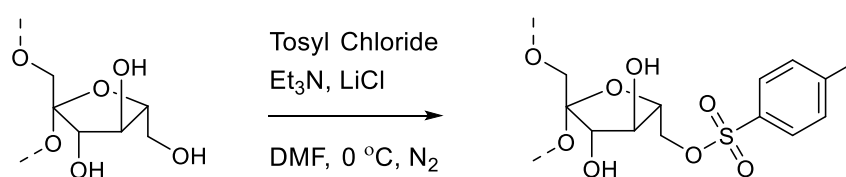


Scheme 7 - Formation of epichlorohydrin activated Inulin^{164,165}

The resulting epoxide unit is susceptible to nucleophilic attack by amines, allowing for a structure to be conjugated to the polysaccharide. Another advantage of this method is that

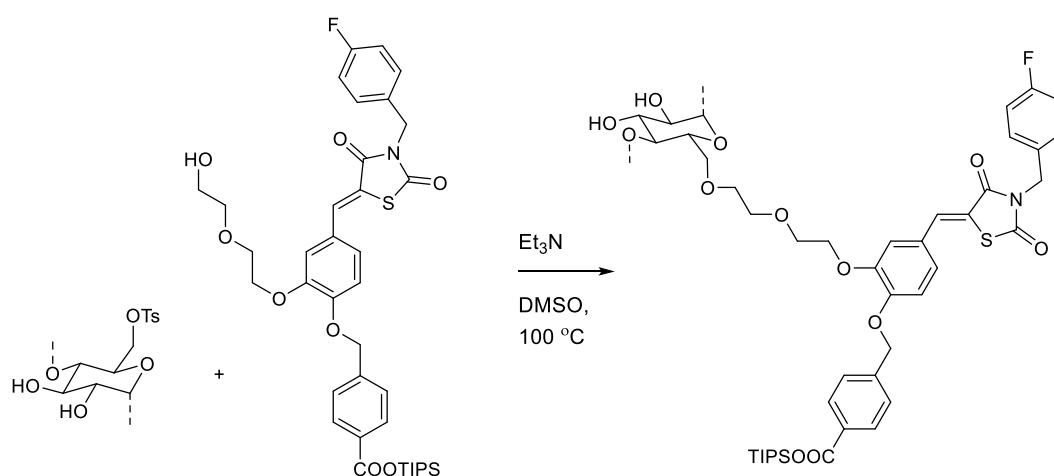
it has been employed successfully on multiple polysaccharides, such as dextrans and would therefore have potential to be used with IDX.¹⁶⁴ Ideally, this procedure would be applicable to alcohols as well, however there remains a paucity of evidence in the literature to suggest that this is possible.¹⁶⁵

An alternative method to form ether linkages with polysaccharides is to install a suitable leaving group in place of the primary hydroxyl.¹⁶⁰ This can then be displaced by nucleophilic attack from a drug molecule to attach the substrate. For example, Inulin has been tosylated by Ren and co-workers, in the presence of LiCl, to disrupt hydrogen bonding within the sugar (Scheme 8).¹⁶⁶



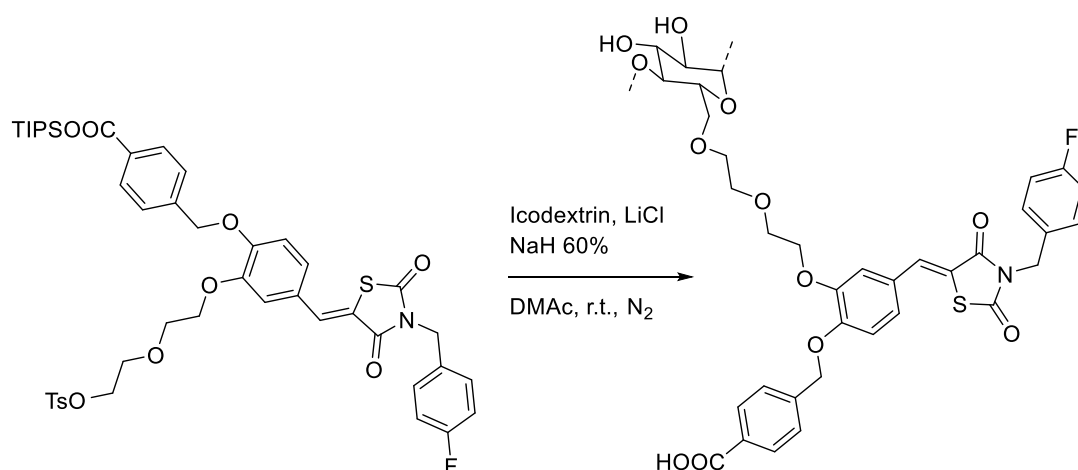
Scheme 8 - Synthesis of tosylated Inulin ¹⁶⁶

Hienze and co-workers have also applied this method to cellulose under similar conditions and more interestingly efforts by our own group have shown coupling to Icodextrin.^{94,167} This strategy proved to be a relatively effective approach in our previous work for attaching an autotaxin inhibitor by a simple S_N2 displacement of the tosylate, by the modified drug molecule (Scheme 9).⁹⁴



Scheme 9 - The addition of an ATX inhibitor to Icodextrin ⁹⁴

This method can also be applied in reverse synthesising a drug molecule modified with a suitable leaving group. The polysaccharide can then be treated with a strong base (typically sodium hydride) to generate an alkoxide which then displaces the tosylate.^{94,160,168} This method has been applied to Icodextrin in our previous research endeavours, by employing a specially modified drug molecule (Scheme 10).⁹⁴



*Scheme 10 - Shows the "reverse" tosylation approach*⁹⁴

Out of the two "tosylation" approaches utilised by us, tosylating the drug prior to conjugation was preferred.⁹⁴ This was because of the greater amount of control available in terms of the stoichiometry of drug-to-polymer, which is harder to control by pre-functionalizing IDX with tosyl chloride, due to it being reliant on every tosyl group reacting with a drug molecule. Otherwise some tosyl residues may be left on the polymer, which is of concern, considering the toxicity generally associated with alkylating agents.¹⁶⁹

1.5.4 Analysis of drug-polymer conjugates

The preferred mode of analysis for the conjugate described in Scheme 10 was ¹H NMR spectroscopy; typical methods of analysis associated with synthetic chemistry are less useful when analysing polymers, this is because of the lack of uniformity / regulation associated with a polymeric system, compared to a small molecule.¹⁴⁷ Mass spectrometry has recently found some use in the analysis of polymers, using "soft" ionisation techniques (such as Matrix Assisted Laser Desorption/Ionization, MALDI), however methods remain in their

infancy for the analysis of polymer drug conjugates.¹⁷⁰ Elemental analysis, FTIR spectroscopy and TGA have also been used in the analysis of the materials. Because of the restricted rotation of the IDX polymeric system, ¹H NMR spectra often lack definition and are unresolved, regardless of temperature. For this reason ¹³C NMR spectroscopy has limited use, with peaks noticeably broad. Nonetheless ¹H NMR spectroscopy offers a convenient means by which to demonstrate the formation of a drug-polymer conjugate, as shown in Figure 20.¹⁷¹

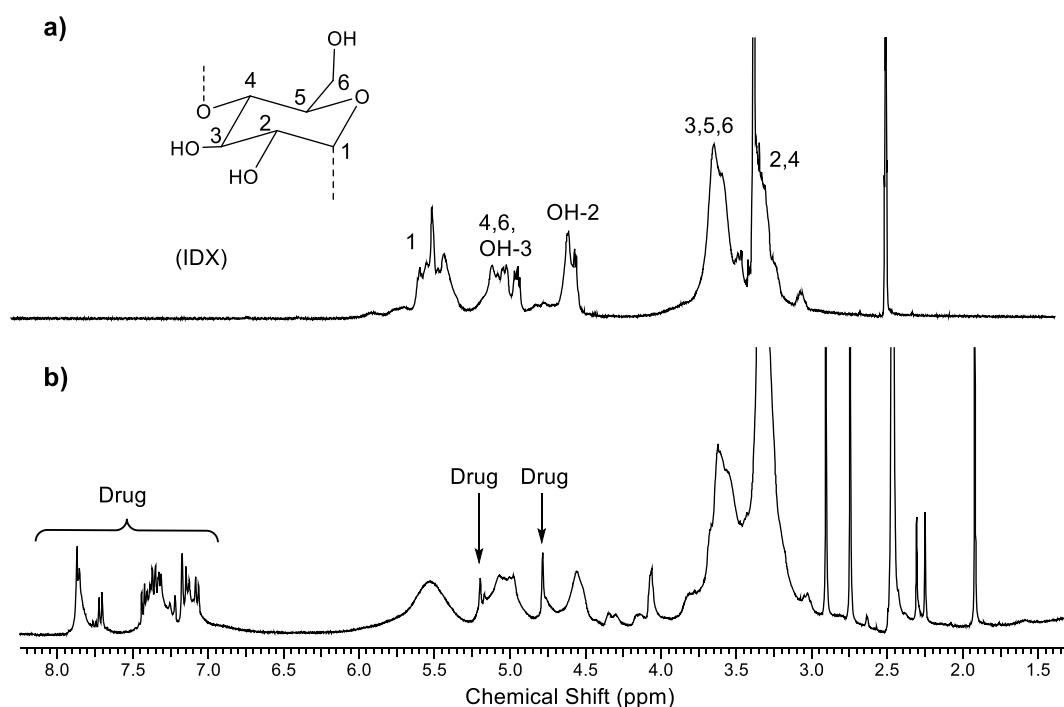


Figure 20 - The ¹H NMR spectra of: a) Icodextrin and b) Drug-IDX conjugate (400 MHz)

The amount of drug molecule attached to the polymer (drug-loading) can be quantified by either fluorescence spectroscopy or elemental analysis. The results can then be expressed as the degree of substitution (DS), which refers to the number of drug molecules attached to the hydroxyl groups of a monomeric unit of the polysaccharide, averaged over the whole polymer.¹⁶⁰ For instance, IDX has a maximum DS value of 3.

It is also worthy to note the selectivity observed in almost all the polymer-conjugation reactions for the primary hydroxyl groups of the sugars. This can be explained in part due to the hydroxyl groups adjacent to the electrophile being electron withdrawing, which disfavours S_N2 displacement.^{160,172} This effect is less prominent for primary electrophiles due to being located further from the alcohol groups. Conversely when the polysaccharide takes

the role of the nucleophile the primary alcohol reacts in preference to the secondary.^{160,172,173} This effect is caused by increased nucleophilicity of the primary hydroxyl group. Although the reaction is not entirely regioselective, with some alkylation occurring with the secondary alcohols, as evidenced by DS (degree of substitution) values of up to 2 reported for some polysaccharides.¹⁷³

1.5.5 Approaches to the synthesis of novel drug-conjugates

Overall, of the different methods available for the covalent attachment of drug molecules to polymers, there are two differing approaches. Firstly, *via* modification of the polymer to increase its reactivity.^{166,167} Or through modification of the substrate so that it reacts with the polymer.^{157,166,167} The latter approach can be divided into two further subtypes: taking an active drug molecule and performing minimal synthetic changes needed for conjugation, or alternatively, a ground-up approach in which an analogue of the intended drug molecule is made. A new synthetic handle is installed on the molecule from which the drug can be attached, at a position that is not likely to disrupt key pharmacophoric interactions with the target. The main problem with the former method is that while it is less synthetically challenging, it relies on pre-existing functionality of the drug molecule. If those functional groups are modified for attachment, then a decrease in potency may be expected. The “ground-up” approach is seen rarely in the literature, likely due to the synthetic challenges posed. Our own previous work utilised this method for the advantages outlined previously.⁹⁴

1.5.6 The use of linker / spacer units in drug polymer conjugates

On the topic of drug modification for attachment, one additional modification to a drug compound may be to include a spacer / linker unit (Figure 21).^{174,175}

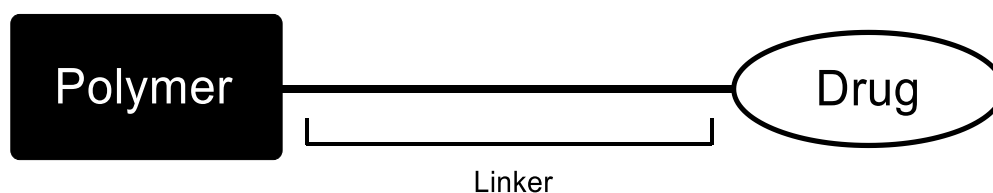


Figure 21 – Use of a linker to separate a polymer from a drug

Spacer groups are used to alleviate unfavourable steric interactions that may occur as a consequence of attaching a drug to a polymer. When one considers the highly branched and bulky nature of a polysaccharide, it can be envisaged that this may disrupt the interaction of a drug molecule and the active site of the target. The effect may lead to a loss in potency of the drug-conjugate (compared to the free drug) and therefore the dosage would need to be increased. Using a spacing unit between the drug molecule and a polysaccharide should reduce the effect of unfavourable steric interactions with the polymer, by introducing a suitable distance between each entity. This principle has been utilised by Caron and co-workers who synthesised dextran-alprenolol conjugates incorporating an alkyl spacing unit.¹⁷⁴ Additionally, Infante and co-workers have also using alkyl linkers in the preparation of Inulin conjugates.¹⁷⁵ Our work has also previously employed a spacer unit comprised of diethylene glycol, chosen to closely mimic the environment of Icodextrin, rather than an alkyl linker which may act to reduce aqueous solubility of the conjugate.⁹⁴

1.6 Relevance to previous work

The work described within this thesis builds upon an investigation previously described by us, *J. Med. Chem.*, 2018, **61**, 7942–7951.¹⁴⁷ In those studies, we presented a novel drug delivery strategy for use within the peritoneal cavity. Many autotaxin inhibitors have been found to be highly potent *in vitro*, but when they have been tested within a living organism, they often perform poorly. One reason suggested for this reduced activity was the drug is rapidly eliminated from the peritoneal cavity and then metabolised. To increase the residence time of an ATX inhibitor within the peritoneal cavity, a polymer therapeutic approach was taken. An analogue of the potent autotaxin inhibitor, HA155 (Table 2) was attached to Icodextrin using the “tosylated-drug method” (Chapter 1.5.3). Icodextrin was viewed as an ideal polymer support, based upon its desirable pharmacokinetic properties, in which it has been shown to be retained within the peritoneal cavity for up to several days by virtue of its high molecular weight. Following the attachment of the ATX inhibitor to IDX, we postulated that the resulting drug-conjugate (Figure 22) would demonstrate significantly improved peritoneal retention whilst maintaining its inherent biological activity.

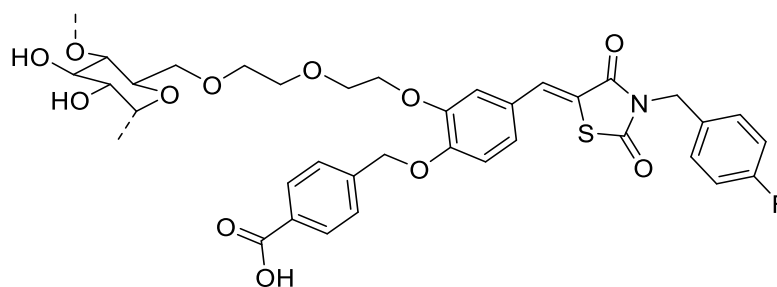


Figure 22 - Icodextrin-drug conjugate

The resulting conjugate was then evaluated for biological activity *in vitro* using two artificial substrate enzyme assays (bis *p*-NPP and FS-3). The drug residue was found to retain much of its original potency following conjugation to the polymer: $0.86 \pm 0.13 \mu\text{g mL}^{-1}$ (FS-3) and $0.94 \pm 0.12 \mu\text{g mL}^{-1}$ (bis-*p*NPP) compared to the free inhibitor, $0.297 \pm 0.08 \mu\text{g mL}^{-1}$.¹⁴⁷ A wound closure assay was then performed on OVCAR-3 cells, in the presence of the free-inhibitor, the icodextrin-drug conjugate, parent-Icodextrin and a control (DMSO). The results are shown in Figure 23.¹⁴⁷ Both the icodextrin-drug conjugate and the free autotaxin inhibitor reduced wound closure by approximately 50% compared with cells exposed to DMSO.¹⁴⁷

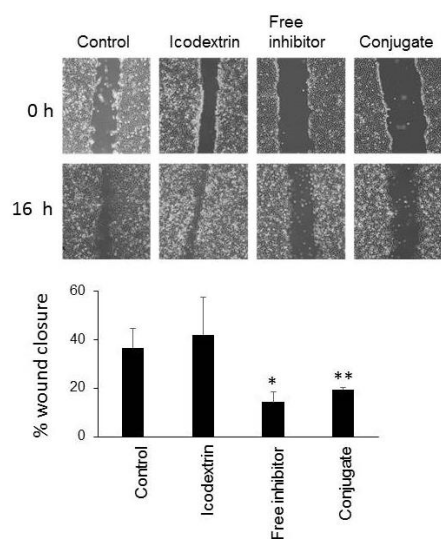


Figure 23 - Effect of percentage wound closure by IDX, IDX-drug conjugate and free-inhibitor

Most significantly the peritoneal retention of the drug conjugate was tested within mice and was found to be retained up to 30% of its original concentration after 24 hours.¹⁴⁷ This significantly increased the residence time of the drug in the peritoneal cavity, in comparison <0.1 % of the free-drug equivalent was observed after 24 hours.¹⁴⁷

1.7 Project outline

The work described above, functioned as proof of concept for our novel drug delivery strategy, designed specifically for use within the peritoneal cavity, as a treatment for ovarian cancer. In this thesis we describe a new application of the carbohydrate-based polymer Icodextrin in drug-conjugate synthesis, and our approach to the synthesis of conjugated analogues of recently published autotaxin inhibitors (Figure 24).⁸⁸

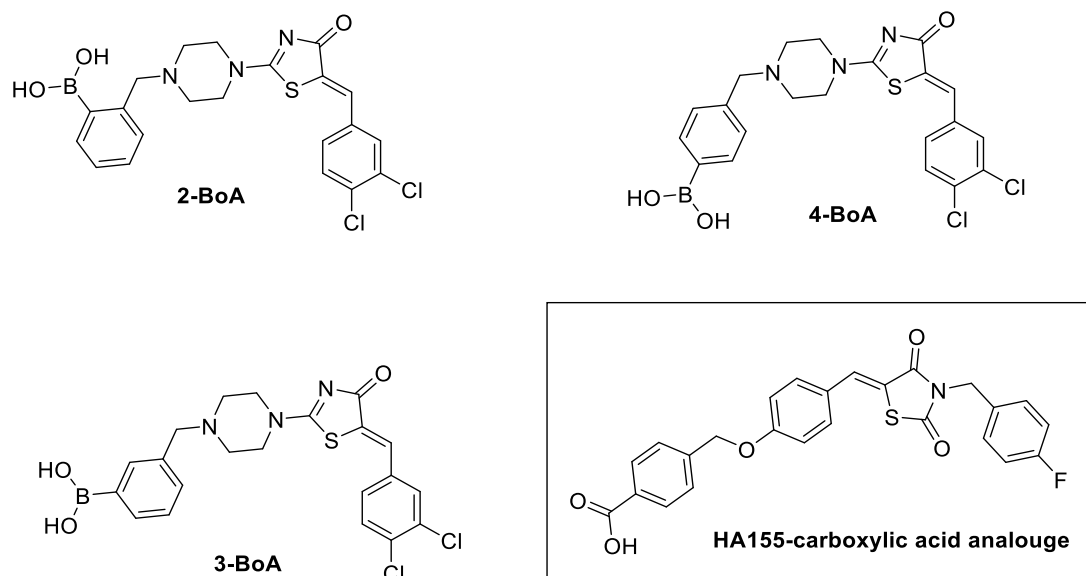


Figure 24 - Three potent ATX inhibitors from a study by Nagano and co-workers and the HA155-carboxylic acid analogue previously investigated by us.⁸⁸

These inhibitors contain a boronic acid moiety instead of a carboxylic acid group employed in our previous efforts.⁹⁴ Carboxylic acids are less synthetically challenging to install compared to boronic acids. Indeed, even as of 2018, there remains few reliable synthetic methods to install boronic acids.¹⁷⁶⁻¹⁷⁹ Boronic acid ATX inhibitors are known to be significantly more potent than their carboxylic acid counterpart, such as HA155, described by Albers and co-workers, with an IC_{50} value of 5.7 nM.⁴³ This is due to the covalent bond between the boronic acid group and the Thr209 residue on ATX, with two zinc atoms holding the substrate in place, in a similar manner to the interaction between LPC and ATX (Figure 25a).^{42,43,88}

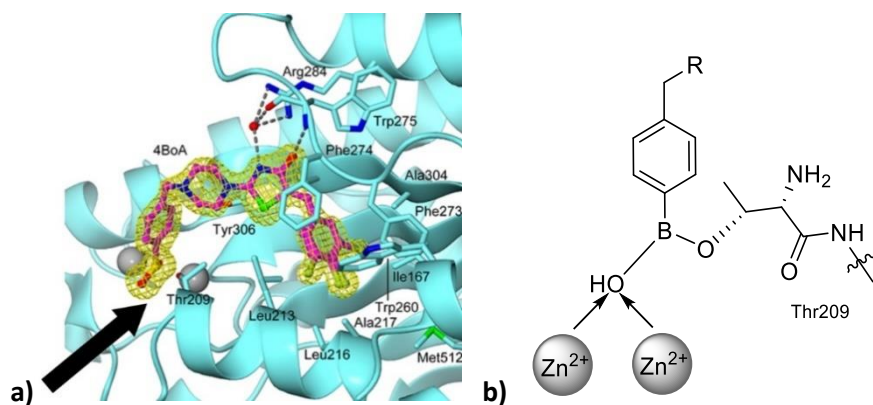


Figure 25 – a) 4-BoA bound to the active site of ATX, b) the boronic acid group coordinating to zinc and covalently bonded to Thr209.⁸⁸

As denoted by the arrow in Figure 25a, one hydroxyl group from the boronic acid sits between two zinc atoms (grey spheres) and coordinates to these ions.⁸⁸ The nucleophilic hydroxyl group of Thr209 forms reversibly a covalent bond with the boronic acid, which accounts for the high level of activity attributed to 4-BoA.^{43,88}

Novel Inulin (INU) drug conjugates will also be produced, and explored as an alternative to Icodextrin, given Icodextrin's susceptibility to hydrolysis by amylase in rodents.¹⁴⁹ It is envisaged that the complementary Inulin conjugates could be synthesised in a similar manner to the Icodextrin conjugates.⁹⁴ The importance of this is that for an IDX conjugate to be compared to an INU equivalent, the linker chemistry used to attach the drug to the polymer must be equivalent, in order to determine which polymer is the more suitable for use in the peritoneal cavity.

As in our previous work, the ATX inhibitor will be modified to incorporate a linker unit, with a suitable point of attachment having been identified (Figure 26).¹⁴⁷ The site was chosen so that it would not interfere with those key groups that are involved in binding to the active site, based on the X-ray crystal structure (Figure 26) of 4-BoA bound to autotaxin.⁸⁸

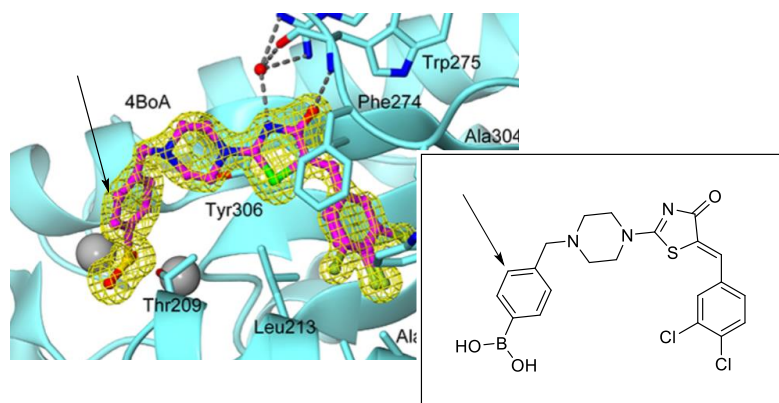


Figure 26 - The proposed point of attachment

It was anticipated that the necessary functionality could be installed by adapting the synthetic route published by Nagano, by directly substituting the starting materials to incorporate the desired synthetic handle.⁸⁸

The initial work for this project will involve the synthesis of three different drug-linker, based around the three most potent inhibitors from Nagano's original publication, 2-BoA, 3-BoA, 4-BoA (Figure 27).⁸⁸ These ATX inhibitor analogues will then be used to produce drug-conjugates with Icodextrin and Inulin, yielding six conjugates in total for the initial study.

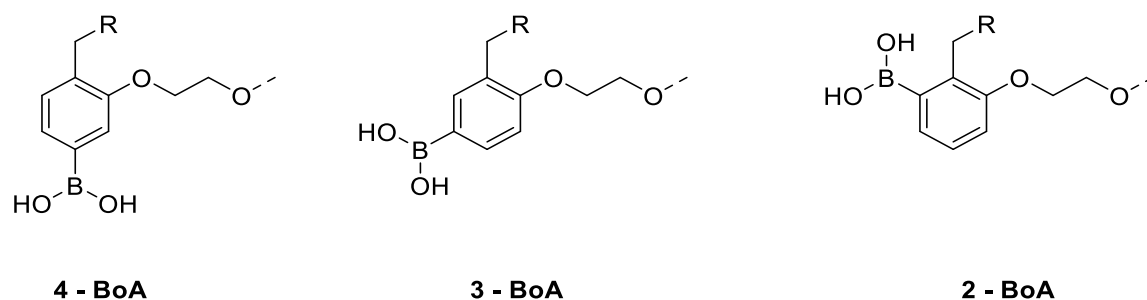


Figure 27 - Three drug-linker compounds that will be produced for this project

These 1st generation conjugates will be evaluated for biological activity using *in vitro* enzyme assays, such as a bis pNPP artificial substrate assay and a FS-3 fluorescence assay, to quantify the inhibition of ATX. A peritoneal-retention study will also be conducted to measure the residence time of a drug-conjugate within the peritoneal cavity.⁹⁴ These results will be used to guide the approach taken for the subsequent studies. As alluded to earlier, conjugating a drug to a polymer is likely to result in a loss of potency (compared to the free drug).

Therefore, efforts should be made to increase potency of the drug conjugate so that it is similar to that of the parent drug. There are several ways this can potentially be achieved. For example, linker length is very likely to be an important factor in determining activity. As suggested by Caron and co-workers, increasing the degree of separation between the drug pharmacophore and the polymeric backbone can potentially reduce any unfavourable steric interactions caused by the polymer. By using a longer linker one could expect a rise in potency to be observed.¹⁷⁴ Another possible modification may be to change the position of the linker on the drug. Due to the significance of the interaction between B(OH)₂ and ATX, the close proximity of the linker may result in the conjugate losing activity (compared to the free drug). A more suitable point of attachment may be the piperazine moiety of the inhibitor, which in itself does not interact with ATX. The chemistry used to establish this functionality could be based upon the work of Berkheij *et al*, involving direct α -lithiation of *N*-Boc piperazine.¹⁸⁰ Another less well-studied modification is the effect on activity of the drug loading on the polymer. Whilst one might expect that the highest drug loading possible may lead to a highly potent conjugate, somewhat counterintuitively this may not be the case. This is because a high degree of substitution may actually reduce the total available pharmacophore because the neighbouring drug molecules could prevent the drug from interacting with ATX, through steric hindrance. It would therefore be beneficial to produce a series of drug conjugates with differing quantities of drug bound to the polymer, to determine the optimum drug loading.

Additional investigations will include the conjugation of other autotaxin inhibitors to Icodextrin and Inulin. A search of the literature highlighted three potential drug molecules that appeared suitable for modification to allow conjugation (Figure 28). These were chosen in part due to their high potency, but were also those felt to be the least challenging, synthetically, to produce drug-linker analogues.^{43,67,87}

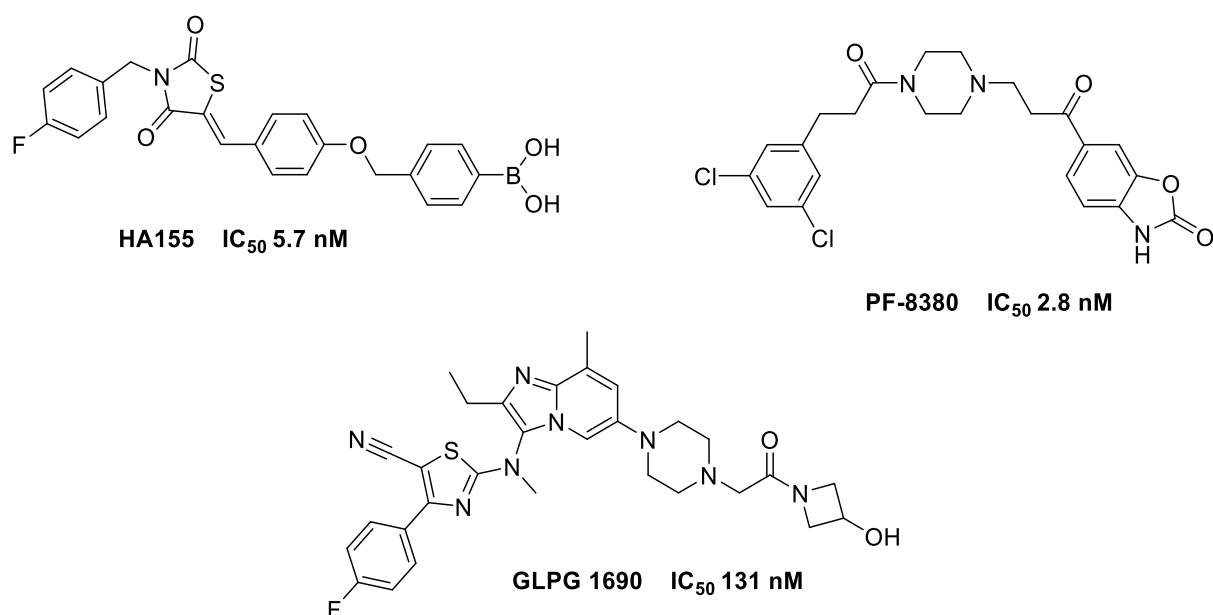


Figure 28 – Other potential ATX inhibitors that could be conjugated to a polymer ^{43,67,87}

GLPG 1690 (Figure 28) would contrast particularly well to the other ATX inhibitors featured, as it employs an alternative binding mode, interacting with the hydrophobic pocket and tunnel of ATX rather than its active site.⁶⁷

1.8 Significance of drug-conjugation for potential treatment in the clinic

As stated earlier, it is common for patients with ovarian cancer to have elevated levels of ascites fluid in their peritoneal cavity, aggravated by tumour growth. The fluid is typically drained as a matter of course in their treatment regime.⁴⁶ Icodextrin is commonly used to achieve peritoneal dialysis, under the tradename “Extraneal”.¹⁸¹ This is a major advantage for our study as this polymer is known to be safe and is regularly used in the clinic and so forms an ideal base for potential drug conjugation.^{142,181} It should be noted that there have been no previous reports of Icodextrin being used as a basis for a drug polymer-conjugate.¹⁴⁷ We propose that an Icodextrin / Inulin drug conjugate could be administered during or after this ascites drainage procedure.¹⁸² This is likely to cause minimal inconvenience to the patient and potentially require fewer repeat dosages, by virtue of the improved pharmacokinetic properties offered by this drug-delivery system. We envisage that the ATX inhibitor conjugate would be taken in combination with a commonly used chemotherapeutic

agent such as taxol, to augment the properties of the conjugate and hopefully lead to a reduction in tumour size.^{73,183}

1.9 Aims of this work

The overall aim of this study is to investigate the use of two polysaccharides Inulin and icodextrin as novel drug delivery systems, in order to improve the pharmacokinetic properties of a number of autotaxin inhibitors as a potential new treatment for ovarian cancer. To date, ATX inhibitors typically perform poorly *in vivo* as ovarian cancer therapies, because they rapidly diffuse through the peritoneal cavity into the systemic circulation where they are metabolised readily. Through the use of a drug-polymer conjugate, a localised concentration of the drug should be established within the peritoneal cavity from where it can then act. Autotaxin is an enzyme known to be an autocrine motility factor; through its inhibition, the mechanisms by which ovarian cancer cells survive, proliferate and become resistant to chemotherapy will be disrupted.^{93,94,147}

The aims of this project can thus be summarised as follows:

- To synthesise new analogues of autotaxin inhibitors based on BoA 2, 3 and 4, to incorporate a suitable linker unit.⁸⁸
- To produce novel drug-polymer conjugates using those modified ATX inhibitors, based on the use of both Icodextrin and Inulin.
- To evaluate the biological activity of the novel drug conjugates *in vitro* and assess the extent to which the drug conjugates retain potency compared to their free-drug equivalents.
- Through animal studies, to compare the peritoneal retention of IDX-conjugates and INU-conjugates to determine which polymer offers the longer residence time in the peritoneal cavity.
- To produce a series of 2nd generation drug-conjugates, to increase their potency, in anticipation of a loss of activity (compared to the free drug) associated with the drug being attached to a polymer. Areas identified for investigation include: length of spacing group, the position of attachment for the linker, the degree of drug loading and alternative autotaxin inhibitors.

Chapter 2:

The synthesis of Icodextrin-drug conjugates

Chapter 2: Synthesis of Icodextrin drug-polymer conjugates

2.1 Synthesis of 3-BoA linker analogue, initial route

The starting point for this investigation was to synthesise analogues of a series of boronic acid-containing ATX inhibitors, incorporating a linker unit (Figure 29).⁸⁸

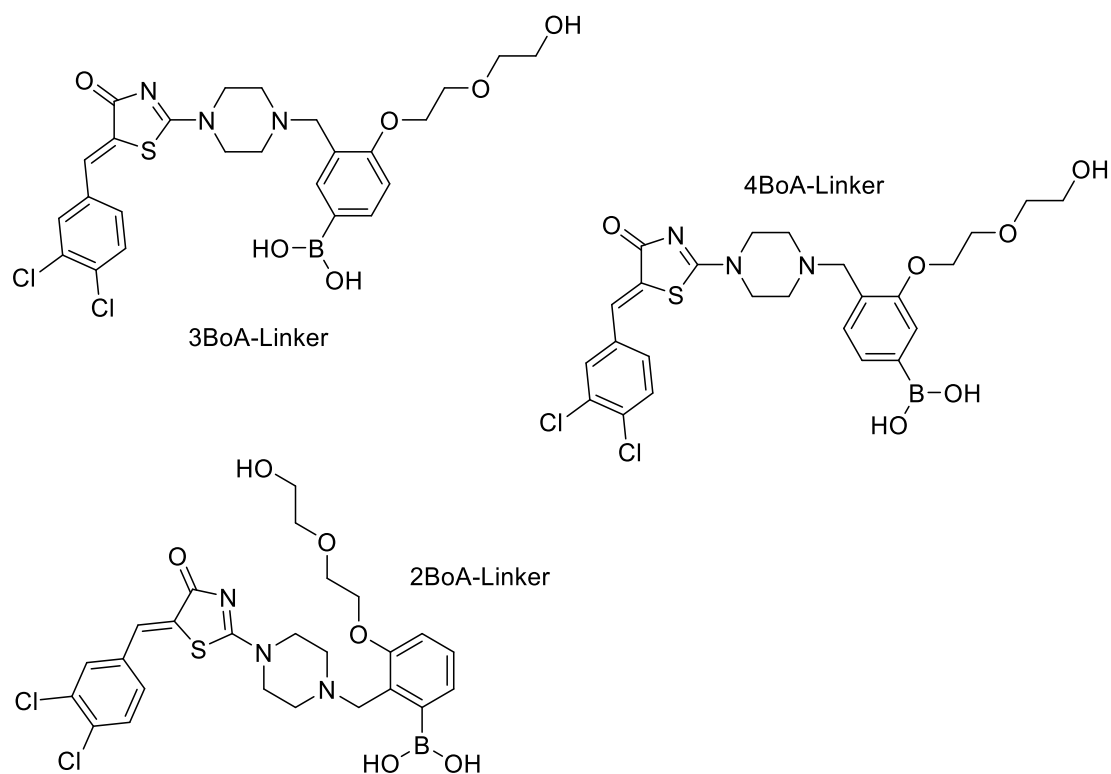
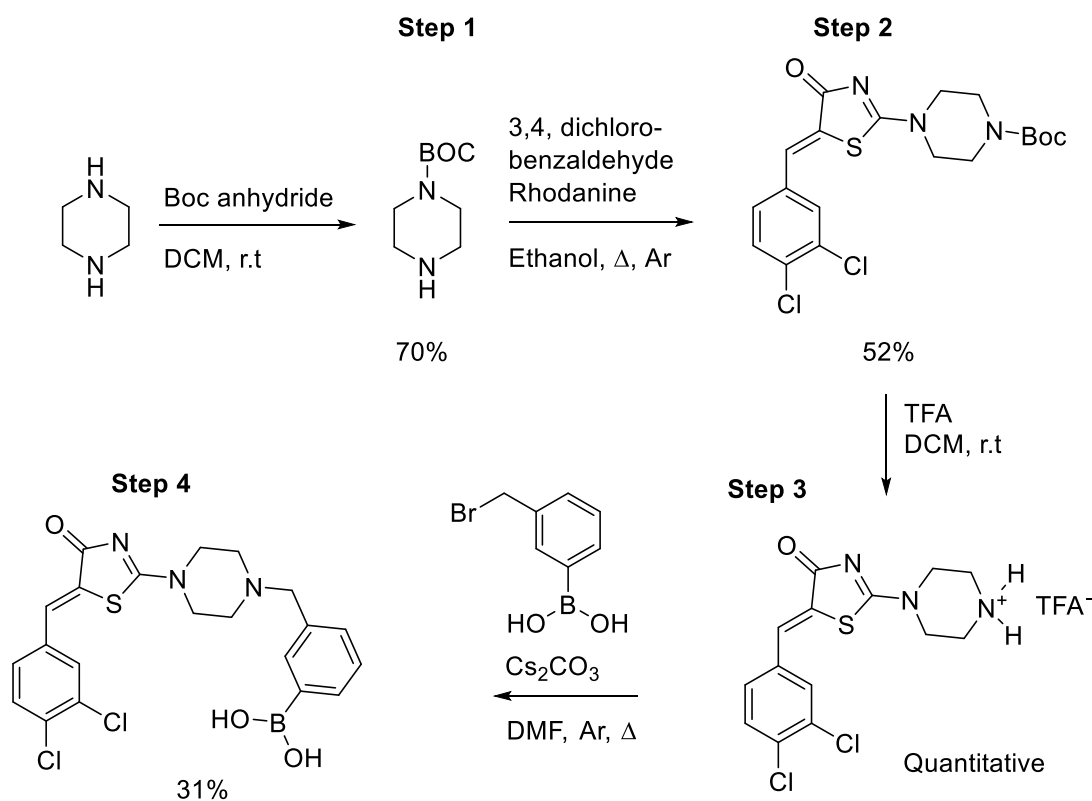


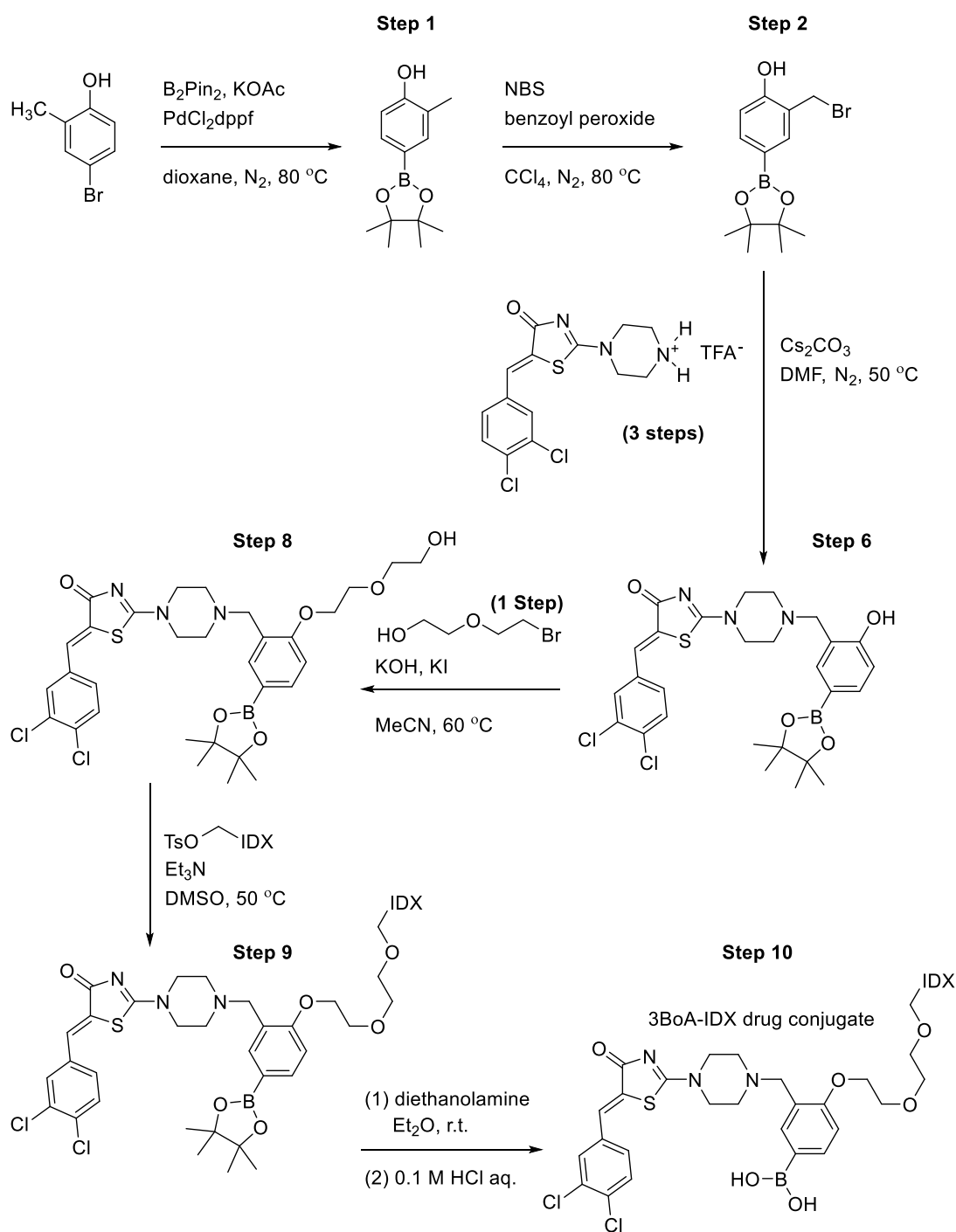
Figure 29 - A representation of the target drug-linker analogues

It was decided that 3BoA-linker would be synthesised first because it was likely to be the most potent (with reference to Nagano's study, free-drug inhibition = 13 nM).⁸⁸ Once a synthetic route had been established, it was anticipated that the two additional analogues (4BoA-linker and 2BoA-linker, Figure 29) could be prepared by similarly using the appropriate starting material. It was our original intention to base the synthetic route for 3BoA-linker on the route published by Nagano for the parent drug (Scheme 11).⁸⁸



Scheme 11- Nagano's synthesis of 3BoA⁸⁸

The synthetic route shown in Scheme 11 has an overall yield of 11%, over four steps.⁸⁸ Whilst Nagano's route was a useful starting point, there were some challenges that would need to be addressed. For instance, 3BoA was synthesised as part of a compound library. In total 31 mg was made as part of the study and the compound was purified by HPLC.⁸⁸ For our purposes, 3BoA-linker is required in multigram quantities so the chemistry used to synthesise it should be robust and relatively facile. Additionally, the synthetic route chosen must account for the difficulties posed in working with boronic acid groups, namely; they react with silica gel so cannot be purified by column chromatography; they are generally insoluble in common organic solvents; there are comparatively few reliable methods by which they can be synthesised; they are sometimes unstable and are susceptible to dimerization or trimerization. Therefore, a sensible approach would be to install the boronic acid group as the last synthetic step, post conjugation. Our initial synthetic route for the 3BoA-Icodextrin drug conjugate is shown in Scheme 12.



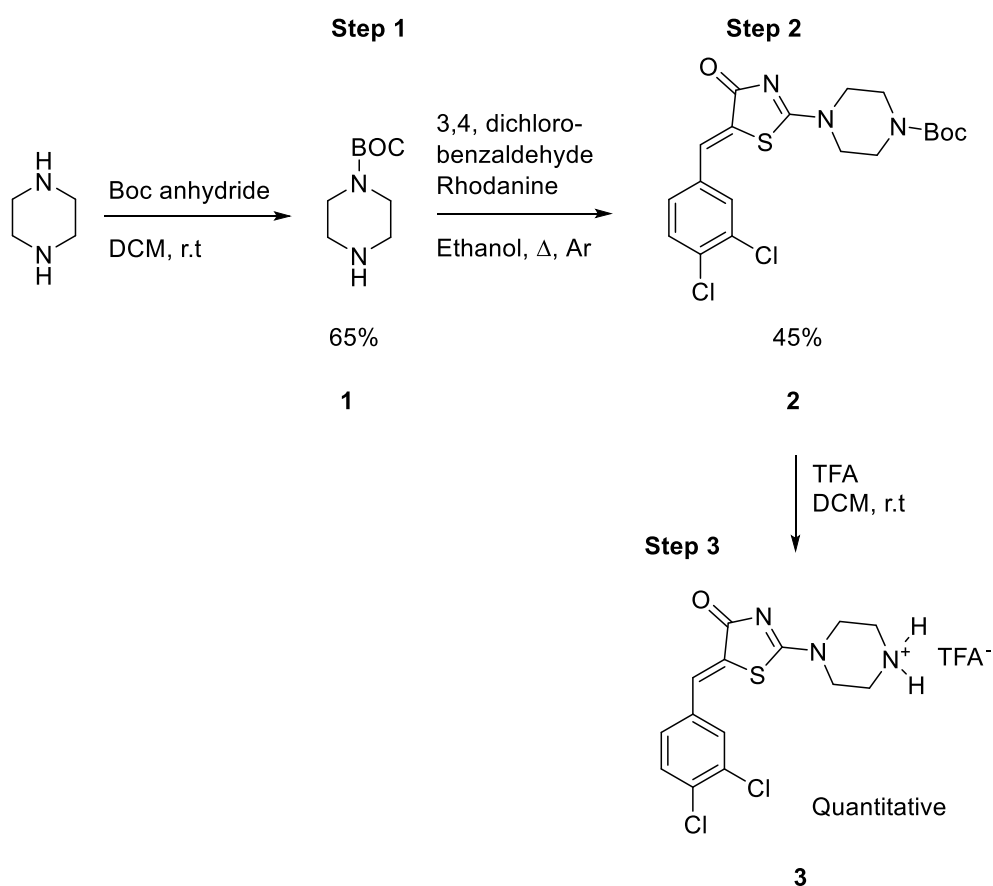
Scheme 12 - Proposed synthesis route for 3BoA-IDX drug conjugate

The route shown in Scheme 12 employs a convergent approach, using three separate fragments: Nagano's heterocycle, an aryl boronic ester and the diethylene glycol linker. Ten synthetic steps are involved, with seven as the longest linear sequence. The route has been designed so that the final step is the hydrolysis of the boronate ester group of the drug, several methods exist for this transformation. Boronate esters, in particular the BPin moiety,

offer a convenient approach to install what are essentially, “boronic acid protection groups” on to aromatic systems, through the Miyaura borylation reaction or CH Borylation developed by Hartwig and co-workers.^{184,185} In order to attach the drug-linker compound to IDX our previously developed “tosylated icodextrin” method will be used in preference to the reverse approach (tosylated drug). This is because the “tosylated IDX” method uses a much milder base (Et₃N, compared to NaH), which is unlikely to compromise the integrity of the BPin moiety, of which are known to degrade in the presence of a strong base.

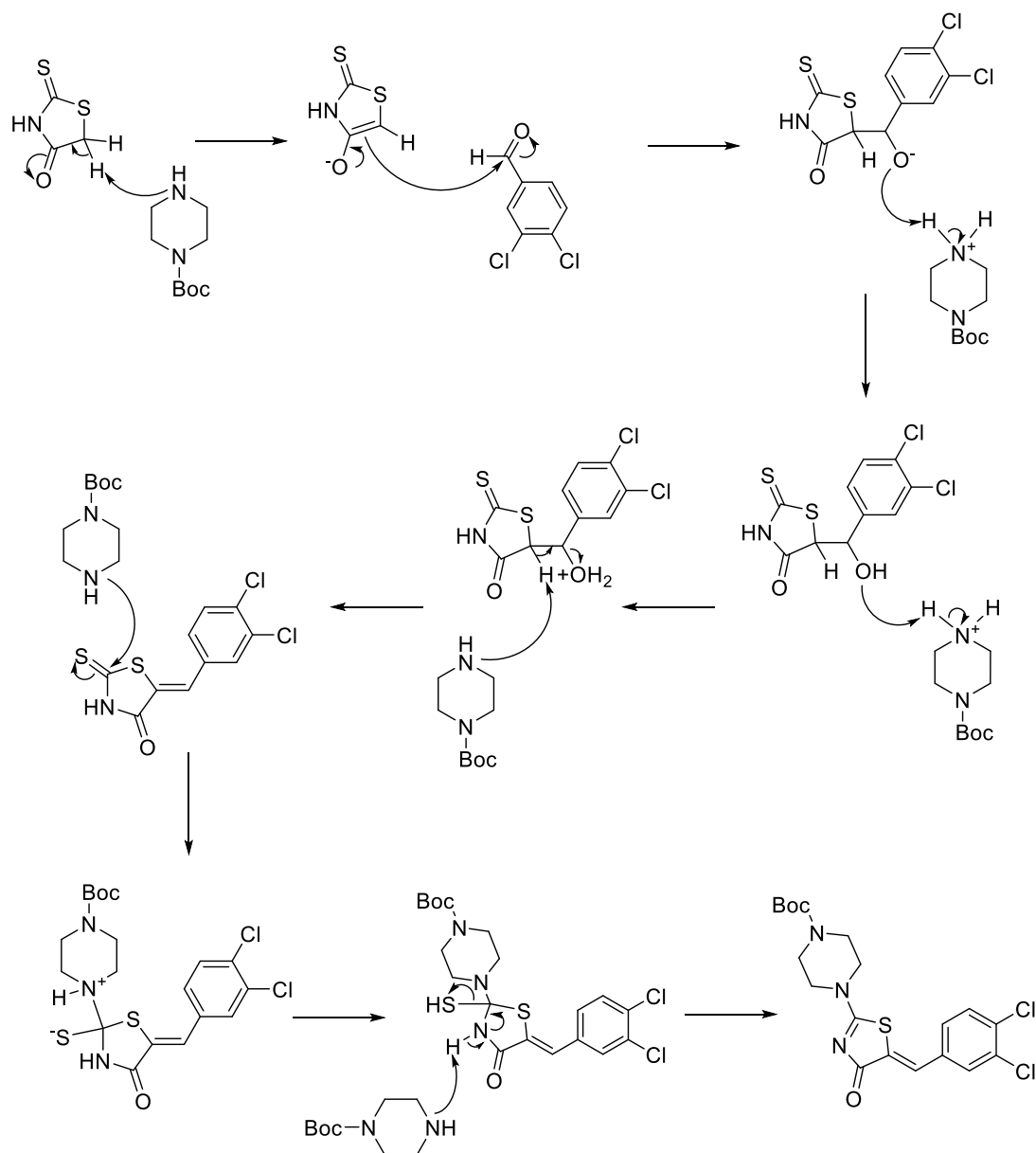
2.1.1 Preparation of Nagano’s heterocycle

Synthesis began with the construction of Nagano’s heterocyclic compound according to the literature procedure, starting with the Boc protection of 1,4 piperazine using Boc anhydride, *N*-Boc piperazine **1** was then reacted with rhodanine and 3,4-dichlorobenzaldehyde in a multicomponent “Knoevenagel reaction, to give **2** (Scheme 13). Finally, the *N*-Boc protecting group was removed from the heterocycle **2**, in the presence of TFA (Scheme 13).⁸⁸



Scheme 13 - Synthesis the heterocycle **3**, over three steps

During the formation of heterocycle **2**, N-Boc piperazine acts as both a base and a nucleophile. Hydrogen sulfide gas and water is given off as a by-product, the suggested mechanism for the formation of **2** is shown in Mechanism 1.

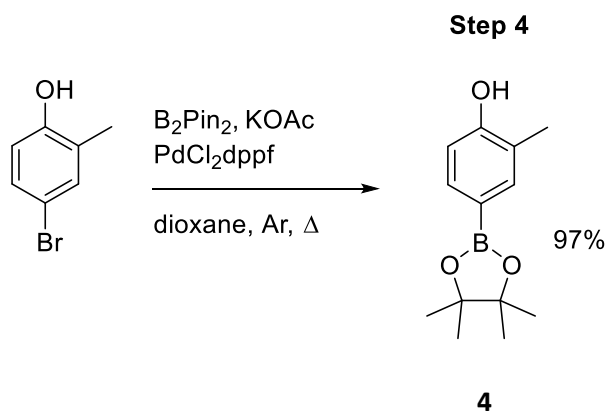


Mechanism 1 – Suggested mechanism of the formation of 2

Heterocycle **3**, resulting from the N-Boc deprotection of **2** formed a salt with trifluoroacetic acid (N-TFA). Nagano suggested that this could be released *in situ* during the S_N2 displacement reaction with the phenyl boronic acid compound (Step 4, Scheme 11), in the presence of Cs₂CO₃.⁸⁸

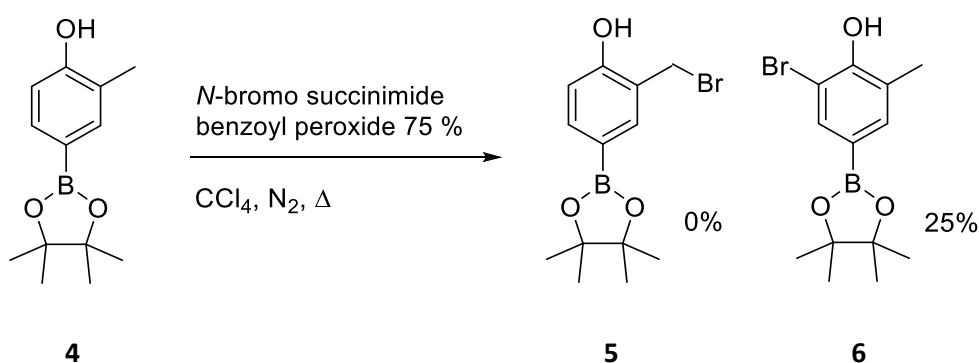
2.1.2 Synthesis of the boronic ester fragment

With Nagano's heterocycle in hand, the boronate ester fragment could now be synthesised, (Scheme 14).



*Scheme 14 - The first step in the synthesis of the boronate ester fragment, **4***¹⁸⁶

The Miyaura borylation reaction proceeded smoothly and in excellent yield, on a multigram scale. The next step was to install a suitable leaving group at the methyl position. It was felt the most convenient way this could be achieved was through radical bromination. Phenol **4** was subjected to standard radical bromination conditions in CCl_4 (Scheme 15).¹⁸⁷

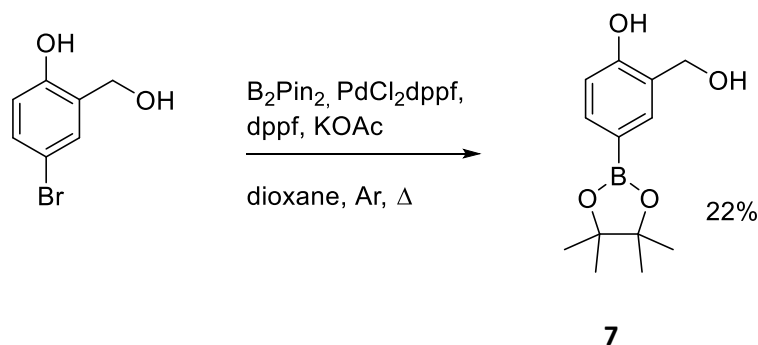


*Scheme 15 - Attempted radical bromination of **4***

The intended bromo species **5** was not isolated, instead it appeared that an electrophilic aromatic bromination reaction had occurred **6**. Typically, for an electrophilic aromatic

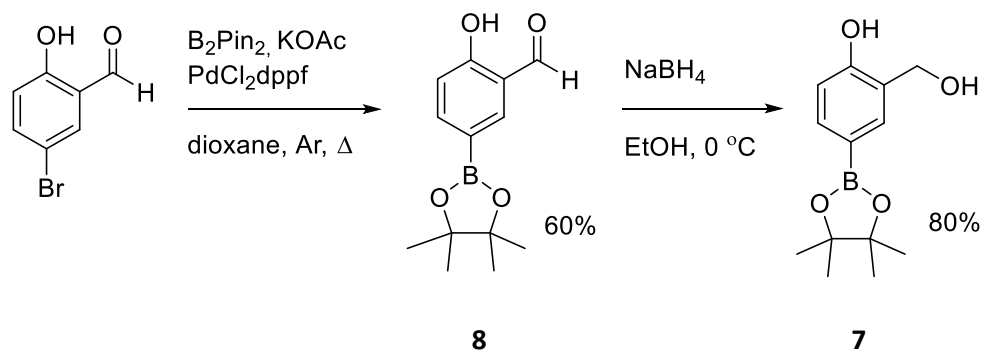
bromination to occur, the reaction must be performed in the presence of a catalyst. However it is known that when a substituent has a strong activating effect, for example an alcohol, a catalyst may not be required.¹⁸⁸ Indeed, this appears to be the case with the phenol **4**. The OH group is strongly electron donating and it causes aromatic bromination to be favoured over radical bromination of the methyl group. Bromination would have also very likely occurred at the *para* position in addition to the *ortho*, had the *para* position not been occupied by the BPin group.¹⁸⁸ The reaction was repeated under the same reaction conditions, but the same result was replicated. No reaction was observed at room temperature, highlighting the importance of temperature in the electrophilic aromatic bromination reaction.

An alternative method to synthesise phenol **5** was investigated, using a different boronate ester substrate **7** (Scheme 16).



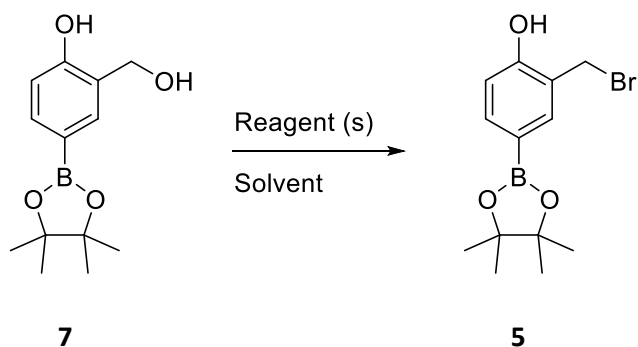
Scheme 16 - The synthesis of 7

This approach used a boronate ester with a benzylic alcohol as a useful synthetic handle from which a leaving group could be installed. As can be seen in Scheme 16, the yield was very low and the majority of starting material was recovered. Repeat reactions saw little improvement. Additionally, the starting material was expensive. Consequently, a much more efficient method was developed using a considerably cheaper substrate (Scheme 17).



Scheme 17 - Alternative synthesis of phenol 7

The route delivered **7** in an overall yield of 48% over the two steps in multigram quantities. With the desired boronate ester, various methods were attempted to generate the desired bromide, as summarised in Table 4.



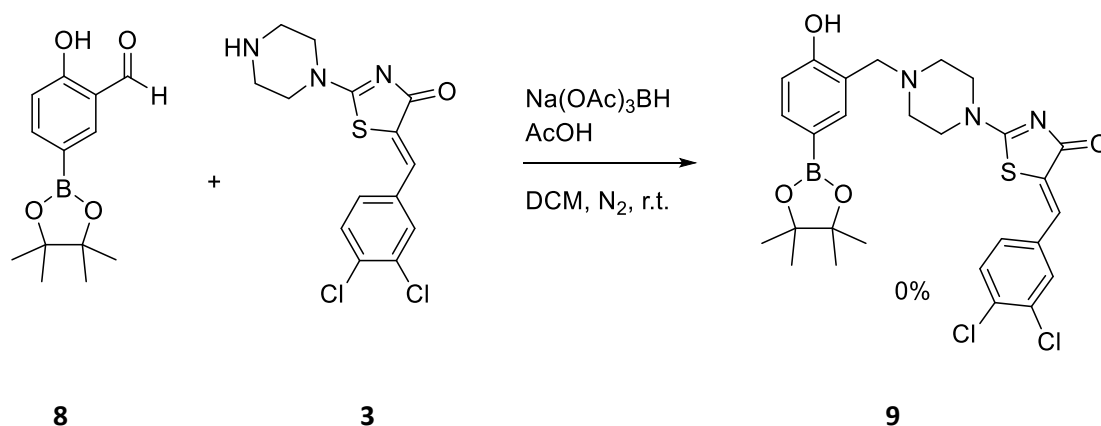
Scheme 18 - General reaction scheme for Table 4

Reagent (s)	Solvent / Conditions	Yield
HBr 48% aq.	Toluene, reflux	0%
PBr ₃	CHCl ₃ , r.t.	0%
Xtalfluor-E, 2,6 Lutidine, Tetrabutyl ammonium bromide ¹⁸⁹	DCM (anhydrous) Ar, r.t	0%

Table 4 - The attempted bromination reactions with 7

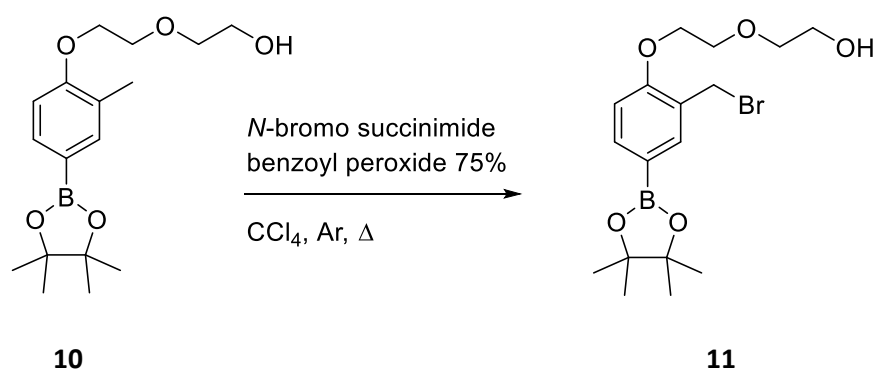
Disappointingly, the desired compound could not be synthesised, in all cases only unreacted starting material was collected. Alternative methods were then investigated. A synthetically

attractive reductive amination reaction between aldehyde **8** and Nagano's heterocycle **3** was attempted (Scheme 19) which had the potential to reduce the overall number of synthetic steps.



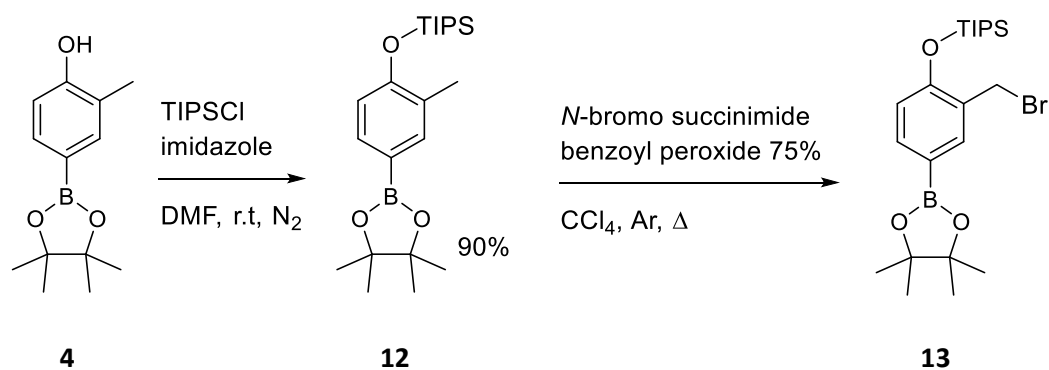
Scheme 19 - The attempted reductive amination between heterocycle **3** and aldehyde **8**¹⁹⁰

This reaction was unsuccessful, possibly due to the low solubility of Nagano's heterocycle in DCM. Attention was then turned back to the radical bromination reaction. A diethylene glycol linker version of phenol **4** was synthesised. Compound **10** was then exposed to radical bromination conditions (Scheme 20). The rationale behind this was two-fold: by converting the alcohol to an ether it may cause the substituent to become subtly less electron donating, encouraging desired radical bromination to occur. Secondly using the same linker that would otherwise be installed at a later stage in preference to another protecting group, such as a methoxy group, would reduce the total number of synthetic steps required.



Scheme 20 - Attempted radical bromination of **10**

Inspection of the crude material by ^1H NMR spectroscopy showed some indication of the formation of the desired product, indicated by the appearance of a methylene peak at 4.52 ppm. However, the material soon appeared to degrade (by ^1H NMR). Encouraged by these results, a TIPS-protected version of Compound **4** was synthesised, to give compound **12**, radical bromination was then attempted with this compound (Scheme 21).



*Scheme 21 - Attempted radical bromination reaction with Compound **12***

Analysis of the crude reaction mixture by ^1H NMR spectroscopy strongly suggested the formation of the desired compound by the appearance of a new methylene singlet at 4.61 ppm. Despite a reaction time of two days, only 50 % of the material had been converted to the halogenated species. Unfortunately, the mixture could not be purified by column chromatography. It can be speculated that the bulky TIPS group adjacent to the methyl group hinders the approach of the bromine radical, accounting for the poor conversion. One could easily envisage complete conversion to the brominated compound if a TMS protection group was used. However, this was not necessary, taking into account the change in reactivity observed by converting the phenol to an ether. Compound **12** was converted to an ester following treatment with acetic anhydride (Scheme 22).¹⁹¹ Esters are less electron donating than alcohol or ether groups so it was anticipated that radical bromination of acetate **14** would proceed in preference to aromatic bromination.¹⁶¹

The reaction conditions used resulted in a mixture of materials being returned, with little indication of the desired product. The likely cause of this was using 4 eq. of Cs_2CO_3 , as described in Nagano's paper, to remove the TFA salt *in situ* from the heterocycle, exposing the amine so that it could displace bromide in the substitution reaction.⁸⁸ Under these conditions the BPin group of compound **15** appeared to degrade, giving rise to a complex mixture. It was decided that the *N*-TFA salt of heterocycle **3** should be removed prior to the substitution reaction. Therefore only one equivalent of carbonate base would be required, conditions for which BPin groups are known to be tolerant.¹⁹² Several methods were found to generate the free amine, such as treatment of the heterocycle with a basic ion exchange resin (Amberlyst® A21) in DCM.¹⁹³ The most suitable method, applicable on multigram scales, was to make a basic aqueous solution of heterocycle **3** basic with sodium carbonate and then use continuous liquid-liquid extraction in CHCl_3 to isolate the desired heterocycle **17**. The difficulty in isolating the free amine was compounded by its poor solubility in low-boiling point organic solvents. An X-ray crystal structure was obtained for the free-amine heterocycle **17**, confirming the *Z*-geometry about the double bond (Figure 30).

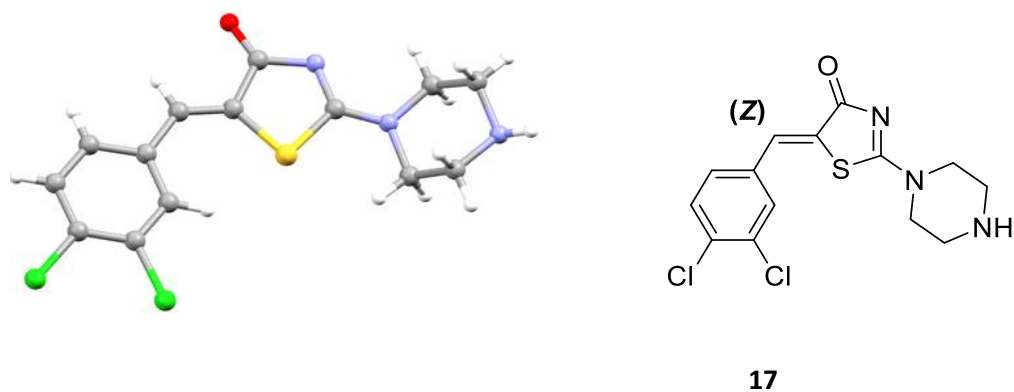
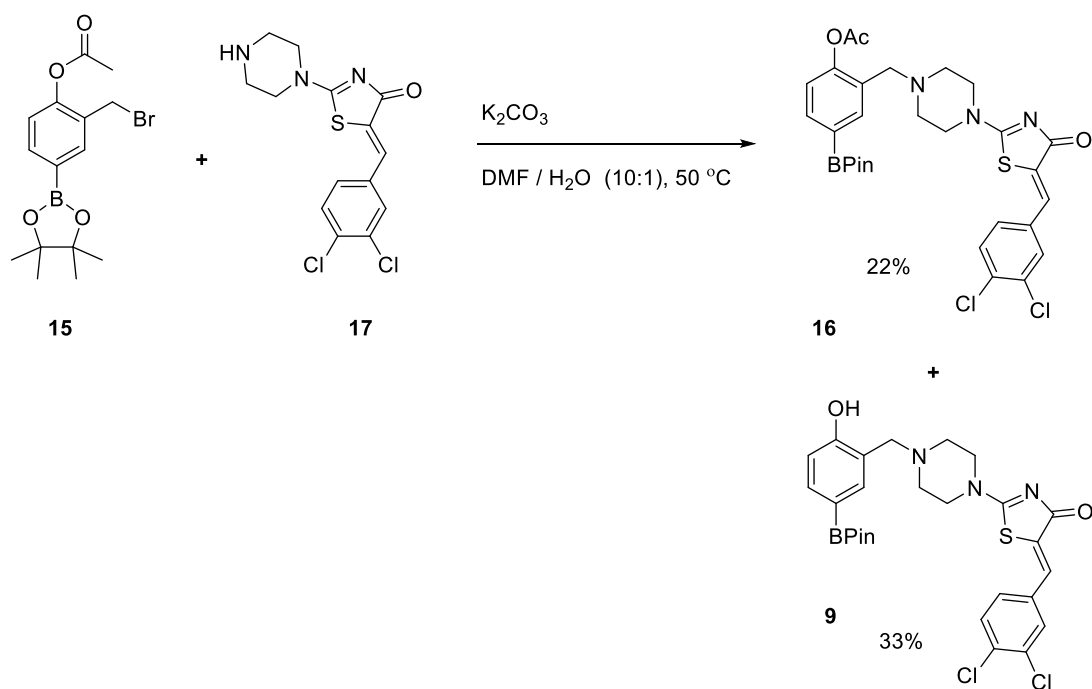


Figure 30 - X-ray crystal structure of free amine **17**

Bromide **15** was then reacted with piperazine **17**, using slightly modified reaction conditions to those used previously (Scheme 24).



Scheme 24 – S_N2 coupling reaction between piperazine **17** and bromide **15**¹⁹²

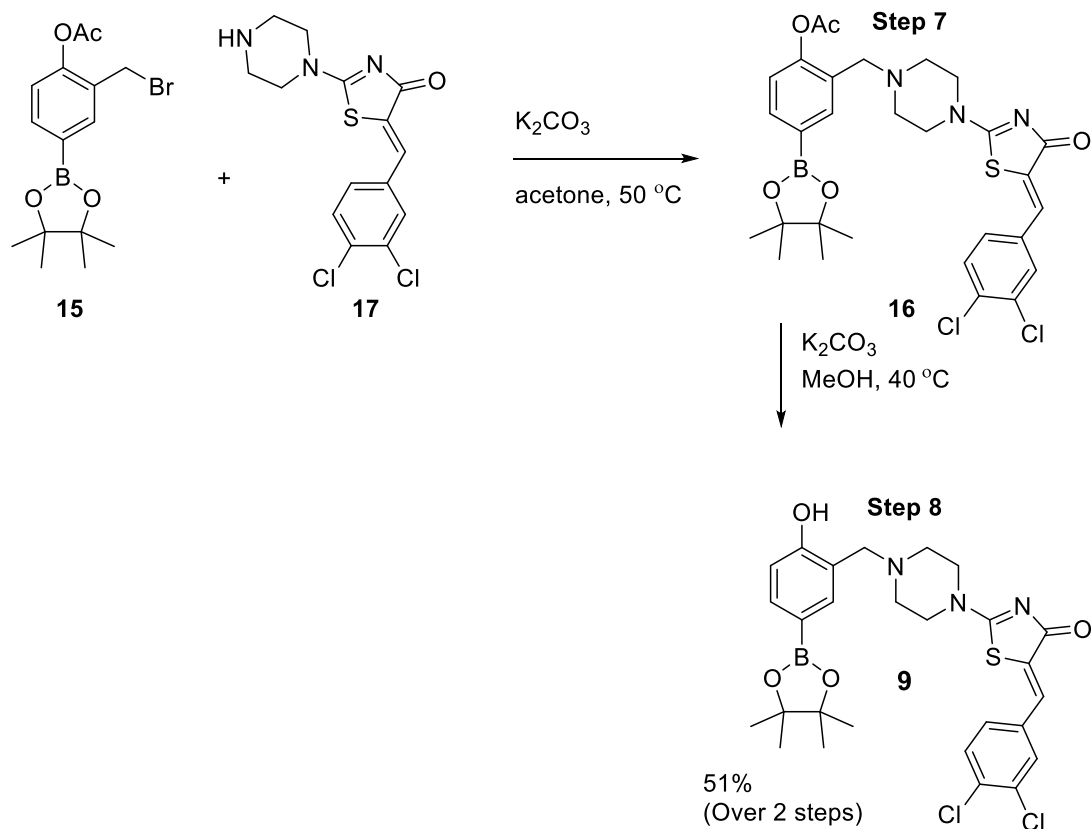
The reaction resulted in an overall conversion of approx. 60% (as measured by ^1H NMR spectroscopy on the crude material). Under the conditions described, the acetate group also underwent hydrolysis to expose the phenol. Whilst this was not undesirable in principle, considering that acetate hydrolysis would be the next synthetic step, both compounds closely eluted with one another. This made them difficult to purify by column chromatography. Additionally, this method did not favour the transition to a larger scale, with a decrease in yield being observed. Attempts were made to completely deacetylate acetate **16** after the substitution reaction *in situ*, however this was unsuccessful.

A suitable method was found for acetyl deprotection that was sufficiently mild to maintain the integrity of the BPin ring, as summarised in Table 5.

Conditions:	Comment:
NaOAc H ₂ O / EtOH, reflux ¹⁹⁴	Partial hydrolysis resulting in a complex mixture
NaHCO ₃ H ₂ O / MeOH, N ₂ , r.t ¹⁹⁴	No reaction
2M NaOH aq. EtOH, r.t ¹⁹⁴	Caused the hydrolysis of the boronate ester, with no deacetylation observed
K ₂ CO ₃ DMF / H ₂ O, 50 °C	Compound degraded, no deacetylation observed
K ₂ CO ₃ (0.1 eq.) MeOH, 40 °C	Quantitative deacetylation

*Table 5 - Different reaction conditions explored in the deacetylation of acetate **16***

Deacetylation of acetate **16** was effected in the presence of K₂CO₃ (0.1 eq.) and MeOH, without any hydrolysis of the BPin group. With deacetylation conditions in hand, attention turned back to the S_N2 coupling reaction. The solvent was changed to acetone from DMF / H₂O, which resulted in formation of mostly the acetate **16**, with only around 5-10 % of the deprotected form (**9**) being produced. The mixture was then exposed to the deacetylation conditions previously established (Scheme 25).

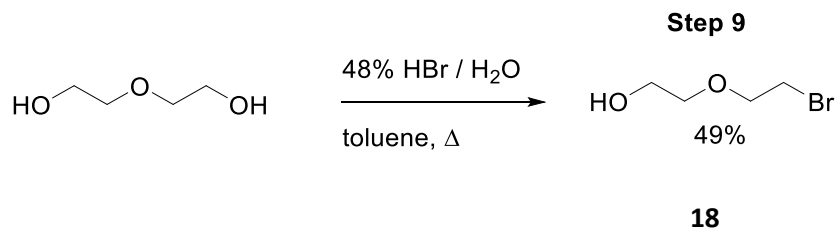


Scheme 25 - Final version of the S_N2 coupling reaction and subsequent deacetylation

The method shown in Scheme 25 was used to produce phenol **9** in multi gram quantities, our attention then turned to the attachment of the diethylene glycol linker.

2.1.4 Attachment of the linker to phenol **9**

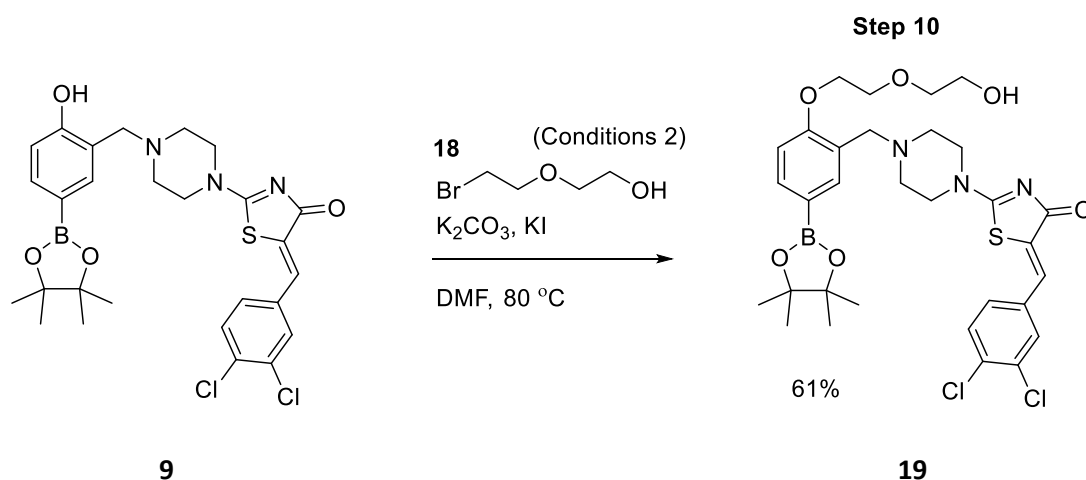
Ether **18** was synthesised by the treatment of diethylene glycol with hydrobromic acid (aq.) in toluene, under Dean-Stark conditions (Scheme 26).



*Scheme 26 – Synthesis of ether **18***

It was found that, due to stability issues, it was essential to synthesise ether **18** and use it directly in subsequent reactions. Substituting ether **18** for the commercially available (and shelf stable) chloro-analogue led to negligible yields in the linker addition reaction; interestingly with other drug compounds (Chapter 2.4) the chloro ether gave yields of up to 95 %.

Using a method described by Maccarrone and co-workers phenol **9** was reacted with ether **18** through an *in situ* Finkelstein reaction with KI (Conditions 1), these were then modified to facilitate the synthesis of ether **19** (Conditions 2) (Scheme 27).¹⁹⁵



Scheme 27 – Attempted linker addition reaction between phenol **9** and ether **18** (Conditions 1: KOH, KI, MeCN, 60 °C, 0 %)

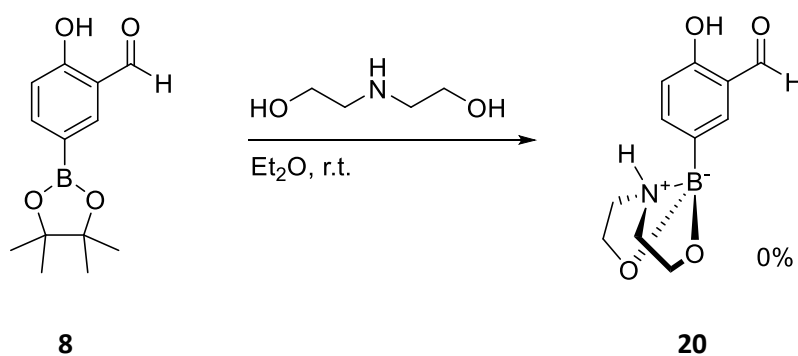
Conditions 1 were found to be too harsh (KOH) and heterocycle **9** had low solubility in acetonitrile, resulting in the need to use conditions 2. Conditions 2 (Scheme 27) resulted in the successful synthesis of ether **19**, in reasonable yield.

2.1.5 The conversion of ether **19** to a boronic acid

As per the synthetic route originally proposed, at this stage ether **19** would be attached to icodextrin (using the “tosylated-icodextrin” approach), then as the final step, the boronate ester would be converted to a boronic acid. However, to ensure that this proposition was feasible, ether **19** would be converted to a boronic acid in a test reaction and to obtain a complete data set, confirming the presence of a boronic acid functional group. Once ether

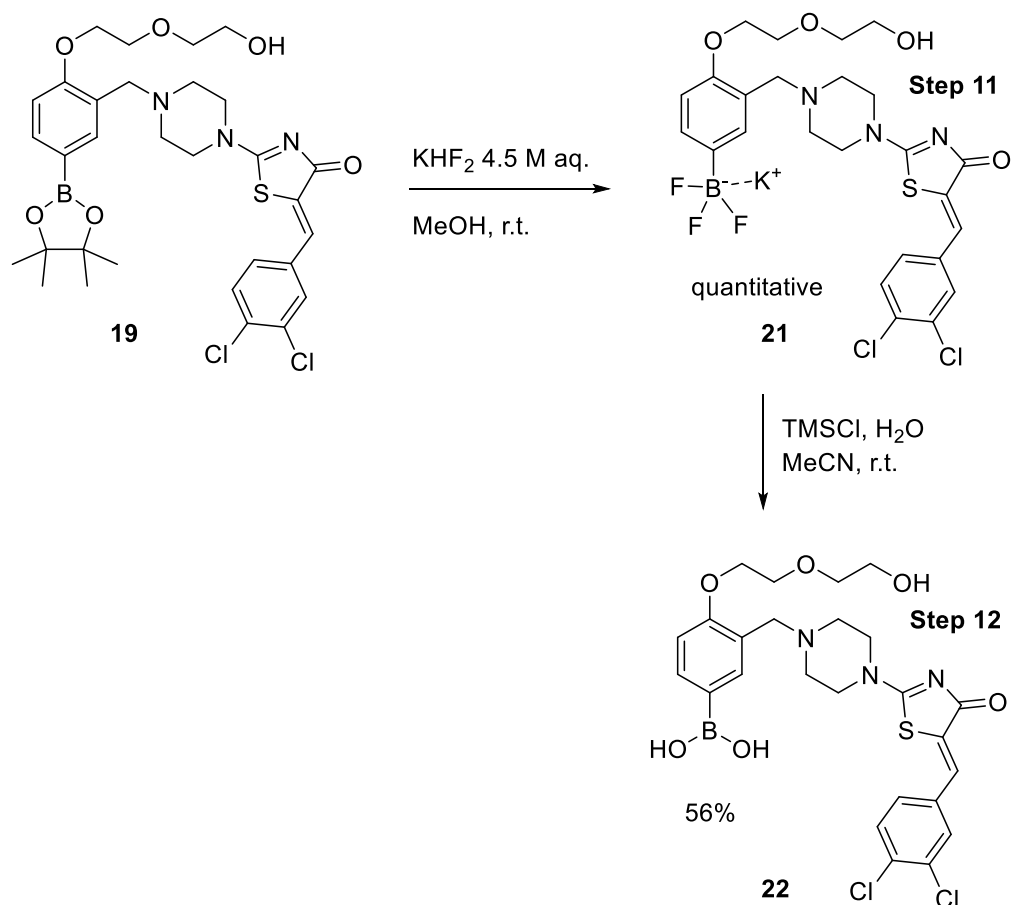
19 was attached to IDX there would be few analytical techniques for analysing the resulting conjugate; following deprotection of the boronate ester the key piece of evidence would be the loss of the distinctive (BPin) 12 H singlet in the ^1H NMR spectrum. The data from the boronic acid version of **19**, the ^1H NMR spectrum of the final conjugate (showing the loss of the distinctive BPin singlet) and high potency *in vitro* of the conjugate would serve as evidence that the boronate ester had been successfully converted to a boronic acid.

Using a method devised by Sun and co-workers, a test reaction was attempted with aldehyde **8** to convert the BPin group to a sp^3 -hybridized boron · DEA adduct, which can then be hydrolysed to a boronic acid in the presence of dilute HCl aq. (Scheme 28).¹⁷⁶



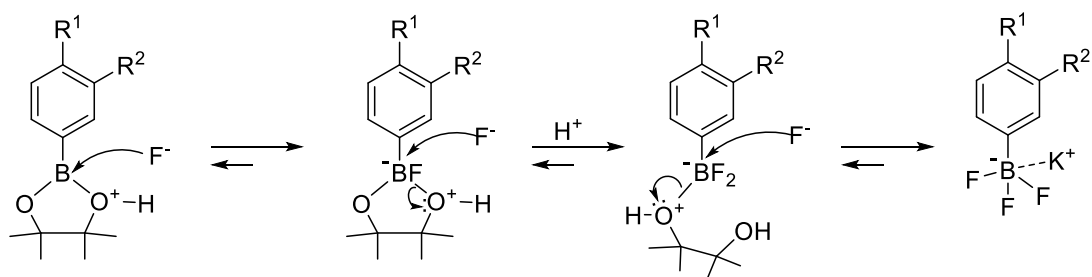
*Scheme 28 - Attempted synthesis of a sp^3 -hybridized boron · DEA adduct of aldehyde **8***

The test reaction was unsuccessful. An alternative method was then explored in which the boronate ester was first converted to the corresponding trifluoroborate salt, which was then successfully hydrolysed to the boronic acid.^{178,196,197} These conditions were then applied to ether **19**.



Scheme 29 - The conversion of ether **19** to BF_3K salt **21** and the subsequent hydrolysis to boronic acid **22**

Trifluoroborate **21** was produced in a quantitative yield, with minimal purification being necessary (Scheme 29). The reaction is reversible although favouring the BF_3K salt (Mechanism 2). Methodology developed by Aggarwal and co-workers was applied to the isolation of trifluoroborate **21**; thus the pinacol by-product was removed by azeotropic distillation using $\text{MeOH} / \text{H}_2\text{O}$ as an evaporation partner, to drive the reaction to completion.¹⁹⁷



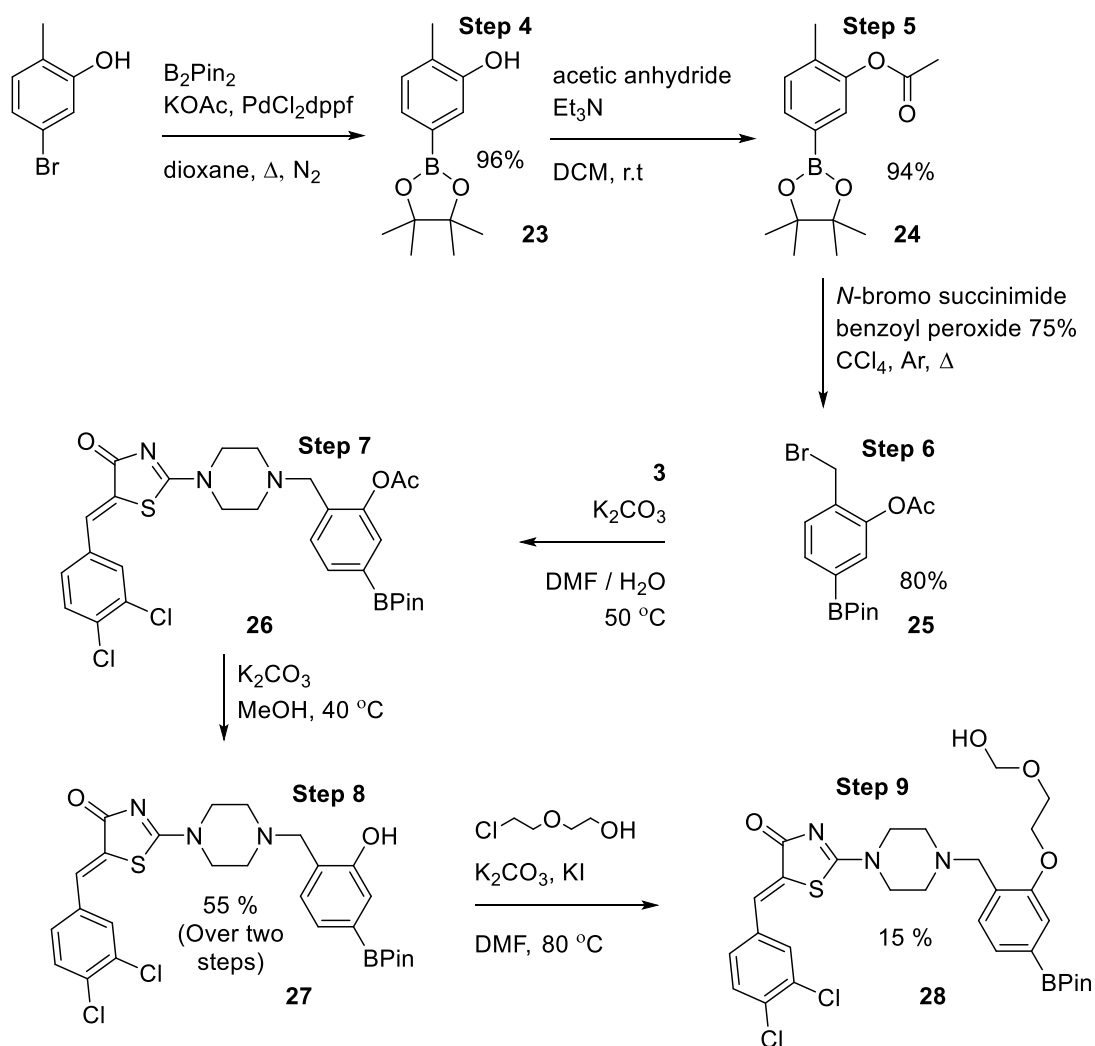
Mechanism 2 – Suggested mechanism for the conversion of ester **19** into BF_3K salt **21**

Trifluoroborate **21** was then hydrolysed in MeCN in the presence of trimethylsilyl chloride and H₂O to give the corresponding boronic acid **22** (Scheme 29). The resulting boronic acid **22** was produced in acceptable yield, with minimal purification being necessary. This study demonstrated that ether **19** could be converted to boronic acid **22** and indicating, in principle, that such a transformation would be possible with the polymer conjugate.

2.1.6 Synthesis of 3-BoA linker, summary

The complete synthetic route for boronic acid **22** has an overall percentage yield of 16.1 % and employed 12 synthetic steps, with the longest linear sequence being 8 steps. Our attention then turned to the preparation of 4BoA linker analogue.

With a viable synthetic route to synthesise drug-linker analogues now established, the same methodology was applied to the 4BoA linker compound. Boronate ester fragment **25** was first synthesised, then reacted with heterocycle **3** (Scheme 30). Acetate **26** was then converted to phenol **27** and then reacted with 2-(2-chloroethoxy) ethanol in the presence of KI, to give the corresponding ether **28**.



Scheme 30 - The synthesis of 4 BoA linker 28

The yield of ether **28** was disappointingly low, but based on experience from the synthesis of ether **19**, it can be speculated that had 2-(2-bromoethoxy)ethanol (ether **18**) been used, the yield would have been much higher. Consequently, the overall yield for ether **28** was 6 %, employing nine synthetic steps, with the longest linear sequence being six steps.

2.2 The attempted preparation of a 3-BoA-Icodextrin conjugate using the “tosylated IDX method”

With the boronate ester derivative of 4BoA-linker now complete, work could begin on the attachment of drug-linker compounds to Icodextrin. Using a stock of tosylated IDX (Figure 31) small-scale drug-IDX couplings were then attempted.

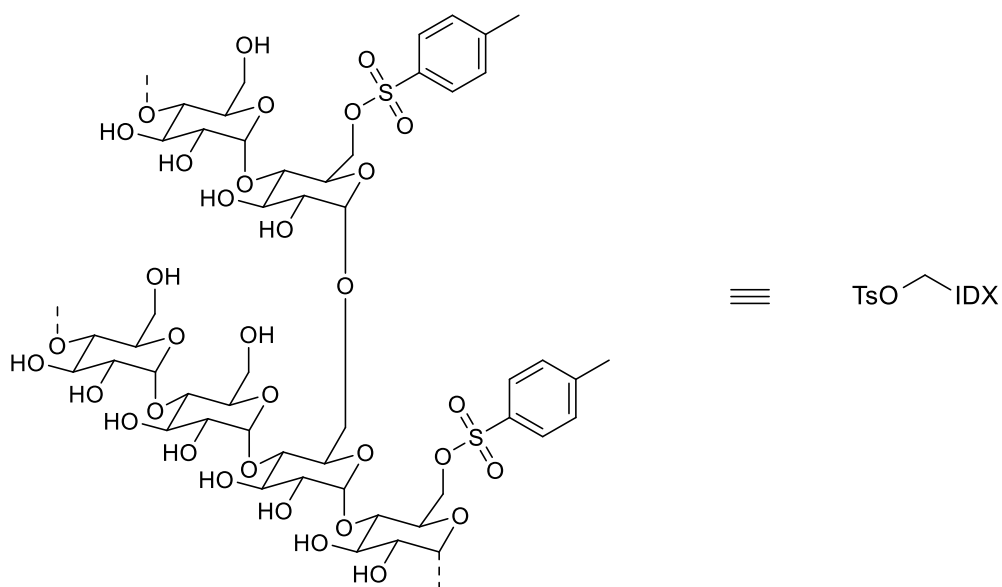
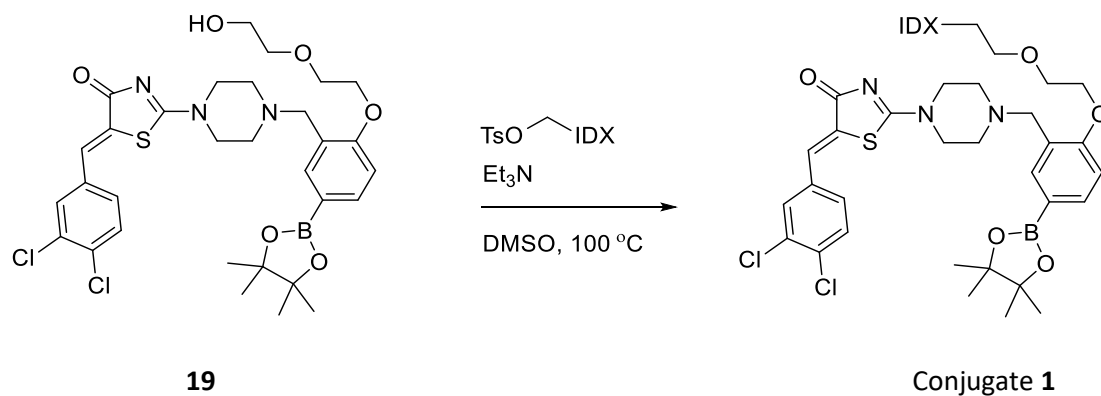


Figure 31 - Representation of tosylated Icodextrin

The boronate ester version of 3BoA-linker **19** was reacted with tosylated Icodextrin (Scheme 31).



Scheme 31 - The coupling of ether **19** with IDX to give Conjugate **1**

After the reaction mixture was heated at 100 °C for two days, the crude mixture was purified by dialysis. In a relatively simple procedure, the material was transferred to a dialysis membrane and then submerged in a volume of water / methanol of around 100 times greater than the membrane contents. Molecules smaller than the molecular weight cut off value (MWCO) of the membrane (typically 8 kDa), will move through the membrane and into the solvent by diffusion. The dialysis fluid is then changed regularly (> 10 times) to ensure that only the polymeric material is retained, by virtue of its high molecular weight.

The results of this first conjugation reaction were disappointing, although there was some evidence (by ^1H NMR spectroscopy) to suggest that the reaction was successful. This was indicated by the incorporation of material relating to ether **19** within the ^1H NMR spectrum of Conjugate **1** (Figure 32). Despite this, the aromatic region was noticeably different, suggesting a loss of structural integrity of the molecule.

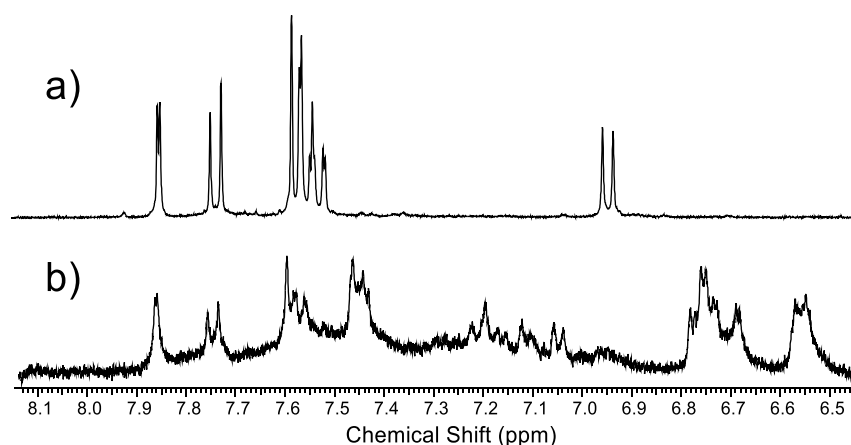
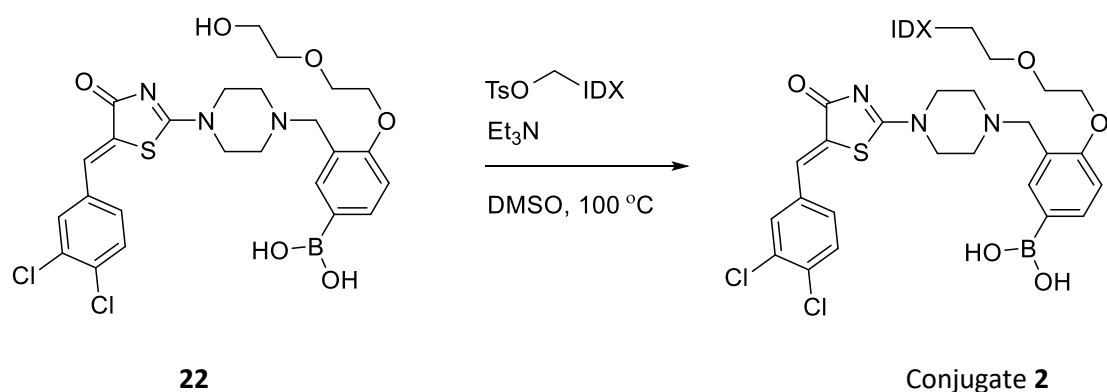


Figure 32 – ^1H NMR spectra comparison (400 MHz, DMSO-d_6) a) the aromatic region of **19** and b) the aromatic region of Conjugate **1**

Due to the high level of derivatisation observed for Conjugate **1**, an alternative approach was investigated. An attempt was made to directly conjugate boronic acid **22** to IDX (Scheme 32).

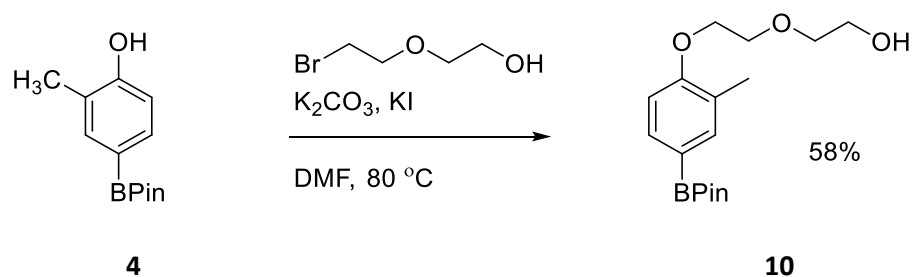


Scheme 32 - Attempted synthesis of Conjugate 2

After dialysis, the reaction returned tosylated IDX without any drug attachment being observed. The reaction conditions were then modified, increasing the number of equivalents of boronic acid **22** from 1.3 eq. to 1.7 eq. (relative to 1 eq. of the polysaccharide, determined by the equivalent molecular weight of the monosaccharide) although this was found to have no improvement.

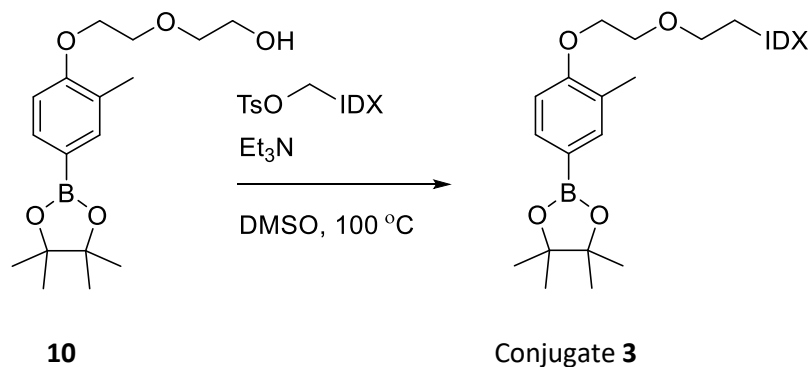
2.2.1 Tosylated icodextrin approach, model study

Due to the discouraging results seen with Conjugate **1** and **2** a “model study” was then conducted, using a model of the drug molecule, ether **10**. Which could be synthesised quickly and on a larger scale (Scheme 33). This was done in order to evaluate the feasibility of attachment by this method and potentially optimise the reaction conditions.



Scheme 33 - Synthesis of 10

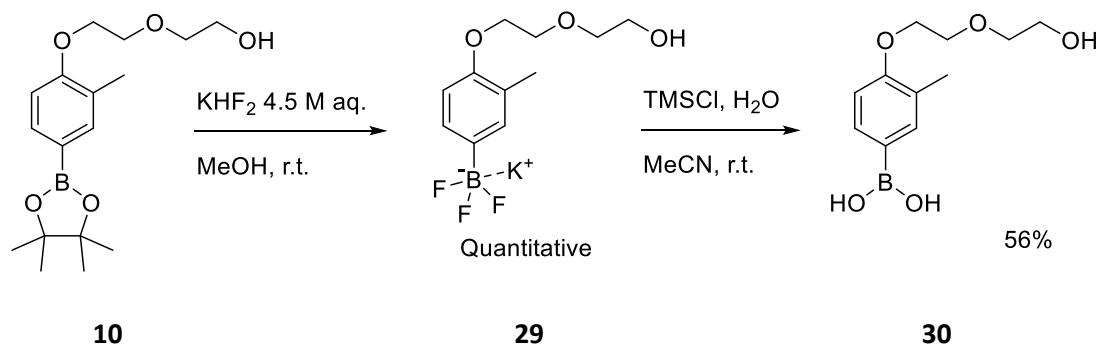
Alcohol **10** was then reacted with tosylated IDX in the same manner as Conjugate **1** and **2** (Scheme 34).



Scheme 34 - Attempted synthesis of Conjugate **3**

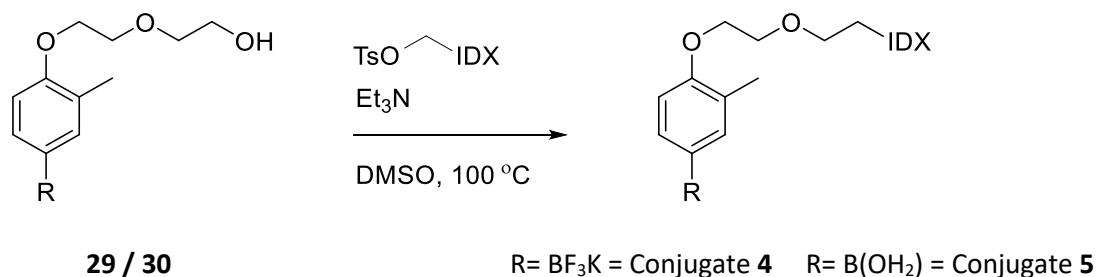
Inspection of the ^1H NMR spectrum of the material, after dialysis indicated that the model drug **10** had not been attached. The reaction was repeated at a lower temperature ($75\text{ }^\circ\text{C}$), known not to cause the molecule to degrade and separately, over a longer reaction time (three days). Both modifications had no effect on the stated outcome.

The effect of changing the BPin group of the alcohol **10** for either a trifluoroborate salt or a boronic acid group was also investigated. Alcohol **10** was converted to BF_3K salt **29**, a portion of which was hydrolysed to the corresponding boronic acid **30** (Scheme 35).



Scheme 35 - Synthesis of BF_3K salt **29** and boronic acid **30**

The two compounds were then reacted (separately) with tosylated IDX, in the same manner as previously stated (Scheme 36).

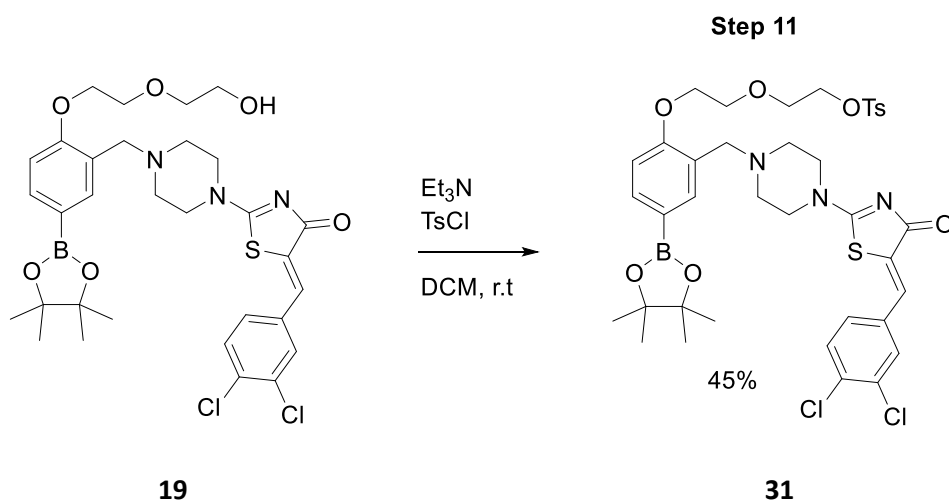


Scheme 36 - Attempted synthesis of Conjugate 4 and 5

After dialysis the isolated product compounds were analysed using ¹H NMR spectroscopy. Both reactions were unsuccessful, so at this stage it was decided that the tosylated IDX conjugation method would not be explored further. Instead, the “tosylated drug” approach would be used from hereon in.

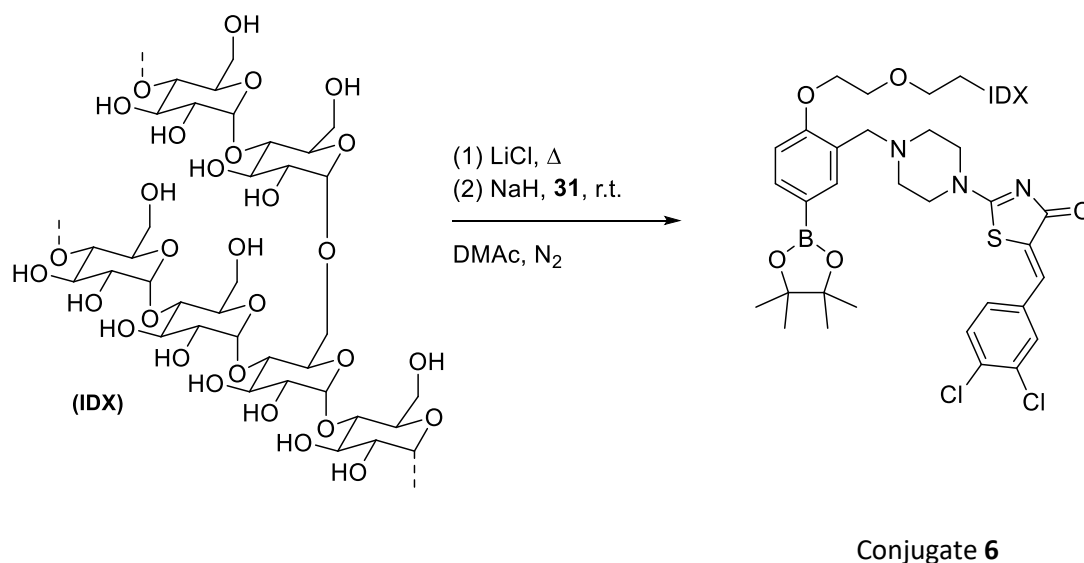
2.2.2 The attempted preparation of a 3-BoA-Icodextrin conjugate, using the “tosylated drug method”

In our previous work the “tosylated drug method” was extensively used, but as explained, the “tosylated IDX method” was initially preferred for this work due to it using milder reaction conditions. A tosylated version of ether **19** was therefore synthesised, by reacting ether **19** with tosyl chloride in the presence of triethylamine (Scheme 37).



Scheme 37 - Synthesis of tosylate 31

Using the same conjugation methodology applied in our previous work, an attempt was made to attach tosylate **31** to IDX (Scheme 38). Icodextrin was first solubilised in (anhydrous) dimethylacetamide (DMAc) / LiCl co-solvent system at 160 °C. LiCl is used to disrupt the extensive hydrogen bonding network that is established within IDX, increasing its solubility and accessibility towards reactants. Solubilised IDX was then treated with NaH (60% mineral oil dispersion), to generate an alkoxide on IDX, which then displaces the tosyl group on the drug-linker compound, yielding a drug-IDX conjugate.



*Scheme 38 - Attempted conjugation reaction between IDX and tosylate **31***

After stirring the reaction mixture for 16 hours at room temperature, the mixture was dialysed and then analysed by ¹H NMR spectroscopy. Unfortunately, no conjugation product was observed. The reaction time was increased to 10 days, which led to a small amount of material being incorporated onto the polymer, as indicated by the ¹H NMR spectrum shown (Figure 33).

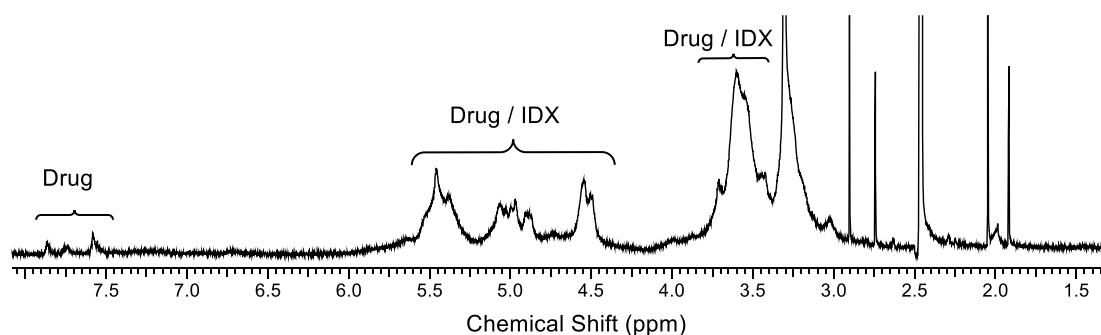
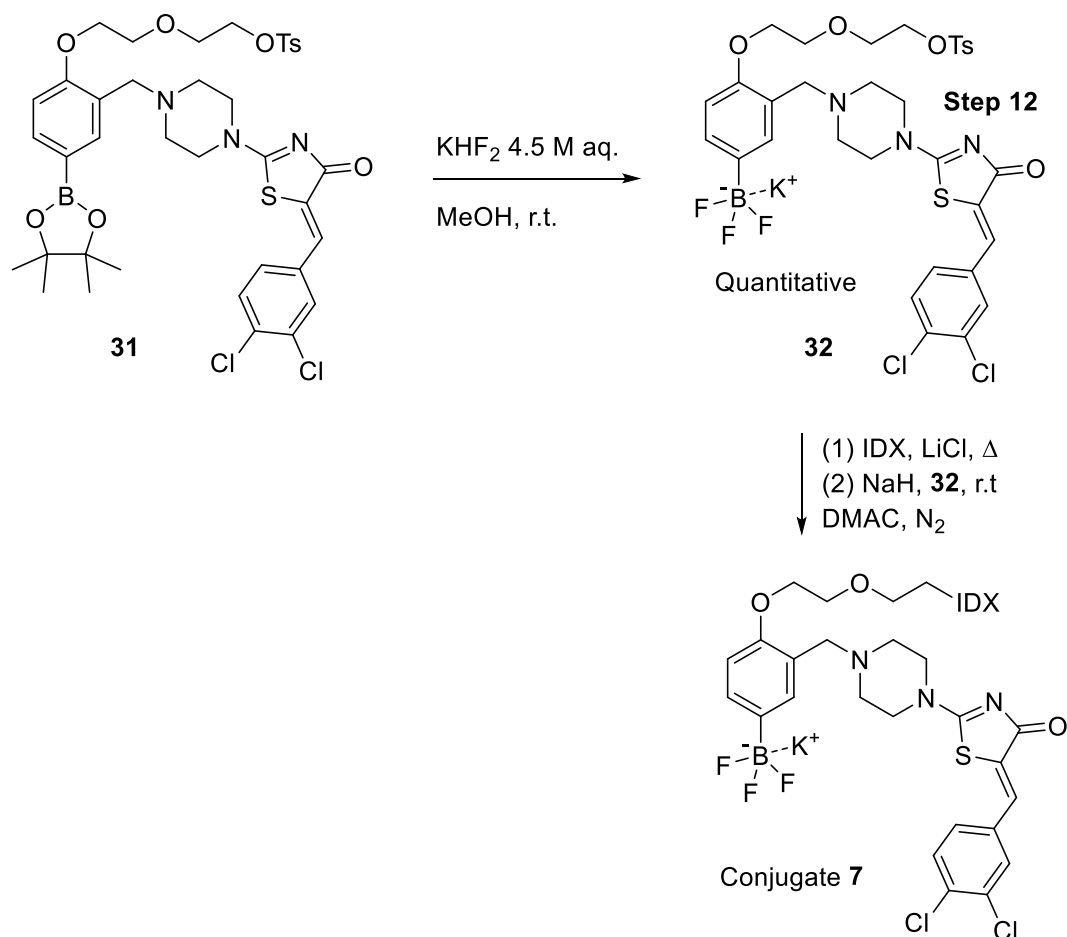


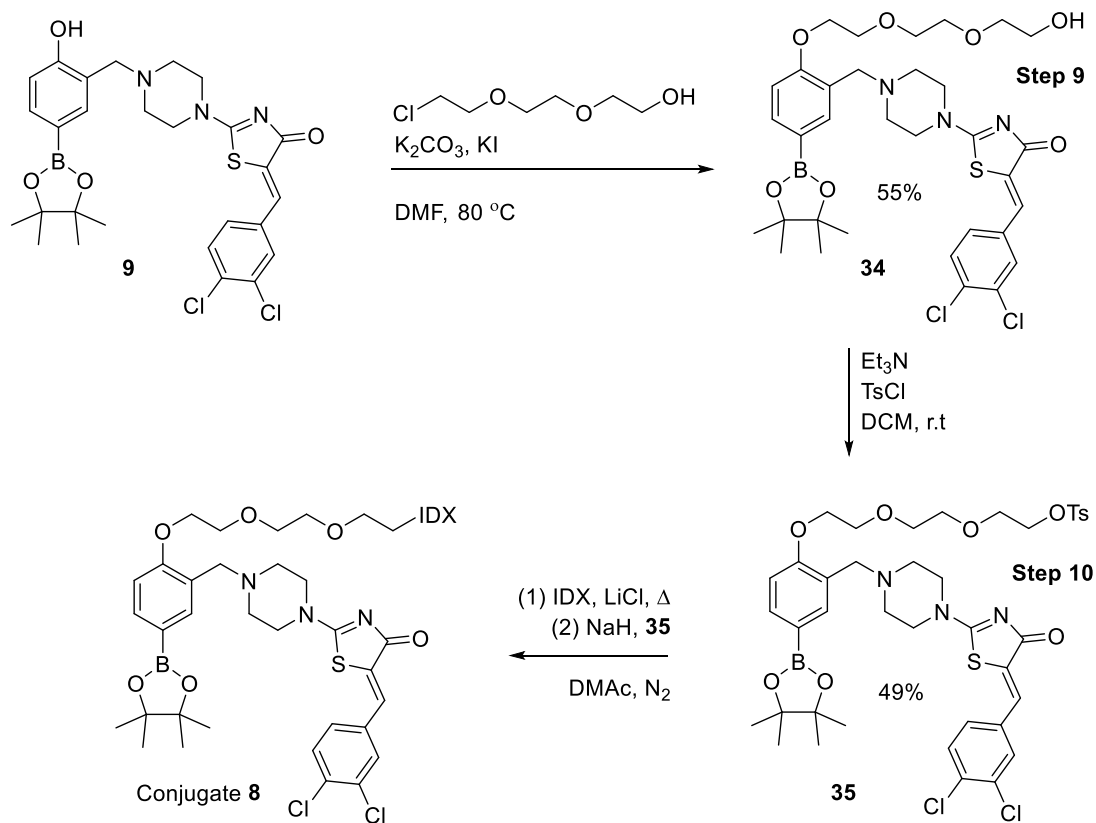
*Figure 33 - The ¹H NMR spectra of Conjugate **6** (400 MHz, DMSO-d₆)*

As can be seen in Figure 33, only a very small amount of material was added to IDX, estimated (by the relative integration of drug and IDX peaks) to be 1 in 30 monomeric units that incorporated drug material. This was felt to be an unacceptably low level of drug loading to have therapeutic benefit, especially considering the length of time needed to synthesise the conjugate. Instead, an alternative route was evaluated, whereby boronate ester **31** was converted to BF_3K salt **32**, then reacted with IDX (Scheme 39).



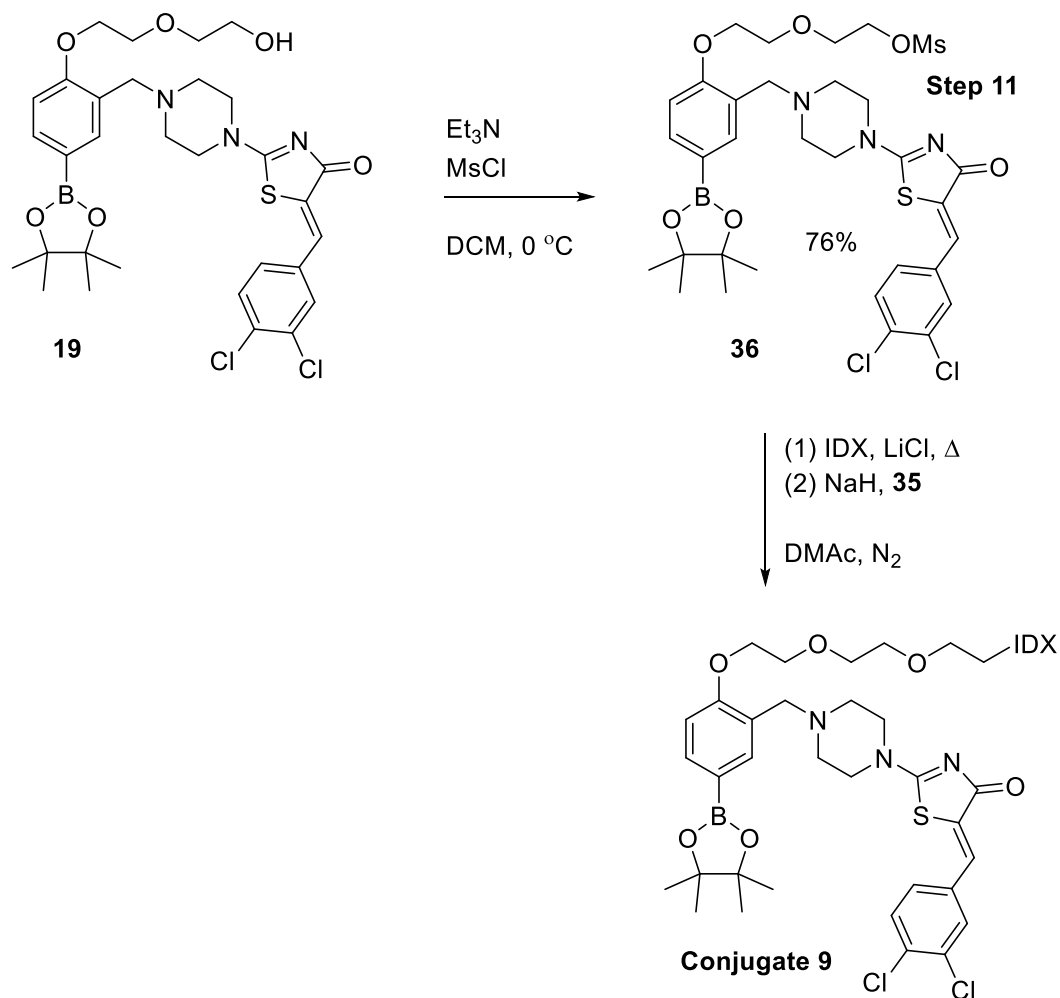
*Scheme 39 - Conversion of boronate **31** to BF_3K salt **32**, and subsequent reaction with IDX*

Unfortunately, no attachment of trifluoroborate salt **32** to IDX was observed by ^1H NMR spectroscopy, and so the synthesis of a boronic acid version of BF_3K salt **32** was attempted (Scheme 40).



Scheme 41 – Attempted synthesis of Conjugate 8

After reacting for two days, the material was dialysed and analysed by ^1H NMR spectroscopy. Unfortunately no conjugation was observed. It was then decided to investigate the effect of the leaving group size /ability on the degree of conjugation observed. Mesylate **36** was synthesised by reacting ether **19** with methanesulfonyl chloride and triethylamine and then reacted with icodextrin (Scheme 42).



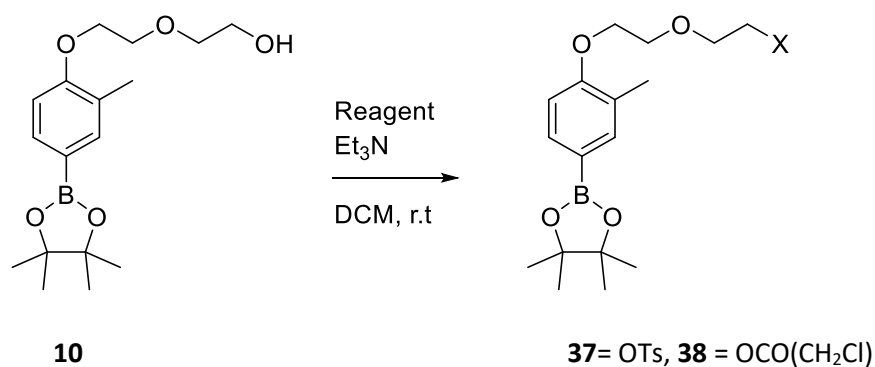
Scheme 42 - The mesylation of ether **19** and its subsequent reaction with IDX

Unfortunately, no conjugation was observed, despite a reaction time of 5 days, which in consideration of Conjugate **6**, one would have expected to see at least an equal amount of drug incorporation, as it is said that the leaving group ability of mesylates and tosylates are similar.¹⁶¹

The reaction conditions for the “tosylated drug” method were then changed to include one equivalent of NaI. It was hoped that the tosylate **31** would give an iodide species *in situ*, which would then be displaced by IDX. The new method was trialed and allowed to react for 5 days, however there was no improvement compared to Conjugate **6**.

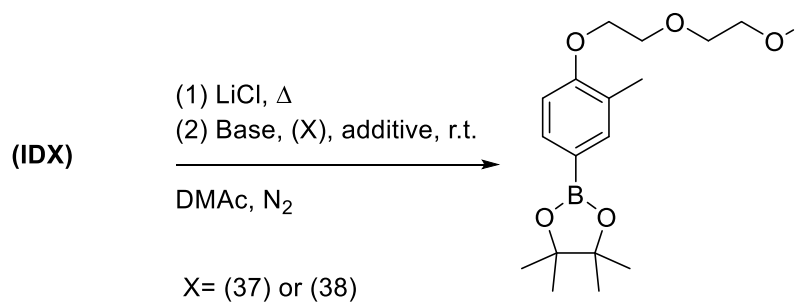
2.2.4 Tosylated drug approach, model drug study

At this stage a number of “model drug” studies were conducted, to attempt to find a method suitable for the attachment of boronate esters to IDX, by varying the base, leaving group and reaction conditions. To facilitate this, two “model drugs” were prepared (Scheme 43).



*Scheme 43 – General scheme for the synthesis of tosylate **37**, in the presence of TsCl and chloroacetate **38**, in the presence of chloroacetyl chloride*

The “model drugs” were then used in various test reactions, based on the generic reaction (Scheme 44), the results of which are listed in Table 6.



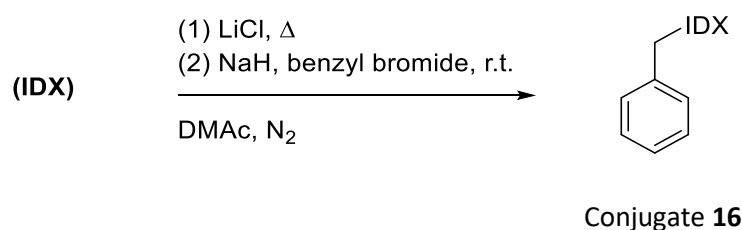
Scheme 44 - Generic reaction scheme for the test reactions

Name (Conjugate)	Leaving group	Reagents	Comment	Result
10	OTs (37)	NaH		No conjugation observed
11	OTs (37)	NaH, 15-Crown 5	15-Crown 5 coordinates to the Na counter ion, preventing ion-pairing to give a “naked” IDX anion (better nucleophile)	No conjugation observed
12	OTs (37)	KH	KH is a stronger base than NaH, more likely to generate the anion	No conjugation observed
13	OTs (37)	KH, 18-Crown 6	18-Crown 6 coordinates to K counter ion, preventing ion-pairing to give a “naked” IDX anion (better nucleophile)	No conjugation observed
14	OTs (37)	BTPP (P1-t-Bu- tris(tetramethylene)	Uses a phosphazene “super base”, $PK_{BH^+} = 28.4$, containing no counterion, therefore IDX anion will be a better nucleophile ^{198,199}	No conjugation observed
15	Cl (38)	DMAP, Pyridine	Mild reaction conditions, literature precedent for coupling to occur with non-polymeric systems	No conjugation observed

Table 6 – A table to summarise the results of the test reactions attempted

Despite a number of different approaches being taken, conjugation did not occur in any of the test reactions and considering the number of attempts made up to this point, this was of concern.

Working on the hypothesis that, compared to the carboxylic acid drug used in our previous work, the presence of the boronate ester and related functionality was causing an inherent loss in reactivity within the conjugation reaction. A simple test substrate was used in place of tosylate **37**. IDX was reacted with benzyl bromide using the exact same procedure as before (Scheme 45). The benzylation of sugars is widely known, so it would be almost certainly expected for IDX to be successfully benzylation. This was also an effective way to remove any doubt in the experimental rigour of the previous conjugation reactions, regarding our air sensitive-techniques.



Scheme 45 - The benzylation of Icodextrin

After leaving the reaction for two days, the mixture was dialysed, then precipitated in acetone. The resulting solid was collected by vacuum filtration and analysed by ^1H NMR spectroscopy. The spectrum for Conjugate **16** strongly suggested the successful benzylation of Icodextrin had been achieved, as shown in Figure 34.

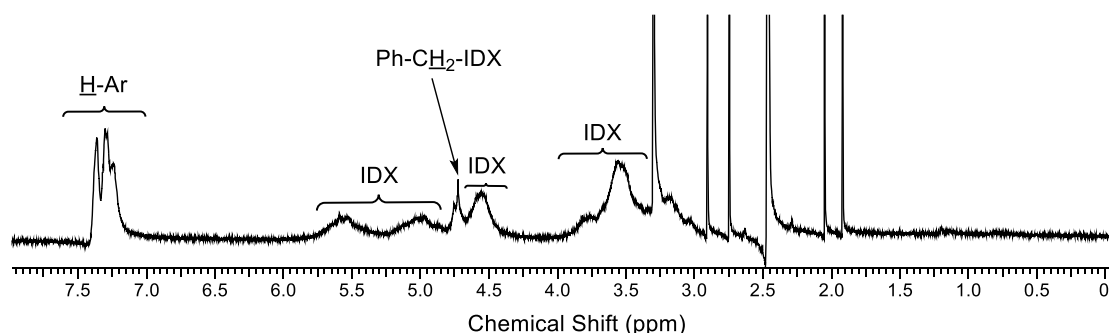


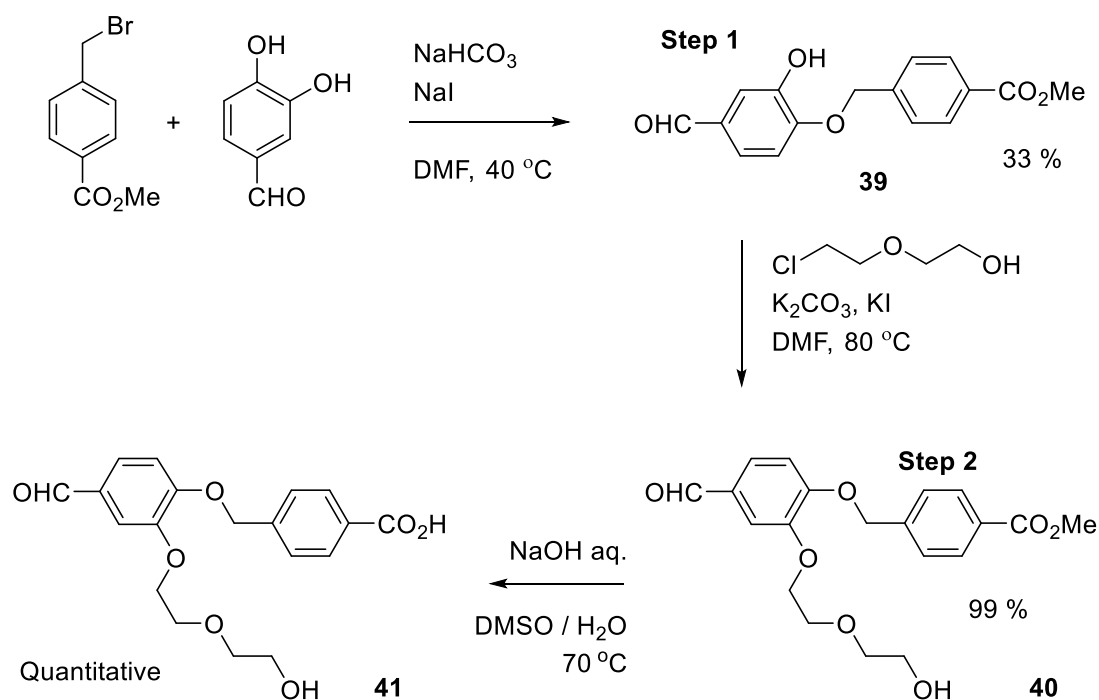
*Figure 34 - The ^1H NMR spectrum of Conjugate **16** (400 MHz, DMSO- d_6)*

The successful benzylation of IDX should be taken as a proof-in-principle of the efficacy of the conjugation methodology. Additionally, the positive result does suggest that boron functionality has some retarding effect on the attachment of the substrates previously investigated (Conjugates **1-15**). To that end, no further attempts were made to attach analogues of Nagano's BoA series to IDX. This decision was taken because of the significant amount of time already devoted to their synthesis with little progress. It was felt that the remaining time would be better spent working on a different drug series, to complement the study and to increase the chance of producing drug-IDX conjugates for biological evaluation.

2.3 Re-synthesis of HA155 analogue **45**

Despite the successful benzylation of IDX Conjugate **16**, there was some concern with work undertaken by a previous student regarding the attachment of an ATX inhibitor containing a carboxylic acid group to IDX, as featured in Chapter 1. On review, it became apparent that several key pieces of data were incomplete or missing, which considering the significance that it had on the foundation of this current work, was worthy of re-investigation. Work therefore began with the resynthesis of the drug-linker compound.

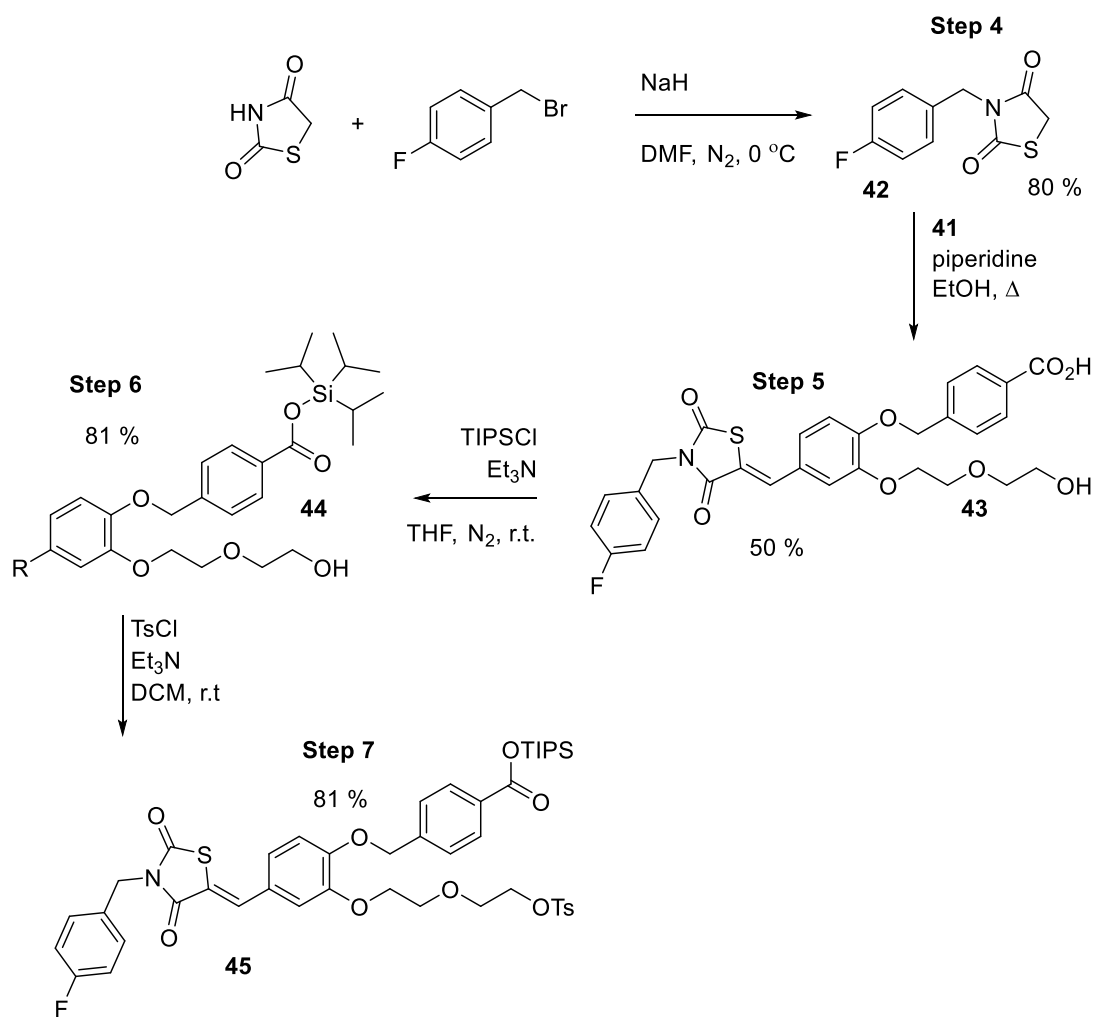
The first part of the synthetic route was to prepare the linker fragment, and this was achieved in three steps. Firstly 3,4-dihydroxybenzaldehyde was regioselectively alkylated with methyl-4-(bromomethyl)-benzoate at the *para* hydroxy position *via* an S_N2 displacement, using a method described by Plourde and co-workers (Scheme 46).²⁰⁰ Ester **39** was then reacted with 2-(2-chloroethoxy) ethanol and the corresponding ether **40** was hydrolysed in the presence of sodium hydroxide to a carboxylic acid.



Scheme 46- Synthesis of carboxylic acid **41**

The regioselectivity observed in this reaction can be rationalized since the aldehyde group, being electron withdrawing, causes the proton of the hydroxyl group *para* to the aldehyde to be more acidic, since the resulting conjugate base is stabilised by resonance through to the aldehyde group. Deprotonation of the alternative OH group cannot lead to this resonance stabilisation.

With carboxylic acid **41** in hand, heterocycle **42** was synthesised in one step by reacting 4-fluorobenzyl bromide with thiazolidine-2,4-dione, in the presence of sodium hydride (Scheme 47). Heterocycle **42** was then reacted carboxylic acid **41**, *via* a Knoevenagel condensation. Carboxylic acid **43** was then protected using triisopropylsilyl chloride and silane **44** reacted with tosyl chloride.

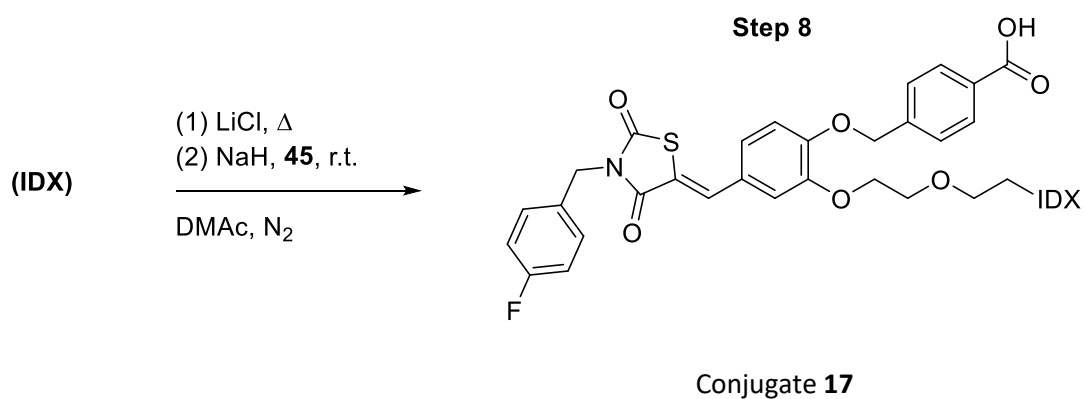


Scheme 47 - The synthesis of heterocycle **45**

Carboxylic acid **43** was protected with TIPS Cl to ensure the carboxylic acid group did not react with IDX in the conjugation reaction (step 8).

2.3.1 Conjugation of **45** to IDX (Conjugate **17**)

Compound **45** was synthesised in 7 steps, with the longest linear sequence being 6 steps, with an overall yield of 8 %. Using the resulting drug-linker compound **45**, a conjugation reaction with IDX was attempted, with the same reaction conditions utilised previously in this study (Scheme 48).



Scheme 48 – Conjugation of heterocycle 45 to IDX

After dialysis, the product was analysed by ^1H NMR spectroscopy (Figure 35), the resulting spectra showed the incorporation of drug material on to IDX, which was comparable to that obtained by the previous student. Additionally, in agreement with our previous findings, the TIPS protection group had been removed during the course of the reaction. This was evidenced by the disappearance of peaks corresponding to the TIPS group in the ^1H NMR spectrum, so the conjugate required no further modification.

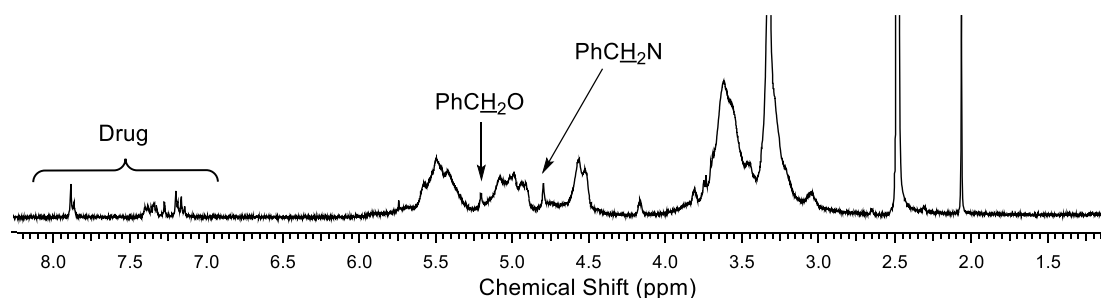


Figure 35 - The ^1H NMR spectrum of Conjugate 17 (400 MHz, DMSO- d_6)

Repeating the synthesis of Conjugate **17** showed that carboxylic acid-based ATX inhibitors could be attached to IDX. The data set obtained for each compound was used as part of the experimental section in our recent publication in the *Journal of Medicinal Chemistry (J. Med. Chem., 2018, 61, 7942–7951)*.¹⁴⁷

By demonstrating the successful conjugation of tosylate **45** to IDX, one may question as to why the many attempts to attach the BoA series to IDX failed? As mentioned previously, the presence of boron-containing functionality was a prime suspect in the difficulties encountered.

The carboxylic acid drug used in our previous investigation was modelled on a boronic acid inhibitor (HA155) reported by Albers and co-workers (Figure 36).⁴²

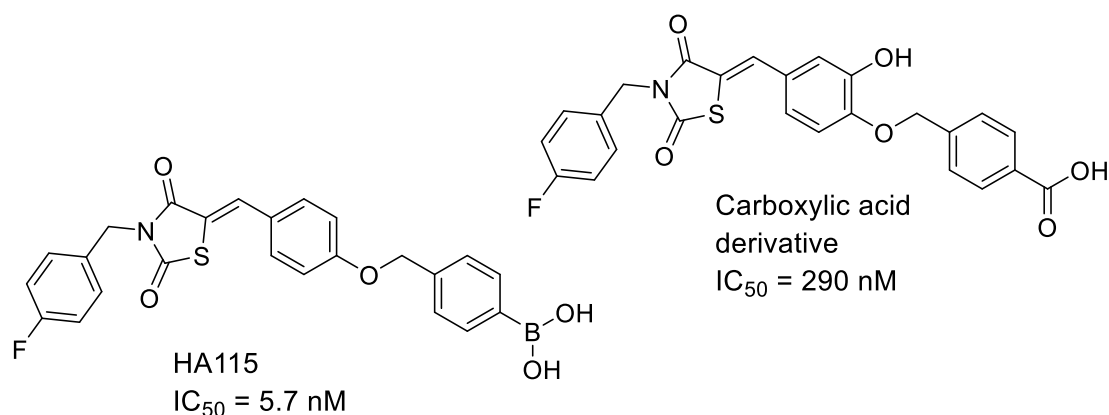


Figure 36 - HA155 and the carboxylic acid derivative^{43,147}

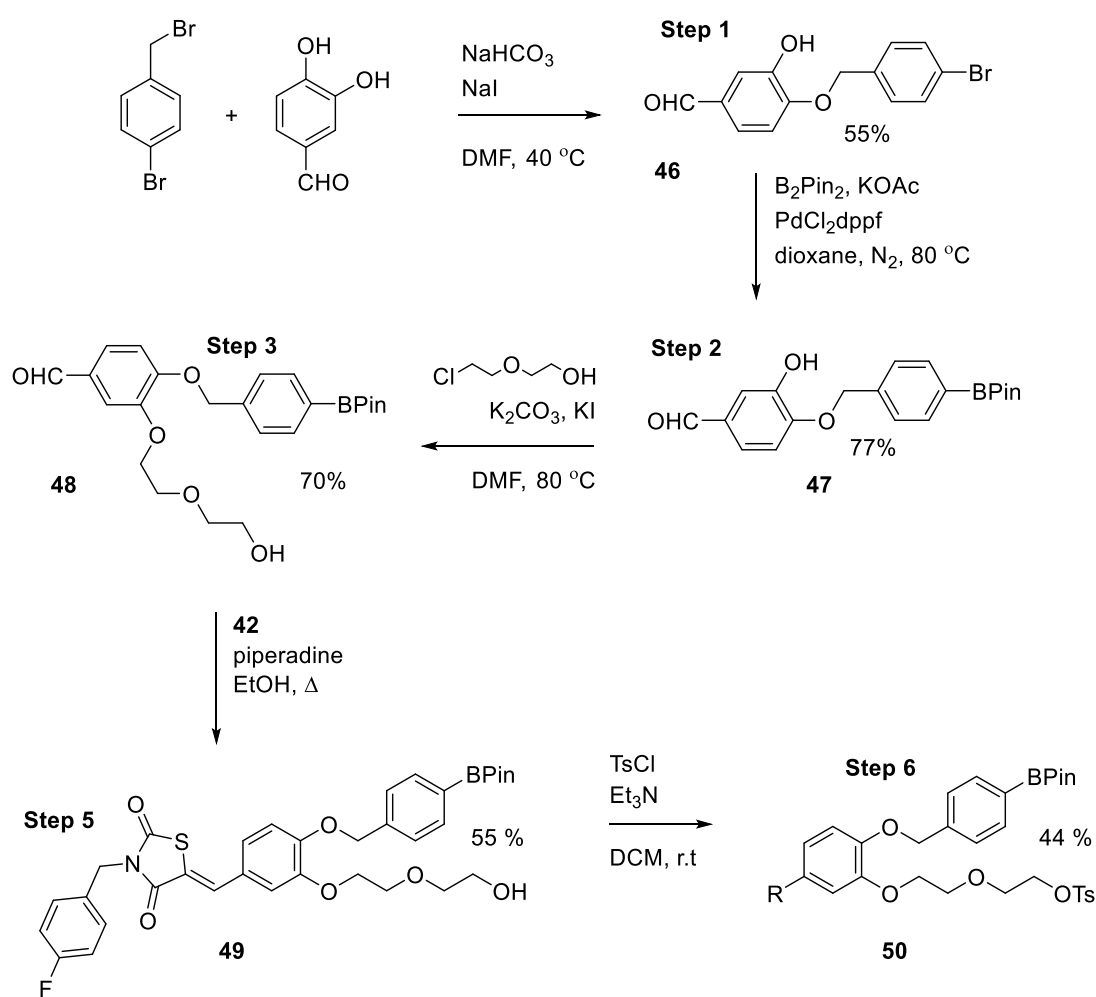
2.4 The attempted synthesis of a HA155-IDX conjugate, using the “tosylated drug method”

The carboxylic acid analogue of HA155 was chosen in our original study due to its relative ease of synthesis in comparison to the corresponding boronic acids. Biologically, the carboxylic acid group was expected to behave in the same way as a boronic acid at the active site of ATX, so would serve as an appropriate mimic. Therefore because of its structural similarity, a linker analogue of HA155 would be expected to react with IDX, based on the precedent set by its carboxylic acid equivalent, giving the best chance of producing a novel IDX drug conjugate. A HA155-IDX conjugate would be expected to be superior to its carboxylic acid counterpart, as indicated by HA155 being much more potent than the carboxylic acid analogue. On the other hand, if the conjugation reaction between HA155-linker and IDX was unsuccessful, it can be concluded that the presence of boron functionality leads to an inherent decrease in reactivity under the reaction conditions.

2.4.1 The preparation of a boronic acid, HA155 linker analogue

To that effect, a boronate ester linker analogue of HA155 was synthesised. As with the work on the BoA series it was intended for the BPin unit to serve as a boronic acid protecting

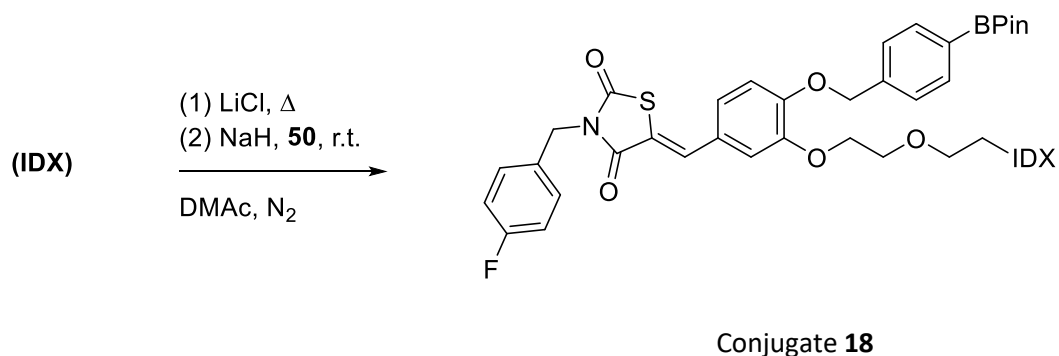
group, which could be removed, post conjugation, to expose the boronic acid. In the first step 3,4-dihydroxybenzaldehyde was reacted with 4-bromobenzyl bromide in a regioselective manner, using methodology published by Plourde and co-workers (Scheme 49).²⁰⁰ Bromide **46** was then converted to boronate ester **47**, via the Miyaura borylation reaction, the diethylene glycol linker was then installed to give ether **48**. Ether **48** was then reacted with heterocycle **42** in a Knoevenagel condensation, alcohol **49** was tosylated to afford the target compound, tosylate **50**.



Scheme 49 - Synthesis of tosylate **50**

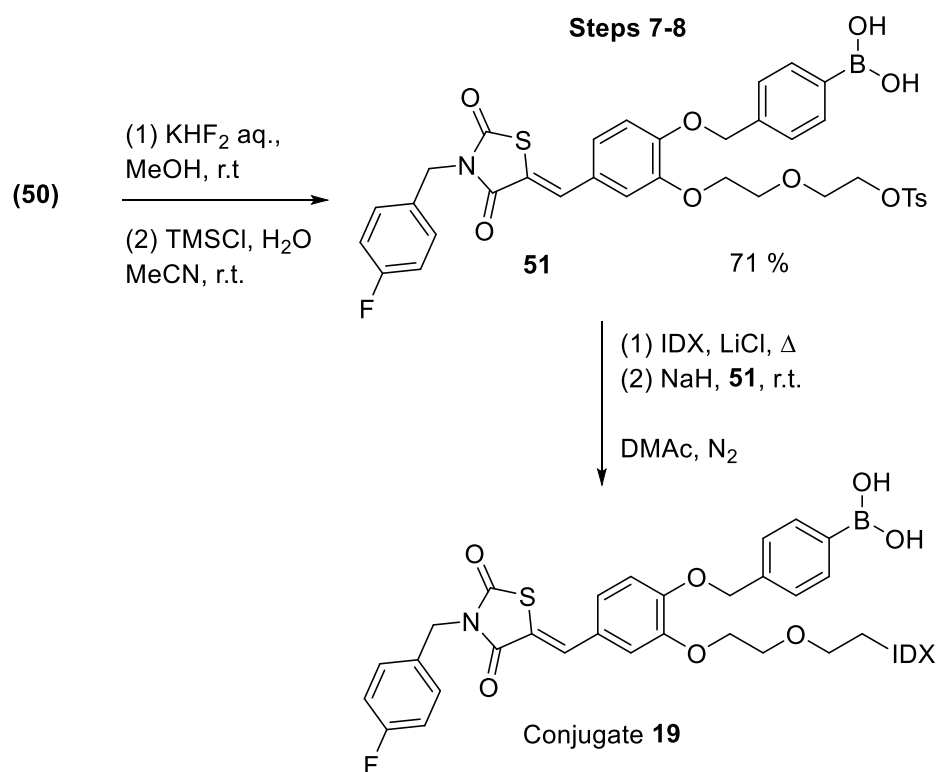
2.5 The attempted conjugation of a linker analogue of HA155 to IDX

The six-step synthesis of tosylate **50** was achieved with an overall yield of 7 %, in five linear steps. The material was then reacted with Icodextrin using our standard conjugation conditions (Scheme 50).



*Scheme 50 - The attempted conjugation of tosylate **50** to IDX*

Disappointingly, the conjugation reaction was unsuccessful, with only unreacted IDX being observed (by ^1H NMR spectroscopy) after dialysis. To attempt to effect conjugation an alternative approach was taken in which the boronic acid version of tosylate **50** was synthesised (Scheme 51), boronic acid **51** was then reacted with IDX.



Scheme 51 - The conversion of tosylate 50 to boronic acid 51 and its reaction with IDX

2.6 Discussion of the difficulties encountered with attaching drug-linker analogues to IDX

Again, no conjugation was observed after dialysis. Though the results were discouraging, an important conclusion can be made. The only difference between tosylate **45** and tosylate **50** is the presence of boron functionality in place of a carboxylic acid group, they are otherwise identical. It has been shown that tosylate **45** can be attached to IDX, whereas the conjugation of boronate ester **50** and boronic acid **51** were unsuccessful. This result strongly suggests that the presence of a boronate ester / boronic acid functional group has a strong attenuating effect on the conjugation reaction. To explain why this effect is observed is extremely difficult, especially considering the possible contribution by the polymeric system to the reduction in reactivity observed. Boronate esters and even boronic acids are widely known to participate in nucleophilic substitution reactions, without any indication of causing a retarding effect on reactivity.^{42,88,192} There are however, some factors which are likely to contribute to the reduction in reactivity observed in the conjugation reactions.

On the occasions where limited attachment of boronate ester compounds to IDX was observed, such as Conjugate **6** there was an interesting observation regarding the ^1H NMR spectra of the conjugates. The region at approximately 1.15-1.35 ppm was noticeably derivatised, BPin groups have a characteristic 12 H singlet at 1.20 ppm (DMSO- d_6), whereas in those spectra there was two singlets in its place (Figure 37).

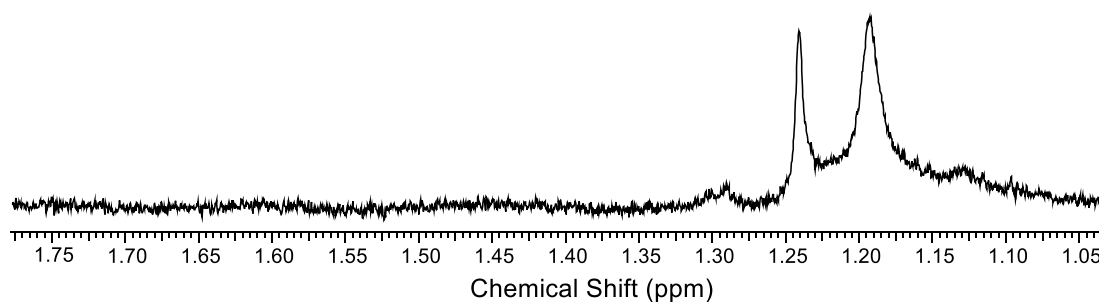


Figure 37 - The ^1H NMR spectrum of Conjugate **6** in the region 1.00 - 1.75 ppm (400 MHz, DMSO- d_6)

It is felt that the appearance of the two singlets could indicate the partial hydrolysis or transesterification of the BPin group in the presence of sodium hydride (Figure 38).

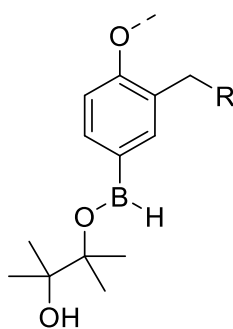
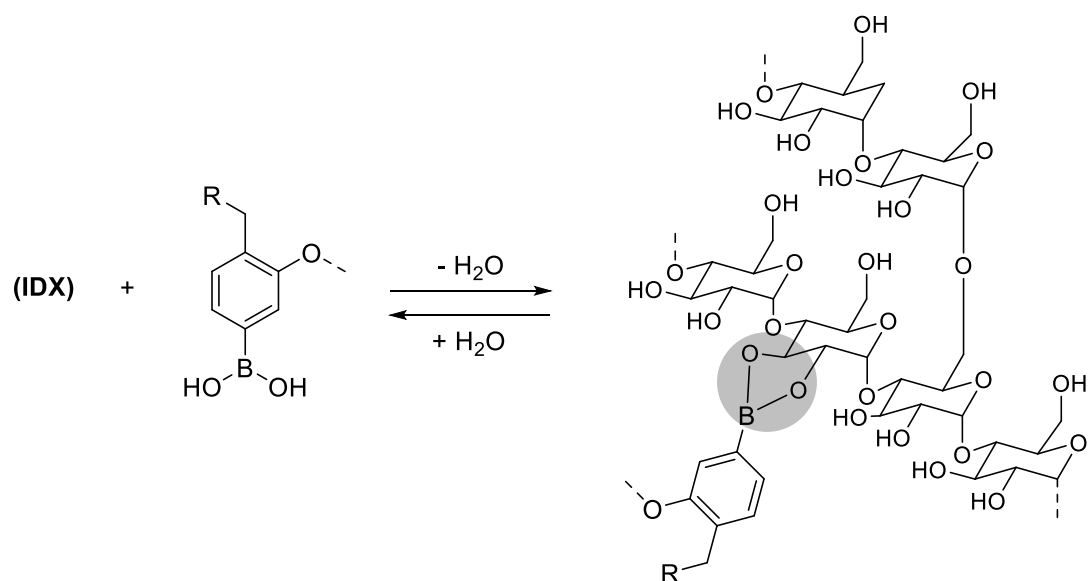


Figure 38 - The proposed partial hydrolysis / transesterification product

Further to this, boronic acids are known to react with sugars in a reversible manner, through boronic acid-diol interactions. This effect is widely known and has been exploited in materials chemistry applications in which boronic acid compounds / bound polymers act as glucose sensors, by measuring the fluorescence of the resulting sugar-boronic acid complex (Scheme 52).^{177,201,202}



Scheme 52 – Proposed IDX-boronic acid complex formation

It can be suggested that the anhydrous conditions used in the conjugation reaction could actively promote this reaction to occur. In the absence of water, the equilibrium will be driven to the right (boronic acid-IDX complex). However, the liberation of a water molecule will either immediately quench the IDX anion or react with NaH and be consumed. Either consequence will disfavour the conjugation reaction. With the drug bound to the polymer (via its boronic acid group) it will have restricted movement, which is necessary for the correct orientation in the displacement of the tosyl group. Once the material is dialysed, water present in the dialysis fluid will push the equilibrium to the left, to give the parent boronic acid and polymer. It may also be possible for IDX to interact with the hydrolysed material (Figure 38) and form a complex.

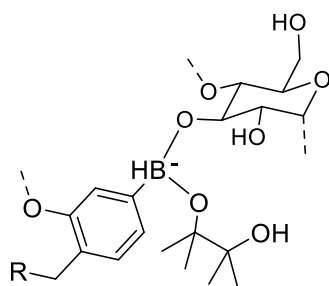


Figure 39 – Proposed structure of the partially hydrolysed boronate ester reacting with IDX

There is also the possibility that the IDX may directly attack the boronate ester, causing the partial hydrolysis of BPin observed in a similar manner to bis-benzoboroxole oligosaccharide detectors developed by Hall and co-workers.²⁰³

In a similar vein, boronic acids are also known to react with themselves, forming dimers and even cyclic trimers (Figure 40).^{204–206} This, like the reaction with oligosaccharides is reversible, however because of the anhydrous conditions used in the coupling reaction it will push the equilibrium towards the dimer / trimer.^{204–206}

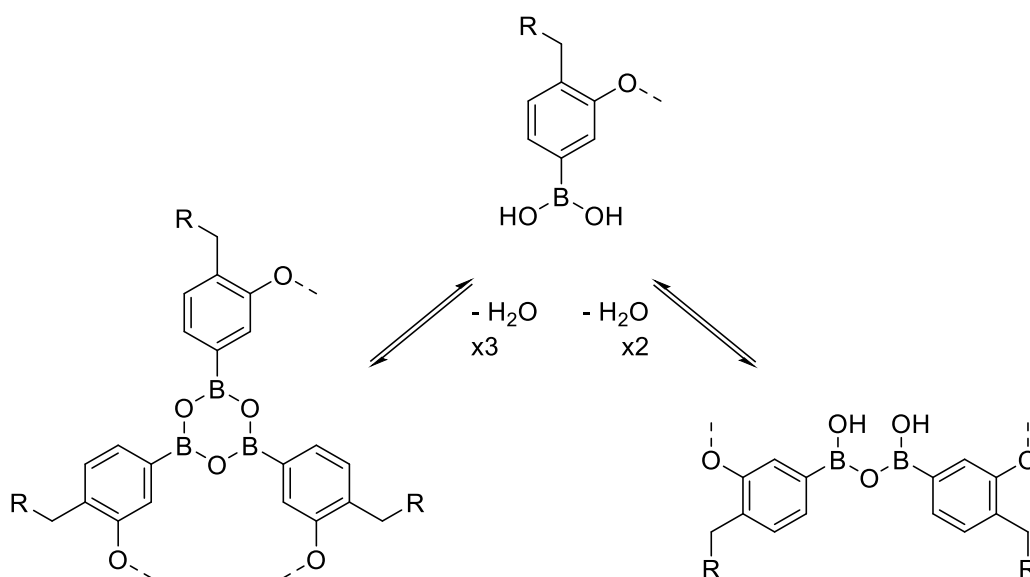


Figure 40 – The suggested boronic anhydride formation of the drug linker compound

When dialysed, the equilibrium will be pushed back to the left and the anhydride will be “broken-up”. The formation of a boronic anhydride is anticipated to have a negative effect on the conjugation of the drug-linker compound to IDX, making it less accessible to nucleophilic attack.

2.7 Alternative approaches to the preparation of boronic acid ATX inhibitor-IDX conjugates

Considering the ideas presented above, a conclusion could be drawn regarding how best to proceed with the conjugation reactions. Although the BPin moiety is a synthetically useful method to introduce a boron functionality into a system, it is potentially susceptible to hydrolysis and is therefore not suited to the reaction conditions used in the conjugation reactions in this study. Secondly if a boronic acid drug-linker compound is used in the

conjugation reaction, then water should be used as an additive to frustrate the formation of boronic anhydrides.

To that effect, three additional conjugation reactions were planned:

- The conjugation of boronic acid **51** to IDX in an aqueous environment, using potassium carbonate as a base.
- The attachment of a MIDA-protected boronic acid version of HA155 to IDX, using the “tosylated drug approach”.
- A “late-stage borylation” approach, involving the attachment of an aryl bromide version of HA155, with a view to borylate the drug post-conjugation.

2.7.1 MIDA protected boronic acid approach

MIDA boronates (Figure 41) are widely used as boronic acid protecting groups.²⁰⁷ Unlike BPin, they can be considered “true” boronic acid protecting groups. This is because for their deprotection they do not need to be converted to an intermediate and can be “put on and taken off”.^{207,208} Another reason for the MIDA group being used is that it is known to be tolerant of NaH, albeit for short reaction times (approx. 30 minutes), so it was felt to be suitable for application in our proposed conjugation reactions.²⁰⁷

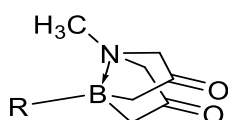
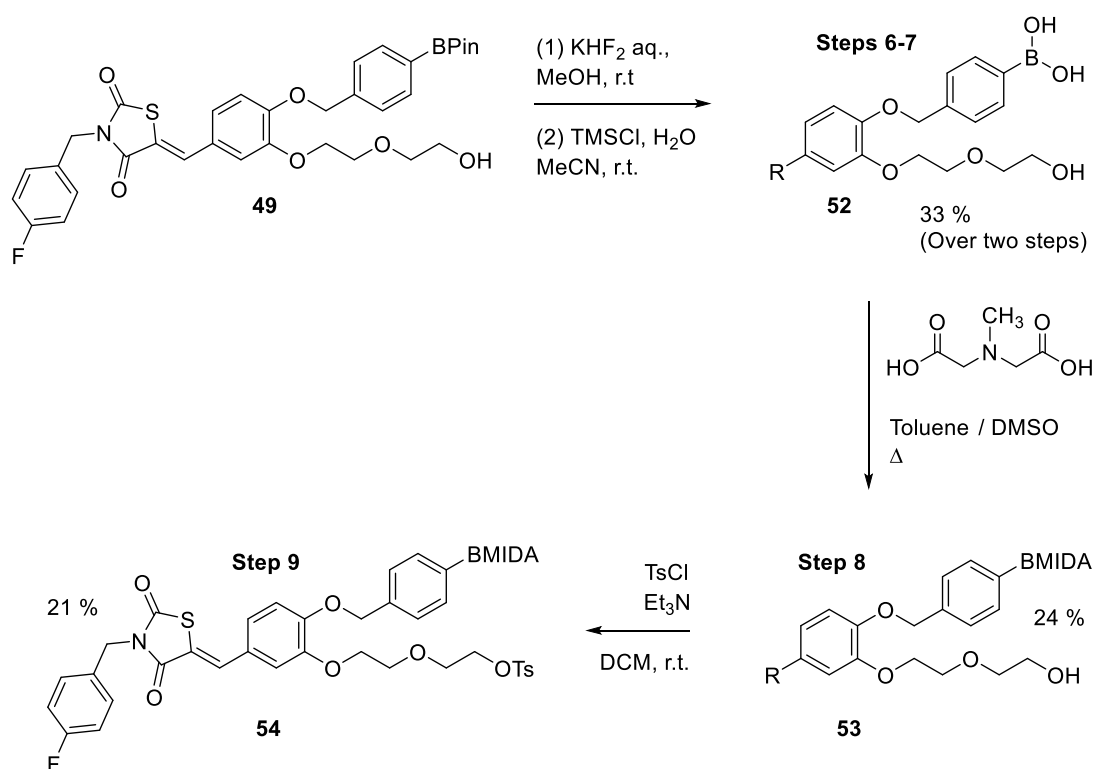


Figure 41 - MIDA boronate

A MIDA boronate version of boronic acid **51** was synthesised as follows: boronate ester **49** was converted to boronic acid **52**, in a two-step process (Scheme 53). Boronic acid **52** was then reacted with *N*-methyliminodiacetic acid under Dean-Stark conditions, followed by tosylation of MIDA boronate **53**, to give tosylate **54**.



*Scheme 53 - Shows the conversion of heterocycle **49** to a tosylate **54***

Tosylate **54** was synthesised in nine steps, the longest linear sequence was eight steps, and the overall yield was 0.3 %. The low overall yield was likely the result of boronic acid **52** and MIDA boronate's **53** low solubility in most organic solvents, which resulted in long reaction times.

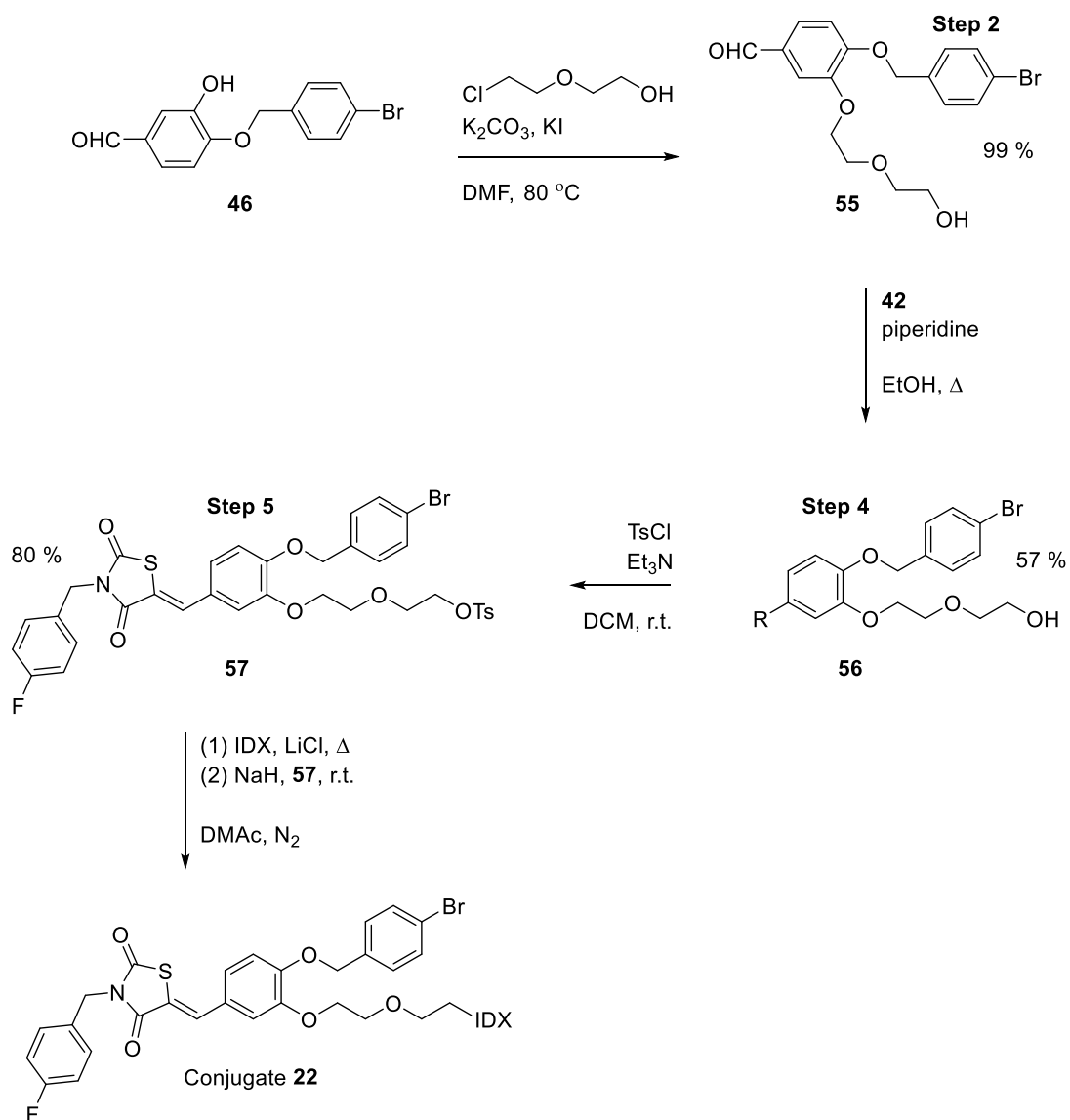
Tosylate **54** was then reacted with IDX using the standard conjugation reaction conditions (Scheme 48).

This was not originally planned, as it was intended to mimic the conditions previously used in the conjugation reaction, i.e. reaction at room temperature. Despite heating, the material was still only slightly soluble. It is also worth noting that boronate anhydrides are reported to form more readily at elevated temperatures (above room temperature).²⁰⁶ Another factor is the nucleophilicity of the primary alcohol group of IDX, because of the electron withdrawing effects of the neighbouring hydroxyl groups, the 1° alcohol may not be sufficiently nucleophilic to displace the tosylate on boronic acid **51**. If the reaction had been repeated, then a water-soluble base such as NaOH could have been more suitable. The solvent ratio would have also been changed to favour the organic solvent (perhaps 10:1 DMF / H₂O) to improve solubility, removing the need to heat the mixture. Because of the subsequent success enjoyed by us with the “epichlorohydrin method”(described in chapter 3), this approach was not investigated further.

2.7.3 “Late-stage” borylation approach

With the difficulties encountered in attaching drugs with boron functionality to IDX in mind, this approach was intended to circumvent this issue. It was postulated that if a version of tosylate **50** with an aryl bromide in place of the BPin group was attached to IDX, then the necessary synthetic handle would be in place to install a BPin group post conjugation. The boronate ester could be subsequently converted to a boronic acid.

The target compound was synthesised over 5 steps by adapting the previously established synthetic route, in an overall yield of 25%. Bromide **57** was then reacted with IDX (Scheme 56).



Scheme 56 – Synthesis of bromide **57** and its conjugation to IDX

After reacting for 5 days, the material was dialysed and then analysed by ^1H NMR spectroscopy. As anticipated, by using this new approach, the spectrum strongly suggested that drug material had been incorporated within IDX. This was evidenced by the appearance of new peaks in the aromatic region of the spectrum (Figure 42).

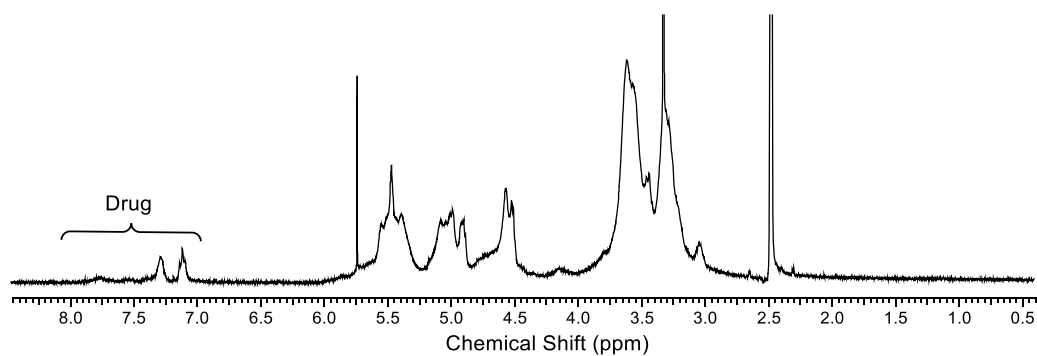


Figure 42 – The ^1H NMR spectrum of Conjugate **22** (400 MHz, DMSO-d_6)

While this attempt at conjugation to IDX can be considered successful, in parallel to these studies, work on an “epichlorohydrin activation method” was being undertaken (Chapter 3) and was showing very promising results. Since these conjugation studies appeared to require significant additional optimisation in order to improve drug-loading and three additional synthetic steps to install a boronic acid group, it was decided not to pursue this route development any further. Ultimately this decision proved to be well founded, taking into account the success enjoyed with the alternative epichlorohydrin method.

The work presented in this chapter demonstrated the preparation of a number of novel ATX inhibitor analogues. Attempts were made to attach these compounds to the polymer: Icodextrin. This was done through two methods that were previously developed by us, “the tosylated IDX method” and the “tosylated drug method”. In both cases only a limited success was observed. Modifications were then made to attempt to effect conjugation, however this was not wholly successful.

Chapter 3:

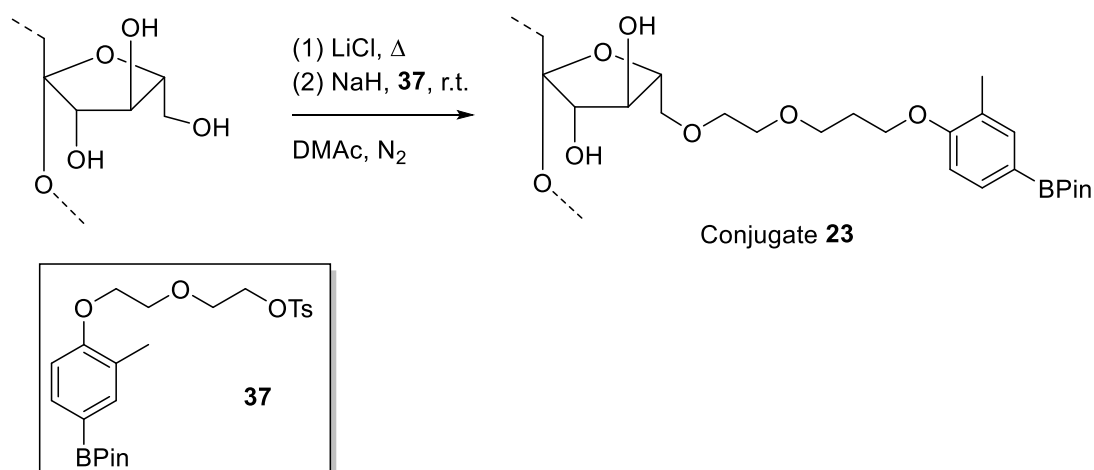
Synthesis of Inulin drug conjugates
and the development of the
“epichlorohydrin activation
method” for both Inulin and IDX

Chapter 3: Synthesis of Inulin drug conjugates and the development of the “epichlorohydrin activation method” for both Inulin and IDX

3.1 Attempted preparation of Inulin drug conjugates, using the “tosylated drug method”

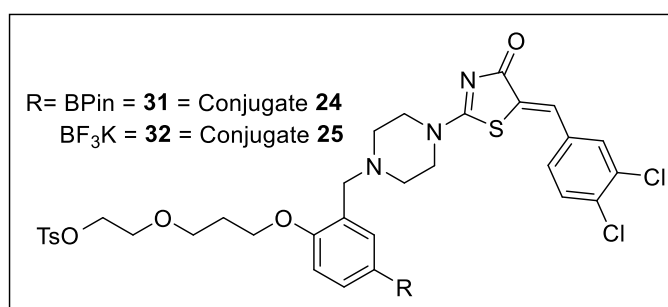
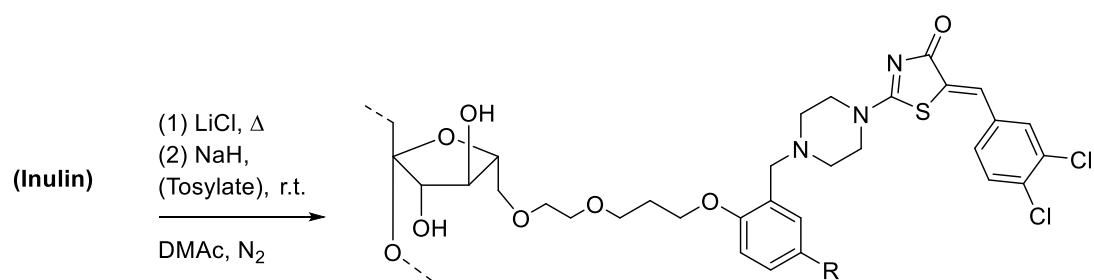
In parallel with the investigation described in Chapter 2, regarding Icodextrin, attempts were also made to attach drug-linker analogues of ATX inhibitors to Inulin.

As an initial investigation into the feasibility of attaching a drug linker compound to Inulin *via* the “tosylated-drug” method, a “model study” was attempted (Scheme 57) using tosylate **37** as a representation of 3BoA-drug linker **22**.



Scheme 57 - Model study of the attempted conjugation of tosylate **37** to Inulin

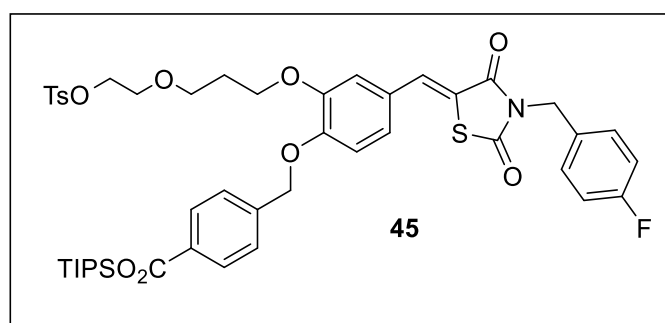
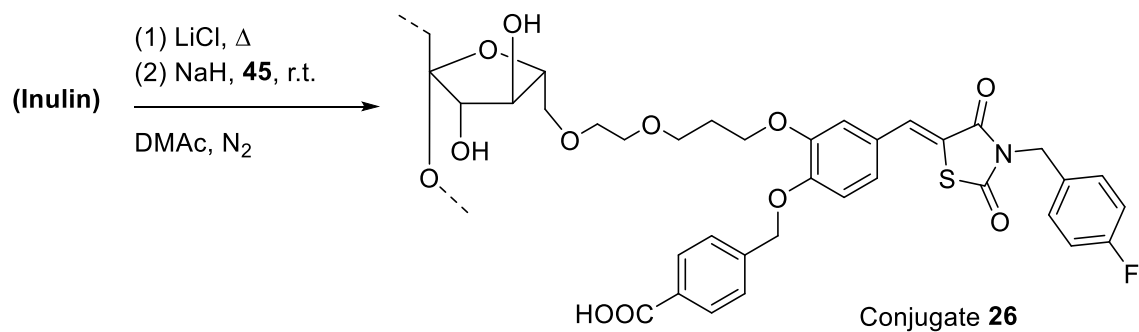
Despite there being strong literature precedent to suggest that the 1° alcohols in Inulin would displace a suitable leaving group in the presence of a strong base, this reaction was unsuccessful.^{157,160} Not discouraged by this, the methodology was applied separately with the drug linker compounds tosylate **31** and tosylate **32** (boronic acid “protected” versions of 3BoA-linker) (Scheme 58).



*Scheme 58 - The attempted attachment of **31** and **32** Inulin to give Conjugate **24** and **25***

Unfortunately, no conjugation was observed (by ¹H NMR spectroscopy). Mirroring the decision taken in Chapter 2, work concerning the attachment of analogues of Nagano's BoA series was discontinued. To complement the synthesis of Conjugate **17** an attempt was made to produce an Inulin version of Conjugate **17**. This would allow for the two polymers to be evaluated against one another for retention within the peritoneal cavity.

To that end, in the same manner as Conjugate **17** tosylate **45** was reacted with Inulin (Scheme 59).



*Scheme 59 - Attachment of tosylate **44** to Inulin to give Conjugate **26***

The material was then purified by dialysis, and the polymer product analysed by ¹H NMR spectroscopy. Pleasingly, a small amount of material appeared to have been conjugated to inulin (Figure 43).

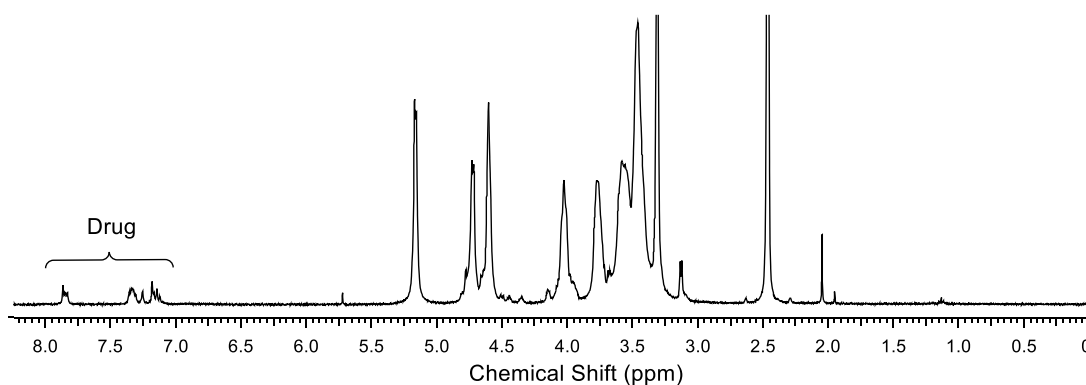


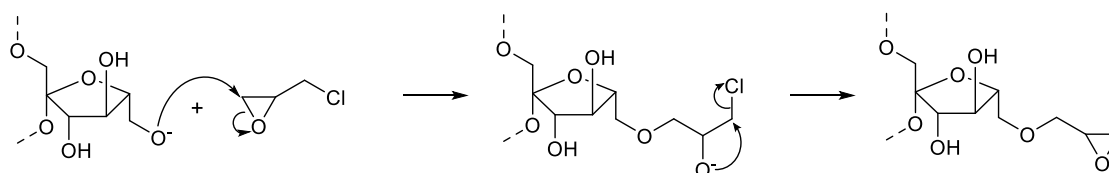
*Figure 43 - The ¹H NMR spectrum of Conjugate **26**, (400 MHz DMSO-d₆)*

Despite the drug loading appearing to be significantly lower than its IDX counterpart Conjugate **17** (by comparing the relative integration of the “drug” peaks to the polymer), the reaction was very promising. It was anticipated that with a small optimisation study, the drug

loading could be increased. However, despite this apparent success of this “tosylated-drug” approach in application with Inulin, the method was not investigated any further, due to the progress being made with an “epichlorohydrin activation method”. Had the epichlorohydrin method not shown such encouraging results, it is likely the “tosylated-drug approach” would have proven to be a useful method from which to conjugate ATX inhibitors to Inulin.

3.2 The development of the “epichlorohydrin activation method” for Inulin, introduction

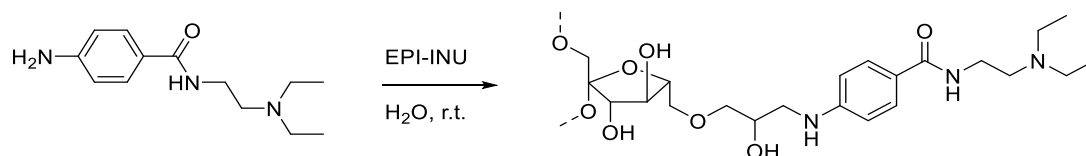
Because of the many challenges experienced throughout this project, in the attempted synthesis of drug-polymer conjugates, an alternative conjugation method was sought. Ideally this alternate method would address the shortcomings noted in the “tosylated IDX” method and the “tosylated drug” method. Fortunately, several methods have been previously reported for the attachment of various substrates to Inulin, as detailed in Chapter 1. Of most interest to us was a method developed by Molteni, in which Inulin was treated with epichlorohydrin in basic aqueous media.¹⁶⁵ The highly reactive epoxide group on epichlorohydrin was found to be susceptible to nucleophilic attack by the hydroxyl groups present on Inulin. This caused a ring-opening reaction to occur that exposed a hydroxyl group, at the alpha position relative to the chloro group (Mechanism 3).



Mechanism 3 - The epichlorohydrin activation of Inulin

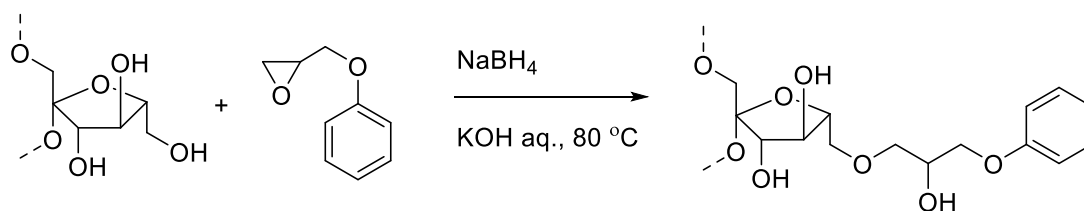
In the presence of dilute base, the alkoxide group will displace the chloro group intramolecularly to form a second epoxide, this is termed the “activation step”.^{165,209} Epichlorohydrin-activated Inulin (EPI-INU) reportedly can be isolated as a powder and stored for many months without it degrading, or more conveniently generated *in situ*.¹⁶⁵ The epoxide residues contained within EPI-INU are able to react with nucleophiles, facilitating the attachment of a drug molecule to Inulin. In a study by Remon and co-workers the

antiarrhythmic drug procainamide was attached to EPI-INU in this manner *via* the aniline group present within its structure (Scheme 60).



Scheme 60 - The addition of procainamide to EPI-INU

A consequence of the epoxide ring opening by procainamide is the formation of a secondary hydroxyl group. Whilst introducing additional functionality into the polymer was less than ideal for our purposes. It was postulated that the alcohol group would unlikely affect the binding of any drug to ATX, considering the structure of Inulin / IDX. Intrigued by the potential application of this method for our own work, the possibility of attaching a drug-linker analogue to Inulin using this method was investigated. It was decided, that despite there being a literature precedent for the attachment of aniline groups to EPI-INU, the drug-linker compounds developed for this project would not be modified further. The primary alcohol of the drug linker compounds would act as the nucleophile.²⁰⁹ This was reasoned due to a desire not to introduce additional functionality into the linker that may potentially interfere or compete with the interaction of key functional groups on the drug. However, there was concern that a primary alcohol group would not be sufficiently nucleophilic to be able to attack an epoxide residue on EPI-INU. In one book Chapter from the mid-seventies, it is suggested (by Molteni) that alcohols can act as suitable nucleophiles for EPI-INU although this is never substantiated with experimental details or references to similar studies.¹⁶⁵ A thorough examination of the literature revealed a similar approach had been taken by Infante and co-workers. In their method, the epichlorohydrin activation method had been applied in “reverse”, in which a phenyl epoxide compound was reacted with Inulin (Scheme 61).¹⁷⁵



*Scheme 61 - Addition of a phenyl-epoxy compound to Inulin, as described by Infante and co-workers.*¹⁷⁵

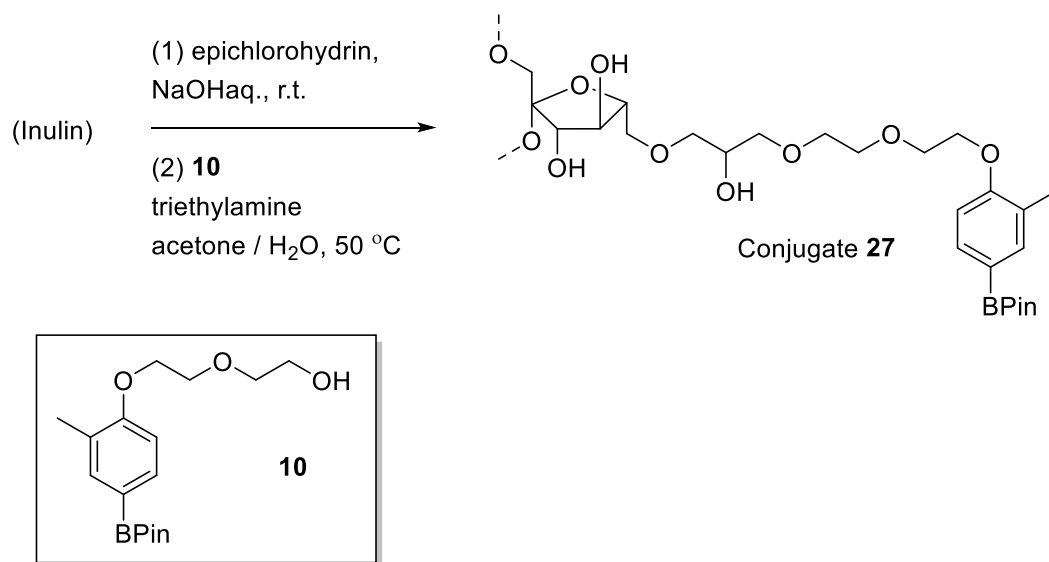
3.2.1 Trial reactions

Whilst not identical to the suggested nucleophilic attack by the alcohol group of the drug linker compound, the literature precedent was encouraging. The feasibility of using a “reversal” of the epichlorohydrin method for our purposes was investigated by reacting a “model” drug-linker compound (ether **10**) with epichlorohydrin. However, in both attempts the compound could not be isolated, likely due to the highly reactive epoxide group degrading.

A trial conjugation reaction was attempted: EPI-INU was prepared by reacting Inulin with epichlorohydrin in the presence of dilute NaOH aq. for 16 hours. The material was then neutralised with dilute hydrochloric acid. In the presence of triethylamine, ether **10** was added as a solution in acetone and reacted for 5 days (Scheme 62).

The reaction conditions are worthy of comment, for example the reason the EPI-INU is neutralised and then triethylamine is added afterwards is due to the desire to avoid the use of a NaOH in the presence of a boronic ester, as explained previously. Triethylamine was chosen as it is miscible in water and from our own investigations, does not act to degrade boronate esters. EPI-INU and ether **10** were reacted in an acetone / H₂O co-solvent system, due to the low solubility of Inulin in common organic solvents and the very low solubility of ether **10** in water. By using a mixture of two solvents that are miscible in one another, Inulin and ether **10** became homogeneous at an elevated temperature (50 °C), which proved essential for the etherification reaction to occur. Using a co-solvent system avoided the need to use a phase-transfer catalyst such as tetra-*N*-butylammonium bromide, as has been applied in other studies.¹⁷⁵ When this method has been applied to other drug-linker compounds it has often been found to be necessary to change the solvent ratio to achieve complete dissolution of both components at 50 °C. If this method were to be applied to drug

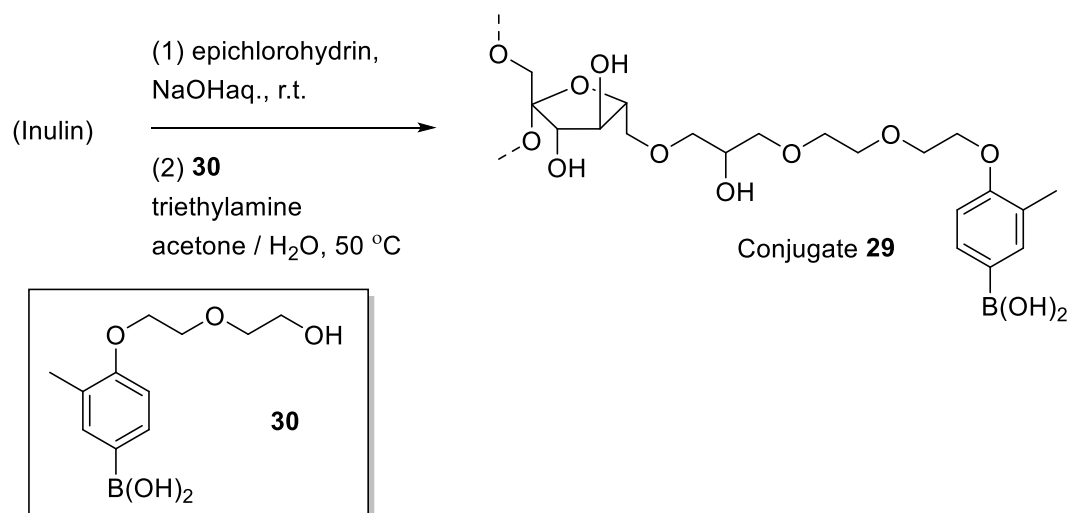
molecules outside the remit of this thesis, the minimum amount of organic solvent should be used to solubilise the drug compound at an elevated temperature, so as not to precipitate the polysaccharide. If acetone was found to be unsuitable, other water miscible organic solvents such as IPA, DMF, MeCN, DMAc or DMSO could be used.



*Scheme 62 - Attachment of ether **10** to EPI-INU to give Conjugate **27***

The reaction was left for 5 days, then the material was precipitated in acetone and dialysed and analysed by ^1H NMR spectroscopy. To our delight, the model drug (ether **10**) appeared to have attached to EPI-INU with an acceptable drug loading (Figure 44).

Interestingly, after dialysis, the only material to be recovered was epichlorohydrin activated Inulin, suggesting that the BF_3K group had a direct effect on the conjugation reaction inhibiting the reaction. We then decided to investigate if a boronic acid “model drug” (boronic acid **30**) could be directly conjugated to EPI-INU (Scheme 64).



*Scheme 64 - Coupling of boronic acid **30** to EPI-INU to give Conjugate **29***

Pleasingly, inspection of the ^1H NMR spectrum of the dialysed product indicated the successful attachment of boronic acid **30** to INU (Figure 45).

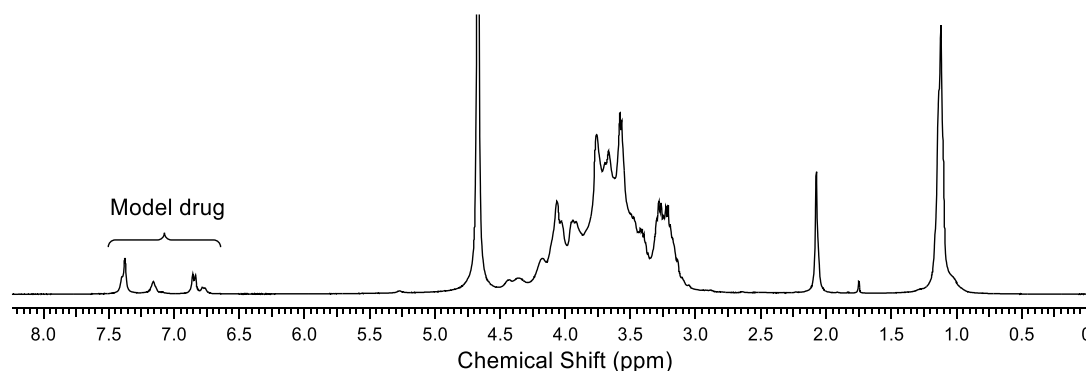


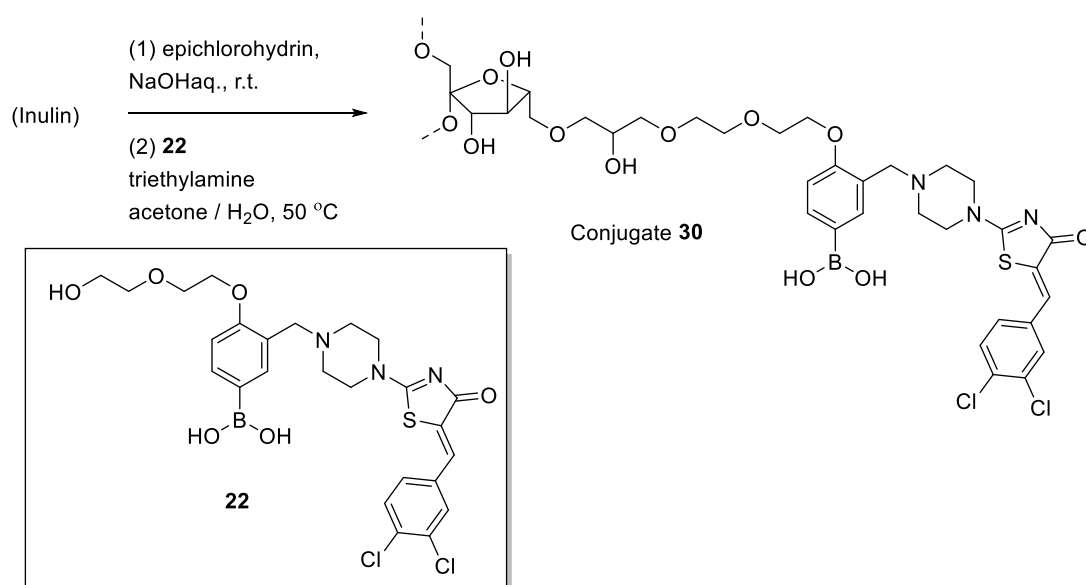
*Figure 45 - The ^1H NMR spectrum of Conjugate **29** (400 MHz, D_2O)*

With the knowledge that the boronic acid “model drug” could be directly conjugated to EPI-INU, logically the next step of this investigation was to attempt to attach the drug linker analogue of 3BoA (ether **22**) to Inulin. But before this was attempted there was one concern that needed to be resolved. In the ^1H NMR spectra of Conjugates **27** and **29** (Figure 44 and Figure 45) there is a broad singlet at approx. 1.12 ppm. This peak could be assigned as a BPin

12 H singlet for Conjugate **27**. However, the peak is also visible in the spectra of Conjugate **29** which contained no boronate ester. A clue to the peaks origin was provided in the ^1H NMR spectrum of Conjugate **28**, despite no material coupling to Inulin, the singlet was still visible. This strongly suggesting that the new peak was a consequence of the conditions / reagents used in the conjugation reaction. To test this hypothesis a test reaction was conducted, mimicking the method used for Conjugate **27** except for the addition of ether **10**. The resulting product was dialysed and analysed *via* ^1H NMR spectroscopy, as predicted the resonance at 1.12 ppm was visible. A sample of EPI-INU was also prepared and analysed in the same manner; in this case, there was no such peak observed. It can therefore be concluded that the resonance 1.12 ppm forms when the model drug is added to the reaction mixture, but occurs independently of the drug itself, for example as a result of heating. Whilst the identity of the peak was not yet confirmed (discussed in Chapter 3.5) it was felt that the conditions could be modified at a later stage in this study to attenuate its appearance.

3.2.2 Attempted preparation of a 3-BoA-Inulin conjugate using the “epichlorohydrin activation method”

Having demonstrated that a boronic acid “model drug” could be directly attached to Inulin, an attempt was made to attach the drug-linker analogue (ether **22**) to EPI-INU, in the same manner as conjugates **27** and **29** (Scheme 65).

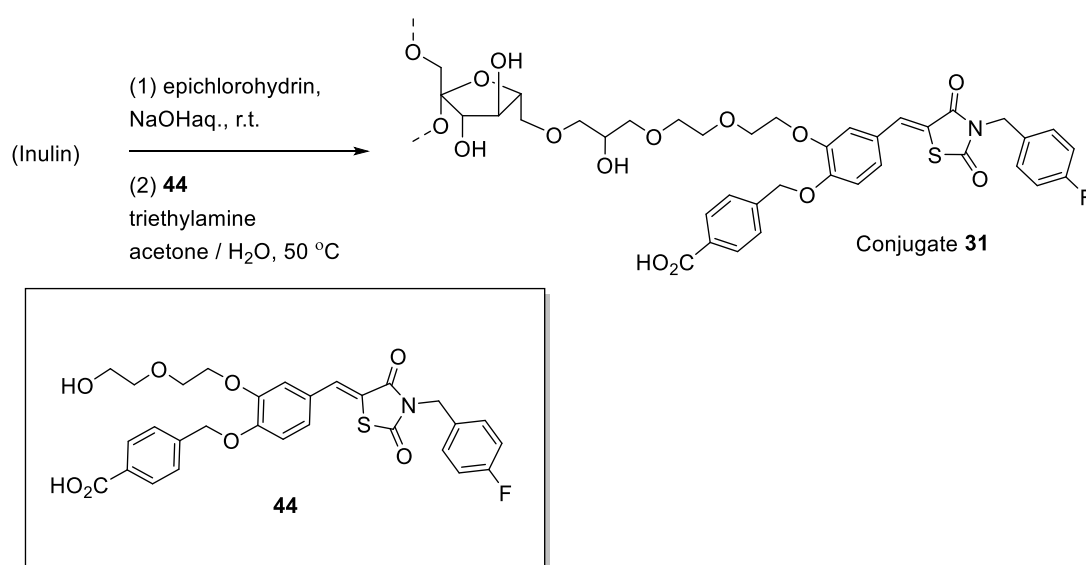


Scheme 65 - Attempted synthesis of Conjugate **30**

Disappointingly, the conjugation reaction was not successful. A likely cause of this lack of success may be the thermal stability of the drug-linker analogue, considering compound **22** was typically stored at -18 °C. However, this could not be confirmed as the material was dialysed over several litres of solvent, making its recovery impractical. At this point in time our focus moved away from the BoA series and towards inhibitors based around the HA155 scaffold.

3.2.3 Preparation of carboxylic acid-ATX inhibitor Inulin conjugates, early method

As was stated earlier, it was desirable to prepare an Inulin equivalent of Conjugate **17** for the peritoneal retention of IDX and Inulin to be effectively evaluated. With limited success using our “tosylated-drug” approach, it was decided that ether **44** would be attached to Inulin using the “epichlorohydrin activation method” (Scheme 66).



Scheme 66 – The preparation of Conjugate **31**

In this first study, the TIPS-protected version of the drug-linker analogue (ether **44**) was used in the conjugation reaction rather than the unprotected carboxylic acid equivalent, in order to prevent side reactions from occurring with the carboxylic acid. Additionally, ether **44** was more soluble in a variety of organic solvents compared to the carboxylic acid version, which from a practical viewpoint made it considerably easier to manipulate. When the same

conjugation reaction was attempted with carboxylic acid **43**, it did not dissolve in an acetone / H₂O co-solvent system and required the addition of DMF for complete dissolution.

Gratifyingly, the conjugation reaction (Scheme 66) proceeded smoothly and the drug-linker compound (ether **44**) was successfully reacted with EPI-INU, as evidenced by the ¹H NMR spectrum of Conjugate **31** (Figure 46).

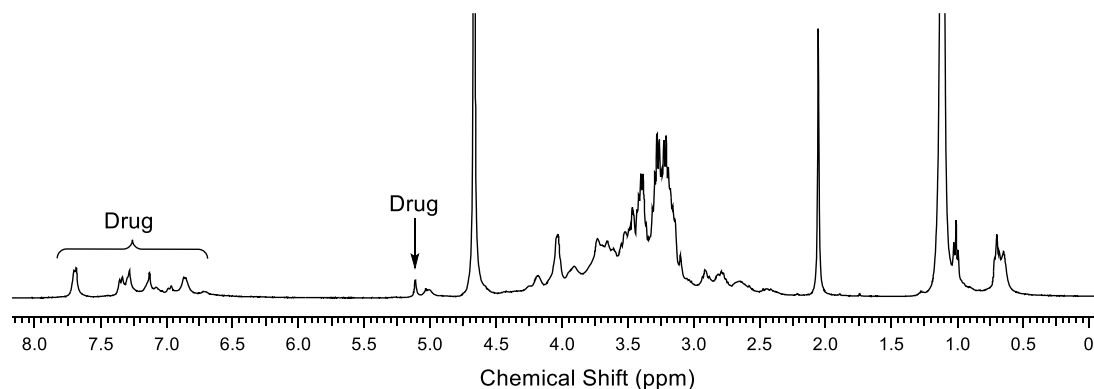


Figure 46 - The ¹H NMR spectrum of Conjugate **31** (D₂O, 400 MHz)

In agreement with findings in our previous studies, the TIPS ester group had undergone hydrolysis under the reaction conditions, which meant the conjugate required no further chemical modification, post conjugation.

3.3 The development of the “epichlorohydrin activation method” for IDX

In comparison to Conjugate **17** (attached to IDX *via* the “tosylated drug” method), the drug conjugates synthesised with Inulin using the “epichlorohydrin activation” method are almost structurally identical (except for the polymer). However, the drug is attached to Inulin through a secondary alcohol bridged-ether chain, whereas Conjugate **17** is linked by a straight alkyl ether chain. The difference in linkage to each polymer is not anticipated to have any significant change on activity (the linker unit is believed to be completely inert). But for Inulin and IDX drug conjugates to be directly comparable, it was felt the drug should be attached to each polymer using the same conjugation chemistry. As detailed earlier (Chapter 3.1), the “tosylated drug method” was used to limited effect on Inulin, so to complement those studies a series of IDX drug conjugates using the “epichlorohydrin method” would be made.

To that end, the feasibility of producing EPI-IDX drug conjugates was investigated by reacting Icodextrin with epichlorohydrin in the same manner as with Inulin, under the standard reaction time of 16 hours. The material was then neutralised, evaporated and triturated in acetone to give a white powder. This was then analysed by ^1H NMR spectroscopy, the results are shown in Figure 47.

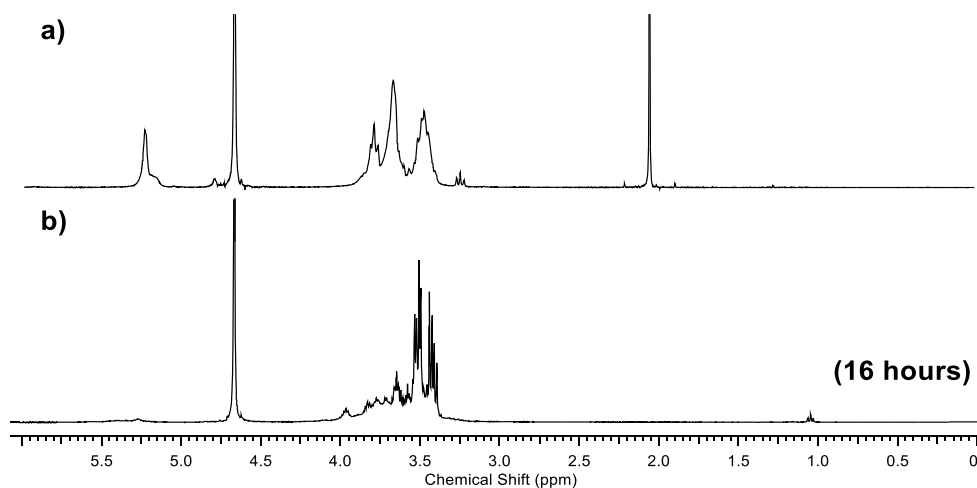
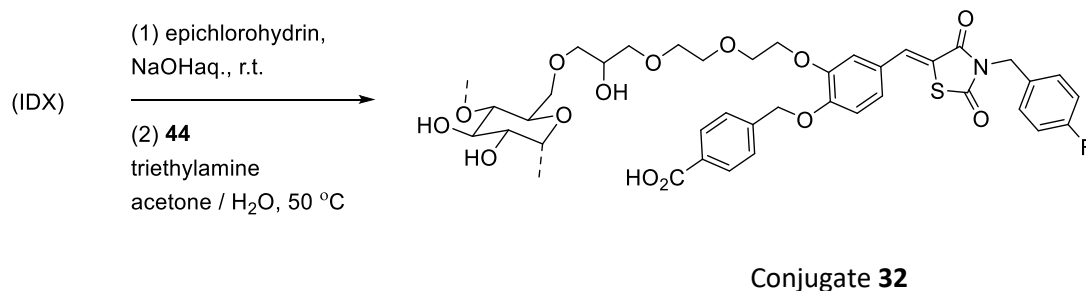


Figure 47 - ^1H NMR spectra of a) IDX and b) epichlorohydrin-activated IDX (D_2O , 400 MHz)

As can be seen in Figure 47b the spectrum is noticeably different to that of IDX (Figure 47a), with the multiplet at 3.40-3.55 ppm (Figure 47b) appearing to have incorporated new material, in comparison to pure IDX. This suggested that epichlorohydrin may have reacted with IDX. This may also indicate that intra polymer cross-linking has occurred with the attached epoxide groups and the hydroxyl groups on neighbouring sugars.²¹¹

It is thought that, in keeping with our previous assertion, the primary hydroxyl group of IDX will react preferentially with epichlorohydrin due to it being more nucleophilic than the secondary alcohol groups also present. This is substantiated by other studies on epoxide addition to glucose-containing polysaccharides.^{211,212} However, the epoxide may also react with secondary alcohol groups contained within the sugar, considering the precedent set in the epoxidation of Inulin, with DS values of up to 2 being reported.¹⁶⁵

Having evidence that IDX will react with epichlorohydrin, a conjugation reaction was attempted. Epichlorohydrin-activated IDX (EPI-IDX) was prepared by reacting IDX with epichlorohydrin for 16 hours. The pH was then adjusted to neutral (using dilute HCl aq.). In the same manner as Conjugate **31**, EPI-IDX was reacted with triethylamine and ether **44** for 2 days at 50 °C (Scheme 67).



Scheme 67 - The attempted synthesis of Conjugate 32

The product was analysed by ^1H NMR spectroscopy. To our disappointment, no drug material appeared to have been attached to IDX. In attempting to discern why the reaction failed, attention was drawn to the ^1H NMR spectrum in Figure 47b, regarding the change in appearance within the spectrum. If it was the case that IDX had crosslinked with itself (as represented in Figure 48) then it could have a negative effect on the conjugation reaction.

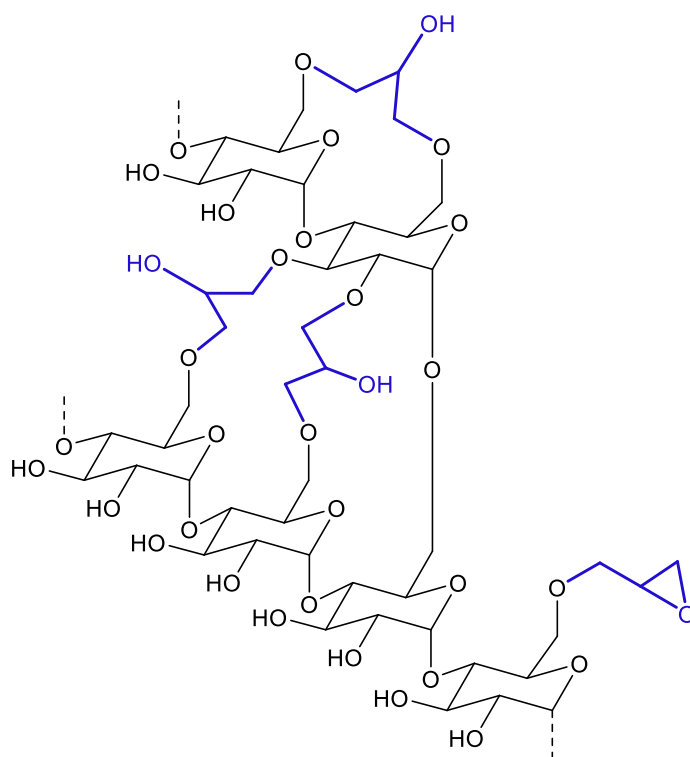


Figure 48 - Intra IDX crosslinking, (cross-linking highlighted in blue)

Intra molecular and (possibly) inter molecular cross-linking will have two main consequences with regard to the conjugation reaction: there will be fewer epoxide units with which the drug can react, reducing the total amount of drug that can be theoretically attached.

Secondly, cross-linking may hinder the approach of the drug molecule, making conjugation less likely. Cross-linking may also cause the polymer to fold in on itself, in the same manner as a tertiary protein structure. Potentially, this agglomeration may mean that any un-reacted epoxide units are inaccessible to the drug molecule.

3.3.1 ¹H NMR Study of the reaction between epichlorohydrin and IDX over time

Working on the hypothesis that the cross-linking effect was occurring over time, a study was undertaken to evaluate the reaction between epichlorohydrin and IDX over time. Icodextrin was reacted with epichlorohydrin for set time periods, then worked-up as previously described. The isolated material was then analysed by ¹H NMR spectroscopy (Figure 49).

The study gave a valuable insight into the reaction of epichlorohydrin with IDX. As can be seen from the spectra in Figure 49, IDX loses much of its structural definition after 4 hours, with reference to the ¹H NMR spectra of pure IDX. It is suggested that the gradual change in shape of the peaks at 3.20 - 4.00 ppm is the result of cross-linking enveloping IDX. After 16 hours IDX is likely to be highly crosslinked. It can be concluded that when the conjugation reaction was attempted using EPI-IDX with a 16-hour reaction time (Scheme 67), the approach of tosylate **44** was likely to be extremely hindered. This study highlights the importance of time on the activation step. It is indicated that the intra IDX cross-linking process occurs over several hours, so if the activation time was reduced, there is likely to be less internal cross-linking within IDX, but potentially still be sufficient epoxide residues with which drug-linker molecules can react with. The study also revealed the gradual loss of the anomeric proton within the structure of IDX. The broad singlet at 5.25 ppm diminished in intensity and eventually (after 12 hours) disappeared. This was taken to show the degradation of the polymer over time.

The study also revealed a second process, which we also feel is important to the attachment of drug molecules to IDX. After 10 minutes, the NMR spectrum reveals two small multiplets at 2.58 – 2.61 ppm and 2.74 – 2.79 ppm (Figure 50). At 30 minutes their intensity (by relative integration) has increased, which was mirrored at 1 hour and by 4 hours these were at their most intense. After 4 hours, these multiplets slowly decreased in size, and by 16 hours they have disappeared.

It is believed that these peaks indicate the formation of the epoxide group on IDX (following the attachment epichlorohydrin to IDX). The evidence for this is that if it were the hydroxy-chloro version of IDX it would be expected to have a different splitting pattern and be shifted downfield to approx. 3.50 ppm (using the ^1H NMR spectrum of epichlorohydrin as a guide). The formation of the epoxide group is probably essential for the successful addition of a drug molecule to IDX and additionally is a process that intra IDX cross-linking is reliant upon for it to occur. This is evidenced by the gradual reduction and eventual disappearance of the epoxide peak over time. Implying that the epoxide has been consumed in the cross-linking process, to expose the hydroxyl group, which is obscured by the main bulk of IDX in the spectrum, though the epoxide could be ring-opened by H_2O . The epoxide ring opening will most probably take preference in the drug addition / cross-linking reaction, over direct displacement of the chloro group of hydroxy chloro IDX although the same result will be obtained regardless.

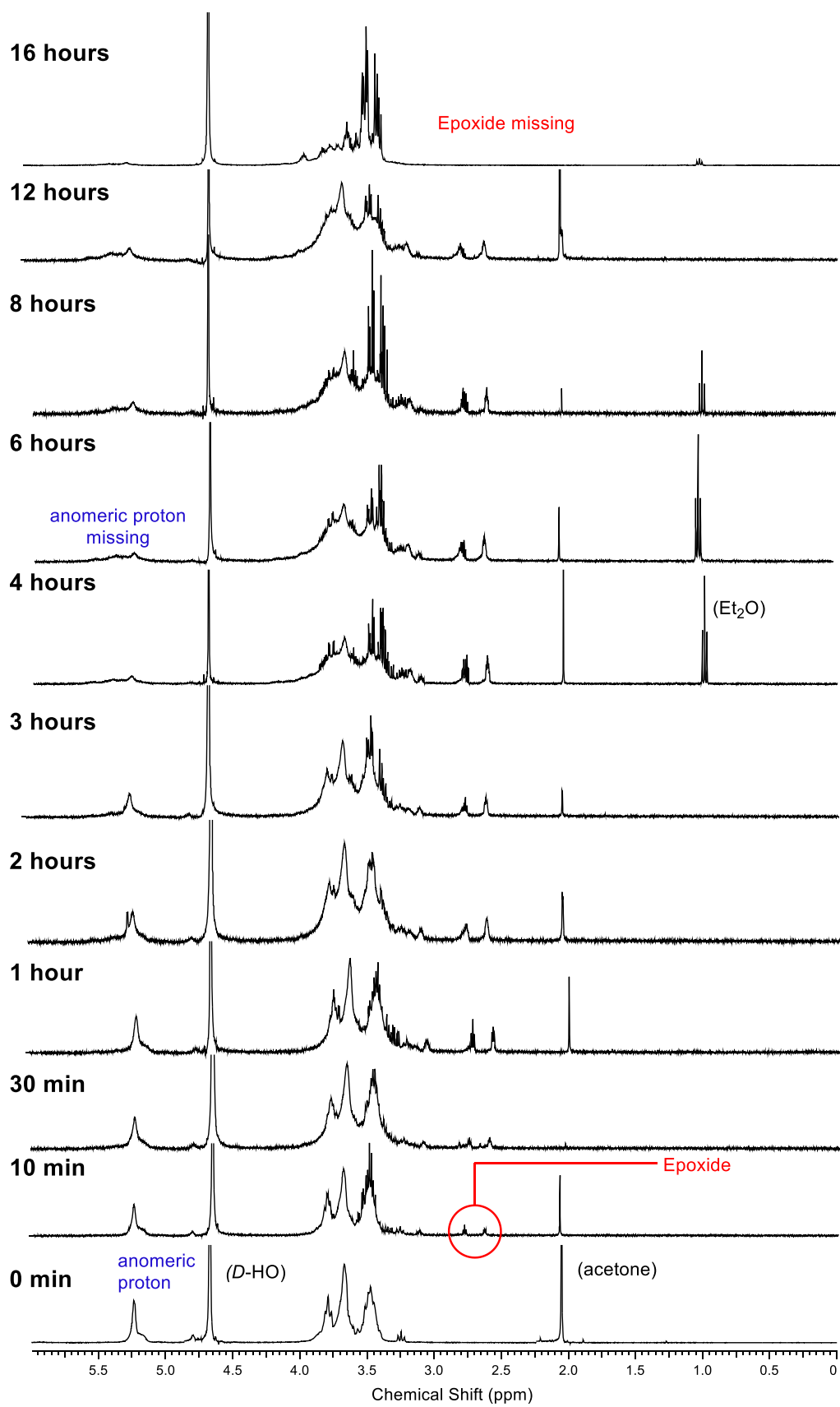


Figure 49 - The ¹H NMR spectra of epichlorohydrin activated IDX with differing reaction times (D₂O, 400 MHz)

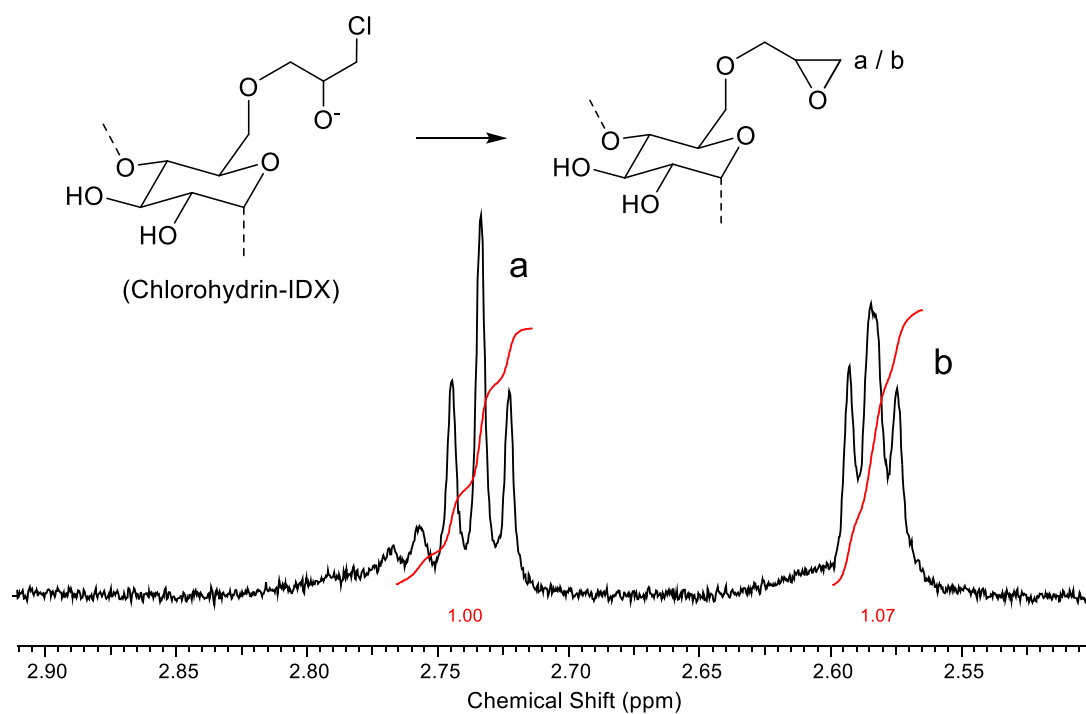


Figure 50 - The formation of an epoxide on IDX and the spectral assignment of the new peaks

3.3.2 Refinement of the epichlorohydrin method for IDX

Using the insight afforded by the ^1H NMR study, the conjugation reaction between IDX and ether **44** was re-attempted, using a 1-hour activation time. Because although after 4 hours (Figure 49) the epoxide peaks were at their most intense, suggesting that there are the most epoxide residues available to react with IDX, after this time the spectrum began to lose its resolution, indicating cross-linking was occurring. At 1 hour, the epoxide peaks are still intense, but the resonances remain well resolved. After one hour, the reaction mixture was neutralised and the product isolated as a solid and used immediately in the drug coupling step.

To our delight, the conjugation reaction appeared to be successful, with ether **44** appearing to be incorporated into IDX, as shown in the ^1H NMR spectrum of Conjugate **33** (Figure 51).

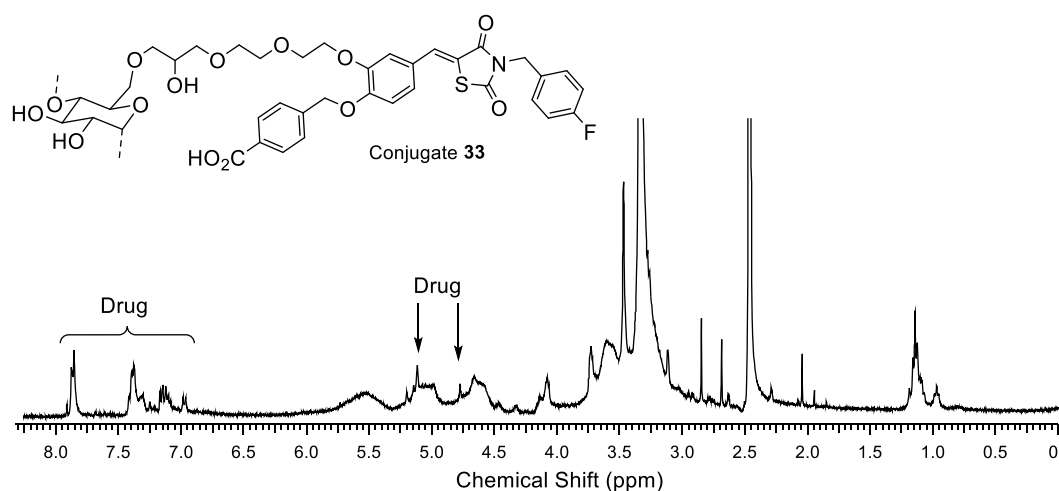


Figure 51 - ^1H NMR spectrum of Conjugate **33** after dialysis (DMSO- d_6 , 400 MHz)

3.4 Further refinement of the “epichlorohydrin activation method” for Inulin and IDX

When the conjugation reaction was repeated using EPI-IDX with activation times of 4 and 8 hours, interestingly no conjugation was observed despite there being epoxide residues present on the polymer as suggested by ^1H NMR spectroscopy (Figure 49). This observation highlights the significance that cross-linking has on the reactivity of EPI-IDX, presumably by hindering the approach of the drug-linker compound. It can therefore be said that intra polymer cross-linking and epoxide formation both have a significant effect on the ability to attach a drug molecule to a polymer using this method. These factors must be taken into account if the epichlorohydrin activation method is applied to other polysaccharides such as dextran.

As previously stated, the Inulin drug-conjugate Conjugate **31** was prepared with an activation time of 16 hours, whereas IDX required an activation time no longer than 1 hour. One may question as to why the two polymers behaved so differently. To answer this, a study similar to that shown in Figure 49 was conducted. Inulin was reacted with epichlorohydrin for set periods of time, then isolated as a solid by precipitation in acetone and analysed by ^1H NMR spectroscopy (Figure 52).

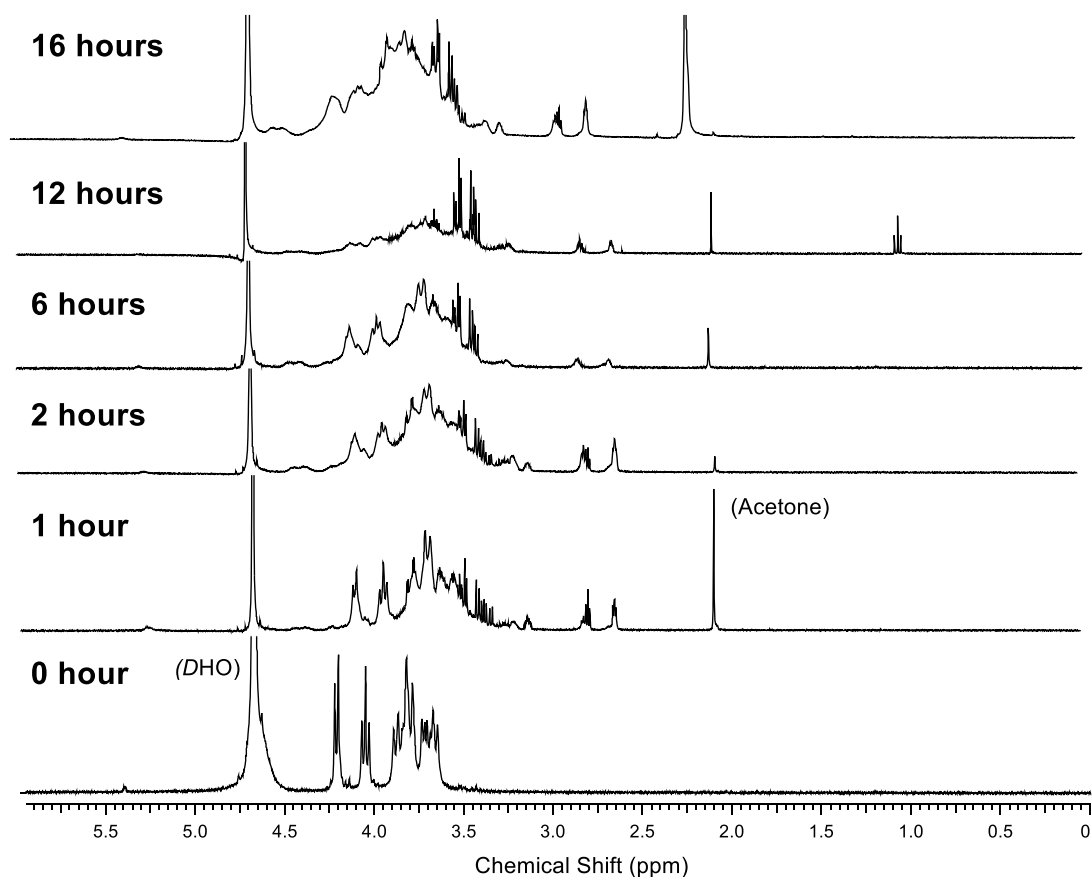


Figure 52 - The ^1H NMR spectra of the reaction between Inulin and epichlorohydrin at different periods of time (D_2O , 400 MHz)

The rate at which resolution of the spectrum is lost is significantly slower than that of IDX (Figure 49), suggesting that intra Inulin cross-linking occurs at a reduced rate. Additionally, at 16 hours, epoxide peaks are still visible. Indicating that only partial cross-linking has occurred, which explains why the conjugation reaction still proceeded at 16 hours. When the structure of IDX and Inulin are compared (Figure 53) the reason for the difference in the rate of cross-linking is clear. The main difference between IDX and Inulin, aside from the number of carbon atoms in their rings, is that IDX is a branched polymer whereas Inulin is more akin to a linear polymer. We suggest that the structure of IDX, through its α (1,6) branching increases its propensity to cross-link with itself because of neighbouring sugar units being held in close proximity.

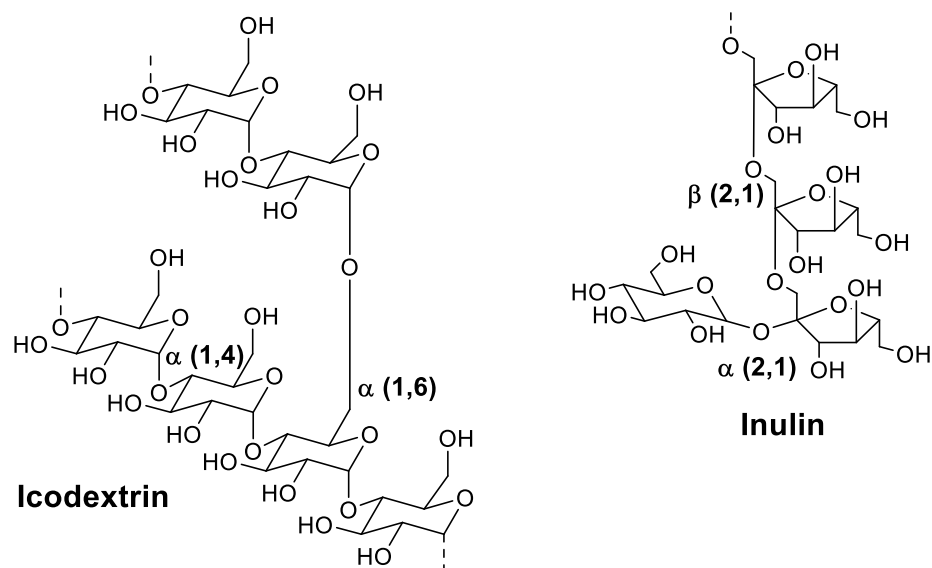


Figure 53 - The structure of IDX and Inulin

3.5 Final reaction optimisation

A further modification was made to the procedure used to make the Inulin Conjugate **31**: instead of leaving Inulin to react with epichlorohydrin for 16 hours, the time would be reduced to 80 minutes (the conditions would otherwise be kept the same). This resulted in the successful conjugation of ether **44** to Inulin, however the loss of resolution observed (by ^1H NMR) in conjugate **31** (using a 16-hour activation time) was reduced. It was felt that this would make conjugates produced with Icodextrin and Inulin more comparable, as they should have similar levels of crosslinking, which would be beneficial for their biological evaluation.

Before the conjugation methodology for IDX and Inulin could be finalised, there was one additional factor to be resolved. As mentioned earlier in this Chapter, for every conjugation reaction attempted with both IDX and Inulin, a multiplet at approx. 1.05-1.20 ppm was visible (Figure 51, for example). In the case of Conjugate **31**, this was initially explained by the TIPS protection group being retained post conjugation. Elemental analysis showed a much higher percentage of nitrogen than could arise from the drug, a likely culprit for the increase in nitrogen was felt to be triethylamine: used in the conjugation reaction (though it did not match its associated reference data).²¹³ A solution to this problem was found by using a different base. On a small scale, potassium carbonate was substituted for triethylamine (the conjugation reaction conditions were otherwise kept the same). The resulting conjugate

showed no indication of the aforementioned peak, and also demonstrated the removal of the TIPS group, exposing the carboxylic acid. This modification was also applied to IDX, which satisfyingly, saw the disappearance of the multiplet.

3.6 Synthesis of IDX and Inulin drug conjugates, optimised conditions

With the optimised conjugation condition conditions in hand, work began on the synthesis of IDX and Inulin drug conjugates for biological evaluation. Using the optimised conditions, 1.2 eq. of ether **44** was reacted with EPI-INU in the presence of K_2CO_3 .

An equivalent is defined as being relative to the number of moles of polysaccharide used in the reaction, determined by the molecular weight of the equivalent monosaccharide (IDX = 161 g / mol, INU = 162 g / mol).

After the material had been dialysed, it was analysed by 1H NMR spectroscopy (Figure 54).

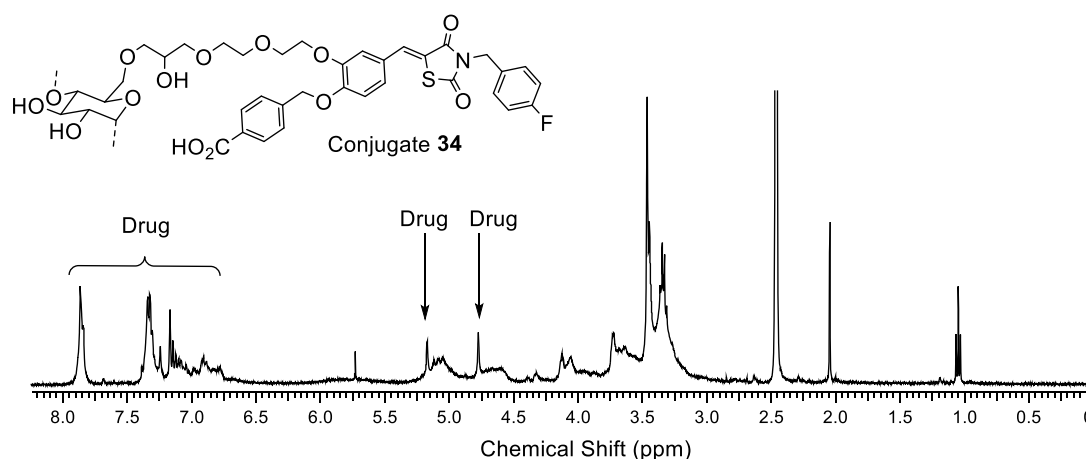


Figure 54 - The 1H NMR spectrum of Conjugate **34** ($DMSO-d_6$, 400 MHz)

As can be seen in Figure 54, a significant amount of compound **44** was incorporated within IDX. The same methodology was then applied to Inulin, the material was then analysed by 1H NMR spectroscopy (Figure 55).

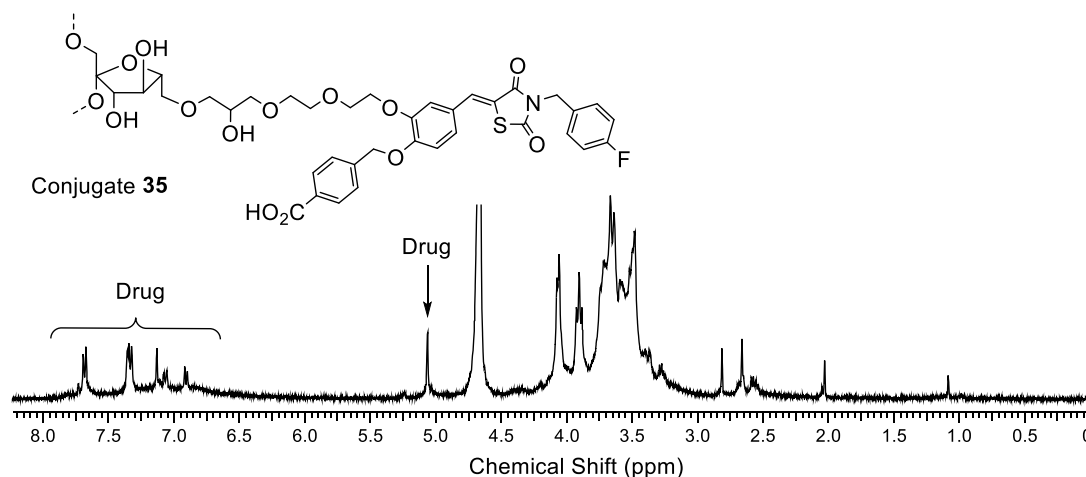


Figure 55 -The ^1H NMR spectrum of Conjugate **35** (D_2O , 400 MHz)

The spectrum in Figure 55 showed the incorporation of drug onto Inulin. An additional purification step was used from Conjugate **34** onwards. It was found that the polymer conjugates precipitated in a 1:1 mixture of DMF / acetone whilst the drug material stayed in solution. The liquid was decanted, the procedure was then repeated 10 times. The advantage to this method is the free-drug is completely removed from the mixture before it is dialysed, ensuring that no free-drug material is present in the final product.

3.7 Drug loading study

Now that the versatility of the epichlorohydrin activation method had been proven for both Inulin and IDX, it was decided that to complement this study conjugates with different drug loadings would be investigated. Conjugates of different drug loadings are of interest because differing drug concentrations may result in a change in biological activity. The results of this study can be exploited to enhance the design of polymer-drug conjugates.

Starting with Inulin, the number of equivalents of ether **44** used in the conjugation reaction were varied. Using the original 1.2 eq. as a starting point, the following equivalents of drug were investigated: 1.7, 0.8, 0.5 and 0.3 eq., otherwise the conditions were kept the same. It was hoped that by varying the amount of the drug available to react with EPI-INU the degree of substitution of the drug bound to the polymer could be manipulated. Each polymer conjugate was purified as previously described and then analysed by ^1H NMR spectroscopy (Figure 56).

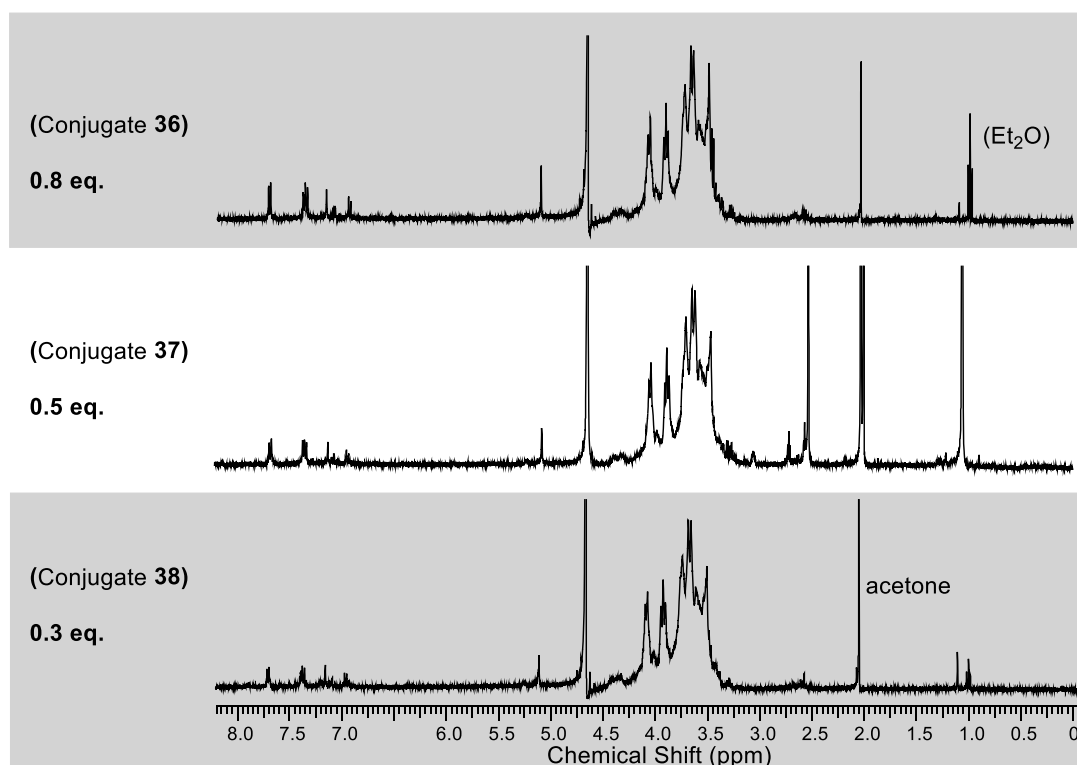


Figure 56 - The ^1H NMR spectra of Conjugates **36**, **37** and **38** (D_2O , 400 MHz)

The drug loading of Inulin was successfully manipulated by changing the number of equivalents of drug used in the conjugation reaction. However, when the number of equivalents were increased to 1.7 (Conjugate **39**) from 1.2 eq., there was no change in the amount of drug attached (by comparing the relative integration of the drug peaks to Inulin peaks for each conjugate). Therefore, using between 0.8 - 1.2 eq. of ether **44** in the conjugation reaction gave the maximum amount of drug that can be attached to Inulin, using the epichlorohydrin activation method.

A series of conjugates with decreasing drug loadings were then made with IDX, using: 0.8, 0.5 and 0.3 equivalents of ether **44**. The results of this study are shown in Figure 57.

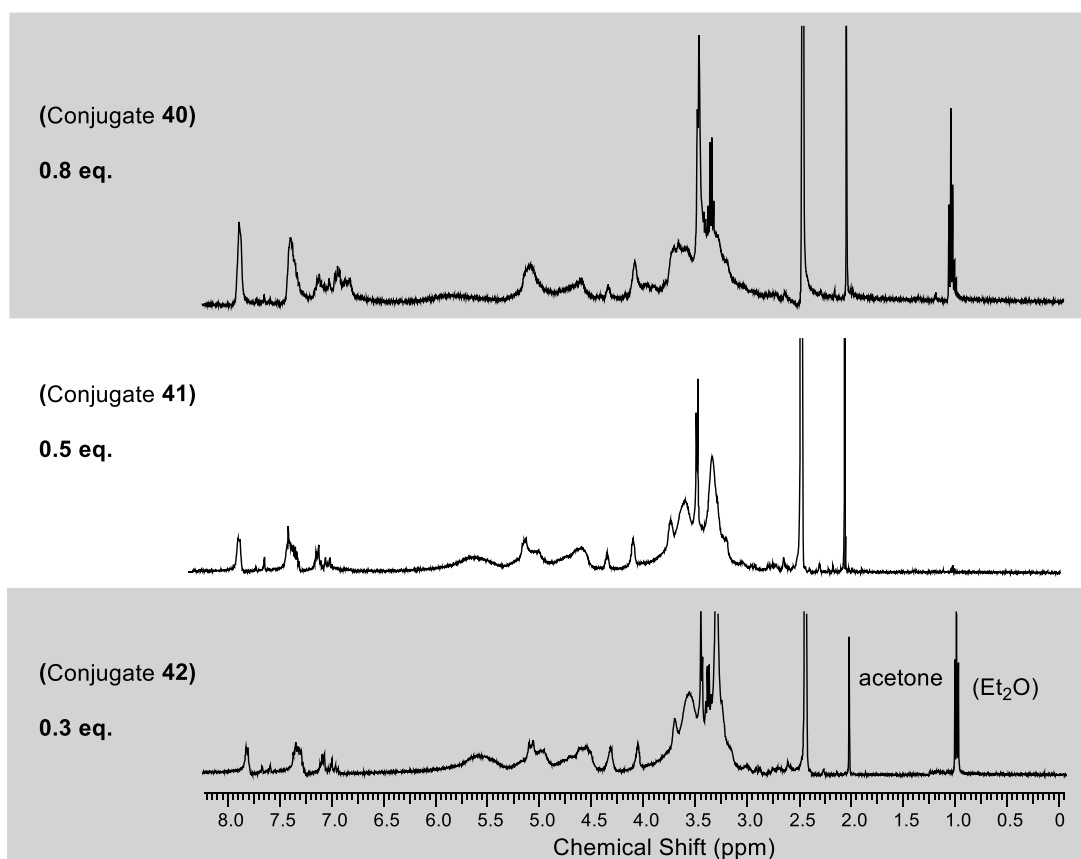


Figure 57 - The ^1H NMR spectra of Conjugates **40**, **41** and **42** (DMSO- d_6 400 MHz)

3.7.1 Quantification of drug loading: determining the degree of substitution (DS)

The quantity of drug present in the polymer conjugates and degree of substitution was then calculated for each material. A convenient method for quantification of the drug was found in microanalysis. Ether **44** possesses one nitrogen, EPI-IDX or EPI-INU have no nitrogen content. Therefore, the amount of nitrogen, determined by elemental analysis, will relate directly to the amount of drug material present within the polymer conjugate. Each drug-conjugate was analysed by elemental analysis, then using an equation adapted from a publication by Domb and co-workers (Equation 1) the degree of substitution was calculated.²¹⁴

$$DS = \frac{M_{SU} \times \%N}{(M_N \times 100) - (M_{DRUG} \times \%N)}$$

Equation 1 - Equation to calculate the degree of substitution (DS), M_{SU} = Molecular weight of saccharide monomeric unit, M_N = molecular weight of nitrogen, M_{DRUG} = molecular weight of drug

The results of this study are shown in Table 7 and Table 8.

Conjugate	Number of eq. of drug (44)	% N (By elemental analysis)	DS (degree of substitution)	% of drug in conjugate
35	1.2	1.74	0.68	70%
36	0.8	1.35	0.35	55%
37	0.5	1.30	0.32	52%
38	0.3	1.16	0.25	47%
EPI-INU	-	<0.1	-	0%

Table 7 - Table to show the degree of substitution for Inulin drug conjugates

Conjugate	Number of eq. of drug (44)	% N (By elemental analysis)	DS (degree of substitution)	% of drug in conjugate
34	1.2	1.80	0.76	73%
40	0.8	1.50	0.44	61%
41	0.5	1.38	0.36	56%
42	0.3	1.13	0.24	46%
EPI-IDX	-	<0.1	-	0%

Table 8 - Table to show the degree of substitution for IDX drug conjugates

3.8 Synthesis of a highly crosslinked Icodextrin drug-conjugate

While it has previously been stated that intra polymer cross-linking would likely have a negative effect on activity, this may not be the case from a pharmacokinetics standpoint. IDX crosslinked “bridges” may provide a non-hydrolysable barrier to attack from α -amylase, increasing its residence time in the peritoneal cavity. Additionally, if inter IDX cross-linking occurs between different IDX polymer chains, then one could anticipate a large increase in molecular weight from the standard weight of 13-19 kDa. This attribute has been shown to be beneficial to the retention of a material in the peritoneal cavity.¹³²

By purposely designing an IDX drug conjugate with increased crosslinking, it will allow the effect of cross-linking on biological activity to be studied and the influence that it has on peritoneal retention to be evaluated.

To synthesise a highly crosslinked drug-conjugate, the conjugation procedure was modified. 1 eq. of epichlorohydrin was reacted with IDX for two hours. EPI-IDX was isolated by precipitation then immediately reacted with ether **44** for two days. The drug conjugate was isolated by precipitation in 1:1 acetone / DMF, reacted with 3 eq. of epichlorohydrin for 18 hours and then isolated by dialysis. The results of this study are shown in Figure 58.

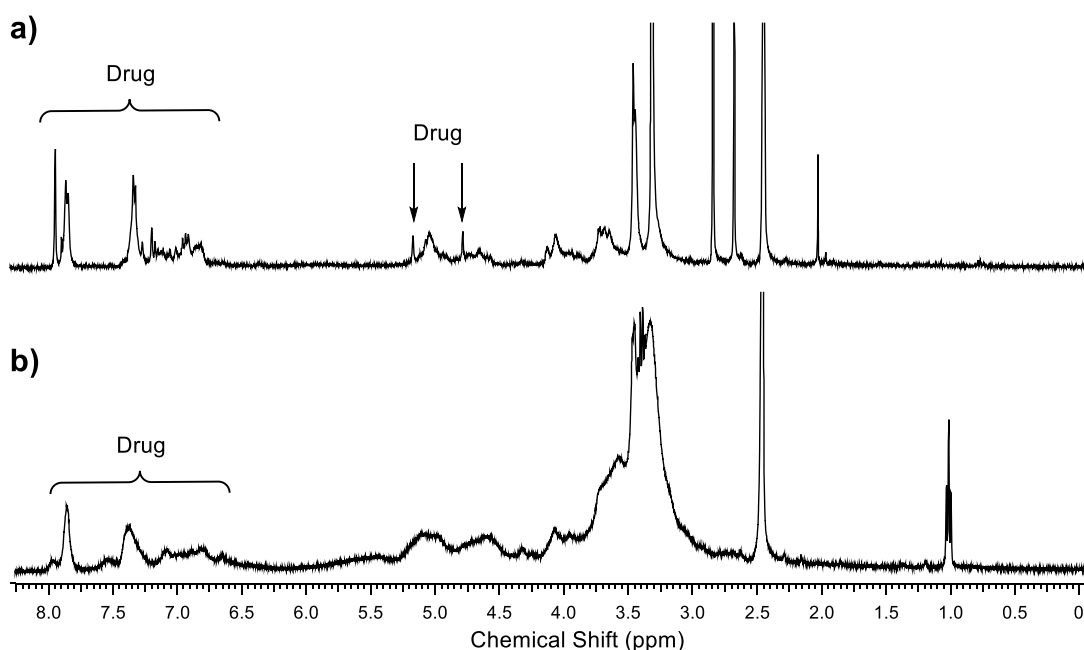


Figure 58 ^1H NMR spectra comparison of a) Conjugate **43** b) Conjugate **43** after treatment with 3 eq. of epichlorohydrin (DMSO- d_6 , 400 MHz)

Conjugate **43** DS = 0.2

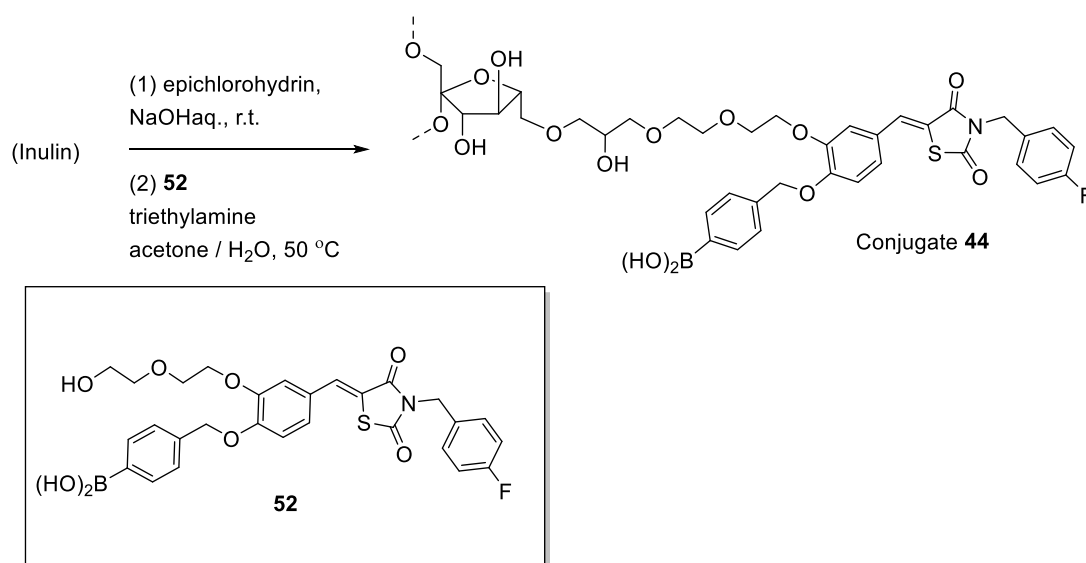
There is a clear difference in structure between Figure 58 a) and b). Following the addition of epichlorohydrin (3 eq.) the spectrum of Conjugate 43 loses much of its structural definition, becoming considerably less resolved than any conjugate previously synthesised. This was interpreted that the polymer was highly cross-linked.

3.9 Boronic acid ATX inhibitor IDX / Inulin conjugates, using the epichlorohydrin method

In Chapter 2 a number of different methods were attempted with the aim of attaching an ATX inhibitor containing a boronic acid moiety to IDX and to Inulin (Chapter 3). It was postulated that these boronic acid ATX inhibitors would be significantly more potent than the carboxylic-acid containing drug used in our previous investigation.⁴² Despite these efforts, a suitable method for the conjugation of boron-containing drug-linker analogues was not found. However, as stated in Chapter 2, it was hypothesised that one of the possible reasons for the lack of success was because the boronic acid group may interact with itself and form a boroxine anhydride and/or react with the polysaccharide support itself. It was felt that these side reactions would be detrimental to the conjugation reaction. This effect may have been potentiated by the conjugation reaction being performed under anhydrous conditions, which in the absence of water would push the equilibrium towards forming anhydrides, and reactions with the polysaccharide.

It was decided that the epichlorohydrin activation method would be used to attempt to attach boronic acid **52** (a drug-linker analogue of the potent ATX inhibitor HA155) to IDX and Inulin. It was thought that the reaction conditions used for the epichlorohydrin activation method may overcome the obstacles previously encountered in the attempted conjugation reactions. This is because the epichlorohydrin method uses an acetone / H₂O co-solvent system. The presence of water in the reaction mixture may help to push the equilibrium back to the boronic acid, so the drug linker can react with the epoxide residues present on each polymer.

EPI-INU was reacted with 1.2 eq. of boronic acid **52** for two days (Scheme 68).



Scheme 68 - The synthesis of Conjugate **44**

The material was worked-up and dialysed, as previously described, then analysed by ^1H NMR spectroscopy, the results of which are shown in Figure 59.

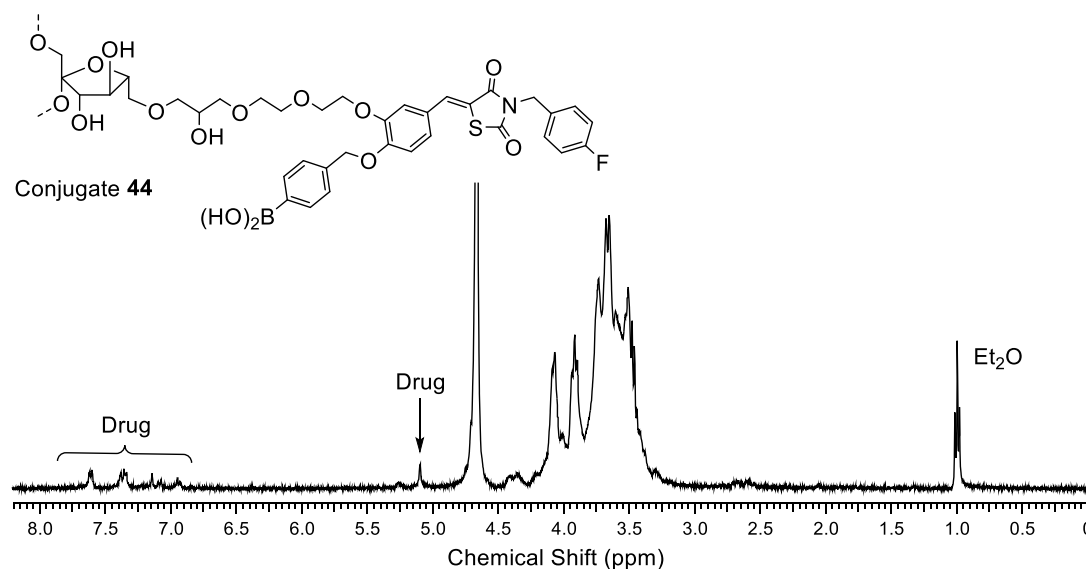


Figure 59 - The ^1H NMR spectrum of Conjugate **44** (D_2O , 400 MHz)

DS (Conjugate **44**) = 0.2

Pleasingly the reaction proceeded smoothly, with boronic acid **52** reacting with EPI-INU, albeit at a lower degree of substitution than the equivalent carboxylic acid drug conjugate (Conjugate **35**).

The method was then applied to Icodextrin, using the same conditions and number of equivalents of boronic acid **52**. The material was worked-up and dialysed as previously described, then analysed by ^1H NMR spectroscopy (Figure 60).

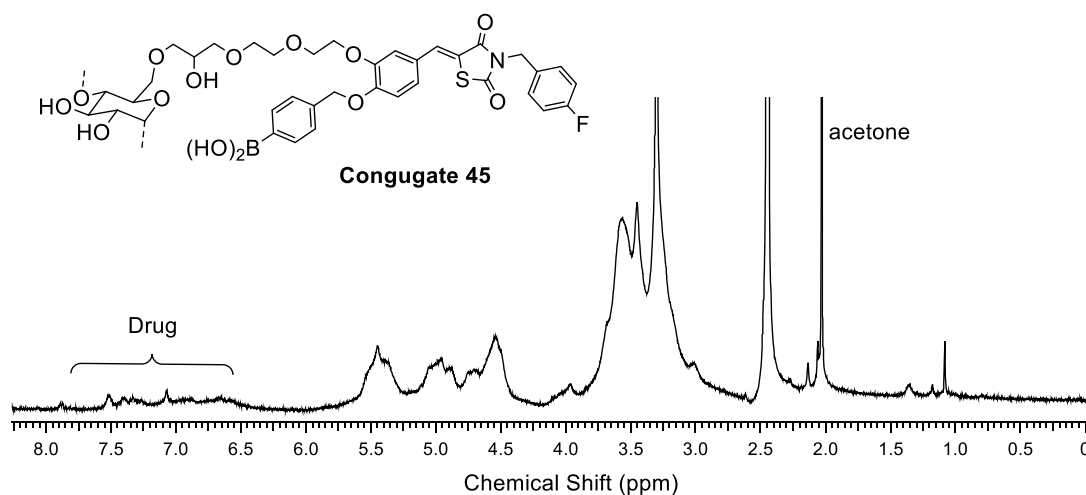


Figure 60 - ^1H NMR spectrum of Conjugate **45** (DMSO- d_6 , 400 MHz)

DS (Conjugate **45**) = 0.07

As can be seen in Figure 60, the reaction appears to have been successful, indicating that boronic acid **52** had been conjugated to IDX. The DS value for Conjugate **45** is quite low. However, when the many unsuccessful attempts to attach boronic acid compounds to IDX are considered, it is still a notable achievement. Additionally, with a DS value of 0.07, 22% of the conjugate (by mass) corresponds to the drug, which is not insignificant considering the low nanomolar potency of the parent drug.

3.9.1 Synthesis of boronic acid “free-drug”

The 11 drug conjugates synthesised *via* the epichlorohydrin method were then evaluated for biological activity (Chapter 4). As per our previous work, the conjugates would be tested against a non-polymeric equivalent of the parent drug (Figure 61).

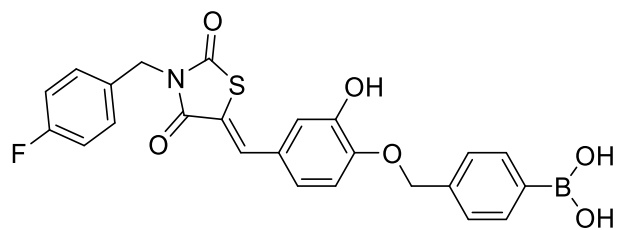
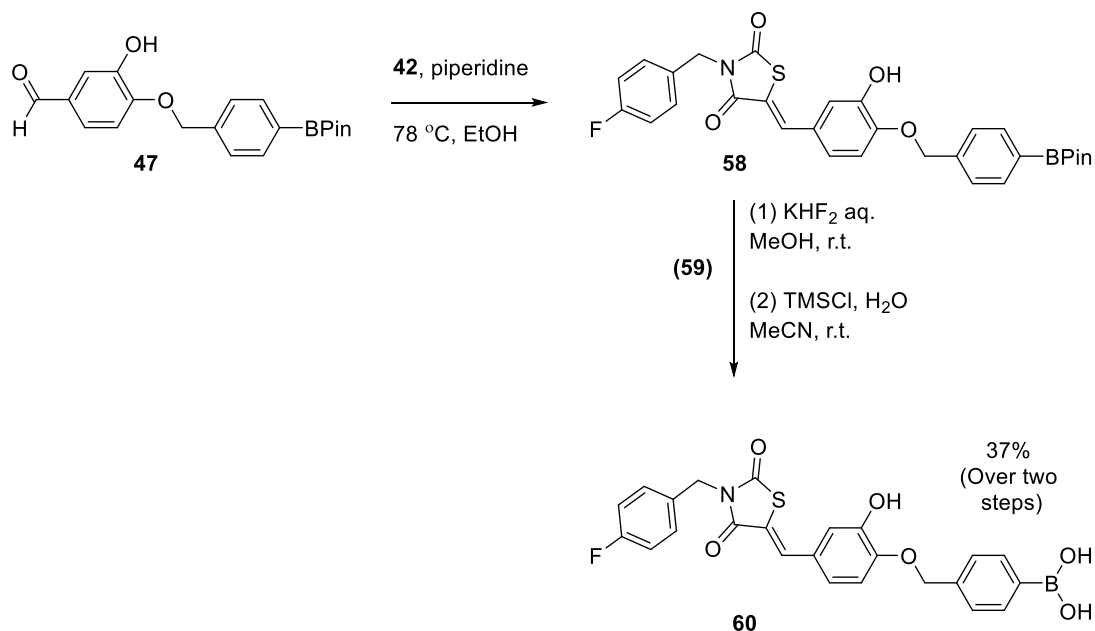


Figure 61 - The "free-drug" target

A hydroxyl group was included at the position usually occupied by the linker unit, this was seen as an effective way to mimic the drug-linker compound in its "free-form".

The free-drug was synthesised to provide a comparison between the free drug and the drug-conjugate. In the case of observed activity, this will indicate any loss in potency which results from the attachment of the drug to a polymer. From a pharmacokinetics standpoint it will provide a reference for the residence time of the free-drug within the peritoneal cavity, to demonstrate the effect of conjugation on peritoneal retention.

The boronic acid "free-drug" was synthesised in six synthetic steps, boronate ester **47** was reacted with heterocycle **42** in a Knoevenagel condensation, to give boronate **58**. Boronate **58** was converted to its BF_3K salt **59**, then hydrolysed to the corresponding boronic acid to give the target compound (Scheme 69).



Scheme 69 – Synthesis of boronic acid **60**

The free drug was synthesised with a respectable overall yield of 8 %, and was tested alongside the drug conjugates, when they were evaluated for biological activity (Chapter 4).

3.10 Attempted conjugation of GLPG 1690 to IDX and Inulin

3.10.1 Introduction

With the epichlorohydrin activation method now proven to be an effective and versatile approach to the formation of drug-polymer conjugates, in the final stage of this project our attention was drawn to a recently published autotaxin inhibitor: GLPG 1690 (Figure 62). As mentioned in Chapter 1, this drug is of interest for two reasons: it is the only autotaxin inhibitor to enter clinical trials (to date) and second, it displays an alternative binding mode compared to the ATX inhibitors previously studied (3BoA and HA155) which would complement our investigation.^{65,67}

By examining the X-ray crystal structure of GLPG 1690 bound to ATX, a suitable position for attachment was determined (Figure 62).⁶⁷ The hydroxyazetidide terminus is not reported to have a significant role in the binding of GLPG 1690 to ATX, so is an ideal location for the diethylene glycol linker unit to be attached.⁶⁷

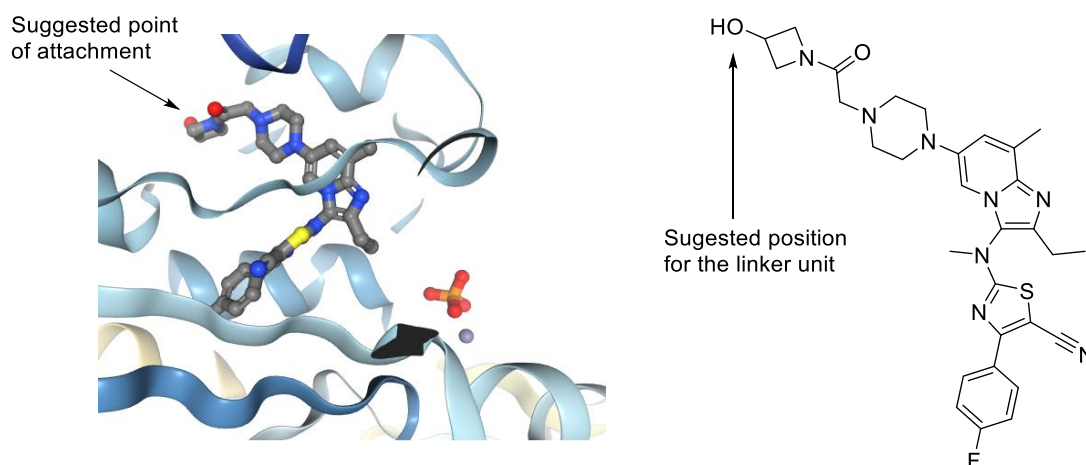


Figure 62 - The crystal structure of GLPG 1690 bound to ATX and the position determined for the attachment of a linker unit.⁶⁷

From a synthetic perspective, GLPG 1690 is an attractive substrate from which a drug-linker analogue can be made, this is because the drug can be synthesized as per its literature

preparation and then as the final synthetic step the linker unit can be installed. This means that the drug-linker analogue of GLPG 1690 (Figure 63) should be synthesised with relative ease.

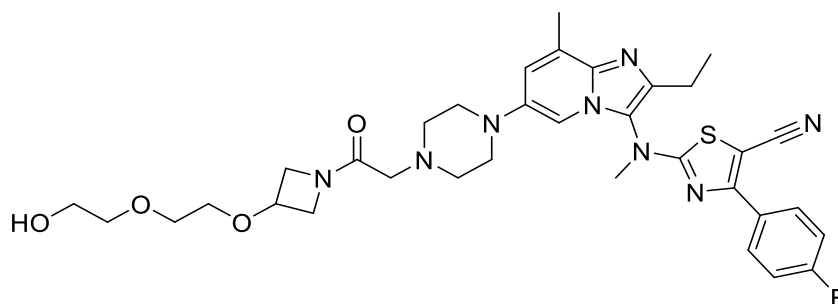
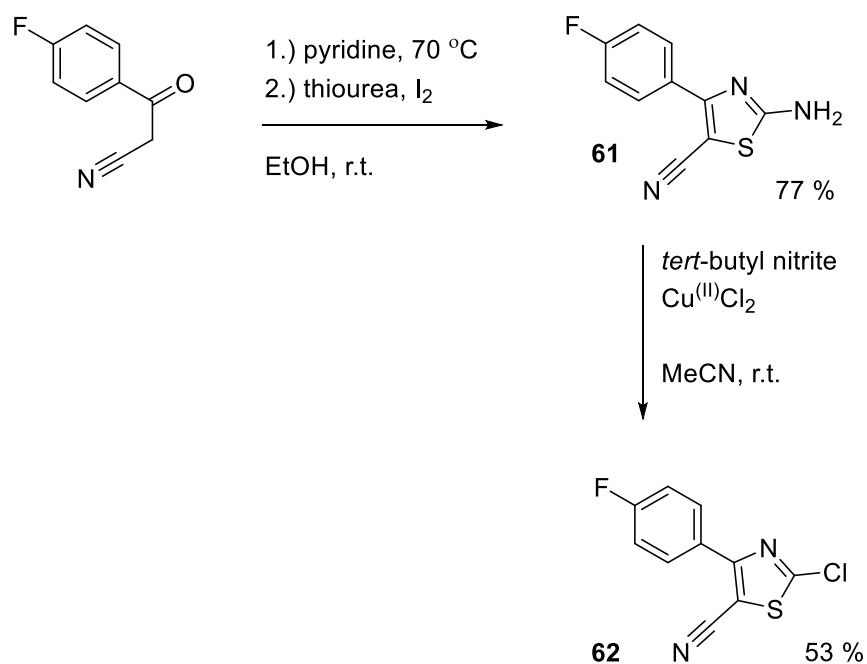


Figure 63 - Target compound: GLPG 1690 linker-analogue

3.10.2 Synthesis of GLPG 1690

3.10.2.1 Fragment 1

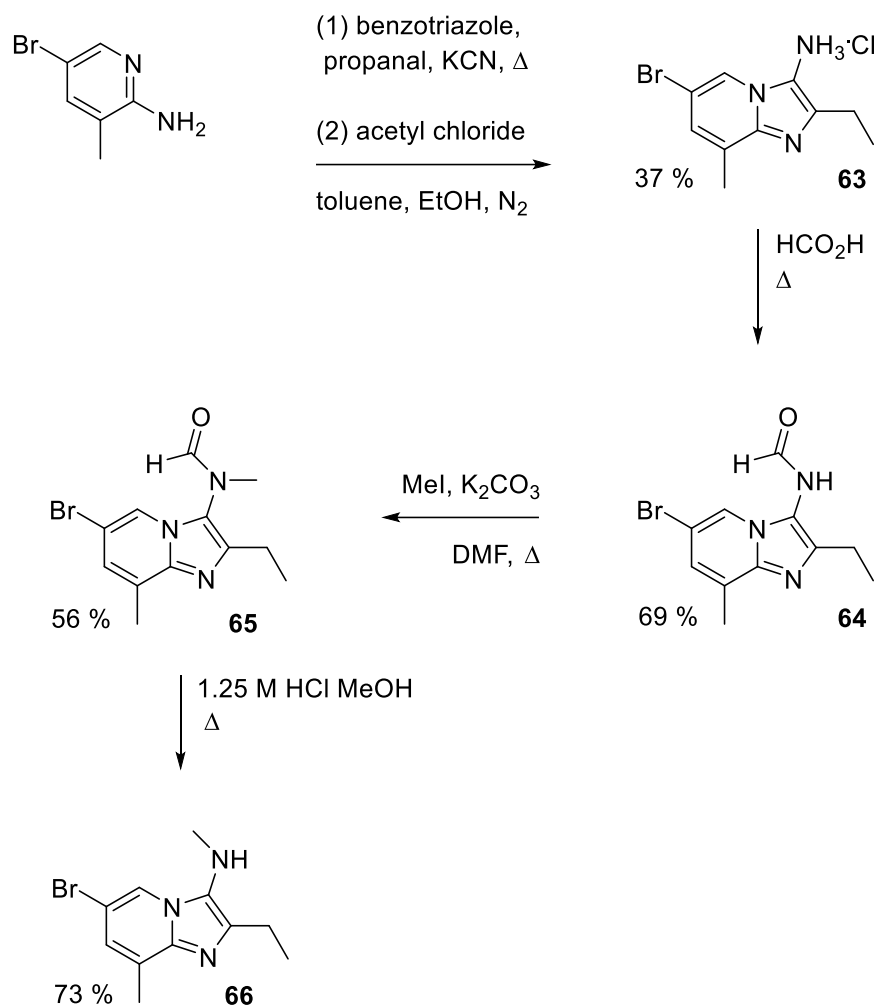
GLPG 1690 was synthesised according to the procedure outlined in the original publication by Heckman and co-workers, although it is worthy of note that some of the procedures required modification for the stated reaction to be reproducible in our hands. The synthetic route employed a divergent strategy using three fragments. The first fragment was synthesised in two synthetic steps (Scheme 70). The formation of the thiazole component proceeded *via* the cyclisation of thiourea and the aromatic ketone in the presence of iodine. Amine **60** was then converted to a chloride, through the Sandmeyer reaction, following treatment with *tert*-butyl nitrite and CuCl_2 and dilute HCl aq.^{215,216}



Scheme 70 – The synthesis of chloride **62**

3.10.3 Synthesis of fragment 2

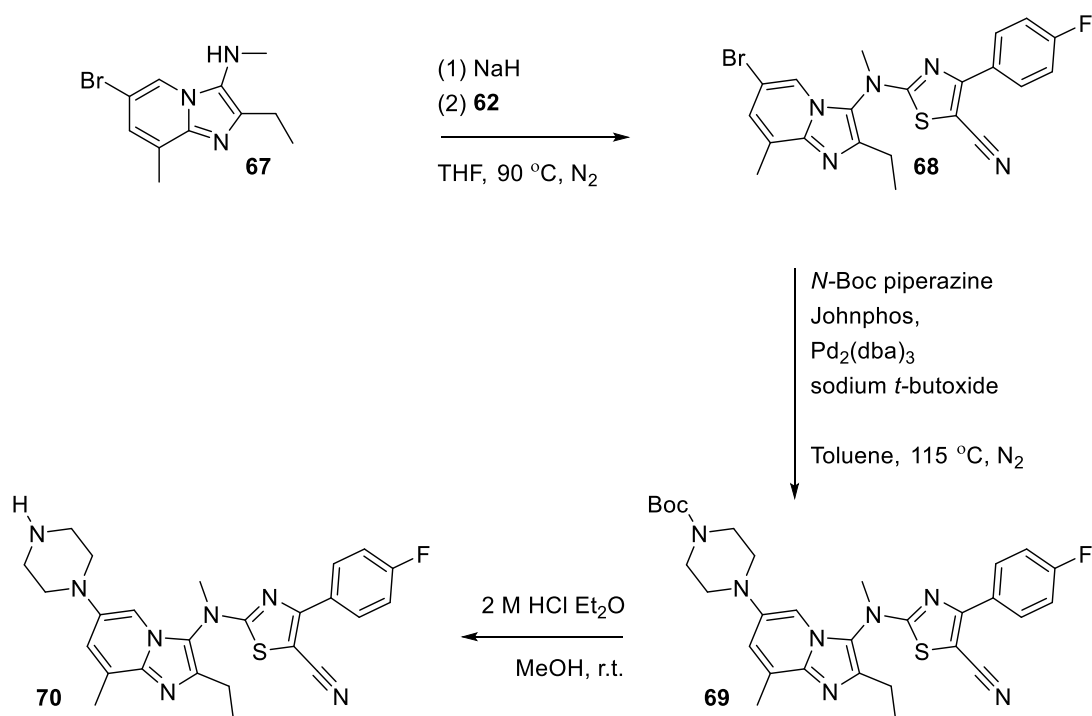
With chloride **62** in hand, work then proceeded towards the synthesis of the second fragment with the first synthetic step involving a multi-component Groebke-Blackburn-Bienayme reaction (Scheme 71).^{217,218} Amine **63** was then stirred in neat formic acid to give the corresponding amide **64**, which was then methylated, using methyl iodide and potassium carbonate. Amide **65** was then converted to its corresponding amine.



Scheme 71 - The synthesis of amine **66**

3.10.4 Coupling reaction between amine **66** and chloride **62** and proceeding transformations

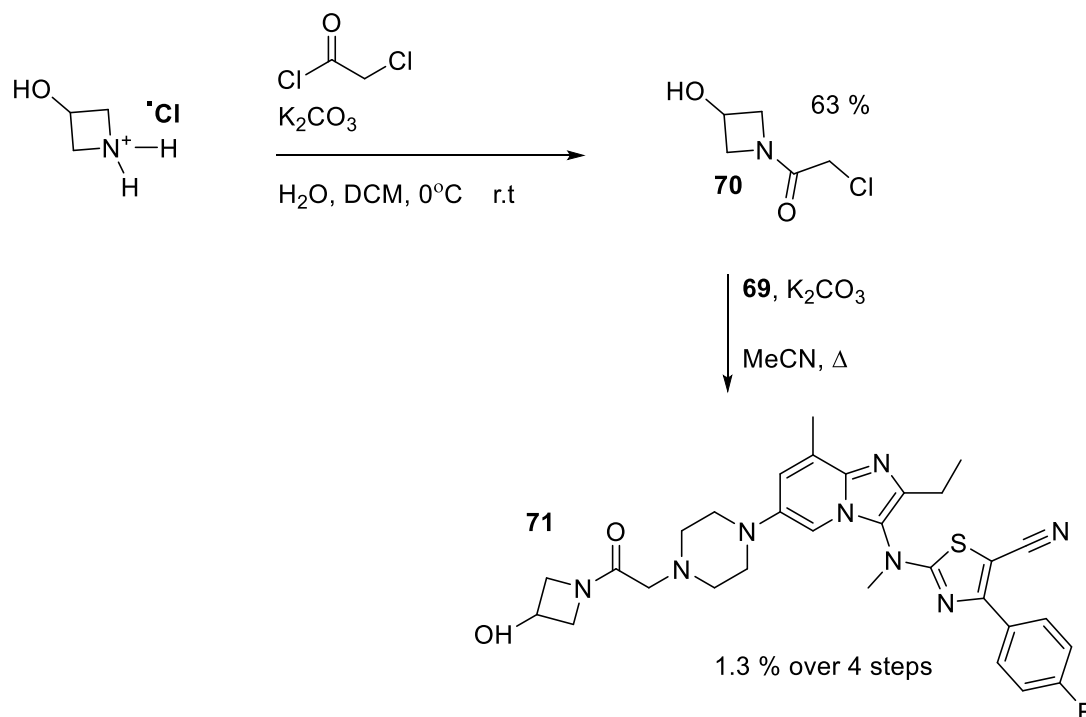
Fragments **62** and **66** were then coupled together by an S_NAr displacement, in the presence of sodium hydride, heterocycle **67** then underwent a Buchwald-Hartwig coupling with *N*-Boc piperazine. The Boc protecting group was then removed from *N*-Boc piperazine **68** using ethereal HCl (Scheme 72).



*Scheme 72 - Synthesis of heterocycle **70** (material carried through to the next step without isolation)*

3.10.5 The preparation of fragment 3 and synthesis of GLPG 1690

GLPG 1690 (Compound **71**) was prepared by reacting azetidine hydrochloride with 2-chloroacetyl chloride, in the presence of potassium carbonate. Azetidine **70** was then reacted with piperazine **69** in a S_N2 reaction to give GLPG 1690 (Scheme 73).

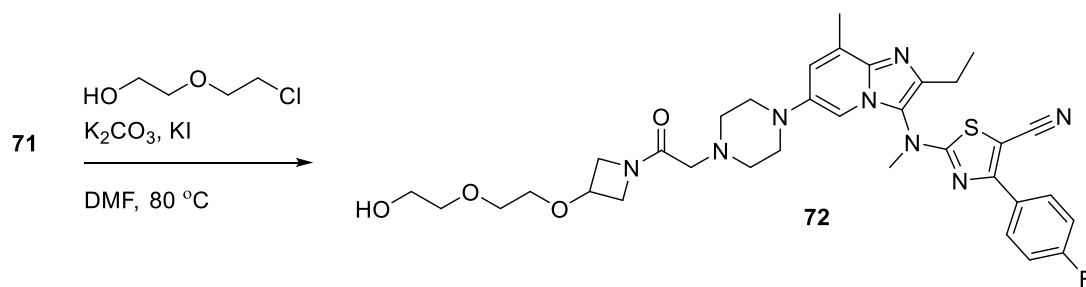


Scheme 73 - The synthesis of GLPG 1690 (Compound 71)

GLPG 1690 (**Compound 71**) was synthesised over 12 synthetic steps, with the longest linear sequence using 8 steps. The overall yield was very low at 0.14 %, however this was caused by the low return in material following the Buchwald Hartwig coupling. This significantly affected the subsequent synthetic steps. Had the reaction been repeated the conversion could possibly have been improved. Notwithstanding this, a small amount of GLPG 1690 was available to evaluate if a linker group can be directly attached to its hydroxyazetididine terminus.

3.11 Attempted attachment of a diethylene glycol linker to GLPG 1690

In line with our previous work, 2-(2-chloroethoxy)ethanol was reacted with GLPG 1690 (**Compound 71**) in the presence of K_2CO_3 and KI (Scheme 74).



*Scheme 74 - Shows the attempted linker addition to GLPG 1690 (Compound **71**)*

Disappointingly, there was little evidence to show that the reaction had been successful. The crude material was very polar, making column chromatography with normal phase silica gel difficult. Had the reaction been repeated, a more suitable approach may be to attach the linker to fragment 3 (azetidine **70**) prior to the coupling reaction in Scheme 73. Time constraints towards the end of this research project prevented the further development of a GLPG 1690-linker analogue and so the study was not pursued any further.

3.12 Summary of Chapter 2 and 3

The attachment of drug-linker analogues of ATX inhibitors containing boronic acid groups to Icodextrin and Inulin is an extremely challenging undertaking, and reasons for the difficulties encountered have been suggested. Despite this, a novel conjugation method developed during this project has allowed the synthesis of boronic acid ATX inhibitor polymer conjugates. From the work described in Chapters 2 and 3, eleven testable drug polymer conjugates have been prepared using two alternative polymer supports (IDX and Inulin) and using two separate drug-linker series. These novel polymer conjugates and their free-drug counterparts were then evaluated for biological activity, using enzyme assays and for peritoneal retention studies, animal models. This work is described in Chapter 4.

Chapter 4:

The biological evaluation of novel
ATX inhibitor-IDX and ATX inhibitor-
Inulin drug conjugates

Chapter 4: The biological evaluation of novel ATX inhibitor-IDX and ATX inhibitor-Inulin drug conjugates

4.1 Introduction

Resulting from the work described within Chapters 2 and 3, eleven drug conjugates were prepared for biological evaluation. This study involved both *in vitro* and *in vivo* investigations and provided significant information regarding the efficacy of the drug conjugate approach explored throughout this thesis. Of particular interest to us was the biological activity of the drug conjugates, as one might anticipate a loss in activity of the drug following polymeric attachment. Additionally, there was some concern that the intra-polymer cross linking that occurs as a consequence of the conjugation reaction may lead to a further reduction in activity. An effective method from which to assess the activity of the conjugates was therefore required. It was decided that two separate enzyme assays would be used to evaluate conjugate activity, the key reason for this is that the assays will use two sources of ATX, one commercial and the other obtained in-house. These assays have been used to evaluate the activity of drug conjugates in our previous work in this area and additionally have been widely used in the literature.^{73,78,147,219–222}

The second part of our biological investigation was an animal study in which the peritoneal retention of an Inulin-drug conjugate would be measured in mice. This was the first time that the residence time of Inulin in the peritoneal cavity had been compared to IDX and would allow us to determine which polymer offers superior peritoneal retention. The study also had the potential to provide a valuable insight into how a drug-polymer conjugate may perform in the human body.

4.2 Autotaxin inhibition assays

The enzyme assays used in this investigation are known as “artificial substrate assays” in which a substrate mimicking LPC, containing a phosphodiester bond, is used in place of LPC. It is then assumed that ATX will hydrolyse the material in the same manner as LPC because of the substrate’s structural similarity.²¹⁹ The concentration of the hydrolysed substrate can then be measured by fluorescence or absorbance spectroscopy. It follows that the amount

of hydrolysed material produced is a measure of the enzyme's activity and in the presence of an inhibitor will be reduced. Over the last decade there have been many artificial substrate assays developed, such as a fluorescence probe developed by Nagano and co-workers. However, for this study we chose the two most widely used, which will assist in comparing the results to other studies.^{88,219}

4.2.1 Bis(*para*-nitrophenyl) phosphate (Bis-*p*NPP) artificial substrate assay

Bis-*p*NPP is understood to be hydrolysed in the same manner as LPC (Chapter 1). A product of this reaction is the chromophore: *p*-nitrophenol the concentration of which can be measured at 405 nm by absorbance spectroscopy (Figure 64). Therefore, the concentration of the hydrolysis product (*p*-nitrophenol) provides a useful indication as to the activity of ATX and in the presence of an inhibitor. This was done by measuring the absorbance of *p*-nitrophenol in the presence of a drug conjugate, which was used to determine the IC₅₀ value for each material.

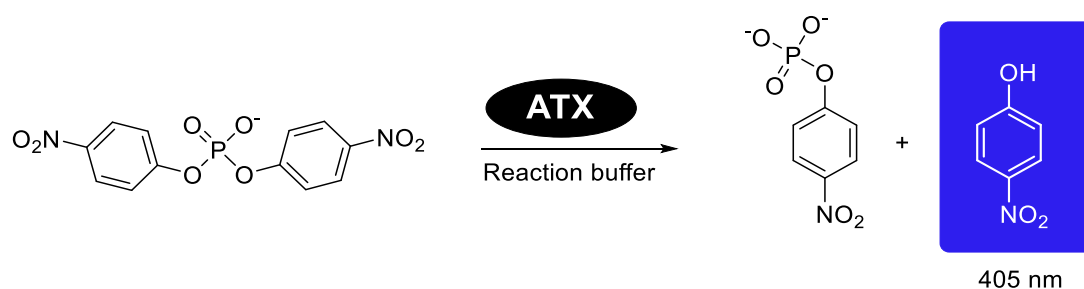


Figure 64 - The hydrolysis of bis-*p*NPP by ATX

Recombinant ATX, obtained from 3E3 cells that were genetically engineered to overexpress ATX, was purified by passing the material through a Sepharose column, and then dialysed. The drug conjugates were diluted to a concentration appropriate to their predicted activity in distilled water. A 3-fold dilution series was then prepared (final concentration = 0 µg / mL, well H = distilled water). A solution of autotaxin, reaction buffer, bis-*p*NPP and conjugate at its respective concentration were mixed in a 96-well plate and incubated for 4 hours at 37 °C. The absorbance of the plate was measured at a wavelength of 405 nm, and the resulting data were analysed using Graph Pad Prism software. Non-linear regression was used to fit a 4 parameter (Hill equation) dose-response curve to determine the IC₅₀ value for each

conjugate. The free drug equivalents of each inhibitor were also analysed in this manner, as well as samples of the “parent” Icodextrin and Inulin (150 µg / mL) polymers and it was found that they no inhibitory action on ATX. Each experiment was repeated a minimum of 3 times for each conjugate / free-drug, on separate days, using different batches of purified ATX.

4.2.1.1 Dose response curves for Bis-pNPP

The dose response curves obtained for each sample tested are featured in Figure 65 and Figure 66.

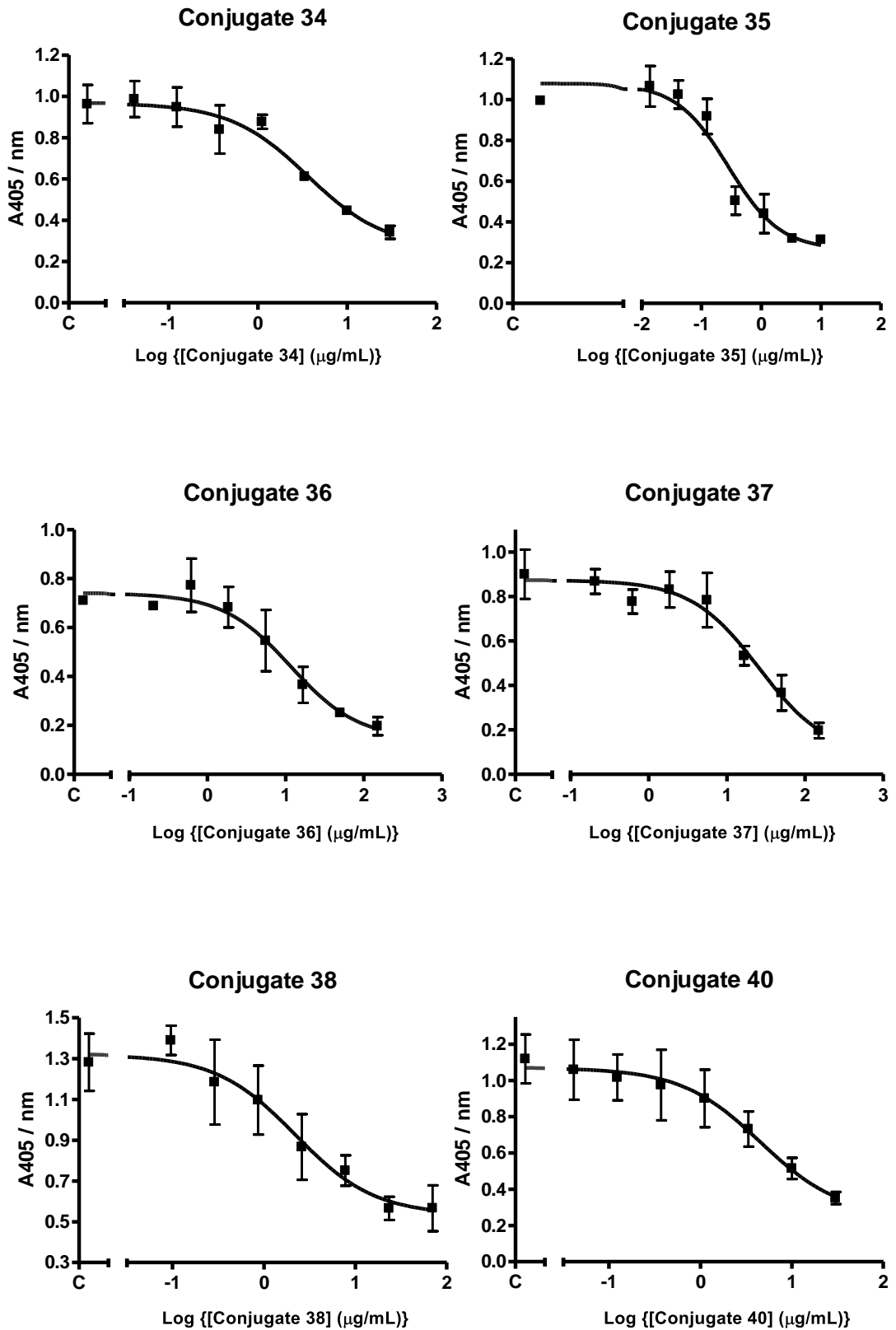


Figure 65 - Shows the dose response curves for Conjugates 34-40

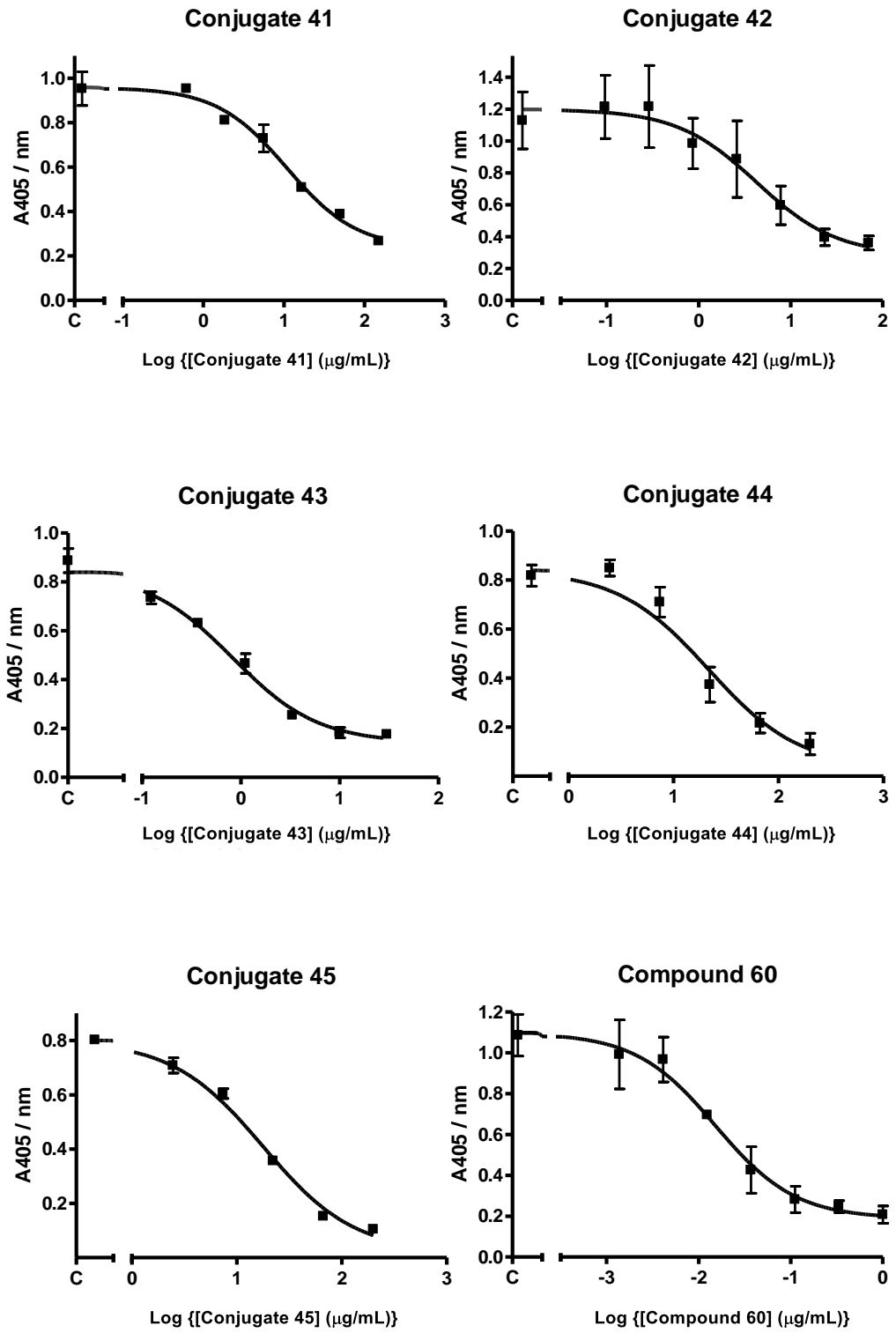


Figure 66 - Shows the dose response curves for Conjugates 41-45 and Compound 60

4.2.1.2 Bis-pNPP assay results

The IC₅₀ values determined for the Icodextrin-drug conjugates (Figure 67) are shown in Table 9.

Sample	IC ₅₀ / $\mu\text{g mL}^{-1}$ (n=3)	Degree of substitution / DS
Conjugate 34	3.22 ± 0.15	0.76
Conjugate 40	4.41 ± 1.21	0.44
Conjugate 41	12.41 ± 1.33	0.36
Conjugate 42	4.45 ± 1.43	0.24
Conjugate 43 (High cross-linking)	0.70 ± 0.29	0.20
Conjugate 45	16.92 ± 1.79	0.07
Icodextrin	0	n / a

Table 9 - Shows the results of the bis-pNPP assay for IDX-drug conjugates

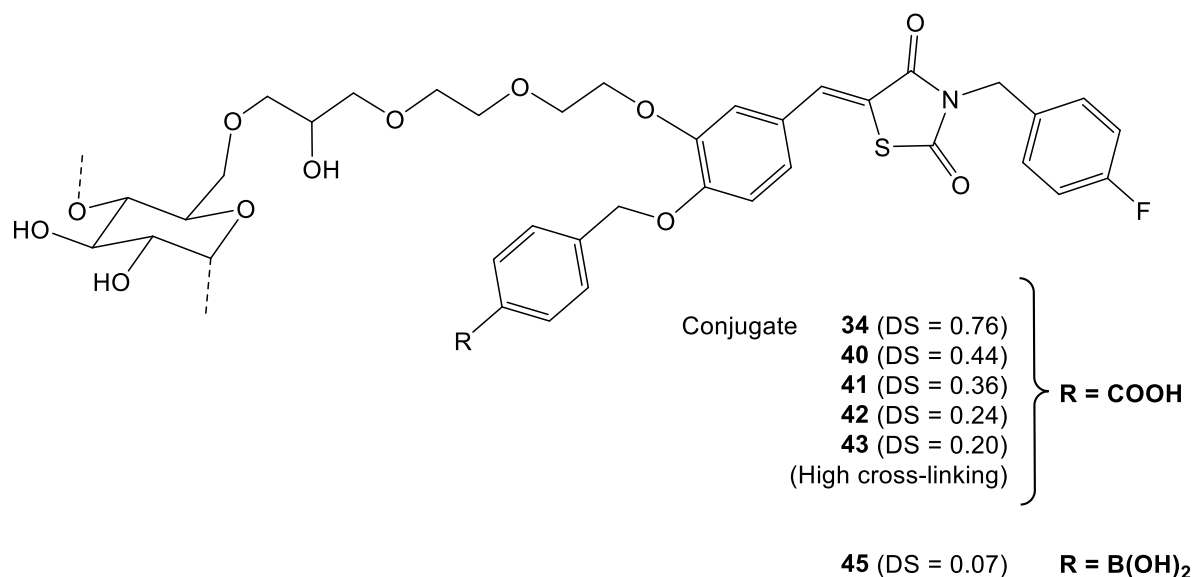


Figure 67 - Diagram to show the structure of each conjugate that was tested

The IC₅₀ value of compound **60** "free-drug" (Figure 68) was 0.019 ± 0.008 $\mu\text{g} / \text{mL}$ or 39.67 ± 16.70 nM

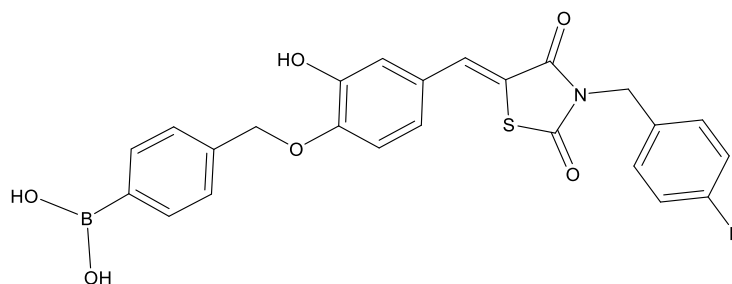
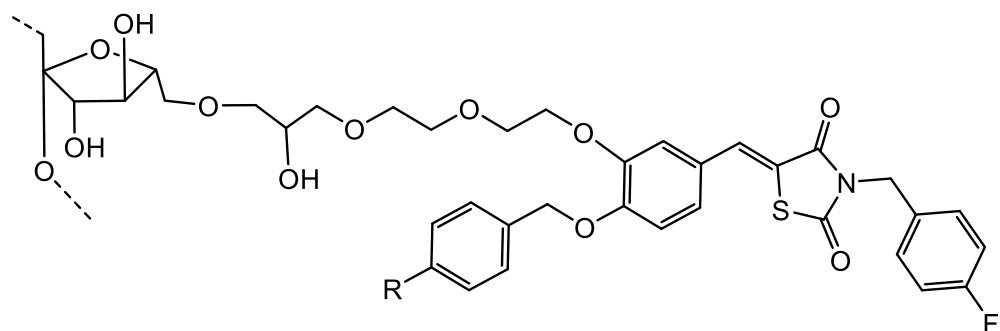


Figure 68 – Boronic acid **60**

The IC₅₀ values for the Inulin-drug conjugates (Figure 69) were then calculated (Table 10)

Sample	IC ₅₀ / $\mu\text{g mL}^{-1}$ (n=3)	Degree of substitution / DS
Conjugate 35	0.30 ± 0.04	0.68
Conjugate 36	22.35 ± 1.51	0.35
Conjugate 37	23.88 ± 2.45	0.32
Conjugate 38	3.14 ± 0.45	0.25
Conjugate 44	21.88 ± 1.28	0.20
Inulin	0	n / a

Table 10 - Shows the results of the bis-pNPP assay for Inulin conjugates



Conjugate	35 (DS = 0.68)	} R = COOH
	36 (DS = 0.35)	
	37 (DS = 0.32)	
	38 (DS = 0.25)	
	44 (DS = 0.20)	R = B(OH)₂

Figure 69 - Diagram to show the structure of each Inulin conjugate that was tested

Additionally, both Icodextrin and Inulin were found to have no measurable inhibitory action on ATX, at 150 $\mu\text{g} / \text{mL}$.

4.2.2 Fluorogenic substrate-3 (FS-3) artificial substrate assay

FS-3 artificial substrate assays are a widely used and convenient method for screening potential autotaxin inhibitors. They are commercially available as an enzyme assay kit from Echelon biosciences Inc.^{40,220,221,223} In a similar manner to bis-*p*NPP, FS-3 closely mimics the structure of LPC. Following the hydrolysis of its phosphodiester bond a fluorophore “tag” is released which can then be detected at 485 nm excitation / 528 nm emission, as shown in Figure 70. Additionally, the FS3-3 substrate has a quenching tag at the “choline terminus”. The FS-3 assay has a number of advantages over bis-*p*NPP; for example, the substrate is designed to mimic the structure of LPC. As can be seen in Figure 71, the substrate is of a similar length to LPC and contains linear alkyl chains, it is therefore anticipated to adopt a similar binding mode to LPC in the active site of ATX. Rather than simply measuring the rate of hydrolysis of a phosphodiester bond (in the case of the bis-*p*NPP assay), the FS-3 substrate

should realistically depict the rate of hydrolysis of LPC and provide a more representative value for the inhibitory potential of each conjugate.

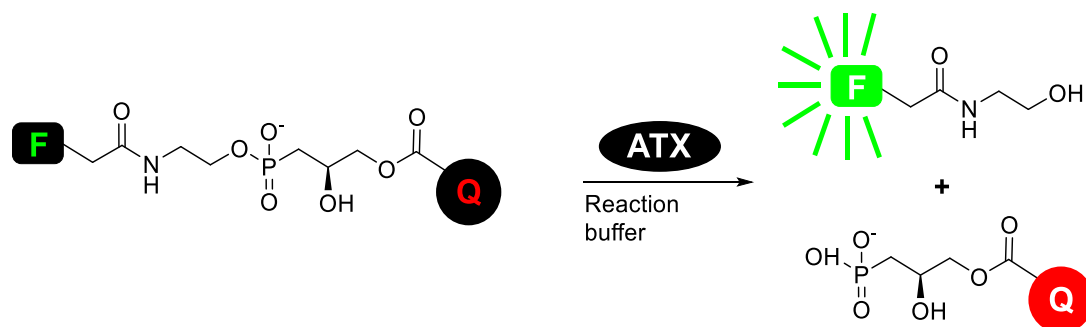


Figure 70 - The hydrolysis of FS-3 by ATX

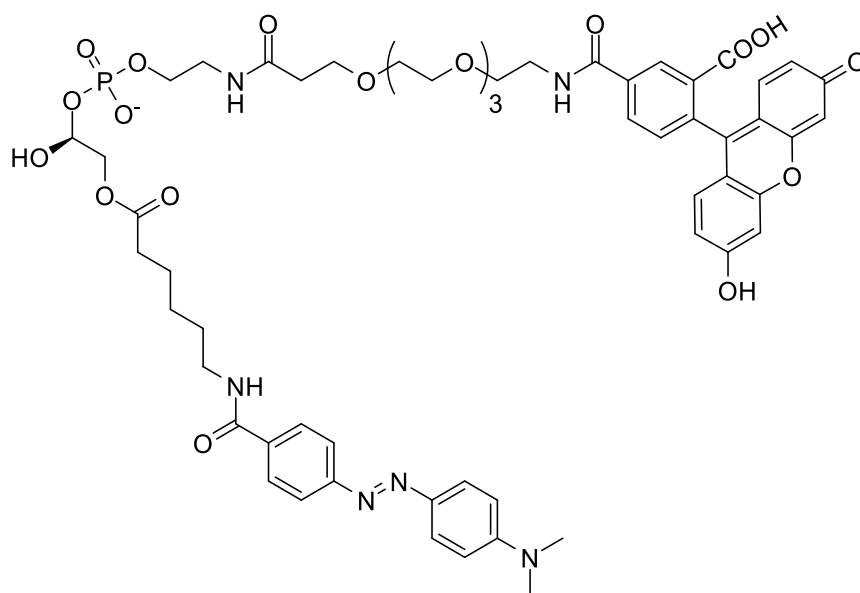


Figure 71 - The structure of FS-3²²³

The drug conjugates were diluted to a concentration appropriate to their predicted activity in distilled water and a 3-fold dilution series was prepared. The assay was then performed as follows: ATX (supplied by Echelon) as a solution in reaction buffer was mixed with the drug-conjugate (at each concentration of the dilution series), in a 96-well plate. A solution of FS-3 substrate was then added to each well. The fluorescence was then read immediately ($\lambda_{\text{Ex}} = 485 \text{ nm}$, $\lambda_{\text{Em}} = 528 \text{ nm}$) and every two minutes thereafter, for 30 minutes in total (at room temperature). Fluorescence for each concentration was plotted as a function against time. A linear regression was then fitted to the graph. Non-linear regression was then used to fit a 4 parameter (Hill equation) dose-response curve to the rate of reaction for each concentration in order to determine the IC₅₀ value for each conjugate. An internal replicate was used for

each drug-conjugate analysed. Each experiment was repeated a minimum of three times (n=3) over multiple days. A secondary screen was performed with each conjugate to ensure the fluorescence reading was not a false positive due to interference with the fluorescence of hydrolysed FS-3. The results of this study are shown in Figure 72 and Figure 73.

Owing to restrictions on the number of compounds that could be assayed, using the results obtained from the bis-*p*-NPP assay only the 8 most promising candidates were carried forward to this assay; thus Conjugates **36**, **37**, **40** and **41** were omitted from this study.

4.2.2.1 FS-3 Dose response curves

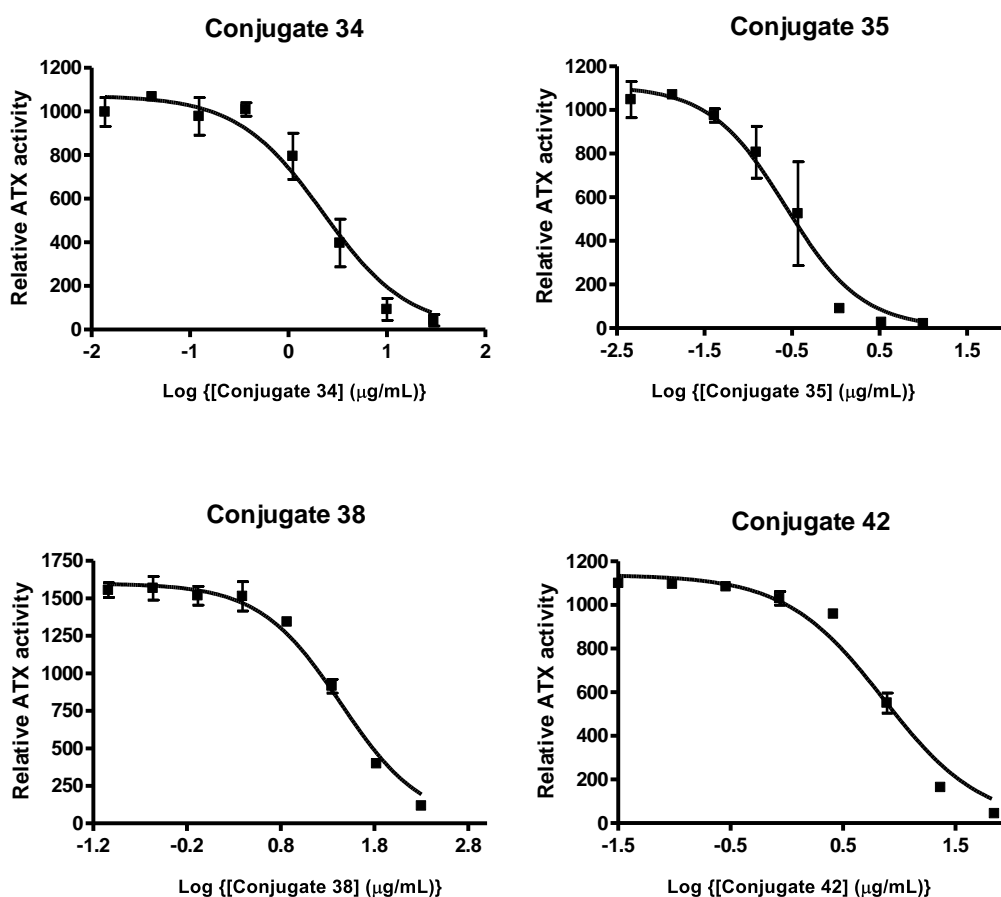


Figure 72 - The dose response curves for Conjugates **34-35**, **38** and **42**, obtained via the FS-3 artificial substrate assay

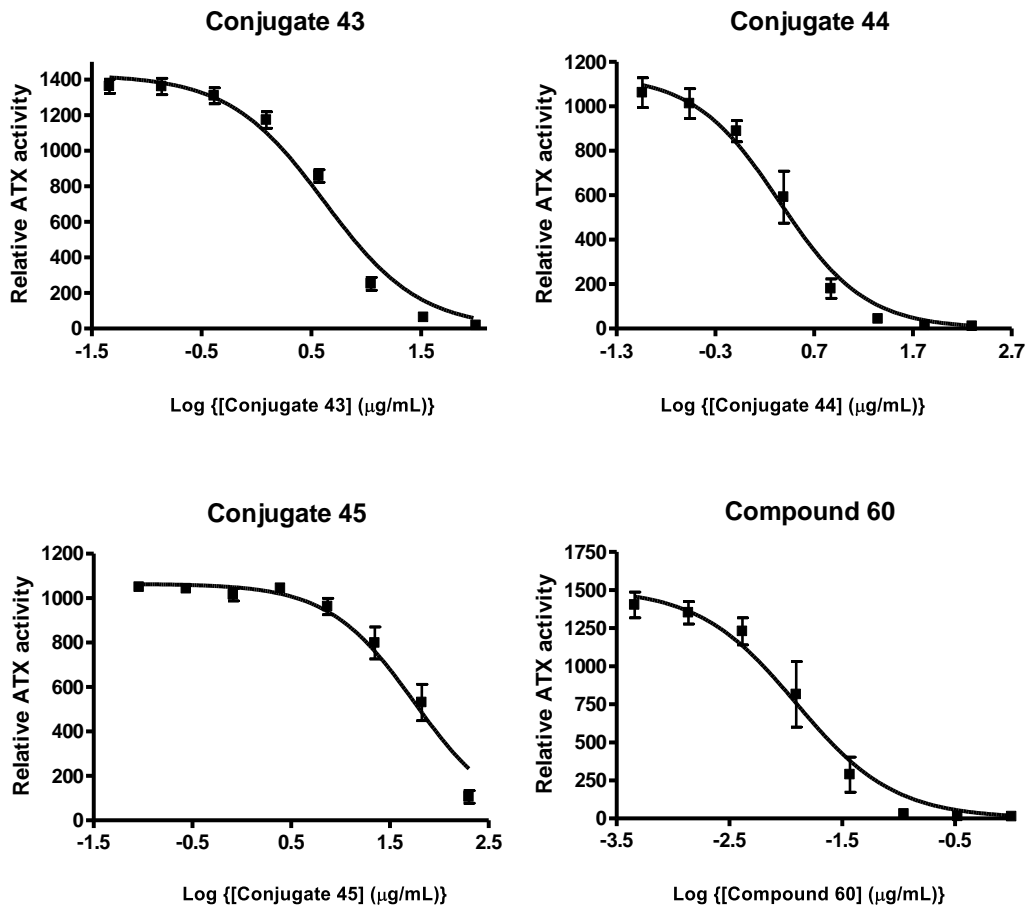


Figure 73 - The dose response curves for Conjugates **43-45** and compound **60**, obtained via the FS-3 artificial substrate assay

4.2.2.2 FS-3 assay results

The mean IC₅₀ values (n=3), and standard deviation for this assay are shown in Table 11.

Sample	IC ₅₀ / $\mu\text{g mL}^{-1}$ (n=3)	Degree of substitution / DS
Conjugate 34	2.00 \pm 0.78	0.76
Conjugate 42	6.89 \pm 0.92	0.24
Conjugate 43	4.18 \pm 0.56	0.20
Conjugate 45	53.60 \pm 8.02	0.07
Conjugate 35	0.24 \pm 0.18	0.68
Conjugate 38	30.51 \pm 6.35	0.25
Conjugate 44	2.42 \pm 1.15	0.20
Compound 60	0.014 \pm 8.02 (29.33 \pm 14.61 nM)	n/a

Table 11 - Shows the IC₅₀ values for samples assayed using the FS-3 substrate (pink = IDX, blue = Inulin)

The structure of each conjugate / drug is shown in Figure 67, Figure 68 and Figure 69.

4.3 Discussion of results

Pleasingly, as can be seen from the IC₅₀ values featured in Table 9, Table 10 and Table 11, the drug-linker analogues retained a significant level of potency when attached to Inulin and IDX. The data obtained from the bis-*p*NPP assay (Table 9 and Table 10) appears to be in agreement with those from the FS-3 assay (Table 11), with the same trends observed within the data replicated in each Table. There is of course, some slight difference in the activity for each compound across each assay, however this is negligible considering the difference in substrate specificity, therefore the two assays provide a useful assessment of the ATX inhibitory potential of each conjugate.

The most active Icodextrin conjugate (prepared using the standard epichlorohydrin activation method), was Conjugate **34** (Figure 74) which had an IC_{50} value of $3.22 \pm 0.15 \mu\text{g mL}^{-1}$ (Bis-pNPP).

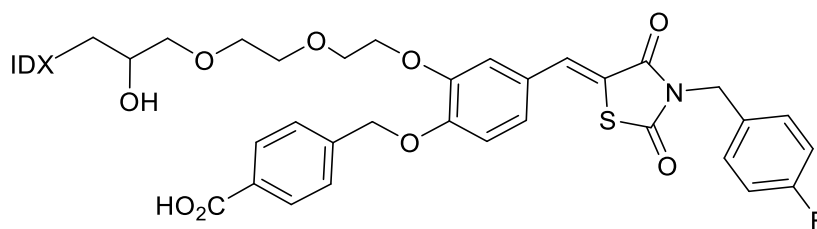


Figure 74 - Conjugate **34**

The most potent drug conjugate produced in this study was one prepared from Inulin, Conjugate **35** (Figure 75), which had an activity of $0.30 \pm 0.04 \mu\text{g mL}^{-1}$ and is the most potent drug conjugate synthesised by us to date.

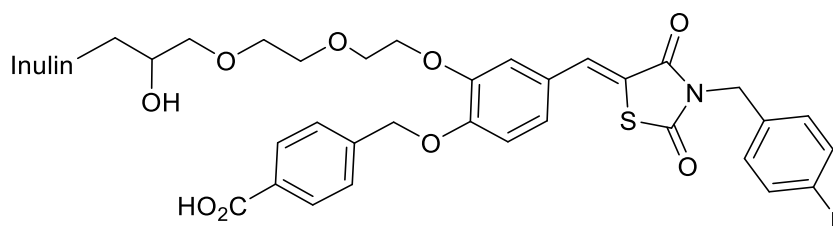


Figure 75 - Conjugate **35**

With regards to the carboxylic acid-functionalised inhibitor used in this study, the activity obtained by the corresponding Conjugate **35** (Figure 75), is at the upper-limit of what could be expected, considering that the activity of the "model" free drug (Figure 76) is stated to be $0.14 \pm 0.08 \mu\text{g mL}^{-1}$.¹⁴⁷

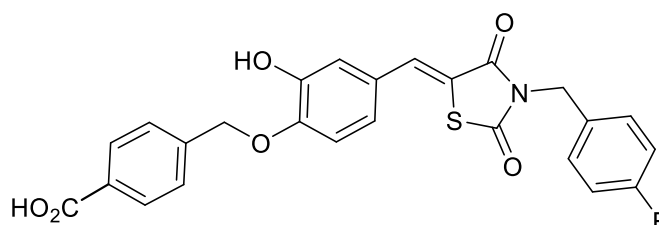


Figure 76 - Carboxylic acid "free-drug"

To achieve even greater potencies in the future, alternative ATX inhibitors should be investigated. The likely reason for the differences in potency between Conjugate **34** (IDX) and Conjugate **35** (Inulin) (Figure 74 and Figure 75 respectively) is that despite having comparable degree of substitution (DS) values, there is a difference in structure between the two polymers. As explained previously, IDX is highly branched whereas Inulin is more “linear”. This could make the drug molecules bound to Inulin more accessible to the active site of ATX.

The HA155-polymer conjugates (Conjugates **44** and **45**, Figure 77) incorporated a boronic acid group, when compared to a corresponding carboxylic acid moiety, also performed satisfactorily in both assays.

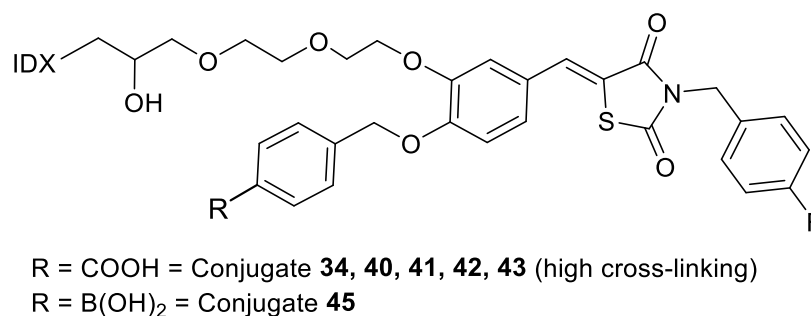


Figure 77 - Conjugate **44** and **45**

Of the two conjugates, Conjugate **44** (Figure 77) appeared to be the more potent, with an IC₅₀ value of 2.42 ± 1.15 µg mL⁻¹ (FS-3). Though if the potency of the model “free drug” (compound **60**, Figure 68) is considered (0.014 ± 0.007 µg mL⁻¹, FS-3) then the drug has lost a significant amount of activity, post conjugation. This could be explained by the low drug loading of the two conjugates; however, as explained in the next paragraph, a low DS value may not necessarily lead to a reduction in potency. A more subtle reason may be (as stated in Chapter 2) that the boronic acid group of the drug is able to react with the hydroxyl groups present on each polymer, in the same manner as “glucose sensing biomaterials” featured in the literature.²⁰¹ This reversible interaction may compete with that of ATX and the inhibitor, giving rise to the reduced potency observed in Conjugate **44** (Figure 77), compared to the free drug (Figure 68). In the future, if drug loading cannot be improved by reaction optimisation, potentially a more potent HA155-polymer conjugate could be prepared by synthesising a highly-crosslinked version as per Conjugate **43** (Figure 81), which would, in effect “cap-off” any free hydroxyl groups present on the polymer.

4.3.1 The effect of drug loading on activity

4.3.1.1 Introduction

The most intriguing part of the biological activity study is revealed when the effect of drug loading on activity is examined; for clarity, the results have been re-tabulated in Table 12 and Table 13, the structure of each conjugate is shown in Figure 78 .

Icodextrin

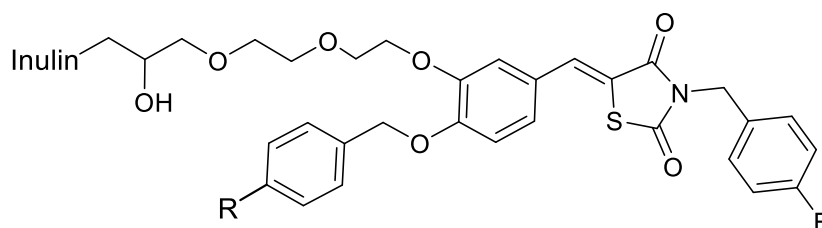
Sample	Degree of substitution (DS)	IC ₅₀ / $\mu\text{g mL}^{-1}$ (n=3)
Conjugate 34	0.76	2.00 \pm 0.78
Conjugate 40	0.44	4.41 \pm 1.21
Conjugate 41	0.36	12.41 \pm 1.33
Conjugate 42	0.24	4.45 \pm 1.43

Table 12 - Icodextrin drug-loading study results

Inulin

Sample	Degree of substitution (DS)	IC ₅₀ / $\mu\text{g mL}^{-1}$ (n=3)
Conjugate 35	0.68	0.30 \pm 0.04
Conjugate 36	0.35	22.35 \pm 1.51
Conjugate 37	0.32	23.88 \pm 2.45
Conjugate 38	0.25	3.14 \pm 0.45

Table 13 - Inulin drug-loading study results



R = COOH = Conjugate **35, 36, 37, 38**

R = B(OH)₂ = Conjugate **44**

Figure 78 - The structure of each IDX and Inulin conjugate prepared for this study

Inspection of Table 12 and Table 13, showed an interesting and unexpected trend: as the degree of substitution decreases then activity decreases, as would be anticipated. However, as the DS further decreases the activity increases again - this trend is demonstrated across both polymer series, as shown in Figure 79.

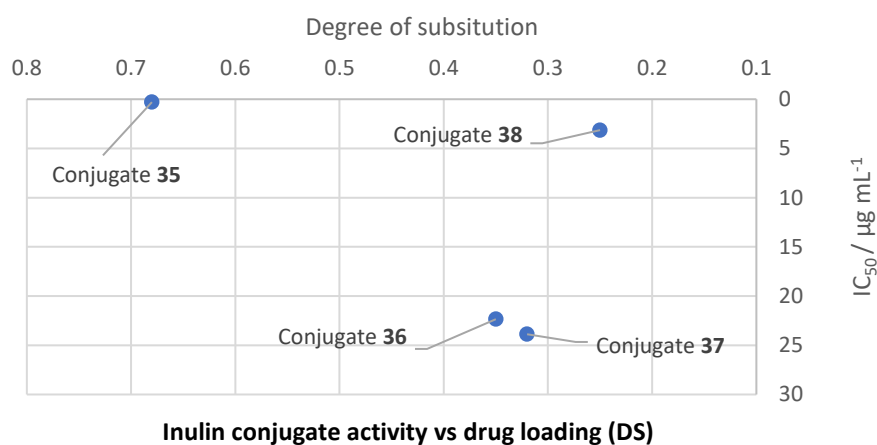
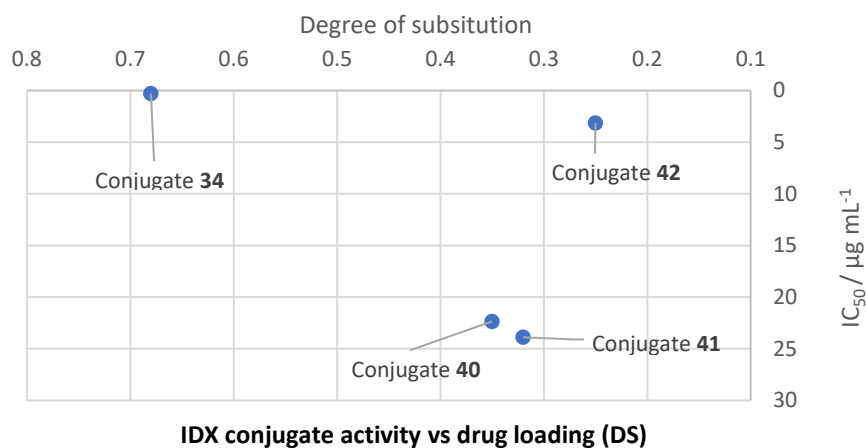


Figure 79 - The effect of drug loading on activity

Further to this, the trend observed with IDX is continued in Conjugate **43** (Figure 81, highly cross-linked drug conjugate). As a consequence of the conditions used in its preparation, the material had a low DS value of 0.20, but was had an activity of $0.70 \pm 0.29 \mu\text{g mL}^{-1}$. Which makes Conjugate **43** the most potent IDX-drug conjugate produced by us, to date.

4.3.1.2 Discussion of results for the drug loading study

Despite this effect of drug loading on activity being unexpected, the fact that it was observed in both IDX and Inulin suggests that it has significance and is not merely an anomaly - to our knowledge this is the first time that such a trend has been observed. It can possibly be explained by considering the environment that is created by changing the degree of substitution of the drug (Figure 80), although it should be noted that we have not carried out any investigations on the structural and conformational properties of these polymeric conjugates at this stage.

With the lowest loaded polymer conjugates (Conjugates **38** and **42**, Figure 78), each drug molecule is effectively in isolation from its neighbour and is therefore not affected by steric or electronic effects due to the other drug molecules on the polymer, as shown in Figure 80c, and the polymer may remain relatively linear in structure. Therefore, in this environment the pharmacophore is able to interact relatively unimpeded with the ATX active site, with the polymer displaying levels of activity which are dependent upon the properties of the drug.

As the loading is increased to produce conjugates with “medium” levels of drug loading (such as Conjugates **37** and **41**, Figure 78) one might then expect an increase in steric and electronic effects to occur between the more closely situated drug molecules, leading to a possible change in conformation of the polymer backbone. Further to this, medium-loaded drug molecules will likely have a distinct hydrophobic region (the drug) and a hydrophilic region (the polymer). In an aqueous environment (such as that which the conjugates were tested in), an Inulin-ibuprofen conjugate was observed to form a micelle, which would in effect encapsulate the drug, with the polymer backbone on the outside.¹⁰⁴ This change in conformation may therefore manifest itself in the reduced accessibility of pharmacophores to allow successful binding to the active site of ATX (Figure 80b).

For highly loaded conjugates (such as Conjugates **34** and **35**, Figure 78) nearly every sugar unit has a drug molecule attached to it (according to the DS calculation). The “swamping” of the polymer with drug molecules in this manner, causing maximum steric and electronic effects between closely situated drug moieties, this may have the effect of forcing the drug units to repel one another to such a degree that may prevent the formation of a micelle. This effect would act to restrict the conformational change which affects the positioning of the drug molecules on the medium-loaded conjugate and now ensures that there is more likely

to be an available drug molecule on the surface of the polymer for binding to ATX. Hence, the activity of the conjugate is seen to increase, compared to medium-loaded conjugates.

It is suggested by us that the effect of drug loading on activity is a dynamic process and will change subtly across different polymers and different drugs. The influence of linker length may also play a part in the overall result. The results of this study strongly indicate that to assume the amount of drug attached to a polymer will directly correlate to the activity observed, is a misnomer. A linear rise in potency may be observed in conjugates of a low loading (such as those with a DS value lower than 0.25), but at higher loadings, steric hindrance caused by neighbouring drug molecules will have a stronger influence on binding to ATX – which in that instance means that although every drug residue is capable of interacting with ATX, they are not all able to interact at the same time.

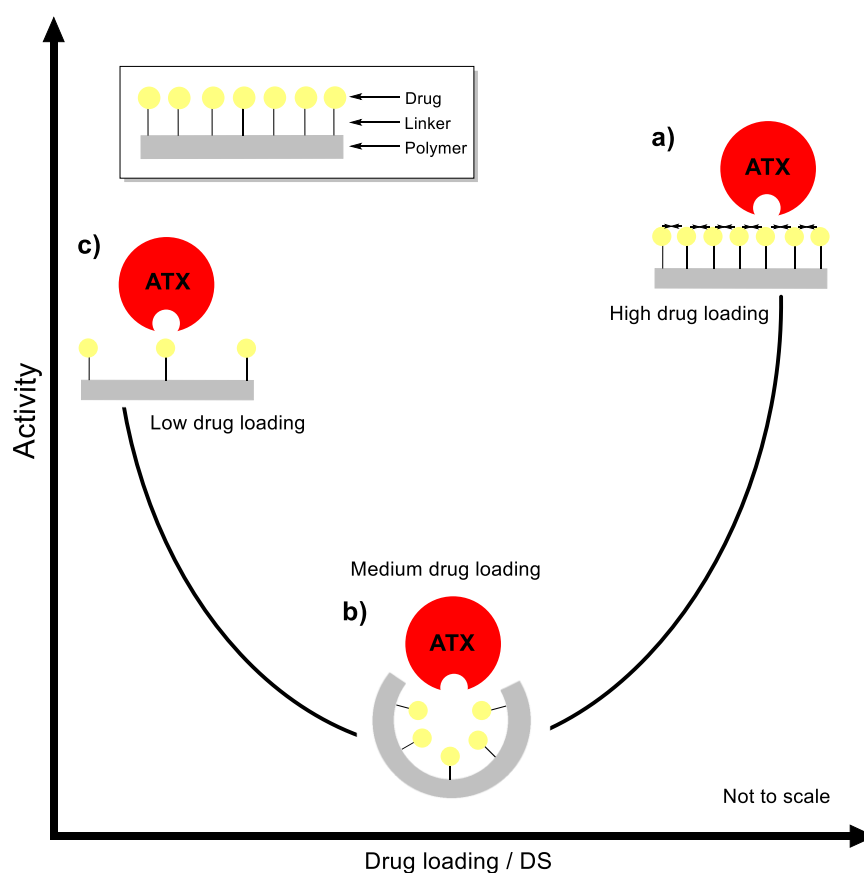


Figure 80 - A diagram to explain the effect of drug loading on activity

The effect of drug loading on activity could be exploited in the design of future drug conjugates. Rather than concentrating efforts on preparing materials with the highest drug loading, a more constructive approach may be to focus on conjugates of a lower loading. By tailoring a series of low DS drug conjugates, with small changes in loading, a potency equal

4.4 Peritoneal retention study

4.4.1 Introduction

In our previous work, a peritoneal retention study was used to demonstrate that the residence time of a drug was significantly improved following attachment to IDX.¹⁴⁷ 30 % of the drug-conjugate was found to be retained within the peritoneal cavity of mice after 24 hours.¹⁴⁷ The limitations with this study were detailed in Chapter 1: rodents are known to have higher levels of the enzyme amylase, which means that they metabolise IDX faster than humans do.¹⁵¹ Based on information published on the peritoneal retention of Icodextrin, it would be expected that the IDX-inhibitor conjugate previously prepared by us would be retained at a quantity greater than 30 % after 24 hours if it were tested in a human.¹³⁹ The limitations of this study were the driving force behind our interest in Inulin as a polymer support for our current work because, the polysaccharide Inulin is resistant to amylase, although has a molecular weight similar to IDX. Inulin drug conjugates may therefore display superior peritoneal retention in comparison to IDX conjugates, in rodent models.

4.4.2 Method

The peritoneal retention of Conjugate **35** was evaluated using a method similar to that used in our previous investigation. A 0.2 mg / mL solution of Conjugate **35** in PBS was made up, and this was then filtered through a syringe filter in order to sterilise the solution. In addition, a 0.2 mg / mL solution of Inulin was prepared and sterilised in the same manner as described above. 7-Week old nude mice were allowed to acclimatize for one week before the experiment began. Mice were injected with a solution of Conjugate **35** (0.4 mL) in their lower left quadrant at pre-determined timepoints (0 min, 30 min, 1 hour, 3 , 6 and 24 hours). The mice were then dispatched by cervical dislocation, this entire process was performed in triplicate. The peritoneal cavity was washed with PBS solution (0.4 mL), and the washings were collected, centrifuged, and the supernatant was then collected. As a control, three mice were injected with a solution of Inulin and then immediately dispatched and processed, as described previously. The peritoneal washings were analysed using fluorescence spectroscopy ($\lambda_{\text{EX}} = 360 \text{ nm}$, $\lambda_{\text{EM}} = 485 \text{ nm}$), alongside a calibration curve prepared with

conjugate 35, (2-fold dilution, 0.2 µg / mL, top conc.) in order to determine the concentration of the conjugate present in each sample.

4.4.3 Discussion of results

To our disappointment, the data obtained initially suggested that there was no drug conjugate present in the peritoneal cavity of the mice, even for those dispatched at 0 minutes. However, it became apparent that drug conjugate may never have actually been injected into the mice, the original solution of Conjugate **35** was analysed by fluorescence spectroscopy and found to contain no drug. It was concluded that the test drug must have been removed from solution during the filtration step and therefore only PBS solution was injected into the mice, giving rise to the results observed.

Due to time and financial constraints the experiment could not be immediately repeated, but if it were an alternative method of sterilisation should be used for the conjugate / Inulin.

4.5 Conclusion

Though the failed peritoneal retention study was disappointing, it should not have any negative bearing on similar studies conducted in the future, which should demonstrate that the drug-conjugate approach taken in this thesis will significantly enhance the residence time of a drug in the peritoneal cavity. Based on our previous findings concerning the peritoneal retention of Icodextrin drug conjugates, we would anticipate that the IDX drug conjugates produced in this study to show a similar level of peritoneal retention (30% removed after 24 hours). Notwithstanding this, the two enzyme assays performed in this study (bis-pNPP and FS-3) have shown that the drug-linker analogues retain their potency, following conjugation to a polymer. Many of the conjugates produced by us have been shown to be very potent, such as Conjugate **35** and **43**. Additionally, the effect of changing the degree of substitution on activity has been revealed, which has the potential to influence the design of drug conjugates in the future.

Chapter 5:

Novel approaches to the asymmetric synthesis of 3-substituted isoindolin-1-ones

Chapter 5: Novel approaches to the asymmetric synthesis of 3-substituted isoindolin-1-ones

The work described within this chapter was completed alongside my work on the synthesis and biological evaluation of ATX inhibitor polymer conjugates. It is entirely separate from that work and is included for the sake of completeness.

5.1 Introduction

Isoindolinones are a family of compounds that have numerous medicinal properties that are of therapeutic benefit. For instance isoindolinones act as anti-inflammatory, antihypertensive, antipsychotic and anaesthetic agents, as well as many other biological activities such as vasodilatory, antiulcer, antiviral, and antileukemic properties.^{224–230} Indeed, our own research endeavours have seen them evaluated as novel NMDA receptor antagonists as a treatment for Alzheimer's disease and as antimicrobial agents.²³¹ As shown in Figure 82, the isoindolinone framework is incorporated into a variety of biologically active drugs.²²⁷

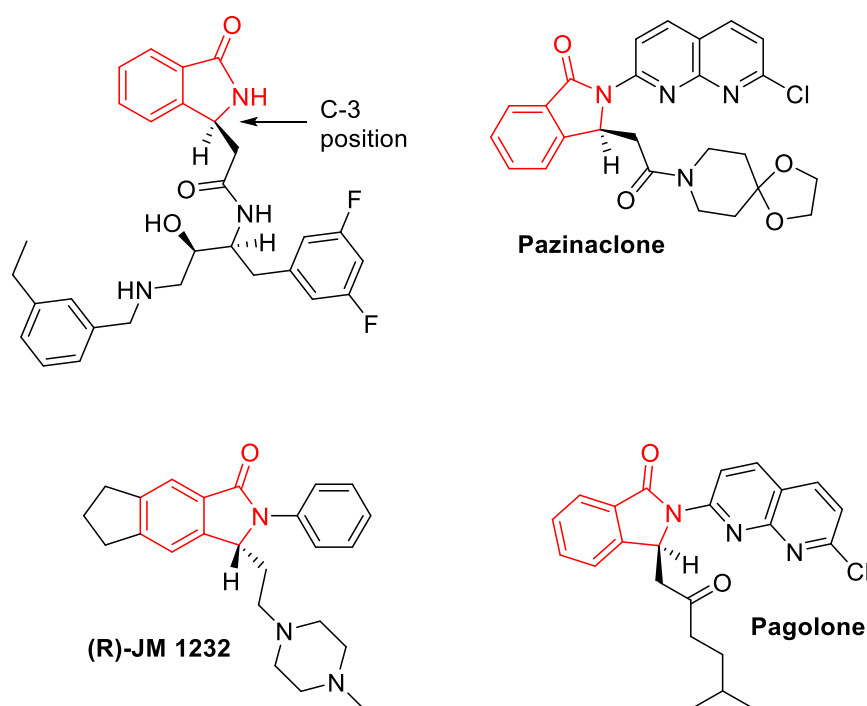
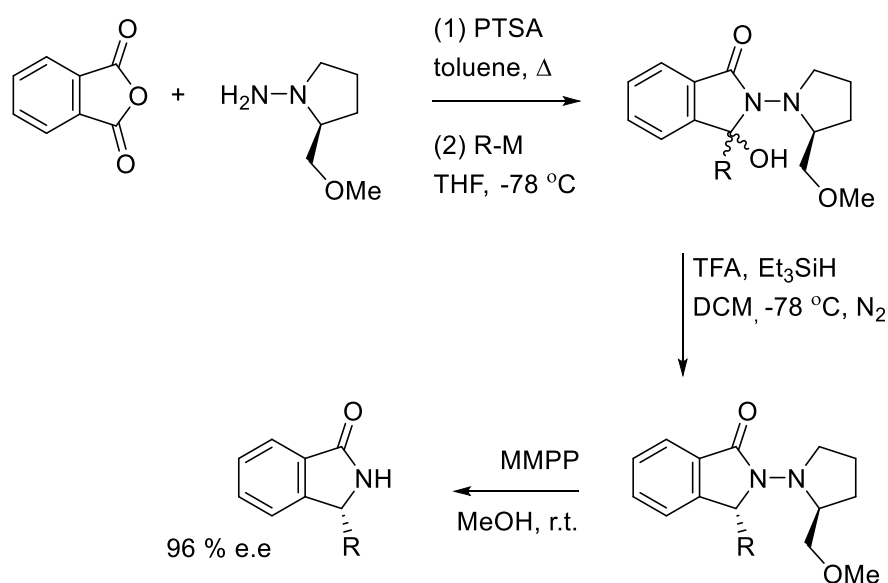


Figure 82 - A selection of therapeutic agents that incorporate the isoindolinone motif (shown in red)

Based on the numerous biological systems that isoindolinones are known to target, the indolinone framework could be described as a privileged structure and is therefore of significant interest to the pharmaceutical industry. A complication in the synthesis of isoindolinones is that they commonly contain a stereogenic centre at the C-3 position (as denoted in Figure 82).²³² Functionality at the C-3 position is often essential to the biological activity of isoindolinone drugs.^{227,232} In recent times it has become less acceptable to administer a drug as a racemate, and it is preferred that the active component is synthesised as a single enantiomer.²³³ Unsurprisingly, considering their therapeutic potential, there have been a number of efforts towards the enantioselective synthesis of 3-substituted isoindolinones.^{230,234,235}

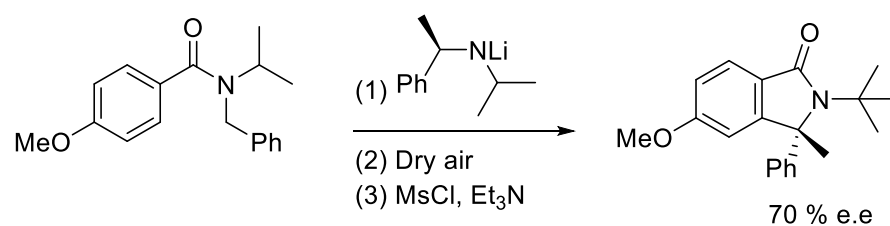
5.1.1 Approaches of to the stereoselective synthesis of isoindolinones in the literature

Deniau and co-workers pioneered a chiral auxiliary-hemiaminal approach, in which an intermediate was constructed by condensing phthalic anhydride with (*S*)-1-amino-2-methoxymethylpyrrolidine. Groups could then be introduced to the C-3 position *via* a Grignard reagent and later, as featured in the work of Couture and co-workers, using an alkenoyl alkylation strategy (Scheme 75).^{232,236,237} Upon the treatment of triethylsilane, the approach of the nucleophile is hindered by the chiral auxiliary, which gives rise to a preferred diastereomer. The chiral auxiliary was then easily removed by oxidative cleavage.^{236,237}



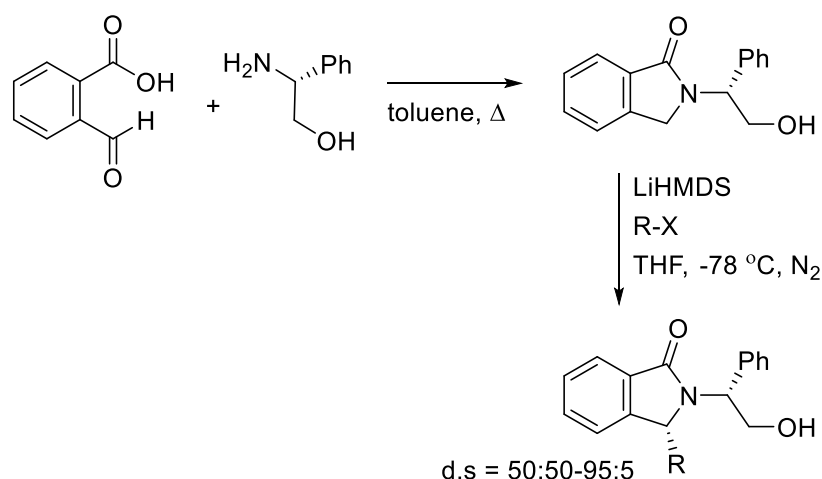
Scheme 75 - The chiral auxiliary approach used by Deniau and co-workers.

Clayden and co-workers were able to exert stereocontrol at the C-3 position of isoindolinones through cyclization and re-aromatisation of lithiated benzamides, which were formed using a chiral nucleophile.²³⁸ For the reaction to proceed in an enantioselective manner, the method required the presence of an *N-tert*-butyl group on the indolinone framework, which was synthetically difficult to remove, thus limiting the scope of the procedure. (Scheme 76).²³⁸



Scheme 76 - The enantioselective isoindolinone synthesis strategy used by Clayden and colleagues.

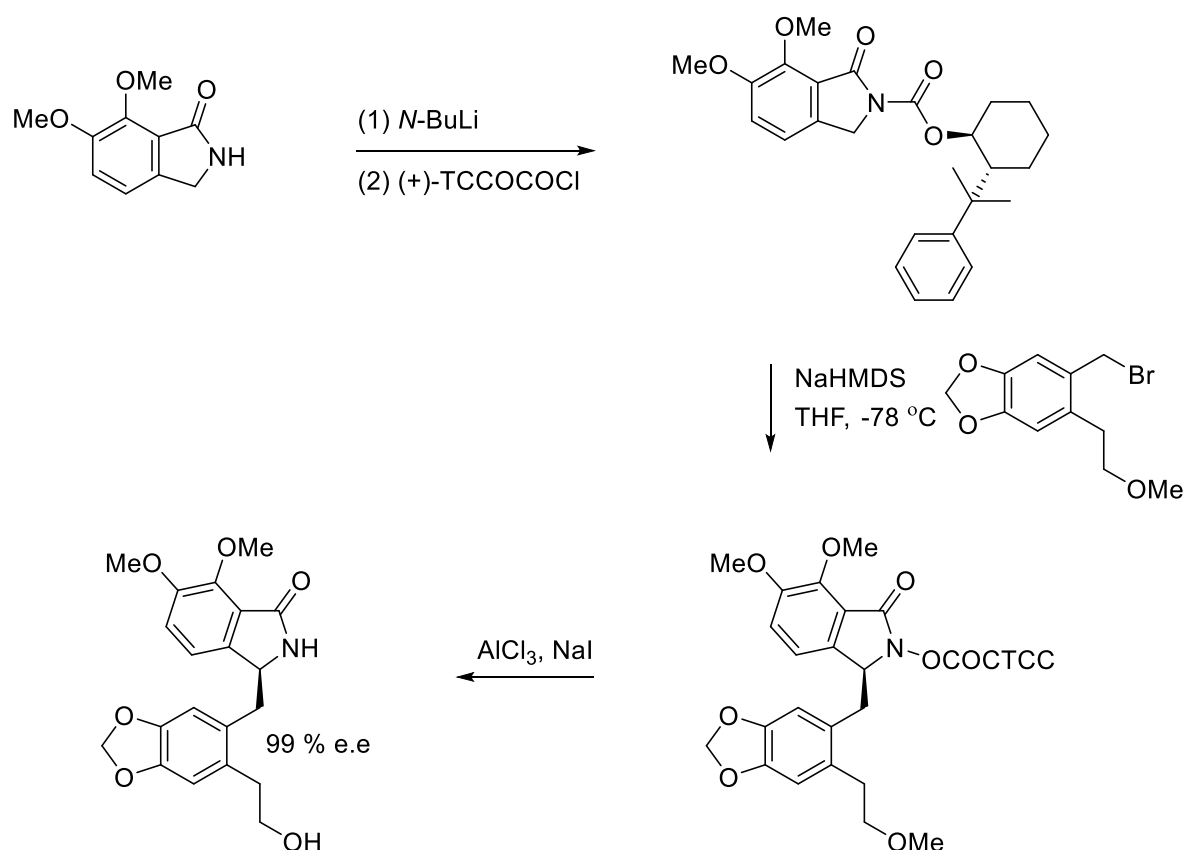
Royer and co-workers demonstrated a diastereoselective metalation / α -amino alkylation reaction (Scheme 77). The approach of the electrophile was guided by conformational control of the chiral auxiliary. The auxiliary could then be removed using a method previously developed by our own group, though the authors elected that this be a formal synthesis only (Scheme 82).^{234,239}



Scheme 77 - The diastereoselective alkylation strategy used by Royer and co-workers.

Despite the elegance of their methodology and the potential scope of the substituents that could be introduced to the C-3 position, the procedure suffered from inconsistent diastereoselectivities and issues with purification that may prevent wider application.²³⁹

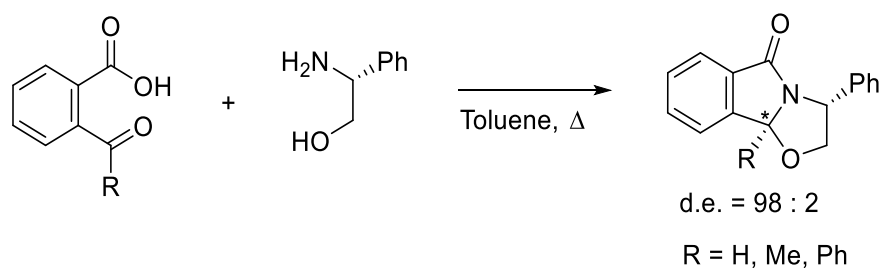
Comins and co-workers used a chiral auxiliary mediated approach towards the asymmetric synthesis of isoindolinones, the versatility of this method was demonstrated when it was employed to construct the biologically active alkaloid: (+)-Lennoxamine in high enantiomeric excess (Scheme 78).²³⁵



Scheme 78 - The diastereoselective synthesis strategy used to prepare (+)-Lennoxamine by Comins and co-workers

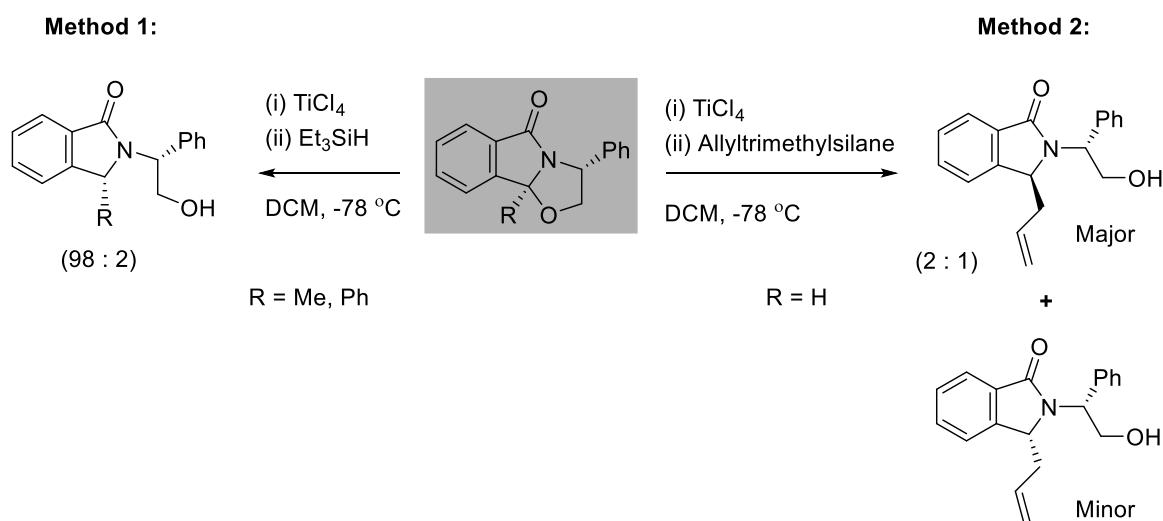
5.1.2 Our previous work

Our own efforts in this area have been concerned with the development of a stereoselective route towards the synthesis of tricyclic γ -lactams, from readily available keto-acids and enantiomerically pure amino-alcohols (which themselves can be derived easily from amino acids or can be purchased) (Scheme 79).^{234,240–242}



Scheme 79 - The cyclo-condensation reaction to give a tricyclic γ -lactam, under Dean-Stark conditions

The induced stereochemistry at the stereocentre formed at the C-3 position of the isoindolin-1-one ring (denoted by *) is determined by the stereochemistry of the amino alcohol used in the cyclo-condensation reaction.²⁴⁰ This reaction is highly diastereoselective and was used to prepare tricyclic lactams on multigram quantities, with minimal purification.²³⁴ In our previous work the tricyclic lactam scaffold served as a template from which two methods were developed to access chiral 3-substituted isoindolin-1-one's (Scheme 80).^{234,240-242}



Scheme 80 - The two methods applied by our group for the synthesis of 3-substituted isoindolin-1-ones

In Method 1 (Scheme 80), the tricyclic lactam template was reacted with a Lewis acid (TiCl_4) and a hydride source (triethylsilane) to give the ring-opened product. This reaction was found to be highly diastereoselective, effectively only giving one diastereomer as the product.²³⁴ The stereochemical outcome can be rationalised by considering the mechanism of the ring-

opening reaction and the preferred conformation of the reactive intermediate, as shown in Figure 83.²³⁴

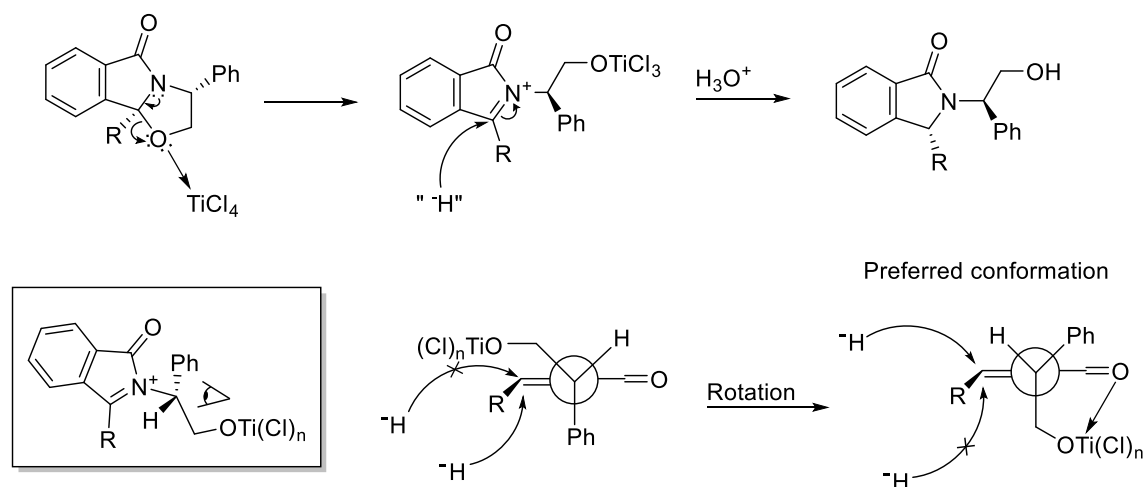


Figure 83 - The mechanism for the ring-opening reaction and the conformational rationalisation of the stereochemical outcome²³⁴

The Lewis acid is expected to coordinate to the ether oxygen of the lactam substrate, this assists in the generation of the crucial *N*-acyliminium ion, through the ring-opening reaction promoted by the *N*-lone pair.^{234,241,242} Triethylsilane then attacks the *N*-acyliminium species to yield the *N*-substituted isoindolinone intermediate, following an acidic work-up.^{234,241,242} The high diastereoselectivity observed with this method is attributed to the chelation control (Figure 83) and the presence of the angular R group which gives one preferred conformer.^{234,241,242} Consequently, triethylsilane will approach from the less hindered face of the planar acyliminium species.^{234,241,242} When a non-coordinating Lewis acid was used in place of TiCl_4 , the diastereoselectivity was reduced to 4 : 1, which highlights the significance of chelation in the stereochemical outcome of the reaction.²³⁴ The obvious benefit to this method is the high diastereoselectivity observed, however its synthetic utility is limited, due to there being few commercially available ketoacids that have different substitutions at the R position (R = Ph, Me in our study). While it is possible to synthesise ketoacids with the appropriate substitution, the chemistry used to achieve this is not trivial.

Based on the limited substitution patterns that could be accessed from Method 1, Method 2 (Scheme 80) served as a complementary approach.²³⁴ In this approach a carbon nucleophile was used in place of hydride, with the aim of increasing the variety of substitution patterns available at the C-3 position. However, the C-3 Hydrogen lacks the steric bulk of the methyl

or phenyl groups in method 1 to differentiate between the different conformations, as shown in Figure 84. This leads to a considerable drop in diastereoselectivity.

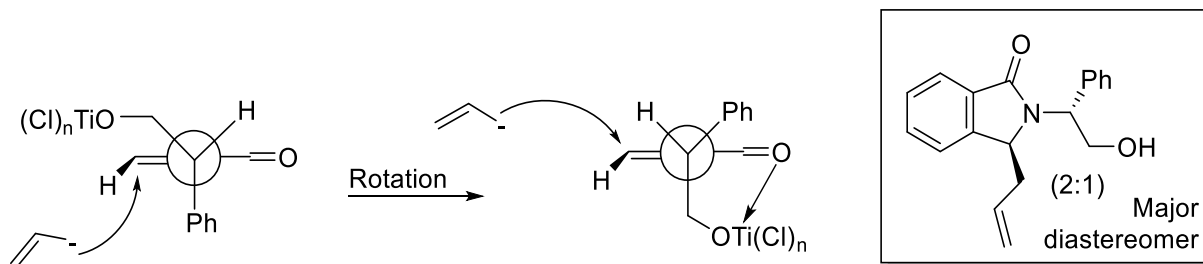
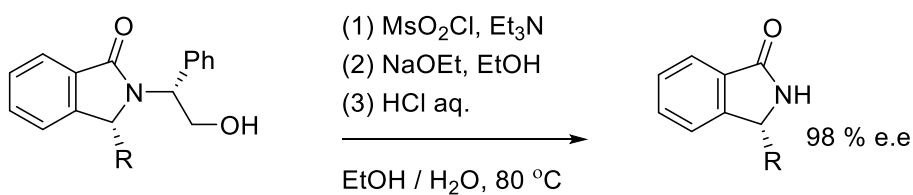


Figure 84 - The mechanism for method 2, with regard to the stereochemical outcome

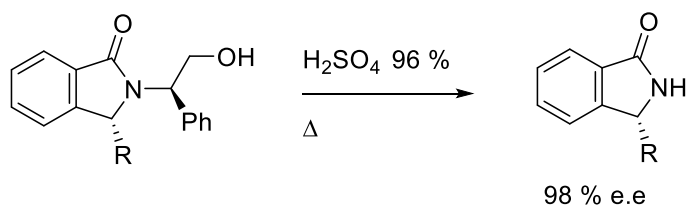
With this method there is a clear advantage over Method 1 in the wider variety of compounds that can be prepared, however it does result in much poorer levels of product diastereoselectivity, especially in comparison to Method 1.²³⁴

Two methods that did not lead to racemisation of the product were developed to remove the chiral auxiliary and yield the desired 3-substituted isoindolin-1-one targets.²³⁴ Methodology developed by Vernon and co-workers was applied, in which the auxiliary was removed through a three-step (one-pot method) by converting the alcohol group to a mesylate, which was then converted to the *N*-H isoindolinone, following a base-induced elimination to give an enamide, followed by acidic hydrolysis (Scheme 81).^{234,243}



Scheme 81 - Methodology by Vernon and co-workers, for the removal of a chiral auxiliary

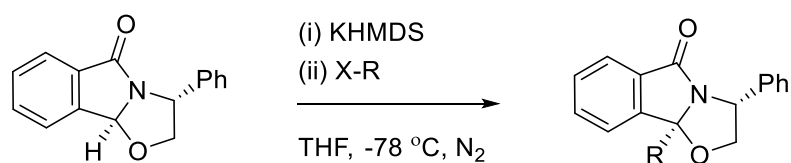
The chiral auxiliary could also be removed from the *N*-substituted isoindolinone intermediates by reaction with concentrated sulfuric acid to form the enamine intermediate, as per Vernon's methodology (Scheme 82).²³⁴



Scheme 82 - The removal of the chiral auxiliary, using concentrated sulfuric acid.

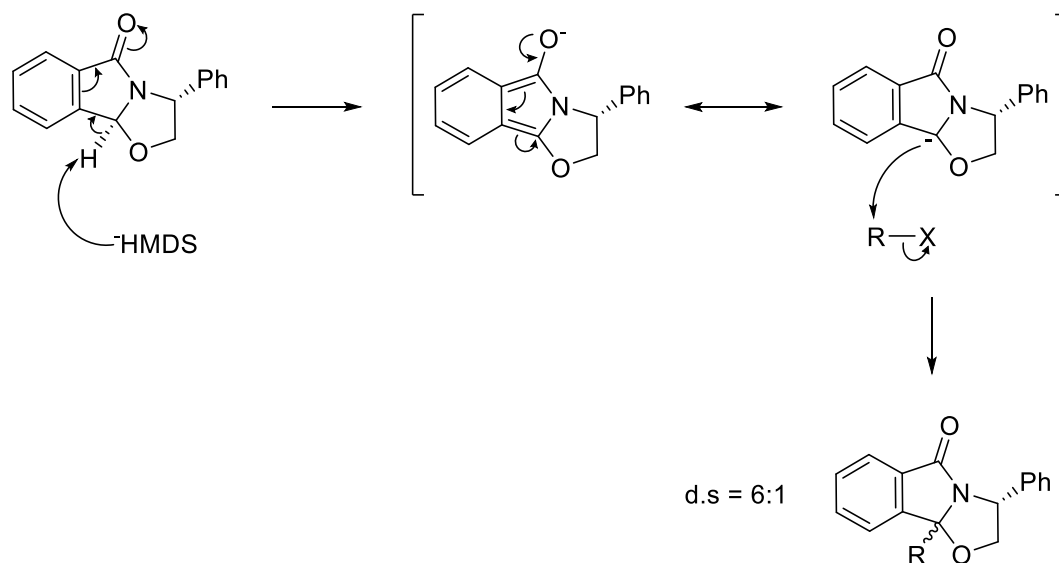
The product formed was found to have a very high level of enantiomeric excess (*e.e.*), as determined by chiral HPLC.²³⁴

In later studies carried out alongside the work in this thesis, we were interested in producing a series of C-3 substituted tricyclic γ -lactams as potential NMDA receptor antagonists.²³¹ We were inspired by the work of Couture and co-workers in which the stereoselective alkylation of an isoindolinone-like compound was demonstrated. This approach is in itself, an extension of "Meyers", polycyclic lactam methodology.^{237,244,245} Based upon the literature precedent, we hoped that the phenyl group contained within the lactam structure would help guide the approach of an incoming electrophile and result in a high level of diastereoselectivity, as indicated in Scheme 83.^{231,237} Lactam template was treated with KHMDS at -78 °C, then an alkyl halide was added and the mixture warmed to room temperature.



Scheme 83 – Attempted stereoselective alkylation of a tricyclic lactam template

The alkylation reaction (Mechanism 4) was attempted with a small number of alkyl, allyl and benzyl halides and was found to be successful, but to our disappointment was not particularly diastereoselective, despite the literature precedent to the contrary on similar substrates.^{231,237}



*Mechanism 4 - Mechanism for the alkylation of a tricyclic lactam template*²³⁷

Attempts were then made to influence the diastereoselectivity by altering the counterion present on the base, as per the work of Royer and co-workers. The results of this study are shown in Table 14.²³⁹

Base	Alkyl halide	Diastereoselectivity	% Conversion
LiHMDS	Me-I	1:1	50
LiHMDS	Benzyl-Br	3:1	94
LiHMDS	Allyl-Br	4:1	96
NaHMDS	Allyl-Br	9:1	50
KHMDS	Allyl-Br	6:1	57

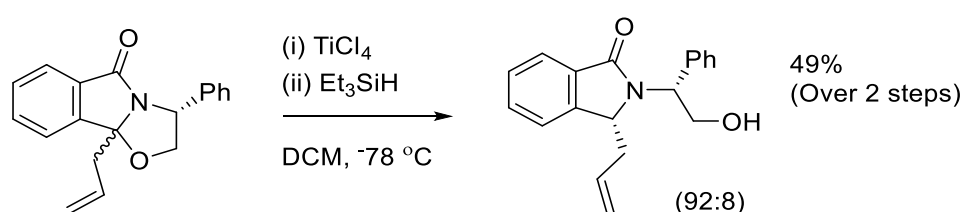
*Table 14 – Alkylation of tricyclic lactam templates using alternative base, and electrophiles (% conversion determined by ¹H NMR spectroscopy, of the crude material)*²³¹

The study revealed that NaHMDS gives a sharp rise in diastereoselectivity compared to LiHMDS, however this was at the expense of conversion.²³¹ Diastereoselectivity was also influenced by the relative “size” of the electrophile, as evidenced with LiHMDS: methyl iodide gave a d.e. of 1:1, which increased to 3:1 for benzyl bromide and to 4:1 for allyl bromide.²³¹ Despite these modifications there was little real benefit, because the two product

diastereomers could not be separated using column chromatography, and also co-eluted with unreacted starting material.²³¹

While this was disappointing, the study also revealed that if LiHMDS was used as the base, a high level of conversion could be achieved, which suggested that the reaction could be used in an alternative approach.²³¹ We decided to attempt to use this approach in combination with Method 1 (Scheme 80), as a novel method to access 3-substituted isoindolin-1-ones. As stated above, when the *N*-acyliminium ion is generated in the ring-opening reaction (Figure 83), any stereochemistry present at the C-3 position is lost, meaning that the diastereoselectivity of the intermediate alkylation step is of no significance.²³⁴ The stereocentre can be re-established with high levels of stereoselectivity when the intermediate *N*-acyliminium ion is reduced with triethylsilane with chelation control. Only a single diastereomer should be observed, resulting in a convenient method from which to synthesise a wide range of *N*-substituted isoindolinone targets.²³⁴

In the an initial experiment the tricyclic lactam template **73** was alkylated using allyl bromide, to give the intermediate compound (Scheme 84).²³¹ This 4:1 mixture of diastereomers was carried through to the next reaction along with unreacted starting material, following an aqueous workup.²³¹ This mixture was treated with TiCl₄ and triethylsilane to give the ring-opened product with an excellent level of diastereoselectivity (92:8), and the target could be isolated as a crystalline solid *via* flash column chromatography (Scheme 84).

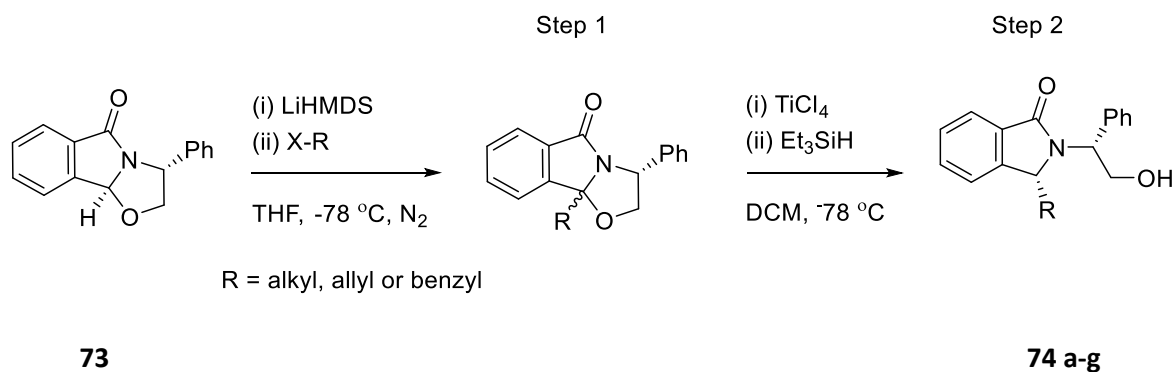


Scheme 84 - The diastereoselective ring-opening of the allyl intermediate

The approach shown in Scheme 84 overcomes the shortcomings of both Methods 1 and 2 (Scheme 80) because it can be used to introduce a wide variety of substituents at the C-3 position and is highly diastereoselective.

5.2 Application to the synthesis of a range of 3-substituted isoindolin-1-one targets

The tricyclic lactam template **73** was deprotonated with LiHMDS and the anion reacted with an alkyl, allyl or benzyl halide. The crude alkylation product was then carried through to the ring-opening reaction (Scheme 85).



*Scheme 85 - The 2-step synthetic route to prepare N-substituted isoindolinone targets from a common template **73***

Seven compounds were prepared using this method, with diastereoselectivities >92:8 (determined by ^1H NMR spectroscopy of crude material) and in acceptable to good yields (when the percentage conversion in Step 1 is considered). The results of the study are shown in Table 15.

Alkyl halide	ds (Step 1)	Product (74)	Ds (Step 2)	yield (%)
Methyl iodide	1.3:1	a	≥93:7	32
Ethyl iodide	1:1	b	≥94:6	47
Propyl iodide	2:1	c	≥94:6	32
Allyl bromide	4:1	d	≥92:8	49
Benzyl bromide	1.5:1	e	≥93:7	35
2-Fluorobenzyl bromide	5:1	f	≥93:7	65
3-Methoxybenzyl bromide	4:1	g	≥94:6	61

Table 15 - The results of the two-step alkylation and ring-opening procedure

A consistently high level of diastereoselectivity was observed for every substrate in Step 2. To confirm the structure of the major diastereomer of the reductive ring-opening reaction, X-ray crystal structures were obtained for the major diastereomers of compounds **74b**, **d** and **e** (**74e** shown in Figure 85).

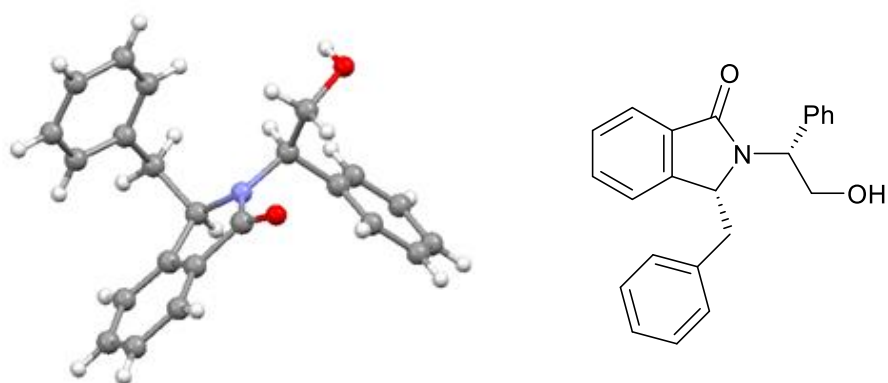
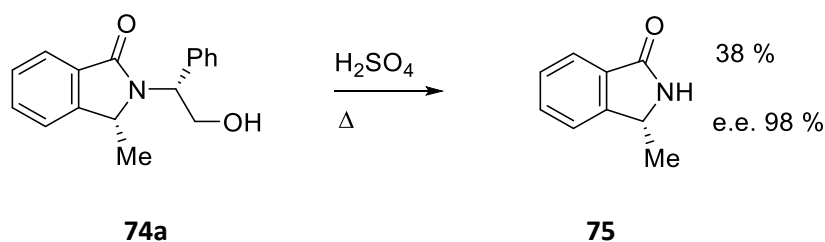


Figure 85 - The X-ray crystal structure of compound **74e** and the structure showing the observed (*R, R*) stereochemistry

The (*R, R*)-stereochemistry shown in Figure 85 for compound **74e** was also observed for compounds **74b** and **74d**. This confirmed our previous assertion that the reductive ring-opening reaction followed the proposed conformational model (Figure 83).²³⁴

5.2.1 Removal of the chiral auxiliary

With a range of *N*-substituted isoindolinone intermediates in hand (Table 15), we decided to complete the synthesis of a 3-substituted *NH*-isoindolin-1-one, by applying our previously established strategy for removal of the chiral auxiliary (Scheme 86).²³⁴ Compound **74a** was dissolved in concentrated sulfuric acid, then heated over a steam bath for precisely 2 minutes (longer reaction times led to racemisation of the C-3 stereocentre), then worked-up and purified by preparative chromatography.



Scheme 86 - The chiral auxiliary removal of compound **74a**

The purified material was then analysed independently by Reach Separations (BioCity, Nottingham) using chiral HPLC, by comparing the enantio-enriched compound to the racemic version of (**75**) that was also prepared by us. To our delight, the enantiomeric excess was determined to be 98%, meaning that no loss of stereochemical integrity had occurred during the acid-mediated cleavage of the auxiliary group.

5.3 Attempted enantioselective synthesis of an isoindolinone drug molecule

With an effective synthetic route towards the synthesis of 3-substituted isoindolin-1-ones having been established, our attention turned towards applying it to the enantioselective synthesis of an isoindolinone drug molecule. A particular target of interest was (*S*)-PD 172938, a potent dopamine D4 ligand (Figure 86).

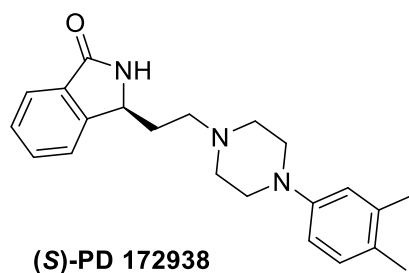
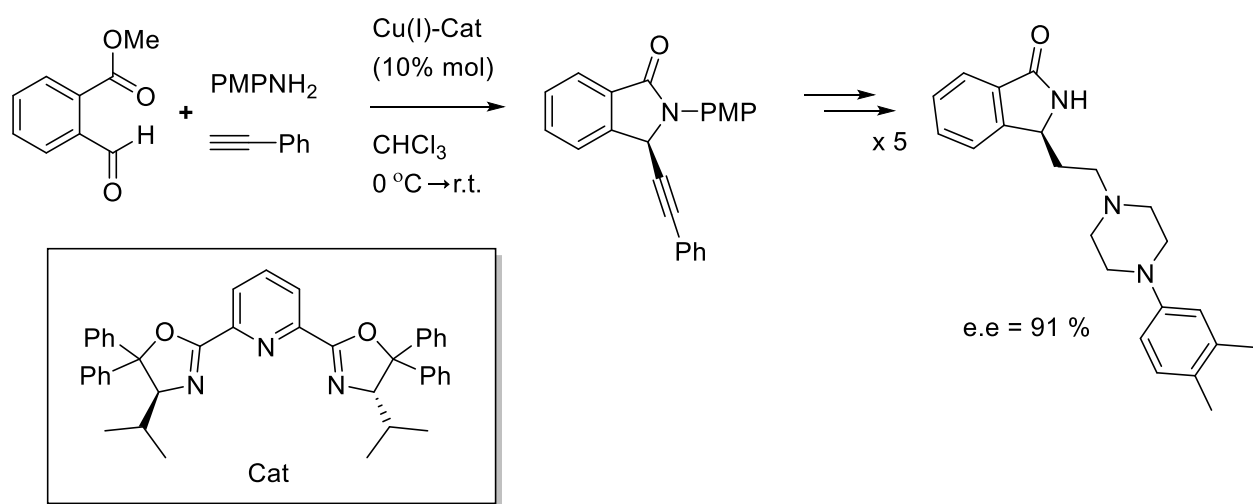


Figure 86 - The structure of (S)-PD 172938

In the original publication in which (S)-PD 172938 first featured, Belliotti and co-workers prepared the compound as a racemate and the two enantiomers were then separated *via* chiral resolution as the final step (using chiral HPLC).²⁴⁶ The obvious problem with the approach used by Belliotti was that of waste, since the (*R*)-enantiomer of PD 172938 is inactive at the dopamine receptor.²⁴⁶ There is a clear need for an asymmetric approach for the preparation of these compounds in the spirit of atom economy and for a cost-effective synthesis. Singh and co-workers presented their domino enantioselective alkyne/ lactamization method to construct an indolinone template with a suitable synthetic handle, which was then transformed in five additional synthetic steps to give (S)-PD 172938, in reasonable overall yield and e.e. of 91 % (Scheme 87).²²⁷

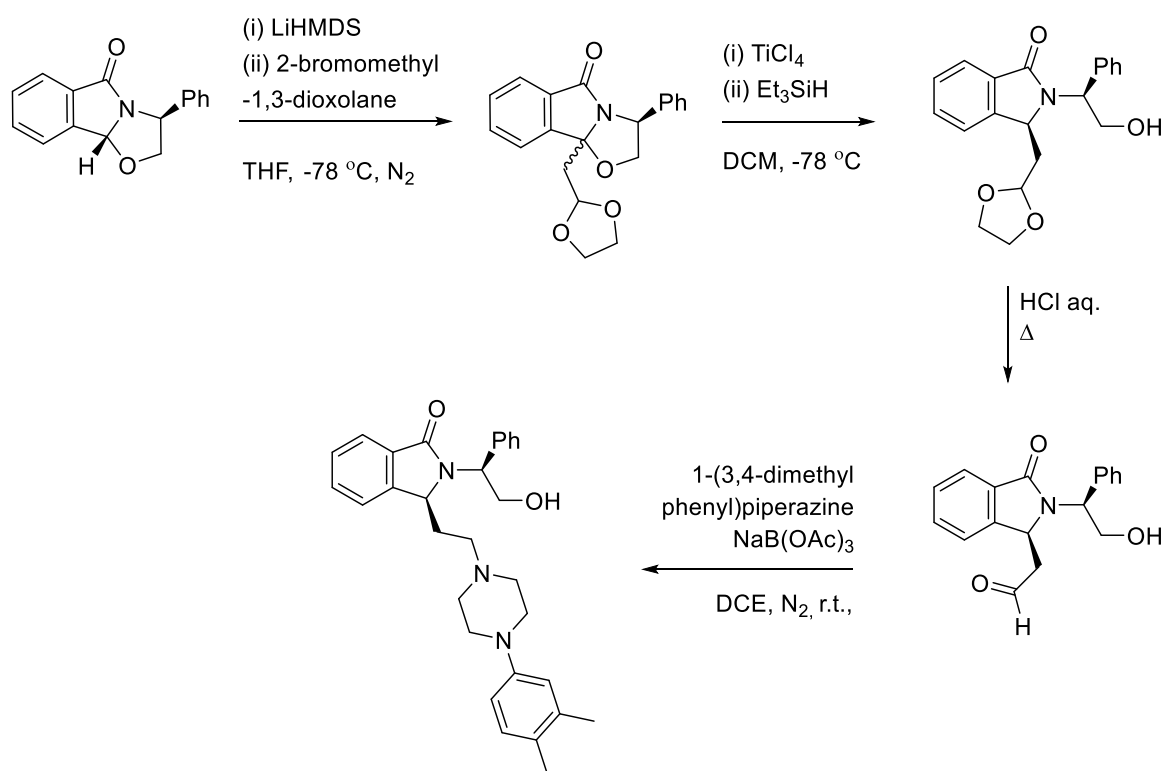


Scheme 87 - The approach taken by Singh and co-workers, to synthesise (S)-PD 172938²²⁷

The catalytic asymmetric approach taken by Singh (Scheme 87), could be considered superior to our own method to construct isoindolinones, due to it being necessary in our method to remove the chiral auxiliary as the final step, which is inherently wasteful.^{227,234} However, the

organo-copper catalyst employed in their approach has to be prepared, adding an additional synthetic step. Additionally, to install the piperazine moiety requires the installation of aryl and mesyl groups, that are removed in subsequent steps.²²⁷ The chiral auxiliary used in our approach is derived from inexpensive amino acids meaning that a synthetic route employing our methodology is likely to be much more cost effective.

We designed a synthetic route using our alkylation / ring-opening methodology employing 2-bromomethyl-1,3-dioxolane as the electrophile in order to install a synthetic handle from which the piperazine moiety (commercially available) could be introduced. It was intended for reductive amination to be used to couple the two fragments, the chiral auxiliary would then be removed as the final step (Scheme 88).

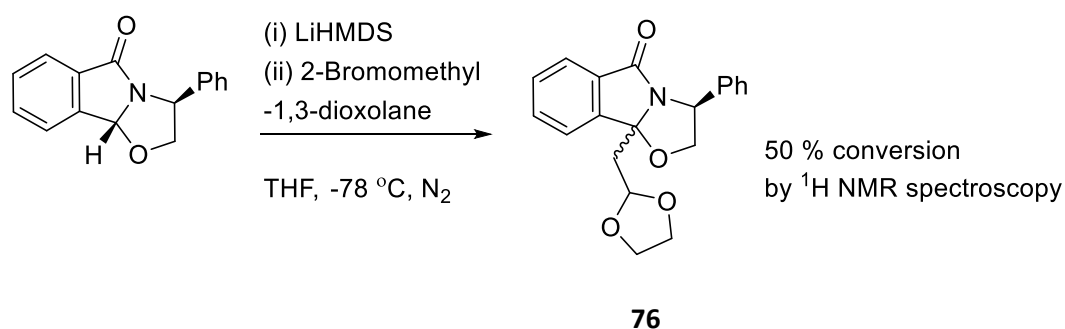


Scheme 88 - The proposed synthetic route for the preparation of (S)-PD 172938

It is worth noting that a number of other electrophiles were considered, such as bromomethyl acetate, however when this reaction was attempted, it was found to be unsuccessful (on multiple occasions) so the route was not pursued further. The aldehyde intermediate (*Scheme 88*) was of particular synthetic utility, as this handle could be used to synthesise multiple classes of isoindolinone drugs, pazinaclone and (*R*)-JM 1232 contain a common methyl amide linkage at the C-3 position (Figure 82).²²⁷ The synthetic route could

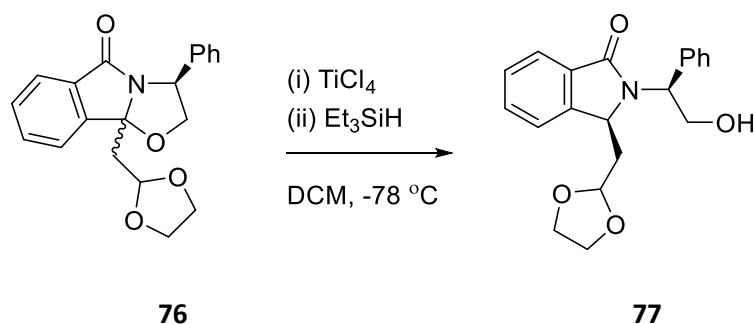
be easily adapted to prepare targets of this type, by oxidising the aldehyde to a carboxylic acid, followed by amide bond formation.

In a similar manner to our previous investigation, the (*S*)-tricyclic lactam template was alkylated with bromomethyl-1,3-dioxolane, using LiHMDS as a base (Scheme 89).



Scheme 89 - The synthesis of dioxolane 76

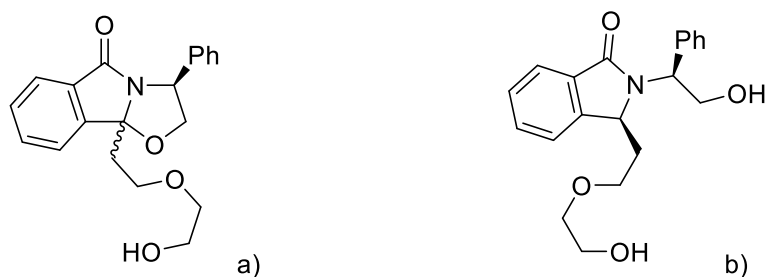
The crude material was then analysed *via* ¹H NMR spectroscopy, which strongly indicated that the desired product had formed (by the appearance of resonances thought to belong to the dioxolane group), with a conversion of around 50 % and a d.s. of 1:1. As per usual, the material was carried through to the next step without further purification (Scheme 90).



Scheme 90 - The synthesis of 77

To our disappointment, the reaction gave an inseparable mixture of components which could not be purified by column chromatography. This result was unexpected as the reaction usually proceeded smoothly and the product was relatively easy to purify. The reason for this was identified in the published synthesis of Tamiflu® by Hoffmann-La Roche. In their synthetic route, a dioxolane moiety was treated TiCl₄ and triethylsilane in near identical

conditions to that of the reductive ring-opening reaction attempted by us.^{247,248} They demonstrated that under those conditions, a dioxolane is susceptible to ring-opening. Therefore, when **76** was treated with TiCl₄ and triethylsilane, at least 2 competing reactions occurred, the alternative reaction product is shown in Scheme 91a.^{247,248}



Scheme 91 - The alternative reaction products

Though it is quite possible that both competing ring-opening reactions could occur on the same substrate (Scheme 91b), there was evidence to suggest that this may be observed in the ¹H NMR spectra of the crude product mixture. Despite it being inconvenient that this side reaction occurred, it was felt that the order in which each synthetic manipulation was performed could be an important factor in successfully preparing (*S*)-PD 172938. For instance, taking our previous findings into account, it may be prudent to convert the dioxolane intermediate **76** into an aldehyde, prior to the ring opening reaction, if the conversion is sufficiently mild, this could be done as part of the work-up, by washing in dilute HCl. This work on the preparation of (*S*)-PD 172938 was passed over to a project student and is still under investigation by our group.

5.4 Conclusion

In summary, the work described within this Chapter demonstrates a significant advance on previously developed strategies for the synthesis of 3-substituted isoindolinones. The alkylation / reductive ring-opening methodology developed by us expands the scope of substitution patterns accessible at the C-3 position, limited only by the availability of alkylating agents. Our previously established strategy for the removal of the auxiliary group was applied to a ring-opened template **74a**, to obtain an *N*-H isoindolinone with a high level of enantiomeric excess of 98 %. An attempt was then made to apply our alkylation / reductive ring-opening methodology towards the synthesis of an enantio-enriched drug target.

Chapter 6:

Conclusion, future work and final
comments

Chapter 6: Conclusion, future work and final comments

6.1 Conclusion

The work described within this thesis concerns the synthesis and biological evaluation of novel autotaxin inhibitor-polymer conjugates as a potential treatment for ovarian cancer.

In Chapter 1 the case for ATX as a target for ovarian cancer was made. ATX has been linked to ovarian cancer cells developing resistance to a number of chemotherapeutic agents. It is thought that reduced sensitivity towards anti-cancer drugs is a major factor in the poor survival rate observed in patients with ovarian cancer.²⁷ Further to this, ATX has been found to instigate many of the processes which are conducive to the proliferation metastasis and survival of ovarian cancer cells. It is suggested that by inhibiting autotaxin, using a small drug molecule, the mechanisms by which ovarian cancer cells rely on for multi-drug resistance will be disrupted. However, it has been noted that many ATX inhibitors perform poorly *in vivo*, most likely due to the drug being rapidly eliminated from the peritoneal cavity and away from the tumour. We have proposed a novel polymer drug delivery strategy to increase the residence time of an ATX inhibitor within the peritoneal cavity, building upon our previous work in this field.¹⁴⁷ Two separate polymers were identified for this study, to maximise peritoneal retention, and several autotaxin inhibitors were also chosen for this investigation.

In Chapter 2 the 12-step preparation of an analogue of the potent ATX inhibitor, 3-BoA, was presented. The same methodology was applied to the 4-BoA isomer.⁸⁸ Chapter 2 documented the attempted attachment of the 3BoA-linker intermediate to IDX. However, this was largely unsuccessful. The re-synthesis of an HA155 analogue (Compound **45**) was described and as explained, the data-set obtained for this compound and its intermediates were published in the *Journal of Medicinal Chemistry*.¹⁴⁷

Chapter 3 described the attempted preparation of Inulin drug conjugates using similar conjugation chemistries used in Chapter 3 and this was also found to be mostly unsuccessful. A new method for the covalent attachment of ATX inhibitors to IDX and Inulin was therefore developed by studying the reaction between IDX and epichlorohydrin over time. This new “epichlorohydrin activation” method was used to great effect to prepare a range of drug conjugates from both Inulin and Icodextrin and has the potential to be applied to many other polysaccharides. The effect of changing the drug loading on activity was investigated by

preparing a series of drug conjugates with different degrees of substitution. A highly cross-linked IDX drug conjugate was also prepared in order to investigate the effect of cross-linking on biological activity. The epichlorohydrin method was also used to synthesise drug conjugates containing a boronic acid moiety (an analogue of the potent ATX inhibitor HA155), which would not have been possible using previous conjugation chemistry.⁴³

Chapter 4 described the biological evaluation of the conjugates prepared in Chapter 3. To our delight the drugs used in this investigation retained their potency following attachment to Icodextrin and Inulin, using both Bis-*p*NPP and FS-3 as the substrate. A number of conjugates tested were found to be highly potent. Conjugate **43** had an IC₅₀ value of 0.70 ± 0.29 µg mL⁻¹, which is the most potent IDX-drug conjugate prepared by us to date. Additionally, the Inulin drug conjugate, Conjugate **35**, was found to be extremely potent, with an IC₅₀ value of 0.30 ± 0.04 µg mL⁻¹. To our surprise, intra polymer cross-linking appeared to have no effect on the conjugate's *in vitro* activity. We postulate that cross-linking improves resistance to amylase and increases peritoneal retention. If this is the case, such a feature can then be incorporated into the design of future drug conjugates. A non-linear relationship between polymer drug loading and activity was established. This study suggests that a polymer conjugate with a low DS could have a comparable or higher activity than a conjugate with a high DS value. This discovery will influence the design of drug conjugates in the future and could result in conjugates displaying improved solubility and high activity, which are cheaper and to prepare.

Chapter 5 demonstrated a significant advantage to previously developed strategies for the synthesis of 3-substituted isoindolinones. The alkylation / reductive ring-opening methodology developed by us, expands the scope of substitution patterns accessible at the C-3 position, limited only by the availability of alkylating agents. This was achieved while maintaining a high level of diastereoselectivity. Our previously established chiral auxiliary removal strategy was applied to a ring-opened template to obtain the product with an exceptional enantiomeric excess of 98 %. An attempt was then made to apply our alkylation / reductive ring-opening methodology towards the synthesis of an enantioenriched drug targets.

6.2 Future work

While undertaking the work described within this thesis, it became apparent that additional avenues of investigation could be explored. Most evident, was an extension of the biological evaluation of the drug conjugates, described in Chapter 4. In particular, the peritoneal retention study of Conjugate **35** should be repeated. It was postulated that the most likely reason the peritoneal retention study was not successful was due to the sterilisation method chosen. The experiment should therefore be repeated using a freeze-drying sterilization method. The peritoneal retention study will also give an early indication of any issues with toxicity surrounding the conjugates. The results of the peritoneal retention study should indicate which polymer (IDX or Inulin) has the longest residence time in the peritoneal cavity (in mice) and is therefore most suited as a polymeric support for use in a drug conjugate. Moving forward, the next biological investigation should be to examine the inhibition of ATX *in vivo*, within the peritoneal cavity of mice, by directly monitoring the LPA concentration at set time periods after administration of the drug conjugate.

As stated in Chapter 4, based on the findings from the drug loading study, a more extensive investigation should be conducted. The study should involve the preparation of around 10 drug conjugates of DS values increasing in 0.05 increments, using the epichlorohydrin activation method. This should provide a greater understanding of the effect of drug loading on activity, the predicted trend that could be observed is shown in Figure 87.

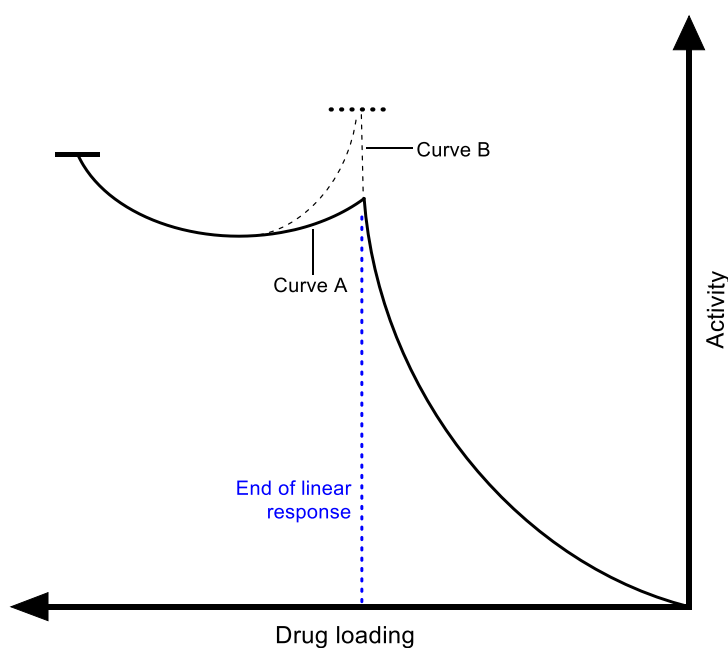


Figure 87 – The predicted response to increased drug loading, from zero.

The trend predicted in Figure 87 shows how the effect of drug loading may influence activity, based upon the experimental observations featured in Chapter 4. As drug loading is increased from zero, activity should increase in a linear fashion. At low levels of drug loading, neighbouring drug molecules attached to the polymer should have little to no influence on the interaction of ATX. As the degree of loading increases, neighbouring drug molecules may begin to influence the interaction between the binding drug and ATX and may encourage the formation of a micelle, further restricting access of ATX to the pharmacophore. At this stage a linear response to increased drug loading will end (Figure 87). The graph should then follow a similar “bowl shaped” curve, as observed in the data collected in Chapter 4. There was some experimental evidence that a lower drug loading may result in a conjugate with a higher potency, in comparison to a conjugate with the maximum loading that is available *via* the epichlorohydrin activation method. This is indicated in curve B (Figure 87). This study will better inform the design of polymer therapeutics in the future and help to understand the effect of drug loading on activity, which to our knowledge has not been studied before.

When the drug polymer conjugate approach described within this thesis and our earlier work is considered, it should be clear that its application should not be limited to autotaxin inhibitors and ovarian cancer. One can imagine a whole host of drugs that could benefit from enhancement in this manner as novel treatments for a variety of diseases. For example, it could be envisaged that a linker analogue of 18-hydroxycorticosterone could be synthesised and attached to Icodextrin. This polymer conjugate could be used as a new arthritis therapy. It is believed that attachment to IDX will improve the pharmacokinetics properties of corticosterone.^{249,250} When the material is injected into the joints, a localised concentration of the drug may be established, which could increase the half-life of the drug and reduce the time between repeated injections.^{249,250}

As stated in Chapter 1, there is little evidence to suggest that ATX inhibitors have any inherent cytotoxic properties and will therefore not act to reduce the size of a tumour. For the effective treatment of ovarian cancer, an ATX inhibitor should be used in combination with a conventional chemotherapeutic agent. For the reasons outlined previously, it would be beneficial to extend the residence time of paclitaxel within the peritoneal cavity. Additionally, by attaching taxol to IDX, its aqueous solubility would likely be significantly improved. We propose that if the number of equivalents of epichlorohydrin are carefully controlled in the preparation of an ATX inhibitor polymer conjugate, then there may be sufficient hydroxyl residues left, from which to attach a linker analogue of paclitaxel. The resulting conjugate (Figure 88) would therefore have a dual-action: the inhibition of ATX,

disrupting the mechanisms that govern chemoresistance, proliferation and metastasis in ovarian cancer cells and the inhibition of mitosis (by paclitaxel), leading to cell death. While to synthesise an analogue of paclitaxel is far from trivial, there are many examples of the structural modification of paclitaxel in the literature to assist in this endeavour. For instance, it is known that the alcohol group at the C'2 position of paclitaxel (Figure 88) can be selectively alkylated with a carboxylic acid, to give the corresponding ester (which retains activity). This chemistry appears to be robust and does not result in racemisation of any stereocentres.^{251–253} This method could be used to install the diethylene glycol linker, previously employed in our investigations, to give a paclitaxel-linker analogue.

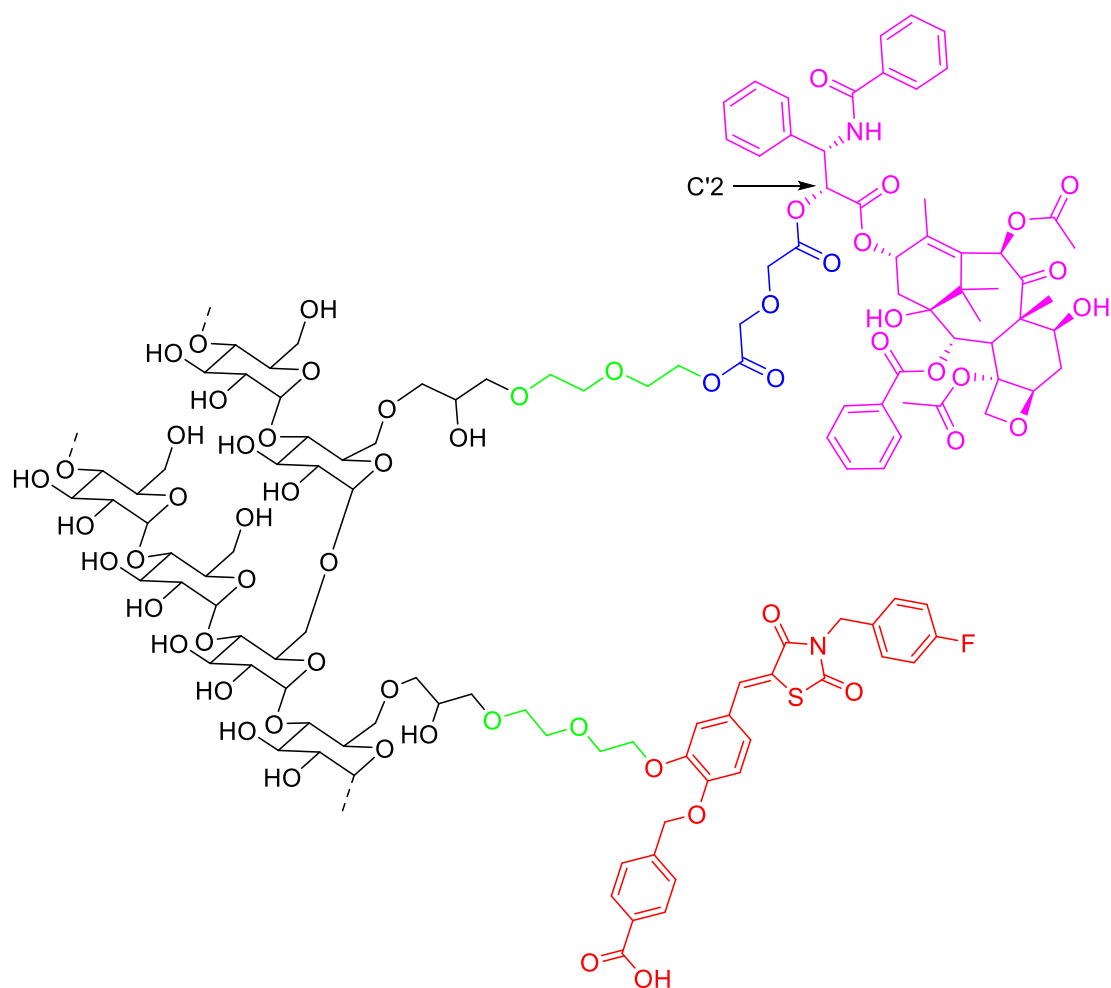


Figure 88 - The proposed IDX-paclitaxel conjugate, **44** = red, paclitaxel = pink, linker = green, succinate ether chain = blue and EPI-IDX = black.

6.3 Concluding remarks

Ovarian cancer is responsible for over 4200 deaths each year in the UK. There is clearly a need for new drugs to be developed and strategies found to combat chemoresistance, which is linked to the poor survival rate associated with ovarian cancer.¹

The work described within this thesis has produced 11 drug conjugates, using both IDX and Inulin as a polymer support, all of which were found to be highly potent. The effect of intra polymer cross-linking and drug loading on activity has been investigated and has the potential to impact on the design of drug conjugates in the future. The results of these investigations will be published in due course. Overall the new ATX inhibitor polymer conjugate approach described within this thesis could provide the basis for an effective new therapeutic strategy for the treatment of ovarian cancer and could help overcome the problems associated with multi-drug resistance in chemotherapy.

Chapter 7:

Experimental methodology

Chapter 7: Experimental methodology

Solvents were removed under reduced pressure with a Büchi rotary evaporator. Any remaining solvent was removed under high vacuum. The progress of the reactions was monitored by TLC analysis, using glass pre-coated silica gel plates (Merck) visualised by UV irradiation at a wavelength of 254 nm or using a potassium permanganate stain. Flash column chromatography was carried out on silica gel 60 (43-60 mesh); columns were slurry packed in the appropriate eluent mixture and samples were added as a concentrated solution or pre-absorbed onto silica. Dialysis was carried out using 20 kDa, 8 kDa, 3.5 kDa MWCO (Bioscience) and 1 kDa MWCO (Spectrum) dialysis membrane tubing, where stated. H₂O was of distilled grade or higher.

¹H- and ¹³C-nuclear magnetic resonance (NMR) spectra were measured on a Jeol eclipse 400 MHz Fourier transform spectrometer using D₆-DMSO, CDCl₃, D₂O, D₆-acetone, D₄-methanol and D₃-acetonitrile solvents. Chemical shifts are quoted in ppm downfield from TMS; coupling constants (*J*) are quoted in Hertz (Hz). TMS was defined as 0 ppm in ¹H NMR spectra and the residual chloroform triplet as 77.10 ppm in ¹³C NMR spectra. The following abbreviations were used in analysis: broad (br), singlet (s), doublet (d), triplet (t), quartet (q), double doublet (dd), doublet of doublet of doublets (ddd), doublet of triplets (dt) and multiplet (m).

Infra-red (IR) spectra were recorded in their natural state on a Perkin Elmer spectrum 100 FT-IR spectrometer and the vibrational frequencies were recorded in the range 4000-600 cm⁻¹. Mass spectra were obtained from the EPSRC UK National Mass Spectrometry Facility at Swansea University, using electron spray ionization (ESI) or atmospheric pressure chemical ionization (APCI) in positive or negative mode. Optical rotation measurements were obtained from a Bellingham and Stanley ADP440+ Polarimeter, at 23.9 °C, at a concentration of 0.5 g/100 ml, with a cell length of 5 cm. Melting points were measured on a Stuart SMP10 melting point apparatus. Elemental analysis was performed by the elemental analysis service at London Metropolitan University. Enantiomeric excess (*e.e.*) was determined independently by Reach Separations Ltd. Analysis was carried out using a chiral stationary phase, Chiralpak IC column, 4.6 mm x 250 mm, 5 μm, (Daicel Chemical Industries). The isocratic mobile phase comprised of 20:80 MeOH:CO₂ (0.2% v/v NH₃). The flow rate of the mobile phase was 4.0 mL min⁻¹. A detector wavelength of 210-400 nm was utilised. The column temperature was maintained at 40 °C and the injection volume was 1.0 μL. The sample was compared to a racemic compound in order to determine the enantiomeric excess, (*e.e.*)

Reagents and solvents were purchased from Sigma-Aldrich, Acros Organics, Fluorochem, Fisher Scientific Alfa Aesar, and were used without further purification. Anhydrous solvents (used where specified) were purchased and used without further drying. Reactions were

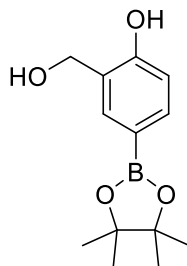
carried out under a flow of nitrogen gas, where specified. Dry ice/acetone baths were used to cool reactions to -78 °C. Solvents were degassed by injection of a flow of nitrogen gas, connected to a suitable outlet.

Note: the relaxation time between a C-B bond is too long for the respective ^{13}C NMR resonance to be observed (caused by broadening of the peak) in ^{13}C NMR spectroscopy and hence is reported as missing / not visible.

7.1 Synthetic chemistry

7.1.1 2-(Hydroxymethyl)-4-(4,4,5,5-tetramethyl-1,3,2-dioxaborolan-2-yl)phenol, (**7**)

Method 1



B₂Pin₂ (1.04 g, 4.10 mmol, 1.2 eq.), dppf (83 mg, 0.15 mmol, 0.05 eq.) and KOAc (1.08 g, 11.00 mmol, 3.5 eq.) were added to 5-bromo-2-hydroxy benzyl alcohol (0.80 g, 3.10 mmol, 1.0 eq.) dissolved in anhydrous dioxane (20 mL), under N₂. The resulting mixture was degassed under N₂, for 5 min, PdCl₂dppf (0.12 g, 0.15 mmol, 0.05 eq.) was then added and the resulting mixture heated at 80 °C and stirred overnight. The mixture was then heated under reflux with activated charcoal (8 mg) for 10 min and then cooled to room temperature. The crude mixture was filtered through celite (prepared with EtOAc), then the filtrate was evaporated under reduced pressure to obtain a brown oil. The material was purified by flash column chromatography, 50 % EtOAc / 50 % hexanes, to afford boronate ester **7** as an off-white solid (192 mg, 23 %).

¹H NMR (400 MHz, CDCl₃) δ = 7.67 (dd, *J* = 8.1, 1.4 Hz, 2H), 7.49 (s, 1H), 6.89 (d, *J* = 8.1 Hz, 1H), 4.88 (br s, 2H), 1.33 (s, 12H)

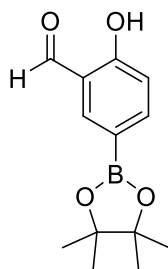
(¹H NMR spectrum identical to that reported by Xiao-Ling and co-workers)²⁵⁴

Method 2

To a solution of 2-hydroxy-5-(4,4,5,5-tetramethyl-1,3,2-dioxaborolan-2-yl)benzaldehyde (0.55 g, 2.22 mmol, 1.0 eq.), in ethanol (35 mL) cooled to 0 °C, NaBH₄ (42 mg, 1.11 mmol, 0.5 eq.) was added, and the resulting mixture was stirred for 2 h. The solvent was then evaporated under reduced pressure to yield a white solid. The material was dissolved in HCl aq. (1 M, 60 mL) and extracted with EtOAc (3 x 60 mL). The organic extracts were combined, dried over anhydrous MgSO₄, filtered and evaporated to obtain boronate ester **7** as an off-white solid, that was used without further purification (0.44 g, 80 %).

The sample was analysed by ¹H NMR spectroscopy (CDCl₃) and found to be in agreement the compound generated according to method 1 and literature values.

7.1.2 2-Hydroxy-5-(4,4,5,5-tetramethyl-1,3,2-dioxaborolan-2-yl)benzaldehyde, (**8**)

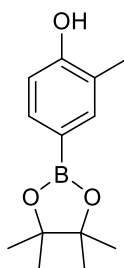


B_2Pin_2 (2.08 g, 8.2 mmol, 1.1 eq.), KOAc (2.20 g, 22.3 mmol, 3.0 eq.) and PdCl_2dppf (0.31 g, 0.37 mmol, 0.05 eq.) were added to 5-bromo-2-hydroxybenzaldehyde (1.50 g, 7.46 mmol, 1.0 eq.) dissolved in anhydrous dioxane (20 mL), under N_2 . The resulting mixture was degassed under N_2 , for 10 min, then heated to 110 °C and stirred overnight. The cooled reaction mixture was filtered through celite (DCM), concentrated under reduced pressure and purified by flash column chromatography, to afford aldehyde **8** as a white crystalline solid, (1.09 g, 59 %).

^1H NMR (400 MHz, CDCl_3) δ = 11.23 (s, 1H), 9.92 (s, 1H), 8.05 (d, J = 1.6 Hz, 1H), 7.95 (dd, J = 8.4, 1.7 Hz, 1H), 6.98 (d, J = 8.3 Hz, 1H), 1.35 (s, 12H)

^1H NMR spectrum identical to that reported by Lee and co-workers.²⁵⁵

7.1.3 2-Methyl-4-(4,4,5,5-tetramethyl-1,3,2-dioxaborolan-2-yl)phenol, (**4**)



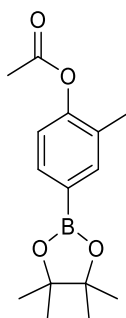
4-Bromo-2-methyl phenol (1.80 g, 9.6 mmol, 1 eq.), B₂Pin₂ (2.70 g, 10.6 mmol, 1.1 equiv.) and KOAc (2.84 g, 28.8 mmol, 3 eq.) were degassed under nitrogen in anhydrous dioxane (35 mL) for 10 min. PdCl₂dppf (0.39 g, 0.48 mmol, 0.05 eq.) was added. The mixture was then heated to 80 °C and stirred for 16 h. The mixture was cooled to room temperature, then filtered through a plug of silica (DCM), the filtrate was then filtered through a second plug of silica and evaporated under reduced pressure to give a golden-brown oil.

The crude product was purified *via* flash column chromatography, (30% EtOAc / 70 % light petroleum ether), to afford phenol **4** as a white crystalline solid (2.17 g, 97 %).

¹H NMR (400 MHz, CDCl₃) δ = 7.59 (s, 1 H), 7.54 (dd, *J* = 8.1, 1.3 Hz, 1 H), 6.75 (d, *J* = 8.0 Hz, 1 H), 5.10 (s, 1 H), 2.24 (s, 3 H), 1.33 (s, 12 H).

¹H NMR Data identical to that reported by Hanson and co-workers¹⁸⁶

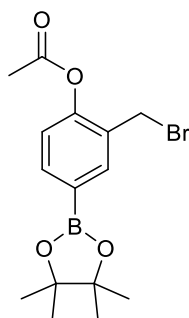
7.1.4 2-Methyl-4-(4,4,5,5-tetramethyl-1,3,2-dioxaborolan-2-yl)phenyl acetate, (**14**)



Triethylamine (1.88 mL, 13.5 mmol, 1.5 eq.) was added to a solution of 2-methyl-4-(4,4,5,5-tetramethyl-1,3,2-dioxaborolan-2-yl)phenol (2.11 g, 9.0 mmol, 1 eq.) in DCM (30 mL). Acetic anhydride (1.7 mL, 18.0 mmol, 2 eq.) was then added dropwise over 2 minutes and the resulting mixture stirred for 16 h at room temperature. The volatiles were then removed under reduced pressure to obtain a rose-pink solid. The material was diluted in H₂O (30 mL) and extracted with DCM (3 x 30 mL). The organic extracts were combined, washed with brine (30 mL), dried over anhydrous MgSO₄, filtered and evaporated to obtain acetyl **14** as an off-white crystalline solid (2.43g, 98%).

¹H NMR (400 MHz, CDCl₃) δ = 7.69 (s, 1 H, C(BPin)CHC(CH₃)), 7.65 (dd, *J* = 8.1, 1.6 Hz, 1 H, C(BPin)CHCH), 7.01 (d, *J* = 8.0 Hz, 1 H, C(BPin)CHCH), 2.31 (s, 3 H, ArOCOCH₃), 2.18 (s, 3 H, ArCH₃), 1.33 (s, 12 H, BO₂C₂(CH₃)₄); ¹³C NMR (100 MHz, CDCl₃) δ = 168.98, 151.84, 137.75, 133.60, 129.37, 121.31, 83.76, 24.76, 20.77, 15.86, C-BPin not visible; IR (neat) 2978, 2929, 1764, 1606, 1559, 1354, 1280, 1168, 1118 cm⁻¹; HRMS (ESI) [M + H]⁺ calcd for C₁₅H₂₁¹¹BO₄, 277.1606 found 277.1606.

7.1.5 2-(Bromomethyl)-4-(4,4,5,5-tetramethyl-1,3,2-dioxaborolan-2-yl)phenyl acetate, (**15**)



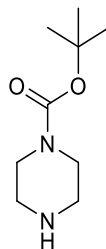
N-Bromo succinimide (1.51 g, 8.5 mmol, 1.1 eq.) and benzoyl peroxide (75 % in H₂O, 99 mg, 0.3 mmol, 0.04 eq.), under a flow of argon, were added to a solution of 2-methyl-4-(4,4,5,5-tetramethyl-1,3,2-dioxaborolan-2-yl)phenyl acetate (2.12 g, 7.7 mmol, 1 eq.) in CCl₄ (20 mL). The resulting mixture was heated to 84 °C and stirred for 20 h. The mixture was then cooled to 0 °C and the resulting precipitate removed by filtration. The filtrate was then evaporated to a yellow oil, dissolved in DCM (10 mL) and diluted with H₂O (20 mL). The organic phase was extracted with DCM (3 x 30 mL), combined, dried over anhydrous MgSO₄, filtered and evaporated under reduced pressure to obtain bromide **15** as an off-white crystalline solid, (2.46 g, 90 %).

The material was used without further purification in subsequent reactions*

¹H NMR (400 MHz, CDCl₃) δ = 7.85 (d, *J* = 1.4 Hz, 1 H, C(CH₂Br)CHC(BPin)), 7.79 (dd, *J* = 8.1, 1.5 Hz, 1 H, CHCHC(BPin)), 7.14 (d, *J* = 8.0 Hz, 1 H, CHCHC(BPin)), 4.43 (s, 2 H, CH₂Br), 2.37 (s, 3 H, ArCO₂CH₃), 1.34 (s, 12 H, BO₂C₂(CH₃)₄); ¹³C NMR (100 MHz, CDCl₃) δ = 137.63, 136.64, 129.01, 122.72, 84.23, 27.82, 24.97, 21.15, C-B not visible; IR (neat) 2978, 2929, 1721, 1618, 1411, 1311, 1233, 1198, 1122, 990, 856, 799, 655 cm⁻¹; HRMS (ESI) [M - H]⁺ calcd for C₁₅H₁₉¹¹B ⁷⁹BrO₄, 354.0562 found 353.0558; Mp = 81 - 83 °C.

*After approx. three weeks the material tended to strongly discolour (red/purple), regardless of storage conditions (-18°C / N₂), however inspection by ¹H NMR spectroscopy showed retention of the titular compound without any degradation of the structure.

7.1.6 *tert*-Butyl piperazine-1-carboxylate, (**1**)

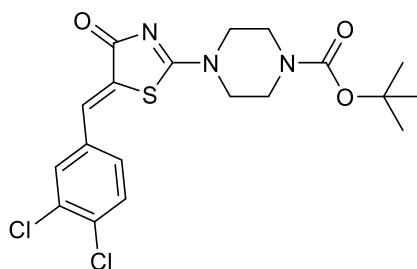


To a stirring solution of 1,4 piperazine (6.90 g, 80.0 mmol, 1 eq.) in DCM (200 mL) a solution of di-*tert*-butyl dicarbonate (9.60 g, 44.0 mmol, 0.55 eq.) in DCM (100 mL) was added dropwise over a period of 1 h, at room temperature, then stirred for 16 h. The volatiles were removed under reduced pressure to expose a white oily residue, H₂O (200 mL) was then added, causing the precipitation of a white solid which was filtered under gravity. The filtrate was extracted in DCM (3 x 200 mL), combined, dried over anhydrous MgSO₄, filtered and evaporated to obtain *N*-Boc piperazine **1** as a white crystalline solid (5.34 g, 65%).

¹H NMR (400 MHz, CDCl₃) δ = 3.40 - 3.35 (m, 4 H), 2.82 - 2.76 (m, 4 H), 1.45 (s, 9 H)

The ¹H NMR data was found to be in agreement with that of Nagano and co-workers.⁸⁸

7.1.7 *tert*-Butyl-(*Z*)-4-(5-(3,4-dichlorobenzylidene)-4-oxo-4,5-dihydrothiazol-2-yl)piperazine-1-carboxylate, (**2**)

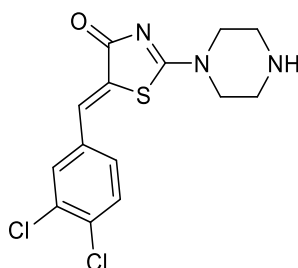


A solution of *tert*-butyl piperazine-1-carboxylate (4.50 g, 24.0 mmol, 2.4 eq.) and 3,4 dichloro benzaldehyde (2.10 g, 12.0 mmol, 1.3 eq.) in anhydrous ethanol (10 mL) was added dropwise to a solution of rhodanine (1.30 g, 10.0 mmol, 1 eq.), in anhydrous ethanol (20 mL), under nitrogen. The resulting mixture was then heated to 70 °C and stirred for 16 h. The mixture was evaporated under reduced pressure and under high vacuum give to a viscous red / orange oil. The oil was triturated in cold ethanol (10 mL) which precipitated a yellow solid, that was collected *via* vacuum filtration to give heterocycle **2** (2.17 g, 49 %).

¹H NMR (400 MHz ,DMSO-*d*₆) δ = 7.86 (d, *J* = 2.2 Hz, 1 H), 7.76 (d, *J* = 8.5 Hz, 1 H), 7.62 (s, 1 H), 7.57 (dd, *J* = 8.4, 2.1 Hz, 1 H), 3.91 - 3.86 (m, 2 H), 3.67 - 3.61 (m, 2 H), 3.52 - 3.43 (m, 4 H), 1.39 (s, 9 H)

The ¹H NMR spectroscopy data was found to be in agreement with that of Nagano and co-workers.⁸⁸

7.1.8 (Z)-5-(3,4-Dichlorobenzylidene)-2-(piperazin-1-yl)thiazol-4(5H)-one, (**17**)



A solution of trifluoroacetic acid (8.44 mL, 27.5 mmol, 25 eq.), in DCM (50 mL) was added dropwise over 1 h to a solution of *tert*-butyl (Z)-4-(5-(3,4-dichlorobenzylidene)-4-oxo-4,5-dihydrothiazol-2-yl)piperazine-1-carboxylate (2.00 g, 1.1 mmol, 1 eq.) in DCM (100 mL). The mixture was stirred for 1 h at room temperature. The mixture was evaporated under reduced pressure to a golden oil. The crude material was re-dissolved in DCM (approx. 30 mL) and evaporated under reduced pressure. This process was repeated five times to completely remove excess TFA from the material, whereupon it transformed to a yellow solid, *N*-TFA salt form **3** (quantitative).

$^1\text{H NMR}$ (400 MHz, DMSO-d_6) δ = 7.87 (d, J = 2.1 Hz, 1 H), 7.78 (d, J = 8.9 Hz, 1 H), 7.66 (s, 1 H), 7.58 (dd, J = 8.5, 2.2 Hz, 1 H), 4.12 - 4.04 (m, 2 H), 3.91 - 3.81 (m, 2 H), 3.27 (br. s., 4 H) (The $^1\text{H NMR}$ data were in agreement with that of Nagano and co-workers.⁸⁸)

The *N*-TFA salt was ground to a fine powder and dissolved in the minimum amount of water to make a thick syrup. Sodium carbonate was then added portion wise to basify the mixture to pH 12, to expose the titular compound in its free base form.

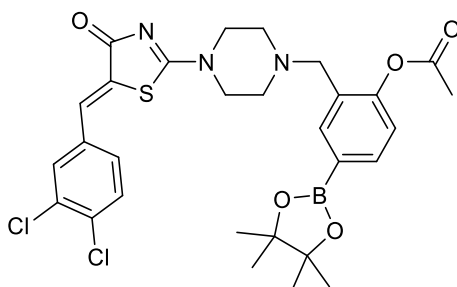
The product was then isolated by continuous liquid-liquid extraction in chloroform over a period of two days, to give piperazine **17** as a yellow powder (3.01 g, 80 %).

$^1\text{H NMR}$ (400 MHz, CDCl_3) δ = 7.66 (s, 1 H, $\text{C}=\underline{\text{CH}}$), 7.58 (d, J = 2.1 Hz, 1 H, $\text{C}(\text{Cl})\underline{\text{CH}}\text{C}(\text{HC}=\text{C})$), 7.49 (d, J = 8.3 Hz, 1 H, $\text{C}(\text{C}=\text{C})\underline{\text{CH}}\text{CH}$), 7.33 (dd, J = 8.2, 2.1 Hz, 1 H, $\text{C}(\text{C}=\text{C})\underline{\text{CH}}\text{CH}$), 4.06 (d, J = 5.0 Hz, 2 H, $\text{NCH}_2\underline{\text{CH}}_2\text{NH}$), 3.68 - 3.57 (m, 2 H, $\text{NCH}_2\underline{\text{CH}}_2\text{NH}$), 3.08 - 2.93 (m, 4 H, $(\text{NCH}_2\underline{\text{CH}}_2\text{NH}) \times 2$); $^{13}\text{C NMR}$ (100 MHz, CDCl_3) δ = 180.4, 174.6, 134.4, 133.7, 133.4, 131.0, 130.9, 130.0, 128.9, 128.8, 50.4, 50.1, 46.1, 45.7; IR (neat) 2998, 2735, 1664, 1541, 1448, 1356, 1284, 1194, 1123, 1028 cm^{-1} ; HRMS (ESI) $[\text{M} + \text{H}]^+$ calcd for $\text{C}_{14}\text{H}_{13}^{35}\text{Cl}_2\text{N}_3\text{OS}$, 342.0229 found 342.0234; Mp = 223 – 225 °C.

A single crystal was grown by slow evaporation in chloroform, and submitted for analysis by single crystal X-Ray diffraction, confirming the Z geometry of the double bond.

A suitable crystal was obtained by slow evaporation in chloroform. Diffraction data (7683 total reflections with $R_{\text{int}} = 0.0331$) were collected on a Rigaku Oxford Diffraction Excalibur diffractometer at $T = 150$ K using graphite-monochromated Mo-K α radiation. The structure was solved and refined using the SHELXS-2016 and SHELXL-2016 programs.²⁵⁶ Crystal data: $\text{C}_{14}\text{H}_{12}\text{N}_3\text{O}_1\text{S}_1\text{Cl}_2$, $M = 341.24$, orange plate, $0.378 \times 0.359 \times 0.290$ mm³, monoclinic, space group $P2_1/C$, $V = 1455.74(14)$ Å³, $Z = 4$, $D_c = 1.5568$ g/cm³, $F_{000} = 700$, Xcalibur, Sapphire3, Gemini, Mo K α radiation, $\lambda = 0.71073$ Å, $T = 150.00(10)$ K, $2\theta_{\text{max}} = 58.6^\circ$, 7683 reflections collected, 3362 unique ($R_{\text{int}} = 0.0331$). Final $Goof = 1.062$, $RI = 0.0588$, $wR2 = 0.1566$, R indices based on 2661 reflections with $I > 2(I)$ (refinement on F^2), 190 parameters, 0 restraints. Lp and absorption corrections applied, $\mu = 0.082$ mm⁻¹.

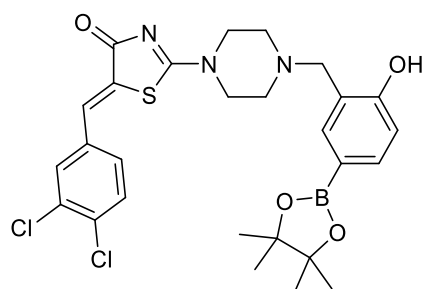
7.1.9 (Z)-2-((4-(5-(3,4-Dichlorobenzylidene)-4-oxo-4,5-dihydrothiazol-2-yl)piperazin-1-yl)methyl)-4-(4,4,5,5-tetramethyl-1,3,2-dioxaborolan-2-yl)phenyl acetate, (**16**)



2-(Bromomethyl)-4-(4,4,5,5-tetramethyl-1,3,2-dioxaborolan-2-yl)phenyl acetate (2.50 g, 7.0 mmol, 1.2 eq.) and K_2CO_3 (0.81 g, 5.9 mmol, 1.0 eq.) were added to a solution of (Z)-5-(3,4-dichlorobenzylidene)-2-(piperazin-1-yl)thiazol-4(5H)-one, (2.01 g, 5.9 mmol, 1.0 eq.) in acetone (160 mL), the resulting mixture was heated to 50°C and stirred for two days. The mixture was then evaporated under reduced pressure to obtain a light tan powder, which was dissolved in EtOAc (100 mL) and diluted with water (100 mL). The organic portion was extracted with EtOAc (5 x 50 mL), combined, washed with brine (200 mL), dried over anhydrous $MgSO_4$, filtered and evaporated to a yellow solid, as the crude product **16**.

The crude material: containing a mixture of starting materials and product as well as a small amount (10% approx.) of the Ar-OH deprotected form This was used directly in the next step without further purification

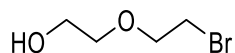
7.1.10 (Z)-5-(3,4-Dichlorobenzylidene)-2-(4-(2-hydroxy-5-(4,4,5,5-tetramethyl-1,3,2-dioxaborolan-2-yl)benzyl)piperazin-1-yl)thiazol-4(5H)-one, (**9**)



A flask was charged with, (Z)-2-((4-(5-(3,4-dichlorobenzylidene)-4-oxo-4,5-dihydrothiazol-2-yl)piperazin-1-yl)methyl)-4-(4,4,5,5-tetramethyl-1,3,2-dioxaborolan-2-yl)phenyl acetate (crude) (2.00 g, 3.30 mmol, 1.0 eq.) and dissolved in methanol (120 mL). K_2CO_3 (46 mg, 0.03 mmol, 0.10 eq.) was added. The mixture was heated to 40 °C and stirred over two days and then evaporated under reduced pressure to give a light-yellow solid, which was purified *via* flash column chromatography (100% EtOAc), to afford phenol **9** as a light-yellow powder, (1.54 g, 51%, over two steps).

1H NMR (400 MHz, DMSO- d_6) δ = 7.90 (d, J = 2.2 Hz, 1H, C(HC=C)CHC(Cl)), 7.78 (d, J = 8.5 Hz, 1H, C(Cl)CHCH), 7.64 (s, C=CH, 1H), 7.59 (dd, J = 8.8, 2.2 Hz, 1H, C(Cl)CHCH), 7.49 (d, J = 1.5 Hz, 1H, C(BPin)CHC(HC=C)), 7.44 (dd, J = 8.0, 1.6 Hz, 1H, C(BPin)CHCH), 6.80 (d, J = 8.0 Hz, 1H, C(BPin)CHCH), 3.91 (br. s., 2 H, $CH_2NCH_2CH_2$), 3.66 (br. s., 2 H, $CH_2NCH_2CH_2$), 3.59 (s, 2 H, $CH_2NCH_2CH_2$), 2.63 - 2.49 (m, 4 H, $(CH_2NCH_2CH_2) \times 2$), 1.24 (s, 12 H, $BO_2C_2(CH_3)_4$); ^{13}C NMR (100 MHz, DMSO- d_6) δ = 179.47, 174.05, 159.96, 137.75, 135.87, 135.26, 132.55, 132.51, 131.86, 131.72, 131.32, 129.41, 127.83, 122.52, 115.64, 83.87, 57.16, 52.35, 51.9, 49.00, 48.62, 25.23; IR (neat) 2975, 1681, 1612, 1558, 1470, 1351, 1294, 1243, 1141 cm^{-1} ; HRMS (ESI) $[M + H]^+$ calcd for $C_{27}H_{30}^{11}B^{35}Cl_2N_3O_4S$, 574.1505 found 574.1502; Mp = 226 – 229 °C.

7.1.11 2-(2-Bromoethoxy)ethan-1-ol, (**18**)



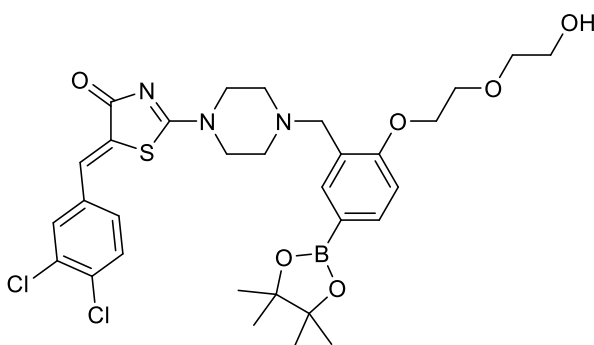
Freshly procured / distilled diethylene glycol (4.46 mL, 47.1 mmol, 1.0 eq.), was mixed in toluene (150 mL) with HBr (48% in H₂O, 5.32 mL, 47.1 mmol, 1.0 eq.). The mixture was then heated under dean-stark conditions for 4 h, upon which it was cooled to 0 °C and quenched with NaOH aq. (1 M, 50 mL). The mixture was diluted with H₂O (200 mL) and extracted with EtOAc (2 x 200 mL), combines, washed with brine (200 mL), dried over anhydrous MgSO₄, filtered and evaporated under reduced pressure to a pale-yellow oil. The crude material was purified by flash column chromatography (40% EtOAc / 60% hexanes), to afford ether **18** as a pale-yellow oil, (3.13 g, 40 %).*

¹H NMR (400 MHz, CDCl₃) δ = 3.83 (t, *J* = 6.0 Hz, 2H), 3.79 - 3.73 (m, 2H), 3.63 (d, *J* = 4.3 Hz, 2H), 3.51 (t, *J* = 6.0 Hz, 2H), 2.12 - 2.01 (m, 1H).

*It was found that for best results, 2-(2-bromoethoxy)ethan-1-ol should be used immediately after purification in the next reaction, dues to issues with shelf stability.

Data in agreement with that stated by Koley and co-workers.²⁵⁷

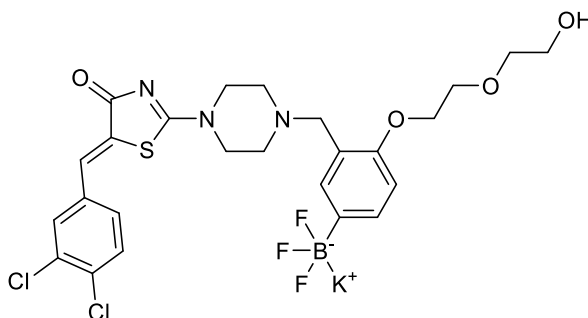
7.1.12 (Z)-5-(3,4-Dichlorobenzylidene)-2-(4-(2-(2-(2-hydroxyethoxy)ethoxy)-5-(4,4,5,5-tetramethyl-1,3,2-dioxaborolan-2-yl)benzyl)piperazin-1-yl)thiazol-4(5H)-one, (**19**)



K_2CO_3 (0.32 g, 2.3 mmol, 1.5 eq.) was added to a solution of (Z)-5-(3,4-dichlorobenzylidene)-2-(4-(2-hydroxy-5-(4,4,5,5-tetramethyl-1,3,2-dioxaborolan-2-yl)benzyl)piperazin-1-yl)thiazol-4(5H)-one (0.89 g, 1.6 mmol, 1 eq.) in DMF (25 mL). This was followed by a solution of 2-(2-bromoethoxy)ethan-1-ol (0.76 g, 4.5 mmol, 2.9 eq.) dissolved in DMF, added dropwise and lastly KI (0.26 g, 1.6 mmol, 1.0 eq.). The mixture was heated to 80 °C and stirred for 20 h, then cooled to room temperature, diluted with H_2O (50 mL). The organic portion was extracted with EtOAc (3 x 75 mL), washed with a solution of 5 % LiCl aq. (3 x 100 ml), dried over anhydrous magnesium sulfate, filtered and evaporated to brown oil. The crude material was then purified by flash column chromatography (90% EtOAc / 10% acetone \rightarrow 100% acetone) to obtain alcohol **19** as a golden-brown oil (0.48 g, 61 %).

^1H NMR (400 MHz, CDCl_3) δ = 7.71 (dd, J = 8.2, 1.8 Hz, 1 H, $\text{CHCHC}(\text{BPin})$), 7.66 (d, J = 1.8 Hz, 1 H, $\text{C}(\text{CH}_2)\text{CHC}(\text{BPin})$), 7.62 (s, 1 H, $\text{C}=\text{CH}$), 7.55 (d, J = 2.3 Hz, 1 H, $\text{CHCHC}(\text{Cl})\text{C}(\text{Cl})\text{CH}$), 7.47 (d, J = 8.7 Hz, 1 H, $\text{CHCHC}(\text{Cl})\text{C}(\text{Cl})\text{CH}$), 7.31 (dd, J = 8.5, 2.1, 1 H, $\text{CHCHC}(\text{Cl})\text{C}(\text{Cl})\text{CH}$), 6.86 (d, J = 8.2 Hz, 1 H, $\text{CHCHC}(\text{BPin})$), 4.19 - 4.13 (m, 2 H, $\text{ArOCH}_2\text{CH}_2$), 4.09 - 4.02 (m, 2 H, $\text{CH}_2\text{NCH}_2\text{CH}_2$), 3.92-3.88 (m, 2 H, $\text{ArOCH}_2\text{CH}_2$), 3.76 - 3.69 (m, 2 H, OHCH_2CH_2), 3.67 - 3.58 (m, 6 H, ArCH_2 , OHCH_2CH_2 , $\text{CH}_2\text{NCH}_2\text{CH}_2$), 2.71 - 2.57 (m, 5 H, $(\text{CH}_2\text{NCH}_2\text{CH}_2) \times 2$, OH), 1.32 (s, 12 H, $\text{BO}_2\text{C}_2(\text{CH}_3)_4$); ^{13}C NMR (100 MHz, CDCl_3) δ = 180.55, 174.32, 159.87, 138.41, 136.4, 134.59, 133.66, 133.48, 131.11, 130.96, 130.24, 128.92, 128.72, 124.12, 111.06, 83.88, 72.56, 69.58, 67.38, 61.76, 56.29, 52.54, 52.29, 49.01, 48.88, 25.08, C-BPin not visible; IR (neat) 3350, 2931, 2868, 1673, 1604, 1556, 1386, 1272, 1252, 1131, 993 cm^{-1} ; HRMS (ESI) $[\text{M} + \text{H}]^+$ calcd for $\text{C}_{31}\text{H}_{38}^{11}\text{B}^{35}\text{Cl}_2\text{N}_3\text{O}_6\text{S}$, 662.2030 found 662.2017.

7.1.13 Potassium (Z)-3-((4-(5-(3,4-dichlorobenzylidene)-4-oxo-4,5-dihydrothiazol-2-yl)piperazin-1-yl)methyl)-4-(2-(2-hydroxyethoxy)ethoxy)phenyl)trifluoroborate, (**21**)



To a solution of (Z)-5-(3,4-dichlorobenzylidene)-2-(4-(2-(2-(2-hydroxyethoxy)ethoxy)-5-(4,4,5,5-tetramethyl-1,3,2-dioxaborolan-2-yl)benzyl)piperazin-1-yl)thiazol-4(5H)-one (57 mg, 0.1 mmol, 1.0 eq.) in methanol (2 mL), a solution of KHF_2 aq. (4.5 M, 0.11 mL, 0.5 mmol, 5.65 eq.) was added in one portion. The mixture was stirred for 1 h at room temperature and then acetone (10 mL) was added. The solution filtered, and the filtrate evaporated under reduced pressure to give a tacky white residue. The residue was then co-evaporated with a 1:1 mixture of H_2O / methanol 4 times (procedure described below). The reaction was then repeated again using the crude material, then purified in the same manner, to obtain trifluoroborate **21** as a white crystalline solid (quantitative). This was used immediately in the next reaction.

^1H NMR data included for reference:

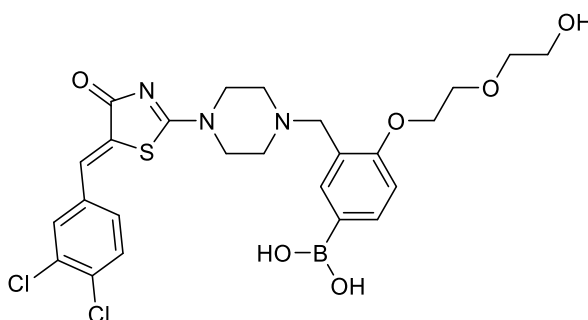
^1H NMR (400 MHz, MeOH-D_3) δ = 7.74 (d, J = 2.1 Hz, 1H), 7.70 - 7.59 (m, 2H), 7.52 (dd, J = 8.2, 1.9 Hz, 1H), 7.45 - 7.38 (m, 2H), 6.84 (d, J = 8.3 Hz, 1H), 4.25 - 4.09 (m, 2H), 4.06 - 3.94 (m, 2H), 3.85 (dd, J = 5.3, 3.8 Hz, 2H), 3.78 - 3.58 (m, 8H), 2.81 - 2.60 (m, 4H)

The material was then used immediately as an intermediate for the next reaction

Evaporation procedure:

The material was dissolved in 1:1 H_2O / methanol, using a volume approx. $\frac{1}{4}$ that of the round bottom flask, and evaporated under reduced pressure, starting at 200 mbar (50 °C water bath, approx. 180 rpm) then the vacuum was increased in 10 mbar increments to 50 mbar over a period of 3-4 min, taking care not to “bump” the material. Once 50 mbar was attained the material could be held under continuous vacuum.

7.1.14 (Z)-3-((4-(5-(3,4-Dichlorobenzylidene)-4-oxo-4,5-dihydrothiazol-2-yl)piperazin-1-yl)methyl)-4-(2-(2-hydroxyethoxy)ethoxy)phenyl)boronic acid, (**22**)

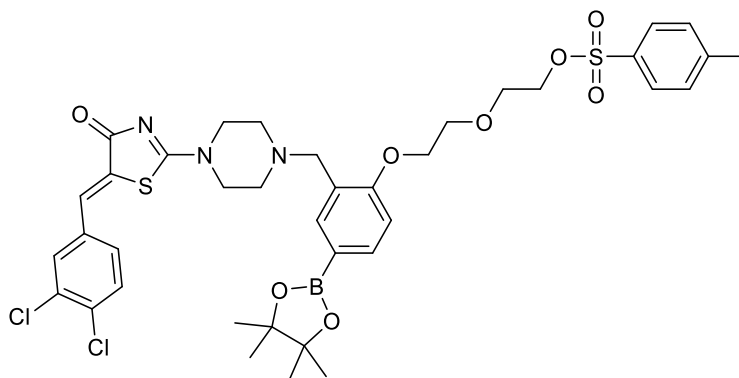


Trimethylsilyl chloride (0.03 mL, 0.26 mmol, 3.0 eq.) and H₂O (5 μ L, 0.26 mmol, 3.0 eq.) were added to a solution of potassium (Z)-3-((4-(5-(3,4-dichlorobenzylidene)-4-oxo-4,5-dihydrothiazol-2-yl)piperazin-1-yl)methyl)-4-(2-(2-hydroxyethoxy)ethoxy)phenyl tri fluoroborate (55 mg, 0.09 mmol, 1.0 eq.) in MeCN (2 mL). The mixture was stirred for 1 h at room temperature. A solution of sodium bicarbonate sat. aq. (0.2 mL) was added to the mixture, which was then dried using anhydrous sodium sulfate, filtered and evaporated under reduced pressure to obtain boronic acid **22** as a crystalline cream solid (29 mg, 59%).

¹H NMR (400 MHz, MeOH-D₃) δ = 7.73 - 7.61 (m, 1H, C(HC=C)CHC(Cl)), 7.61 - 7.51 (m, 3H, C=CH, C(Cl)CHCH, C(B(OH)₂)CHC(CH₂)), 7.43 (dd, *J* = 8.5, 2.1 Hz, 1H, C(Cl)CHCH), 7.07 - 6.89 (m, 1H, C(B(OH)₂)CHCH), 4.24 - 4.12 (m, 2H, ArOCH₂CH₂), 4.07 - 3.97 (m, 2H, NCH₂CH₂NCH₂Ar), 3.91 - 3.82 (m, 2H, ArOCH₂CH₂), 3.77 - 3.62 (m, 8H, NCH₂CH₂NCH₂Ar, CH₂CH₂OH, NCH₂Ar), 2.84 - 2.63 (m, 4H, (NCH₂CH₂NCH₂Ar) x 2), CHC(OCH₂CH₂) not visible; ¹³C NMR (100 MHz, MeOH-D₃) δ = 180.85, 174.80, 137.30, 135.17, 134.43, 133.29, 132.87, 131.05, 130.96, 130.02, 128.76, 128.51, 123.25, 120.41, 110.73, 72.47, 69.43, 67.43, 60.96, 55.43, 51.83, 51.60, 48.77, 44.03, C-B(OH)₂ not visible; IR (neat); 3234, 2921, 1675, 1605, 1555, 1470, 1444, 1341, 1288, 1181 cm⁻¹; HRMS (ESI) (Sample + ethylene glycol) [M + H]⁺ calcd for C₂₇H₃₂ ¹¹B ³⁵Cl₂N₃O₆S, 606.1409 found 606.1400*; Mp = 85 – 88 °C.

*Molecular ion peak was not detected by the EPSRC national mass spectrometry facility, a problem found to not be uncommon with boronic acid compounds. Instead the sample was reacted with a small amount of ethylene glycol, to give the corresponding boronic ester, allowing the acquisition of the molecular ion for the devitalised compound.²⁵⁸

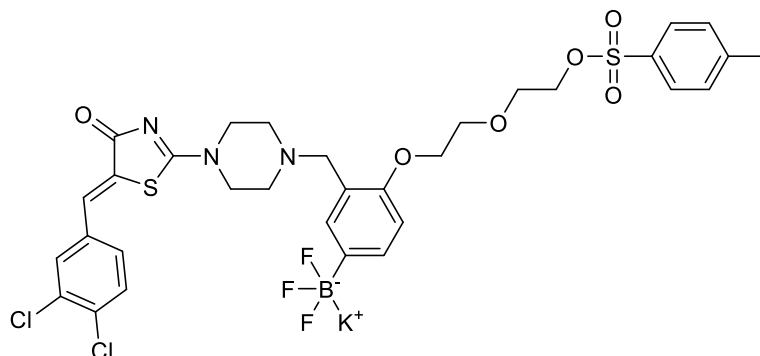
7.1.15 (Z)-2-(2-(2-((4-(5-(3,4-Dichlorobenzylidene)-4-oxo-4,5-dihydrothiazol-2-yl)piperazin-1-yl)methyl)-4-(4,4,5,5-tetramethyl-1,3,2-dioxaborolan-2-yl)phenoxy)ethoxy)ethyl 4-methylbenzenesulfonate, (**31**)



Tosyl chloride (0.14 g, 0.7 mmol, 1.3 eq.) and triethylamine (0.15 mL, 1.1 mmol, 2.0 eq.) were added to a solution of (Z)-5-(3,4-dichlorobenzylidene)-2-(4-(2-(2-(2-hydroxyethoxy)ethoxy)-5-(4,4,5,5-tetramethyl-1,3,2-dioxaborolan-2-yl)benzyl)piperazin-1-yl)thiazol-4(5H)-one, (0.37 g, 0.6 mmol, 1.0 eq.) in DCM (20 mL). The resulting mixture was stirred at room temperature for two days. The volatiles were then removed under reduced pressure to obtain a yellow residue which was purified *via* flash column chromatography (100% EtOAc) to afford a tosylate **31** as a yellow oil (0.20 g, 45%).

^1H NMR (400 MHz, CDCl_3) δ = 7.78 (d, J = 8.2 Hz, 2H, (SO₃)CCH), 7.75 - 7.70 (m, 2H, C(BPin)CHC(CH₂), C(BPin)CHCH), 7.65 (s, 1H, C=CH), 7.58 (d, J = 2.3 Hz, 1H, C(HC=C)CHC(Cl)), 7.49 (d, J = 8.2 Hz, 1H, CHCHC(Cl)), 7.34 (dd, J = 8.2, 2.3 Hz, 1H, CHCHC(Cl)), 7.30 (d, J = 8.2 Hz, 2H, C(CH₃)CH), 6.85 (d, J = 8.2 Hz, 1H, C(BPin)CHCH), 4.20 - 4.15 (m, 2H, ArOCH₂CH₂), 4.10 (dd, J = 5.3, 3.9 Hz, 2H, CH₂CH₂OTs), 4.08 - 4.03 (m, 2H, NCH₂CH₂NCH₂), 3.82 (dd, J = 5.3, 3.9 Hz, 2H, CH₂CH₂OTs), 3.78 - 3.74 (m, 2H, PhOCH₂CH₂), 3.69 - 3.61 (m, 4H, NCH₂CH₂NCH₂, ArCH₂), 2.69 - 2.59 (m, 4H, (NCH₂CH₂NCH₂) x2), 2.41 (s, 3H, ArCH₃), 1.35 (s, 12H, BO₂C₂(CH₃)₄); ^{13}C NMR (100 MHz, CDCl_3) δ = 180.5, 174.4, 159.7, 145.0, 138.1, 136.2, 134.5, 133.6, 133.4, 132.9, 131.0, 131.0, 130.3, 130.0, 128.8, 128.6, 128.0, 124.4, 111.1, 83.8, 69.9, 69.4, 69.0, 67.5, 55.7, 52.2, 51.9, 49.2, 48.9, 25.0, 21.8, C-BPin not visible; IR (neat) 2978, 2926, 2245, 1686, 1604, 1558, 1353, 1284, 1254, 1174, 1133 cm^{-1} ; HRMS (ESI) $[\text{M} + \text{H}]^+$ calcd for C₃₈H₄₄ ^{11}B $^{35}\text{Cl}_2\text{N}_3\text{O}_8\text{S}_2$, 816.2225 found 816.2211.

7.1.16 Potassium (Z)-3-((4-(5-(3,4-dichlorobenzylidene)-4-oxo-4,5-dihydrothiazol-2-yl)piperazin-1-yl)methyl)-4-(2-(2-(tosyloxy)ethoxy)ethoxy)phenyl)trifluoroborate, (**32**)

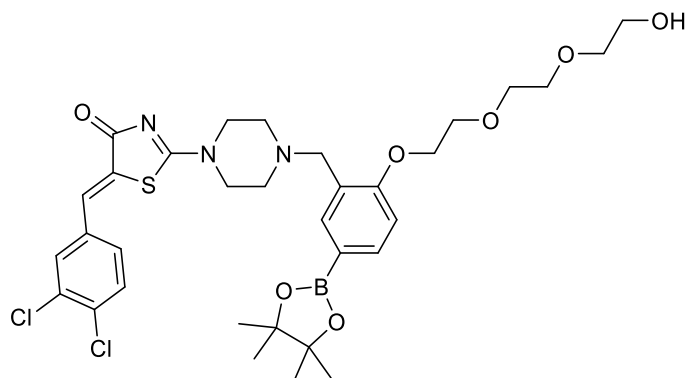


KHF₂ aq. (4.5 M, 0.44 mL, 2.0 mmol, 10.0 eq.) was added in one portion to a solution of (Z)-2-(2-(2-((4-(5-(3,4-dichlorobenzylidene)-4-oxo-4,5-dihydrothiazol-2-yl)piperazin-1-yl)methyl)-4-(4,4,5,5-tetramethyl-1,3,2dioxaborolan-2-yl)phenoxy)ethoxy)ethyl -4-methyl benzenesulfonate (0.16 g, 0.2 mmol, 1.0 eq.) in MeOH (5 mL). The mixture was stirred for 1 h at room temperature. Acetone (7 mL) was added, the solution was then filtered and evaporated under reduced pressure to give a golden brown solid. The solid was then co-evaporated with a 1:1 mixture of H₂O / MeOH 3 times. The entire reaction / purification procedure was then repeated with the product, to obtain trifluoroborate **32** as an orange crystalline solid (quantitative).

¹H NMR (400 MHz, DMSO-d₆) δ = 7.86 (d, *J* = 1.8 Hz, 1H, C(HC=C)CHC(Cl)), 7.77 - 7.70 (m, 3H, C(SO₃)CH, C(Cl)CHCH), 7.60 (s, 1H, HC=C), 7.58 (dd, *J* = 8.2, 1.8 Hz, 1H, C(Cl)CHCH), 7.38 (br d, *J* = 7.8 Hz, 2H, C(CH₃)CH), 7.21 (d, *J* = 0.9 Hz, 1H, C(BF₃K)CHC(CH₂)), 7.14 (d, *J* = 8.2 Hz, 1H, C(BF₃K)CHCH), 6.66 (d, *J* = 8.2 Hz, 1H, C(BF₃K)CHCH), 4.19 - 4.07 (m, 2H, ArOCH₂CH₂), 3.97 - 3.80 (m, 2H, CH₂CH₂OTs), 3.70 - 3.56 (m, 6H, NCH₂CH₂NCH₂Ar, ArOCH₂CH₂, CH₂CH₂OTs), 3.51 - 3.40 (m, 2H, NCH₂Ar), 2.40 - 2.32 (m, 3H, ArCH₃)*; ¹³C NMR (100 MHz, DMSO-d₆) δ = 179.47, 173.86, 155.44, 145.42, 135.33, 135.16, 135.14, 132.97, 132.55, 132.01, 131.93, 131.82, 131.41, 130.66, 129.38, 128.11, 127.64, 123.0, 111.17, 70.67, 69.73, 68.62, 68.04, 56.27, 52.35, 52.22, 49.31, 48.96, 21.61, (C-BF₃K not visible); IR (neat) 3673, 2986, 2900, 1679, 1600, 1555, 1447, 1348, 1130 cm⁻¹; HRMS (ESI) [M - K]⁻ calcd for C₃₂H₃₂ ¹¹B ³⁵Cl₂F₃N₃O₈S₂, 756.1166 found 756.1173.

*(NCH₂CH₂NCH₂Ar) x2 obscured by DMSO residual solvent

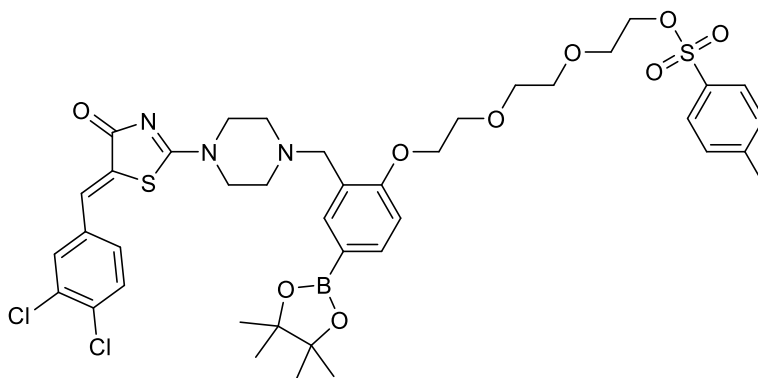
7.1.17 (Z)-5-(3,4-Dichlorobenzylidene)-2-(4-(2-(2-(2-(2-hydroxyethoxy)ethoxy)ethoxy)ethoxy)-5-(4,4,5,5-tetramethyl-1,3,2-dioxaborolan-2-yl)benzyl)piperazin-1-yl)thiazol-4(5H)-one, (**34**)



To a solution of (Z)-5-(3,4-dichlorobenzylidene)-2-(4-(2-hydroxy-5-(4,4,5,5-tetramethyl-1,3,2-dioxaborolan-2-yl)benzyl)piperazin-1-yl)thiazol-4(5H)-one (0.29 g, 0.5 mmol, 1.0 eq.) in DMF (5 mL) K_2CO_3 (0.11 g, 0.8 mmol, 1.5 eq.), a solution of 2-[2-(2-chloroethoxy)ethoxy] ethanol (0.22 ml, 1.5 mmol, 3.0 eq.) dissolved in DMF (1 mL) (dropwise, over 1 min) and KI (81 mg, 0.5 mmol, 1.0 eq.) were added. The resulting mixture was heated to 75°C and stirred for 16 h, cooled and then concentrated under reduced pressure to give a brown oil. The material was diluted with H_2O (30 mL), extracted with EtOAc (3 x 50 mL), combined, dried over anhydrous MgSO_4 and evaporated to obtain a light brown oil. The crude product was purified *via* flash column chromatography (80% EtOAc / 20% acetone \rightarrow 100% acetone), to afford alcohol **34** as a yellow oil which overnight crystallised to a golden solid (195 mg, 55 %).

^1H NMR (400 MHz, CDCl_3) δ = 7.69 (dd, J = 8.2, 1.8 Hz, 1H, C(BPin)CHCH), 7.65 (d, J = 1.6 Hz, 1H, C(BPin)CHC(CH₂)), 7.60 (s, 1H, HC=C), 7.53 (d, J = 2.3 Hz, 1H, C(HC=C)CHC(Cl)), 7.45 (d, J = 8.2 Hz, 1H, C(Cl)CHCH), 7.29 (dd, J = 8.2, 2.3 Hz, 1H, C(Cl)CHCH), 6.85 (d, J = 8.2 Hz, 1H, C(BPin)CHCH), 4.19 - 4.10 (m, 2H, ArOCH₂CH₂), 4.08 - 3.93 (m, 2H, NCH₂CH₂NCH₂), 3.88 - 3.78 (m, 2H, ArOCH₂CH₂), 3.75 - 3.56 (m, 12H, NCH₂CH₂NCH₂, ArCH₂, CH₂OCH₂CH₂OCH₂, CH₂CH₂OH), 2.72 - 2.59 (m, 4H, (NCH₂CH₂NCH₂) x2), 1.31 (s, 12H, $\text{BO}_2\text{C}_2(\text{CH}_3)_4$); ^{13}C NMR (100 MHz, CDCl_3) δ = 180.27, 174.08, 159.64, 138.10, 136.13, 134.25, 133.38, 133.19, 130.83, 130.67, 129.99, 128.66, 128.40, 123.83, 110.97, 83.58, 72.60, 70.69, 70.26, 69.54, 67.29, 61.59, 55.49, 51.85, 51.59, 48.92, 48.66, 24.78; IR (neat) 3402, 2974, 2926, 2870, 1690, 1604, 1557, 1470, 1446, 1387, 1353, 1133 cm^{-1} ; HRMS (ESI) $[\text{M} + \text{H}]^+$ calcd for $\text{C}_{33}\text{H}_{42}^{11}\text{B}^{35}\text{Cl}_2\text{N}_3\text{O}_7\text{S}$, 706.2292 found 706.2281; Mp = 65-67 °C.

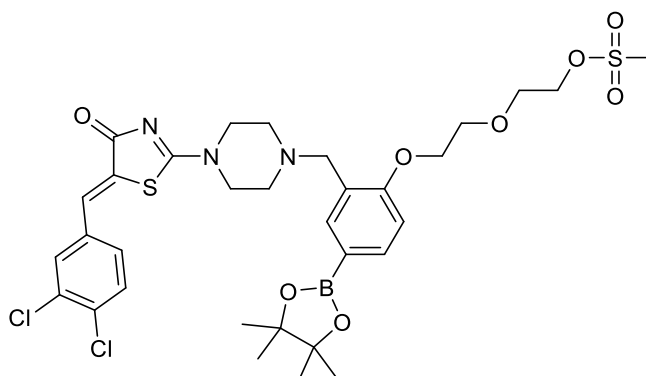
7.1.18 (Z)-2-(2-(2-(2-((4-(5-(3,4-Dichlorobenzylidene)-4-oxo-4,5-dihydrothiazol-2-yl) piperazin-1-yl)methyl)-4-(4,4,5,5-tetramethyl-1,3,2-dioxaborolan-2-yl)phenoxy)ethoxy)ethoxy)ethyl 4-methylbenzenesulfonate, (**35**)



Triethylamine (0.08 mL, 0.5 mmol, 2.0 eq.) and tosyl chloride (103 mg, 0.5 mmol, 2.0 eq.) was added to a solution of (Z)-5-(3,4-dichlorobenzylidene)-2-(4-(2-(2-(2-(2-hydroxyethoxy)ethoxy)ethoxy)ethoxy)-5-(4,4,5,5-tetramethyl-1,3,2-dioxaborolan-2-yl)benzyl)piperazin-1-yl)thiazol-4(5H)-one (0.19 g, 0.3 mmol, 1.0 eq.) in DCM (5 mL). The resulting mixture was stirred at room temperature for 4 days, and then evaporated to an orange residue. The residue was re-dissolved in DCM (30 mL), washed in brine (20 mL), dried over anhydrous MgSO₄ and evaporated to obtain an orange oil. The crude material was purified *via* flash column chromatography (95% EtOAc / 5% acetone) to afford tosylate **35** as a yellow oil (114 mg, 49 %).

¹H NMR (400 MHz, CDCl₃) δ = 7.75 (d, *J* = 8.2 Hz, 2 H, (SO₃)CCH), 7.72 - 7.68 (m, 2 H, C(HC=C)CH(Cl), C(BPin)CHCH), 7.61 (s, 1 H, C=CH), 7.54 (d, *J* = 1.8 Hz, 1 H, C(BPin)CHC(CH₂)), 7.46 (d, *J* = 8.7 Hz, 1 H, C(Cl)CHCH), 7.34 - 7.26 (m, 3 H, C(CH₃)CH, C(Cl)CHCH), 6.85 (d, *J* = 8.2 Hz, 1 H, C(BPin)CHCH), 4.15 - 4.10 (m, 4 H, ArOCH₂CH₂, CH₂CH₂OTs), 4.06 - 4.00 (m, 2 H, NCH₂CH₂NCH₂), 3.85 - 3.79 (m, 2 H, ArOCH₂CH₂), 3.69 - 3.56 (m, 10 H, ArCH₂, CH₂OCH₂CH₂OCH₂, CH₂CH₂OTs, NCH₂CH₂NCH₂), 2.67-2.58 (m, 4 H, (NCH₂CH₂NCH₂) x2), 1.32 (s, 12 H, BO₂C₂(CH₃)₄); ¹³C NMR (100 MHz, CDCl₃) δ = 180.42, 174.31, 159.84, 144.97, 138.05, 136.27, 134.59, 133.53, 133.44, 133.02, 131.01, 130.97, 130.33, 129.95, 128.87, 128.53, 128.05, 111.16, 83.85, 76.43, 70.92, 70.72, 69.88, 69.38, 68.83, 67.66, 55.77, 52.32, 52.02, 49.25, 48.98, 25.02, 21.72, C-BPin missing; IR (neat) cm⁻¹; HRMS (ESI) [M + H]⁺ calcd for C₄₀H₄₈¹¹B ³⁵Cl₂N₃O₉S₂, 860.2382 found 860.2373.

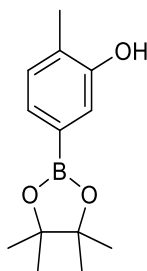
7.1.19 (Z)-2-(2-(2-((4-(5-(3,4-Dichlorobenzylidene)-4-oxo-4,5-dihydrothiazol-2-yl)piperazin-1-yl)methyl)-4-(4,4,5,5-tetramethyl-1,3,2-dioxaborolan-2-yl)phenoxy)ethoxy)ethylmethanesulfonate, (**36**)



Triethylamine (0.05 mL, 0.4 mmol, 2.0 eq.) was added to a stirring solution of (Z)-5-(3,4-dichlorobenzylidene)-2-(4-(2-(2-(2-hydroxyethoxy)ethoxy)-5-(4,4,5,5-tetramethyl-1,3,2-dioxaborolan-2-yl)benzyl)piperazin-1-yl)thiazol-4(5H)-one (125 mg, 0.2 mmol, 1.0 eq.) in DCM (10 mL) cooled to 0 °C. Methanesulfonyl chloride (0.03 mL, 0.4 mmol, 2.0 eq.) was added dropwise over 2 min. The reaction mixture was then warmed to room temperature and stirred for 18 h. The mixture was diluted with H₂O (10 mL), the organic portion extracted with DCM (3 x 30 mL), combined, dried over anhydrous MgSO₄ and evaporated under reduced pressure. The crude material was purified by column chromatography (85% EtOAc / 15% acetone → 100% acetone) to afford mesylate **36** as a yellow oil (0.11 g, 76 %).

¹H NMR (400 MHz, MeOH-D₃) δ = 7.75 (br s, 1H, C=CH), 7.73 - 7.69 (m, 2H, C(HC=C)CHC(Cl), CHCHC(BPin)), 7.64 - 7.59 (m, 2H, C(HC=C)CHCH, C(CH₂)CHC(BPin)), 7.49 (dd, *J* = 8.6, 1.9 Hz, 1H, C(HC=C)CHCH), 7.02 (d, *J* = 8.2 Hz, 1H, CHCHC(BPin)), 4.43 - 4.35 (m, 2H, ArOCH₂CH₂), 4.25 - 4.18 (m, 2H, CH₂CH₂OMs), 4.05 (br s, 2H, NCH₂CH₂NCH₂Ar), 3.96 - 3.74 (m, 8H, CH₂CH₂OMs, NCH₂CH₂NCH₂Ar, ArOCH₂CH₂, NCH₂Ar), 3.06 (s, 3H, SO₃CH₃), 2.94 - 2.79 (m, 4H, (NCH₂CH₂NCH₂Ar) x2), 1.32 (s, 12H, (CH₃)₄); ¹³C NMR (100 MHz, MeOH-D₃) δ = 182.23, 176.47, 161.39, 139.57, 137.82, 137.85, 135.86, 134.67, 134.24, 132.46, 132.31, 131.47, 130.07, 129.99, 112.34, 85.02, 70.96, 70.72, 70.28, 68.77, 56.52, 52.97, 52.79, 37.37, 25.21, C-BPin not visible, NCH₂CH₂NCH₂Ar obscured by residual solvent peak; IR (neat) 2976, 2927, 2243, 1686, 1604, 1559, 1470, 1353, 1284, 1174, 1133 cm⁻¹; HRMS (ESI) [M + H₃O]⁺ calcd for 759.1989 C₃₂H₄₄¹¹B³⁵Cl₂N₃O₉S₂, found 759.1980.

7.1.20 2-Methyl-5-(4,4,5,5-tetramethyl-1,3,2-dioxaborolan-2-yl)phenol, (**23**)

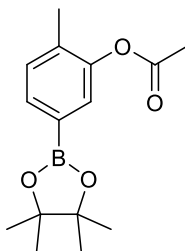


B₂Pin₂ (2.09 g, 8.3 mmol, 1.10 eq.) and KOAc (2.42 g, 24.7 mmol, 3.00 eq.) were added to a solution 5-Bromo-2-methyl phenol (1.40 g, 7.50 mmol, 1.0 eq.) in anhydrous dioxane (25 mL), then the resulting mixture was degassed under N₂ for 10 min. PdCl₂dppf (0.31 g, 0.4 mmol, 0.05 eq.) was added and then the mixture was stirred at 80 °C for 16 h. The reaction mixture was cooled to room temperature, upon which it was filtered through a plug of silica, eluting with DCM, the filtrate was then filtered through a second plug of silica and then evaporated to a golden-brown oil. The crude product was purified *via* flash column chromatography (30% EtOAc / 70% light petroleum ether) to afford boronate ester **23** as a cream crystalline solid (1.68g, 96%).

¹H NMR (400 MHz, CDCl₃) δ = 7.29 (dd, *J* = 7.3, 0.8 Hz, 1H, C(BPin)CH₂CH), 7.19 (s, 1H, C(BPin)CH₂CH(OH)), 7.13 (d, *J* = 7.3 Hz, 1H, C(BPin)CH₂CH), 5.12 (s, 1H, OH), 2.26 (s, 3H, ArCH₃), 1.31 (s, 12H, BO₂C₂(CH₃)₄); ¹³C NMR (100 MHz, CDCl₃) δ = 153.36, 130.67, 127.77, 127.12, 120.57, 83.76, 24.76, 16.04, C-BPin not visible.

Data in agreement to that reported by Hoheisel and co-workers.²⁵⁹

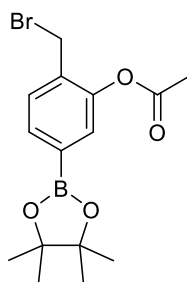
7.1.21 2-Methyl-5-(4,4,5,5-tetramethyl-1,3,2-dioxaborolan-2-yl)phenyl acetate, (**24**)



Triethylamine (0.9 mL, 6.4 mmol, 1.5 eq.) was added to a solution of 2-methyl-5-(4,4,5,5-tetramethyl-1,3,2-dioxaborolan-2-yl)phenol (1.00 g, 4.2 mmol, 1.0 eq.) in DCM (25 mL). Acetic anhydride (0.81 mL, 8.5 mmol, 2.0 eq.) was added dropwise to the mixture, and stirred for 16 h at room temperature. The volatiles were then removed under reduced pressure to yield a yellow oil as the crude product, the oil was then partitioned between EtOAc (30 mL) and H₂O (40 mL) and extracted with EtOAc (3 x 30 mL), combined, dried over anhydrous MgSO₄ and evaporated to obtain acetyl **24** as a cream crystalline solid (1.17g, 94 %).

¹H NMR (400 MHz, CDCl₃) δ = 7.57 (dd, *J* = 7.5, 0.9 Hz, 1 H, C(BPin)CHCH), 7.42 (s, 1 H, C(BPin)CHC(OAc)), 7.23 (d, *J* = 7.4 Hz, 1 H, C(BPin)CHCH), 2.29 (s, 3 H, ArCH₃), 2.19 (s, 3 H, ArOC(O)CH₃), 1.31 (s, 12 H, BO₂C₂(CH₃)₄); ¹³C NMR (100 MHz, CDCl₃) δ = 169.41, 149.19, 133.76, 132.64, 130.88, 128.03, 83.96, 24.96, 20.94, 16.58, C-BPin not visible; IR (neat) 2978, 2929, 1764, 1608, 1559, 1356, 1207, 1170, 1120 cm⁻¹; HRMS (ESI) [M + NH₄]⁺ calcd for C₁₅H₂₅¹¹BO₄N, 294.1871 found 294.1871, Mp = 127-130 °C.

7.1.22 2-(Bromomethyl)-5-(4,4,5,5-tetramethyl-1,3,2-dioxaborolan-2-yl)phenyl acetate, (**25**)

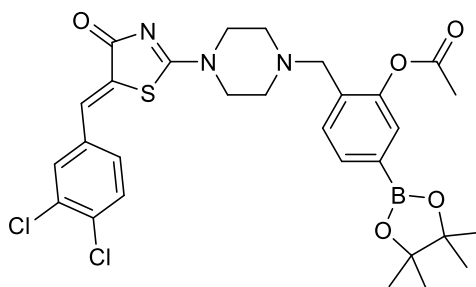


Freshly recrystallized *N*-bromo succinimide (0.71 g, 3.9 mmol, 1.10 eq.) and benzoyl peroxide (75 % in H₂O, 47 mg, 0.1 mmol, 0.04 eq.) was added to a solution of 2-methyl-5-(4,4,5,5-tetramethyl-1,3,2-dioxaborolan-2-yl)phenyl acetate (1.00 g, 3.6 mmol, 1.0 eq.) in anhydrous CCl₄ (20 mL), under a flow of argon. The resulting mixture was heated to 85 °C and stirred for two days. The reaction mixture was then cooled to 0 °C and the solids removed by gravity filtration, the filtrate was evaporated under reduced pressure to a yellow oil. The crude material was diluted with H₂O (20 mL) and extracted with DCM (4 x 25 mL). The combined organic extracts were then dried over anhydrous MgSO₄, filtered and evaporated under reduced pressure to afford bromide **25** as a pale-yellow oil (1.02 g, 80%).

The material was used in the next reaction without any further purification.

¹H NMR (400 MHz, CDCl₃) δ = 7.64 (dd, *J* = 7.4, 0.9 Hz, 1 H, C(BPin)CHCH), 7.51 (s, 1 H, C(BPin)CHC(OAc)), 7.41 (d, *J* = 7.5 Hz, 1 H, C(BPin)CHCH), 4.41 (s, 2 H, CH₂Br), 2.36 (s, 3 H, ArOC(O)CH₃), 1.32 (s, 12 H, BO₂C₂(CH₃)₄); ¹³C NMR (100 MHz, CDCl₃) δ = 169.24, 148.65, 132.73, 132.62, 130.45, 129.27, 84.28, 27.53, 25.05, 21.03, C-BPin not visible; IR (neat) 2969, 2262, 2104, 1686, 1604, 1436, 1192, 924 cm⁻¹; HRMS (ESI) [M + H]⁺ calcd for C₁₅H₂₀¹¹B³⁵BrO₄, 355.0544 found 355.0597.

7.1.23 (*Z*)-2-((4-(5-(3,4-dichlorobenzylidene)-4-oxo-4,5-dihydrothiazol-2-yl)piperazin-1-yl)methyl)-5-(4,4,5,5-tetramethyl-1,3,2-dioxaborolan-2-yl)phenyl acetate, (**26**)

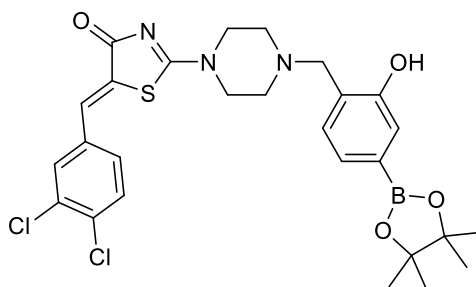


(*Z*)-5-(3,4-Dichlorobenzylidene)-2-(piperazin-1-yl)thiazol-4(*5H*)-one (0.40 g, 1.2 mmol, 1.0 eq.) was added to a solution of 2-(bromomethyl)-5-(4,4,5,5-tetramethyl-1,3,2-dioxaborolan-2-yl)phenyl acetate (0.50 g, 1.5 mmol, 1.2 equiv.) in DMF / H₂O 10:1 (22 mL). K₂CO₃ (0.16 g, 1.2 mmol, 1.0 eq.) was added, the solution was heated to 50°C and stirred for two days.

The reaction mixture was then evaporated under reduced pressure to dryness obtain an orange residue. The residue was dissolved in EtOAc (10 mL) and the insoluble material filtered and discarded, the filtrate was then evaporated to yield a yellow solid as the crude product.

Flash column chromatography (100% EtOAc) was used to isolate acetyl and phenol (de-protected) derivatives as a mixture. The isolated mixture (acetyl **26** and phenol **27**) were used directly without further purification.

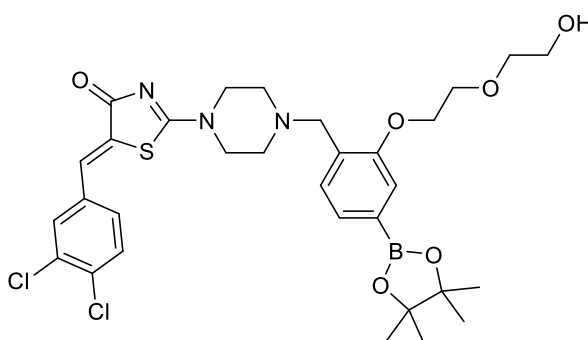
7.1.24 (Z)-5-(3,4-Dichlorobenzylidene)-2-(4-(2-hydroxy-4-(4,4,5,5-tetramethyl-1,3,2-dioxaborolan-2-yl)benzyl)piperazin-1-yl)thiazol-4(5H)-one, (**27**)



K_2CO_3 (8 mg, 0.1 mmol, 0.12 eq.) was added to a solution of (Z)-2-((4-(5-(3,4-dichlorobenzylidene)-4-oxo-4,5-dihydrothiazol-2-yl)piperazin-1-yl)methyl)-5-(4,4,5,5-tetramethyl-1,3,2-dioxaborolan-2-yl)phenyl acetate, as a mixture, (0.28 g, 0.5 mmol, 1.0 eq., MAX) in MeOH (12 mL). The resulting mixture was heated to 40 °C and stirred for 2 days. At which point the reaction was quenched following the addition of a solution of 0.1 M aq. HCl to pH 7. The volatiles were removed under reduced pressure to obtain a white solid, this was then partitioned between DCM (25 mL) and H_2O (30 mL). The organic portion was extracted using DCM (4 x 25 ml), combined, dried over anhydrous MgSO_4 , and evaporated under reduced pressure to obtain phenol **27** as a white solid (0.37 g, 55 %, over two steps).

^1H NMR (400 MHz, CDCl_3) δ = 7.68 (s, 1 H, C=CH), 7.57 (d, J = 2.3 Hz, 1 H, C(Cl)CHCH), 7.50 (d, J = 8.2 Hz, 1 H, C(Cl)CHC(HC=C)), 7.33 (dd, J = 8.4, 2.1 Hz, 1 H, C(Cl)CHCH), 7.31 (s, 1 H, C(BPin)CHC(OH)), 7.27 (d, J = 7.3 Hz, 1 H, C(BPin)CHCH), 7.01 (d, J = 7.3 Hz, 1 H, C(BPin)CHCH), 4.18 - 4.07 (m, 2 H, $\text{NCH}_2\text{CH}_2\text{NCH}_2$), 3.79 (s, 2 H, ArCH_2), 3.71 - 3.67 (m, 2 H, $\text{NCH}_2\text{CH}_2\text{NCH}_2$), 2.77 - 2.66 (m, 4 H, ($\text{NCH}_2\text{CH}_2\text{NCH}_2$) x2), 1.33 (s, 12 H, $\text{BO}_2\text{C}_2(\text{CH}_3)_4$); ^{13}C NMR (100 MHz, CDCl_3) δ = 180.38, 174.94, 156.66, 134.33, 133.95, 133.53, 131.16, 130.98, 129.86, 129.54, 128.96, 128.73, 126.22, 123.21, 122.43, 84.02, 61.38, 52.16, 51.94, 48.53, 48.37, 24.94, C-BPin not visible; IR (neat): 3691, 2978, 1677, 1606, 1559, 1351, 1293, 1246, 1172, 1120, 993 cm^{-1} ; HRMS (ESI) $[\text{M} + \text{H}]^+$ calcd for $\text{C}_{27}\text{H}_{30}^{11}\text{B}^{35}\text{Cl}_2\text{N}_3\text{O}_4\text{S}$, 574.1505 found 574.1497; Mp = 193-195 °C.

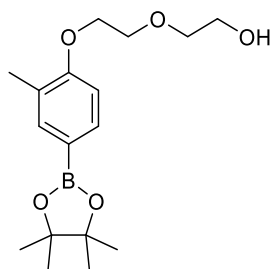
7.1.25 (Z)-5-(3,4-Dichlorobenzylidene)-2-(4-(2-(2-(2-hydroxyethoxy)ethoxy)-4-(4,4,5,5-tetramethyl-1,3,2-dioxaborolan-2-yl)benzyl)piperazin-1-yl)thiazol-4(5H)-one, (**28**)



2-(2-Chloroethoxy)ethanol (57 mg, 0.5 mmol, 3.0 eq.), K_2CO_3 (65 mg, 0.5 mmol, 3.0 eq.) and KI (26 mg, 0.2 mmol, 1.0 eq.) were added to a solution of (Z)-5-(3,4-dichlorobenzylidene)-2-(4-(2-hydroxy-4-(4,4,5,5-tetramethyl-1,3,2-dioxaborolan-2-yl)benzyl)piperazin-1-yl)thiazol-4(5H)-one (90 mg, 0.2 mmol, 1.0 eq.) in DMF (10 mL). The resulting mixture was stirred at 75 °C for 24 h. The reaction mixture was cooled to room temperature, then evaporated under reduced pressure to obtain an orange residue which was dissolved in EtOAc (30 mL) and diluted with H_2O (30 mL). The organic portion was extracted using EtOAc (3 x 20 mL), then DCM (1 x 20 mL), combined, dried over anhydrous $MgSO_4$, filtered and evaporated to give a yellow oil. This was then purified using flash column chromatography (90 % EtOAc / 10 % acetone \rightarrow 100 % acetone) to afford alcohol **28** as a yellow oil, (15 mg, 15 %).

1H NMR (400 MHz, $CDCl_3$) δ = 7.66 (s, 1H, C=CH), 7.58 (d, J = 2.3 Hz, 1H, C(Cl)CHC(HC=C)), 7.50 (d, J = 8.2 Hz, 1H, C(Cl)CHCH), 7.43 (d, J = 7.3 Hz, 1H, C(BPin)CHCH), 7.37 - 7.30 (m, 3H, C(BPin)CHCH, C(BPin)CHC(OCH₂), C(Cl)CHCH), 4.26 - 4.19 (m, 2H, ArOCH₂CH₂), 4.13 - 4.04 (m, 2H, NCH₂CH₂NCH₂), 3.92 - 3.84 (m, 2H, ArOCH₂CH₂), 3.78 - 3.63 (m, 8H, CH₂CH₂OH, NCH₂CH₂NCH₂, NCH₂CH₂NCH₂), 2.79 - 2.63 (m, 4H, (NCH₂CH₂NCH₂) x2), 1.35 (s, 12H, $BO_2C_2(CH_3)_4$); ^{13}C NMR (100 MHz, $CDCl_3$) δ = 180.33, 179.34, 174.34, 156.59, 134.28, 133.57, 133.33, 130.92, 130.82, 130.72, 129.94, 128.76, 128.72, 127.39, 117.54, 83.95, 72.36, 69.72, 67.58, 61.65, 56.02, 52.35, 51.94, 48.71, 48.46, 24.81, C-BPin not visible; IR (neat) cm^{-1} : 3363, 2931, 2868, 1682, 1604, 1559, 1470, 1354, 1285, 1135; HRMS (ESI) $[M + H]^+$ calcd for $C_{31}H_{39}BCl_2N_3O_6S$ 662.2030, found 662.2021.

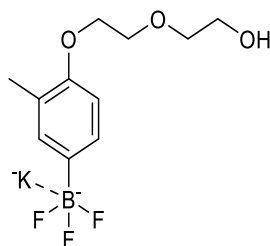
7.1.26 2-(2-(2-Methyl-4-(4,4,5,5-tetramethyl-1,3,2-dioxaborolan-2-yl)phenoxy)ethoxy)ethan-1-ol, (**10**)



A solution of 2-(2-bromoethoxy)ethan-1-ol, (0.96 g, 5.7 mmol, 2.9 eq.) dissolved in DMF (2 mL) was added dropwise (over 1 min) to a solution of 2-methyl-4-(4,4,5,5-tetramethyl-1,3,2-dioxaborolan-2-yl)phenol, (0.45 g, 1.9 mmol, 1.0 eq.) in DMF (15 mL). K_2CO_3 (0.53 g, 3.8 mmol, 2.0 eq.) was then added, followed by KI (0.32 g, 1.9 mmol, 1.0 eq.), the resulting mixture was heated to 80 °C and stirred for 16 h. The mixture was evaporated under reduced pressure, diluted in H_2O (50 mL) and extracted using EtOAc (4 x 40 mL). The combined organic extracts were dried over anhydrous $MgSO_4$ and evaporated under reduced pressure to a brown oil. The crude product was purified *via* flash column chromatography (50% EtOAc / 50% light petroleum ether) to afford alcohol **10** as a pale-yellow oil (0.35 g, 58%).

1H NMR (400 MHz, $DMSO-d_6$) δ = 7.46 (dd, J = 8.1, 1.3 Hz, 1H, $CHCHC(BPin)$), 7.42 (s, 1H, $C(CH_3)CHC(BPin)$), 6.91 (d, J = 8.2 Hz, 1H, $CHCHC(BPin)$), 4.73 - 4.51 (m, 1H, OH), 4.17 - 3.98 (m, 2H, $ArOCH_2CH_2$), 3.81 - 3.66 (m, 2H, $ArOCH_2CH_2$), 3.54 - 3.43 (m, 4H, CH_2CH_2OH), 2.12 (s, 3H, $ArCH_3$), 1.22 (s, 12H, $B(O_2C_2(CH_3)_4)$); ^{13}C NMR (100 MHz, $DMSO-d_6$) δ = 159.31, 136.79, 134.10, 125.19, 110.72, 83.27, 72.58, 68.91, 67.10, 60.26, 24.69, 15.83, C-BPin Not visible; IR (neat) 3436, 2980, 1604, 1405, 1351, 1321, 1285, 1254, 1131, 1069 cm^{-1} ; m/z (ESI) $[M + Na]^+$ 345.34

7.1.27 Potassium trifluoro(4-(2-(2-hydroxyethoxy)ethoxy)-3-methylphenyl)borate, (**29**)

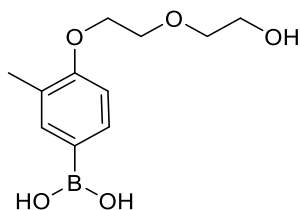


KHF₂ aq. (4.5 M, 1.37 mL, 6.2 mmol, 5.65 eq.) was added to 2-(2-(2-methyl-4-(4,4,5,5-tetramethyl-1,3,2-dioxaborolan-2-yl)phenoxy)ethoxy)ethan-1-ol (0.35 g, 1.1 mmol, 1.0 eq.) in MeOH (7 mL) and stirred for 1 h at room temperature. The reaction mixture was diluted with acetone (10 mL) and filtered. The filtrate was evaporated under reduced pressure to give a white residue. The residue was then subjected to three evaporation cycles in MeOH / H₂O 1:1 (15 mL), as described previously.

The procedure above was repeated entirely using the crude reaction mixture, to ensure the material fully reacted, to give trifluoroborate **29** as a white solid (quantitative).

¹H NMR (400 MHz, DMSO-d₆) δ = 7.09 - 6.95 (m, 2 H, C(BF₃K)CHCH, C(BF₃K)CHC(CH₃)), 6.60 (d, *J* = 8.3 Hz, 1 H, C(BF₃K)CHCH), 4.61 (br. s., 1 H, OH), 4.04 - 3.88 (m, 2 H, ArOCH₂CH₂), 3.72 - 3.62 (m, 2 H, ArOCH₂CH₂), 3.47 (s, 4 H, CH₂CH₂OH), 2.04 (s, 3 H, ArCH₃); ¹³C NMR (100 MHz, DMSO-d₆) δ = 155.06, 134.67, 130.25, 123.56, 110.58, 73.14, 69.84, 67.83, 60.82, 16.74, C-BF₃K (not visible); IR (neat) 2923, 2881, 1603, 1501, 1451, 1405, 1367, 1249, 1123, 1056 cm⁻¹; m/z (ESI) [M - K]⁺ 263.22; Mp = 215 - 218 °C (decomposed)

7.1.28 (4-(2-(2-Hydroxyethoxy)ethoxy)-3-methylphenyl)boronic acid, (**30**)

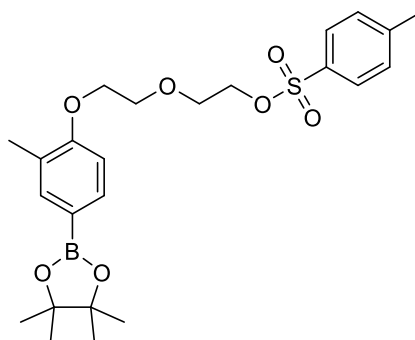


Trimethylsilyl chloride (0.56 mL, 4.5 mmol, 6.0 eq.) and H₂O (0.08 mL, 4.5 mmol, 6.0 eq.) was added to potassium trifluoro(4-(2-(2-hydroxyethoxy)ethoxy)-3-methylphenyl)borate (0.225 g, 0.80 mmol, 1.0 eq.) dissolved in MeCN (9 ml) and stirred for 1 h at room temperature. Sat. aq. sodium bicarbonate solution (0.8 mL) was added. The mixture was dried over anhydrous Na₂SO₄, filtered and evaporated to give a boronic acid **30** as a white solid (0.10 g, 56%).

¹H NMR (400 MHz, MeOH-D₃) δ = 7.49 - 7.23 (m, 2H, Ar-H), 7.10 - 6.88 (m, 1H, Ar-H), 6.83 - 6.55 (m, 1H, Ar-H), 4.08 - 3.91 (m, 2H, ArOCH₂CH₂O), 3.80 - 3.65 (m, 2H, ArCH₂CH₂O), 3.63 - 3.45 (m, 4H, CH₂CH₂), 2.08 (s, 3H, CH₃)*

* ¹H NMR indicated the formation of dimers / trimers within the structure, after 1 day the material was found to have degraded (by ¹H NMR), which prevented further analysis. Compound synthesised just prior to use in subsequent reactions.

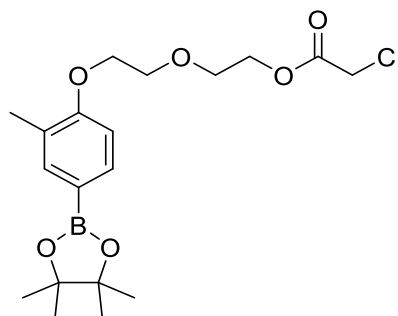
7.1.29 2-(2-(2-Methyl-4-(4,4,5,5-tetramethyl-1,3,2-dioxaborolan-2-yl)phenoxy)ethoxy)ethyl 4-methylbenzenesulfonate, (**37**)



Triethylamine (0.22 mL, 1.5 mmol, 2.0 eq.) and tosyl chloride (0.29 g, 1.5 mmol, 2.0 eq.) were added to a stirring solution of 2-(2-(2-methyl-4-(4,4,5,5-tetramethyl-1,3,2-dioxaborolan-2-yl)phenoxy)ethoxy)ethan-1-ol (0.25 g, 0.8 mmol, 1.0 eq.) in DCM (10 ml). The resulting mixture was left stir at room temperature for 24 h. It was then diluted with H₂O (40 mL), extracted in DCM (4 x 30 mL). The combined organic extracts were dried over anhydrous MgSO₄, filtered and evaporated. The crude product was purified *via* flash column chromatography (30% EtOAc / 70% light petroleum ether), to yield tosylate **37** as a pale-yellow oil (0.37 g, 74%).

¹H NMR (400 MHz, DMSO-d₆) δ = 7.75 (d, *J* = 8.2 Hz, 2H, CHCHC(SO₃)), 7.46 (d, *J* = 8.1 Hz, 1H, CHCHC(BPin)), 7.43 (s, 1H, C(CH₃)CHC(BPin)), 7.40 (d, *J* = 8.5 Hz, 2H, CHCHC(SO₃)), 6.88 (d, *J* = 8.1 Hz, 1H, CHCHC(BPin)), 4.18 - 4.08 (m, 2H, ArOCH₂CH₂), 4.06 - 3.96 (m, 2H, CH₂CH₂OTs), 3.74 - 3.62 (m, 4H, CH₂CH₂OTs, ArOCH₂CH₂), 2.36 (s, 3H, CH₃TsO), 2.10 (s, 3H, ArCH₃), 1.26 (s, 12H, B(O₂C₂(CH₃)₄)); ¹³C NMR (100 MHz, CDCl₃) δ = 159.35, 144.73, 137.14, 134.07, 132.77, 129.71, 127.84, 125.97, 110.12, 83.43, 69.75, 69.24, 68.84, 67.34, 24.76, 21.53, 15.96, C-BPin Not visible; m/z (ESI) [M + Na]⁺ 499.41

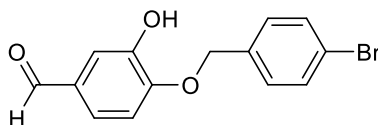
7.1.30 2-(2-(2-methyl-4-(4,4,5,5-tetramethyl-1,3,2-dioxaborolan-2-yl)phenoxy)ethoxy)ethyl 2-chloroacetate, (**38**)



To a solution of 2-(2-(2-methyl-4-(4,4,5,5-tetramethyl-1,3,2-dioxaborolan-2-yl)phenoxy)ethoxy)ethan-1-ol, (0.16 g, 0.5 mmol, 1.0 eq.) dissolved in DCM (3 mL), under a flow of N₂. Pyridine (0.04 mL, 0.5 mmol, 1.0 eq.) was added. Chloroacetyl chloride (0.08 mL, 1.0 mmol, 2.0 eq.) was then added dropwise, and stirred at room temperature for 2 h. The reaction was quenched following the addition of H₂O (10 mL) and diluted with DCM (30 mL), then washed with H₂O (2 x 10 mL), NaOH aq. 0.1 M (1 x 20 mL) and 1 x 0.1M HCl aq. The organic component was dried over anhydrous MgSO₄, the volatiles were then removed under reduced pressure to give a golden-brown oil. The crude material was purified *via* flash column chromatography eluting with 40% EtOAc / 60 % light petroleum ether, to afford chloride **38** as a yellow oil (0.16 g, 81%).

¹H NMR (400 MHz, CDCl₃) δ = 7.62 (d, *J* = 8.1 Hz, 1H, CHCHC(BPin)), 7.60 (s, 1H, C(CH₃)CHC(BPin)), 6.81 (d, *J* = 8.1 Hz, 1H, CHCHC(BPin)), 4.39 - 4.34 (m, 2H, ArOCH₂CH₂), 4.18 - 4.14 (m, 2H, CH₂CH₂CO₂Cl), 4.07 (s, 2H, CH₂Cl), 3.91 - 3.86 (m, 2H, CH₂CH₂CO₂Cl), 3.85 - 3.80 (m, 2H, ArOCH₂CH₂), 2.22 (s, 3H, ArCH₃), 1.33 (s, 12H, (CH₃)₄); ¹³C NMR (100 MHz, CDCl₃) δ = 167.46, 159.56, 137.35, 134.25, 126.20, 110.38, 83.62, 69.88, 69.15, 67.58, 65.37, 40.92, 24.94, 16.15, C-BPin not visible; IR (neat) 2976, 2342, 1759, 1604, 1407, 1354, 1287, 1135, 965 cm⁻¹; HRMS (ESI) [M + H]⁺ calcd for C₁₉H₂₈ ¹¹B ³⁵ClO₆, 398.1662 found 398.1659

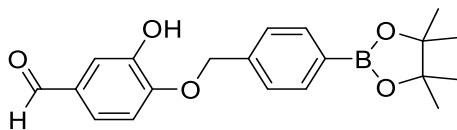
7.1.31 4-((4-Bromobenzyl)oxy)-3-hydroxybenzaldehyde, (**46**)



3,4-Dihydroxybenzaldehyde (0.55 g, 4.0 mmol, 1 eq.) was added to a stirring solution of 4-bromo benzyl bromide (2.00 g, 8.0 mmol, 2 eq.) in DMF (20 mL), followed by the addition of NaHCO_3 (0.50 g, 6.0 mmol, 1.5 eq.) and NaI (0.18 g, 1.2 mmol, 0.3 eq.). The resulting mixture was heated at 40 °C for 24 h. The reaction was quenched by the addition of a solution of 1 M HCl aq. (10 mL) and then diluted with 5% LiCl aq. solution (50 mL). The organic portion was extracted using EtOAc (1 x 50 mL) and washed with 5 % LiCl solution (2 x 50 ml). The organic extract was dried over anhydrous MgSO_4 , filtered and evaporated to give a light brown solid. The crude mixture was purified by flash column chromatography using 40 % EtOAc / 60 % light petroleum ether as the eluent to give aldehyde **46** as an off-white crystalline solid (0.68 g, 55 %). An analytical sample was obtained by recrystallization using DCM and hexanes, to afford a white crystalline solid.

^1H NMR (400 MHz, CDCl_3) δ = 9.83 (s, 1 H, C(O)H), 7.55 (d, J = 8.2 Hz, 2 H, CHCBr), 7.45 (d, J = 2.3 Hz, 1 H, C(CHO)CHC(OH)), 7.40 (dd, J = 8.7, 2.1 Hz, 1 H, C(CHO)CHCH), 7.29 (d, J = 8.2 Hz, 2 H, C(CH₂)CH), 6.99 (d, J = 8.7 Hz, 1 H, CHCHC(OCH₂ArBr)), 5.79 (br. s., 1 H, C(OH)), 5.15 (s, 2 H, CH₂); ^{13}C NMR (100 MHz, CDCl_3) δ = 191.15, 150.79, 146.39, 134.36, 132.27, 131.16, 129.68, 124.44, 123.03, 114.76, 111.62, 70.66; IR (neat) 3210.33, 2807.11, 1660.83, 1601.18, 1503.99, 1412.22, 1274.37, 1127.60, 1007.14, 798.73 cm^{-1} ; HRMS (ESI) $[\text{M} + \text{H}]^+$ calcd for $\text{C}_{14}\text{H}_{11}^{11}\text{BrO}_3$, 306.9964 found 306.9968; Mp = 131 - 134 °C

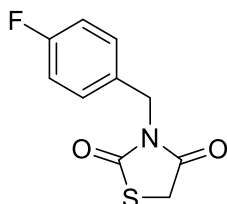
7.1.32 3-Hydroxy-4-((4-(4,4,5,5-tetramethyl-1,3,2-dioxaborolan-2-yl)benzyl)oxy)benzaldehyde, (**47**)



B₂Pin₂ (0.38 g, 1.5 mmol, 1.1 eq.) and KOAc (0.40 g, 4.1 mmol, 3.0 eq.) were added to a solution of 4-((4-bromobenzyl)oxy)-3-hydroxybenzaldehyde (0.42 g, 1.4 mmol, 1 eq.) in anhydrous dioxane (15 mL), the resulting mixture was degassed under nitrogen for 5 min. The flask was then charged with PdCl₂dppf (56 mg, 0.7 mmol, 0.05 eq.) and heated to 80 °C, under a flow of nitrogen for 48 h. The reaction mixture was then cooled to room temperature, filtered through a pad of silica (prepared with DCM) and flushed through with additional DCM (100 mL). This process was repeated once more using the filtrate. The volatiles were then removed under reduced pressure to obtain a golden-brown oil. The crude mixture was purified using column chromatography, 50% EtOAc / 50% light petroleum ether eluent. Evaporation of desired fractions afforded boronate ester **47** as a pale-yellow solid (0.39 g, 77%). An analytical sample was obtained by recrystallization using DCM and hexanes, to afford a white crystalline solid.

¹H NMR (400 MHz, CDCl₃) δ = 9.82 (s, 1 H, C(O)H), 7.85 (d, *J* = 7.9 Hz, 2 H, CHC(Br)), 7.45 (d, *J* = 2.0 Hz, 1 H, C(CHO)CHC(OH)), 7.41 (d, *J* = 7.9 Hz, 2 H, C(CH₂)CH), 7.38 (dd, *J* = 8.2, 2.0 Hz, 1 H, C(CHO)CHCH), 6.99 (d, *J* = 8.2 Hz, 1 H, CHCHC(OCH₂ArBPin), 5.81 (s, 1 H, ArOH), 5.22 (s, 2 H, CH₂), 1.34 (s, 12 H, (CH₃)₄); ¹³C NMR (100 MHz, CDCl₃) δ = 191.12, 150.98, 146.49, 138.27, 135.49, 131.07, 127.08, 124.49, 114.55, 111.69, 84.19, 71.34, 24.98, C-BPin missing; IR (neat) 3546, 3226, 2982, 2871, 1655, 1603, 1583, 1456, 1323, 1283, 1087, 1020, 963 cm⁻¹; HRMS (ESI) [M + H]⁺ calcd for C₂₀H₂₃¹¹BO₅, 355.1711 found 355.1705; Mp = 120 – 122 °C.

7.1.33 3-(4-Fluorobenzyl)thiazolidine-2,4-dione, (**42**)



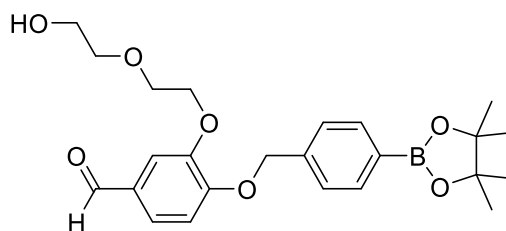
2,4-Thiazolidindione (2.94 g, 25.0 mmol, 1.5 eq.) was added to anhydrous DMF (50 mL) and the stirred solution was cooled to 0 °C, under N₂. NaH was then added as a 60 % mineral oil dispersion (0.92 g, 23.0 mmol, 1.35 eq.), followed by 4-fluoro benzyl bromide (2.1 mL, 17 mmol, 1 eq.) as a solution in anhydrous DMF (10 mL). The resulting solution was left to warm to room temperature over a period 90 min and then stirred for a further 5 h.

The reaction mixture was poured over crushed ice / water (100 mL), hexanes (50 mL) were then added to give a loose cream precipitate. The mixture was refrigerated at 4 °C for a period of 12 h. On decanting the liquid portion in to a separate flask, a white solid was spontaneously formed. This left an oily residue on the base of the original flask, which precipitated a white solid upon the addition of hexanes (100 mL). The precipitates from both flasks were collected by vacuum filtration, washed with cold hexanes and combined to give an off-white solid. The solid was then dissolved in DCM (250 mL) and washed with 5% aq. LiCl solution (1 x 200 mL, then 2 x 100 mL). The organic layer was then dried over anhydrous MgSO₄, filtered and evaporated to yield heterocycle **42** as an off-white crystalline solid, 3.26 g 80%.

¹H NMR (400 MHz, CDCl₃) δ = 7.46 - 7.35 (m, 2H), 7.08 - 6.94 (m, 2H), 4.73 (s, 2H), 3.95 (s, 2H)

¹H NMR data was in agreement with that published by Albers and co-workers.⁴³

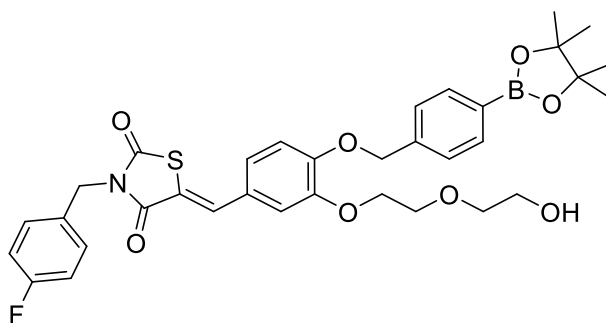
7.1.34 3-(2-(2-hydroxyethoxy)ethoxy)-4-((4-(4,4,5,5-tetramethyl-1,3,2-dioxaborolan-2-yl)benzyl)oxy)benzaldehyde, (**48**)



To a stirring solution of 3-hydroxy-4-((4-(4,4,5,5-tetramethyl-1,3,2-dioxaborolan-2-yl)benzyl)oxy)benzaldehyde (0.27 g, 0.7 mmol, 1 eq.) in DMF (5 mL), potassium carbonate (0.15 g, 1.1 mmol, 1.5 eq.) was added. 2-chloro-2-ethoxy ethanol (0.23 mL, 2.2 mmol, 3 eq.) dissolved in DMF (1 mL) was then added dropwise (over 1 minute) to the mixture, followed by the addition of KI (0.18 g, 0.7 mmol, 1 eq.). The resulting mixture was heated to 75 °C and stirred for 36 h. The solvent was then evaporated under reduced pressure to obtain a brown oil, which was dissolved in H₂O (30 mL). The organic portion extracted with EtOAc (3 x 30 mL). The combined organic extracts were then dried over anhydrous MgSO₄, filtered and evaporated to obtain brown oil. The crude material was purified by flash column chromatography (50 % EtOAc / 50 % light petroleum ether) to afford alcohol **48** as a pale-yellow oil (0.26 g, 70 %).

¹H NMR (400 MHz, CDCl₃) δ = 9.79 (s, 1 H, CHO), 7.80 (d, *J* = 8.2 Hz, 2 H, C(BPin)CH), 7.45 (d, *J* = 2.3 Hz, 1 H, C(CHO)CHC(OCH₂)), 7.37 (dd, *J* = 8.2, 2.1 Hz, 1 H, C(CHO)CHCH), 6.94 (d, *J* = 8.2 Hz, 1 H, C(CHO)CHCH), 5.23 (s, 2 H, CH₂ArBPin), 4.26 - 4.21 (m, 2 H, ArOCH₂CH₂), 3.95 - 3.86 (m, 2 H, ArOCH₂CH₂), 3.78 - 3.59 (m, 5 H, OHCH₂CH₂, OHCH₂CH₂, OHCH₂CH₂), 1.32 (s, 12 H, BO₂(CH₃)₄); ¹³C NMR (100 MHz, CDCl₃) δ = 191.08, 154.08, 149.37, 139.24, 135.23, 130.38, 127.03, 126.43, 112.93, 111.58, 84.06, 72.81, 70.83, 69.57, 68.93, 61.98, 25.02, C-BPin not visible; IR (neat) 3423, 3978, 3931, 2871, 1583, 1655, 1584, 1508, 1268 cm⁻¹; HRMS (ESI) [M + H]⁺ calcd for C₂₄H₃₁¹¹BO₇, 443.2236 found 443.2228

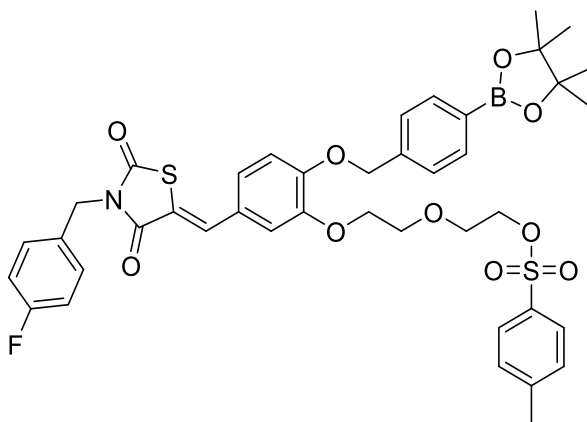
7.1.35 (Z)-3-(4-Fluorobenzyl)-5-(3-(2-(2-hydroxyethoxy)ethoxy)-4-((4-(4,4,5,5-tetramethyl-1,3,2-dioxaborolan-2-yl)benzyl)oxy)benzylidene)thiazolidine-2,4-dione, (**49**)



3-(4-Fluorobenzyl)thiazolidine-2,4-dione (0.1 g, 0.4 mmol, 1 eq.) was added to a solution of 3-(2-(2-hydroxyethoxy)ethoxy)-4-((4-(4,4,5,5-tetramethyl-1,3,2-dioxaborolan-2-yl)benzyl)oxy)benzaldehyde (0.2 g, 0.4 mmol, 1 eq.) in ethanol (5 mL), followed by piperidine (45 μ L, 0.4 mmol, 1 eq.). The resulting mixture was heated to 78 °C and stirred for 24 h. The solution was cooled to room temperature and evaporated to an orange residue. This was then purified by flash column chromatography (50 % EtOAc / 50 % light petroleum ether) to afford alcohol **49** as a yellow oil (0.16 g, 55 %).

^1H NMR (400 MHz, CDCl_3) δ = 7.83 - 7.77 (m, 3 H, $\text{C}=\underline{\text{C}}\text{H}$, $\text{C}(\text{BPin})\underline{\text{C}}\text{H}$), 7.44 - 7.38 (m, 4 H, $\text{C}(\text{CH}_2\text{O})\underline{\text{C}}\text{H}$, $\text{C}(\text{CH}_2\text{N})\underline{\text{C}}\text{H}$), 7.07 - 6.96 (m, 4 H, $\text{C}(\text{HC}=\text{C})\underline{\text{C}}\text{H}\underline{\text{C}}\text{H}$, $\text{C}(\text{HC}=\text{C})\underline{\text{C}}\text{H}\underline{\text{C}}(\text{OCH}_2)$, $\text{C}(\text{F})\underline{\text{C}}\text{H}$), 6.91 (d, J = 9.1 Hz, 1 H, $\text{C}(\text{HC}=\text{C})\underline{\text{C}}\text{H}\underline{\text{C}}\text{H}$), 5.20 (s, 2 H, $\underline{\text{C}}\text{H}_2\text{ArBPin}$), 4.84 (s, 2 H, $\underline{\text{C}}\text{H}_2\text{ArF}$), 4.24 - 4.18 (m, 2 H, $\text{ArO}\underline{\text{C}}\text{H}_2\underline{\text{C}}\text{H}_2$), 3.95 - 3.89 (m, 2 H, $\text{ArO}\underline{\text{C}}\text{H}_2\underline{\text{C}}\text{H}_2$), 3.75 - 3.65 (m, 4 H, $\text{OH}\underline{\text{C}}\text{H}_2\underline{\text{C}}\text{H}_2$, $\text{OH}\underline{\text{C}}\text{H}_2\underline{\text{C}}\text{H}_2$), 1.33 (s, 12 H, $\text{BO}_2(\underline{\text{C}}\text{H}_3)_4$); ^{13}C NMR (100 MHz, CDCl_3) δ = 167.91, 166.25, 162.69 (d, $^1J_{\text{C-F}}$ = 247.28 Hz), 150.95, 149.11, 139.41, 135.17, 134.25, 131.17 (d, $^4J_{\text{C-F}}$ = 2.88 Hz), 130.97 (d, $^3J_{\text{C-F}}$ = 7.67 Hz), 126.47, 126.38, 125.31, 118.81, 115.71 (d, $^2J_{\text{C-F}}$ = 21.09 Hz), 115.32, 114.10, 83.97, 72.78, 70.84, 69.54, 69.12, 61.92, 44.53, 24.95, C-BPin not visible; IR (neat): 3672, 2974, 2902, 2298, 2108, 1734, 1676, 1590, 1508, 1311 cm^{-1} ; HRMS (ESI $^+$) (m/z) calcd for $\text{C}_{34}\text{H}_{37}^{11}\text{BFNO}_7\text{S}^+$ [M + H] $^+$ 650.2396, found 650.2396.

7.1.36 (Z)-2-(2-(5-((3-(4-Fluorobenzyl)-2,4-dioxothiazolidin-5-ylidene)methyl)-2-((4-(4,4,5,5-tetramethyl-1,3,2-dioxaborolan-2-yl)benzyl)oxy)phenoxy)ethoxy)ethyl 4-methyl benzenesulfonate, (**50**)



Method 1:

Triethylamine (0.04 mL, 0.3 mmol 2 eq.) was added slowly (over 1 min) to a solution of (Z)-3-(4-fluorobenzyl)-5-(3-(2-(2-hydroxyethoxy)ethoxy)-4-((4-(4,4,5,5-tetramethyl-1,3,2-dioxaborolan-2-yl)benzyl)oxy)benzylidene)thiazolidine-2,4-dione (84 mg, 0.1 mmol, 1 eq.) in DCM (5 mL), followed by tosyl chloride (49 mg, 0.3 mmol, 2 eq.). This was then stirred at room temperature for 36 h. The reaction mixture was diluted with H₂O (50 mL) and the organic layer extracted with DCM (3 x 25 mL). The combined organic extracts were then dried over anhydrous MgSO₄, filtered and evaporated to obtain a yellow oil.

The crude mixture was purified *via* flash column chromatography (35 % EtOAc / 65 % petroleum ether to afford tosylate **50** as a yellow oil (44 mg, 44 %).

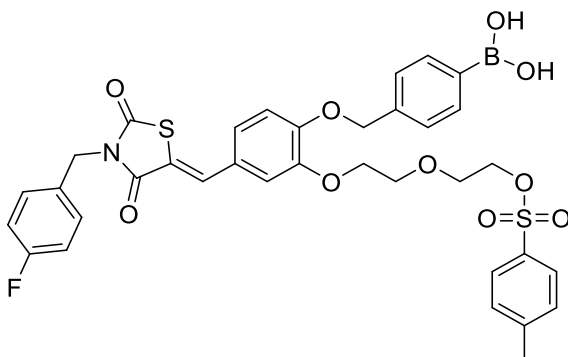
¹H NMR (400 MHz, CDCl₃) δ = 7.81 - 7.75 (m, 5 H, CHC(SO₃), CHC(BPin), C=CH), 7.44 - 7.37 (m, 4 H, C(CH₂O)CH, C(CH₂N)CH), 7.27 (d, *J* = 8.1 Hz, 2 H, C(CH₃)CH), 7.06 - 6.96 (m, 4 H, C(HC=C)CHCH, C(F)CH, C(HC=C)CHC(OCH₂)), 6.91 (d, *J* = 8.3 Hz, 1 H, C(HC=C)CHCH), 5.17 (s, 2 H, CH₂Ar(BPin)), 4.84 (s, 2 H, NCH₂Ar(F)), 4.14 - 4.11 (m, 4 H, ArOCH₂CH₂, CH₂CH₂OTs), 3.84 - 3.78 (m, 2 H, CH₂CH₂OTs), 3.77 - 3.74 (m, 2 H, ArOCH₂CH₂), 2.38 (s, 3 H, CH₃Ar), 1.34 (s, 12 H, BO₂(CH₃)₄); ¹³C NMR (100 MHz, CDCl₃) δ = 167.90, 166.24, 162.68 (d, ¹*J*_{C-F} = 250.84 Hz), 151.04, 149.11, 144.83, 139.47, 135.15, 134.23, 133.06, 131.19 (d, ⁴*J*_{C-F} = 2.31 Hz), 130.96 (d, ³*J*_{C-F} = 9.25 Hz), 129.87, 128.06, 126.49, 126.40, 125.28, 118.83, 115.70 (d, ²*J*_{C-F} = 20.81 Hz), 115.56, 114.21, 83.99, 70.85, 69.80, 69.36, 69.22, 69.16, 44.52, 24.98, 21.72, C-BPin not visible; IR (solid): 3671, 2974, 1917, 1734, 1677, 1592, 1508, 1454, 1355 cm⁻¹; HRMS (ESI⁺) (*m/z*) calcd for C₄₁H₄₃¹¹BFNO₁₀S₂ [M + H]⁺ 821.2744, found 821.2756.

Method 2:

B₂Pin₂ (0.22 g, 0.90 mmol, 1.1 eq.), KOAc (0.23 g, 2.40 mmol, 3.0 eq.) and PdCl₂dppf (33 mg, 0.04 mmol, 0.05 eq.) was added to a solution of (Z)-2-(2-(2-((4-bromobenzyl)oxy)-5-((3-(4-fluorobenzyl)-2,4-dioxothiazolidin-5-ylidene)methyl)phenoxy)ethoxy)ethyl 4-methyl benzenesulfonate (0.60 g, 0.79 mmol, 1.0 eq.), in anhydrous dioxane (25 mL). The resulting mixture was heated to 80°C for 24 h, then cooled to room temperature. The resulting slurry was filtered through a plug of silica, eluting with DCM (100 mL) and the filtrate filtered through a second silica plug. The filtrate was then evaporated to a brown oil which was purified by flash column chromatography (50% EtOAc / 50% light petroleum ether) to afford tosylate **50** as a yellow oil (0.63 g, 64 %).

The material was analysed *via* ¹H NMR spectroscopy, (CDCl₃) and was found to be in agreement with that of method 1.

7.1.37 (Z)-4-((4-((3-(4-fluorobenzyl)-2,4-dioxothiazolidin-5-ylidene)methyl)-2-(2-(2-(tosyloxy)ethoxy)ethoxy)phenoxy)methyl)phenyl)boronic acid, (**51**)

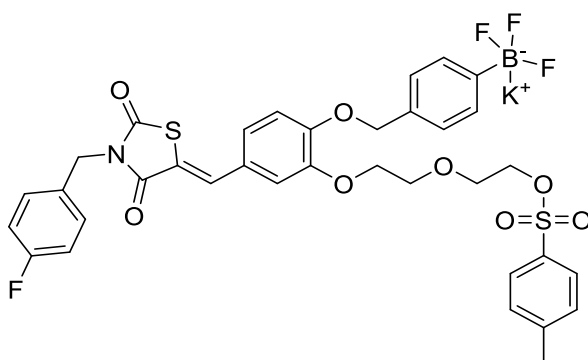


Method 1:

NaIO₄ (70 mg, 3.3 mmol, 6 eq.) was added to a solution of (Z)-2-(2-(5-((3-(4-fluorobenzyl)-2,4-dioxothiazolidin-5-ylidene)methyl)-2-((4-(4,4,5,5-tetramethyl-1,3,2-dioxaborolan-2-yl)benzyl)oxy)phenoxy)ethoxy)ethyl 4-methylbenzenesulfonate (43 mg, 0.5 mmol, 1eq.) in THF/ H₂O 1:4 (1 mL) and the resulting mixture stirred for 30 min at room temperature. 1 M HCl aq. (0.2 mL) was then added and stirred for 2 h. A second portion of NaIO₄ (47 mg, 2.2 mmol, 4 eq.) was added and this was stirred for 14 h. The reaction mixture was diluted with H₂O (20 mL) and extracted with EtOAc (3 x 15 mL). The organic extracts were combined, dried over anhydrous MgSO₄, filtered and evaporated to obtain a grainy yellow oil. MeCN (3 mL) was added, which effected the precipitation of boronic acid **51** as a yellow crystalline solid, that was then decanted and the solid dried (10 mg, 25 %).

¹H NMR (400 MHz, ACETONE-d₆) δ = 7.87 (d, *J* = 7.8 Hz, 2 H, C(B(OH)₂)CH), 7.83 (s, 1 H, C=CH), 7.75 (d, *J* = 8.2 Hz, 2 H, C(SO₃)CH), 7.46 - 7.41 (m, 4 H, C(CH₂N)CH, C(CH₂O)CH), 7.37 (d, *J* = 8.2 Hz, 2 H, C(CH₃)CH), 7.22 - 7.19 (m, 3 H, C(HC=C)CHCH, C(HC=C)CHCH, C(HC=C)CHC(OCH₂)), 7.13 - 7.06 (m, 2 H, C(F)CH), 5.22 (s, 2 H, CH₂ArB(OH)₂), 4.86 (s, 2 H, NCH₂), 4.19 - 4.10 (m, 4 H, ArOCH₂CH₂, CH₂CH₂OTs), 3.82 - 3.72 (m, 4 H, ArOCH₂CH₂, CH₂CH₂OTs), 2.35 (s, 3H, ArCH₃); ¹³C NMR (100 MHz, ACETONE-d₆) δ = 167.37, 165.80, 162.43 (d, *J* = 245.37 Hz), 151.08, 149.36, 144.89, 139.07, 134.37, 133.59, 133.43, 132.20 (d, *J* = 2.88 Hz), 130.54 (d, *J* = 7.67 Hz), 129.95, 127.89, 126.61, 126.57, 124.59, 118.87, 115.57, 115.36 (d, *J* = 21.09 Hz), 114.45, 70.53, 69.91, 69.39, 69.03, 68.82, 44.11, 20.69, C-B(OH)₂ Not visible; ; IR (solid): 3334, 2932, 1733, 1672, 1590, 1513, 1345, 1270 cm⁻¹; HRMS (ESI⁺) (*m/z*) calcd for C₃₅H₃₃¹¹BFNO₁₀S₂ [M + H]⁺ 722.1702, found 722.1701; Mp = 139 – 142 °C.

7.1.38 Potassium (Z)-trifluoro(4-((4-((3-(4-fluorobenzyl)-2,4-dioxothiazolidin-5-ylidene)methyl)-2-(2-(2-(tosyloxy)ethoxy)ethoxy)phenoxy)methyl)phenyl)borate



KHF_2 4.5M aq. (1.42 mL, 6.4 mmol, 10 eq.) was added in one portion to a solution of (Z)-2-(2-(5-((3-(4-fluorobenzyl)-2,4-dioxothiazolidin-5-ylidene)methyl)-2-((4-(4,4,5,5-tetramethyl-1,3,2-dioxaborolan-2-yl)benzyl)oxy)phenoxy)ethoxy)ethyl 4-methylbenzenesulfonate (0.50 g, 0.6 mmol, 1.0 eq.) in MeOH (10 mL), then stirred for 1 h at room temperature. Acetone (15 mL) was then added. The solution was filtered under gravity, and the filtrate was then evaporated under reduced pressure to give an oily yellow residue. The residue was subjected to MeOH / H₂O 1:1 evaporation cycles (as previously described). The entire reaction was repeated with the yellow solid obtained and then worked-up as described, to obtain a yellow crystalline solid (quantitative).

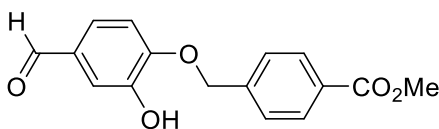
The material was then carried through to the next reaction without any further purification as an intermediate.

Trimethylsilyl chloride (0.40 mL, 3.1 mmol, 5.0 eq.) and H₂O (60 μL , 3.1 mmol, 5.0 eq.) were added to a solution of potassium (Z)-trifluoro(4-((4-((3-(4-fluorobenzyl)-2,4-dioxothiazolidin-5-ylidene)methyl)-2-(2-(2-(tosyloxy)ethoxy)ethoxy)phenoxy)methyl)phenyl)borate (0.49 g, 0.6 mmol, 1 eq.) in MeCN (10 mL) and stirred for 1 h at room temperature. A solution of sodium bicarbonate sat. aq. (1 mL) was added. The mixture was then dried using anhydrous sodium sulfate, filtered and evaporated to give a yellow solid.

This was purified *via* flash column chromatography (90% Acetone / 10% light petroleum ether) to give boronic acid **51** as a yellow solid (0.34 g, 71%).

The material was analysed *via* ¹H NMR spectroscopy (Acetone-D₆) and in agreement with that of method 1, (boronic acid **51**).

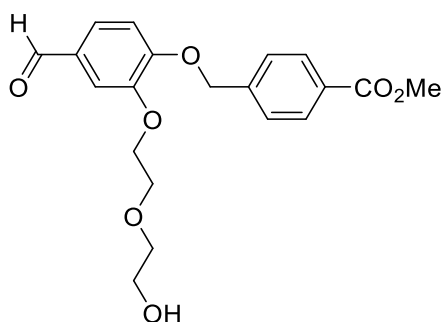
7.1.39 Methyl 4-((4-formyl-2-hydroxyphenoxy)methyl)benzoate, (**39**)



3,4-Dihydroxybenzaldehyde (1.51 g, 10.9 mmol, 1.0 eq.) was stirred in DMF (40 mL), sodium bicarbonate (1.29 g, 15.3 mmol, 1.5 eq.), methyl-4-(bromomethyl)-benzoate (5.00 g, 21.8 mmol, 2.0 eq.) and sodium iodide (0.49 g, 3.3 mmol, 0.3 eq.) was added. The reaction mixture stirred for 2 days at 40 °C. The reaction was quenched using 1M HCl aq. (100 mL) and then diluted with H₂O (100 mL). The organic portion was extracted with EtOAc (3 x 200 mL), combined, washed with a solution of 5% LiCl aq. (3 x 250 mL), then brine (1 x 400 mL), dried over anhydrous MgSO₄, filtered and evaporated under reduced pressure to obtain a light brown solid. This was then recrystallized using a mixture of EtOAc / hexanes to obtain ester **39** as a tan crystalline solid (1.00 g, 32 %).

¹H NMR (400 MHz, CDCl₃) δ = 9.85 (s, 1H, CHO), 8.09 (d, *J* = 8.3 Hz, 2H, C(CO₂Me)CH), 7.62 - 7.46 (m, 3H, C(CO₂Me)CHCH, C(CHO)CHC(OH)), 7.41 (dd, *J* = 8.5, 1.9 Hz, 1H, C(CHO)CHCH), 7.00 (d, *J* = 8.2 Hz, 1H, C(CHO)CHCH), 5.81 (s, 1H, C(OH)), 5.28 (s, 2H, O(CH)), 3.94 (s, 3H, CO₂CH₃); ¹³C NMR (100 MHz, CDCl₃) δ = 191.08, 166.67, 150.68, 146.36, 140.30, 131.13, 130.54, 130.26, 127.50, 124.40, 114.76, 111.65, 70.61, 52.41; IR (neat) cm⁻¹; 3270, 2952, 2361, 1710, 1673, 1608, 1582, 1505, 1436, 1278, 1110; HRMS (ESI) [M + H]⁺ calcd for C₁₆H₁₄O₅, 287.0914 found 287.0916, Mp = 138 – 140 °C.

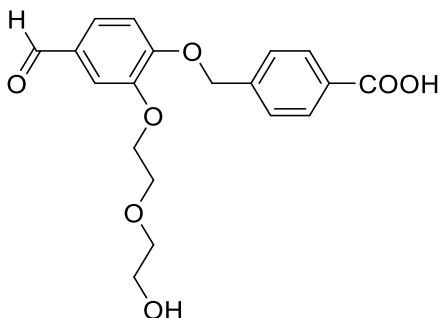
7.1.40 Methyl 4-((4-formyl-2-(2-(2-hydroxyethoxy)ethoxy)phenoxy)methyl)benzoate, (**40**)



Potassium carbonate (0.92 g, 6.6 mmol, 2.0 eq.), potassium iodide (0.55 g, 3.3 mmol, 1.0 eq.) and 2-(2-chloro-ethoxy)-ethanol (1.05 mL, 10.0 mmol, 3.0 eq.) was added to a solution of methyl 4-((4-formyl-2-hydroxyphenoxy)methyl)benzoate (0.95 g, 3.32 mmol, 1.0 eq.) in DMF (20 mL). The resulting mixture was heated to 70 °C for 40 h. The solution was diluted with H₂O (70 mL) and extracted with EtOAc (3 x 100 mL), the organic extracts were combined, washed with a solution of 5% LiCl aq. (3 x 200 mL) and brine (2 x 300 mL), dried over anhydrous MgSO₄, filtered and evaporated to brown oil. The crude material was purified *via* flash column chromatography (70% EtOAc / light petroleum ether → 100% EtOAc) to give alcohol **40** as a white solid (1.12 g, 95 %).

¹H NMR (400 MHz, CDCl₃) δ = 9.83 (s, 1H, CHO), 8.06 (d, *J* = 8.3, 2H, C(CO₂Me)CH), 7.60 - 7.45 (m, 3H, C(CO₂Me)CHCH, C(CHO)CHC(OCH₂CH₂)), 7.41 (dd, *J* = 8.2, 2.1, 1H, C(CHO)CHCH), 6.97 (d, *J* = 8.5, 1H, C(CHO)CHCH), 5.28 (s, 2H, OCH₂ArCO₂Me), 4.33 - 4.19 (m, 2H, ArOCH₂CH₂O), 4.02 - 3.86 (m, 5H, ArOCH₂CH₂O, CO₂Me), 3.79 - 3.56 (m, 4H, CH₂CH₂OH); ¹³C NMR (100 MHz, CDCl₃) δ = 195.14, 171.00, 157.84, 153.53, 145.50, 134.80, 134.24, 134.17, 131.25, 131.09, 117.08, 115.67, 76.96, 74.46, 73.70, 73.01, 66.08, 56.48. IR (solid): 3671, 3504, 3442, 3407, 2908, 1722, 1685, 1584 cm⁻¹; HRMS (ESI⁺) calcd for C₂₀H₂₂O₇ [M + H]⁺ 375.1438, found 375.1441. Mp = 56-59 °C.

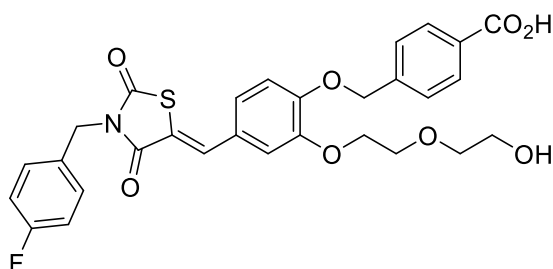
7.1.41 4-((4-Formyl-2-(2-(2-hydroxyethoxy)ethoxy)phenoxy)methyl)benzoic acid, (**41**)



Methyl 4-((4-formyl-2-(2-(2-hydroxyethoxy)ethoxy)phenoxy)methyl)benzoate (1.09 g, 3.1 mmol, 1.0 eq.) was dissolved in DMSO (18 mL). H₂O (12 mL) was added followed by NaOH aq. (1M, 3.07 mL, 3.1 mmol, 1.0 eq.), the mixture was then heated to 70 °C for 1 h, and then cooled to room temperature. The pH was adjusted to pH 2 *via* the careful addition of 1 M HCl aq. effecting the precipitation of a white solid, which was collected through vacuum filtration. The filter cake was then dried under reduced pressure to obtain carboxylic acid **41** as a white powder, (quantitative).

¹H NMR (400 MHz, CDCl₃) δ = 9.84 (s, 1H, ArCHO), 8.09 (d, *J* = 8.3 Hz, 2H, C(COOH)CH), 7.54 (d, *J* = 8.3 Hz, 2H, C(COOH)CHCH), 7.50 (d, *J* = 1.8 Hz, 1H, C(OCH₂CH₂)CHC(CHO)), 7.42 (dd, *J* = 8.1, 1.8 Hz, 1H, C(CHO)CHCH), 6.98 (d, *J* = 8.2 Hz, 1H, C(CHO)CHCH), 5.30 (s, 2H, CH₂ArCOOH), 4.29 (dd, *J* = 5.3, 3.8 Hz, 2H, ArOCH₂CH₂), 3.97 (dd, *J* = 5.3, 3.7 Hz, 2H, ArOCH₂CH₂), 3.81 - 3.64 (m, 4H, CH₂CH₂OH); ¹³C NMR (100 MHz, CDCl₃) δ = 191.01, 170.55, 153.60, 149.31, 142.05, 130.63, 130.07, 129.27, 127.09, 126.94, 112.85, 111.42, 72.75, 70.24, 69.50, 68.74, 61.85. IR (solid): 3347, 2861, 1678, 1584, 1508 cm⁻¹; HRMS (ESI⁺) calcd for C₁₉H₂₀O₇ [M + H]⁺ 361.1282, found 361.1286. Mp = 116-119 °C.

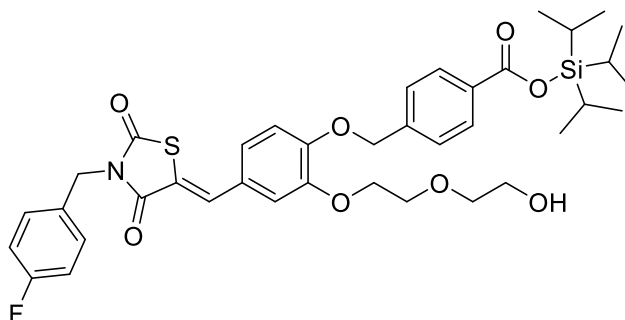
7.1.42 (Z)-4-((4-((3-(4-Fluorobenzyl)-2,4-dioxothiazolidin-5-ylidene)methyl)-2-(2-(2-hydroxyethoxy)ethoxy)phenoxy)methyl)benzoic acid, (**43**)



Piperidine (0.26 mL, 2.6 mmol, 1.0 eq.) and 4-((4-formyl-2-(2-(2-hydroxyethoxy)ethoxy)phenoxy)methyl)benzoic acid (0.94 g, 2.6 mmol, 1.0 eq.) was added to a solution of 3-(4-fluorobenzyl)-1,3-thiazolane-2,4-dione (0.59 g, 2.6 mmol, 1.0 eq.) in EtOH (10 mL). The solution was heated to 78 °C for 24 h. The mixture was cooled to room temperature and the resulting precipitate was collected *via* vacuum filtration to yield heterocycle **43** as a pale-yellow powder (0.72 g, 50%).

$^1\text{H NMR}$ (400 MHz, DMSO- d_6) δ = 8.01 (d, J = 8.2, 2H, C(CH₂OAr)CH), 7.90 (s, 1H, C=CH), 7.60 (d, J = 8.2, 2H, C(COOH)CH), 7.39 (dd, J = 8.6, 5.5, 2H, C(CH₂N)CH), 7.31 - 7.05 (m, 5H, C(HC=C)CHCH, C(HC=C)CHCH, C(HC=C)CHC(OCH₂CH₂), C(F)CH), 5.30 (s, 2H, CH₂Ar(COOH)), 4.83 (s, 2H, CH₂Ar(F)), 4.30 - 4.08 (m, 2H, ArOCH₂CH₂), 3.88 - 3.74 (m, 2H, ArOCH₂CH₂), 3.57 (s, 4H, OHCH₂CH₂, OHCH₂CH₂). $^{13}\text{C NMR}$ (100 MHz, DMSO- d_6) δ = 167.88, 167.63, 166.03, 162.20 (d, $^1J_{\text{C-F}}$ = 243.5 Hz), 150.54, 149.08, 142.23, 134.23, 132.28 (d, $^4J_{\text{C-F}}$ = 2.9 Hz), 130.78, 130.49 (d, $^3J_{\text{C-F}}$ = 7.7 Hz), 130.03, 127.75, 126.63, 124.51, 118.78, 115.97 (d, $^2J_{\text{C-F}}$ = 22.0 Hz), 114.72, 73.14, 69.87, 69.31, 68.91, 60.82, 44.38, 22.68. IR (solid): 3672, 3448, 2972, 2902, 1729, 1678, 1509 cm^{-1} ; HRMS (ESI⁺) (m/z) calcd for C₂₉H₂₆FNO₈S [M + H]⁺ 568.1436, found 568.1430; (Found: C, 61.15; H, 4.73; N, 2.61. C₂₉H₂₆FNO₈S requires C, 61.37; H, 4.62; N, 2.47%); Mp = 188-191 °C.

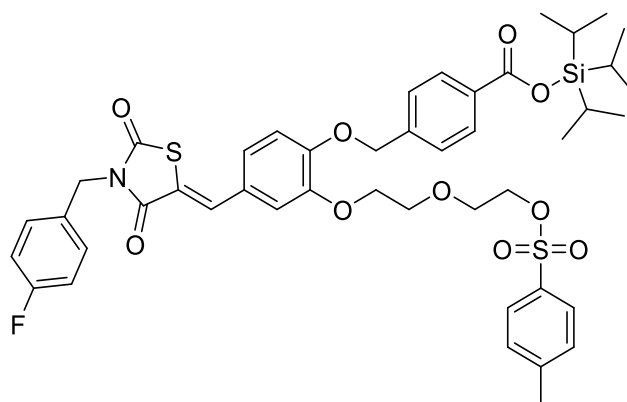
7.1.43 Triisopropylsilyl-(Z)-4-((4-((3-(4-fluorobenzyl)-2,4-dioxothiazolidin-5-ylidene)methyl)-2-(2-(2-hydroxyethoxy)ethoxy)phenoxy)methyl)benzoate, (**44**)



Triisopropylsilyl chloride (0.38 mL, 1.8 mmol, 1.40 eq.) was added to a solution of (Z)-4-((4-((3-(4-fluorobenzyl)-2,4-dioxothiazolidin-5-ylidene)methyl)-2-(2-(2-hydroxyethoxy)ethoxy)phenoxy)methyl)benzoic acid (0.72 g, 1.3 mmol, 1.0 eq.) in anhydrous THF (30 mL). Triethylamine (0.16 mL, 1.4 mmol, 1.1 eq.) was then added and the reaction mixture was stirred for 1 h at room temperature. The resulting mixture was then diluted with Et₂O (20 mL) and then evaporated to give an oily yellow solid. The crude material was purified by flash column chromatography (60% EtOAc / light petroleum ether) to yield TIPS ester **44** as a bright yellow powder (0.92 g, 81 %).

¹H NMR (400 MHz, CDCl₃) δ = 8.07 (d, *J* = 8.3, 2H, C(COOTIPS)CH), 7.80 (s, 1H, C=CH), 7.51 (d, *J* = 8.3, 2H, C(CH₂O)CH), 7.46 - 7.39 (m, 2H, C(CH₂N)CH), 7.09 - 6.89 (m, 5H, C(HC=C)CHCH, C(HC=C)CHC(OCH₂), C(HC=C)CHCH), 5.26 (s, 2H, CH₂Ar(COOTIPS)), 4.85 (s, 2H, CH₂ArF), 4.30 - 4.11 (dd, *J* = 5.2, 4.0, 2H, ArOCH₂CH₂), 3.95 (dd, *J* = 5.3, 4.0, 2H, ArOCH₂CH₂), 3.75 - 3.42 (m, 4H, OHCH₂CH₂, OHCH₂CH₂), 1.52 - 1.31 (m, 3H, Si(CH(CH₃)₂)₃), 1.12 (d, *J* = 7.4, 18H, Si(CH(CH₃)₂)₃). ¹³C NMR (100 MHz, CDCl₃) δ = 167.84, 166.22, 165.99, 162.70 (d, ¹*J*_{C-F} = 246.3 Hz, 1C), 150.61, 149.14, 141.47, 134.10, 131.34, 131.15 (d, ⁴*J*_{C-F} = 2.9 Hz, 1C), 130.98 (d, ³*J*_{C-F} = 7.7 Hz, 1C), 130.63, 126.85, 126.75, 125.20, 119.06, 115.72 (d, ²*J*_{C-F} = 21.1 Hz, 1C), 115.23, 114.10, 72.75, 70.32, 69.52, 69.01, 61.88, 44.55, 17.96, 12.14; IR (solid): 3536, 2944, 2868, 1728, 1669, 1510 cm⁻¹; HRMS (ESI⁺) (*m/z*) calcd for C₃₈H₄₆FNO₈SSi⁺ [M + H]⁺ 724.2770, found 724.2774. (Found: C, 62.96; H, 6.53; N, 2.04. C₃₈H₄₆FNO₈SSi requires C, 63.05; H, 6.41; N, 1.93%). Mp = 107-109 °C.

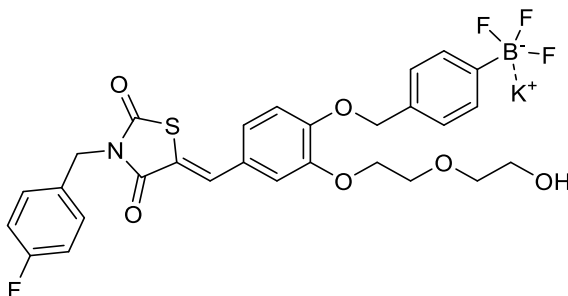
7.1.44 Triisopropylsilyl(Z)-4-((4-((3-(4-fluorobenzyl)-2,4-dioxothiazolidin-5-ylidene)methyl)-2-(2-(2-(tosyloxy)ethoxy)ethoxy)phenoxy)methyl)benzoate, (**45**)



Tosyl chloride (0.21 g, 1.1 mmol, 2.0 eq.) and triethylamine (0.15 mL, 1.1 mmol, 2.0 eq.) were added to a solution of triisopropylsilyl (Z)-4-((4-((3-(4-fluorobenzyl)-2,4-dioxothiazolidin-5-ylidene)methyl)-2-(2-(2-hydroxyethoxy)ethoxy)phenoxy)methyl)benzoate (0.40 g, 0.6 mmol, 1.0 eq.) in DCM (12 mL). The reaction mixture was stirred at room temperature for 36 h, then evaporated to a yellow residue which was purified by flash column chromatography (50% EtOAc / 50 % light petroleum ether) to afford tosylate **45** as a yellow crystalline solid (0.30 g, 61 %).

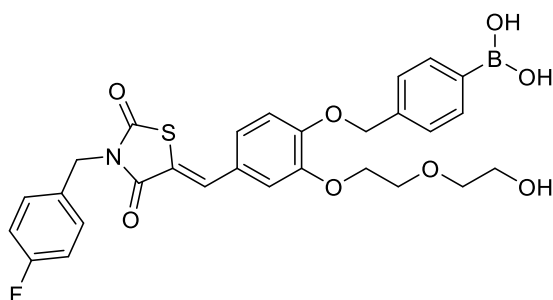
^1H NMR (400 MHz, ACETONE- d_6) δ = 8.08 (d, J = 8.2, 2H, C(COOTIPS)CH), 7.84 (s, 1H, C=CH), 7.76 (d, J = 8.2, 2H, C(SO₃)CH), 7.64 (d, J = 8.2, 2H, C(CH₂O)CH), 7.48 - 7.41 (m, 2H, C(CH₂N)CH), 7.37 (d, J = 8.2, 2H, C(CH₃)CH), 7.25 - 7.18 (m, 3H, C(HC=C)CHCH, C(HC=C)CHCH, C(HC=C)CHC(OCH₂)), 7.15 - 7.07 (m, 2H, C(F)CH), 5.33 (s, 1H, CH₂ArCOOH), 4.87 (s, 2H, CH₂ArF), 4.23 - 4.14 (m, 4H, ArOCH₂CH₂, TsOCH₂CH₂), 3.86 - 3.75 (m, 4H, ArOCH₂CH₂, TsOCH₂CH₂), 2.36 (s, 3H, CH₃), 1.49 - 1.36 (m, 3H, Si(CH(CH₃)₂)₃), 1.14 (d, J = 7.3, 18H, Si(CH(CH₃)₂)₃). ^{13}C NMR (100 MHz, ACETONE- d_6) δ = 168.10, 166.55, 166.34, 163.21 (d, $^1J_{\text{C-F}}$ = 245.4 Hz), 151.48, 150.17, 145.61, 143.39, 134.27, 134.24, 132.94 (d, $^4J_{\text{C-F}}$ = 3.8 Hz), 131.69, 131.32 (d, $^3J_{\text{C-F}}$ = 8.6 Hz), 130.99, 130.68, 128.65, 128.16, 127.62, 125.24, 119.83, 116.28, 116.13 (d, $^2J_{\text{C-F}}$ = 21.1 Hz), IR (solid) 115.36, 70.69, 70.64, 70.17, 69.69, 69.55, 44.88, 21.46, 18.16, 12.72 cm^{-1} (solid): 2926, 2867, 2667, 1731, 1681, 1592. HRMS (ESI⁺) (m/z) calcd for C₄₅H₅₂FNO₁₀S₂SiNH₄⁺ [M + NH₄]⁺ 896.3124, found 896.3123. (Found: C, 61.44 ; H, 5.79 ; N, 1.71 . C₃₈H₄₆FNO₈SSi requires C, 61.55; H, 5.97; N, 1.60%). Mp = 72-75 °C.

7.1.45 Potassium (Z)-trifluoro(4-((4-((3-(4-fluorobenzyl)-2,4-dioxothiazolidin-5-ylidene)methyl)-2-(2-(2-hydroxyethoxy)ethoxy)phenoxy)methyl)phenyl)borate (**51**)



A solution of KHF_2 aq. (4.5 M, 5.1 mL, 23.1 mmol, 10.0 eq.) was added to a solution of (Z)-3-(4-fluorobenzyl)-5-(3-(2-(2-hydroxyethoxy)ethoxy)-4-((4-(4,4,5,5-tetramethyl-1,3,2-dioxaborolan-2-yl)benzyl)oxy)benzylidene)thiophene-2,4(3H,5H)-dione (1.50 g, 2.3 mmol, 1.0 eq.) in MeOH (25 mL). The solution was stirred at room temperature for 1 h, after which acetone (100 mL) was added resulting in the precipitation of a white solid, which was then filtered. The filtrate was evaporated under reduced pressure to give a yellow residue that was then co-evaporated with MeOH / H_2O 1:1, 3 times (as previously described). The entire process was repeated once more with the crude product, to yield trifluoroborate **51** as a yellow solid (0.76 g, 52 %), which was used immediately.

7.1.46 (Z)-4-((4-((3-(4-fluorobenzyl)-2,4-dioxothiazolidin-5-ylidene)methyl)-2-(2-(2-hydroxyethoxy)ethoxy)phenoxy)methyl)phenyl)boronic acid, (**52**)

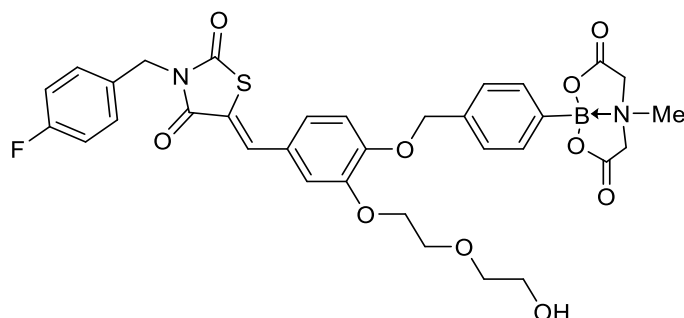


H₂O (0.10 mL, 5.7 mmol, 5 eq.) and trimethylsilyl chloride (0.73 mL, 5.7 mmol, 5 eq.) was added to a solution of potassium (Z)-trifluoro(4-((4-((3-(4-fluorobenzyl)-2,4-dioxothiazolidin-5-ylidene)methyl)-2-(2-(2-hydroxyethoxy)ethoxy)phenoxy)methyl)phenyl) borate (0.72 g, 1.1 mmol, 1.0 eq.) in MeCN (12 mL). The resulting mixture was stirred at room temperature for 30 min, then H₂O (0.5 mL) was added followed by MeCN (20 mL), effecting the precipitation of a light-yellow solid. The liquid was carefully decanted and the solid re-suspended in MeCN (10 mL), the liquid was then decanted. This process was repeated three additional times. The solid was thoroughly dried under high vacuum, then finally washed in hexanes and dried, to obtain boronic acid **51** as a light-yellow powder (0.43 g, 67 %).

¹H NMR (400 MHz, DMSO-d₆) δ = 7.90 (s, 1H, C=CH), 7.81 (d, *J* = 8.10 Hz, 2H, C(B(OH)₂CH), 7.36 (d, *J* = 7.90 Hz, 2H, C(B(OH)₂CHCH), 7.34 - 7.30 (m, 2H, (NCH₂)CCH), 7.25 (br. s, 1H, (HC=C)CCHC(OCH₂CH₂)), 7.18 - 7.12 (m, 4H, C(HC=C)CHCH, C(F)CH), 5.23 (s, 2H, CH₂ArB(OH)₂), 4.86 - 4.75 (m, 1H, CH₂CH₂OH), 4.18 - 4.08 (m, 2H, ArOCH₂CH₂), 3.84 - 3.70 (m, 2H, ArOCH₂CH₂), 3.61 - 3.44 (m, 4H, CH₂CH₂OH); ¹³C NMR (100 MHz, DMSO-d₆) δ = 167.42, 165.57, 161.67 (d, ¹*J*_{C-F} = 244.4 Hz, 1C), 150.27, 148.53, 138.41, 134.29, 133.79, 131.82 (d, ⁴*J*_{C-F} = 2.9 Hz), 129.94 (d, ³*J*_{C-F} = 8.6 Hz), 126.50, 125.89, 124.04, 118.20, 115.50 (d, ²*J*_{C-F} = 22.0 Hz), 114.22, 72.57, 69.89, 68.77, 68.35, 60.24, 43.89, C-B(OH)₂ not visible; IR (neat) 3374, 2937, 1730, 1677, 1590, 1509, 1380, 1334, 1276, 1143 cm⁻¹; HRMS (ESI) (Sample + ethylene glycol) [M + H]⁺ calcd for C₃₁H₃₁¹¹BFNO₈S, 594.1774 found 594.1774*; Mp = 115 - 118 °C

*Sample analysed reacted with diethylene glycol by the National Mass Spectrometry Facility at Swansea, to obtain the accurate mass for the boronate ester adduct.²⁵⁸

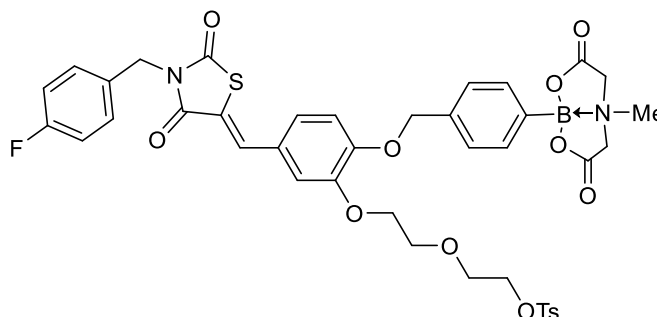
7.1.47 (Z)-2-(4-((4-((3-(4-Fluorobenzyl)-2,4-dioxothiazolidin-5-ylidene)methyl)-2-(2-(2-hydroxyethoxy)ethoxy)phenoxy)methyl)phenyl)-6-methyl-1,3,6,2-dioxazaborocane-4,8-dione, (**53**)



(Z)-4-((4-((3-(4-Fluorobenzyl)-2,4-dioxothiazolidin-5-ylidene)methyl)-2-(2-(2-hydroxyethoxy)ethoxy)phenoxy)methyl)phenyl)boronic acid (0.34 g, 0.6 mmol, 1.0 eq.) and *N*-methyl imonodicacetic acid (109 mg, 0.7 mmol, 1.2 eq.) were heated under Dean-Stark conditions, in a 15:1 mixture of toluene and DMSO (32 mL), for 16 h. The crude mixture was stripped of solvent as far as possible by evaporation under reduced pressure, to obtain a yellow residue. Following the addition of MeCN (10 mL) a white precipitate formed which was filtered and washed with additional MeCN. The filtrate was evaporated under reduced pressure to obtain a yellow solid, which was triturated in hexanes (2 x 5 mL) and the remaining solid dried. The crude material was purified by flash column chromatography (50 % EtOAc / 50 % acetone) to obtain MIDA boronate **53** as a bright yellow solid (97 mg, 24 %).

^1H NMR (400 MHz, ACETONE- d_6) δ = 7.82 (s, 1 H, C=CH), 7.55 (d, J = 8.7 Hz, 2 H, C(BO₂)CH), 7.50 (d, J = 8.7 Hz, 2 H, C(CH₂O)CH), 7.46 - 7.40 (m, 2 H, C(CH₂N)CH), 7.26 - 7.17 (m, 3 H, C(OCH₂)CHCH, C(OCH₂)CHCH, C(HC=C)CHC(O)), 7.13 - 7.06 (m, 2 H, C(F)CH, 2 H), 5.23 (s, CH₂ArMIDA), 4.85 (s, 2 H, CH₂ArF), 4.33 (d, J = 16.9 Hz, 2 H, CH₂NMe), 4.26 - 4.20 (m, 2 H, ArOCH₂CH₂), 4.13 (d, J = 16.9 Hz, 2 H, CH₂NMe), 3.88 - 3.82 (m, 2 H, ArOCH₂CH₂), 3.60 (s, 4 H, OHCH₂CH₂, OHCH₂CH₂), 2.72 (s, 3 H, NCH₃); ^{13}C NMR (100 MHz, ACETONE- d_6) δ = 168.50, 167.40, 165.79, 162.35 (d, $^1J_{\text{C-F}}$ = 243.45 Hz), 151.11, 149.48, 137.85, 133.64, 132.77, 132.20 (d, $^4J_{\text{C-F}}$ = 2.88 Hz), 130.55 (d, $^3J_{\text{C-F}}$ = 8.63 Hz), 127.03, 126.56, 124.57, 118.80, 115.51, 115.36 (d, $^2J_{\text{C-F}}$ = 22.04 Hz), 114.43, 102.91, 72.95, 70.54, 69.32, 68.98, 61.91, 61.21, 47.44, 44.1; IR (solid) 3455, 2952, 1731, 1678, 1590, 1509, 1494, 1423, 1380 cm^{-1} ; HRMS (ESI) $[\text{M} + \text{NH}_4]^+$ calcd for C₃₃H₃₂¹¹BFN₂O₁₀SNH₄, 696.2199 found 696.2195; HRMS (ESI) $[\text{M} + \text{Na}]^+$ calcd for C₃₃H₃₂¹¹BFN₂O₁₀SNa, 701.1753 found 701.1745; Mp = 186 – 186 °C.

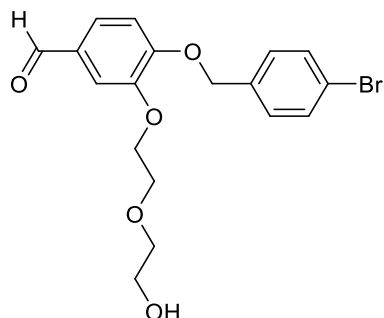
7.1.48 (Z)-2-(2-(5-((3-(4-Fluorobenzyl)-2,4-dioxothiazolidin-5-ylidene)methyl)-2-((4-(6-methyl-4,8-dioxo-1,3,6,2-dioxazaborocan-2-yl)benzyl)oxy)phenoxy)ethoxy)ethyl 4methylbenzenesulfonate, (**54**)



Triethylamine (30 μ L, 0.2 mmol, 2.0 eq.) and tosyl chloride (46 mg, 0.2 mmol, 2.0 eq.) was added to a solution of (Z)-2-(4-((4-((3-(4-fluorobenzyl)-2,4-dioxothiazolidin-5-ylidene)methyl)-2-(2-(2-hydroxyethoxy)ethoxy)phenoxy)methyl)phenyl)-6-methyl-1,3,6,2-dioxazaborocane-4,8-dione (80 mg, 0.1 mmol, 1.0 eq.) in DCM (5 mL). The resulting mixture was stirred at room temperature for 5 days. The solvent was evaporated under reduced pressure to obtain a yellow residue, which was purified by flash column chromatography (100 % EtOAc) to yield tosylate **54** as a pale-yellow oil (21 mg, 21 %).

^1H NMR (400 MHz, CDCl_3) δ = 7.79 (s, 1 H, C=CH), 7.72 (d, J = 8.2 Hz, 2 H, C(SO₃)CH), 7.55 (d, J = 7.8 Hz, 2 H, CHC(BMIDA)), 7.47 - 7.38 (m, 4 H, NCH₂CH, C(CH₂O)CH), 7.27 (d, J = 8.2 Hz, 2 H, C(CH₃)CH), 7.08 (dd, J = 8.7 2.3 Hz, 1 H, C(HC=C)CHCH), 7.03 - 6.96 (m, 4 H, C(HC=C)CHCH, C(F)CH, C(HC=C)CHCOCH₂), 5.13 (s, 2 H, CH₂ArBMIDA), 4.84 (s, 2 H, CH₂ArF), 4.14 - 4.06 (m, 4 H, ArOCH₂CH₂, CH₂CH₂OTs), 3.97 (d, J = 16.9 Hz, 2 H, N(CH₃)CH₂), 3.85 (d, J = 16.9 Hz, 2 H, N(CH₃)CH₂), 3.82 - 3.79 (m, 2 H, ArOCH₂CH₂), 3.78 - 3.74 (m, 2 H, CH₂CH₂OTs), 2.55 (s, 3 H, N(CH₃)), 2.37 (s, 3 H, CH₃ArSO₃); ^{13}C NMR (100 MHz, CDCl_3) δ = 167.84, 166.22, 164.76 162.69 (d, $^1J_{\text{C-F}}$ = 247.28 Hz), 150.96, 149.09, 145.10, 137.92, 134.18, 132.78, 132.62, 131.16 (d, $^4J_{\text{C-F}}$ = 2.88 Hz), 130.97 (d, $^3J_{\text{C-F}}$ = 8.63 Hz), 129.99, 128.05, 127.18, 126.57, 125.30, 118.89, 115.72 (d, $^2J_{\text{C-F}}$ = 22.04 Hz), 115.04, 113.99, 102.87 70.70, 69.69, 69.54, 69.23, 69.18, 62.02, 47.73, 44.55, 21.74; IR (neat) 2897, 1719, 1643, 1564, 1504, 1473, 1455, 1398, 1350, 1301 cm^{-1} ; HRMS (ESI) $[\text{M} + \text{H}]^+$ calcd for $\text{C}_{40}\text{H}_{38}^{11}\text{BFN}_2\text{O}_{12}\text{S}_2\text{H}$, 833.2023 found 833.2023; HRMS (ESI) $[\text{M} + 2\text{H}]^+$ calcd for $\text{C}_{40}\text{H}_{38}^{11}\text{BFN}_2\text{O}_{12}\text{S}_2\text{H}_2$, 834.2050 found 834.2047

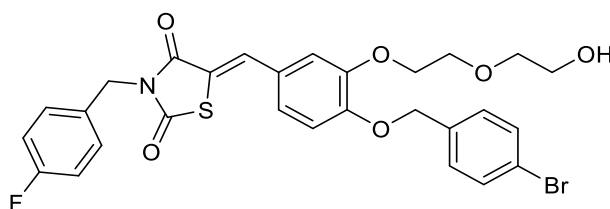
7.1.49 4-((4-bromobenzyl)oxy)-3-(2-(2-hydroxyethoxy)ethoxy)benzaldehyde, (**55**)



A solution of 2-chloro-2-ethoxy ethanol (1.49 mL, 14.1 mmol, 3.0 eq.) in DMF (1 mL) was added dropwise (over 1 min) to a solution of 4-((4-bromobenzyl)oxy)-3-hydroxybenzaldehyde (1.44 g, 4.7 mmol, 1.0 eq.) in DMF (20 mL). K_2CO_3 (0.98 g, 7.1 mmol, 1.5 eq.) and KI (0.75 g, 4.7 mmol, 1.0 eq.) were added, and the resulting mixture was then stirred at 75 °C for two days. The solution was cooled to room temperature, diluted with H_2O (200 mL) and extracted with EtOAc (3 x 150 mL). The combined organic extracts were washed with a solution of 5% LiCl aq. (2 x 250) and brine (2 x 400 mL). The organic portion was dried over anhydrous $MgSO_4$, filtered and evaporated to obtain a dark brown oil. The crude material was purified by flash column chromatography (80% EtOAc / 20% light petroleum ether), to afford ether **55** as a yellow oil (1.84 g, 99%).

1H NMR (400 MHz, $CDCl_3$) δ = 9.82 (s, 1 H, $\underline{C}HO$), 7.51 (d, J = 8.2 Hz, 2 H, $\underline{C}HCB$ r), 7.47 (d, J = 1.8 Hz, 1 H, $\underline{C}HCO$ H), 7.40 (dd, J = 8.2 1.8 Hz, 1 H, $C(\underline{C}HO)\underline{C}H$), 7.31 (d, $C(\underline{C}H_2)\underline{C}H$, J = 8.2 Hz, 2 H), 6.96 (d, $C(O)\underline{C}H$, J = 7.8 Hz, 1 H), 5.16 (s, $Ar\underline{C}H_2$, 2 H), 4.27 - 4.23 (m, $ArO\underline{C}H_2CH_2$, 2 H), 3.95 - 3.91 (m, $ArO\underline{C}H_2CH_2$, 2 H), 3.74 - 3.65 (m, $\underline{C}H_2CH_2OH$, 4 H), 2.33 (t, $\underline{O}H$, J = 5.7 Hz, 1 H); ^{13}C NMR (100 MHz, $CDCl_3$) δ = 191.01, 153.72, 149.34, 135.22, 131.91, 130.56, 129.06, 127.03, 122.23, 112.82, 111.47, 72.77, 70.26, 69.55, 68.83, 61.91; IR (neat) 3425, 2872, 1681, 1584, 1507, 1434, 1263, 1123 cm^{-1} ; HRMS (ESI) $[M + H]^+$ calcd for $C_{18}H_{19}^{79}BrO_5$, 395.0489 found 395.0491.

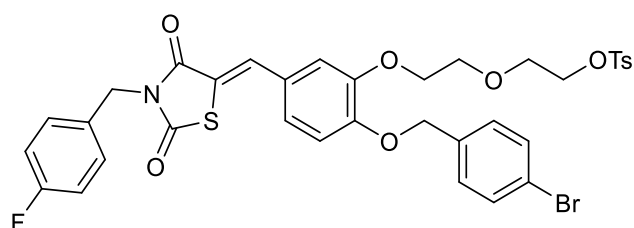
7.1.50 (Z)-5-(4-((4-Bromobenzyl)oxy)-3-(2-(2-hydroxyethoxy)ethoxy)benzylidene)-3-(4-fluorobenzyl)thiazolidine-2,4-dione, (**56**)



3-(4-Fluorobenzyl)thiazolidine-2,4-dione (1.08 g, 4.7 mmol, 1.0 eq.) and piperadine (0.47 mL, 4.7 mmol, 1.0 eq.) were added to a solution of 4-((4-bromobenzyl)oxy)-3-(2-(2-hydroxyethoxy)ethoxy)benzaldehyde (1.46 g, 4.7 mmol, 1.0 eq.) dissolved in ethanol (50 mL). The mixture was then stirred at 78 °C for 16 h. The solution was cooled to room temperature and left to stand for 1 h, which effected the precipitation of a yellow solid. This was collected by vacuum filtration and thoroughly dried to obtain bromide **56** as a yellow powder (1.62 g, 57 %).

^1H NMR (400 MHz, CDCl_3) δ = 7.79 (s, 1 H, $\text{C}=\text{CH}$), 7.49 (d, J = 8.2 Hz, 2 H, CBrCH), 7.45 - 7.39 (m, 2 H, $\text{CHC}(\text{CH}_2\text{N})$), 7.30 (d, J = 8.2 Hz, 2 H, $\text{C}(\text{CH}_2\text{CH})$), 7.08 - 6.96 (m, 4 H, $\text{C}(\text{O})\text{CHCH}$, $\text{C}(\text{CH}=\text{C})\text{CH}$, $\text{C}(\text{F})\text{CH}$), 6.91 (d, J = 8.2 Hz, 1 H, $\text{C}(\text{O})\text{CH}$), 5.12 (s, 2 H, ArCH_2), 4.84 (s, 2 H, NCH_2), 4.26 - 4.14 (m, 2 H, $\text{ArOCH}_2\text{CH}_2$), 3.97 - 3.84 (m, 2 H, $\text{ArOCH}_2\text{CH}_2$), 3.77 - 3.62 (m, 4 H, $\text{CH}_2\text{CH}_2\text{OH}$), 2.28 (br. s., 1 H, OH); ^{13}C NMR (100 MHz, CDCl_3) δ = 167.85, 166.22, 162.69 (d, $^1J_{\text{C-F}}$ = 248.24 Hz), 150.60, 149.12, 135.35, 134.12, 131.88, 131.15 (d, $^4J_{\text{C-F}}$ = 2.90 Hz), 130.99 (d, $^3J_{\text{C-F}}$ = 7.67 Hz), 128.99, 126.70, 125.19, 122.20, 119.02, 115.72 (d, $^2J_{\text{C-F}}$ = 21.09 Hz), 115.12, 114.08, 102.88, 72.74, 70.22, 69.48, 68.97, 61.88, 44.55; IR (neat) 3394, 2930, 2876, 1731, 1678, 1591, 1508, 1425, 1378 cm^{-1} ; HRMS (ESI) $[\text{M} + \text{H}]^+$ calcd for $\text{C}_{28}\text{H}_{25}^{79}\text{BrFNO}_6\text{S}$, 602.0648 found 602.0651; Mp = 143 – 144 °C.

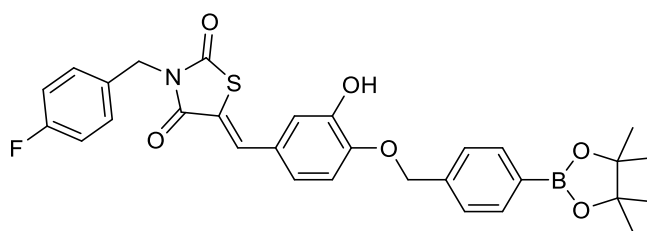
7.1.51 (Z)-2-(2-(2-((4-Bromobenzyl)oxy)-5-((3-(4-fluorobenzyl)-2,4-dioxothiazolidin-5-ylidene)methyl)phenoxy)ethoxy)ethyl 4-methylbenzenesulfonate, (**57**)



Tosyl chloride (0.98 g, 5.1 mmol, 2.0 eq.) and triethylamine (0.72 mL, 5.1 mmol, 2.0 eq.) were added to a solution of (Z)-5-(4-((4-bromobenzyl)oxy)-3-(2-(2-hydroxyethoxy)ethoxy)benzylidene)-3-(4-fluorobenzyl)thiazolidine-2,4-dione (1.55 g, 2.5 mmol, 1.0 eq.) in DCM, (25 mL) and stirred at room temperature for 2.5 days. The mixture was then evaporated to a yellow residue, which was purified *via* flash column chromatography (50% EtOAc / 50% light petroleum ether) to afford tosylate **57** as a pale-yellow oil (1.55 g, 80 %).

^1H NMR (400 MHz, CDCl_3) δ = 7.79 (s, 1 H, C=CH), 7.75 (d, J = 8.2 Hz, 2 H, C(SO₃)CH), 7.47 (d, J = 10.1 Hz, 2 H, C(Br)CH), 7.44 - 7.39 (m, 2 H, C(CH₂N)CH), 7.30 - 7.24 (m, 4 H, C(CH₃)CH, C(CH₂O)CH), 7.05 (dd, J = 8.1, 2.1 Hz, 1 H, C(HC=C)CHCH), 7.02 - 6.97 (m, 3 H, C(HC=C)CHC(O), C(F)CH), 6.92 (d, J = 8.7 Hz, 1 H, C(OCH₂ArBr)CH), 5.09 (s, 2 H, CH₂ArBr), 4.84 (s, 2 H, CH₂ArF), 4.15 - 4.10 (m, 4 H, ArOCH₂CH₂, CH₂CH₂OTs), 3.85 - 3.80 (m, 2 H, ArOCH₂CH₂), 3.78 - 3.73 (m, 2 H, CH₂CH₂OTs), 2.38 (s, 3 H, CH₃); ^{13}C NMR (100 MHz, CDCl_3) δ = 167.84, 166.20, 162.68 (d, $^1J_{\text{C-F}}$ = 246.33 Hz), 150.71, 149.17, 144.90, 135.44, 134.12, 133.02, 131.85, 131.18 (d, $^4J_{\text{C-F}}$ = 2.87 Hz), 130.98 (d, $^3J_{\text{C-F}}$ = 8.63 Hz), 129.91, 129.04, 128.04, 126.74, 125.16, 122.16, 119.02, 115.71 (d, $^2J_{\text{C-F}}$ = 21.09 Hz), 115.33, 114.30, 70.27, 69.79, 69.34, 69.17, 69.09, 44.55, 21.74; IR (neat) 3665, 2988, 1731, 1682, 1589, 1509, 1489, 1424, 1378, cm^{-1} ; HRMS (ESI) $[\text{M} + \text{H}]^+$ calcd for $\text{C}_{35}\text{H}_{31}^{79}\text{BrFNO}_8\text{S}_2$, 756.0737 found 756.0736; Mp = 61 – 63 °C.

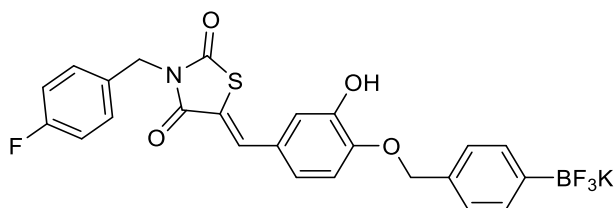
7.1.52 (Z)-3-(4-Fluorobenzyl)-5-(3-hydroxy-4-((4-(4,4,5,5-tetramethyl-1,3,2-dioxaborolan-2-yl)benzyl)oxy)benzylidene)thiazolidine-2,4-dione, (**58**)



3-(4-Fluorobenzyl)thiazolidine-2,4-dione (0.47 g, 2.1 mmol, 1 eq.) and piperidine (0.21 mL, 2.08 mmol, 1 eq.) were added to a solution of 3-hydroxy-4-((4-(4,4,5,5-tetramethyl-1,3,2-dioxaborolan-2-yl)benzyl)oxy)benzaldehyde (0.77 g, 2.1 mmol, 1.0 eq.) in ethanol (20 mL) and stirred at 78 °C and for 22 h. The reaction mixture was then slowly cooled to 0 °C which effected the precipitation of a tan solid, that was collected by vacuum filtration to give boronate ester **58** as a tan crystalline solid (0.56 g, 48 %).

$^1\text{H NMR}$ (400 MHz, CDCl_3) δ = 7.84 (d, J = 7.8 Hz, 2 H, C(BPin)CH), 7.78 (s, 1 H, C=CH), 7.45 - 7.38 (m, 4 H, C(BPin)CHCH, C(CH₂N)CH), 7.08 (d, J = 2.3 Hz, 1 H, C(HC=C)CHC(OH)), 7.03 - 6.92 (m, 4 H, C(F)CH, C(OCH₂)CHCH), 5.75 (br s, 1 H, OH), 5.18 (s, 2 H, OCH₂), 4.84 (s, 2 H, NCH₂), 1.34 (s, 12 H, $\text{BO}_2\text{C}_2(\text{CH}_3)_4$); $^{13}\text{C NMR}$ (100 MHz, CDCl_3) δ = 168.09, 166.33, 162.68 (d, $^1J_{\text{C-F}}$, J =247.28 Hz), 147.82, 146.29, 138.43, 135.37, 134.30, 134.28, 131.19 (d, $^4J_{\text{C-F}}$, J =2.88 Hz), 131.00 (d, $^3J_{\text{C-F}}$, J =8.63 Hz), 127.02, 124.04, 119.18, 115.99, 115.71 (d, $^3J_{\text{C-F}}$, J =22.04 Hz), 112.34, 84.08, 71.18, 44.50, 24.95, C-BPin not visible; IR (neat) 3475, 2981, 2936, 2114, 1911, 1728, 1596, 1505, 1450, 1355, 1269, 1208, 1133, 1082 cm^{-1} ; HRMS (ESI) $[\text{M} + \text{H}]^+$ calcd for $\text{C}_{30}\text{H}_{29}^{11}\text{BFNO}_6\text{S}$, 562.1871 found 562.1862; Mp = 168 - 169 °C.

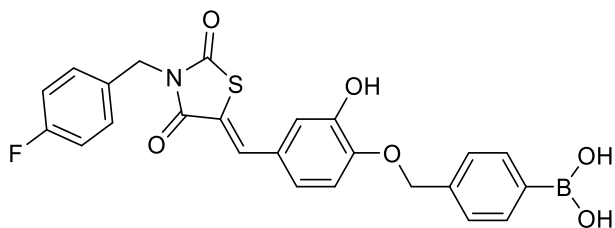
7.1.53 (Z)-3-(4-Fluorobenzyl)-5-(3-hydroxy-4-((4-(trifluoro-14-boraneyl)benzyl)oxy)benzylidene)thiazolidine-2,4-dione, potassium salt, (**59**)



A solution of KHF_2 aq. (4.5M, 1.2 mL, 5.3 mmol, 10.0 eq.) was added in one portion to a solution of (Z)-3-(4-fluorobenzyl)-5-(3-hydroxy-4-((4-(4,4,5,5-tetramethyl-1,3,2dioxaborolan-2-yl)benzyl)oxy)benzylidene)thiazolidine-2,4-dione (0.30 g, 0.5 mmol, 1 eq.) in a 5:1 mixture of MeOH / DCM (20 mL), the solution was then stirred for 1 h at room temperature. The mixture was diluted in acetone (150 mL), filtered, the filtrate was then evaporated under reduced pressure. Four MeOH / H_2O evaporation cycles were then applied to the residue (as described previously). The reaction / work-up procedure was repeated in its entirety, to obtain trifluoroborate **59** as a fine yellow powder (0.29 g, 76 %).

^1H NMR (400 MHz, DMSO-d_6) δ = 7.71 (s, 1 H, $\text{C}=\underline{\text{CH}}$), 7.36 - 7.26 (m, 4 H, $\text{CHC}\underline{\text{H}}\text{C}(\text{CH}_2\text{N})$, $\text{C}(\text{BF}_3\text{K})\underline{\text{C}}\text{HCH}$), 7.17 - 7.08 (m, 4 H, $\text{C}(\text{BF}_3\text{K})\underline{\text{C}}\text{HCH}$, $\text{C}(\text{F})\underline{\text{C}}\text{H}$), 7.04 - 6.97 (m, 2 H, $\text{C}(\text{OCH}_2)\underline{\text{C}}\text{HCH}$, $\text{C}(\text{HC}=\text{C})\underline{\text{C}}\text{HCH}(\text{OH})$), 6.91 (d, $J = 7.3$ Hz, 1 H, $\text{C}(\text{OCH}_2)\underline{\text{C}}\text{HCH}$), 5.02 (s, 2 H, OCH_2), 4.75 (s, 2 H, NCH_2); ^{13}C NMR (100 MHz, DMSO-d_6) δ = 168.13, 166.14, 162.26 (d, $^1J_{\text{C-F}}$, $J=240.57$ Hz), 135.02, 134.98, 134.95, 133.58, 132.43 (d, $^4J_{\text{C-F}}$, $J=2.88$ Hz), 132.08, 131.83, 130.43 (d, $^3J_{\text{C-F}}$, $J=8.63$ Hz), 126.59, 126.42, 126.08, 116.68, 115.98 (d, $^2J_{\text{C-F}}$, $J=21.09$ Hz), 114.40, 70.94, 44.28, C- BF_3K not visible; IR (neat) 3445, 2115, 1724, 1669, 1592, 1508, 1437, 1329, 1283, 1224, 1129, 975 cm^{-1} ; HRMS (ESI) $[\text{M} - \text{K}]^-$ calcd for $\text{C}_{24}\text{H}_{17}^{11}\text{BF}_4\text{KNO}_4\text{S}$, 502.0917 found 502.0919; Mp = 211 – 213 °C (decomposed).

7.1.54 (Z)-4-((4-((3-(4-Fluorobenzyl)-2,4-dioxothiazolidin-5-ylidene)methyl)-2-hydroxyphenoxy)methyl)phenyl)boronic acid, (**60**)



Trimethylsilyl chloride (0.23 mL, 1.8 mmol, 5.0 eq.) and H₂O (30 μL, 1.8 mmol, 5 eq.) were added to a solution of (Z)-3-(4-fluorobenzyl)-5-(3-hydroxy-4-((4-(trifluoro-14-boranyl)benzyl)oxy)benzylidene)thiazolidine-2,4-dione, potassium salt (0.20 g, 0.4 mmol, 1.0 eq.) in MeCN (3 mL), the resulting solution was stirred at room temperature for three h. H₂O (0.3 mL) was added to the reaction mixture, followed by MeCN (30 mL), precipitating an off-white solid, which was filtered, the filtrate was then evaporated to obtain boronic acid **60** as a yellow powder (84 mg, 48 %).

¹H NMR (400 MHz, ACETONE-d₆) δ = 7.89 (d, *J* = 8.2 Hz, 2H, C(B(OH)₂)CHCH), 7.79 (s, 1H, C=CH), 7.51 - 7.40 (m, 4H, C(B(OH)₂)CHCH, NCH₂CCH), 7.21 - 7.01 (m, 5H, C(F)CH, C(OCH₂)CHCH, C(OCH₂)CHCH, C(OH)CH), 5.26 (s, 2H, COCH₂), 4.86 (s, 2H, NCH₂); ¹³C NMR (100 MHz, ACETONE-d₆) δ = 167.43, 165.84, 162.44 (d, ¹*J*_{C-F}, *J* = 244.4 Hz), 149.13, 147.42, 138.65, 134.37, 133.70, 132.22 (d, ⁴*J*_{C-F}, *J* = 2.9 Hz), 130.56 (d, ³*J*_{C-F}, *J* = 7.7 Hz), 127.05, 126.65, 123.66, 118.60, 116.59, 115.36 (d, ²*J*_{C-F}, *J* = 22.0 Hz), 113.43, 70.47, 44.08, C-B(OH)₂ not visible; IR (neat) 3315, 3215, 2114, 1730, 1661, 1595, 1512, 1438, 1333, 1286, 1215 cm⁻¹; HRMS (ESI) [M + H]⁺ calcd for C₂₄H₁₉¹¹BFNO₆S, 480.1087 found 480.1080; Mp = 176 – 179 °C.

7.1.55 Procedure for the isolation of solid Icodextrin from Adept® adhesion reduction solution:

Adept® solution (150 mL approx.) was dialysed against H₂O (1 L, 20 kDa). The water was changed 9 times over a period of 3 days. The contents of the dialysis membranes were transferred to a beaker, acetone (200 mL) was then added, which caused the solution to turn cloudy, the beaker was then left to stand for 1 h at room temperature. The liquid portion was then decanted, leaving a thick tacky residue on the bottom of the beaker. A further portion of acetone (50 mL) was added which precipitated a white solid. The solid was collected *via* vacuum filtration and dried under high vacuum, to afford a white powder, 10.4 g.

Anhydrous Icodextrin was prepared by heating a flask of stirring finely powdered IDX at 50 °C, under high vacuum (0.1 mbar minimum) for two days.

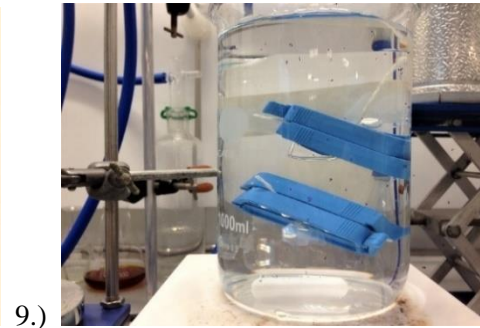
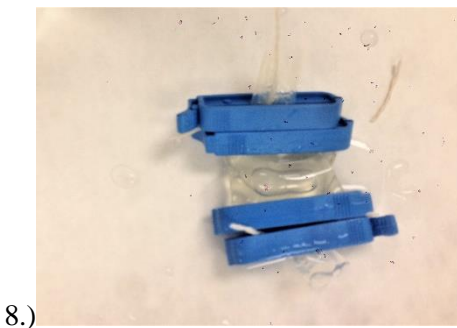
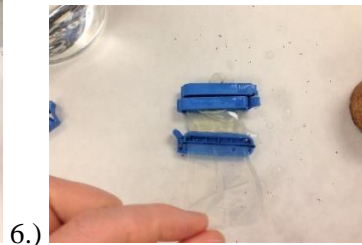
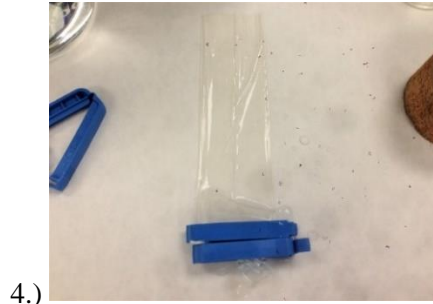
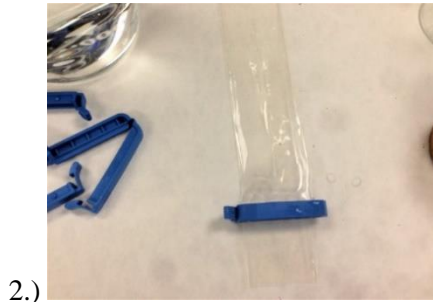
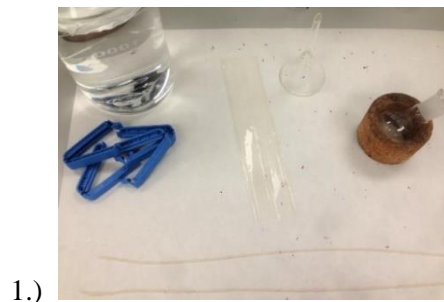
Dialysis procedure:

(As shown in photos on the next page)

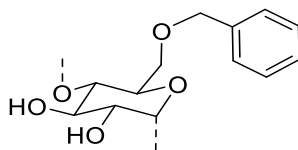
- 1.) The dialysis membrane pre-soaked in distilled water for one h and then “opened-out”, distilled water was run through the inside of the membrane.
- 2.) 1 closure secured approx. 5 cm from one end of the membrane
- 3.) Thin parcel string (wet) was used to tie the end securely, then excess membrane and string was trimmed.
- 4.) A second closure was placed over the knot.
- 5.) Using a funnel or syringe, the material (dissolved in water) was added to the membrane, excess material was washed with distilled water.
- 6.) The free-end was secured with a closure, approx. 0.5 cm above the top of the material.
- 7.) The membrane was then tied using wet string, excess membrane was trimmed away.
- 8.) A second closure was placed above the knot.
- 9.) The membrane was placed in a beaker containing a suitable dialysis solvent, (and a stirrer bar) and was suspended approx. 4 cm above the stirrer bar and secured to the beaker using excess string (attached to the membrane) and masking tape. Solvent changed as specified.

Note: Care should be taken to ensure the membrane is not punctured or damaged, such as keeping the membrane wet throughout the procedure and away from abrasive surfaces.

7.1.56 Photos to demonstrate dialysis procedure:



7.1.57 Benzyl Icodextrin conjugate, (Conjugate **16**)

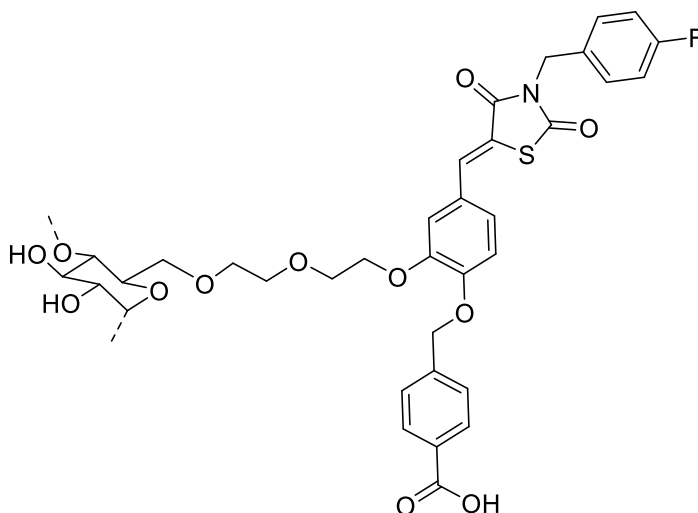


A solution of anhydrous Icodextrin (0.50 g, 3.1 mmol, 1.0 eq.) in anhydrous DMAc (3 mL) was heated to 160 °C, under a flow of N₂, for 90 min, until IDX completely dissolved. The mixture was cooled to 100 °C, where upon anhydrous LiCl (0.50 g (w / w IDX)) was added. The resulting mixture was then stirred overnight. The solution was cooled to room temperature, then a mineral oil dispersion of NaH (60 %, 0.19 g, 4.7 mmol, 1.75 eq.) was added and the solution was stirred for 4 h. Benzyl bromide (1.63 mL, 13.4 mmol, 5 eq.) was then added dropwise and the reaction mixture stirred for 2 days.

The material was dialysed against MeOH (1 L, 8 kDa MWCO), the methanol was changed twice over a period of 4 h. The contents of the dialysis membrane were transferred to a beaker, a solid was precipitated following the addition of cold acetone (20 mL). The material was then collected *via* vacuum filtration and washed with additional cold acetone. The solid was dried over a high vacuum for 4 h to afford Conjugate **16** as an off-white solid (0.36 g).

¹H NMR (400 MHz, DMSO-d₆) δ = 7.42 - 7.16 (m, Ph-H), 5.71 - 5.39 (m, IDX-H), 5.16 - 4.87 (m, IDX-H), 4.79 - 4.70 (m, CH₂Ph), 4.56 (br. s., IDX-H), 3.87 - 3.33 (m, IDX-H)

7.1.58 Icodextrin-**44** conjugate, (Conjugate **17**)

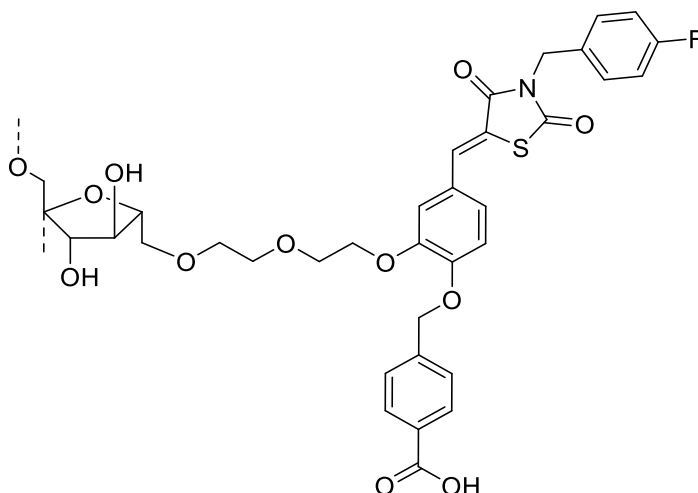


Anhydrous Icodextrin (0.12 g, 0.2 mmol, 1.00 eq.) was suspended in anhydrous DMAc (5 mL) with anhydrous LiCl (0.12 g, w / w IDX) under a flow of nitrogen and the mixture was heated to 132 °C until all of the IDX had dissolved. The solution was then cooled to room temperature and sodium hydride (60% mineral oil dispersion, (40 mg, 1.0 mmol, 0.67 eq.) was added and the reaction mixture and stirred for 4 h. A solution of triisopropylsilyl-(Z)-4-((4-((3-(4-fluorobenzyl)-2,4-dioxothiazolidin-5-ylidene)methyl)-2-(2-(2-(tosyloxy)ethoxy)ethoxy)phenoxy)methyl)benzoate (0.45 g, 0.5 mmol, 0.33 eq.) in anhydrous DMAc (1 mL) was added dropwise (over 2 minutes) to the reaction mixture and then stirred for 16 h. The reaction mixture was then dialysed against MeOH (1 L, 8 kDa MWCO), the methanol was changed 9 times over a period of 3 days. The contents of the dialysis membrane were then evaporated to yield an off-white solid which was precipitated from methanol (3 mL). The liquid was then carefully decanted and the retained solid washed twice with methanol (3 mL) and once with DCM (3 mL). The remaining solid was then dried under high vacuum to yield Conjugate **17** as an off-white solid (81 mg).

$^1\text{H NMR}$ (400 MHz, DMSO- d_6) δ = 7.87 (s, Ar-H), 7.43 - 7.29 (m, Ar-H), 7.29 - 7.20 (m, Ar-H), 7.19 - 7.06 (m, Ar-H), 5.68 - 5.28 (m, IDX-H), 5.20 (s, CH₂ArCOOH), 5.14 - 4.84 (m, IDX-H), 4.80 (m, IDX-H), 4.63 - 4.41 (s, IDX-H), 4.19 - 4.07 (m, ArCH₂CH₂O), 3.83 - 3.39 (m, IDX-H)

* $^1\text{H NMR}$ data in agreement our previous findings ¹⁴⁷

7.1.59 Inulin-(**44**) conjugate, (Conjugate **26**)



Anhydrous Inulin (0.13 g, 0.8 mmol, 1.0 eq.) was suspended in anhydrous DMAc (5 mL) with anhydrous LiCl (0.13 g, w / w INU) under a flow of nitrogen and heated to 116 °C until completely dissolved. The solution was then cooled to room temperature and sodium hydride (60% mineral oil dispersion, (24 mg, 0.6 mmol, 0.8 eq.) was added. The reaction mixture was stirred for 4 h. A solution of triisopropylsilyl-(*Z*)-4-((3-(4-fluorobenzyl)-2,4-dioxothiazolidin-5-ylidene)methyl)-2-(2-(2-(tosyloxy)ethoxy)ethoxy)phenoxy)methyl benzoate (0.24 g, 0.3 mmol, 0.4 eq.) in anhydrous DMAc (1 mL) was added dropwise (over 2 min) to the reaction mixture and then stirred for 16 h. The reaction mixture was then dialysed against MeOH (1 L, 1 kDa MWCO), the methanol was changed 7 times over a period of 2 days. The contents of the dialysis membrane were then evaporated to yield a pale-yellow solid which was precipitated from methanol (3 mL), the liquid was then carefully decanted, and the retained solid washed twice with methanol (3 mL) and twice with DCM (3 mL). The remaining solid was then dried under high vacuum to yield Conjugate **26** as a pale-yellow solid (93 mg).

7.1.61 Inulin-(**44**) conjugate, (Conjugate **36**)

Inulin, (5000 Da, 39 mg, 0.2 mmol, 1 eq.), was dissolved in a solution of NaOH aq. (0.5 M, 2 mL), and (±)-epichlorohydrin (0.04 mL, 0.5 mmol, 2 eq.) was added. The resulting mixture was then stirred at room temperature for 80 min. To quench the reaction, HCl aq. (0.1 M) was added to adjust the pH to pH 7, to give epichlorohydrin-activated Inulin (EPI-INU). Triisopropylsilyl-(*Z*)-4-((4-((3-(4-fluorobenzyl)-2,4-dioxothiazolidin-5-ylidene)methyl)-2-(2-(2-hydroxyethoxy)ethoxy)phenoxy)methyl)benzoate, (0.14 g, 0.2 mmol, 0.8 eq.) was dissolved in acetone, (6 mL) and added dropwise to the reaction mixture. K₂CO₃ (66 mg, 0.5 mmol, 2.0 eq.), was added and the reaction was heated to 50 °C for 2 days. The reaction mixture was then evaporated under reduced pressure to obtain a light-yellow residue. An off-white solid was precipitated by trituration in 1:1 acetone / DMF (5 mL). The liquid portion was decanted and the remaining solid re-suspended in 1:1 acetone / DMF, (5 mL). The liquid was then decanted, this process was repeated 10 times (until liquid became clear), followed by acetone (5 x 5 mL). The solid was then dissolved in H₂O (5 mL) and dialysed against H₂O (dist.) (1L, 1 kDa MWCO). The water was changed 9 times over a period of 2 days, followed by IMS, 0.6 L, which was changed 5 times in total, over a period of 24 h (at room temperature throughout). The contents of the dialysis membrane were evaporated under reduced pressure and then dried under vacuum to obtain Conjugate **36** as a white solid (11 mg).

¹H NMR (400 MHz, DEUTERIUM OXIDE) δ = 7.75 - 7.69 (m, Ar-H (Drug)), 7.41 - 7.35 (m, Ar-H (Drug)), 7.19 - 7.16 (m, Ar-H (Drug)), 7.13 - 7.07 (m, Ar-H (Drug)), 6.98 - 6.93 (m, Ar-H (Drug)), 5.12 - 5.10 (br. s, CH₂OAr(COOH) (Drug)), 4.71 (br. s, NCH₂Ar(F) (Drug)), 4.13 - 4.03 (m, (Drug / INU)), 3.96 - 3.88 (m, (Drug / INU)), 3.80 - 3.44 (m, (Drug / INU)); IR (neat) 3293, 3929, 2106, 1776, 1595, 1508, 1450, 1375, 1266, 1112, 1020, 933 cm⁻¹; Elemental analysis (Found: C, 48.67; H, 6.18; N, 1.35, Ds = 0.35).

7.1.62 Inulin-(**44**) conjugate, (Conjugate **37**)

Inulin, (5000 Da, 39 mg, 0.2 mmol, 1 eq.), was dissolved in a solution of NaOH aq. (0.5 M, 2 mL), and (±)-epichlorohydrin (0.04 mL, 0.5 mmol, 2 eq.) was added. The resulting mixture was then stirred at room temperature for 80 min. To quench the reaction, HCl aq. (0.1 M) was added to adjust the pH to pH 7, to give epichlorohydrin-activated Inulin (EPI-INU). Triisopropylsilyl-(Z)-4-((4-((3-(4-fluorobenzyl)-2,4-dioxothiazolidin-5-ylidene)methyl)-2-(2-(2-hydroxyethoxy)ethoxy)phenoxy)methyl)benzoate, (87 mg, 0.1 mmol, 0.5 eq.) was dissolved in acetone (6 mL) and added dropwise to the reaction mixture. K₂CO₃ (66 mg, 0.50 mmol, 2.0 eq.), was added and the reaction was heated to 50°C for 48 h. The reaction mixture was then evaporated under reduced pressure to obtain a light-yellow residue, an off-white solid was precipitated by trituration in 1:1 acetone / DMF (5 mL). The liquid portion was decanted and the remaining solid re-suspended in 1:1 acetone / DMF (5 mL), then the liquid decanted, this process was repeated 10 times in total (until liquid became clear), followed by acetone (5 x 5 mL). The solid was then dissolved in H₂O (dist.) (5 mL) and dialysed against H₂O (dist.) (1L, 1 kDa MWCO). The water was changed 9 times over a period of 2 days, followed by IMS (0.6 L) which was changed 5 times in total, over a period of 24 h (at room temperature throughout). The contents of the dialysis membrane were evaporated under reduced pressure and then dried under vacuum to obtain Conjugate **37** as a white crystalline solid (13 mg).

¹H NMR (400 MHz, DEUTERIUM OXIDE) δ = 7.72 - 7.64 (m, Ar-H (Drug)), 7.41 - 7.32 (m, Ar-H (Drug)), 7.17 - 7.06 (m, Ar-H (Drug)), 6.99 - 6.93 (m, Ar-H (Drug)), 5.10 (br.s, CH₂OAr(COOH) (Drug)), 4.71 (br. s, NCH₂Ar(F) (Drug)), 4.11 - 4.03 (m, (Drug / INU)), 3.96 - 3.86 (m, (Drug / INU)), 3.80 - 3.44 (m, (Drug / INU)); IR (neat) 3309, 2925, 2473, 2118, 1596, 1550, 1508, 1377, 1268, 1112, 1017, 931 cm⁻¹; Elemental analysis (Found: C, 48.79; H, 6.11; N, 1.30, Ds = 0.32).

7.1.63 Inulin-(**44**) conjugate, (Conjugate **38**)

Inulin, (5000 Da, 39 mg, 0.2 mmol, 1 eq.), was dissolved in a solution of NaOH aq. (0.5 M, 2 mL), and (±)-epichlorohydrin (0.04 mL, 0.5 mmol, 2 eq.) was added. The resulting mixture was then stirred at room temperature for 80 min. To quench the reaction, HCl aq. (0.1 M) was added to adjust the pH to pH 7, to give epichlorohydrin-activated Inulin (EPI-INU). Triisopropylsilyl-(Z)-4-((4-((3-(4-fluorobenzyl)-2,4-dioxothiazolidin-5-ylidene)methyl)-2-(2-(2-hydroxyethoxy)ethoxy)phenoxy)methyl)benzoate, (52 mg, 0.07 mmol, 0.3 mmol) was dissolved in acetone (6 mL) and added dropwise to the reaction mixture. K₂CO₃ (66 mg, 0.5 mmol, 2.0 eq.), was added and the reaction heated to 50 °C for 48 h. The reaction mixture was then evaporated under reduced pressure to obtain a cream coloured residue. An off-white solid was precipitated by trituration in 1:1 acetone / DMF (5 mL). The liquid portion was decanted and the remaining solid re-suspended in 1:1 acetone / DMF (5 mL), then the liquid decanted, this process was repeated 10 times in total (until liquid became clear), followed by acetone (5 x 5 mL). The solid was then dissolved in H₂O (5 mL) and dialysed against H₂O (1L, 1 kDa MWCO). The water was changed 9 times over a period of 2 days, followed by IMS (0.6 L) which was changed 5 times in total, over a period of 24 h (at room temperature throughout). The contents of the dialysis membrane were evaporated under reduced pressure, washed / decanted in acetone (5 x 3 mL) and then dried under vacuum to obtain Conjugate **38** as a white crystalline solid (25 mg).

¹H NMR (400 MHz, DEUTERIUM OXIDE) δ = 7.75 - 7.66 (m, Ar-H (Drug)), 7.43 - 7.31 (m, Ar-H (Drug)), 7.18 - 7.08 (m, Ar-H (Drug)), 7.00 - 6.89 (m, Ar-H (Drug)), 5.10 (br.s, CH₂OAr(COOH) (Drug)), 4.61 (br. s, NCH₂Ar(F) (Drug)), 4.13 - 4.05 (m, (Drug / INU)), 4.00 - 3.85 (m, (Drug / INU)), 3.84 - 3.45 (m, (Drug / INU)); IR (neat) 3302, 2925, 2107, 1715, 1636, 1595, 1508, 1412, 1376, 1266, 1221, 1108, 1016, 931 cm⁻¹; Elemental analysis (Found: C, 48.57; H, 4.90; N, 1.16, Ds = 0.25).

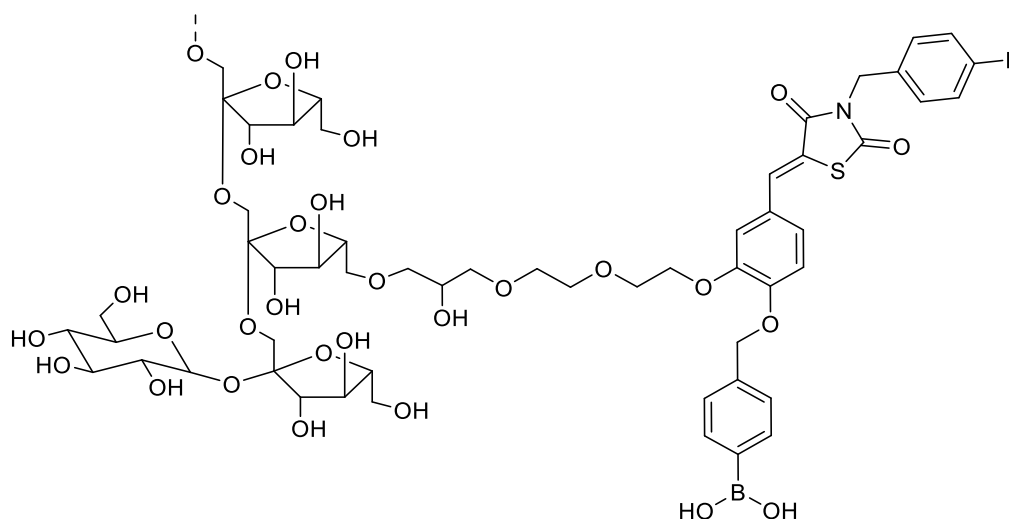
7.1.64 Inulin-(**44**) conjugate, (Conjugate **39**)

Inulin, (5000 Da, 39 mg, 0.2 mmol, 1 eq.), was dissolved in a solution of NaOH aq. (0.5 M, 2 mL), and (±)-epichlorohydrin (0.04 mL, 0.5 mmol, 2 eq.) was added. The resulting mixture was then stirred at room temperature for 80 min. To quench the reaction, HCl aq. (0.1 M) was added to adjust the pH to pH 7, to give epichlorohydrin-activated Inulin (EPI-INU). Triisopropylsilyl-(Z)-4-((4-((3-(4-fluorobenzyl)-2,4-dioxothiazolidin-5-ylidene)methyl)-2-(2-(2-hydroxyethoxy)ethoxy)phenoxy)methyl)benzoate (0.30 g, 0.40 mmol, 1.7 eq.) was dissolved in acetone (8 mL) and added dropwise to stirring the mixture. K₂CO₃ (66 mg, 0.5 mmol, 2.0 eq.), was added and the reaction heated to 50 °C for 2 days. The mixture was then evaporated under reduced pressure to obtain a cream coloured residue, a cream solid was precipitated by trituration in 1:1 acetone / DMF (5 mL). The liquid portion was decanted and the remaining solid re-suspended in 1:1 acetone / DMF (5 mL). The liquid was then decanted, this process was repeated 10 times in total (until liquid became clear), followed by acetone (5 x 5 mL). The solid was then dissolved in H₂O (5 mL) and dialysed against H₂O (1L, 1 kDa MWCO). The water was changed 8 times over a period of 2 days, followed by IMS, (0.6 L) which was changed 6 times in total, over a period of 24 h (at room temperature throughout). The contents of the dialysis membrane were evaporated under reduced pressure, the resulting solid was further washed with acetone (5 x 3 mL) and then dried under vacuum to obtain Conjugate **39** as an off-white solid (31 mg).

¹H NMR (400 MHz ,DEUTERIUM OXIDE) δ = 7.72 - 7.67 (m, Ar-H (Drug)), 7.40 - 7.33 (m, Ar-H (Drug)), 7.16 - 7.13 (m, Ar-H (Drug)), 7.12 - 7.07 (m, Ar-H (Drug)), 6.98 - 6.93 (m, Ar-H (Drug)), 5.11 (br.s, CH₂OAr(COOH) (Drug)), 4.13 - 4.03 (m, (Drug / INU)), 3.96 - 3.86 (m, (Drug / INU)), 3.81 - 3.45 (m, (Drug / INU))

N.B. Inspection of the H¹ NMR spectrum of Conjugate **39** compared to Conjugate **35**, showed a negligible increase in drug loading.

7.1.65 Inulin-(**52**) conjugate, (Conjugate **44**)

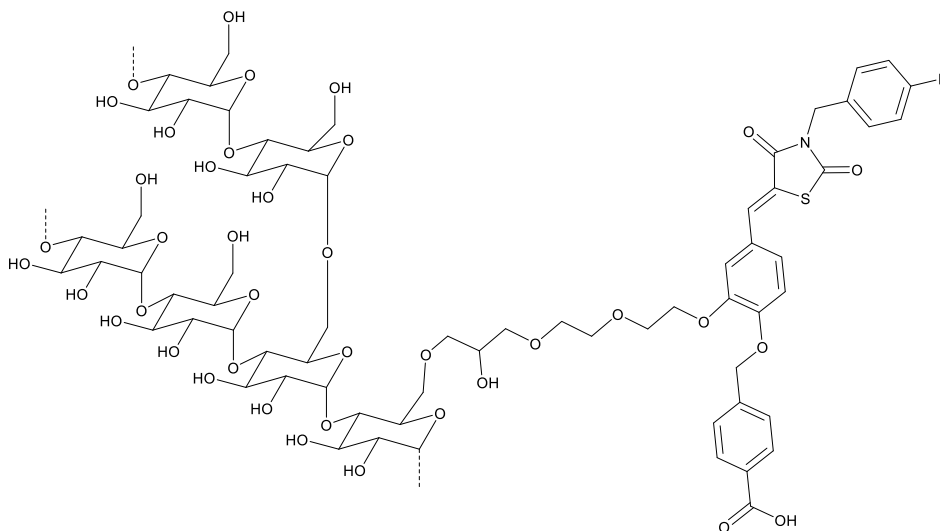


Inulin, (5000 Da, 27 mg, 0.2 mmol, 1 eq.), was dissolved in a solution of NaOH aq. (0.5 M, 1.5 mL), and (\pm)-epichlorohydrin (0.026 mL, 0.5 mmol, 2 eq.) was added. The resulting mixture was then stirred at room temperature for 80 min. To quench the reaction, HCl aq. (0.1 M) was added to adjust the pH to pH 7, to give epichlorohydrin-activated Inulin (EPI-INU). (Z)-4-(((4-((3-(4-fluorobenzyl)-2,4-dioxothiazolidin-5-ylidene)methyl)-2-(2-(2-hydroxyethoxy)ethoxy)phenoxy)methyl)phenyl)boronic acid, (0.11 g, 0.2 mmol, 1.2 eq.), was added dropwise, as a solution in acetone (4.5 mL). K_2CO_3 (45 mg, 0.3 mmol, 2.0 eq.) was then added and the resulting mixture was heated to 50 °C and stirred for 1.5 days. The reaction mixture was then cooled to room temperature and evaporated under reduced pressure, to expose a yellow residue. A light cream solid was obtained by precipitating the residue in 1:1 acetone / DMF (5 mL). The liquid was discarded and the solid re-suspended in acetone / DMF (5 mL), then the liquid decanted, this process was repeated 10 times in total. Then with 5 additional times with acetone (5 mL). The resulting solid was dissolved in H_2O (10 mL) and dialysed against H_2O (1L, 1 kDa MWCO). The water was changed 9 times over a period of 2 days, then IMS, (0.6 L) which was changed 5 times. The contents of the dialysis membrane were then evaporated under reduced pressure and dried under high vacuum, to obtain Conjugate **44** as an off-white solid (11 mg).

1H NMR (400 MHz, DEUTERIUM OXIDE) δ = 7.66 - 7.56 (m, Ar-H (Drug)), 7.42 - 7.31 (m, Ar-H (Drug)), 7.19 - 7.11 (m, Ar-H (Drug)), 7.09 - 7.03 (m, Ar-H (Drug)), 6.95 - 6.88 (m, Ar-H (Drug)), 5.09 (br.s, $CH_2OAr(B(OH)_2)$ (Drug)), 4.14 - 4.04 (m, (Drug / INU)), 3.98 - 3.38 (m, (Drug / INU)); IR (neat) 3299, 2932, 2882, 1650, 1503, 1460, 1270, 1190, 1107, 1015,

925 cm^{-1} ; Elemental analysis (Found: C, 43.16; H, 6.90; N, 1.03, Ds (degree of substitution) = 0.20).

7.1.66 Icodextrin-(**44**) conjugate, (Conjugate **34**)



(\pm)-Epichlorohydrin (0.04 mL, 0.5 mmol, 2 eq.) was added to Icodextrin (39 mg, 0.2 mmol, 1 eq.) in a solution of NaOH aq. (0.5 M, 2 mL) and stirred for 80 min, at room temperature. The pH was carefully adjusted to pH 7, using a solution of HCl aq. (0.1 M). The solvent was removed under reduced pressure, to obtain a grainy white residue. The residue was triturated in acetone (5 mL), which precipitated a white solid, the liquid was then carefully decanted. The solid was re-suspended in acetone and the process repeated 5 additional times, then the resulting white powder dried under reduced pressure, to obtain epichlorohydrin activated Icodextrin (EPI-IDX), which was used without further purification in the next reaction.

Triisopropylsilyl-(Z)-4-((4-((3-(4-fluorobenzyl)-2,4-dioxothiazolidin-5-ylidene)methyl)-2-(2-(2-hydroxyethoxy)ethoxy)phenoxy)methyl)benzoate, (0.21 g, 0.3 mmol, 1.2 eq.) in a solution of acetone, (6 mL), was added to EPI-IDX in H_2O (2 mL), (3:1 acetone / H_2O). K_2CO_3 (66 mg, 0.5 mmol, 2.0 eq.) was then added and the resulting mixture heated to 50 $^\circ\text{C}$ for 2.5 days. The mixture was evaporated under reduced pressure to give a residue, which was then suspended in a mixture of acetone / DMF (1:1) and the liquid decanted, this process was repeated 10 times, then acetone (5 x 5 mL). The yellow solid was dissolved in H_2O (10 mL) and then dialysed against H_2O (1 L, 3.5 kDa MWCO). The water was changed 9 times in total, over a period of 2 days, then IMS (0.6 L), which was changed 5 times, over 1.5 days. The contents of the dialysis membrane were then evaporated under reduced pressure and dried under high vacuum to obtain as Conjugate **34** as a yellow solid (56 mg).

^1H NMR (400 MHz, DMSO- d_6) δ = 8.14 - 7.74 (m, Ar-H (Drug)), 7.49 - 7.29 (m, Ar-H (Drug)), 7.27 - 6.75 (m, Ar-H (Drug)), 5.25 - 4.96 (m, CH₂OAr(COOH), IDX), 4.90 - 4.42 (m, NCH₂Ar(F), IDX), 4.27 - 3.93 (m, (Drug / IDX)), 3.87 - 3.41 (m, (Drug / IDX)); IR (neat) 3334, 2928, 2871, 1676, 1594, 1550, 1507, 1375, 1262, 1220, 1135, 1015 cm^{-1} ; Elemental analysis (Found: C, 52.57; H, 4.24; N, 1.0, Ds (degree of substitution) = 0.76).

7.1.67 Icodextrin-(**44**) conjugate, (Conjugate **40**)

EPI-IDX was prepared in the same manner as Conjugate **34**, using the exact same quantities of reagents.

Triisopropylsilyl-(*Z*)-4-((4-((3-(4-fluorobenzyl)-2,4-dioxothiazolidin-5-ylidene)methyl)-2-(2-(2-hydroxyethoxy)ethoxy)phenoxy)methyl)benzoate, (0.14 g, 0.18 mmol, 0.8 eq.) in a solution of acetone (6 mL) was added to EPI-IDX in H₂O (2 mL), (3:1 acetone / H₂O). K₂CO₃ (66 mg, 0.5 mmol, 2.0 eq.) was then added and the resulting mixture heated to 50 °C for 2.5 days. The mixture was evaporated under reduced pressure to give an orange residue, which was then suspended in a mixture of acetone / DMF (1:1) and the liquid decanted, this process was repeated 10 times, followed by acetone (5 x 5 mL). The yellow solid was dissolved in H₂O (10 mL) and then dialysed against H₂O (1 L, 3.5 kDa MWCO). The water was changed 8 times over a period of 2 days, then IMS (0.6 L), which was changed 5 times, over 1.5 days. The contents of the dialysis membrane were evaporated under reduced pressure, and dried under high vacuum to obtain Conjugate **40** as a light yellow solid (34 mg).

¹H NMR (400 MHz, DMSO-*d*₆) δ = 7.89 (br s, Ar-H (Drug)), 7.49 - 7.23 (m, Ar-H (Drug)), 7.20 - 6.74 (m, Ar-H (Drug)), 5.45 - 4.54 (m, Drug / IDX), 4.49 - 4.16 (m, Drug / IDX), 4.15 - 3.39 (m, Drug / IDX); IR (neat) 3348, 2924, 2875, 1596, 1551, 1507, 1375, 1260, 1220, 1118, 1014, 769 cm⁻¹; Elemental analysis (Found: C, 47.77; H, 4.57; N, 1.50, Ds (degree of substitution) = 0.44).

7.1.68 Icodextrin-(**44**) conjugate, (Conjugate **41**)

EPI-IDX was prepared in the same manner as Conjugate **34**, using the exact same quantities of reagents.

Triisopropylsilyl-(*Z*)-4-((4-((3-(4-fluorobenzyl)-2,4-dioxothiazolidin-5-ylidene)methyl)-2-(2-(2-hydroxyethoxy)ethoxy)phenoxy)methyl)benzoate, (87 mg, 0.12 mmol, 0.5 eq.) in a solution of acetone (6 mL) was added to EPI-IDX in H₂O (2 mL) (3:1 acetone / H₂O). K₂CO₃ (66 mg, 0.5 mmol, 2.0 eq.) was then added and the resulting mixture heated to 50 °C for 2 days. The mixture was evaporated under reduced pressure to give a yellow residue, which was then suspended in a mixture of acetone / DMF (1:1) and the liquid decanted; this process was repeated 10 times, followed by acetone (5 x 5 mL). The yellow solid was dissolved in H₂O (10 mL) and then dialysed against H₂O (1 L, 3.5 kDa MWCO). The water was changed 8 times, over a period of 2 days, then IMS (0.6 L), which was changed 5 times, over 1.5 days. The contents of the dialysis membrane were then evaporated under reduced pressure, and dried under high vacuum to obtain Conjugate **41** as a golden solid (28 mg).

¹H NMR (400 MHz, DMSO-d₆) δ = 7.95 - 7.74 (m, Ar-H (Drug)), 7.47 - 7.23 (m, Ar-H (Drug)), 7.21 - 6.88 (m, Ar-H (Drug)), 5.89 - 5.35 (m, IDX), 5.26 - 4.86 (m, CH₂OAr(COOH), IDX), 4.78 - 4.47 (m, Drug / IDX), 4.43 - 4.25 (m, Drug / IDX), 4.19 - 4.01 (m, Drug / IDX), 3.86 - 3.41 (m, Drug / IDX); IR (neat) 3334, 2927, 2458, 2106, 1594, 1551, 1507, 1364, 1262, 1121, 1013 cm⁻¹; Elemental analysis (Found: C, 48.15; H, 4.25; N, 1.38, Ds (degree of substitution) = 0.36).

7.1.69 Icodextrin-(**44**) conjugate, (Conjugate **42**)

EPI-IDX was prepared in the same manner as Conjugate **34**, using the exact same quantities of reagents.

Triisopropylsilyl-(Z)-4-((4-((3-(4-fluorobenzyl)-2,4-dioxothiazolidin-5-ylidene)methyl)-2-(2-(2-hydroxyethoxy)ethoxy)phenoxy)methyl)benzoate, (52 mg, 0.07 mmol, 0.3 eq.) in a solution of acetone (6 mL) was added to EPI-IDX in H₂O (2 mL) (3:1 acetone / H₂O). K₂CO₃ (66 mg, 0.5 mmol, 2.0 eq.) was then added and the resulting mixture heated to 50 °C for 2 days. The mixture was evaporated under reduced pressure to give a yellow residue, which was then suspended in a mixture of acetone / DMF (1:1), and the liquid decanted; this process was repeated 10 times, then acetone (5 x 5 mL). The white solid was dissolved in H₂O (10 mL) and then dialysed against H₂O (1 L, 3.5 kDa MWCO). The water was changed 9 times over a period of 2 days, then IMS (0.6 L), which was changed 6 times over 1.5 days. The contents of the dialysis membrane were then evaporated under reduced pressure and dried further under high vacuum to obtain Conjugate **42** as an off-white solid (25 mg).

¹H NMR (400 MHz, DMSO-d₆) δ = 7.89 - 7.73 (m, Ar-H (Drug)), 7.49 - 7.24 (m, Ar-H (Drug)), 7.22 - 6.84 (m, Ar-H (Drug)), 5.84 - 5.34 (m, IDX), 5.20 - 4.80 (m, Drug / IDX), 4.78 - 4.01 (m, Drug / IDX), 3.79 - 3.33 (m, Drug / IDX); IR (neat) 3307, 2925, 2086, 1596, 1551, 1507, 1364, 1261, 1121, 1013 cm⁻¹; Elemental analysis (Found: C, 44.66; H, 5.72; N, 1.13, Ds (degree of substitution) = 0.24).

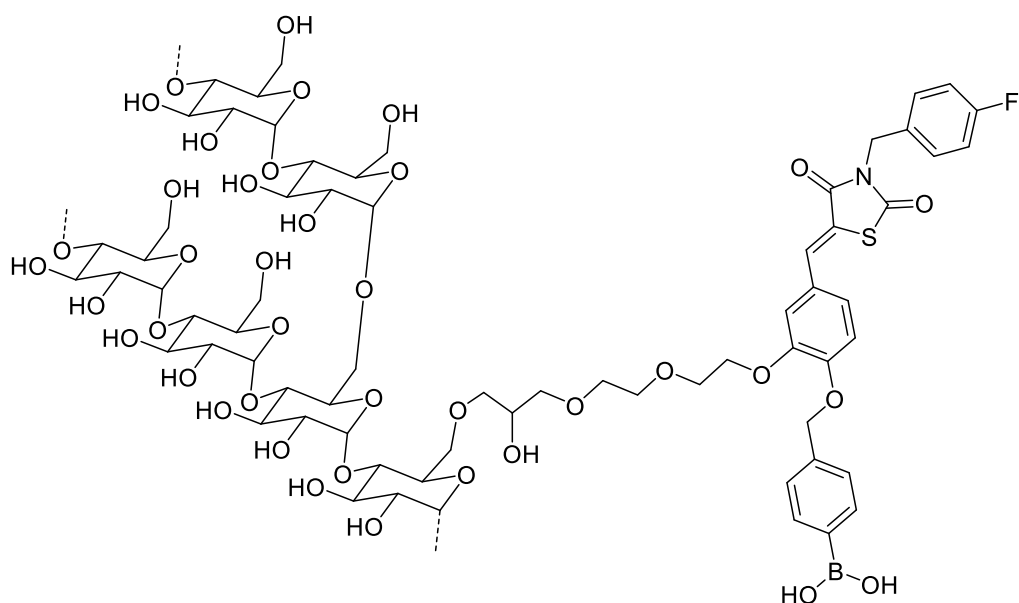
7.1.70 Icodextrin-(**44**) highly cross-linked conjugate, (Conjugate **43**)

EPI-IDX was prepared in the same manner as Conjugate **34**, using the following quantities of reagents: IDX (56 mg, 0.3 mmol, 1.0 eq.), (\pm)-epichlorohydrin (0.03 mL, 0.40 mmol, 1.1 eq.), in NaOH aq. (0.5 M, 3 mL).

Triisopropylsilyl-(Z)-4-((4-((3-(4-fluorobenzyl)-2,4-dioxothiazolidin-5-ylidene)methyl)-2-(2-(2-hydroxyethoxy)ethoxy)phenoxy)methyl)benzoate, (0.30 g, 0.4 mmol, 1.2 eq.) in a solution of acetone (9 mL) was added to EPI-IDX in H₂O (3 mL) (3:1 acetone / H₂O). K₂CO₃ (95 mg, 0.7 mmol, 2.0 eq.) was then added and the resulting mixture heated to 50 °C for 2 days. The mixture was evaporated under reduced pressure to give a yellow residue, which was then suspended in a mixture of acetone / DMF (1:1), and the liquid decanted; this process was repeated 15 times, then acetone (5 x 5 mL). The material was dried under vacuum, to obtain a light-yellow solid. The solid was re-dissolved in a solution of NaOH aq. (0.5 M, 2 mL), then (\pm)-epichlorohydrin (0.08 mL, 1.0 mmol, 3 eq.) was added and the resulting mixture stirred for 18 h at room temperature, the solvent was then evaporated under reduced pressure. The resulting yellow residue was washed / decanted in acetone (5 x 5 mL) to give a yellow powder. This was then dissolved in H₂O (10 mL) and then dialysed against H₂O (1 L, 8 kDa MWCO). The water was changed 9 times in total, over a period of 2 days, then IMS (0.6 L) which was changed 6 times, over 1.5 days. The contents of the dialysis membrane were then evaporated under reduced pressure and dried under high vacuum to obtain Conjugate **43** as a yellow solid (42 mg).

¹H NMR (400 MHz, DMSO-d₆) δ = 8.01 - 7.67 (m, Ar-H (Drug)), 7.52 - 7.16 (m, Ar-H (Drug)), 7.22 - 6.47 (m, Ar-H (Drug)), 5.77 - 5.41 (m, IDX), 5.38 - 4.42 (m, Drug / IDX), 4.24 - 3.12 (m, Drug / IDX); IR (neat) 2322, 2873, 2115, 1701, 1597, 1507, 1375, 1261, 1120, 1013 cm⁻¹; Elemental analysis (Found: C, 47.07; H, 5.94; N, 1.03, Ds (degree of substitution) = 0.20).

7.1.71 Icodextrin-(**52**) conjugate, (Conjugate **45**)

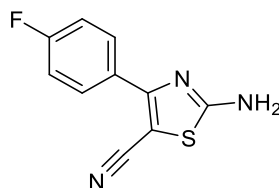


(±)-Epichlorohydrin (0.035 mL, 0.44 mmol, 2 eq.) was added to Icodextrin (35 mg, 0.22 mmol, 1 eq.) in a solution of NaOH aq. (0.5 M, 2 mL) and stirred for 80 min, at room temperature. The pH was carefully adjusted to pH 7, using a solution of HCl aq. (0.1 M). The solvent was removed under reduced pressure, to obtain a grainy white residue. The residue was triturated in acetone (5 mL), which precipitated a white solid. The liquid was then carefully decanted. The solid was then re-suspended in acetone and the process repeated five additional times. The resulting white powder was dried under reduced pressure, to obtain epichlorohydrin activated Icodextrin (EPI-IDX), which was used without further purification in the next reaction.

(Z)-4-((4-((3-(4-Fluorobenzyl)-2,4-dioxothiazolidin-5-ylidene)methyl)-2-(2-(2-hydroxyethoxy)ethoxy)phenoxy)methyl)phenyl)boronic acid (0.15 g, 0.3 mmol, 1.2 eq.) in acetone (6 mL) was added to EPI-IDX dissolved in H₂O (2 mL) (3:1 acetone / H₂O). K₂CO₃ (61 mg, 0.4 mmol, 2.0 eq.) was then added and the resulting mixture heated to 50 °C for 2.5 days. The mixture was evaporated under reduced pressure to give a brown residue, which was then suspended in a mixture of acetone / DMF (1:1), and the liquid decanted. This process was repeated 10 times, then acetone (5 mL) x 5. The brown solid was dissolved in H₂O (10 mL) and then dialysed against H₂O (1 L, 3.5 kDa MWCO). The water was changed 12 times, over a period of 2.5 days, then IMS (0.6 L), which was changed 5 times, over 1.5 days. The contents of the dialysis membrane were then evaporated under reduced pressure and dried further under high vacuum to obtain Conjugate **45** as a light brown solid (27 mg).

^1H NMR (400 MHz, DMSO- d_6) δ = 7.64 - 7.26 (m, Ar-H (Drug)), 7.16 - 7.05 (m, Ar-H (Drug)), 5.65 - 5.25 (m, CH₂OAr(B(OH)₂), 5.20 - 4.43 (m, (Drug / IDX)), 4.03 - 3.42 (m, (Drug / INU)); IR (neat) 3312, 2925, 2103, 1699, 1596, 1510, 1363, 1148, 1016 cm^{-1} ; Elemental analysis (Found: C, 54.79; H, 5.33; N, 0.5, Ds (degree of substitution) = 0.07).

7.1.72 2-Amino-4-(4-fluorophenyl)thiazole-5-carbonitrile, (**61**)

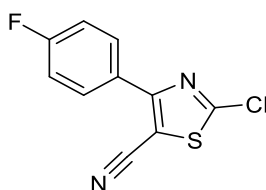


Pyridine (1.23 mL, 15.3 mmol, 1 eq.) was added to a solution of 4-fluorobenzoyl acetonitrile (2.50 g, 15.3 mmol, 1 eq.) in ethanol (30 mL) and stirred at 70 °C for 15 min. The solution was then cooled to room temperature, where upon a slurry of thiourea (2.33 g, 30.6 mmol, 2 eq.) and I₂ (3.88 g, 15.3 mmol, 1 eq.) in ethanol (15 mL) was added to the reaction mixture. This was then stirred for 1.5 h at room temperature. A solution of Na₂S₃O₃ aq. (1 M, 20 mL) was added, effecting the precipitation of a heterocycle **61** as a cream solid, which was collected by vacuum filtration and thoroughly dried (2.61 g, 77 %).

¹H NMR (400 MHz, DMSO-d₆) δ = 8.25 (s, 2H), 8.06 - 7.90 (m, 2H), 7.35 (t, *J* = 8.1 Hz, 2H)

The ¹H NMR spectrum was found to be in agreement with that of Heckman and co-workers.⁶⁷

7.1.73 2-Chloro-4-(4-fluorophenyl)thiazole-5-carbonitrile, (**62**)



tert-Butyl nitrite (1.53 mL, 12.9 mmol, 1.5 eq.) was added dropwise (over 2 minutes) to CuCl₂ (1.38 g, 10.3 mmol, 1.2 eq.) in MeCN (20 mL) and stirred for 30 min at room temperature, to obtain a dark green precipitate. 2-Amino-4-(4-fluorophenyl)thiazole-5-carbonitrile (1.91 g, 8.6 mmol, 1.0 eq.) was then added portion wise (over 5 min) and stirred for 1 h at room temperature. The reaction was quenched following the addition of a solution of HCl aq. (1 M, 25 mL) and stirred for an additional 15 min. The reaction mixture was then diluted with H₂O (20 mL) and extracted with EtOAc (3 x 50 mL). The combined organic extracts were washed

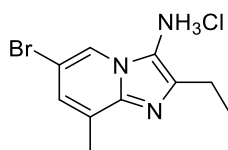
with brine (100 mL), dried over anhydrous MgSO_4 , filtered and evaporated to obtain an orange residue.

The residue was dissolved in DCM (5 mL) and the mixture filtered through a plug of silica gel (prepared with DCM), the filtrate was evaporated under reduced pressure to obtain a golden-brown residue. The residue was then triturated in heptane to obtain chloride **62** as an orange powder, which was collected by decanting the liquid and drying the solid under high vacuum, (1.10 g, 53 %).

^1H NMR (400 MHz, DMSO-d_6) δ = 8.13 - 7.96 (m, 2H), 7.44 (t, J = 8.1 Hz, 2H)

The ^1H NMR spectrum was found to be in agreement with that of Heckman and co-workers.⁶⁷

7.1.74 6-Bromo-3-(chloro-15-azaneyl)-2-ethyl-8-methylimidazo[1,2-a]pyridine, (**63**)



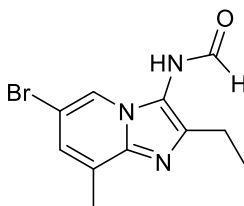
Benzotriazole (2.67 g, 2.2 mmol, 1.05 eq.) and propanal (2.29 mL, 3.2 mmol, 1.50 eq.) were added to 5-bromo-3-methylpyridine (4.00 g, 2.1 mmol, 1.00 eq.) in a solution of anhydrous toluene (15 mL), under a flow of nitrogen and stirred for 4 h at room temperature. Then, EtOH (30 mL) was added, followed by KCN (1.66 g, 2.6 mmol, 1.20 eq.) and the resulting mixture stirred for 16 h, at room temperature, then for 2 h at 75 °C. The reaction mixture was cooled to room temperature and quenched using a solution of NaOH aq. (2.5 M, 20 mL). The solution was diluted with H_2O (30 mL) and extracted with EtOAc (4 x 50 mL). The organic extracts were combined, washed with NaOH aq. (2M, 2 x 50 mL), dried over anhydrous Na_2SO_4 , filtered and evaporated to give the free amine product: 6-bromo-2-ethyl-8-methylimidazo[1,2-a]pyridin-3-amine, as an orange oil, used immediately.

Acetyl chloride (2.43 mL, 3.41 mmol, 1.60 eq.) was added to 6-bromo-2-ethyl-8-methylimidazo[1,2-a]pyridin-3-amine as solution in ethanol (20 mL) and stirred at room temperature for 16 h, then evaporated. The oil was triturated in Et_2O (15 mL), effecting the precipitation of a solid, which was washed / decanted in DCM (5 x 15 mL), then thoroughly dried to obtain hydrochloride salt (**63**) as a light brown solid (2.31 g, 37 %).

^1H NMR (400 MHz, DMSO- d_6) δ = 8.67 - 8.54 (m, 1H), 7.74 - 7.55 (m, 1H), 2.75 (q, J = 7.5 Hz, 2H), 2.49 (s, 3H), 1.18 (t, J = 7.5 Hz, 3H)

The ^1H NMR spectrum was found to be in agreement with that of Heckman and co-workers⁶⁷

7.1.75 *N*-(6-Bromo-2-ethyl-8-methylimidazo[1,2-*a*]pyridin-3-yl)formamide, (**64**)

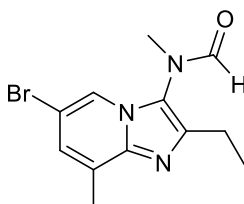


6-Bromo-3-(chloro-15-azaneyl)-2-ethyl-8-methylimidazo[1,2-*a*]pyridine (2.3 g, 7.91 mmol, 1.0 eq.) was stirred in formic acid (2.1 mL, 55.3 mmol, 7.0 eq.) at 80 °C, for 4 h then cooled to room temperature. A solution of NaOH aq. (3 M, 6 mL) was added, then the pH adjusted to 8-9 using a solution of NaHCO₃ sat. aq. (approx. 50 mL), which resulted in the precipitation of a brown solid. The solid was collected by vacuum filtration, then slurried in toluene (3 mL), then MTBE (20 mL) (1:7) which gave a light brown precipitate. The liquid portion was decanted and the solid then re-suspended in MTBE (10 mL), then decanted once more, this process was repeated 3 times. The resulting cream solid (amide **64**) was thoroughly dried under vacuum (1.41 g, 69 %).

^1H NMR (400 MHz, DMSO- d_6), presence of two rotomers δ = 9.91 (br s, 1H), 8.23 (br s, 1H), 8.10 (br s, 1H), 7.95 (br s, 1H), 7.13 (br s, 1H), 7.09 (br s, 1H), 2.57 - 2.41 (m, 2H), 2.38 (br s, 3H), 2.34 (br s, 3H), 1.21 - 0.89 (m, 3H)

The ^1H NMR spectrum was found to be in agreement with that of Heckman and co-workers⁶⁷

7.1.76 *N*-(6-Bromo-2-ethyl-8-methylimidazo[1,2-*a*]pyridin-3-yl)-*N*-methylformamide, (**65**)

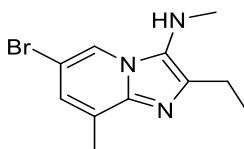


Methyl iodide (0.46 mL, 7.4 mmol, 1.5 eq.) and K_2CO_3 (2.06 g, 14.9 mmol, 3.0 eq.) was added to *N*-(6-bromo-2-ethyl-8-methylimidazo[1,2-*a*]pyridin-3-yl)formamide (1.40 g, 4.9 mmol, 1.0 eq.) in DMF (9 mL). The resulting mixture was heated at 80 °C, for 10 min. The reaction mixture was diluted with H_2O (100 mL), then extracted with DCM (4 x 50 mL). The combined organic extracts were then washed with a solution of 5% LiCl aq. (3 x 50 mL), dried over anhydrous $MgSO_4$, filtered and evaporated to obtain methyl amide **65** as a crystalline solid (0.82 g, 56 %).

1H NMR (400 MHz, $CDCl_3$), presence of two rotomers δ = 8.49 (s, 1H), 8.19 (s, 1H), 7.84 - 7.73 (m, 1H), 7.67 - 7.63 (m, 1H), 7.31 - 7.23 (m, 1H), 7.18 - 7.12 (m, 1H), 7.10 - 7.06 (m, 1H), 3.36 (s, 3H), 3.24 (s, 3H), 2.80 - 2.66 (m, 2H), 2.64 - 2.59 (m, 3H), 1.31 (t, J = 7.8 Hz, 3H)

The 1H NMR spectrum was found to be in agreement with that of Heckman and co-workers.⁶⁷

7.1.77 6-Bromo-2-ethyl-*N*,8-dimethylimidazo[1,2-*a*]pyridin-3-amine, (**66**)



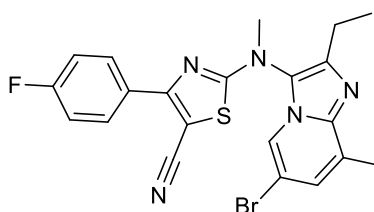
N-(6-bromo-2-ethyl-8-methylimidazo[1,2-*a*]pyridin-3-yl)-*N*-methylformamide was added to a solution of HCl in methanol (1.25 M, 5.6 mL, 2.50 eq.) and stirred at 80 °C for 4 h. A second portion of HCl in methanol (1.25 M, 2.3 mL, 1.25 eq.) was added and stirred for 2 h. The reaction mixture was then evaporated under reduced pressure to obtain a brown oil which was diluted with H_2O (50 mL). Powdered $NaHCO_3$ was added to bring the pH to 9. The organic layer was extracted using DCM (4 x 50 mL), then combined, washed with $NaHCO_3$ sat. aq.

(70 mL), brine (70 mL), dried over anhydrous MgSO_4 , filtered and evaporated to obtain amine **66** as a light brown crystalline solid (0.55 g, 73%).

^1H NMR (400 MHz, CDCl_3) δ = 8.03 - 7.84 (m, 1H), 7.03 - 6.84 (m, 1H), 2.92 - 2.74 (m, 5H), 2.66 (s, 3H), 1.31 (t, J = 7.7 Hz, 3H)

The ^1H NMR spectrum was found to be in agreement with that of Heckman and co-workers.⁶⁷

7.1.78 2-((6-Bromo-2-ethyl-8-methylimidazo[1,2-a]pyridin-3-yl)(methyl)amino)-4-(4-fluorophenyl)thiazole-5-carbonitrile, (**67**)

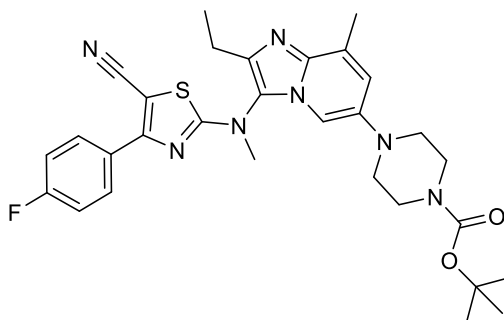


NaH as a dispersion in mineral oil, 60 %, (0.86 g, 4.6 mmol, 3.0 eq.) was added to 6-bromo-2-ethyl-*N*,8-dimethylimidazo[1,2-*a*]pyridin-3-amine (0.42 g, 1.5 mmol, 1.0 eq.) dissolved in anhydrous THF (7 mL), under a flow of N_2 . The resulting mixture was heated to 90 °C for 30 min and then cooled to 40 °C. This was followed by the addition of 2-Chloro-4-(4-fluorophenyl)thiazole-5-carbonitrile (0.44 g, 1.9 mmol, 1.2 eq.). The temperature was increased to 90 °C, and the mixture stirred for 1.5 h. The reaction was quenched following the addition of H_2O (70 mL). The organic portion was extracted with EtOAc (6 x 30 mL), combined, dried over anhydrous MgSO_4 , filtered and evaporated to obtain heterocycle **67** as a brown solid, which was used without any further purification as an intermediate.

^1H NMR (400 MHz, CDCl_3) δ = 8.20 - 8.09 (m, 2H), 7.77 (s, 1H), 7.24 - 7.12 (m, 3H), 3.62 (s, 3H), 2.81 - 2.71 (m, 2H), 2.61 (s, 3H), 1.35 (t, J = 7.7 Hz, 3H)

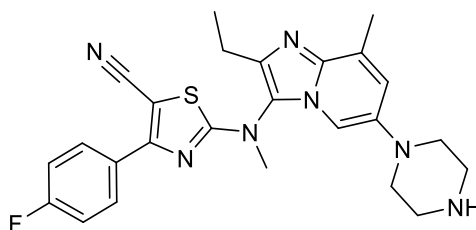
The ^1H NMR spectrum was found to be in agreement with that of Heckman and co-workers⁶⁷

7.1.79 *tert*-Butyl 4-(3-((5-cyano-4-(4-fluorophenyl)thiazol-2-yl)(methyl)amino)-2-ethyl-8-methylimidazo[1,2-a]pyridin-6-yl)piperazine-1-carboxylate, (**68**)



N-Boc piperazine (0.60 g, 3.0 mmol, 1.50 eq.), sodium *tert* butoxide (0.38 g, 4.0 mmol, 2.00 eq.), John phos (60 mg, 0.02 mmol, 0.10 eq.) and Pd₂(dba)₃ (92 mg, 0.01 mmol, 0.05 eq.) was added to 2-((6-bromo-2-ethyl-8-methylimidazo[1,2-a]pyridin-3-yl)(methyl)amino)-4-(4-fluorophenyl)thiazole-5-carbonitrile (0.94 g, 2 mmol, 1.00 eq.) in a solution of toluene (15 mL), under a flow of N₂. The reaction mixture was heated to 115 °C, for 1 h, then cooled to room temperature. The crude mixture was filtered through a plug of silica (EtOAc), and the filtrate evaporated under reduced pressure to obtain piperazine **68** as a brown oil (0.18 g) which was used without further purification in the next reaction.

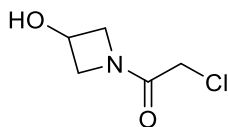
7.1.80 2-((2-Ethyl-8-methyl-6-(piperazin-1-yl)imidazo[1,2-a]pyridin-3-yl)(methyl)amino)-4-(4-fluorophenyl)thiazole-5-carbonitrile, (**69**)



HCl in Et₂O (2 M, 0.96 mL, 6.0 eq.) was added to *tert*-butyl 4-(3-((5-cyano-4-(4-fluorophenyl)thiazol-2-yl)(methyl)amino)-2-ethyl-8-methylimidazo[1,2-a]pyridin-6-yl)piperazine-1-carboxylate (0.18 g, 0.3 mmol, 1.0 eq.) dissolved in methanol (1 mL) and stirred for 3 h at room temperature. The reaction mixture was then evaporated under reduced pressure to obtain an oily residue. The oil was layered under EtOAc (20 mL) and then basified with NaOH aq. (1 M) (pH 8-9). The organic layer was extracted with EtOAc (3 x 20 mL), combined, washed with brine (30 mL), dried over anhydrous MgSO₄, filtered and evaporated

under reduced pressure, to give piperazine **69** as a brown oil (0.11 g). The crude material was carried through to the next reaction, without further purification.

7.1.81 2-Chloro-1-(3-hydroxyazetid-1-yl)ethan-1-one, (**70**)

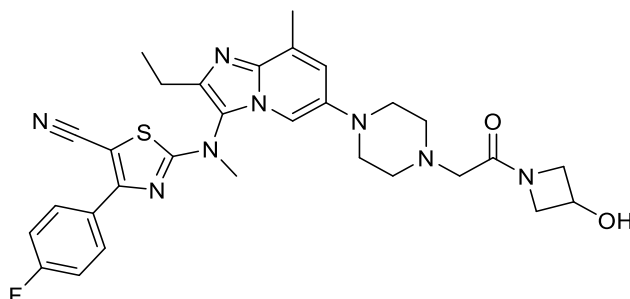


To a solution of 3-hydroxyazetid-1-yl hydrochloride (1.00 g, 9.1 mmol, 1 eq.) in H₂O (20 mL), K₂CO₃ (1.39 g, 10.0 mmol, 1.1 eq.) was added, this was stirred for 30 min at room temperature. DCM (4 mL) was added and the reaction mixture cooled to 0 °C. 2-Chloroacetyl chloride (1.46 mL, 18.3 mmol, 2.0 eq.) dissolved in DCM (3 mL) was added dropwise. The solution was then warmed to room temperature and stirred overnight. The organic portion was extracted with EtOAc / Butanol 1:1 (4 x 10 mL), the extracts were combined, dried over anhydrous MgSO₄, filtered and evaporated to obtain a light green oil. The oil was dissolved in acetone (10 mL) and stirred vigorously for 10 min, then filtered under gravity. The filtrate was then evaporated under reduced pressure to give azetidine **70** as a pale orange oil (0.86 g, 63 %).

¹H NMR (400 MHz, CDCl₃) δ = 4.82 - 4.66 (m, 1H), 4.58 - 4.46 (m, 1H), 4.34 (dd, *J* = 10.7, 6.7 Hz, 1H), 4.25 - 4.17 (m, 1H), 3.99 (br dd, *J* = 11.0, 3.9 Hz, 1H), 3.94 (s, 2H)

The ¹H NMR spectrum was found to be in agreement with that of Heckman and co-workers.⁶⁷

7.1.82 2-((2-Ethyl-6-(4-(2-(3-hydroxyazetidin-1-yl)-2-oxoethyl)piperazin-1-yl)-8-methylimidazo[1,2-a]pyridin-3-yl)(methyl)amino)-4-(4-fluorophenyl)thiazole-5-carbonitrile, **(71)**

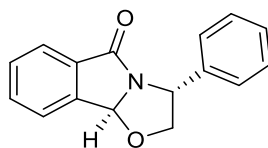


2-Chloro-1-(3-hydroxyazetidin-1-yl)ethan-1-one (45 mg, 0.3 mmol, 1.3 eq.) and K_2CO_3 (64 mg, 0.5 mmol, 2.0 eq.) was added to 2-((2-ethyl-8-methyl-6-(piperazin-1-yl)imidazo[1,2-a]pyridin-3-yl)(methyl)amino)-4-(4-fluorophenyl)thiazole-5-carbonitrile (0.11 g, 0.2 mmol, 1.0 eq.) dissolved in MeCN (2 mL) and the resulting mixture stirred at 80 °C for one day. The solution was cooled to room temperature, diluted with MeCN (10 mL), then filtered. The filtrate was evaporated under reduced pressure to give a brown oil. The crude material was purified *via* flash column chromatography (100 % acetone), to give heterocycle **71** (GLPG 1690) as a white solid (12 mg, 1.3 %, over 4 steps)

1H NMR (400 MHz, $CDCl_3$) δ = 8.12 - 8.08 (m, 2H), 7.17 - 7.02 (m, 2H), 6.97 - 6.80 (m, 2H), 4.75 - 4.56 (m, 1H), 4.43 - 4.29 (m, 1H), 4.27 - 4.14 (m, 1H), 4.07 - 3.95 (m, 1H), 3.91 - 3.79 (m, 1H), 3.61 - 3.48 (m, 3H), 3.05 (br d, J = 3.7 Hz, 4H), 2.78 - 2.59 (m, 6H), 2.54 (s, 3H), 1.26 (t, J = 7.7 Hz, 3H)

The 1H NMR spectrum was found to be in agreement with that of Heckman and co-workers.⁶⁷

7.1.83 (3*R*,9*bS*)-3-Phenyl-2,3-dihydrooxazolo[2,3-*a*]isoindol-5(9*bH*)-one, (**73**)

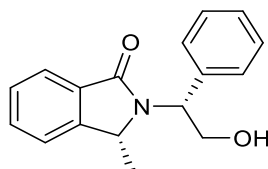


(*R*)-Phenyl glycinol, (5.00 g, 36.0 mmol, 1 eq.) was heated for 48 h with 2-carboxy benzaldehyde (6.02 g, 40.0 mmol, 1.1 eq.) in toluene (300 mL) under Dean-Stark conditions. The crude mixture was then evaporated to an oil and purified via flash column chromatography, (50 % Et₂O / 50 % light petroleum ether), to afford lactam **73** as a white crystalline solid (6.45 g, 88 %).

¹H NMR (400 MHz, CDCl₃) δ = 7.97 - 7.78 (m, 1H), 7.71 - 7.55 (m, 3H), 7.51 - 7.29 (m, 5H), 6.06 (s, 1H), 5.23 (t, *J* = 7.4, 1H), 4.85 (dd, *J* = 8.7, 7.7, 1H), 4.17 (dd, *J* = 8.8, 7.4, 1H)

¹HNMR Spectrum identical to that reported by Allin and co-workers.²³⁴

7.1.84 (*R*)-2-((*R*)-2-Hydroxy-1-phenylethyl)-3-methylisoindolin-1-one, (**74a**)

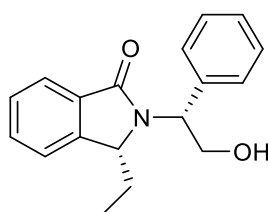


To a stirring solution of (3*R*,9*bS*)-3-phenyl-2,3-dihydrooxazolo[2,3-*a*]isoindol-5(9*bH*)-one, (1.00 g, 3.9 mmol, 1.0 eq.) in anhydrous THF (15 mL), under N₂, cooled to -78 °C, was added LiHMDS as a solution in THF (1M, 4.36 mL, 4.4 mmol, 1.1 eq.) dropwise (over 5 min) and the resulting mixture stirred for 30 min. Methyl iodide (0.30 mL, 4.8 mmol, 1.2 eq.) was then added dropwise (over 2 min). The solution was warmed to room temperature overnight. NH₄Cl sat. aq. (20 mL) was added to quench the reaction, then diluted with H₂O (20 mL). The organic portion was extracted with Et₂O (5 x 30 mL) and washed with brine (30 mL), dried with anhydrous MgSO₄, filtered and evaporated to a light brown oil, to yield crude intermediate (3*R*)-9*b*-methyl-3-phenyl-2,3-dihydrooxazolo[2,3-*a*]isoindol-5(9*bH*)-one, used immediately without purification.

TiCl₄ as a solution in DCM (1 M, 5.94 mL, 5.9 mmol, 1.5 eq.) was added dropwise (over 2 min) to (3*R*)-9*b*-methyl-3-phenyl-2,3-dihydrooxazolo[2,3-*a*]isoindol-5(9*bH*)-one (1.059 g, 3.9 mmol, 1.0 eq.) in anhydrous DCM (15 mL), under N₂, at -78 °C and stirred for 30 min. Triethylsilane (0.95 mL, 5.9 mmol, 1.5 eq.) was added dropwise (over 1 min) to the mixture, then after 10 min warmed to room temperature overnight. The reaction was quenched using NH₄Cl sat. aq. (20 mL) and then diluted with H₂O (20 mL). The organic portion was extracted with DCM (3 x 40 mL) washed with brine (30 mL), dried over anhydrous MgSO₄, filtered and evaporated to a light brown residue. This was then purified by flash column chromatography (100% light petroleum ether), to afford isoindolinone **74a** as a yellow oil (0.34 g, 32 %).

¹H NMR (400 MHz, CDCl₃) δ 7.88 (d, *J* = 7.4, Ar-H, 1H), 7.62 - 7.44 (m, 2H, Ar-H), 7.39 - 7.26 (m, 6H, Ar-H), 5.00 - 4.89 (m, 1H, CH₂OH), 4.77 (dd, *J* = 8.0, 3.4, 1H, NCHAr), 4.53 - 4.43 (m, 1H, CHHOH), 4.34 (q, *J* = 6.7, 1H, CH(CH₃)), 4.18 - 4.05 (m, 1H, CHHOH), 1.46 (d, *J* = 6.7, 3H, CH₃); ¹³C NMR (100 MHz, CDCl₃) δ 169.75, 147.14, 137.96, 132.13, 128.93, 128.42, 128.13, 127.32, 123.96, 122.03, 64.73, 62.57, 57.14, 18.45; IR (solid): 3333, 1658, 1469, 1404, 1353 cm⁻¹; HRMS (ESI, *m/z*): calcd. for C₁₇H₁₇NO₂ [M + H]⁺ 268.1332, found: 268.1334; [α]_D = +244 (*c* 0.5, CH₂Cl₂).

7.1.85 (*R*)-3-Ethyl-2-((*R*)-2-hydroxy-1-phenylethyl)isoindolin-1-one, (**74b**)



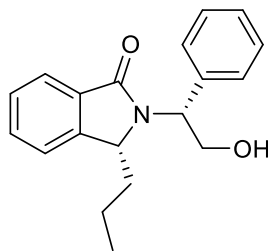
A stirring solution of (3*R*,9*bS*)-3-phenyl-2,3-dihydrooxazolo[2,3-*a*]isoindol-5(9*bH*)-one, (0.50 g, 1.98 mmol, 1.0 eq.) in anhydrous THF (15 mL), under N₂, was cooled to -78 °C. LiHMDS as a solution in THF (1 M, 2.18 mL, 2.2 mmol, 1.1 eq.) was added dropwise (over 5 min) and the resulting mixture stirred for 30 min. Ethyl iodide (0.19 mL, 2.4 mmol, 1.2 eq.) was then added dropwise and the warmed to room temperature overnight. NH₄Cl sat. aq. (15 mL) was added to quench the reaction, which was then diluted with H₂O (20 mL). The organic portion was extracted with Et₂O (5 x 30 mL), washed with brine (30 mL), dried with anhydrous MgSO₄, filtered and evaporated to an orange oil, to yield crude intermediate ((3*R*)-9*b*-ethyl-3-phenyl-2,3-dihydrooxazolo[2,3-*a*]isoindol-5(9*bH*)-one, used in the next step without further purification.

TiCl₄, as a solution in DCM (1 M, 2.97 mL, 2.9 mmol, 1.5 eq.) was added dropwise (over 2 mins) to (3*R*)-9*b*-ethyl-3-phenyl-2,3-dihydrooxazolo[2,3-*a*]isoindol-5(9*bH*)-one (0.55 g, 1.9 mmol, 1.0 eq.) in anhydrous DCM (10 mL), under N₂ at -78 °C and stirred for 30 min. Triethylsilane (0.47 mL, 2.9 mmol, 1.5 eq.) was added dropwise (over 1 min) to the mixture, which after 10 min was warmed to room temperature overnight. The reaction was quenched with NH₄Cl sat. aq. (20 mL) and then diluted with H₂O (20 mL). The organic portion was extracted with DCM (3 x 30 mL), washed with brine (30 mL), dried over anhydrous MgSO₄, filtered and evaporated to a light brown residue. This was then purified by flash column chromatography (80 % EtOAc / 20 % light petroleum ether), to afford isoindolinone **74b** as a yellow crystalline solid (0.26 g, 47 %).

¹H NMR (400 MHz, CDCl₃) δ 7.88 (d, *J* = 7.5, 1H, Ar-H), 7.62 - 7.40 (m, 2H, Ar-H), 7.38 - 7.26 (m, 6H, Ar-H), 7.38 - 7.21 (m, 1H, Ar-H), 5.07 - 4.99 (m, 1H, CH₂OH), 4.62 (dd, *J* = 8.0, 3.3 1H, NCHPh), 4.48 (dt, *J* = 12.5, 7.9, 1H, CHHOH), 4.40 (dd, *J* = 5.1, 2.7, 1H, CHCH₂CH₃), 4.11 (ddd, *J* = 12.5, 7.0, 3.3, 1H, CHHOH), 2.13 - 1.90 (m, 2H, CHCH₂CH₃), 0.55 (t, *J* = 7.4, 3H, CH₂CH₃); ¹³C NMR (100 MHz, CDCl₃) δ 170.47, 144.95, 138.02, 132.94, 132.06, 128.92, 128.47, 128.13, 127.36, 123.84, 122.07, 64.83, 62.86, 61.18, 22.94, 5.97; IR (solid): 3345, 2995, 2876, 1659, 1469, 1407, 1214 cm⁻¹; HRMS (ESI, *m/z*): calcd. for C₁₈H₁₉NO₂ [M + H]⁺ 282.1489, found 282.1489; [α]_D = + 180 (*c* 0.5, CH₂Cl₂); Mp: 101-104 °C

A suitable crystal was obtained by slow evaporation in Et₂O / light petroleum ether). Diffraction data (3135 total reflections with *R*_{int} = 0.0254) were collected on a Rigaku Oxford Diffraction Excalibur diffractometer at *T* = 150 K using graphite-monochromated Mo-Kα radiation. The structure was solved and refined using the SHELXS-2016 and SHELXL-2016 programs.²⁵⁶ Crystal data: C₁₈H₁₉NO₂, *M* = 293.35, colourless plate, 0.454 × 0.384 × 0.277 mm³, orthorhombic, space group *P* 2₁ 2₁ 2₁ (No. 18), *V* = 1504.58(14) Å³, *Z* = 4, *D*_c = 1.2419 g/cm³, *F*₀₀₀ = 600, Xcalibur, Sapphire3, Gemini, Mo Kα radiation, λ = 0.71073 Å, *T* = 150.00(10)K, 2θ_{max} = 58.6°, 4837 reflections collected, 3135 unique (*R*_{int} = 0.0543). Final *Goof* = 0.877, *RI* = 0.0476, *wR2* = 0.1309, *R* indices based on 2711 reflections with *I* > 2(*I*) (refinement on *F*²), 192 parameters, 0 restraints. Lp and absorption corrections applied, μ = 0.082 mm⁻¹. Absolute structure parameter = -0.4(15) (Flack, H. D. *Acta Cryst.* **1983**, *A39*, 876-881).

7.1.86 (*R*)-2-((*R*)-2-Hydroxy-1-phenylethyl)-3-propylisoindolin-1-one, (**74c**)



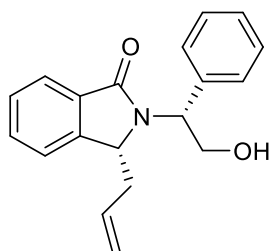
A stirring solution of (*3R,9bS*)-3-phenyl-2,3-dihydrooxazolo[2,3-*a*]isoindol-5(*9bH*)-one (0.50 g, 1.9 mmol, 1.0 eq.) in THF (15 mL), under N₂, was cooled to -78 °C. LiHMDS as a solution in THF (1 M, 2.18 mL, 2.1 mmol, 1.1 eq.) was then added dropwise (over 5 min) and the resulting mixture stirred for 30 min. 1-Iodopropane (0.23 mL, 2.4 mmol, 1.2 eq.) was added dropwise (over 2 min), then warmed to room temperature overnight. NH₄Cl sat. aq. (20mL) was added to quench the reaction, then diluted with H₂O (20 mL). The organic portion was extracted with Et₂O (5 x 30 mL), washed with brine (30 mL), dried with anhydrous MgSO₄, filtered and evaporated to a light brown oil, to yield crude intermediate (*3R*)-3-phenyl-9b-propyl-2,3-dihydrooxazolo[2,3-*a*]isoindol-5(*9bH*)-one, used in the next step without any further purification.

TiCl₄ as a solution in DCM (2.97 mL, 2.9 mmol, 1.5 eq.) was added dropwise to (*3R*)-3-phenyl-9b-propyl-2,3-dihydrooxazolo[2,3-*a*]isoindol-5(*9bH*)-one (0.58 g, 1.9 mmol, 1.0 eq.) in anhydrous DCM (10 mL), under N₂, at -78 °C and stirred for 30 min. Triethylsilane (0.47 mL, 2.9 mmol, 1.5 eq.) was added dropwise to the mixture, which after 10 min was warmed to room temperature overnight. The reaction was quenched with NH₄Cl sat. aq. (20 mL) and then diluted with H₂O (20 mL). The organic portion was extracted with DCM (3 x 30 mL) washed with brine (30 mL), dried over anhydrous MgSO₄, filtered and evaporated to a light brown residue. This was then purified by flash column chromatography (80 % EtOAc / 20 % light petroleum ether), to afford isoindolinone **74c** as a white crystalline solid (0.19 g, 32 %).

¹H NMR (400 MHz, CDCl₃) δ 7.87 (d, *J* = 7.5, 1H, Ar-H), 7.61 - 7.42 (m, 2H, Ar-H), 7.38 - 7.15 (m, 6H, Ar-H), 5.08 - 4.94 (m, 1H, CH₂OH), 4.66 (dd, *J* = 8.0, 3.4, 1H, NCHPh), 4.47 (dt, *J* = 12.5, 7.9, 1H, CHHOH), 4.42 - 4.31 (m, 1H, CHCH₂CH₂CH₃), 4.09 (ddd, *J* = 12.4, 7.3, 3.4, 1H, CHHOH), 2.02 - 1.79 (m, 2H, CHCH₂CH₂CH₃), 0.88 - 0.68 (m, 5H, CHCH₂CH₂CH₃); ¹³C NMR (100 MHz, CDCl₃) δ 170.26, 145.44, 137.92, 132.58, 131.82, 128.84, 128.25, 127.93, 127.18, 123.75, 121.95, 64.74, 62.63, 60.57, 32.35, 15.17, 13.98; IR

(solid): 3300, 2998, 2875, 1660, 1413, 1305, 1216 cm^{-1} HRMS (ESI, m/z): calcd. for $\text{C}_{19}\text{H}_{21}\text{NO}_2$ $[\text{M} + \text{H}]^+$ 296.1645, found 296.1644; $[\alpha]_{\text{D}} = +132$ [c 0.5, CH_2Cl_2]; Mp: 149-151 $^{\circ}\text{C}$.

7.1.87 (*R*)-3-Allyl-2-((*R*)-2-hydroxy-1-phenylethyl)isoindolin-1-one, (**74d**)



A solution of (*3R,9bS*)-3-phenyl-2,3-dihydrooxazolo[2,3-*a*]isoindol-5(*9bH*)-one, (1.00 g, 3.96 mmol, 1.0 eq.) in anhydrous THF (15 mL), under N_2 , was cooled to -78 $^{\circ}\text{C}$. LiHMDS as a solution in THF (1 M, 4.4 mL, 4.36 mmol, 1.1 eq.) was added dropwise (over 5 min) and the resulting mixture stirred for 30 min. Allyl bromide (0.41 mL, 4.8 mmol, 1.2 eq.) was added dropwise (over 2 min), then the solution was warmed to room temperature overnight. NH_4Cl sat. aq. (15 mL) was added to quench the reaction, then further diluted with H_2O (20 mL). The organic portion was extracted with Et_2O (5 x 30 mL), combined, washed with brine (30 mL), dried over anhydrous MgSO_4 , filtered and evaporated to an orange oil, to yield crude intermediate (*3R*)-9b-allyl-3-phenyl-2,3-dihydrooxazolo[2,3-*a*]isoindol-5(*9bH*)-one, which was used without further purification.

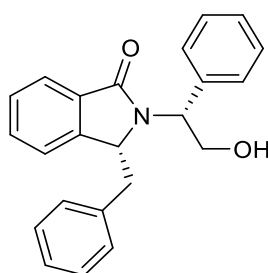
TiCl_4 , as a solution in DCM (5.94 mL, 5.9 mmol, 1.5 eq.) was added to (*3R*)-3-phenyl-9b-propyl-2,3-dihydrooxazolo[2,3-*a*]isoindol-5(*9bH*)-one (1.15 g, 3.9 mmol, 1.0 eq.) in anhydrous DCM (10 mL) was added dropwise (over 2 min), under N_2 and at -78 $^{\circ}\text{C}$ and stirred for 30 min. Triethylsilane (0.95 mL, 5.9 mmol, 1.5 eq.) was added dropwise (over 1 min) to the mixture, which after 10 min was warmed to room temperature overnight. The reaction was quenched by the addition of NH_4Cl sat. aq. (20 mL) and then diluted with H_2O (20 mL). The organic portion was extracted with DCM (3 x 30 mL), washed with brine (30 mL), dried over anhydrous MgSO_4 , filtered and evaporated to a light brown oil. This was then purified by flash column chromatography, (70 % Et_2O / 30 % light petroleum ether) to afford isoindolinone **74d** as a yellow solid (0.57 g, 49 %).

^1H NMR (400 MHz, CDCl_3) δ 7.87 (d, $J = 7.4$, 1H, Ar-H), 7.60 - 7.44 (m, 2H, Ar-H), 7.41 - 7.21 (m, 6H, Ar-H), 5.56 - 5.15 (m, 1H, HC=CH₂), 5.12 - 4.96 (m, 3H, CH₂OH, C=CH₂), 4.74

(dd, $J = 7.7, 3.2$, 1H, NCHPh), 4.49 - 4.36 (m, 2H, CHCH₂CH=CH₂, CHHOH), 4.13 (m, 1H, CHHOH), 2.80 - 2.48 (m, 2H, CH₂CH=CH, 2H); ¹³C NMR (100 MHz, CDCl₃) δ 170.11, 144.88, 137.83, 132.35, 131.83, 130.47, 128.82, 128.31, 127.92, 127.15, 123.73, 122.26, 119.77, 64.53, 62.64, 59.93, 34.92; IR (solid): 3381, 2924, 1725, 1646, 1406 cm⁻¹; HRMS (ESI, m/z): calcd. for C₁₉H₁₉NO₂ [M + H]⁺ 294.1489, found 294.1490. [α]_D = + 104 (c 0.5, CH₂Cl₂); Mp = 108-112 °C.

A suitable crystal was obtained by slow evaporation in Et₂O / light petroleum ether. Diffraction data (5424 total reflections with $R_{\text{int}} = 0.022$) were collected on a Rigaku Oxford Diffraction Excalibur diffractometer at $T = 150$ K using graphite-monochromated Mo-K α radiation. The structure was solved and refined using the SHELXS-2016 and SHELXL-2016 programs.²⁵⁶ Crystal data: C₁₉H₁₉NO₂, $M = 293.35$, colourless needle, 0.454 x 0.384 x 0.277 mm³, space group P212121, $V = 1545.30(10)$ Å³, $Z = 4$, $D_c = 1.261$ g/cm³, $F_{000} = 624$, Xcalibur, Sapphire3, Gemini, MoK α radiation, $\lambda = 0.71073$ Å, $T = 150(2)$ K, $2\theta_{\text{max}} = 58.7^\circ$, 5427 reflections collected, 3364 unique ($R_{\text{int}} = 0.0222$). Final GooF = 1.078, $R_1 = 0.0423$, $wR_2 = 0.0874$, R indices based on 3072 reflections with $I \geq 2(I)$ (refinement on F^2), 205 parameters, 0 restraints. Lp and absorption corrections applied, $m = 0.082$ mm⁻¹. Absolute structure parameter = -0.1(7) (Flack, H. D. Acta Cryst. 1983, A39, 876-881).

7.1.88 (*R*)-3-Benzyl-2-((*R*)-2-hydroxy-1-phenylethyl)isoindolin-1-one, (**74e**)



A solution of (3*R*,9*bS*)-3-phenyl-2,3-dihydrooxazolo[2,3-*a*]isoindol-5(9*bH*)-one, (0.50 g, 1.9 mmol, 1.0 eq.) in anhydrous THF (15 mL), under N₂, was cooled to -78 °C. LiHMDS as a solution in THF (1 M, 2.2 mL, 2.18 mmol, 1.1 eq.) was then added dropwise and the resulting mixture stirred for 30 min. Benzyl bromide (0.31 mL, 2.4 mmol, 1.2 eq.) was added dropwise (over 2 min), then warmed to room temperature overnight. NH₄Cl sat. aq. (20mL) was added to quench the reaction, then diluted with H₂O (20 mL). The organic portion was extracted with

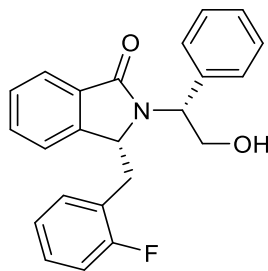
Et₂O (5 x 30 mL), washed with brine (30 mL), combined, dried with anhydrous MgSO₄, filtered and evaporated to a light orange solid, to yield crude intermediate (3*R*)-9*b*-benzyl-3-phenyl-2,3-dihydrooxazolo[2,3-*a*]isoindol-5(9*bH*)-one, used in the next step without further purification.

TiCl₄, as a solution in DCM (1 M, 2.97 mL, 2.9 mmol, 1.5 eq.) was added dropwise (over 2 min) to (3*R*)-9*b*-benzyl-3-phenyl-2,3-dihydrooxazolo[2,3-*a*]isoindol-5(9*bH*)-one (0.676 g, 1.98 mmol, 1.0 eq.) in anhydrous DCM (10 mL), under N₂ at -78 °C. The solution was then stirred for 30 min. Triethylsilane (0.47 mL, 2.9 mmol, 1.5 eq.) was added dropwise (over 1 min) to the mixture, which after 10 min was warmed to room temperature overnight. The reaction was quenched by the addition of NH₄Cl sat. aq. (20 mL) and then diluted with H₂O (20 mL). The organic portion was extracted with DCM (3 x 30 mL), washed with brine (30 mL), dried over anhydrous MgSO₄, filtered and evaporated to a light brown oil. This was then purified by flash column chromatography (90 % Et₂O / 10 % light petroleum ether) to afford isoindolinone **74e** as a white crystalline solid (0.24 g, 35 %).

¹H NMR (400 MHz, CDCl₃) δ 7.84 - 7.74 (m, 1H, Ar-H), 7.51 - 7.14 (m, 10H, Ar-H), 6.98 - 6.91 (m, 2H, Ar-H), 6.88 - 6.78 (m, 1H, Ar-H), 5.10 - 4.95 (m, 1H, CH₂OH), 4.87 (dd, *J* = 7.8, 3.4, 1H, NCHPh), 4.54 (dd, *J* = 7.8, 4.5, 1H, HC(Bn)), 4.46 (dt, *J* = 12.5, 7.7, 1H, CHHOH), 4.09 (ddd, CHHOH, *J* = 12.4, 6.9, 3.3, 1H), 3.37 (dd, CHCHPh, *J* = 13.9, 4.4, 1H), 2.88 (dd, *J* = 13.8, 7.8, 1H, CHCHPh); ¹³C NMR (100 MHz, CDCl₃) δ 169.94, 144.93, 137.97, 135.44, 132.08, 131.49, 129.41, 128.95, 128.42, 128.35, 128.02, 127.14, 127.12, 123.74, 122.82, 64.65, 63.13, 61.75, 38.12; IR (solid): 3380, 2924, 2885, 1649, 1408 cm⁻¹; HRMS (ESI, *m/z*): calcd. for C₂₃H₂₁NO₂ [M + H]⁺ 344.1645, found 344.1643. [α]_D = + 124 (*c* 0.5, CH₂Cl₂); Mp: 174-177 °C.

A suitable crystal was obtained by slow evaporation in diethyl ether / light petroleum ether. Diffraction data (3860 total reflections with *R*_{int} = 0.024) were collected on a Rigaku Oxford Diffraction Excalibur diffractometer at *T* = 150 K using graphite-monochromated Mo-Kα radiation. The structure was solved and refined using the SHELXS-2016 and SHELXL-2016 programs.²⁵⁶ *Crystal data*: C₂₃H₂₁NO₂, *M*_r = 343.41 g mol⁻¹, orthorhombic, *P*2₁2₁2₁, *a* = 8.6454(3), *b* = 10.5715(3), *c* = 20.1931(6) Å, *V* = 1845.55(10) Å³, *Z* = 4, *R*[*F*² > 2σ(*F*²)] = 0.053 for 3401 reflections with *I* > 2σ(*I*), *wR*(*F*²) = 0.097 for all 3860 independent data, GOF = 1.104, 239 refined parameters. The crystallographic data is deposited as CCDC 1583682. These data can be obtained free of charge from The Cambridge Crystallographic Data Centre via www.ccdc.cam.ac.uk/data_request/cif.

7.1.89 (*R*)-3-(2-Fluorobenzyl)-2-((*R*)-2-hydroxy-1-phenylethyl)isoindolin-1-one, (**74f**)



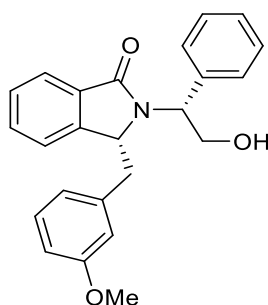
A stirring solution of (*3R,9bS*)-3-phenyl-2,3-dihydrooxazolo[2,3-*a*]isoindol-5(*9bH*)-one, (0.50 g, 1.98 mmol, 1.0 eq.) in anhydrous THF (15 mL), under N₂, was cooled to -78 °C. LiHMDS as a solution in THF (1 M, 2.18 mL, 2.2 mmol, 1.1 eq.) was then added dropwise (over 5 min) and the resulting mixture stirred for 30 min. 2-Fluoro benzyl bromide (0.29 mL, 2.4 mmol, 1.2 eq.) was added dropwise (over 2 min), the solution was then allowed to warm to room temperature overnight. NH₄Cl sat. aq. (10 mL) was added to quench the reaction, then diluted with H₂O (20 mL). The organic portion was then extracted with EtOAc (3 x 40 mL), washed with brine, dried with anhydrous MgSO₄, filtered and evaporated to a light orange oil, to yield crude intermediate (*3R*)-9b-(2-fluorobenzyl)-3-phenyl-2,3-dihydrooxazolo[2,3-*a*]isoindol-5(*9bH*)-one, used in the next step without any further purification.

TiCl₄, as a solution in DCM (1 M, 2.97 mL, 2.9 mmol, 1.5 eq.) was added dropwise to (*3R*)-9b-(2-fluorobenzyl)-3-phenyl-2,3-dihydrooxazolo[2,3-*a*]isoindol-5(*9bH*)-one (0.71 g, 1.9 mmol, 1.0 eq.) in anhydrous DCM (10 mL), under N₂ at -78 °C. The solution was stirred for 30 min. Triethylsilane (0.47 mL, 2.9 mmol, 1.5 eq.) was added dropwise (over 2 min) to the mixture, which after 10 min, was warmed to room temperature overnight. The reaction was quenched by the addition of NH₄Cl sat. aq. (10 mL) and then diluted with H₂O (20 mL). The organic portion was extracted with DCM (3 x 30 mL), washed with brine (30 mL), dried over anhydrous MgSO₄, filtered and evaporated to a light brown oil. This was then purified by flash column chromatography (70 % EtOAc / 30 % light petroleum ether), to afford isoindolinone **74f** as an off-white crystalline solid (0.46 g, 65 %).

¹H NMR (400 MHz, CDCl₃) δ 7.85 - 7.77 (m, 1H, Ar-H), 7.50 - 6.88 (m, 12H, Ar-H), 4.96 - 4.82 (m, 2H, CH₂OH, NCHPh), 4.59 (dd, *J* = 7.7, 4.3, 1H, CHCH₂Ar(F)), 4.48 (dt, *J* = 12.5, 7.8, 1H, CHHOH), 4.13 (ddd, *J* = 12.5, 7.0, 3.4, 1H, CHHOH), 3.43 (dd, *J* = 14.0, 4.2, 1H, CHCHHAr(F)), 2.93 (dd, *J* = 14.0, 7.7, 1H, CHCHHAr(F)); ¹³C NMR (100 MHz, CDCl₃) δ

170.01, 161.23 (d, $^1J_{C-F} = 245.4$ Hz), 144.93, 137.97, 132.14, 131.75 (d, $^3J_{C-F} = 4.8$ Hz), 131.58, 129.16 (d, $^2J_{C-F} = 7.7$ Hz), 128.95, 128.47, 128.08, 127.22, 124.03 (d, $^3J_{C-F} = 3.8$ Hz), 123.84, 122.82, 122.71 (d, $^4J_{C-F} = 15.3$ Hz), 115.43 (d, $^2J_{C-F} = 22.0$ Hz), 64.64, 63.08, 60.58, 31.65; IR (solid): 3313, 2871, 1657, 1491, 1230 cm^{-1} ; HRMS (ESI, m/z): calcd. for $\text{C}_{23}\text{H}_{20}\text{FNO}_2$ $[\text{M} + \text{H}]^+$ 362.1551 found, 362.1550; $[\alpha]_{\text{D}} = +152$ (c 0.5, CH_2Cl_2); Mp = 140-143 $^{\circ}\text{C}$.

7.1.90 (*R*)-2-((*R*)-2-Hydroxy-1-phenylethyl)-3-(3-methoxybenzyl)isoindolin-1-one, (**74g**)



A stirring solution of (*3R,9bS*)-3-phenyl-2,3-dihydrooxazolo[2,3-*a*]isoindol-5(*9bH*)-one, (0.50 g, 1.9 mmol, 1.0 eq.) in anhydrous THF (15 mL) under N_2 , was cooled to -78 $^{\circ}\text{C}$. LiHMDS as a solution in THF (1 M, 2.18 mL, 2.2 mmol, 1.1 eq.) was then added dropwise (over 5 min) and the resulting mixture stirred for 30 min. 3-Methoxy benzyl bromide (0.33 mL, 2.4 mmol, 1.2 eq.) was then added dropwise (over 2 min). The solution was allowed to warm to room temperature. A solution of sat. NH_4Cl aq. (10 mL) was added and then diluted with H_2O (20 mL). The organic portion was extracted with EtOAc (3 x 40 mL) and washed with brine (1 x 30 mL). The combined extracts were then dried with anhydrous MgSO_4 , filtered and evaporated to a light orange oil, to yield crude intermediate (*3R*)-9b-(3-methoxybenzyl)-3-phenyl-2,3-dihydrooxazolo[2,3-*a*]isoindol-5(*9bH*)-one, this was used in the next step without any further purification.

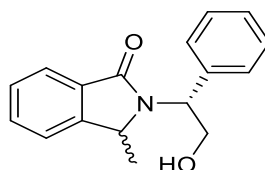
Crude (*3R*)-9b-(3-methoxybenzyl)-3-phenyl-2,3-dihydrooxazolo[2,3-*a*]isoindol-5(*9bH*)-one (0.74 g, 1.9 mmol, 1.0 eq.) was stirred in anhydrous DCM (10 mL), under N_2 and cooled to -78 $^{\circ}\text{C}$. A solution of TiCl_4 (1 M, 2.9 mL, 2.97 mmol, 1.5 eq.) in DCM was added dropwise (over 2 mins) to the reaction mixture and left to stir for 30 minutes at -78 $^{\circ}\text{C}$. Triethylsilane (0.47 mL, 2.9 mmol, 1.5 eq.) was added dropwise (over 1 min) to the reaction mixture, which was then warmed to room temperature overnight. The reaction was quenched following the addition of a solution of sat. NH_4Cl aq. (10 mL) and then diluted with H_2O (20 mL). The organic portion was extracted with DCM (3 x 20 mL), washed with brine (1 x 30 mL), dried

over anhydrous MgSO₄, filtered and evaporated to a light brown oil. This was then purified by flash column chromatography (70 % EtOAc / 30 % light petroleum ether), to afford isoindolinone **74g** as an off-white solid, (0.45 g, 61 %).

¹H NMR (400 MHz, CDCl₃) δ = 7.84 - 7.76 (m, 1H, Ar-H), 7.49 - 7.40 (m, 2H, Ar-H), 7.38 - 7.28 (m, 3H, Ar-H), 7.27 - 7.20 (m, 2H, Ar-H), 7.14 (t, *J* = 7.9, 1H, Ar-H), 6.96 - 6.88 (m, 1H, Ar-H), 6.76 (dd, *J* = 8.2, 2.0, 1H, Ar-H), 6.56 (d, *J* = 7.5, 1H, Ar-H), 6.45 - 6.39 (m, 1H, Ar-H), 5.07 - 5.00 (m, 1H, OH), 4.85 (dd, *J* = 7.8, 3.1, 1H, CHCH₂Ar(OMe)), 4.54 (dd, *J* = 7.7, 4.4, 1H, CHPh), 4.50 - 4.39 (m, 1H, CHCHHAr(OMe)), 4.19 - 4.00 (m, 1H, CHCHHAr(OMe)), 3.68 (s, 3H, OCH₃), 3.34 (dd, *J* = 13.8, 4.3, 1H, CHHOH), 2.86 (dd, *J* = 14.0, 7.8, 1H, CHHOH). ¹³C NMR (100 MHz, CDCl₃) δ = 169.96, 159.47, 145.02, 137.87, 136.93, 132.05, 131.47, 129.41, 128.91, 128.33, 128.03, 127.15, 123.72, 122.80, 121.80, 114.76, 112.65, 64.62, 63.14, 61.64, 55.07, 38.05; IR (neat) 2868, 1715, 1616, 1361, 1311 cm⁻¹; HRMS (ESI⁺) (*m/z*) calcd for C₂₄H₂₃NO₃⁺ [M + H]⁺, 374.1751 found, 374.1749, [α]_D = +40 [c=0.5, CH₂Cl], Mp = 94-96 °C.

7.1.91 Preparation of C-3 racemic compound for chiral HPLC investigation

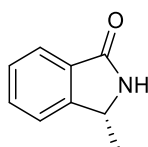
2-((*R*)-2-Hydroxy-1-phenylethyl)-3-methylisindolin-1-one



To a stirring solution of (*R*)-2-((*R*)-2-hydroxy-1-phenylethyl)-3-methylisindolin-1-one, (71 mg, 0.3 mmol, 1 eq.) in acetone / H₂O 3:1 (4 mL), powdered sodium hydroxide (20 mg, 0.5 mmol, 2 eq.) was added and the resulting mixture was stirred at 50 °C for 3 h (until the formation of a second diastereomer was indicated by TLC). The mixture was diluted with H₂O (10 mL) and carefully acidified to pH 7 using a 1 M solution of HCl aq. The organic portion was extracted using EtOAc (3 x 20 mL), combined, washed with brine (40 mL), dried over anhydrous MgSO₄, filtered and evaporated to obtain isindolinone **74a** (racemic) as a pale-yellow oil (71 mg, quantitative).

Inspection of the ¹HNMR (400 MHz, CDCl₃) spectrum indicated formation of a new diastereomer, 6:4 in favour of the starting material. The chiral auxiliary was then removed in the same manner as (*R*)-3-methylisindolin-1-one, **75**.

7.1.92 (*R*)-3-Methylisindolin-1-one, (**75**)



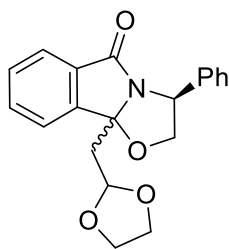
To a test tube, (*R*)-2-((*R*)-2-hydroxy-1-phenylethyl)-3-methylisindolin-1-one, (53 mg, 0.2 mmol, 1.0 eq.) was dissolved in conc. H₂SO₄ (96%, 2 mL). This was then immediately heated for two min in a steam bath, then cooled to room temperature. Cold H₂O (20 mL, 5 °C) was added. The organic portion extracted using DCM (3 x 20 mL), the extracts were pooled, dried over anhydrous MgSO₄, filtered and evaporated to obtain a pale-yellow oil.

The material was then purified using preparative chromatography (80 % EtOAc / 20 % light petroleum ether) to obtain isindolinone **75** as colourless oil (11 mg, 38 %).

¹H NMR (400 MHz, CDCl₃) δ = 7.89 - 7.77 (m, 1H), 7.63 - 7.52 (m, 1H), 7.52 - 7.39 (m, 2H), 4.70 (q, *J* = 6.5, 1H), 1.51 (d, *J* = 6.7, 3H), e.e 98% (determined by chiral HPLC)

¹HNMR Spectrum identical to that reported by Allin and co-workers.²³⁴

7.1.93 (3*S*)-9*b*-((1,3-Dioxolan-2-yl)methyl)-3-phenyl-2,3-dihydrooxazolo[2,3-*a*]isoindol-5(9*bH*)-one, (**76**)



A solution of (3*S*,9*bR*)-3-phenyl-2,3-dihydrooxazolo[2,3-*a*]isoindol-5(9*bH*)-one (1.20 g, 4.7 mmol, 1.0 eq.) in anhydrous THF (20 mL), under a flow of N₂ was cooled to -78 °C. A solution of LiHMDS (1 M, 5.25 mL, 5.2 mmol, 1.1 eq.) in THF, was then added dropwise (over 5 min) to the reaction mixture. After 30 min, a solution of bromomethyl-1,3-dioxolane (0.60 mL, 5.7 mmol, 1.2 eq.) in anhydrous THF (10 mL) was added dropwise. The reaction mixture was then allowed to warm to room temperature overnight. The reaction was quenched using a solution of saturated NH₄Cl aq. (20 mL), diluted with H₂O (20 mL), and then extracted with Et₂O (3 x 50 mL). The combined organic extracts were then washed with brine (1 x 50 mL), dried over anhydrous MgSO₄, filtered and evaporated under reduced pressure to give dioxolane **76** as a yellow oil, (1.86 g).

Analysis by ¹H NMR spectroscopy indicated the formation of the desired product, as a 1:1 mixture of diastereomers, with an approximate conversion of 50 %. The material was used without further purification.

7.2 Biological evaluation

7.2.1 Bis-pNPP assay

Recombinant ATX was obtained from 3E3 cells, that were genetically engineered to overexpress ATX, 3E3 cells were seeded in a T150 x 3 and incubated until 50% confluent. The medium was replaced with serum-free medium (approx. 15 mL) and incubated overnight (37 °C). The supernatant was collected and combined, which was then centrifuged at 16 G for 5 min. The supernatant was then collected, the pellet was discarded. A Sepharose column (HiTrap Con A, 1 mL) was prepared by eluting with Tris buffered saline (TBS, 20 mM, 0.5 M NaCl, pH 7.4, 20 mL), at a flow rate of approximately 1.0 mL / min, 4 °C. The collected supernatant was loaded on to the column at a rate of 0.1 mL / min, and then eluted with TBS (25 mL) at a flow rate of 1 mL / min. A solution of methyl α -D-mannopyranoside in TBS (0.5 M, 2 mL) was passed through the column. The eluent was collected, both the column and the eluent were held at 4 °C overnight. The eluent was then passed through the column and the resulting eluent then dialysed (8 kDa MWCO) against TBS (20 mM, 0.05 M NaCl, pH 7.4, 1 L), at 4 °C, for 2 h. The TBS solution was then changed once. Dialysed ATX was then used without further purification.

The drug conjugates were diluted to a concentration appropriate to their predicted activity in distilled water, a 3-fold dilution series was then prepared (final concentration = 0 μ g / mL), which were additionally diluted 5-fold when added to the assay plate.

In a 96-well plate, reaction buffer (Tris HCl aq. 250 mM, KCl aq. 25 mM, CaCl₂ aq. 5 mM, MgCl₂.6H₂O aq. 5 mM, NaCl aq. 700 mM, pH 7.8, 20 μ L), bis-pNPP aq. (1 mM, 10 μ L), and the test compound (20 μ L) were added to each well, followed by the addition of autotaxin as a solution in TBS (50 μ L). The plate was incubated at 37 °C for 4 h. The absorbance of the plate was measured at a wavelength of 405 nm, using a Synergy 2 multimode microplate reader. The resulting data were analysed using Graph Pad Prism software. Non-linear regression was used to fit a 4 parameter (Hill equation) dose-response curve to determine the IC₅₀ value for each conjugate.

7.2.2 FS3 Assay

The drug conjugates were diluted to a concentration appropriate to their predicted activity in distilled water, a 3-fold dilution series was prepared, which was further diluted 10-fold when added to the assay plate.

The assay was then performed as per instructed in the assay kit supplied by Echelon Biosciences Inc., ATX as a solution in reaction buffer (80 μL) was added to a 96-well plate. The test compound (20 μL), at an appropriate dilution was then added. The plate was then gently mixed by hand for 1 minute and incubated at room temperature for 10 min. A solution of FS-3 substrate (10 μL) was then added to each well and the fluorescence was then read immediately ($\lambda_{\text{Ex}} = 485 \text{ nm}$, $\lambda_{\text{Em}} = 528 \text{ nm}$) using a Synergy 2 multimode microplate reader, every two min, for 30 min in total, at room temperature.

Fluorescence for each concentration was plotted as a function against time. A linear regression was then fitted to the graph. Non-linear regression was then used to fit a 4 parameter (Hill equation) dose-response curve to the rate of reaction for each concentration in order to determine the IC_{50} value for each conjugate.

7.2.3 Peritoneal retention

A solution of Conjugate **35** in PBS (0.2 mg / mL) was sterilised by filtering the solution through a syringe filter. This was repeated with a 0.2 mg / mL solution of Inulin.

7-week old nude mice (supplied by Envigo) were allowed to acclimatize for one week, before the experiment began. Mice were weighed, then injected (using a 26G syringe) with a solution of conjugate 35 (0.4 mL) in their lower left quadrant, at pre-determined timepoints (0 min, 30 min, 1, 3, 6 and 24 h). The mice were then dispatched by cervical dislocation. The entire process was performed in triplicate. Ventral skin was removed and the peritoneal cavity was washed with PBS solution (0.4 mL). The washings were collected, then centrifuged at 2300 rpm, 5 min, 4 °C. The supernatant was collected. As a control, three mice were injected with a solution of Inulin and then immediately dispatched and processed, as described previously.

The peritoneal washings were analysed using fluorescence spectroscopy ($\lambda_{\text{ex}} = 360 \text{ nm}$, $\lambda_{\text{em}} = 485 \text{ nm}$), alongside a calibration curve prepared with Conjugate **35**, (2-fold dilution, 0.2 μg / mL, top conc.) in order to determine the concentration of the conjugate present in each sample.

Mice were monitored through the experiment for any adverse effects.

Animal experiments were performed at Keele University and were approved by the animal welfare commission of Keele University.

Chapter 8: References

- 1 Ovarian cancer, <http://www.cancerresearchuk.org/about-cancer/ovarian-cancer>, (accessed 5 June 2017).
- 2 World Cancer Research Fund International, Ovarian cancer statistics, <https://www.wcrf.org/int/cancer-facts-figures/data-specific-cancers/ovarian-cancer-statistics>, (accessed 6 September 2018).
- 3 J. Prat, *Virchows Arch.*, 2012, **460**, 237–249.
- 4 N. S. Weiss, T. Homonchuk and J. L. Young, *Gynecol. Oncol.*, 1977, **5**, 161–167.
- 5 L. Dubeau, *Gynecol. Oncol.*, 1999, **72**, 437–42.
- 6 J. Prat, *J. Gynecol. Oncol.*, 2015, **26**, 87–9.
- 7 T. Saida, Y. O. Tanaka, K. Matsumoto, T. Satoh, H. Yoshikawa and M. Minami, *Jpn. J. Radiol.*, 2016, **34**, 117–124.
- 8 K. Doufekas and A. Olaitan, *Int. J. Womens. Health*, 2014, **6**, 537–45.
- 9 J. Broggio, N. Bannister, K. Wong, J. Poole, C. Gildea, M. Emmett, M. Luchtenborg, J. Kaur, L. Butler, M. Peet and A. King, *Statistical bulletin: Cancer survival in England: adult, stage at diagnosis and childhood – patients followed up to 2016*, 2017.
- 10 B. J. Monk and P. J. Anastasia, *J. Adv. Pract. Oncol.*, 2016, **7**, 271–273.
- 11 NICE, Ovarian cancer: recognition and initial management | Guidance and guidelines | NICE, <https://www.nice.org.uk/guidance/cg122/chapter/1-Guidance>, (accessed 5 September 2018).
- 12 G. H. Eltabbakh and C. S. Awtrey, *Expert Opin. Pharmacother.*, 2001, **2**, 109–124.
- 13 A. Berkenblit and S. A. Cannistra, *J. Reprod. Med.*, 2005, **50**, 426–38.
- 14 G. C. Jayson, E. C. Kohn, H. C. Kitchener and J. A. Ledermann, *Lancet*, 2014, **384**, 1376–88.
- 15 Z. Lu, J. Wang, G. M. Wientjes and L. Au, *Futur. Oncol.*, 2011, **6**, 1625–1641.
- 16 J. Chien, R. Kuang, C. Landen and V. Shridhar, *Front. Oncol.*, 2013, **3**, 251.
- 17 W. Tarumi, N. Suzuki, N. Takahashi, Y. Kobayashi, K. Kiguchi, K. Sato and B. Ishizuka, *J. Obstet. Gynaecol. Res.*, 2009, **35**, 414–420.
- 18 C. M. Coticchia, J. Yang and M. A. Moses, *J. Natl. Compr. Canc. Netw.*, 2008, **6**, 795–802.
- 19 K.-S. Ling, G.-D. Chen, H.-J. Tsai, M.-S. Lee, P.-H. Wang and F.-S. Liu, *Taiwan. J. Obstet. Gynecol.*, 2005, **44**, 209–217.
- 20 M. M. Gottesman, T. Fojo and S. E. Bates, *Nat. Rev. Cancer*, 2002, **2**, 48–58.
- 21 M. Kavallaris, D. Y. Kuo, C. A. Burkhart, D. L. Regl, M. D. Norris, M. Haber and S. B. Horwitz, *J. Clin. Invest.*, 1997, **100**, 1282–93.
- 22 S. Dasari and P. B. Tchounwou, *Eur. J. Pharmacol.*, 2014, **740**, 364–78.

- 23 W. Zhen, C. J. Link, P. M. O'Connor, E. Reed, R. Parker, S. B. Howell and V. A. Bohr, *Mol. Cell. Biol.*, 1992, **12**, 3689–98.
- 24 S. W. Johnson, R. P. Perez, A. K. Godwin, A. T. Yeung, L. M. Handel, R. F. Ozols and T. C. Hamilton, *Biochem. Pharmacol.*, 1994, **47**, 689–97.
- 25 K. V. Ferry, T. C. Hamilton and S. W. Johnson, *Biochem. Pharmacol.*, 2000, **60**, 1305–13.
- 26 J. L. Nitiss, *Nat. Rev. Cancer*, 2009, **9**, 338–50.
- 27 J. King-underwood, S. M. Allin, C. W. Redman and A. Richardson, *Ovarian Cancer - Basic Science Perspective*, InTech, London, 2012.
- 28 S. W. Nam, T. Clair, C. K. Campo, H. Y. Lee, L. A. Liotta and M. L. Stracke, *Oncogene*, 2000, **19**, 241–247.
- 29 A. Perrakis and W. H. Moolenaar, *J. Lipid Res.*, 2014, **55**, 1010–8.
- 30 N. Samadi, R. Bekele, D. Capatos, G. Venkatraman, M. Sariahmetoglu and D. N. Brindley, *Biochimie*, 2011, **93**, 61–70.
- 31 R. Leblanc and O. Peyruchaud, *Exp. Cell Res.*, 2015, **333**, 183–189.
- 32 J. Hausmann, W. J. Keune, A. L. Hipgrave Ederveen, L. van Zeijl, R. P. Joosten and A. Perrakis, *J. Struct. Biol.*, 2016, **195**, 199–206.
- 33 M. G. K. Benesch, Y. M. Ko, T. P. W. McMullen and D. N. Brindley, *FEBS Lett.*, 2014, **588**, 2712–2727.
- 34 L. A. van Meeteren, P. Ruurs, C. Stortelers, P. Bouwman, M. A. van Rooijen, J. P. Pradère, T. R. Pettit, M. J. O. Wakelam, J. S. Saulnier-Blache, C. L. Mummery, W. H. Moolenaar and J. Jonkers, *Mol. Cell. Biol.*, 2006, **26**, 5015–22.
- 35 L. M. Miller, W. J. Keune, D. Castagna, L. C. Young, E. L. Duffy, F. Potjewyd, F. Salgado-Polo, P. E. Garcia, D. Semaan, J. M. Pritchard, A. Perrakis, S. J. F. MacDonald, C. Jamieson and A. J. B. Watson, *J. Med. Chem.*, 2017, **60**, 722–748.
- 36 S. Knowlden and S. N. Georas, *J. Immunol.*, 2014, **192**, 851–7.
- 37 M. G. K. Benesch, I. T. K. Macintyre, T. P. W. McMullen and D. N. Brindley, *Cancers (Basel)*, 2018, **10**, 73.
- 38 Y.-L. Hu, C. Albanese, R. G. Pestell and R. B. Jaffe, *J. Natl. Cancer Inst.*, 2003, **95**, 733–40.
- 39 D. Meyer zu Heringdorf, H. M. Himmel and K. H. Jakobs, *Biochim. Biophys. Acta - Mol. Cell Biol. Lipids*, 2002, **1582**, 178–189.
- 40 J. I. Fells, S. C. Lee, Y. Fujiwara, D. D. Norman, K. G. Lim, R. Tsukahara, J. Liu, R. Patil, D. D. Miller, R. J. Kirby, S. Nelson, W. Seibel, R. Papoian, A. L. Parrill, D. L. Baker, R. Bittman and G. Tigyi, *Mol. Pharmacol.*, 2013, **84**, 415–424.
- 41 D. N. Brindley, F. Lin and G. J. Tigyi, *Biochim. Biophys. Acta, Mol. Cell Biol. Lipids*, 2013, **1831**, 74–85.

- 42 J. Hausmann, S. Kamtekar, E. Christodoulou, J. E. Day, T. Wu, Z. Fulkerson, H. M. H. G. Albers, L. A. van Meeteren, A. J. S. Houben, L. van Zeijl, S. Jansen, M. Andries, T. Hall, L. E. Pegg, T. E. Benson, M. Kasiem, K. Harlos, C. W. Vander Kooi, S. S. Smyth, H. Ovaa, M. Bollen, A. J. Morris, W. H. Moolenaar and A. Perrakis, *Nat. Struct. Mol. Biol.*, 2011, **18**, 198–204.
- 43 H. M. H. G. Albers, L. J. D. Hendrickx, R. J. P. Van Tol, J. Hausmann, A. Perrakis and H. Ovaa, *J. Med. Chem.*, 2011, **54**, 4619–4626.
- 44 D. Castagna, D. C. Budd, S. J. F. MacDonald, C. Jamieson and A. J. B. Watson, *J. Med. Chem.*, 2016, **59**, 5604–5621.
- 45 J. L. Tanyi, A. J. Morris, J. K. Wolf, X. Fang, Y. Hasegawa, R. Lapushin, N. Auersperg, Y. J. Sigal, R. A. Newman, E. A. Felix, E. N. Atkinson and G. B. Mills, *Cancer Res.*, 2003, **63**, 1073–82.
- 46 Z. Stanojeviæ, G. Ranèiæ, N. Potiæ-Zeèeviaæ, B. Ðorðeviaæ, M. Markoviaæ and I. Todorovska, *Arch Oncol*, 2004, **12**, 115–8.
- 47 R. M. Kortlever, T. R. Brummelkamp, L. A. van Meeteren, W. H. Moolenaar and R. Bernards, *Mol. Cancer Res.*, 2008, **6**, 1452–60.
- 48 R. Y. J. Huang, S. M. Wang, C. Y. Hsieh and J. C. Wu, *Int. J. Cancer*, 2008, **123**, 801–809.
- 49 S.-U. Hwang, K.-J. Kim, E. Kim, J. D. Yoon, K. M. Park, M. Jin, Y. Han, M. Kim, G. Lee and S.-H. Hyun, *Theriogenology*, 2018, **113**, 197–207.
- 50 M. J. Duffy, V. Estrella, J. R. Wiener, M. Mao, A. Eder, M. V. Watt, R. C. Bast and G. B. Mills, *Clin. Cancer Res.*, 1996, **2**, 613–8.
- 51 K. Hindler, *Oncologist*, 2006, **11**, 306–315.
- 52 X. Fang, S. Yu, R. LaPushin, Y. Lu, T. Furui, L. Z. Penn, D. Stokoe, J. R. Erickson, R. C. Bast, G. B. Mills and G. B. Mills, *Biochem. J.*, 2000, **352 Pt 1**, 135–43.
- 53 J. L. Phillips, S. W. Hayward, Y. Wang, J. Vasselli, C. Pavlovich, H. Padilla-Nash, J. R. Pezullo, B. M. Ghadimi, G. D. Grossfeld, A. Rivera, W. M. Linehan, G. R. Cunha and T. Ried, *Cancer Res.*, 2001, **61**, 8143–9.
- 54 M. Kruidering and G. Evan, *IUBMB Life*, 2000, **50**, 85–90.
- 55 R. Mishra, S. K. Panda, P. K. Sahoo, M. S. Bal and A. K. Satapathy, *Parasite Immunol.*, 2017, **39**, 12421.
- 56 D. Westphal, G. Dewson, P. E. Czabotar and R. M. Kluck, *Biochim. Biophys. Acta - Mol. Cell Res.*, 2011, **1813**, 521–531.
- 57 D. N. Brindley, F. T. Lin and G. J. Tigyi, *Biochim. Biophys. Acta - Mol. Cell Biol. Lipids*, 2013, **1831**, 74–85.
- 58 I. Ninou, C. Magkrioti and V. Aidinis, *Front. Med.*, 2018, **5**, 180.
- 59 Z. Lee, R. F. Swaby, Y. Liang, S. Yu, S. Liu, K. H. Lu, R. C. Bast, G. B. Mills and X. Fang, *Cancer Res.*, 2006, **66**, 2740–2748.
- 60 R. Bharadwaj and H. Yu, *Oncogene*, 2004, **23**, 2016–2027.
- 61 D. A. Altomare, H. Q. Wang, K. L. Skele, A. De Rienzo, A. J. Klein-Szanto, A. K. Godwin and J. R. Testa, *Oncogene*, 2004, **23**, 5853–5857.

- 62 L. Hu, J. Hofmann, Y. Lu, G. B. Mills and R. B. Jaffe, *Cancer Res.*, 2002, **62**, 1087–92.
- 63 M. Badinloo and S. Esmaeili-Mahani, *Fundam. Clin. Pharmacol.*, 2014, **28**, 414–422.
- 64 X. Tang, M. G. K. Benesch and D. N. Brindley, *J. Lipid Res.*, 2015, **56**, 2048–60.
- 65 T. M. Maher, E. M. van der Aar, O. Van de Steen, L. Allamassey, J. Desrivot, S. Dupont, L. Fagard, P. Ford, A. Fieuw and W. Wuyts, *Lancet. Respir. Med.*, 2018, **6**, 627–635.
- 66 Idiopathic Pulmonary Fibrosis, <https://www.nhlbi.nih.gov/health-topics/idiopathic-pulmonary-fibrosis>, (accessed 29 July 2018).
- 67 N. Desroy, C. Housseman, X. Bock, A. Joncour, N. Bienvenu, L. Cherel, V. Labeguere, E. Rondet, C. Peixoto, J.-M. Grassot, O. Picolet, D. Annoot, N. Triballeau, A. Monjardet, E. Wakselman, V. Roncoroni, S. Le Tallec, R. Blaque, C. Cottreaux, N. Vandervoort, T. Christophe, P. Mollat, M. Lamers, M. Auberval, B. Hrvacic, J. Ralic, L. Oste, E. van der Aar, R. Brys and B. Heckmann, *J. Med. Chem.*, 2017, **60**, 3580–3590.
- 68 N. Oikonomou, M.-A. Mouratis, A. Tzouveleki, E. Kaffe, C. Valavanis, G. Vilaras, A. Karameris, G. D. Prestwich, D. Bouros and V. Aidinis, *Am. J. Respir. Cell Mol. Biol.*, 2012, **47**, 566–574.
- 69 I. Nikitopoulou, N. Oikonomou, E. Karouzakis, I. Sevastou, N. Nikolaidou-Katsaridou, Z. Zhao, V. Mersinias, M. Armaka, Y. Xu, M. Masu, G. B. Mills, S. Gay, G. Kollias and V. Aidinis, *J. Exp. Med.*, 2012, **209**, 925–33.
- 70 B. Orosa, S. Garcia and C. Conde, *Eur. J. Pharmacol.*, 2015, **765**, 228–233.
- 71 M. F. Gregor and G. S. Hotamisligil, *Annu. Rev. Immunol.*, 2011, **29**, 415–445.
- 72 S. Banerjee, D. D. Norman, S. C. Lee, A. L. Parrill, T. C. T. Pham, D. L. Baker, G. J. Tigyi and D. D. Miller, *J. Med. Chem.*, 2017, **60**, 1309–1324.
- 73 N. Samadi, C. Gaetano, I. S. Goping and D. N. Brindley, *Oncogene*, 2009, **28**, 1028–1039.
- 74 K. Bandoh, J. Aoki, A. Taira, M. Tsujimoto, H. Arai and K. Inoue, *FEBS Lett.*, 2000, **478**, 159–165.
- 75 Y. C. Yung, N. C. Stoddard and J. Chun, *J. Lipid Res.*, 2014, **55**, 1192–214.
- 76 M. R. Steiner, F. W. Holtsberg, J. N. Keller, M. P. Mattson and S. M. Steiner, *Ann. N. Y. Acad. Sci.*, 2000, **905**, 132–41.
- 77 A. Katsifa, E. Kaffe, N. Nikolaidou-Katsaridou, A. N. Economides, S. Newbigging, C. McKerlie and V. Aidinis, *PLoS One*, 2015, **10**, e0143083.
- 78 H. M. H. G. Albers and H. Ovaa, *Chem. Rev.*, 2012, **112**, 2593–2603.
- 79 V. Gududuru, K. Zeng, R. Tsukahara, N. Makarova, Y. Fujiwara, K. R. Pigg, D. L. Baker, G. Tigyi and D. D. Miller, *Bioorg. Med. Chem. Lett.*, 2006, **16**, 451–456.
- 80 D. Baker, Y. Fujiwara, K. Pigg, R. Tsukahara, S. Kobayashi, H. Murofushi, A. Uchiyama, K. Murakami-Murofushi, E. Koh, R. Bandle, H. Byun, R. Bittman, D. Fan, M. Murph, G. Mills and G. Tigyi, *J. Biol. Chem.*, 2006, **281**, 27687.
- 81 L. A. van Meeteren, V. Brinkmann, J. S. Saulnier-Blache, K. R. Lynch and W. H. Moolenaar, *Cancer Lett.*, 2008, **266**, 203–208.
- 82 Patent WO2008157361A1, 2008, 65.

- 83 G. Ferry, N. Moulharat, J.-P. Pradère, P. Desos, A. Try, A. Genton, A. Giganti, M. Beucher-Gaudin, M. Lonchamp, M. Bertrand, J.-S. Saulnier-Blache, G. C. Tucker, A. Cordi and J. A. Boutin, *J. Pharmacol. Exp. Ther.*, 2008, **327**, 809–19.
- 84 PCT Int. Appl. WO2012100018 A1, 2010.
- 85 R. Gupte, A. Siddam, Y. Lu, W. Li, Y. Fujiwara, N. Panupinthu, T.-C. Pham, D. L. Baker, A. L. Parrill, M. Gotoh, K. Murakami-Murofushi, S. Kobayashi, G. B. Mills, G. Tigyi and D. D. Miller, *Bioorg. Med. Chem. Lett.*, 2010, **20**, 7525–7528.
- 86 M. M. Murph, G. W. Jiang, M. K. Altman, W. Jia, D. . Nguyen, W. J. Fambrough, J. M. Hardman, H. T. Nguyen, S. K. Tran, A. A. Alshamrani, D. Madan, J. Zhang and G. D. Prestwich, *Bioorg. Med. Chem.*, 2015, **23**, 5999–6013.
- 87 J. Gierse, A. Thorarensen, K. Beltey, E. Bradshaw-Pierce, L. Cortes-Burgos, T. Hall, A. Johnston, M. Murphy, O. Nemirovskiy, S. Ogawa, L. Pegg, M. Pelc, M. Prinsen, M. Schnute, J. Wendling, S. Wene, R. Weinberg, A. Wittwer, B. Zweifel and J. Masferrer, *J. Pharmacol. Exp. Ther.*, 2010, **334**, 310–7.
- 88 M. Kawaguchi, T. Okabe, S. Okudaira, H. Nishimasu, R. Ishitani, H. Kojima, O. Nureki, J. Aoki and T. Nagano, *ACS Chem. Biol.*, 2013, **8**, 1713–1721.
- 89 PCT Int. Appl. WO2013054185 A1, 2013.
- 90 PCT Int. Appl. WO2015/008229 A1, 2015.
- 91 PCT Int. Appl. WO2014143583 A1, 2014.
- 92 Galapagos, Idiopathic Pulmonary Disease, <http://www.glp.com/IPF>, (accessed 29 July 2018).
- 93 N. Fisher, T. Hilton-Bolt, M. G. Edwards, K. J. Haxton, M. McKenzie, S. M. Allin and A. Richardson, *ACS Med. Chem. Lett.*, 2014, **5**, 34–39.
- 94 N. Fisher, Keele University, 2015.
- 95 R. Duncan, *Nat. Rev. Drug Discov.*, 2003, **2**, 347–360.
- 96 R. Duncan, *J. Control. Release*, 2014, **190**, 371–380.
- 97 N. Kaniwa, N. Aoyagi, H. Ogata, A. Ejima, H. Motoyama and H. Yasumi, *J. Pharmacobiodyn.*, 1988, **11**, 571–575.
- 98 N. Marasini, S. Haque and L. M. Kaminskas, *Curr. Opin. Colloid Interface Sci.*, 2017, **31**, 18–29.
- 99 X. Pang, X. Yang and G. Zhai, *Expert Opin. Drug Deliv.*, 2014, **11**, 1075–1086.
- 100 H. Wu, T. Yin, K. Li, R. Wang, Y. Chen and L. Jing, *Polym. Chem.*, 2018, **9**, 300–306.
- 101 N. Bertrand and J.-C. Leroux, *J. Control. Release*, 2012, **161**, 152–163.
- 102 M. Rivas, C. Janeth, M. Tarhini, W. Badri, K. Miladi, H. Greige-Gerges, Q. A. Nazari, S. A. Galindo Rodríguez, R. Á. Román, H. Fessi and A. Elaissari, *Int. J. Pharm.*, 2017, **532**, 66–81.

- 103 D. López-Molina, S. Chazarra, C. W. How, N. Pruidze, E. Navarro-Perán, F. García-Cánovas, P. A. García-Ruiz, F. Rojas-Melgarejo and J. N. Rodríguez-López, *Int. J. Pharm.*, 2015, **479**, 96–102.
- 104 L. Zhang, Y. Li, C. Wang, G. Li, Y. Zhao and Y. Yang, *Mater. Sci. Eng. C*, 2014, **42**, 111–115.
- 105 M. J. Webber and R. Langer, *Chem. Soc. Rev.*, 2017, **46**, 6600–6620.
- 106 M. Licciardi, C. Scialabba, C. Sardo, G. Cavallaro and G. Giammona, *J. Mater. Chem. B*, 2014, **2**, 4262–4271.
- 107 S. Chen, X. Zhao, J. Chen, J. Chen, L. Kuznetsova, S. S. Wong and I. Ojima, *Bioconjug. Chem.*, 2010, **21**, 979–87.
- 108 G. Russell-Jones, K. McTavish, J. McEwan, J. Rice and D. Nowotnik, *J. Inorg. Biochem.*, 2004, **98**, 1625–1633.
- 109 G. R. Newkome, Z. Yao, G. R. Baker and V. K. Gupta, *J. Org. Chem.*, 1985, **50**, 2003–2004.
- 110 M. T. Morgan, Y. Nakanishi, D. J. Kroll, A. P. Griset, M. A. Carnahan, M. Wathier, N. H. Oberlies, G. Manikumar, M. C. Wani and M. W. Grinstaff, *Cancer Res.*, 2006, **66**, 11913–11921.
- 111 B. Říhová, *Adv. Drug Deliv. Rev.*, 1996, **21**, 157–176.
- 112 A. Abuchowski, T. Van Es, N. C. Palczuk and F. F. Davis, *J. Biol. Chem.*, 1977, **252**, 3578–3581.
- 113 P. Mishra, B. Nayak and R. K. Dey, *Asian J. Pharm. Sci.*, 2016, **11**, 337–348.
- 114 Y. Singh, P. Murat and E. Defrancq, *Chem. Soc. Rev.*, 2010, **39**, 2054.
- 115 J.-F. Liao, J.-C. Lee, C.-K. Lin, K.-C. Wei, P.-Y. Chen and H.-W. Yang, *Theranostics*, 2017, **7**, 2593–2605.
- 116 K. S. Frederiksen, N. Abrahamsen, R. J. Cristiano, L. Damstrup and H. S. Poulsen, *Cancer Gene Ther.*, 2000, **7**, 262–268.
- 117 M. F. Seifu and L. K. Nath, *Polym. Plast. Technol. Eng.*, 2018, 1–14.
- 118 C. A. Schoener, B. Carillo-Conde, H. N. Hutson and N. A. Peppas, *J Drug Deliv Sci Technol.*, 2014, **23**, 111–118.
- 119 J. W. Singer, S. Shaffer, B. Baker, A. Bernareggi, S. Stromatt, D. Nienstedt and M. Besman, *Anticancer. Drugs*, 2005, **16**, 243–54.
- 120 L. Paz-Ares, H. Ross, M. O'Brien, A. Riviere, U. Gatzemeier, J. Von Pawel, E. Kaukel, L. Freitag, W. Digel, H. Bischoff, R. García-Campelo, N. Iannotti, P. Reiterer, I. Bover, J. Prendiville, A. J. Eisenfeld, F. B. Oldham, B. Bandstra, J. W. Singer and P. Bonomi, *Br. J. Cancer*, 2008, **98**, 1608–1613.
- 121 K. Jain, P. Kesharwani, U. Gupta and N. K. Jain, *Int. J. Pharm.*, 2010, **394**, 122–142.
- 122 R. Duncan and M. J. Vicent, *Adv. Drug Deliv. Rev.*, 2013, **65**, 60–70.
- 123 T. Okusaka, S. Okada, H. Ueno, M. Ikeda, R. Iwata, H. Furukawa, K. Takayasu, N. Moriyama, T. Sato and K. Sato, *Oncology*, 2002, **62**, 228–233.

- 124 M. Connock, S. Tubeuf, K. Malottki, A. Uthman, J. Round, S. Bayliss, C. Meads and D. Moore, *Health Technol. Assess. (Rockv).*, 2010, **14**, 1–10.
- 125 L. Frimat, C. Mariat, P. Landais, S. Koné, B. Commenges and G. Choukroun, *BMJ Open*, 2013, **3**, e001888.
- 126 S. J. Matthews and C. McCoy, *Clin. Ther.*, 2004, **26**, 991–1025.
- 127 Z. Zhang and A. Fiorino, *Blood*, 2009, **114**, 3086.
- 128 E. Miele, G. P. Spinelli, E. Miele, F. Tomao and S. Tomao, *Int. J. Nanomedicine*, 2009, **4**, 99–105.
- 129 PMLiVE, Copaxone - sales performance, data and rankings - Top Pharma List, http://www.pmlive.com/top_pharma_list/pharmaceutical_products/copaxone, (accessed 5 September 2018).
- 130 PMLiVE, Neulasta - sales performance, data and rankings - Top Pharma List - PMLiVE, http://www.pmlive.com/top_pharma_list/pharmaceutical_products/neulasta, (accessed 5 September 2018).
- 131 P. G. Blake and J. T. Daugirdas, Physiology of Peritoneal Dialysis, <https://basicmedicalkey.com/physiology-of-peritoneal-dialysis/#F4-21>, (accessed 5 June 2017).
- 132 K. D. Nolph, *Peritoneal dialysis*, Springer Netherlands, Dordrecht, 3rd edn., 1985.
- 133 K. O'Neill, The Peritoneal (Abdominal) Cavity, <http://teachmeanatomy.info/abdomen/areas/peritoneal-cavity/>, (accessed 1 July 2018).
- 134 M. J. E. Gonzalez, R. Green and F. M. Muggia, *Psychiatr. Times*, 2011, 1–9.
- 135 J. K. Leygoldt, *J. Am. Soc. Nephrol.*, 2002, **13**, 84–91.
- 136 K. D. Nolph, R. P. Popovich, A. J. Ghods and Z. Twardowski, *Kidney Int.*, 1978, **13**, 117–123.
- 137 C. E. Douma, J. K. Hiralall, D. R. De Waart, D. G. Strulik and R. T. Krediet, *Kidney Int.*, 1998, **53**, 1014–1021.
- 138 How peritoneal dialysis works, <http://www.mammothmemory.net/biology/organs-and-systems/kidney-disease-and-dialysis/how-peritoneal-dialysis-works.html>, (accessed 1 July 2018).
- 139 E. V. Mishina, A Study to Evaluate the Pharmacokinetics of a Single Exchange of 7.5% Icodextrin, https://www.fda.gov/ohrms/dockets/ac/01/briefing/3775b1_10_biopharm.htm.
- 140 M. S. Finkelstein F, Healy H, Abu-Alfa A, Ahmad S, Brown F, Gehr T, Nash K, Sorkin M, *J Am Soc Nephrol.*, 2005, **16**, 546–554.
- 141 J. R. Pappenheimer, *Physiol. Rev.*, 1953, **33**, 387–423.
- 142 J. . Frampton and G. . Plosker, *Drugs*, 2003, **63**, 2079–2105.
- 143 E. F. Vonesh, K. O. Story, C. E. Douma and R. T. Krediet, *Perit. Dial. Int.*, 2006, **26**, 475–481.

- 144 J. B. Moberly, S. Mujais, T. Gehr, R. Hamburger, S. Sprague, A. Kucharski, R. Reynolds, F. Ogrinc, L. Martis and M. Wolfson, *Kidney Int. Suppl.*, 2002, **62**, S23–S33.
- 145 H. Qi, C. Xu, H. Yan and J. Ma, *Perit. Dial. Int.*, 2011, **31**, 179–88.
- 146 A. Lin, J. Qian, X. Li, X. Yu, W. Liu, Y. Sun, N. Chen and C. Mei, *Clin. J. Am. Soc. Nephrol.*, 2009, **4**, 1799–1804.
- 147 N. Fisher, M. G. Edwards, R. Hemming, S. M. Allin, J. D. Wallis, P. C. Bulman Page, M. J. McKenzie, S. Jones, M. R. J. Elsegood, J. King-Underwood and A. Richardson, *J. Med. Chem.*, 2018, **61**, 7942–7951.
- 148 V. B. Rodriguez, E. J. Alameda, J. F. M. Gallegos, A. R. Lopez and G. Requena, *Biotechnol. Prog.*, 2006, **22**, 718–722.
- 149 E. García-López, K. Pawlaczyk, B. Anderstam, A. R. Qureshi, M. Kuzlan-Pawlaczyk, O. Heimbürger, A. Werynski and B. Lindholm, *Perit. Dial. Int.*, **27**, 415–23.
- 150 M. J. E. C. Van Der Maarel and B. Van Der Veen, 2002, **94**, 137–155.
- 151 A. Akonur, C. J. Holmes and J. K. Leypoldt, *Perit. Dial. Int.*, 2015, **35**, 288–96.
- 152 D. R. de Waart, M. M. Zweers, D. G. Struijk and R. T. Krediet, *Perit. Dial. Int.*, 2001, **21**, 269–274.
- 153 N. Petrovsky, *J. Excipients Food Chem.*, 2010, **1**, 27–50.
- 154 M. A. Mensink, H. W. Frijlink, K. Van Der Voort Maarschalk and W. L. J. Hinrichs, *Carbohydr. Polym.*, 2015, **134**, 418–428.
- 155 M. A. Mensink, H. W. Frijlink, K. Van Der Voort and W. L. J. Hinrichs, *Carbohydr. Polym.*, 2015, **130**, 405–419.
- 156 J. I. M. Felt, C. Richard, C. Mccaffrey and M. Levy, *Kidney Int.*, 1979, **16**, 459–469.
- 157 J. Pitha, K. Kociolek and M. G. Caron, *Eur. J. Biochem.*, 1979, **94**, 11–18.
- 158 C. Sardo, R. Farra, M. Licciardi, B. Dapas, C. Scialabba, G. Giammona, M. Grassi, G. Grassi and G. Cavallaro, *Eur. J. Pharm. Sci.*, 2015, **75**, 60–71.
- 159 G. Pitarresi, G. Tripodo, R. Calabrese, F. Craparo, M. Licciardi and G. Giammona, *Macromol. Biosci.*, 2008, **8**, 891–902.
- 160 I. Cumpstey, *ISRN Org. Chem.*, 2013, **2013**, 1–27.
- 161 J. Clayden, N. Greeves and S. G. Warren, *Organic chemistry*, 2nd edn., 2012.
- 162 K. A. Kristiansen, A. Potthast and B. E. Christensen, *Carbohydr. Res.*, 2010, **345**, 1264–1271.
- 163 M. Yalpani and L. D. Hall, *Macromolecules*, 1984, **17**, 272–281.
- 164 K. J. Widder and R. Green, *Drug and enzyme targeting*, Academic Press, 1985.
- 165 G. Gregoriadis, *Drug Carriers in Biology and Medicine*, Academic Press, London, 1st Editio., 1979.
- 166 J. Ren, P. Wang, F. Dong, Y. Feng, D. Peng and Z. Guo, *Carbohydr. Polym.*, 2012, **87**, 1744–1748.

- 167 S. Schmidt, T. Liebert and T. Heinze, *Green Chem.*, 2014, **16**, 1941–1946.
- 168 J. S. Brimacombe, B. D. Jones, M. Stacey and J. J. Willard, *Carbohydr. Res.*, 1966, **2**, 167–169.
- 169 R. B. Silverman and M. W. Holladay, *The Organic Chemistry of Drug Design and Drug Action*, Elsevier, 3rd Editio., 2014.
- 170 A. Marie, F. Fournier and J. C. Tabet, *Anal. Chem.*, 2000, **72**, 5106–5114.
- 171 D. Das, S. Mukherjee, A. Pal, R. Das, S. G. Sahu and S. Pal, *RSC Adv.*, 2016, **6**, 9352–9359.
- 172 J. M. Sugihara, *Adv. Carbohydr. Chem.*, 1953, **8**, 1–44.
- 173 A. Koschella, T. Leermann, M. Brackhagen and T. Heinze, *J. Appl. Polym. Sci.*, 2006, **100**, 2142–2150.
- 174 J. Pitha, J. Zjawiony, R. J. Lefkowitz and M. G. Caron, *Proc Natl Acad Sci U S A*, 1980, **77**, 2219–2223.
- 175 J. Morros, B. Levecke and R. M. Infante, *Carbohydr. Polym.*, 2010, **82**, 1168–1173.
- 176 J. Sun, M. T. Perfetti and W. L. Santos, *J. Org. Chem.*, 2011, **76**, 3571–5.
- 177 L. Xu, S. Zhang and P. Li, *Chem. Soc. Rev.*, 2015, **44**, 8848–8858.
- 178 Q. I. Churches and C. A. Hutton, in *Boron Reagents in Synthesis*, American Chemical Society, 2016, pp. 357–377.
- 179 E. Vedejs, R. W. Chapman, S. C. Fields, S. Lin and M. R. Schrimpf, *J. Org. Chem.*, 1995, **60**, 3020–3027.
- 180 M. Berkheij, L. van der Sluis, C. Sewing, D. J. den Boer, J. W. Terpstra, H. Hiemstra, W. I. Iwema Bakker, A. van den Hoogenband and J. H. van Maarseveen, *Tetrahedron Lett.*, 2005, **46**, 2369–2371.
- 181 Baxter Healthcare Corporation, *EXTRANEAL (icodextrin) Peritoneal Dialysis Solution Prescribing information*, 2002.
- 182 N. Itami, J. Kimura, S. Ohira, Y. Tsuji and Y. Katsuki, *Perit. Dial. Int.*, 2003, **23**, 170–174.
- 183 L. C. Rogers, R. R. Davis, N. Said, T. Hollis and L. W. Daniel, *Redox Biol.*, 2018, **15**, 380–386.
- 184 J. F. Hartwig, *Acc. Chem. Res.*, 2012, **45**, 864–873.
- 185 T. Ishiyama, M. Murata and N. Miyauro, *J. Org. Chem.*, 1995, **60**, 7508–7510.
- 186 A. B. Williams and R. N. Hanson, *Tetrahedron*, 2012, **68**, 5406–5414.
- 187 D. H. Qu, Q. C. Wang, J. Ren and H. Tian, *Org. Lett.*, 2004, **6**, 2085–2088.
- 188 H. J. Li, Y. C. Wu, J. H. Dai, Y. Song, R. Cheng and Y. Qiao, *Molecules*, 2014, **19**, 3401–3416.
- 189 M. F. Pouliot, O. Mahé, J. D. Hamel, J. Desroches and J. F. Paquin, *Org. Lett.*, 2012, **14**, 5428–5431.
- 190 A. F. Abdel-Magid, K. G. Carson, B. D. Harris, C. A. Maryanoff and R. D. Shah, *J. Org. Chem.*, 1996, **61**, 3849–3862.

- 191 M. Ali, H. Rahaman, S. K. Pal, N. Kar and S. K. Ghosh, *RSC Adv.*, 2015, **5**, 41780–41785.
- 192 J. Spencer, C. B. Baltus, H. Patel, N. J. Press, S. K. Callear, L. Male and S. J. Coles, *ACS Comb. Sci.*, 2011, **13**, 24–31.
- 193 N. Srinivasan, A. Yurek-George and A. Ganesan, *Mol. Divers.*, 2005, **9**, 291–293.
- 194 P. G. M. Wuts and T. W. Greene, *Greene's protective groups in organic synthesis.*, John Wiley & Sons., 4th edn., 2007.
- 195 S. Butini, M. Brindisi, S. Gemma, P. Minetti, W. Cabri, G. Gallo, S. Vincenti, E. Talamonti, F. Borsini, a Caprioli, M. a Stasi, S. Di Serio, S. Ros, G. Borrelli, S. Maramai, F. Fezza, G. Campiani and M. Maccarrone, *J. Med. Chem.*, 2012, **55**, 6898–6915.
- 196 Q. I. Churches, J. F. Hooper and C. A. Hutton, *J. Org. Chem.*, 2015, **80**, 5428–5435.
- 197 V. Bagutski, A. Ros and V. K. Aggarwal, *Tetrahedron*, 2009, **65**, 9956–9960.
- 198 Sigma-Aldrich, Phosphazene Bases,
<https://www.sigmaaldrich.com/chemistry/chemical-synthesis/technology-spotlights/phosphazenes.html>, (accessed 11 August 2018).
- 199 K. Astakhova, A. V. Golovin, I. A. Prokhorenko, A. V. Ustinov, I. A. Stepanova, T. S. Zatsepin and V. A. Korshun, *Tetrahedron*, 2017, **73**, 3220–3230.
- 200 G. Plourde and R. Spaetzel, *Molecules*, 2003, **7**, 697–705.
- 201 G. H.S., R. M. Melavanki, N. D., B. P. and R. A. Kusanur, *J. Mol. Liq.*, 2017, **227**, 37–43.
- 202 B. Pappin, M. J. and T. A., in *Carbohydrates - Comprehensive Studies on Glycobiology and Glycotechnology*, InTech, 2012.
- 203 A. Pal, M. Bérubé and D. G. Hall, *Angew. Chemie Int. Ed.*, 2010, **49**, 1492–1495.
- 204 R. Nishiyabu, Y. Kubo, T. D. James and J. S. Fossey, *Chem. Commun.*, 2011, **47**, 1124–1150.
- 205 H. R. Snyder, J. A. Kuck and J. R. Johnson, *J. Am. Chem. Soc.*, 1938, **60**, 105–111.
- 206 S. R. Chaudhari, *Chem. Phys. Lett.*, 2015, **634**, 95–97.
- 207 E. P. Gillis and M. D. Burke, *J. Am. Chem. Soc.*, 2008, **130**, 14084–14085.
- 208 N. Hiroyoshi, S. Takayuki, C. Chou and M. Sugimoto, *Org. Lett.*, 2008, **10**, 277–280.
- 209 E. Schacht, L. Buys, J. Vermeersch and J. P. Remon, *J. Control. Release*, 1984, **1**, 33–46.
- 210 S. Cérantola, N. Kervarec, R. Pichon, C. Magné, M. A. Bessieres and E. Deslandes, *Carbohydr. Res.*, 2004, **339**, 2445–2449.
- 211 N. Saifuddin, Y. A. A. Nur and S. F. Abdullah, *Asian J. Biochem.*, 2011, **6**, 38–54.
- 212 S. Dinara and N. Saifuddin, *Adv. Nat. Appl. Sci.*, 2012, **6**, 249–267.
- 213 H. E. Gottlieb, V. Kotlyar and A. Nudelman, *J. Org. Chem.*, 1997, **3263**, 7512–7515.
- 214 T. Ehrenfreund-Kleinman, J. Golenser and A. J. Domb, *Biomaterials*, 2004, **25**, 3049–3057.
- 215 F. Csende, *Mini. Rev. Org. Chem.*, 2015, **12**, 127–148.

- 216 F. Mo, G. Dong, Y. Zhang and J. Wang, *Org. Biomol. Chem.*, 2013, **11**, 1582.
- 217 S. Shaaban and B. F. Abdel-Wahab, *Mol. Divers.*, 2016, **20**, 233–254.
- 218 S. K. Guchhait and C. Madaan, *Tetrahedron Lett.*, 2011, **52**, 56–58.
- 219 L. A. van Meeteren, P. Ruurs, E. Christodoulou, J. W. Goding, H. Takakusa, K. Kikuchi, A. Perrakis, T. Nagano and W. H. Moolenaar, *J. Biol. Chem.*, 2005, **280**, 21155–61.
- 220 C. G. Ferguson, C. S. Bigman, R. D. Richardson, L. A. van Meeteren, W. H. Moolenaar and G. D. Prestwich, *Org. Lett.*, 2006, **8**, 2023–2026.
- 221 E. L. Shelton, C. L. Galindo, C. H. Williams, E. Pfaltzgraff, C. C. Hong and D. M. Bader, *PLoS One*, 2013, **8**, e69712.
- 222 F. Salgado-Polo, A. Fish, M.-T. Matsoukas, T. Heidebrecht, W.-J. Keune and A. Perrakis, *J. Biol. Chem.*, 2018, jbc.RA118.004450.
- 223 Echelon Biosciences, Product Details for Autotaxin Inhibitor Screening Kit by EBI : Echelon Biosciences : assay and reagents for drug discovery in lipid signaling pathways, <http://www.echelon-inc.com/index.php?module=Products&func=detail&id=731>, (accessed 29 August 2018).
- 224 M. Linden, D. Hadler and S. Hofmann, *Hum. Psychopharmacol. Clin. Exp.*, 1997, **12**, 445–452.
- 225 J.-M. Ferland, C. A. Demerson and L. G. Humber, *Can. J. Chem.*, 1985, **63**, 361–365.
- 226 Z.-P. Zhuang, M.-P. Kung, M. Mu and H. F. Kung, *J. Med. Chem.*, 1998, **41**, 157–166.
- 227 A. Suneja, V. Bisai and V. K. Singh, *J. Org. Chem.*, 2016, **81**, 4779–4788.
- 228 E. De Clercq, *J. Med. Chem.*, 1995, **38**, 2491–517.
- 229 I. Pendrak, S. Barney, R. Wittrock, D. M. Lambert and W. D. Kingsbury, *J. Org. Chem.*, 1994, **59**, 2623–2625.
- 230 S. Dhanasekaran, A. Kayet, A. Suneja, V. Bisai and V. K. Singh, *Org. Lett.*, 2015, **17**, 2780–2783.
- 231 R. Hemming, 2015.
- 232 E. Deniau, D. Enders, A. Couture and P. Grandclaudon, *Tetrahedron Asymmetry*, 2003, **14**, 2253–2258.
- 233 L. A. Nguyen, H. He and C. Pham-Huy, *Int. J. Biomed. Sci.*, 2006, **2**, 85–100.
- 234 S. M. Allin, C. J. Northfield, M. I. Page and A. M. Z. Slawin, *J. Chem. Soc. Perkin Trans. 1*, 2000, **0**, 1715–1721.
- 235 D. L. Comins, Stefan Schilling and Y. Zhang, *Org. Lett.*, 2005, **7**, 95–98.
- 236 M. Lamblin, A. Couture, E. Deniau and P. Grandclaudon, *Tetrahedron: Asymmetry*, 2008, **19**, 111–123.
- 237 V. Agouridas, F. Capet, A. Couture, E. Deniau and P. Grandclaudon, *Tetrahedron Asymmetry*, 2011, **22**, 1441–1447.
- 238 J. Clayden and C. J. Menet, *Tetrahedron Lett.*, 2003, **44**, 3059–3062.

- 239 J. Perard-Viret, A. Tomas, T. Prange and J. Royer, *Tetrahedron*, 2002, **58**, 5103–5108.
- 240 S. M. Allin, C. J. Northfield, M. I. Page and A. M. . Slawin, *Tetrahedron Lett.*, 1997, **38**, 3627–3630.
- 241 S. M. Allin, C. J. Northfield, M. I. Page and A. M. Z. Slawin, *Tetrahedron Lett.*, 1999, **40**, 141–142.
- 242 S. M. Allin, C. J. Northfield, M. I. Page and A. M. . Slawin, *Tetrahedron Lett.*, 1998, **39**, 4905–4908.
- 243 O. Fains and J. M. Vernon, *Tetrahedron Lett.*, 1997, **38**, 8265–8266.
- 244 L. E. Burgess and A. I. Meyers, *J. Org. Chem.*, 1992, **57**, 1656–1662.
- 245 L. E. Burgess and A. I. Meyers, *J. Am. Chem. Soc.*, 1991, **113**, 9858–9859.
- 246 T. R. Belliotti, W. A. Brink, S. R. Kesten, J. R. Rubin, D. J. Wustrow, K. T. Zoski, S. Z. Whetzel, A. E. Corbin, T. A. Pugsley, T. G. Heffner and L. D. Wise, *Bioorg. Med. Chem. Lett.*, 1998, **8**, 1499–1502.
- 247 P. Laborda, S.-Y. Wang, J. Voglmeir, P. Laborda, S.-Y. Wang and J. Voglmeir, *Molecules*, 2016, **21**, 1513.
- 248 Y. Hayashi, H. Gotoh, T. Hayashi and M. Shoji, *Angew. Chemie Int. Ed.*, 2005, **44**, 4212–4215.
- 249 J. L. Hollander, E. M. Brown, R. A. Jessar and C. Y. Brown, *Ann. Rheum. Dis.*, 1951, **10**, 473–6.
- 250 NHS, Steroid injections, <https://www.nhs.uk/conditions/steroid-injections/>, (accessed 9 September 2018).
- 251 D. Mastropaolo, A. Camerman, Y. Luo, G. D. Brayer and N. Camerman, *Proc. Natl. Acad. Sci. U. S. A.*, 1995, **92**, 6920–4.
- 252 S. M. Ansell, S. A. Johnstone, P. G. Tardi, L. Lo, S. Xie, Y. Shu, T. O. Harasym, N. L. Harasym, L. Williams, D. Bermudes, B. D. Liboiron, W. Saad, R. K. Prud'homme and L. D. Mayer, *J. Med. Chem.*, 2008, **51**, 3288–3296.
- 253 J. S. Sohn, J. Il Jin, M. Hess and B. W. Jo, *Polym. Chem.*, 2010, **1**, 778.
- 254 US20080194546A1, 2007.
- 255 J. Lee, J. Park and V. S. Hong, *Chem. Pharm. Bull.*, 2014, **62**, 906–914.
- 256 G. M. Sheldrick, SHELX, <http://shelx.uni-ac.gwdg.de/SHELX/>.
- 257 D. Koley, Y. Krishna, K. Srinivas, A. A. Khan and R. Kant, *Angew. Chemie Int. Ed.*, 2014, **53**, 13196–13200.
- 258 G. Llewellyn and B. K. Stein, *EPSRC National Mass Spectrometry Centre , Swansea NMSSC Application Note No 6 Boronic Acid Analysis by Mass Spectrometry - I: Cis-diol Derivatisation for EI and CI Analysis*, 2008.
- 259 M. Beier, A. Stephan and J. D. Hoheisel, *Helv. Chim. Acta*, 2001, **84**, 2089–2095.